APR 29 1989

NAS1.55:3031/pt.1

MF-0830-H-10

NASA Conference Publication 3031
Part 1

Recent Advances in Multidisciplinary Analysis and Optimization

Proceedings of a symposium held in
Hampton, Virginia
September 28-30, 1988

NASA

VL

COMPLETED

NASA Conference Publication 3031
Part 1

Recent Advances in Multidisciplinary Analysis and Optimization

Jean-François M. Barthelemy, *Editor*
NASA Langley Research Center
Hampton, Virginia

Proceedings of a symposium cosponsored by
NASA Langley Research Center, NASA Lewis
Research Center, and the Wright Research
Development Center, and held in
Hampton, Virginia
September 28-30, 1988

NASA
National Aeronautics and
Space Administration
Office of Management
Scientific and Technical
Information Division

1989

BLANK PAGE

PREFACE

This publication contains papers presented at the Second NASA/Air Force Symposium on Recent Advances in Multidisciplinary Analysis and Optimization held September 28-30, 1988 in Hampton, Virginia. The symposium was cosponsored by NASA Langley, NASA Lewis, and the Wright Research Development Center. The meeting was attended by 195 participants, with 41% from industry, 35% from academia, and 24% from government organizations.

The aim of the symposium was to provide a forum for researchers, software developers, and practitioners of multidisciplinary analysis and optimization to learn of the latest developments and to exchange experiences in this burgeoning field of engineering.

Ninety-two papers were presented (83 of which are published here). Of the papers originally presented, 58% discussed method development, 30% applications, and 12% software development or implementation. Most (72%) of the contributions to the symposium were strictly multidisciplinary. There were 15 papers dealing with the combination of structures and control systems, 10 with aeroelastic problems, and 5 with aeroservoelastic problems. Eight papers dealt with generic developments in multidisciplinary design. The keynote address was a review of the role of knowledge-based systems in analysis and optimization.

The papers are grouped by sessions and are identified in the Contents. Papers were edited to conform to the technical standards set by NASA for conference publications. A list of addresses of all registered participants is included.

Jean-François M. Barthelemy
Technical Program Chairman

BLANK PAGE

CONTENTS

PREFACE iii

ATTENDEES xiii

Part 1

Session 1: Plenary
Chairman: Owen F. Hughes

APPLICATIONS OF INTEGRATED DESIGN/ANALYSIS SYSTEMS IN AEROSPACE STRUCTURAL DESIGN 3
Philip Mason, Edwin Lerner, and Lawrence Sobel

INTEGRATED DESIGN OPTIMIZATION RESEARCH AND DEVELOPMENT IN AN INDUSTRIAL ENVIRONMENT 39
V. Kumar, M. D. German, and S.-J. Lee

OPTIMIZATION BY DECOMPOSITION: A STEP FROM HIERARCHIC TO NON-HIERARCHIC SYSTEMS 51
Jaroslaw Sobieszczanski-Sobieski

OVERVIEW OF DYNAMICS INTEGRATION RESEARCH (DIR) PROGRAM AT LANGLEY RESEARCH CENTER: Goals and Progress 79
Steven M. Sliwa and Irving Abel

SESSION 2: HELICOPTERS
Chairmen: D. Anderson and R. G. Kvaternik

AN INITIATIVE IN MULTIDISCIPLINARY OPTIMIZATION OF ROTORCRAFT 109
Howard M. Adelman and Wayne R. Mantay

STRUCTURAL OPTIMIZATION OF ROTOR BLADES WITH STRAIGHT AND SWEPT TIPS SUBJECT TO AEROELASTIC CONSTRAINTS 145
Peretz P. Friedmann and Roberto Celi

OPTIMIZATION OF ROTOR BLADES FOR COMBINED STRUCTURAL, PERFORMANCE, AND AEROELASTIC CHARACTERISTICS 163
David A. Peters and Y. P. Cheng

TRANSONIC AIRFOIL DESIGN FOR HELICOPTER ROTOR APPLICATIONS 181
Ahmed A. Hassan and B. Jackson

EFFICIENT SENSITIVITY ANALYSIS AND OPTIMIZATION OF A HELICOPTER ROTOR 195
J. W. Lim and I. Chopra

STRUCTURAL OPTIMIZATION OF ROTOR BLADES WITH INTEGRATED DYNAMICS AND AERODYNAMICS 209
Aditi Chattopadhyay and Joanne L. Walsh

MULTI-OBJECTIVE/LOADING OPTIMIZATION FOR ROTATING COMPOSITE FLEXBEAMS 235
Brian K. Hamilton and James R. Peters

SESSION 3: ARTIFICIAL INTELLIGENCE
Chairmen: K. H. Abbott and P. Hajela

NEW DIRECTIONS FOR ARTIFICIAL INTELLIGENCE (AI) METHODS IN OPTIMUM DESIGN 259
Prabhat Hajela

DEVELOPMENT OF A MICRO-COMPUTER BASED INTEGRATED DESIGN SYSTEM FOR HIGH ALTITUDE LONG ENDURANCE AIRCRAFT 275
David W. Hall and J. Edward Rogan

DEMONSTRATION OF DECOMPOSITION AND OPTIMIZATION IN THE DESIGN OF EXPERIMENTAL SPACE SYSTEMS 297
Sharon L. Padula, Chris A. Sandridge, Raphael T. Haftka, and Joanne L. Walsh

STRUTEX - A PROTOTYPE KNOWLEDGE-BASED SYSTEM FOR INITIALLY CONFIGURING A STRUCTURE TO SUPPORT POINT LOADS IN TWO DIMENSIONS 317
James L. Rogers and Jaroslaw Sobieszczanski-Sobieski

TRUSS: AN INTELLIGENT DESIGN SYSTEM FOR AIRCRAFT WINGS 333
Preston R. Bates and Daniel P. Schrage

REAL-TIME APPLICATION OF KNOWLEDGE-BASED SYSTEMS 357
Randal W. Brumbaugh and Eugene L. Duke

THE DESIGNER OF THE 90'S: A LIVE DEMONSTRATION 373
Tommy L. Green, Basil M. Jordan, Jr., and Timothy L. Oglesby

SESSION 4: AEROELASTIC TAILORING
Chairmen: B. A. Rommel and T. A. Weisshar

STRUCTURAL TAILORING OF COUNTER ROTATION PROPFANS 389
K. W. Brown and D. A. Hopkins

COMPOSITE SIZING AND PLY ORIENTATION FOR STIFFNESS REQUIREMENTS USING A LARGE FINITE ELEMENT STRUCTURAL MODEL 403
N. A. Radovcich and D. P. Gentile

AEROELASTIC TAILORING AND INTEGRATED WING DESIGN 431
Mike Love and Jon Bohlmann

INTEGRATED AERODYNAMIC-STRUCTURAL DESIGN OF A FORWARD-SWEPT TRANSPORT WING 445
R. T. Haftka, B. Grossman, P. J. Kao, D. M. Polen, and J. Sobieszczanski-Sobieski

STATIC AEROELASTIC ANALYSIS AND TAILORING OF MISSILE CONTROL FINS 465
S. C. McIntosh, Jr., and M. F. E. Dillenius

EFFECTS OF NONLINEAR AERODYNAMICS AND STATIC AEROELASTICITY ON MISSION PERFORMANCE CALCULATIONS FOR A FIGHTER AIRCRAFT 477
Gary L. Giles, Kenneth E. Tatum, and William E. Foss, Jr.

OPTIMUM STRUCTURAL DESIGN WITH STATIC AEROELASTIC CONSTRAINTS 497
K. B. Bowman, R. V. Grandhi, and F. E. Eastep

OPTIMUM DESIGN OF SWEPT-FORWARD HIGH-ASPECT-RATIO GRAPHITE-EPOXY WINGS 509
M. J. Shuart, R. T. Haftka, and R. L. Campbell

PART 2*

SESSION 5: SOFTWARE I

Chairmen: G. N. Vanderplaats and R. E. Fulton

ASTROS - A MULTIDISCIPLINARY AUTOMATED STRUCTURAL DESIGN TOOL 529
D. J. Neill

A GENERALIZED SOFTWARE EXECUTIVE FOR MULTIDISCIPLINARY COMPUTATIONAL STRUCTURAL DYNAMICS 545
Alex Berman

RESEARCH ON OPTIMIZATION-BASED DESIGN AT THE ENGINEERING DESIGN METHODS LAB, BRIGHAM YOUNG UNIVERSITY 565
R. J. Balling, A. R. Parkinson, and J. C. Free

RECENT EXPERIENCES USING FINITE-ELEMENT-BASED STRUCTURAL OPTIMIZATION 581
B. K. Paul, J. C. McConnell, and M. H. Love

THE SIZING AND OPTIMIZATION LANGUAGE (SOL) - A COMPUTER LANGUAGE TO IMPROVE THE USER/OPTIMIZER INTERFACE 601
S. H. Lucas and S. J. Scotti

ROBUST COMPUTER-AIDED SYNTHESIS AND OPTIMIZATION OF LINEAR MULTIVARIABLE CONTROL SYSTEMS WITH VARYING PLANT DYNAMICS VIA AUTOCON 621
C. P. Lefkowitz, J. A. Tekawy, P. K. Pujara, and M. G. Safonov

COMPUTERIZED DESIGN SYNTHESIS (CDS), A DATA BASE-DRIVEN MULTIDISCIPLINARY DESIGN TOOL 639
D. M. Anderson and A. O. Bolukbasi

SESSION 6: SENSITIVITY ANALYSIS

Chairmen: R. T. Haftka and B. Prasad

ON EQUIVALENCE OF DISCRETE-DISCRETE AND CONTINUUM-DISCRETE DESIGN SENSITIVITY ANALYSIS 653
Kyung K. Choi and Sung-Ling Twu

AN INVESTIGATION OF USING AN RQP BASED METHOD TO CALCULATE PARAMETER SENSITIVITY DERIVATIVES 673
Todd J. Beltracchi and Gary A. Gabriele

---

*Presented under separate cover.

GRID SENSITIVITY CAPABILITY FOR LARGE SCALE STRUCTURES 697
Gopal K. Nagendra and David V. Wallerstein

ITERATIVE METHODS FOR DESIGN SENSITIVITY ANALYSIS 713
A. D. Belegundu and B. G. Yoon

RESULTS OF AN INTEGRATED STRUCTURE/CONTROL LAW DESIGN SENSITIVITY ANALYSIS 727
Michael G. Gilbert

ON THE CALCULATION OF DERIVATIVES OF EIGENVALUES AND EIGENVECTORS IN THE SIMULTANEOUS DESIGN AND CONTROL OF STRUCTURES 747
Luis Mesquita and Manohar P. Kamat

TREATMENT OF BODY FORCES IN BOUNDARY ELEMENT DESIGN SENSITIVITY ANALYSIS 759
Sunil Saigal, R. Aithal, and Jizu Cheng

DESIGN SENSITIVITY ANALYSIS OF BOUNDARY ELEMENT SUBSTRUCTURES 777
James H. Kane, Sunil Saigal, and Richard H. Gallagher

SESSION 7: CONTROL OF AEROELASTIC STRUCTURES

Chairmen: I. Abel, and N. A. Radovcich

AEROSERVOELASTIC TAILORING FOR LATERAL CONTROL ENHANCEMENT 803
Terrence A. Weisshaar and Changho Nam

RESULTS OF INCLUDING GEOMETRIC NONLINEARITIES IN AN AEROELASTIC MODEL OF AN F/A-18 815
Carey S. Buttrill

FLUTTER SUPPRESSION USING EIGENSPACE FREEDOMS TO MEET REQUIREMENTS 837
William M. Adams, Jr., Robert E. Fennell, and David M. Christhilf

AEROELASTIC MODELING FOR THE FIT TEAM F/A-18 SIMULATION 861
Thomas A. Zeiler and Carol D. Wieseman

DIGITAL ROBUST CONTROL LAW SYNTHESIS USING CONSTRAINED OPTIMIZATION 879
Vivekananda Mukhopadhyay

AN INTEGRATED APPROACH TO THE OPTIMUM DESIGN OF ACTIVELY CONTROLLED COMPOSITE WINGS 897
E. Livne

CONTROL SURFACE SPANWISE PLACEMENT IN ACTIVE FLUTTER SUPPRESSION SYSTEMS 919
E. Nissim and J. J. Burken

SESSION 8: STRUCTURES

Chairmen: R. Levy and P. Papalambros

AN APPROXIMATION FUNCTION FOR FREQUENCY CONSTRAINED STRUCTURAL OPTIMIZATION 937
R. A. Canfield

STRUCTURAL OPTIMIZATION OF FRAMED STRUCTURES USING GENERALIZED OPTIMALITY CRITERIA 955
R. M. Kolonay, V. B. Venkayya, V. A. Tischler, and R. A. Canfield

FINITE ELEMENT FLOW-THERMAL-STRUCTURAL ANALYSIS OF AERODYNAMICALLY HEATED LEADING EDGES 971
Pramote Dechaumphai, Allan R. Wieting, and Ajay K. Pandey

INVOLUTE COMPOSITE DESIGN EVALUATION USING GLOBAL DESIGN SENSITIVITY DERIVATIVES 991
J. K. Hart and E. L. Stanton

OPTIMIZING FOR MINIMUM WEIGHT WHEN TWO DIFFERENT FINITE ELEMENT MODELS AND ANALYSES ARE REQUIRED 1009
Jeffrey C. Hall

PART 3*

SESSION 9: LARGE ENGINEERING SYSTEMS
Chairman: G. L. Giles

ENGINEERING APPLICATIONS OF HEURISTIC MULTILEVEL OPTIMIZATION METHODS 1029
Jean-Francois M. Barthelemy

RECENT DEVELOPMENTS IN MULTILEVEL OPTIMIZATION 1039
G. N. Vanderplaats and D-S Kim

A DECOMPOSITION-BASED DESIGN OPTIMIZATION METHOD WITH APPLICATIONS 1055
S. Azarm, M. Pecht, W.-C. Li, and S. Praharaj

MULTILEVEL DECOMPOSITION OF COMPLETE VEHICLE CONFIGURATION IN A PARALLEL COMPUTING ENVIRONMENT 1069
Vinay Bhatt and K. M. Ragsdell

SESSION 10: SHAPE OPTIMIZATION
Chairman: G. A. Gabriele

DESIGN OPTIMIZATION OF AXISYMMETRIC BODIES IN NONUNIFORM TRANSONIC FLOW 1085
C. Edward Lan

PROCEDURES FOR SHAPE OPTIMIZATION OF GAS TURBINE DISKS 1097
Tsu-Chien Cheu

SESSION 11: ENGINEERING SYSTEM DESIGN
Chairmen: M. D. German and D. P. Schrage

A DECISION-BASED PERSPECTIVE FOR THE DESIGN OF METHODS FOR SYSTEMS DESIGN 1111
Farrokh Mistree, Douglas Muster, Jon A. Shupe, and Janet K. Allen

---

*Presented under separate cover.

THE ART OF SPACECRAFT DESIGN: A MULTIDISCIPLINARY CHALLENGE 1137
F. Abdi, H. Ide, M. Levine, and L. Austel

HYPERSONIC AIRBREATHING VEHICLE CONCEPTUAL DESIGN (FOCUS ON AERO-SPACE PLANE) 1157
James L. Hunt and John G. Martin

OPTIMIZING CONCEPTUAL AIRCRAFT DESIGNS FOR MINIMUM LIFE CYCLE COST 1195
Vicki S. Johnson

AIRCRAFT DESIGN OPTIMIZATION WITH MULTIDISCIPLINARY PERFORMANCE CRITERIA 1219
Stephen Morris and Ilan Kroo

SESSION 12: METHODS
Chairmen: M. P. Kamat and J. E. Rogan

AN INTERPRETATION AND SOLUTION OF ILL-CONDITIONED LINEAR EQUATIONS 1239
I. U. Ojalvo and T. Ting

GENERALIZED MATHEMATICAL MODELS IN DESIGN OPTIMIZATION 1253
Panos Y. Papalambros and J. R. Jagannatha Rao

OPTIMUM DESIGN OF STRUCTURES SUBJECT TO GENERAL PERIODIC LOADS 1265
R. Reiss and B. Qian

FUZZY SET APPLICATIONS IN ENGINEERING OPTIMIZATION 1279
Alejandro R. Diaz

A PENALTY APPROACH FOR NONLINEAR OPTIMIZATION WITH DISCRETE DESIGN VARIABLES 1291
Dong K. Shin, Z. Gurdal, and O. H. Griffin, Jr.

MULTIPLIER-CONTINUATION ALGORITHMS FOR CONSTRAINED OPTIMIZATION 1303
Bruce N. Lundberg, Aubrey B. Poore and Bing Yang

SESSION 13: SOFTWARE II
Chairmen: R. A. Canfield and J. L. Rogers, Jr.

A LARGE SCALE SOFTWARE SYSTEM FOR SIMULATION AND DESIGN OPTIMIZATION OF MECHANICAL SYSTEMS 1319
Bernhard Dopker and Edward J. Haug

THE ROLE OF OPTIMIZATION IN THE NEXT GENERATION OF COMPUTER-BASED DESIGN TOOLS 1335
J. E. Rogan

AN OVERVIEW OF THE DOUGLAS AIRCRAFT COMPANY AEROELASTIC DESIGN OPTIMIZATION PROGRAM (ADOP) 1359
Alan J. Dodd

MEETING THE CHALLENGES WITH THE DOUGLAS AIRCRAFT COMPANY AEROELASTIC DESIGN OPTIMIZATION PROGRAM (ADOP) 1369
Bruce A. Rommel

SESSION 14: DYNAMICS AND CONTROL OF FLEXIBLE STRUCTURES
Chairmen: J.-N. Juang and E. Livne

OPTIMIZATION OF STRUCTURE AND CONTROL SYSTEM 1381
N. S. Khot and R. V. Grandhi

STRUCTURAL OPTIMIZATION AND RECENT LARGE GROUND ANTENNA INSTALLATIONS 1393
Roy Levy

A NOVEL IMPLEMENTATION OF METHOD OF OPTIMALITY CRITERION IN SYNTHESIZING SPACECRAFT STRUCTURES WITH NATURAL FREQUENCY CONSTRAINTS 1417
B. P. Wang and F. H. Chu

COMPUTATIONAL EXPERIMENTS IN THE OPTIMAL SLEWING OF FLEXIBLE STRUCTURES 1427
T. E. Baker and E. Polak

OPTIMAL PLACEMENT OF EXCITATIONS AND SENSORS BY SIMULATED ANNEALING 1441
M. Salama, R. Bruno, G-S. Chen, and J. Garba

EXPERIENCES IN APPLYING OPTIMIZATION TECHNIQUES TO CONFIGURATIONS FOR THE CONTROL OF FLEXIBLE STRUCTURES (COFS) PROGRAM 1459
Joanne L. Walsh

AN IMPROVED ALGORITHM FOR OPTIMUM STRUCTURAL DESIGN WITH MULTIPLE FREQUENCY CONSTRAINTS 1489
Oliver G. McGee and Khing F. Phan

ADDITIONAL PAPERS

The following paper is being included in this publication although time restrictions did not permit its presentation at the September conference.

STRUCTURAL DAMAGE ASSESSMENT AS AN IDENTIFICATION PROBLEM 1507
P. Hajela and F. J. Soeiro

The following paper arrived during the printing process and was originally included in Session I.

RECENT DEVELOPMENTS IN LARGE-SCALE STRUCTURAL OPTIMIZATION 1521
V. B. Venkayya

BLANK PAGE

ATTENDEES

Mrs. Kathy H. Abbott
NASA/Langley Research Center
MS 156A
Hampton, VA 23665-5225

Mr. Irving Abel
NASA/Langley Research Center
MS 242
Hampton, VA 23665-5225

Mr. William M. Adams Jr.
NASA/Langley Research Center
MS 489
Hampton, VA 23665-5225

Dr. Howard M. Adelman
NASA/Langley Research Center
MS 246
Hampton, VA 23665-5225

Dr. Don Anderson
McDonnell Douglas Helicopter Co.
Bldg. 530/B327
5000 E. McDowell Rd.
Mesa, AZ 85205

Mr. Ernest S. Armstrong
NASA/Langley Research Center
MS 499
Hampton, VA 23665-5225

Prof. Shapour Azarm
The University of Maryland
Department of Mechanical
Engineering
College Park, MD 20742

Dr. Richard J. Balling
Brigham Young University
Engineering Design Methods
Laboratory
368R Clyde Building
Provo, UT 84602

Dr. Dey Banerjee
McDonnell Douglas Helicopter Co.
Bldg. 530, MS/B 346
5000 E. McDowell Rd.
Mesa, AZ 85205

Mr. Paul Barnhart
Sverdrup Technology, Inc.
P.O. Box 30650, Midpark Branch
Middleburg Heights, OH 44130

Dr. Bruno Barthelemy
Ford Research and Engineering
Center
Room E3184/SCI-LAB
P. O. Box 2053
Dearborn, MI 48121-2053

Dr. Jean-Francois M. Barthelemy
NASA/Langley Research Center
MS 246
Hampton, VA 23665-5225

Mr. Oscar Barton, Jr.
Howard University
Department of Mechanical
Engineering
2300 6th St. N.W.
Washington, DC 20059

Mr. P. R. Bates
Georgia Institute of Technology
School of Aerospace Engineering
P. O. Box 30302.
Atlanta, GA 30332-0150

Prof. Ashok D. Belegundu
Penn State University
Mechanical Engineering
University Park, PA 16802

Mr. Todd J. Beltracchi
Rensselaer Polytechnic Institute
2418 Huntington Lane #3
Redondo Beach, CA 90278

Dr. Laszlo Berke
NASA/Lewis Research Center
MS 4907
21000 Brookpark Road
Cleveland, OH 44135

Mr. Alex Berman
Kaman Aerospace Corp.
Old Windsor Road
P.O. Box 2
Bloomfield, CT 06002

Mr. Vinay Bhatt
University of Missouri-Columbia
Mechanical and Aerospace
Engineering
1080 Engineering UMC
Columbia, MO 65201

Mr. Robert Blackwell
Sikorsky Aircraft
No. Main Street
Stratford, CT 06601-1381

Mr. Chris Borland
Boeing Military Airplane Co.
P.O. Box 3707
Mail Code 33-04
Seattle, WA 98124

Mr. Keith Bowman
US Air Force
AFWAL/FIBCA
Wright AFB
Wright-Patterson AFB, OH 45433

Mrs. Lynn M. Bowman
Planning Research Corporation
303 Butler Farm Rd, Suite 100
Hampton, VA 23666

Mr. Kenneth W. Brown
Pratt & Whitney Aircraft
400 Main Street, M.S. 163-09
East Hartford, CT 06108

Mr. Randal W. Brumbaugh
Planning Research Corporation
PO Box 273
NASA Dryden Bldg. 4839
Edwards, CA 93523

Mr. Christopher N. Button
Digital Equipment Corporation
4417 Corporation
Virginia Beach, VA 23462

Mr. Carey S. Buttrill
NASA/Langley Research Center
MS 494
Hampton, VA 23665-5225

Mr. Charles Camarda
NASA/Langley Research Center
MS 396
Hampton, VA 23665-5225

Mr. Frank Campisano
Northrop Corporation
One Northrop Ave
Hawthorne, CA 90250

Capt. Robert A. Canfield
AF Wright Aeronautical
Laboratories
AFWAL/FIBRA
Wright-Patterson AFB, OH
45433-6553

Mr. Richard G. Carter
ICASE
NASA/Langley Research Center
MS 132C
Hampton, VA 23665

Mr. Jeffrey A. Cerro
Planning Research Corporation
303 Butler Farm Rd, Suite 100
Suite 100
Hampton, VA 23666

Dr. Christos C. Chamis
NASA/Lewis Research Center
MS 49-8
21000 Brookpark Road
Cleveland, OH 44135

Prof. A. Chandra
University of Arizona
Aerospace and Mechanical
Engineering
Aero Bldg #16
Tucson, AZ 85721

Dr. Kwan J. Chang
Planning Research Corporation
303 Butler Farm Rd, Suite 100
Hampton, VA 23666

Dr. Mladen Chargin
NASA/Ames Research Center
MC 213-3
Moffett Field, CA 94035

Dr. Aditi Chattopadhyay
Analytical Services and
Materials Inc.
NASA/Langley Research Center
MS 246
Hampton, VA 23665-5225

Dr. Tsu-Chien Cheu
Textron Lycoming, Dept. LSK-5
550 S. Main Street
Stratford, CT 06497

Prof. Kyung K. Choi
The University of Iowa
Dept.of Mechanical Engineering
2132 Engineering Bldg
Iowa City, IA 52242

Mr. Choon T. Chon
Ford Motor Company
S-1108, SRL
P.O. Box 2053
Dearborn, MI 48121

Prof. Inderjit Chopra
University of Maryland
Dept. of Aerospace Engineering
College Park, MD 20742

Mr. David M. Christhilf
Planning Research Corporation
NASA/Langley Research Center
MS/489
Hampton, VA 23665-5225

Mr. Ching-Hung Chuang
Old Dominion University
937 Rockbridge Ave. #244
Norfolk, VA 23508

Prof. Young W. Chun
Villanova University
Dept. of Mechanical Engineering
Villanova, PA 19085

Mr. Robert D. Consoli
General Dynamics
P. O. Box 748
Fort Worth, TX 76102

Mr. Mark W. Davis
United Technologies Research
Center
MS 19
Silver Lane
E. Hartford, CT 06108

Mr. Randall C. Davis
NASA/Langley Research Center
MS 396
Hampton, VA 23665-5225

Dr. Pramote Dechaumphai
NASA/Langley Research Center
MS 395
Hampton, VA 23665-5225

Prof. Alojandro Diaz
Michigan State University
Dept. of Mechanical Engineering
Room 200, Engineering Building
East Lansing, MI 48824-1226

Mr. Alan J. Dodd
Douglas Aircraft Company
C1-E84, Mail Code 212-10
3155 Lakewood Blvd.
Long Beach, CA 90815

Mr. Auqustine R. Dovi
Planning Research Corporation
303 Butler Farm Rd, Suite 100
Hampton, VA 23666

Mr. Rodney Dreisbach
The Boeing Company
P. O. Box 707
Mail Stop 9W-22
Seattle, WA

Mr. Delmar W. Drier
NASA/Lewis Research Center
MS 86-12
21000 Brookpark Road
Cleveland, OH 44135

Dr. Ernest D. Eason
Modeling & Computing Services
1153 Bordeaux Drive
Suite 107
Sunnyvale, CA 94089

Dr. Peter A. Fenyes
General Motors Research
Laboratories
Engineering Mechanics Department
30500 Mound Rd Dept 15
Warren, MI 48090-9055

Mr. Brian Fite
NASA/Lewis Research Center
21000 Brookpark Road
MS 86-10
Cleveland, OH 44135

Dr. Donald Flaggs
Lockheed Palo Alto Research
Laboratory
Lockheed M&S 93-30/251
3251 Hanover ST.
Palo Alto, CA 94304

Prof. Claude Fleury
University of California
Dept. of Mech. Aero. & Nuclear
Engrg.
5732 Boelter Hall
Los Angeles, CA 90024

Mr. Williard E. Foss Jr.
NASA/Langley Research Center
MS 412
Hampton, VA 23665

Prof. Joseph Free
Brigham Young University
Department of Mechanical
Engineering
242 Clyde Building
Provo, UT 84602

Prof. Peretz P. Friedmann
University of California-Los
Angeles
5732H Boelter Hall
Los Angeles, CA 90024

Prof. Robert E. Fulton
Georgia institute of Technology
Mechanical Engineering
Atlanta, GA 30332

Dr. Gary A. Gabriele
Rensselaer Polytechnic Institute
Dept. of Mechanical Engineering
Johnson Engineering Center,
Rm. 4026
Troy, NY 12180-3590

Mr. James E. Gardner
NASA/Langley Research Center
MS 246
Hampton, VA 23665

Mrs. Marjorie German
G. E. Research and Development
1 River Road, Bldg. K-1, Room
3A20
Schenectady, NY

Mr. D. Ghosh
Planning Research Corporation
303 Butler Farm Rd, Suite 100
Hampton, VA 23665

Mr. Daniel P. Giesy
Planning Research Corporation
303 Butler Farm Rd, Suite 100
Suite 100
Hampton, Va 23666

Mr. Michael G. Gilbert
NASA/Langley Research Center
MS 243
Hampton, VA 23665-5225

Dr. Gary L. Giles
NASA/Langley Research Center
MS 246
Hampton, VA 23665-5225

Mr. David E. Glass
Analytical Services & Materials
107 Research Drive
Hampton, Va 23666

Prof. Ramana Grandhi
Wright State University
Mechanical Systems and Engineering
Dayton, OH 45435

Mr. Philip C. Graves
Vigyan Research Association
30 Research Drive
Hampton, Va 23666

Mr. Tommy L. Green
LTV Aerospace and Defense Company
Aircraft Products Group
P.O. Box 655907, MS 194-24
Dallas, TX 75265-5907

Mr. William H. Greene
NASA/Langley Research Center
MS 190
Hampton, VA 23665-5225

Prof. Bernard Grossman
Aerospace and Ocean Engineering
VPI & SU
Blacksburg, VA 24061

Prof. Zafer Gurdal
VPI & SU
Engineering Science and Mechanics Dept.
Norris Hall
Blacksburg, VA 24061

Prof. Raphael T. Haftka
VPI&SU
Dept. of Aerospace & Ocean Engineering
Blacksburg, VA 24061

Prof. Prabhat Hajela
University of Florida
Dept. of Aero. Eng., Mech. and Eng. Sci.
231 Aerospace, Aero
Gainesville, FL 32611

Mr. David W. Hall
David Hall Consulting
1158 South Mary Avenue
Sunnyvale, CA 94087-2103

Dr. Jeffrey C. Hall
General Dynamics Corp./Elec. Boat Div.
Department 443
Eastern Point Road
Groton, CT 06340

Mr. Stephen A. Hambric
David Taylor Research Center
Code 1844
Bethesda, MD 20084

Dr. M. Nabil Hamouda
Planning Research Corporation
NASA/Langley Research Center
MS 340
Hampton, VA 23665-5225

Mr. Jonathan K. Hart
PDA Engineering. Inc.
2975 Redhill Avenue
Costa Mesa, CA 92626-5923

Mr. Ahmed A. Hassan
McDonnell Douglas Helicopter Company
5000 E. McDowell
Bldg 530, MS B346
Mesa, AZ 85205-9797

Mr. T. K. Hasselman
Engineering Mechanics Assoc., Inc.
3820 Del Amo Boulevard, Suite 318
Torrance, CA 90503

Ms. Jennifer Heeg
Planning Research Corporation
303 Butler Farm Rd, Suite 100
Hampton, Va 23666

Mr. Charles Holland
AF Office of Scientific Research
Department of the Air Force
Bolling Air Force Base, DC 20332-6458

Prof. Jean Win Hou
Old Dominion University
Dept. Mech. Engineering and Mechanics
Norfolk, VA 23462

Prof. Owen F. Hughes
VPI & SUN
1745 Jefferson Davis Highway
STE 300
Arlington, VA 22202

Mr. Amir Izadpanah
Vigyan Research Association
NASA/Langley Research Center
MS 340
Hampton, VA 23665

Mr. Burton H. Jackson
McDonnell Douglas Helicopter
5000 E. McDowell
Mesa, AZ

MS. Cheryl C. Jackson
Old Dominion University
Dept. of Mech. Eng. and Mech.
Norfolk, VA 23529-0247

Mr. Benjamin B. James III
Planning Research Corporation
303 Butler Farm Rd, Suite 100
Hampton, VA 23666

Ms. Vicki Johnson
NASA/Langley Research Center
MS 412
Hampton, VA 23665-5225

Mr. B. M. Jordan, Jr.
LTV Aerospace & Defense Company
P.O. Box 655907
MS 194-24
Dallas, Texas 75265-5907

Mr. Suresh M. Joshi
NASA/Langley Research Center
MS 161
Hampton, VA 23665-5225

Dr. Jer-Nan Juang
NASA/Langley Research Center
MS 230
Hampton, VA 23665-5225

Prof. Manohar P. Kamat
Georgia Institute of Technology
School of Aerospace Engineering
Atlanta, GA 30332

Mr. James Kane
Clarkson University
Mech. and Ind. Engineering Dept.
Potsdam, NY 13676

Mr. Pi-Jen Kao
VPI&SU
Dept. of Aerospace & Ocean Engineering
Blacksburg, VA 24061

Mr. Mordechay Karpel
Technion -Israel Institute of Technology
Dept. of Aero Engineering
Haifa 32000 Israel

Mr. Sean P. Kenny
Old Dominion University
Norfolk, VA 23508

Mr. Suresh Khandelwal
Sverdrup Technology
16530 Commerce Ct.
Middleburg Hts, OH 44130

Prof. Noboru Kikuchi
University of Michigan
Department of Mechanical
Engineering
Ann Arbor, MI 48109

Prof. Rex K. Kincaid
College of William and Mary
Dept. of Mathematics
Williamsburg, VA 23185

Dr. Norman F. Knight, Jr.
NASA/Langley Research Center
MS 244
Hampton, VA 23665-5225

Mr. Raymond M. Kolonay
AF Wright Aeronautical
Laboratories
AFWAL/FIBRA
Wright-Patterson AFB, OH 45433

Prof. Ilan Kroo
Stanford University
Dept. of Aero/Astro
Stanford, CA 94305

Dr. Raymond G. Kvaternik
NASA/Langley Research Center
MS 340
Hampton, VA 23665-5225

Prof. C. Edward Lan
The University of Kansas
Aerospace Engineering Dept.
Room 2004, Learned Hall
Lawrence, KS 66045

Mr. Jerry Lang
NASA/Lewis Research Center
21000 Brookpark Rd.
Cleveland, OH 44135

Mr. M. Levine
Rockwell International
P.O. Box 92098
Los Angeles, CA 90245

Dr. Roy Levy
Jet Propulsion Laboratory
MS 144-201
4800 Oak Grove Drive
Pasadena, CA 91109

Mr. Joon W. Lim
University of Maryland
College Park, MD

Mr. Kyong B. Lim
Planning Research Corporation
303 Butler Farm Rd
Suite 100
Hampton, Va 23666

Mr. Eli Livne
University of California Los
Angeles
4531 Boelter Hall, UCLA
Los Angeles, CA 90024

Mr. Andrew Logan
McDonnell Douglas Helicopter Co.
Bldg. 503, MSB 325
5000 E. McDowell Rd.
Mesa, AZ 85205

Mr. Michael G. Long
Cray Research. Inc.
1333 Northland Drive
Mendota Heights, MN 55120

Dr. Robert V. Lust
General Motors Research
Laboratories
Engineering Mechanics Department
30500 Mound Road, MS 256 Rm B
Warren, MI 48090-9057

Mr. Peiman G. Maghami
Old Dominion University
Norfolk, VA 23508 23508

Mr. Wayne R. Mantay
US Army Aerostructures
Directorate
NASA/Langley Research Center
MS 266
Hampton, VA 23665-5225

Mr. Carl J. Martin
Planning Research Corporation
303 Butler Farm Rd, Suite 100
Hampton, Va 23666

Mr. John G. Martin
Planning Research Corporation
303 Butler Farm Rd, Suite 100
Hampton, Va 23666

Mr. Zoran N. Martinovic
Analytical Mechanics
Associates, Inc.
17 Research Drive
Hampton, VA 23666

Mr. Philip Mason
Grumman Aerospace Corp.
B-35, Dept. 430
Stewart Ave.
Bethpage, NY 11714

Mr. Oliver G. McGee
Ohio State University
Department of Civil Engineering
417B Hitchcock Hall
Columbus OH 43210

Mr. Niki Mehta
Old Dominion University
Dept. of Mechanical Eng. and
Mechanical
College of Engineering and
Technology
Norfolk, VA 23529-0247

Prof. Luis Mesquita
University of Nebraska
Department of Enigneering
Mechanics
217 Bancroft
Lincoln, NE 68588

Prof. Farrokh Mistree
University of Houston-Univ. Park
Dept. of Mechanical Engineering
4800 Calhoun Road
Houston, TX 77204-4792

Dr. Hiro Miura
NASA/Ames Research Center
Ames Research Center
Attn: 237-11
Moffett Field, CA 94035

Mrs. Arlene A. Moore
Planning Research Corporation
303 Butler Farm Rd, Suite 100
Hampton, Va 23666

Prof Subrata Mukherjee
Cornell University
Dept of T & AM
Kimball Hall
Ithica, NY 14853

Dr. T. Sreekanta Murthy
Planning Research Corporation
MS 340
NASA/Langley Research Center
Hampton, VA 23665-5225

Mr. Evhen M. Mychalowycz
Boeing Vertol Company
MS P32-15
P. O. Box 16858
Philadelphia, PA 19142

Dr. Gopal K. Nagendra
Mac Neal-Schwendler Corp.
815 Colorado Blvd.
Los Angeles, CA 90041-1777

Mr. Changho Nam
Purdue University
School of
Aeronautice/Astronautics
West Lafayette, IN 47907

Mr. D. J. Neill
Northrop Corporation, Aircraft
Division
Dynamics & Loads Research
3854/82
One Northrop Avenue
Hawthorne, CA 90250

Dr. Elli Nissim
NASA Dryden
CODE OFV
Edwards, CA 93523-5000

Mr. Kevin W. Noonan
NASA/Langley Research Center
MS 266
Hampton, VA 23665-5225

Dr. Ahmed K. Noor
The George Washington University
NASA/Langley Research Center
MS269
Hampton, VA 23665-5225

Mr. T. L. Oglesby
LTV Aerospace & Defense Company
P. O. Box 655907
MS 194-24
Dallas, TX 75265-5907

Prof. Irving U. Ojalvo
University of Bridgeport
Dept. of Mechanical Engineering
Bridgeport, CT 06601

Mrs. Sharon L. Padula
NASA/Langley Research Center
IRO Office
MS 246
Hampton, VA 23665

Mr. Ajay K. Pandey
Planning Research Corporation
303 Butler Farm Rd, Suite 100
Hampton, VA 23666

Prof. Alan Parkinson
Department of Mechanical
Engineering
Brigham Young University
242 CB
Provo, UT 84602

Mr. Bernhard Pepker
CCAD, EB
University of Iowa
Iowa City, IA 52242

Prof. David Peters
Georgia Institute of Technology
School of Aerospace Engineering
Atlanta, GA 30332

Mr. James Peters
McDonnell Douglas Helicopter Co.
Bldg. 530/B346
5000 E. McDowell Rd.
Mesa, AZ 85205-9797

Prof. Lucian Elijah Polak
University of California
Dept. of Electrical Engineering
565 Cory Hall
Berkeley, CA 94720

Mr. Dave Polen
VPI&SU
Dept. of Aerospace & Ocean
Engineering
400 H. Foxridge
Blacksburg, VA 24061

Prof. Aubrey Poore
Colorado State University
Dept. of Mathematics
Fort Collins, CO 80523

Dr. Biren Prasad
Electronic Data Systems
Corporation
5555 New King Street
Troy, MI 48007-7019

Dr. Thomas K. Pratt
Pratt & Whitney
Engineering Building, 161-16
400 Main Street
East Hartford, CT 06108

Dr. N. A. Radovcich
Lockheed Aeronautical Systems
Co.
D/76-12, Bldg 63-G, Plant A-1
P.O. Box 551
Burbank, CA 91520

Mr. Charles C. Rankin
Lockheed Missiles and Space
Palo Alto Research Lab.
0/93-30 B/251
Palo Alto, CA 94304-1191

Dr. S. M. Rankin
Mathematics Dept.
Worcester Poly. Tech.
Worcester, Ma 01609

Mr. Jagannatha Rao
The University of Michigan
2212 G. G. Brown Lab.
Ann Arbor, MI 48109

Mr. John J. Rehder
NASA/Langley Research Center
MS 365
Hampton, VA 23665-5225

Prof. Robert Reiss
Howard University
Department of Mechanical
Engineering
2300 Sixth Street, N.W.
Washington, DC 20059

Mr. J. Edward Rogan
Georgia Institute of Technology
School of Aerospace Engineering
Atlanta, GA 30332-0150

Mr. James. L. Rogers
NASA/Langley Research Center
IRO Office
MS 246
Hampton, VA 23665

Mrs. V. Aileen Rogers
Planning Research Corporation
303 Butler Farm Rd, Suite 100
Hampton, VA 23666

Mr. Bruce A. Rommel
Douglas Aircraft Company
C1-E84, Mail Code 212-10
3855 Lakewood Blvd.
Long Beach, CA 90846

Dr. Sunil Saigal
Worcester Polytechnic Institute
Mechanical Engineering
Department
Institute Road
Worcester, Mass 01069

Dr. Moktar Salama
Jet Propulsion Laboratory
Applied Mechanics Div. - MS
157-316
California Institute of
Technology
Pasadena, CA 91109

Mr. Chris A. Sandridge
VPI & SU
Aerospace & Ocean Engineering
Blacksburg, VA 24061

Prof. Lucien A. Schmit
University of California, Los
Angeles
4531K Boelter Hall
Los Angeles, CA 90024

Prof. Daniel P. Schrage
Georgia Institute of Technology
School of Aerospace Engineering
250 Drummen Ct
Atlanta, GA 30332-0150

Mr. Stephen J. Scotti
NASA/Langley Research Center
MS 396
Hampton, VA 23665-5225

Mr. Jeen S. Sheen
Old Dominion University
Dept. of Mechanical Eng. and
Mechanics
College of Engineering and
Technology
Norfolk, VA 23529-0247

Mr. Joram Shenhar
Planning Research Corporation
303 Butler Farm Rd, Suite 100
Hampton, VA 23665

Dr. Mark J. Shuart
NASA/Langley Research Center
MS 190
Hampton, VA 23665-5225

Mr. J. A. Shupe
B. F. Goodrich
9921 Brecksville Road
Brecksville, OH 44141

Mr. Walter A. Silva
Planning Research Corporation
303 Butler Farm Rd, Suite 100
Hampton, VA 23666

Mr. James A. Simak
General Dynamics
Data Systems Division
P.O. Box 748
Fort Worth, TX 76102

Dr. Jaroslaw Sobieski
NASA/Langley Research Center
MS 246
Hampton, VA 23665-5225

Mr. Andy H. Soediono
Georgia Institute of Technology
P. O. Box 34091
225 North Avenue
Atlanta, GA 30332

Dr. James H. Starnes, Jr.
NASA/Langley Research Center
MS 120
Hampton, VA 23665-5225

Mr. Frank J. Tarzanin
Boeing Vertol Company
MS P32-15
P. O. Box 16858
Philadelphia, PA 19142

Mr. Kenneth E. Tatum
Planning Research Corporation
SSD/ATD
303 Butler Farm Rd., Suite 100
Hampton, VA 23666

Mr. Rajiv Thareja
Planning Research Corporation
303 Butler Farm Rd, Suite 100
Hampton, VA 23666

Prof. Garret N. Vanderplaats
University of California, Santa Barbara
Dept. of Mechanical & Environmental Eng.
Santa Barbara, CA 93160

Dr. Vipperla B. Venkayya
AF Wright Aeronautical Laboratories
AFWAL/FIBR
Wright-Patterson AFB, OH 45433

Dr. A. V. Viswanathan
Boeing Commercial Airplane Co.
P. O. Box 3707
Seattle, WA 98124

Mr. A. Von Flotow
MIT
37-335, MIT
Cambridge, MA 02139

Ms. Joanne L. Walsh
NASA/Langley Research Center
MS 246
Hampton, VA 23665-5225

Prof. Bo Ping Wang
The University of Texas
Dept. of Mechanical Engineering
P.O. Box 19023
Arlington, TX 76019

Mr. Bryan Watson
Spectragraphics Corporation
9125 Rehco Road
San Diego, CA 92121

Prof. Terrence A. Weisshaar
Purdue University
School of Aeronautics/Astronautics
West Lafayette, IN 47907

Mr. W. H. Weller
United Technologies Research Center
M. S. 19, Silver Lane
East Hartford, CT 06108

Ms Carol D. Wieseman
NASA/Langley Research Center
MS 243
Hampton, VA 23665-5225

Mr. James L. Williams
NASA/Langley Research Center
MS 499
Hampton, VA 23665-5225

Mrs. Jessica A. Woods
Planning Research Corporation
NASA Langley Research Center
Mail Stop 243
Hampton, VA 23665-5225

Mr. Gregory A. Wrenn
Planning Research Corporation
NASA/Langley Research Center
MS905
Hampton, VA 23665-5225

Mr. Ren-Jye Yang
Ford Motor Company
Scientific Research Labs
P. O. Box 2053, RM E-1134
Dearborn, MI 48212

Dr. E. Carson Yates
NASA/Langley Research Center
MS 246
Hampton, VA 23665-5225

Mr. Chao-Pin Yeh
Georgia Tech
Atlanta, Georgia 30332

Mr. John W. Young
NASA/Langley Research Center
MS 499
Hampton, VA 23665-5225

Mrs. Katherine C. Young
NASA/Langley Research Center
IRO Office
MS 246
Hampton, VA 23665

Mr. Rudy Yurkovich
McDonnell Aircraft Co.
P.O. Box 516
St. Louis, MO 63166

Dr. Thomas A. Zeiler
Planning Research Corporation
NASA/Langley Research Center
MS 243
Hampton, VA 23665-5225

PART I

SESSION 1: PLENARY

Chairman: Owen F. Hughes

BLANK PAGE

APPLICATIONS OF INTEGRATED DESIGN/ANALYSIS SYSTEMS IN AEROSPACE STRUCTURAL DESIGN

Philip Mason, Edwin Lerner, and
Lawrence Sobel
Grumman Aircraft Systems Division
Grumman Corporation
Bethpage, New York

INTRODUCTION

Many papers have been written on structural optimization techniques and integrated design and analysis systems; however, engineering managers, project engineers and design engineers still ask the questions: Are structural optimization techniques of academic interest only, or are they really being used on actual hardware designs in a real production environment? And, if these techniques are being used, do they really contribute to the structural design? Also, are optimization tools being used as an integral part of the overall design/analysis systems that various companies are either currently using or plan on developing? Our paper will attempt to answer these questions by reviewing development efforts and the application of the resulting systems to actual hardware designs that have been developed and manufactured at Grumman Corporation.

Many papers have been written on structural optimization techniques and integrated analysis and design systems. Yet, many design engineers ask

- Are structural optimization techniques of academic interest only, or are they really being used in a production environment? If so, do they really contribute to the design of a structure?

- Are optimization techniques being used as an integral part of the overall design/analysis systems that various companies are currently using and/or developing?

DEVELOPMENT OF AUTOMATED STRUCTURAL DESIGN/ANALYSIS SYSTEMS AT GRUMMAN

Structural engineers at Grumman have been active in developing and applying structural analysis and optimization tools for many years. Grumman was among the pioneers in the development of the force method in the late 1940's (Ref. 1) and continued using that technique on many company projects until the early 1960's. In 1963, we began developing ASTRAL (our Automated Structural Analysis System) which is based on the direct stiffness (displacement) method. The analysis and design of the Lunar Module really forced this to occur, inasmuch as the force method could not cope efficiently nor adequately with the complex structural configuration of that vehicle.

Use of the direct stiffness method led us, in 1964, to develop a program that permitted us to cycle the analysis in conjunction with automated element resizing procedures. Today, we call this approach "Fully Stressed Design" (FSD). Our early FSD program (Refs. 2 and 3) was used in the design of the EA-6B wing and ultimately led to the development of the ASOP program (Automated Structural Optimization Program). Initially, ASOP was developed to handle metallic construction; later, in 1969, it was extended to composites.

- 1948 - Development of force method - Wehle & Lansing
- 1963 - Development of displacement method - ASTRAL system
- 1964 - Development of fully stressed design (FSD) capability
  - ASOP program for metallic structures
- 1967 - Development of IDEAS - integrated analysis procedures in 8 disciplines (Integrated DEsign and Analysis System)
  - applied to design of F-14

DEVELOPMENT OF AUTOMATED STRUCTURAL design/analysis SYSTEMS AT GRUMMAN (CONTINUED)

Obviously, one cannot analyze a structure without applied loads and, likewise, cannot predict flight and ground loads without knowledge of the elasticity of the vehicle. In 1967, when facing a potential, major new design contract (that was to become the F-14), we embarked on the development of a comprehensive computer system that would address the overall external and internal loads problem. We called the system IDEAS (Integrated Design and Analysis System, Ref. 4) and used it extensively in the design of the F-14 fighter and in preliminary designs of the Space Shuttle (Refs. 5 - 7). IDEAS was a batch-oriented system in which special care was given to consistent I/O between the various modules that comprised the system. Later, the concepts behind the IDEAS system were extended to a time share environment and the development of the RAVES system (Rapid Aerospace Vehicle Evaluation System - Ref. 8).

- 1969 - Extension of ASOP to composite construction
- 1972 - Development of RAVES (Rapid Aerospace Vehicle Evaluation System) time share system - considered 15 disciplines
- 1973-1981- Development of FASTOP system
  - flutter constraints, aeroelastic effectiveness, divergence speed
- 1975 - Development of GEMS system -- interactive graphics
  - IBM 2250 --3250 -- 5080 -- GIP system
  - uses CADAM, CATIA on IBM main frames via 5080 scopes

DEVELOPMENT OF AUTOMATED STRUCTURAL DESIGN/ANALYSIS SYSTEMS AT GRUMMAN (CONTINUED)

Between 1973 and 1981, Grumman was active in developing optimization procedures for combined strength and aeroelastic requirements (Refs. 9 - 22). A major computer program that was developed in this time frame was FASTOP (Flutter and Strength Optimization Program). This program, which received Air Force sponsorship, was one of the first major systems to incorporate strength and aeroelastic constraints in one design/analysis system.

In 1975, the company began developing our CAD/CAM "GEMS" system (Grumman Engineering and Manufacturing System). This system embodies various commercial programs such as CADAM, CATIA and PATRAN and operates on IBM mainframes via 5080-type scopes. Our in-house developed design/analysis system, COGS, operates in this same interactive graphics environment, making use of the same equipment used by our designers and manufacturing engineers.

COGS derives its flexibility from the ASTRAL-COMAP system that has been used at Grumman for many years on virtually all major projects that require structural analysis. This system is constantly upgraded to reflect new changes in hardware, software and the interactive graphics environment.

COGS places strong emphasis on interactive graphics and has an extensive analysis capability. For example, using COGS, an engineer can generate a structural finite-element model, a lifting surface airloads model, or a dynamic transient response model. He can calculate aerodynamic influence coefficients, aerodynamic node loads, and inertia loads due to flight or ground loading conditions. He can transform these loads from their respective models to the structural model and can calculate and interactively plot moment, shear and torsion curves, as well as envelopes of these curves, on a 5080 scope. He can also calculate internal loads, stresses and strains, nodal deflections, vibration modes and frequencies, flexibility coefficients, and buckling loads and mode shapes. The system can also perform multilevel substructuring, thermal analysis, plastic analysis, nonlinear variable contact analysis and crack growth analysis. A given model, once analyzed, may be resized for strength or for other constraints such as those dictated by aeroelastic or frequency requirements. (Here, we have incorporated portions of the FASTOP code into COGS.) The user may also perform a wide variety of user-specified matrix operations.

Graphical output may be viewed at the scope or plotted via a batch submittal to a Versatec plotter for hard copy. Buffer plots of any scope display may be obtained by requesting a "buffer dump" at the scope and then plotting these data on the Versatec. In addition, hard copy of color graphics that show contours of stresses, composite ply layups, derivatives of frequency with respect to element gage, plus a wide variety of other information,

DEVELOPMENT OF AUTOMATED STRUCTURAL ANALYSIS/DESIGN SYSTEMS AT GRUMMAN (CONCLUDED)

may be obtained from a Seiko D-SCAN plotter that is attached to selected scopes. We usually plot full E-size or J-size drawings showing such data as internal panel loads, average stresses or strains, ply layups, cap loads and shear flows, element gages, nodal deflections or mode shapes.

As a subsystem of GEMS, COGS runs interactively on the IBM 3090, or compatible mainframes like the NAS 9060. We have attached an FPS-164 to one of the 3090 mainframes in order to provide a 10 Mflops capability for real-time, computer-intensive calculations while, at the same time, off-loading the mainframe so that these calculations do not interfere with other interactive systems. COGS presently interfaces with CADAM and will interface with CATIA in the future. Grumman has worked with PDA Engineering and acted as a beta test site for developing a 5080 fully interactive graphics version of PATRAN. Thus, our COGS structural analysis system is very much entwined with the same computing hardware, software and system that is used to perform computer-aided design and computer-aided manufacturing.

We have used COGS on a wide variety of company projects including: Gulfstream-III, PDX TOKAMAK, M-161 Hydrofoil, F-14, C-2A, E-2C, Dehavilland DASH-8, A-6F, V-22, EA-6B, X-29, Orbiting Maneuvering Vehicle, Space Based Radar, CW/VT (Composite Wing and Vertical Tail Program), and C-17 Control Surfaces.

- 1976 - Development of strength resize capability in ASTRAL
- 1978 - Development of COGS system (subsystem of GEMS)
  Applications: G-III, PDX TOKAMAK, M161 Hydrofoil, F-14, C-2A Reprocurement, E-2C, Dehavilland DASH 8, A-6F, V-22, EA-6B, X-29, OMV, SBR, NPBIE, CW/VT, C-17 control surfaces
- 1983 - Development of COGS system as major interactive graphic structural analysis capability - incorporate FASTOP optimization capability, add flight loads, ground loads, weights, and thermal analysis capability
- 1987 - Conversion of system to PHIGS standard -- increase interactive graphics capability

OBJECTIVE OF THE COGS SYSTEM

The objective of the COGS system is to provide a capability for analyzing and designing structures in a fully integrated interactive graphics environment. The word "analyzing" implies the ability to calculate all external loads due to various conditions such as maneuvers, gusts, landing, catapulting, taxiing, thermal environment as well as calculating the response of the structure to these loads. The word "designing" implies sizing the structure so as to maintain structural integrity and satisfy specified performance requirements throughout the complete flight envelope.

We do not mean to imply that we have linked our finite-element structural analysis and optimization capability directly to CADAM-type shop drawings; however, if we are ever going to achieve this type of objective in the future, the system upon which to build is in place in an interactive graphics environment.

The objective of the COGS system is to provide a capability for

ANALYZING and DESIGNING structures

ANALYZING implies the ability to calculate all external loads due to various conditions such as flight maneuvers, gusts, landing, catapulting, taxiing, thermal environment as well calculating the response of the structure, such as internal loads.

DESIGNING implies sizing the structure so as to maintain structural integrity and specified performance throughout the complete flight spectrum.

THE INTERACTIVE GRAPHICS ENVIRONMENT

Many elements make up the environment for the performance of structural analysis, optimization and design. We certainly need software, and at Grumman our GEMS system embraces and supports CADAM, CATIA, PATRAN, NASTRAN and, of course, our in-house COGS system. GEMS operates on 5080 high-function scopes and utilizes IBM 3090 mainframes. We also have access to a Cray and have an FPS-164 attached to the 3090 to provide on-line computing support and to off-load the mainframe. We have a large number of disk packs for storing data and have design facilities in all of our design and manufacturing plants for properly using the system.

Our trained users are rapidly becoming part of collocated design/analysis/manufacturing teams.

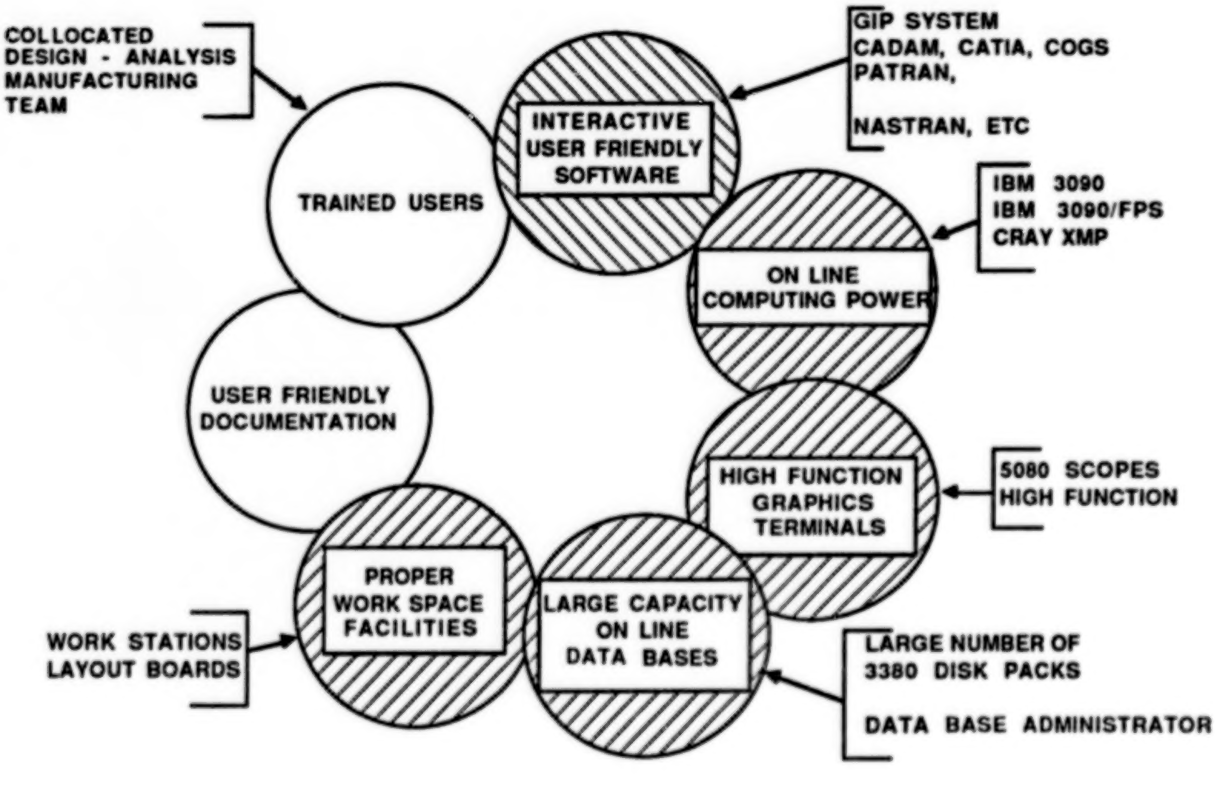
COLLOCATED DESIGN - ANALYSIS MANUFACTURING TEAM
TRAINED USERS
INTERACTIVE USER FRIENDLY SOFTWARE
GIP SYSTEM
CADAM, CATIA, COGS
PATRAN,
NASTRAN, ETC
IBM 3090
IBM 3090/FPS
CRAY XMP
ON LINE COMPUTING POWER
USER FRIENDLY DOCUMENTATION
HIGH FUNCTION GRAPHICS TERMINALS
5080 SCOPES
HIGH FUNCTION
PROPER WORK SPACE FACILITIES
LARGE CAPACITY ON LINE DATA BASES
WORK STATIONS
LAYOUT BOARDS
LARGE NUMBER OF 3380 DISK PACKS
DATA BASE ADMINISTRATOR

DESIGN-USAGE CYCLE

The design-evolution cycle for a given vehicle may be divided into six phases. Phase 1, Conceptual Design, is basically parametric in nature. Finite-element analysis and optimization techniques are usually not applied in this phase. Phase 2, Preliminary Design, begins with a 3-view drawing of the candidate vehicle and progresses until enough information is gained to prepare a proposal for hardware design. Our structural optimization procedures and the COGS system have been used extensively in this phase of design on a wide variety of vehicles. Phase 3, Final Design, begins after award of a hardware proposal and progresses until all drawings have been released to manufacturing. Clearly, structural analysis and optimization techniques play an important role. In Phases 4, Production, and 5, Vehicle Usage, systems such as COGS are used primarily for investigations related to local problem solving. Phase 6, Investigations and Design Modifications, is concerned with design upgrading for improved vehicle performance or extended life.

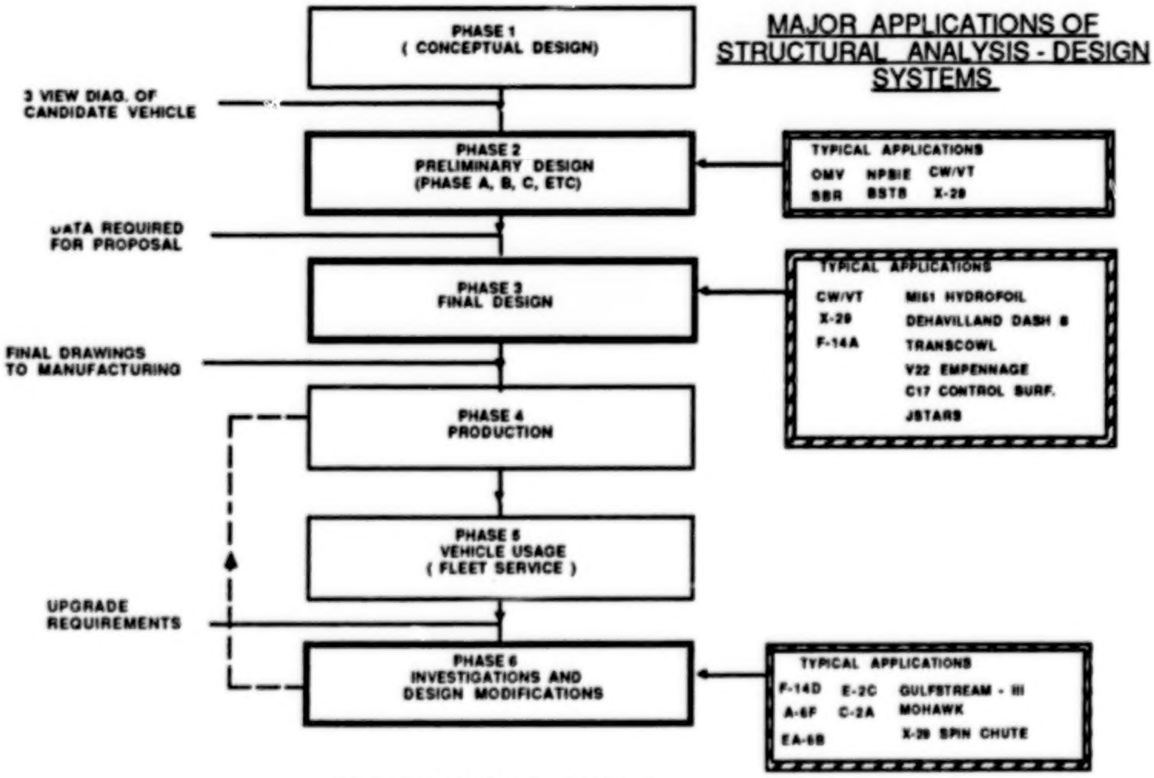

DESIGN-USAGE CYCLE

TYPICAL DESIGN/ANALYSIS CYCLE

The major tasks that are undertaken in a typical analysis/ design cycle are shown in the figure below. This basic flow diagram pertains to the tasks that are performed in Phases 2, 3 and 6, the differences being in the degree of refinement of the analytical models. The arrows indicate the primary direction of the flow of calculation. In actual application, much churning and internal looping is performed which is not shown. This says much about how one must construct rather general analysis modules and supportive data bases which permit entry and exit from almost any task in the cycle. Our intent here is not to discuss the total analysis cycle and its many subtasks, but rather to concentrate on the structural optimization tasks that are shown in boldface.

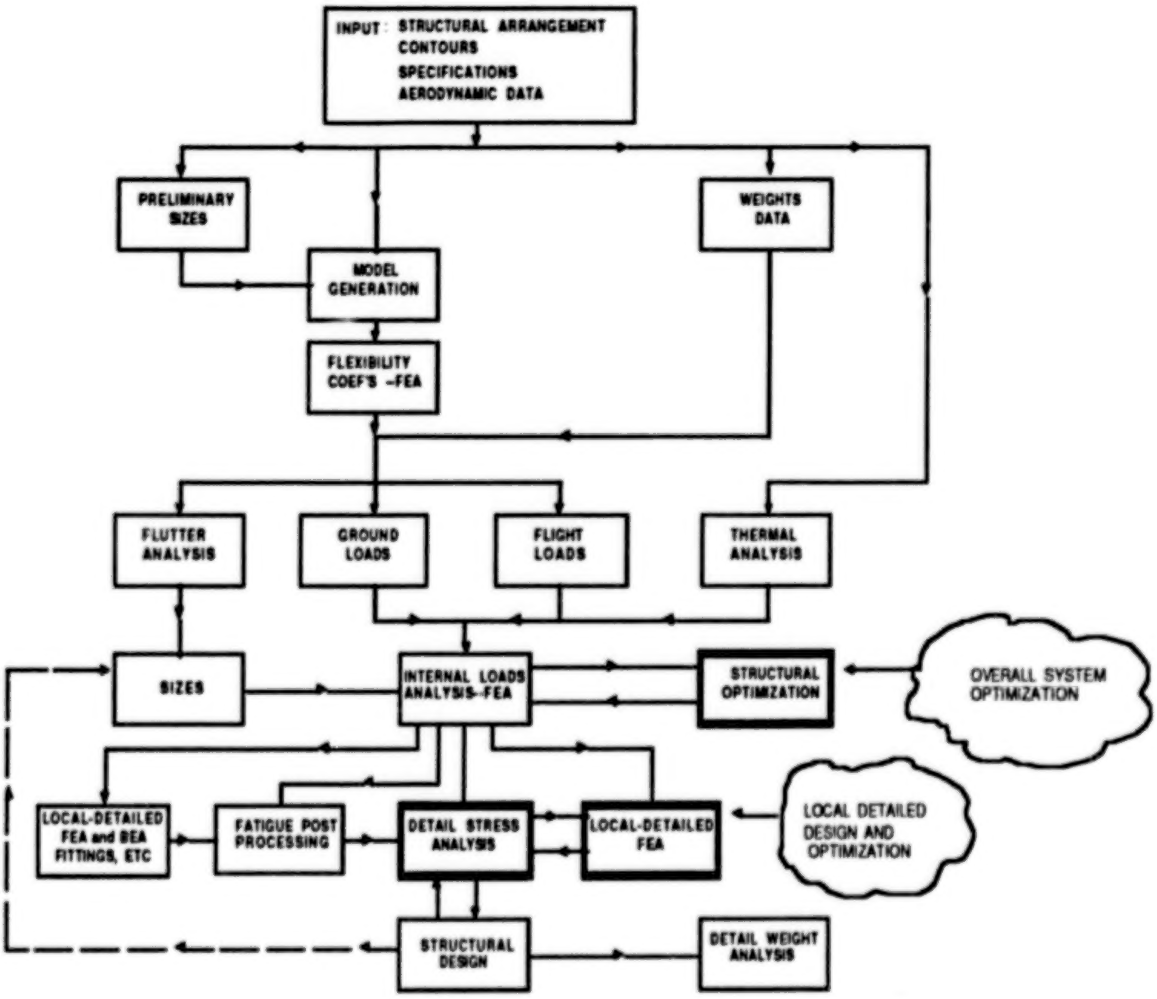

APPLICATIONS OF OPTIMIZATION PROCEDURES TO ACTUAL DESIGN AT GRUMMAN

PHASE 2 -- PRELIMINARY DESIGN

We used the FASTOP system extensively in the preliminary design phases of the X-29 (Ref. 23) and we will elaborate on this later.

We also used our ASTRAL/COGS system to perform element resizing for frequency avoidance on several space type structures. Two examples are the preliminary sizing for the OMV and NPBIE.

PHASE 2 -- PRELIMINARY DESIGN

- X-29 - use of FASTOP to optimize structure for divergence avoidance -- evaluate laminate configurations
- OMV - Orbiting Maneuvering Vehicle
  use of ASTRAL/COGS -- multiple frequency avoidance
- NPBIE - Neutral Particle Beam Ionization Experiment
  use of ASTRAL/COGS -- frequency avoidance

APPLICATIONS OF OPTIMIZATION PROCEDURES TO ACTUAL DESIGN AT GRUMMAN

PHASE 3 -- PRODUCTION

We have employed structural optimization techniques in the production phase on a number of vehicles. In the 1960's, the ASOP program was used to size the EA-6B wing cover (Ref. 2). Later, an upgraded version of this program allowed Grumman to size the F-14 boron-epoxy composite horizontal stabilizer.

The Gulfstream III wing was sized using the fully stressed design capability within ASTRAL-COMAP. Here, a COMAP verb, RESIZE, performs the sizing by calling a subprogram that sizes integrally stiffened construction (Ref. 20).

The X-29 graphite-epoxy, composite, forward-swept wing was sized in the PD phase for divergence avoidance. Gages were maintained as minimums in the final design phase in which the wing was resized for strength using the ASTRAL/COMAP RESIZE capability.

The CW/VT (Composite Wing and Vertical Tail) were sized to meet strength and control-surface effectiveness requirements by making use of the optimization modules contained in our COGS system. We will discuss this in more detail later.

PHASE 3 -- PRODUCTION

- EA-6B wing - use of FSD (early use of ASOP program).
- F-14 boron-epoxy composite horizontal stabilizer - ASOP program.
- Gulfstream-III wing - use of ASTRAL resize capability
  - integrally stiffened panel.
- X-29 graphite-epoxy composite forward-swept wing
  - use of FASTOP in P.D. phase - divergence avoidance
  - use of ASTRAL resize in final design phases.
- CW/VT - composite wing and vertical tail - use of ASTRAL/COGS strength resize and optimization modules for improved control surface effectiveness.
- V-22 empennage - multiple frequency avoidance
  use of ASTRAL/COGS - frequency avoidance optimization.

APPLICATIONS OF STAND-ALONE DETAIL ANALYSIS PROCEDURES TO ACTUAL DESIGN AT GRUMMAN

We have been discussing finite-element analysis and optimization on what we might call the "vehicle system level," where the structure is sized to meet overall design objectives. Automated sizing is also performed on a more detailed component level, in which internal loads are extracted from the analysis and used as input to stand-alone design programs. One might be tempted to call the resizing performed by these programs: "component optimization." We simply refer to the procedures as "component sizing," since we usually have enough manufacturing side constraints that we simply resize by shaving or adding to the basic skin gage. We have used programs that perform this type of resizing on the F-14 wing outer panel, the shuttle wing (which utilized a special hat section), the integrally stiffened construction on the Gulfstream-II wing, and on the CW/VT graphite-epoxy wing to perform local panel-buckling analysis and smoothing of the ply layups.

- F-14 wing outer panel
    - Y stiffener -- upper cover
    - Z stiffener -- lower cover

- Space Shuttle wing
    - special hat section

- Gulfstream-II and III wings
    - integrally stiffened construction

- CW/VT - composite wing and vertical tail
    - graphite/epoxy wing cover -- buckling/smoothing

GRUMMAN OPTIMIZATION PROCEDURES

Grumman uses optimality criteria in structural resizing procedures that involve control effectiveness, divergence avoidance, deflection constraints, frequency constraints, flutter constraints and multiple constraints. The optimality criterion for a single design constraint may be stated simply as

> At minimum weight, the change in the constraint parameter "F" per change in element weight is the same for all elements.

This criterion is the basis for the development of our resizing algorithms.

Grumman uses optimality criteria for overall sizing procedures that involve:

- control effectiveness
- divergence avoidance
- deflection constraints
- frequency constraints
- flutter constraints
- multiple constraints

Optimality Criterion:

$\partial F/\partial w_i$ = constant -- at minimum weight the change in the constraint "F" per change in element weight is the same for all elements.

GRUMMAN OPTIMIZATION PROCEDURES

In sizing for strength, we use resizing procedures that recognize detail design parameters pertinent to the type of construction employed. The appropriate procedure is tied to the "construction code" that is assigned to the element in the member data file. For example:

Construction Code A1 = Metallic - Isotropic construction
The failure criteria give consideration to:

- Principal stress
- Modified effective stress ratio
- Minimum and maximum gages

We use structural sizing procedures that recognize detail design parameters where the structure is sized for strength:

- Metallic -- Isotropic
  - principal stress
  - modified effective stress ratio
  - minimum and maximum gages

GRUMMAN OPTIMIZATION PROCEDURES (CONCLUDED)

Construction Code A3 = Metallic stiffened sheet
The failure criteria give consideration to:

- Stringer compression
- Stringer rigidity (EI/bd)
- Biaxial loading - sheet compression and shear
- Minimum and maximum parameter specification
- Stiffener gage is slaved to skin thickness

Construction Code C1 = Composite construction
The failure criteria give consideration to:

- Multi-ply orientation
- Fiber allowable stresses
- Balanced layer requirements
- Minimum and maximum number of plies in a given layer direction

- Metallic Stiffened Sheet
  - stringer compression
  - stringer rigidity (EI/bd)
  - biaxial loading -- sheet compression and shear
  - minimum and maximum parameter specification
  - stiffener gage is slaved to skin thickness
- Composite Construction
  - multi-ply orientation
  - fiber allowable stresses
  - balanced layer constraints

STRENGTH SIZING SCHEME

The following figure illustrates how our strength resizing scheme works. The illustration pertains to the Gulfstream III wing. The ASTRAL-COMAP member data contain regions that store detailed properties for a given construction as well as the usual finite-element type of data. The detailed construction properties are converted to anisotropic elastic constants and stored in the finite-element regions by appropriate subroutines. The structure is analyzed using standard finite-element techniques, then resized by use of the RESIZE module. This module uses the internal loads and a resizing scheme that utilizes the detail properties stored in the member data to perform rather sophisticated component sizing. The revised properties are output in a new set of member data. Multiple use of the analysis and resizing procedures leads to a fully stressed design that we have found to give realistic results.

We might call this approach "component sizing" within an overall fully stressed design. We use the concept of a "construction code" to imply specified failure criteria for a given type of construction; hence, the finite-element model is merely the device for calculating internal loads. The actual finite-element model sizing is performed using realistic structural quantities that are tracked as attributes of the finite-element data.

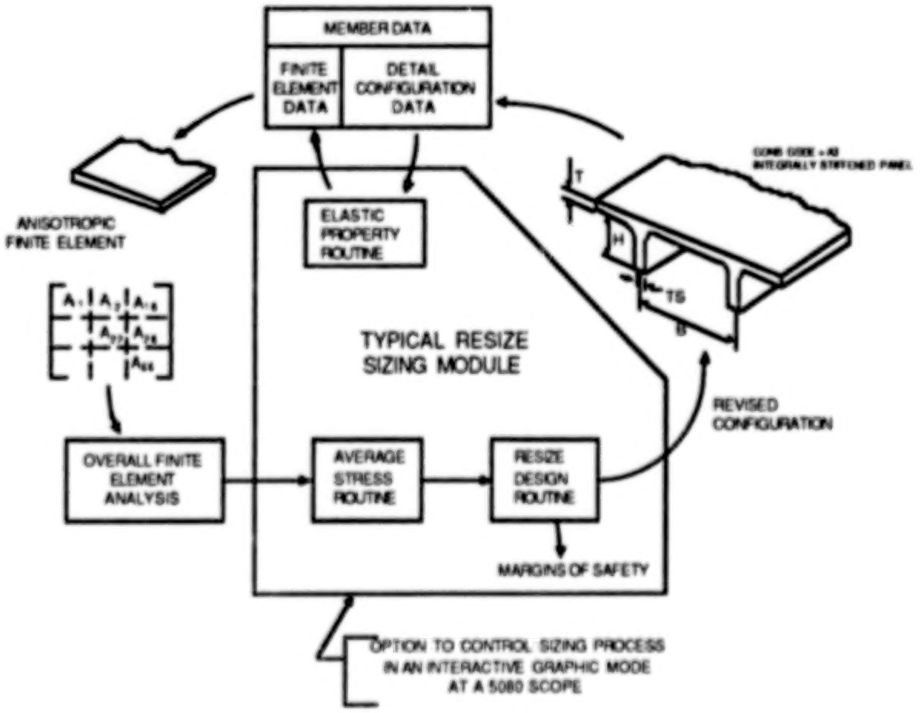
MEMBER DATA
FINITE ELEMENT DATA
DETAIL CONFIGURATION DATA
ANISOTROPIC FINITE ELEMENT
A11 A12 A16
A22 A26
A66
ELASTIC PROPERTY ROUTINE
TYPICAL RESIZE SIZING MODULE
INTEGRALLY STIFFENED PANEL
T
H
TS
B
REVISED CONFIGURATION
OVERALL FINITE ELEMENT ANALYSIS
AVERAGE STRESS ROUTINE
RESIZE DESIGN ROUTINE
MARGINS OF SAFETY
OPTION TO CONTROL SIZING PROCESS IN AN INTERACTIVE GRAPHIC MODE AT A 5080 SCOPE

INTEGRALLY STIFFENED PANEL
CONSTRUCTION CODE A3

Design parameters that are stored for the integral stiffener are shown. This type of construction is used on the Gulfstream III wing, the A-6E inboard wing and the EA-6B inboard wing.

(Gulfstream-III wing, A-6E inboard wing, EA-6B inboard wing)

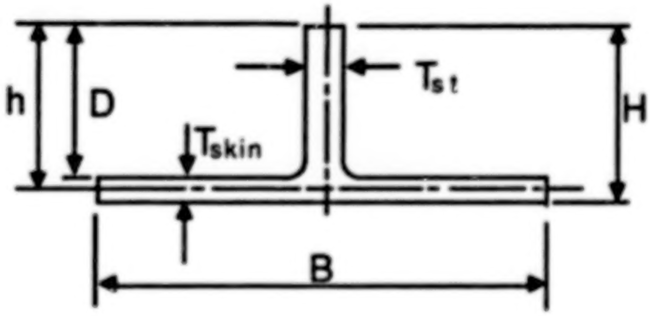

$h = D + (T_{skin}/2)$

$R_B = h/B$

$R_T = T_{st}/T_{skin}$

$A_G = D(T_{st}) + B(T_{skin})$

Z-STIFFENED SHEET
CONSTRUCTION CODE A4

Detail parameters that are stored for the Z-stiffened sheet are shown. This type of construction is used on the E-2C and C-2A wings.

(E-2C and C-2A wing)

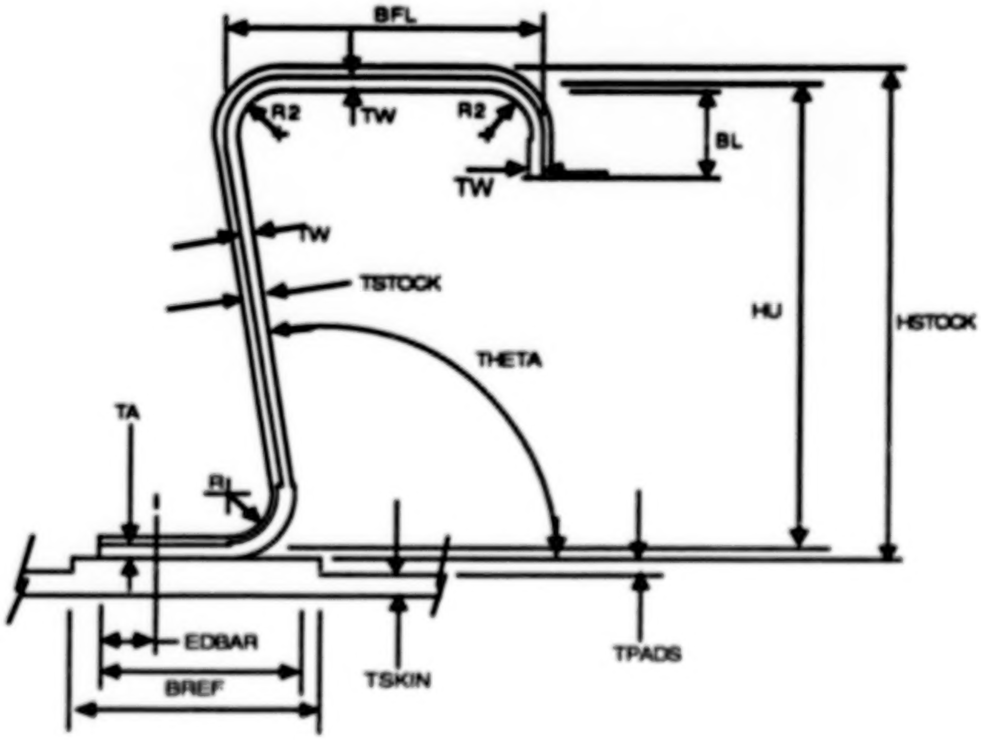

Y-STIFFENED PANEL

Detail parameters that are stored for the Y-stiffened panel are shown. This type of construction is used on upper cover of the F-14 wing outer panel.

(F-14 wing outer panel - upper cover)

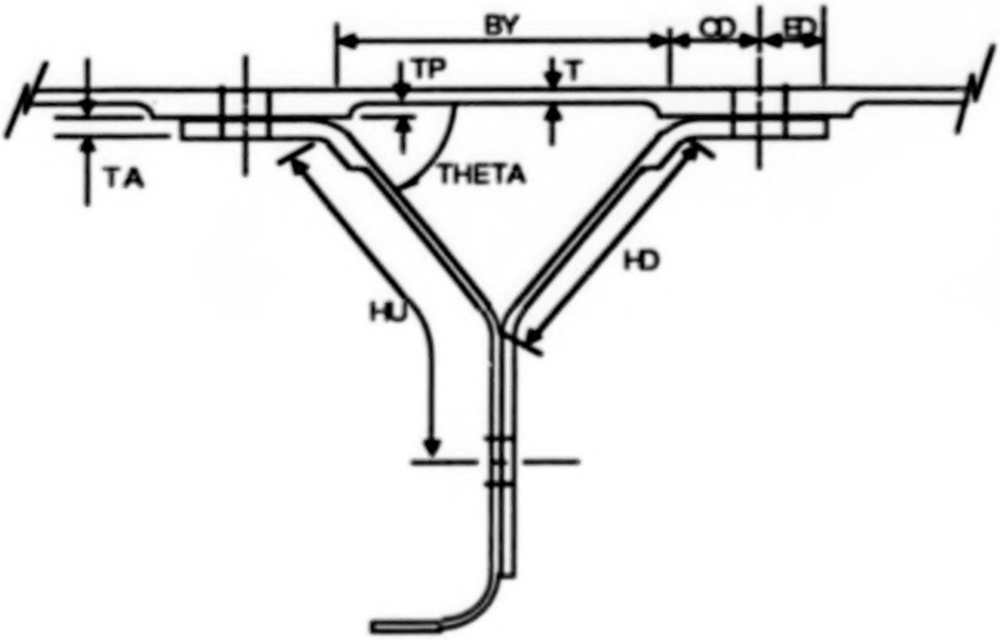

COMPOSITE CONSTRUCTION - CONSTRUCTION CODE C1

Detail parameters that are stored for composite construction are shown. This type of construction was used on the CW/VT wing and vertical tail and the X-29 wing. The code permits up to 6 different ply directions. To indicate what some of the parameters are, in a given direction, L is the number of plies, L_{MIN} and L_{MAX} are minimum and maximum allowed numbers of plies, respectively, L_{BAL} is a balanced layer clue (slaving, e.g., the number of layers in the +45 direction to the number in the -45 direction), L_{EVEN} makes provision to force the number of layers to be even in number, if desired for laminate symmetry.

(CW/VT, X-29 wing)

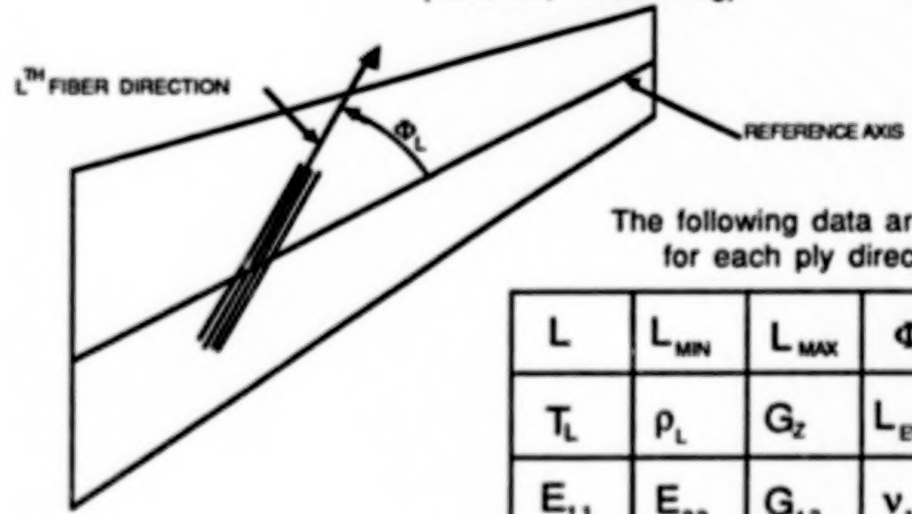

The following data are stored for each ply direction

L	L_{MIN}	L_{MAX}	Φ_L	L_{BAL}
T_L	ρ_L	G_z	L_{EVEN}	L_{ROC}
E_{11}	E_{22}	G_{12}	ν_{12}	
F_{1T}	F_{1C}	F_{2T}	F_{2C}	F_S

STRUCTURAL OPTIMIZATION PROCEDURES

Application of the structural optimization procedures usually begins by performing a structural analysis to obtain displacements and internal loads. This is followed by a strength sizing using the RESIZE module. The analysis and resizing cycle is normally repeated three or four times (our experience indicates that for realistic structures, convergence usually occurs within three to five cycles). We next perform any number of analyses to calculate the specific quantities of interest such as control effectiveness, divergence speed, a specific deflection, modes of vibration, or flutter speeds. This is followed by the calculation of derivatives of these quantities with respect to element weight using modules such as DERIV, DERIVF or DERIVFLT. The derivatives are then used in the resizing modules: AERES which performs resizing for a single constraint, AERESM which is a partially automated procedure for performing resizing when there are multiple constraints or MCRES, which is a fully automated procedure for performing resizing for multiple constraints. The calculation of derivatives and subsequent resizing is cycled until the desired result is obtained.

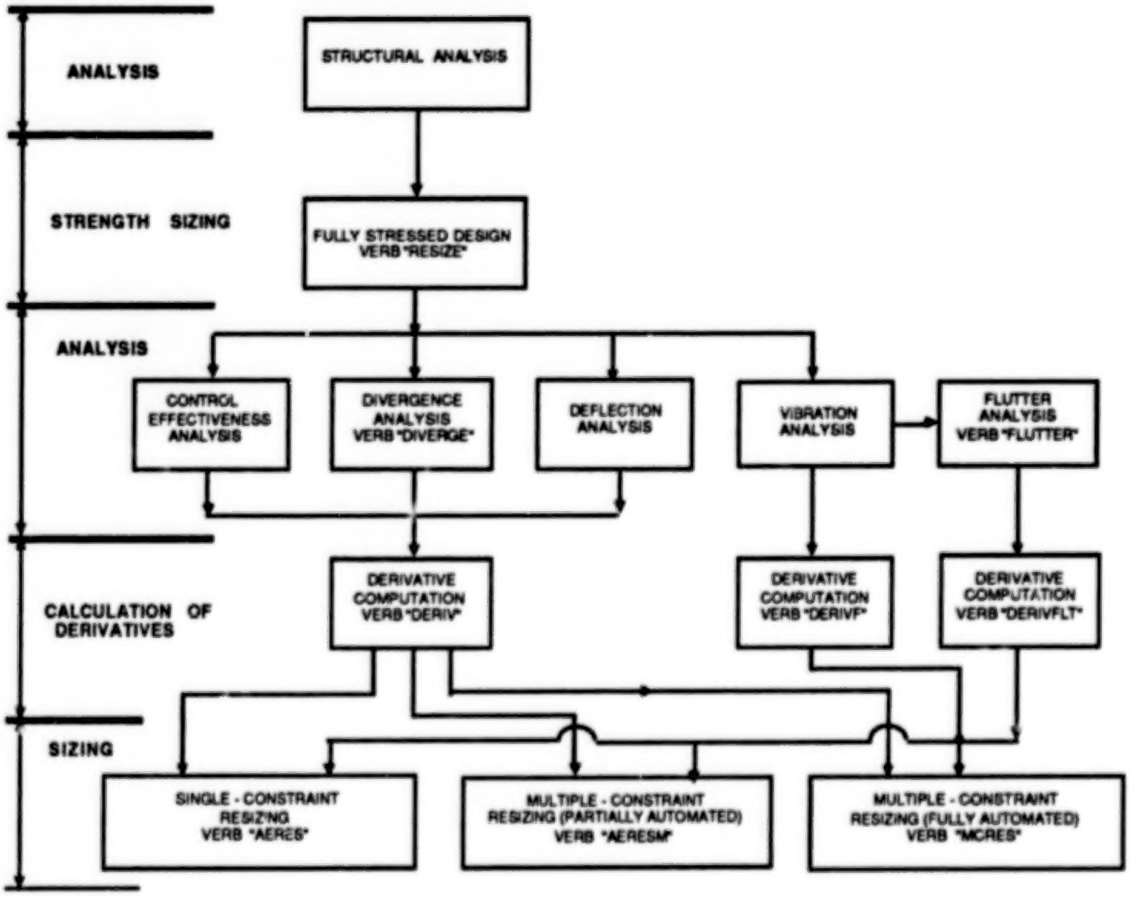
ANALYSIS
STRUCTURAL ANALYSIS
STRENGTH SIZING
FULLY STRESSED DESIGN VERB "RESIZE"
ANALYSIS
CONTROL EFFECTIVENESS ANALYSIS
DIVERGENCE ANALYSIS VERB "DIVERGE"
DEFLECTION ANALYSIS
VIBRATION ANALYSIS
FLUTTER ANALYSIS VERB "FLUTTER"
CALCULATION OF DERIVATIVES
DERIVATIVE COMPUTATION VERB "DERIV"
DERIVATIVE COMPUTATION VERB "DERIVF"
DERIVATIVE COMPUTATION VERB "DERIVFLT"
SIZING
SINGLE - CONSTRAINT RESIZING VERB "AERES"
MULTIPLE - CONSTRAINT RESIZING (PARTIALLY AUTOMATED) VERB "AERESM"
MULTIPLE - CONSTRAINT RESIZING (FULLY AUTOMATED) VERB "MCRES"

THE X-29 FORWARD-SWEPT-WING DEMONSTRATOR AIRCRAFT

Automated design and analysis procedures played a major role in the development of the X-29 demonstrator aircraft. The design of this vehicle incorporates several advanced technology features as shown here. Particularly pertinent to our discussion is the work that was done to incorporate aeroelastic tailoring in the design of the wing covers, with the goal of minimizing the weight increment needed to avoid static divergence. A detailed discussion of the preliminary design work leading to the X-29 is given in Ref. 23.

Grumman/DARPA X-29A Advanced Technology Demonstrator

Technology Features

- Close-Coupled Canard
- Advanced Flight Controls
- Variable Camber

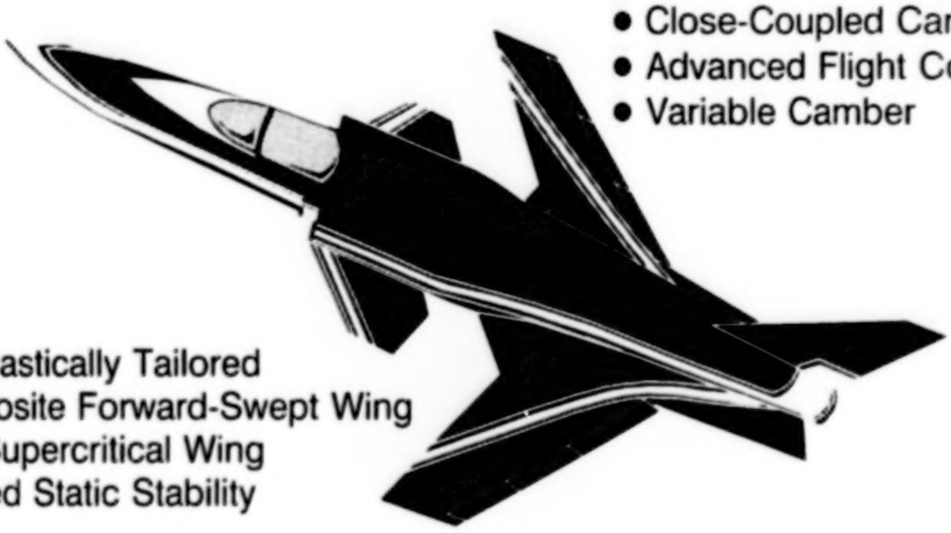

- Aeroelastically Tailored Composite Forward-Swept Wing
- Thin Supercritical Wing
- Relaxed Static Stability

FORWARD-SWEPT WING FEASIBILITY STUDY

Our initial efforts in the design of a forward-swept wing were in a feasibility study we performed for DARPA in 1977. The study examined a relatively high-aspect-ratio wing having variable sweep. A goal was to investigate various configurations of composite cover skins with the objective of minimizing the weight increment required to avoid static divergence. Both beam and coarse-grid, finite-element models were employed to study various materials and laminate configurations with regard to their effect on divergence and flutter characteristics and to identify the weight increments required to avoid divergence. As an example of one part of the study, it was desired to evaluate the benefits of induced bend/twist coupling caused by kicking the spanwise fiber direction forward of the nominal structural axis. Four kick angles were examined with the use of our optimization procedures. Some results are shown in the sketch shown here. We see normalized weight variations for the wing model as obtained for strength-based designs, via fully stressed design, in the lower curve. The upper curve shows the effect on weight when each of the strength designs is stiffened to meet a critical divergence-speed requirement. It may be noted that the optimum kick angle is about 10 degrees.

- Examined feasibility of a variable sweep wing that used advanced composites to minimize weight increment to avoid static divergence
- Used beam and finite-element models and optimization methods to:
  - Assess behavior of various materials & ply configurations for covers
  - Provide estimates of divergence & flutter behavior
  - Estimate weight increments for divergence prevention

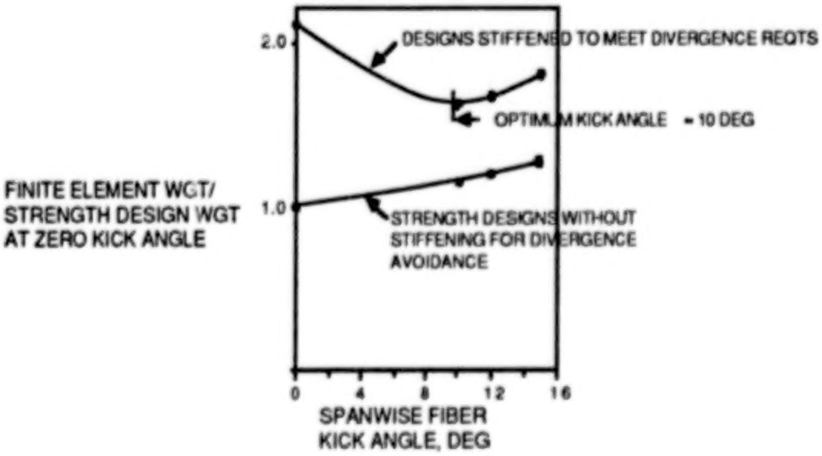

X-29 PRELIMINARY AND FINAL DESIGN

In a later "Forward Swept Wing Demonstrator Technology Integration and Evaluation Study," conducted by Grumman for DARPA and the U.S. Air Force, we transitioned our design concepts to a fixed-wing configuration and utilized structural optimization technology in what was to become a preliminary design effort for the X-29. We adopted a wing cover arrangement that uses 0/90/±45 degree graphite-epoxy laminates which are rotated about 9 degrees forward of the nominal structural axis. This material arrangement offers favorable bend/twist coupling while maintaining high bending stiffness and linear stress/strain behavior. The 9-degree rotation angle comes about from our findings in the feasibility study and the added benefit that fiber continuity is preserved across the airplane centerline. We again used our fully stressed design and divergence optimization tools to size the wing covers and substructure. Gages that were identified as being governed by divergence requirements were maintained as minimums in the subsequent final design effort.

Preliminary Design

- Transitioned to fixed wing configuration utilizing graphite/epoxy cover skins of 0/90/± 45 deg plies. Laminates were balanced in ± 45 deg directions and were rotated approximately 9 deg forward to
  - produce favorable bend/twist coupling
  - maintain high bending stiffness
  - provide linear stress/strain behavior to limit load
  - preserve fiber continuity accross airplane centerline
- Employed fully stressed design and automated optimization to size wing for divergence speed requirements

Final Design

- Increased model complexity and expanded number and type of design loading conditions. Used fully stressed design while maintaining as minimums the numbers of plies identified in the preliminary design as required for divergence avoidance

PRELIMINARY DESIGN DEMONSTRATOR WING AND FINAL X-29 FINITE-ELEMENT MODEL

Here we have a planform of the wing model used in the technology evaluation and preliminary design work. This is followed by an isometric view of the final half-aircraft, finite-element model of the X-29.

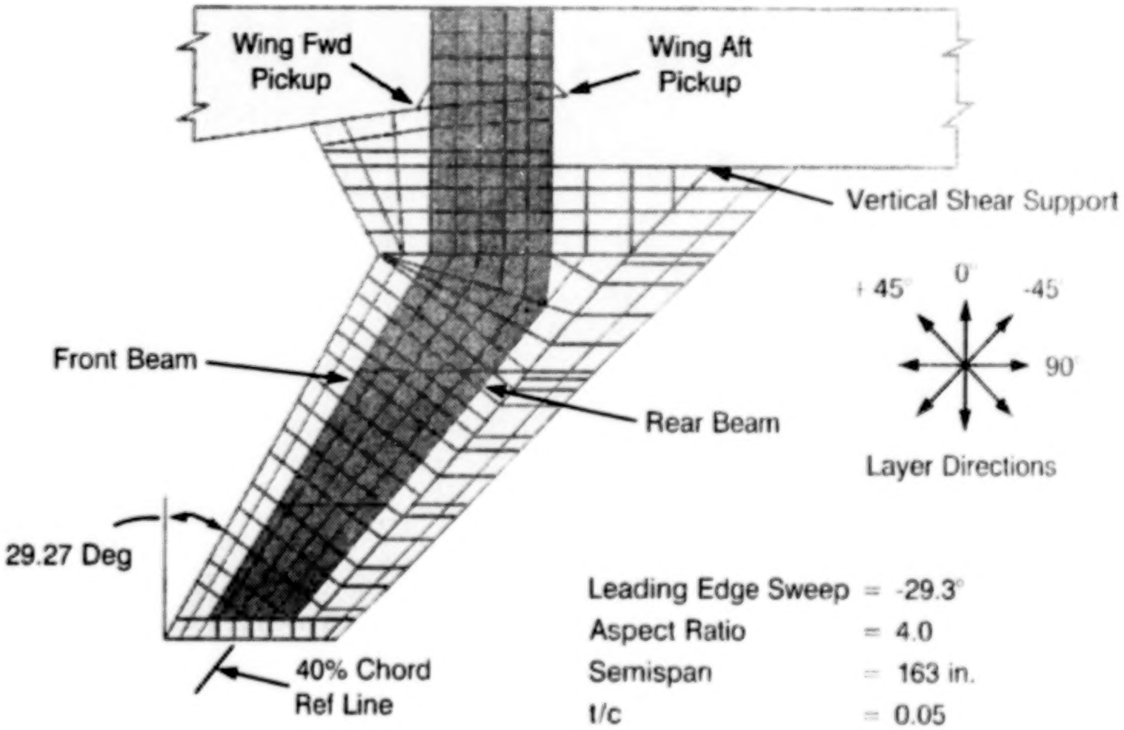

X-29 Forward Swept Wing Demonstrator Aircraft

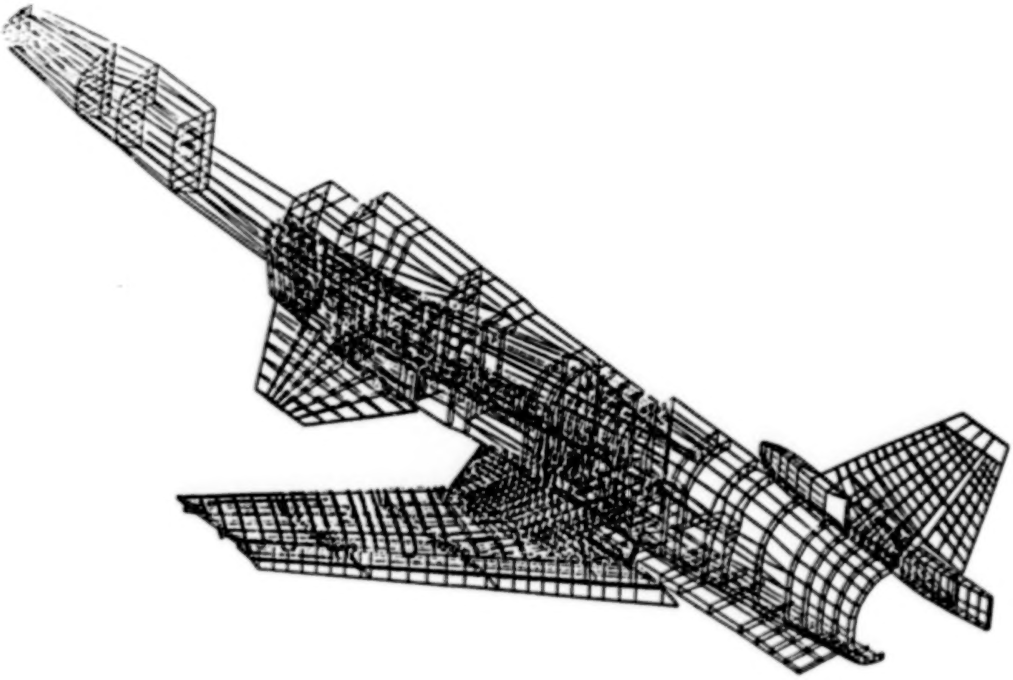

FINITE-ELEMENT MODEL OF CW/VT WING

The CW/VT wing is a multispar configuration having graphite-epoxy covers and metallic substructure. It is attached to the fuselage at 8 points. Movable surfaces consist of a leading-edge flap and inboard and outboard elevons. The covers are modeled as anisotropic membrane panels; ribs and spars are represented by bars and shear panels. The total model contains about 3100 members, 3400 degrees of freedom and approximately 6000 design variables (which account for the individual ply directions in the covers).

The structure was analyzed and sized to meet strength requirements for 102 flight design conditions. For the covers, strength requirements were based on maximum allowed fiber strains and panel buckling avoidance. Control-surface effectiveness requirements also played a major role in the design of this relatively thin wing. These requirements involved both pitch and roll, as well as ratios of pitch moment to hinge moment and roll moment to hinge moment, at Mach 0.9 and 1.2. The design was checked for flutter and leading-edge flap divergence, neither of which had any significant impact on the final design.

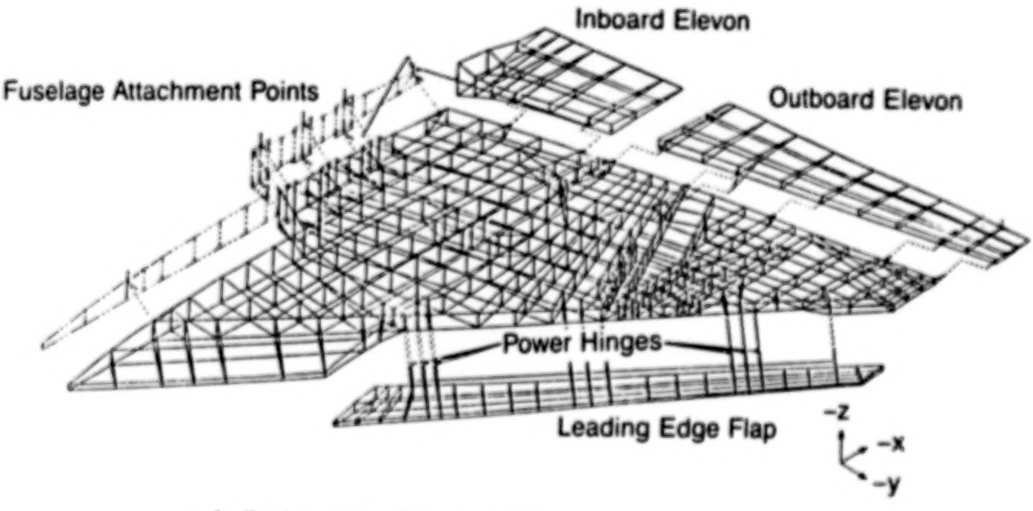

- Indicates store pickup point
- Indicates fuselage attachment point

CW/VT DESIGN/ANALYSIS CYCLE

The design/analysis cycle is shown below. Initial tasks consisted of generating the finite element model using CADAM and our COGS interface. The prime contractor supplied panel-point loads that were transformed to the structural model. They also provided stiffness and mass data for the fuselage. The fuselage stiffness matrix was reduced to the wing and tail attachment points and coupled with the wing and vertical tail stiffness matrices.

Several design/analysis cycles were performed by Grumman for the wing and vertical tail. Based upon experience gained in the early cycles, we established a rather pragmatic approach to obtain a near-minimum-weight design in the final design cycle, in which requirements for strength, panel buckling avoidance and control-surface effectiveness were treated in a somewhat interactive way.

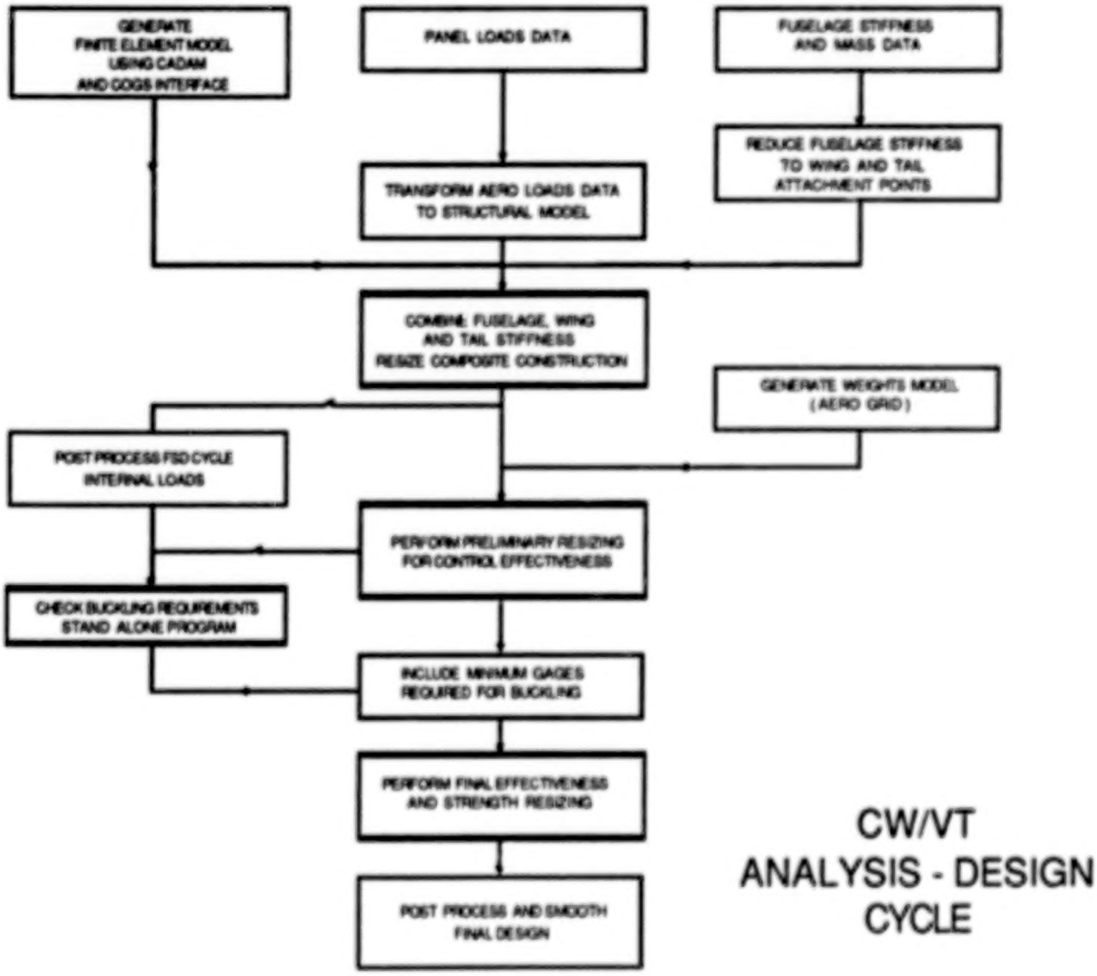
GENERATE FINITE ELEMENT MODEL USING CADAM AND COGS INTERFACE
PANEL LOADS DATA
FUSELAGE STIFFNESS AND MASS DATA
REDUCE FUSELAGE STIFFNESS TO WING AND TAIL ATTACHMENT POINTS
TRANSFORM AERO LOADS DATA TO STRUCTURAL MODEL
COMBINE FUSELAGE, WING AND TAIL STIFFNESS RESIZE COMPOSITE CONSTRUCTION
GENERATE WEIGHTS MODEL (AERO GRID)
POST PROCESS FSD CYCLE INTERNAL LOADS
PERFORM PRELIMINARY RESIZING FOR CONTROL EFFECTIVENESS
CHECK BUCKLING REQUIREMENTS STAND ALONE PROGRAM
INCLUDE MINIMUM GAGES REQUIRED FOR BUCKLING
PERFORM FINAL EFFECTIVENESS AND STRENGTH RESIZING
POST PROCESS AND SMOOTH FINAL DESIGN

CW/VT
ANALYSIS - DESIGN
CYCLE

CW/VT WING SIZING PROCEDURE

The final sizing procedure and results are summarized in the figure below. We have plotted wing finite-element model weight increments along the horizontal axis and the governing control-surface effectiveness parameter along the vertical axis. The required value of the parameter is shown as the horizontal line. Initially, we generated an FSD design for 75% of applied ultimate load. We then performed effectiveness resizing and brought the design to a point where the effectiveness parameter was approximately 80% of its required value. The buckling resizing and adjustments of the ply layups for producibility added additional weight increments and brought the effectiveness parameter to about 85% of the required value. Additional resizing to increase control effectiveness proceeded along the points marked by triangles in the upper portion of the curve. Along with each of these points are side-step increments required to satisfy 100% of ultimate load. All but the last of these latter points (marked by squares) represent designs which satisfy full strength and buckling-avoidance requirements but which compromise the full effectiveness requirement, should such a compromise be desired in the face of the identified weight increments.

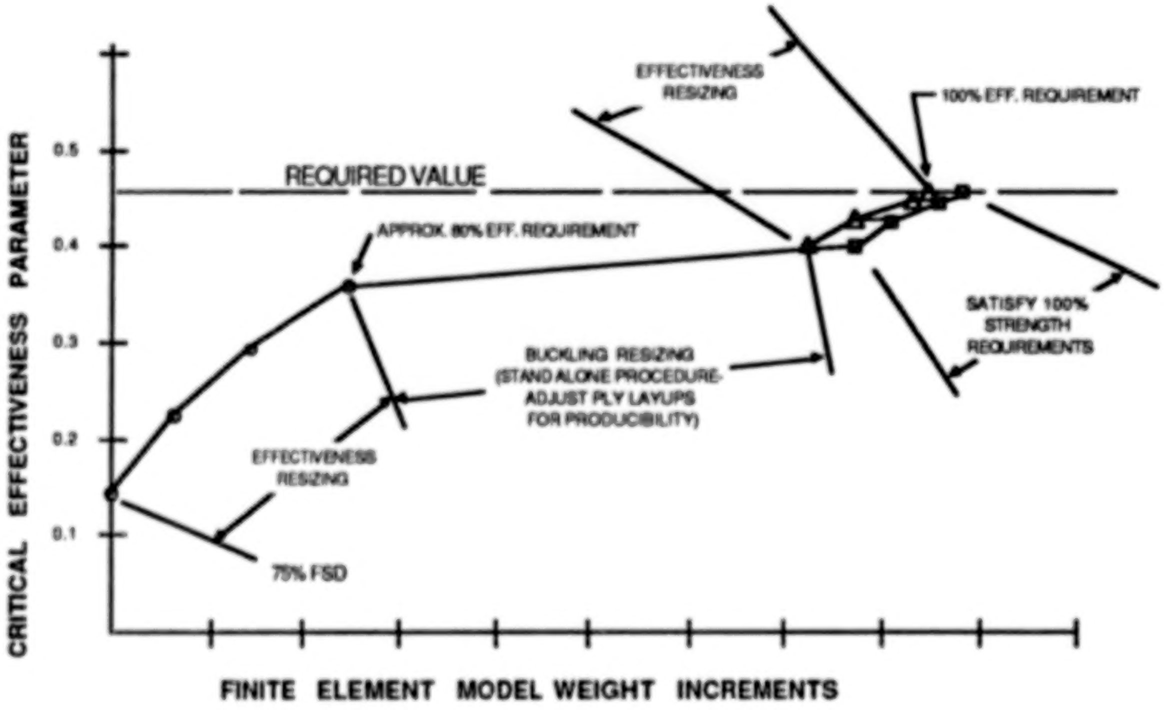

BEST COPY AVAILABLE

CW/VT WING 0° PLY DISTRIBUTION

Here we see the 0°-ply distribution for the lower cover of the CW/VT wing. The number of plys are color coded. The COGS system allows us to display a wide variety of information in an interactive graphics environment. For example, since we store various derivatives within regions of the member data, we can display them as well. We have found displays of this type of information to be particularly useful, not only in giving us important information about the design, but also as an aid in checking the realism of the model.

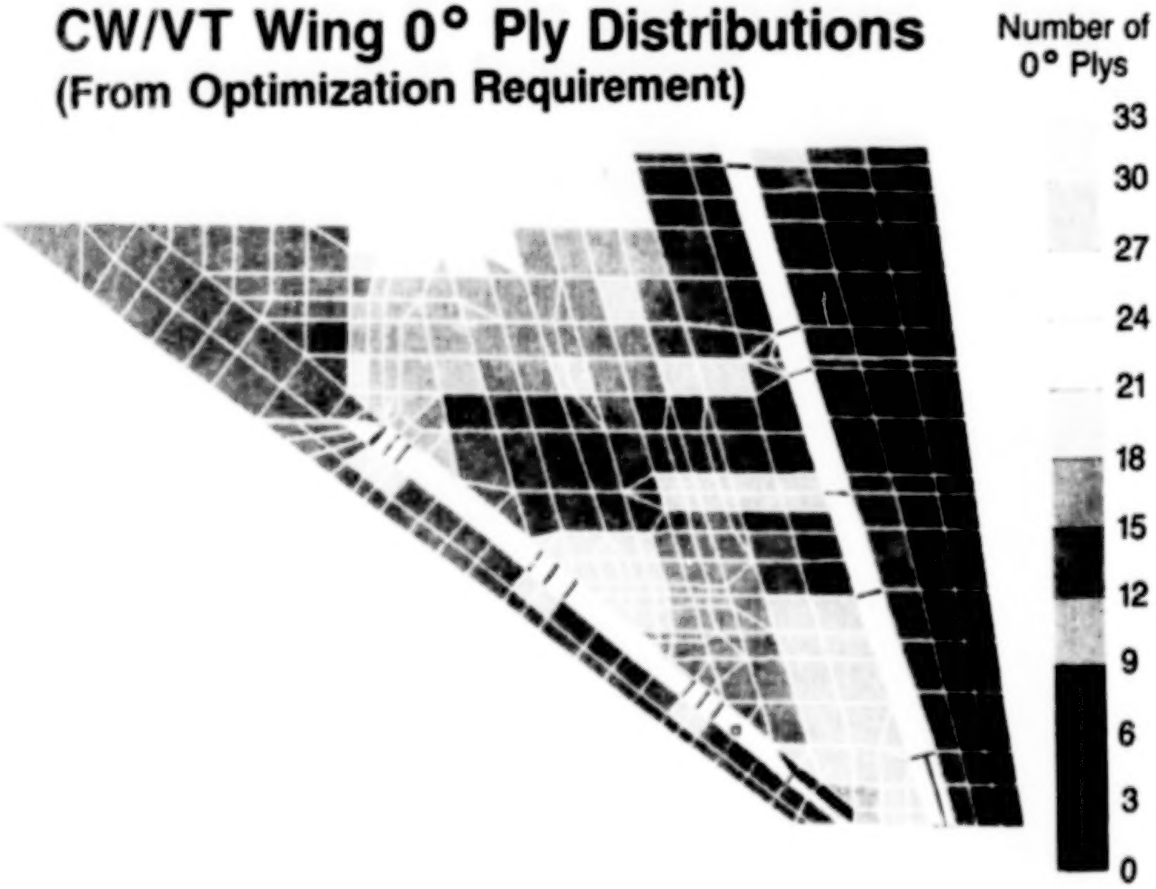

CW/VT Wing 0° Ply Distributions
(From Optimization Requirement)

CONCLUSIONS

Integrated structural analysis and design systems and structural optimization procedures are being used in a production environment. Successful use of these systems requires experienced personnel. Interactive computer graphics can and will play a significant role in the analysis/optimization/design/manufacturing area. Today, we talk about collocating a team of people that include analysts, designers and manufacturing engineers on a given project so that they can interact via a common system. Practical structural optimization procedures are tools that must be made available to the team.

Much work still needs to be done to tie finite-element modeling to actual design details which are being tracked on systems such as CADAM or CATIA.

More work needs to be done to automate the detailed design and analysis process -- more emphasis should be placed on the real design problems.

CONCLUSIONS

Integrated structural design and analysis systems, and structural optimization procedures are being used in the production environment.

- **Successful use of these systems requires experienced personnel.**
- **More work needs to be done in developing data base systems that will track structural detail and permit better means for controlling the finite-element model idealization.**
  (Example: Tie CADAM -- structural modeler -- analysis -- structural design)
- **More work needs to be done to automate the detailed design and analysis process. (Example: Incorporate panel buckling and internal load redistribution due to post buckling)**

REFERENCES

1. Wehle, L.B. and Lansing, W., "A Method for Reducing the Analysis of Complex Structures to a Routine Procedure," Journal of Aeronautical Sciences, Oct. 1952.

2. Dwyer, W., Rosenbaum, J., Shulman, M., and Pardo, H., "Fully Stressed Design of Airframe Redundant Structures," proceedings of the Second Conference on Matrix Methods in Structural Mechanics, Air Force Flight Dynamics Labcratory AFFDL-TR-68-150, Dec. 1969.

3. Lansing, W., Dwyer, W., Emerton, R., and Ranalli, E., "Application of Fully Stressed Design Procedures to Wing and Empennage Structures," Journal of Aircraft, Vol. 9, No. 9, Sept. 1971, pp 683-688.

4. Wennagel, G., Mason, P., and Rosenbaum, J., "IDEAS, Integrated Design and Analysis System," Society of Automotive Engineers, Paper No. 680728, Oct. 1968.

5. Lansing, W., "The Role of Design Analysis Systems for Aerospace Structures and Future Trends," Keynote Address - Third Conference on Matrix Methods in Structural Mechanics, Oct. 1971, published in AFFDL-TR-71-160, Dec. 1973.

6. Lansing, W., Mason, P., Dwyer, W., and Cooper, J.C., "Application of a Design Analysis System to a Space Shuttle Preliminary Design," 2nd Symposium on Structural Optimization, AGARD Conference Proceedings No. 123, April 1973.

7. Mason, P., "Design Experience With an Integrated Design Analysis System," invited panelist, opening session presentation at the 14th SDM (Structures, Dynamics, Materials) Conference, Williamsburg, Virginia, 1973.

8. Wennagel, G.J., Loshigian, H.H., and Rosenbaum, J., "RAVES - Rapid Aerospace Vehicle Evaluation System," ASME Winter Conference, Houston, Texas, Nov.-Dec. 1975.

9. Dwyer, W., Emerton, R.K., and Ojalvo, I.U., "An Automated Procedure for the Optimization of Practical Aerospace Structures," AFFDL-TR-70-118, Vols. I and II, April 1971.

10. Dwyer, W., "Finite Element Modeling and Optimization of Aerospace Structures," AFFDL-TR-72-59, Aug. 1972.

11. Dwyer, W.,"An Improved Automated Optimization Program," AFFDL-TR-74-96, Sept. 1974.

12. Wilkinson, K., et al, "An Automated Procedure for Flutter and Strength Analysis and Optimization of Aerospace Vehicles," Vol. I - Theory, Vol II - Programer User's Manual, AFFDL-TR-75-137, Dec. 1975.

13. Wilkinson, K., Lerner, E., and Taylor R.F., "Practical Design of Minimum-Weight Aircraft Structures for Strength and Flutter Requirements," Journal of Aircraft, Vol. 13, No. 8, Aug. 1976, pp. 614-624. Also presented as Paper 74-986 at the AIAA 6th Aircraft Design, Flight Test and Operations Meeting, Los Angeles, Calif., August 1974.

14. Isakson, G. and Pardo, H., "ASOP-3: A Program for the Minimum-Weight Design of Structures Subject to Strength and Deflection Constraints," AFFDL-TR-76-157, Dec. 1976.

15. Wilkinson, K., Markowitz, J., Lerner, E., George, D., and Batill, S.M., "FASTOP: A Flutter and Strength Optimization Program for Lifting-Surface Structures," Journal of Aircraft, Vol. 14, No. 6, June 1977, pp. 581-587. Also presented at the AIAA/ASME/SAE 17th Structures, Structural Dynamics and Materials Conference, King of Prussia, Pa., May 1976.

16. Lansing, W., Lerner, E., and Taylor, R.F., "Applications of Structural Optimization for Strength and Aeroelastic Design Requirements," AGARD Report No. 664, Sept. 1977. Invited paper presented at the 45th Structures and Materials Panel Meeting, Voss, Norway, September 1977.

17. Markowitz, J., and Isakson, G., "FASTOP-3: A Strength, Deflection and Flutter Optimization Program for Metallic and Composite Structures," Vol. I - Theory and Applications, Vol. II - Programers User's Manual, AFFDL-TR-78-50, May 1978.

18. Austin, F., "A Rapid Optimization Procedure for Structures Subjected to Multiple Constraints," Paper No. 77-374, AIAA/ASME/SAE 18th Structures, Structural Dynamics and Materials Conference, San Diego, Calif., March 1977.

19. Isakson, G., Pardo, H., Lerner, E., and Venkayya, V.B., "ASOP-3: A Program for Optimum Structural Design to Satisfy Strength and Deflection Constraints," Journal of Aircraft, Vol. 15, No. 7, July 1978, pp. 422-428. Also presented as Paper 77-378 at the AIAA/ASME/SAE 18th Structures, Structural Dynamics and Materials Conference, San Diego, Calif., March 1977.

20. Mason, P., Gregory, D., Balderes, T., and Iaccarino, S., "Towards a Realistic Structural Analysis/Design System," Symposium on Future Trends in Computerized Structural Analysis and Synthesis, Oct. 1978, Washington D.C., sponsored by George Washington University and NASA Langley Research Center.

21. Lerner, E., and Markowitz, J., "An Efficient Structural Resizing Procedure for Meeting Static Aeroelastic Design Objectives," Journal of Aircraft, Vol. 16, No. 2, Feb. 1979, pp. 65-71. Also presented as Paper 78-471 at the AIAA/ASME 19th Structures, Structural Dynamics and Materials Conference. Bethesda, Md., April 1978.

22. Mason, P., Balderes, T., and Armen, H., "The Application of Nonlinear Analysis Techniques to Practical Structural Design Problems," Symposium on Advances and Trends in Structural and Solid Mechanics, Oct. 1982, Washington D.C., sponsored by George Washington University and NASA Langley Research Center.

23. Lerner, E., "The Application of Practical Optimization Techniques in the Preliminary Structural Design of a Forward-Swept Wing." Collected papers of the Second International Symposium on Aeroelasticity and Structural Dynamics, Technical University of Aachen, West Germany, April 1985, pp. 381-393.

BLANK PAGE

INTEGRATED DESIGN OPTIMIZATION RESEARCH AND DEVELOPMENT IN AN INDUSTRIAL ENVIRONMENT

V. Kumar
M. D. German
S. -J. Lee
GE Research and Development
Schenectady, New York

ABSTRACT

This paper presents an overview of a design optimization project that is in progress at the GE Research and Development Center for the past few years. The objective of this project is to develop a methodology and a software system for design automation and optimization of structural/mechanical components and systems. The effort focuses on research and development issues and also on optimization applications that can be related to real-life industrial design problems. The overall technical approach is based on integration of numerical optimization techniques, finite element methods, CAE and software engineering, and artificial intelligence/expert systems (AI/ES) concepts. The role of each of these engineering technologies in the development of a unified design methodology is illustrated below in Figure 1. A software system DESIGN-OPT has been developed for both size and shape optimization of structural components subjected to static as well as dynamic loadings. By integrating this software with an automatic mesh generator, a geometric modeler and an attribute specification computer code, a software module SHAPE-OPT has been developed for shape optimization. Details of these software packages together with their applications to some 2- and 3-dimensional design problems will be described later in this presentation.

In regard to the integration with AI/ES, a pilot expert system advisor has been developed to help an engineer use the optimization technology for complex design problems in an effective manner. Some remarks are also made concerning experience with the use of optimization methods for practical design applications. Finally, several topics of future research, like process optimization and simultaneous product and process design, are introduced; and the role of multidisciplinary optimization, multilevel design and decomposition models is highlighted.

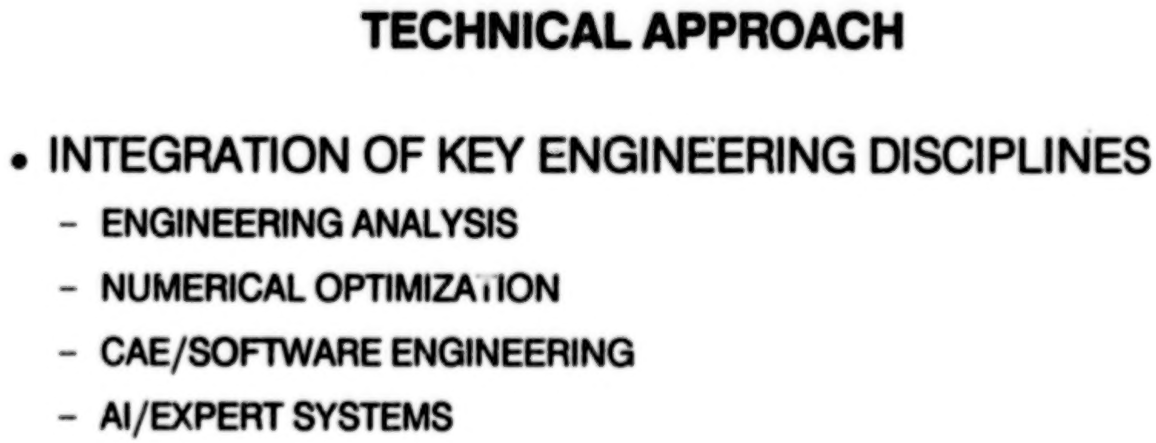

TECHNICAL APPROACH

- INTEGRATION OF KEY ENGINEERING DISCIPLINES
  - ENGINEERING ANALYSIS
  - NUMERICAL OPTIMIZATION
  - CAE/SOFTWARE ENGINEERING
  - AI/EXPERT SYSTEMS

Figure 1

DESIGN-OPT SOFTWARE SYSTEM

A design optimization software system DESIGN-OPT has been developed by integrating the well-known numerical optimization codes COPES/ADS [1], the commercially available analysis codes like ADINA, ADINAT and ANSYS and also some in-house finite element software packages, the pre- and post-processing software packages like MOVIE.BYU, PLOT10 and IDEAS/SUPERTAB, and a number of CAE tools for automatic mesh generation, geometry modeling and attribute specification. A schematic of the software architecture is illustrated in Figure 2. The OPT-AN processor directs the flow of the data from the optimizer to various analysis codes, and update input files to incorporate changes in design parameters at various optimization iterations. It also provides an interface with the SHAPE-OPT module which will be described in a subsequent section. The data flow from the analysis codes to the optimizer occurs through the software module AN-OPT which retrieves relevant information from the finite element output files and utilizes it to compute the objective function, constraints and gradients. In addition, it also provides an interface with various post-processing software packages so that the user can graphically display the structural configuration, stress and temperature contours, mode shapes for dynamic problems, and the iteration histories of objective function and design constraints. Particular emphasis has been placed on the post-processing and interactive aspects for on-line design optimization so that the user can exercise his own judgment during the optimization process. The finite difference method of design sensitivity analysis was used for all the finite element codes mentioned above, except that the implicit differentiation approach was also implemented into the ADINA code. This will be elaborated upon in the next section. Some of the applications include size and shape optimization of 2D/3D structural components subjected to static and dynamic constraints including centrifugal and thermal effects.

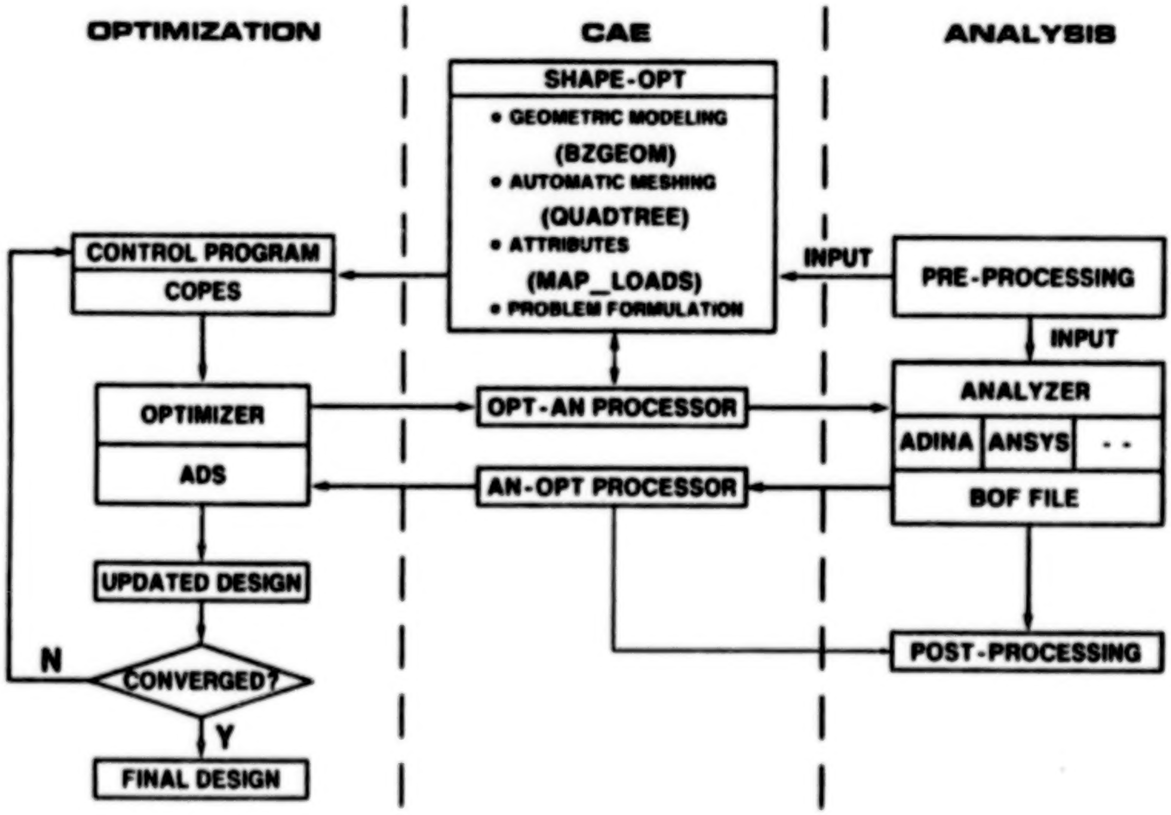

Figure 2

BEST COPY AVAILABLE

DESIGN SENSITIVITY ANALYSIS USING FINITE DIFFERENCE AND IMPLICIT DIFFERENTIATION METHODS

The finite difference method of design sensitivity analysis offers a simple, general and reasonably accurate approach for integrating analysis and optimization codes. The most attractive aspects of this approach are its ease for software implementation and the fact that it can be used external to a finite element code without requiring a source listing. However, it requires (n+1) function evaluations or finite element analyses for sensitivity calculations, n being the number of design variables; therefore, the associated computation time becomes rather large for many practical applications. The implicit differentiation or semi-analytical approach offers an efficient method of design sensitivity analysis requiring only one function evaluation or finite element analysis irrespective of the number of design variables. The implementation in this case, however, is carried out internal to a finite element software; the access to a source finite element code, therefore, becomes essential.In addition,considerable engineering effort and time are required to perform the associated software development. Since the source listing for the finite element code ADINA is available commercially, both the finite difference and implicit differentiation methods were employed when integrating ADINA with the DESIGN-OPT software system as illustrated in Figure 3. These developments were carried out for both size and shape variables, for static as well as dynamic problems, and encompassing a wide range of element types (truss, beam, plate, plane stress, plane strain and axisymmetric). Centrifugal and thermal loadings were also considered. Some closed-form solutions were used to benchmark the ADINA enhancements that were carried out. A comparison of the two approaches was also made in terms of the computational efficiency and solution accuracy. This development is presented in detail in Reference [2].

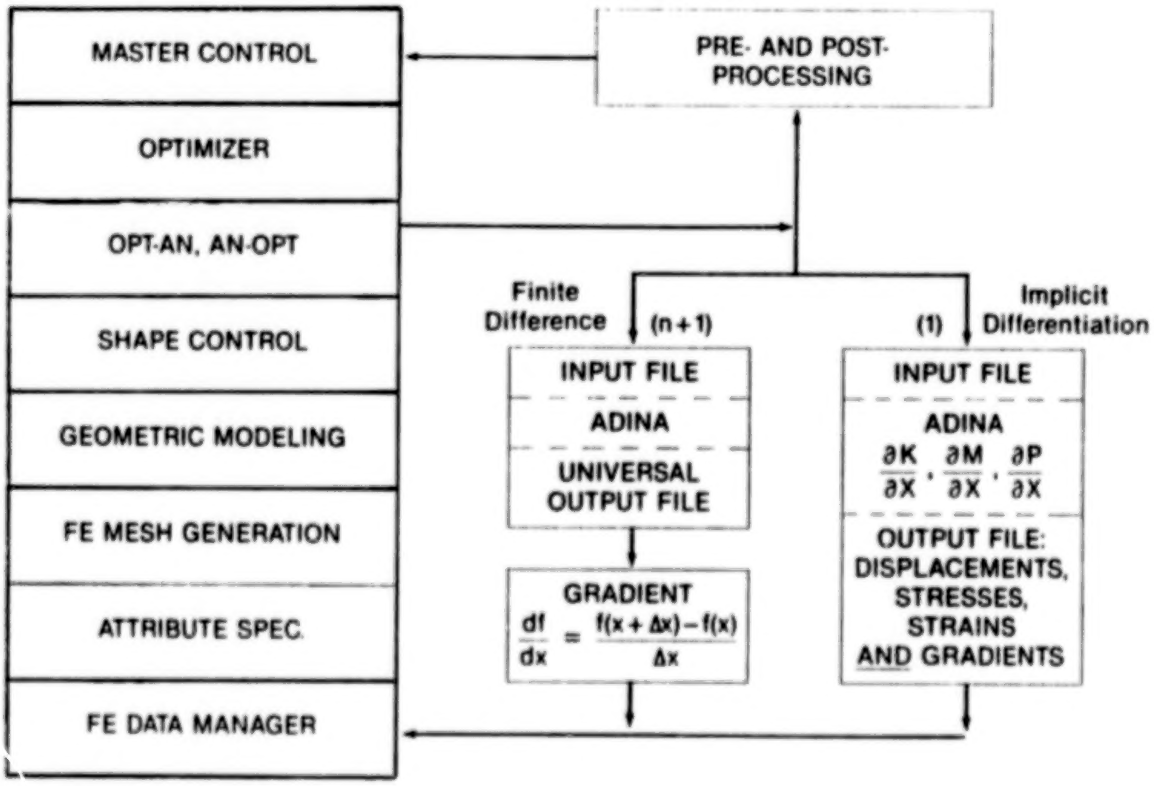

Figure 3

GEOMETRY-BASED SHAPE OPTIMIZATION METHODOLOGY AND THE SHAPE-OPT SOFTWARE

A geometry-based shape optimization methodology and a shape optimization module SHAPE-OPT was developed by integrating DESIGN-OPT with in-house automatic mesh generation, geometric modeler and attribute specification software packages as illustrated conceptually in Figure 4. The overall approach closely parallels the earlier work by Botkin and Bennett [3-5], and is described in some detail in Reference [6]. In this, the geometric modeling techniques (BZGEOM [7]) are employed for shape description in terms of boundary points (fixed as well as design variables) and geometric entities like lines, circular arcs and splines. The optimization formulation is also carried out at the geometry level in that the stress and other design constraints are specified in terms of boundary points, geometric entities and domains rather than individual finite elements or mesh points. An automatic mesh generation capability (QUADTREE [8,9]) is utilized for creating the initial finite element model and also for automatic remeshing as the shape changes during optimization. A strategy was developed for mesh updating between two successive remeshing and for design sensitivity calculations. An in-house software MAP-LOADS [7] is used for specifying attributes (tractions, displacements and temperatures) at the geometry level in an interactive manner via the use of the geometric modeler BZGEOM. A shape control procedure was also introduced for eliminating shape irregularities during optimization iterations; for example, by including constraints on slopes and curvatures at certain boundary points. The experience based upon several practical applications has shown that the geometry-based approach provides an effective method of dealing with different number of nodes and elements that result when using automatic mesh generation at various stages of the optimization process. The task of attribute specification also becomes much easier at the geometry level since the boundary conditions are not tied to finite elements and mesh points.

- **GEOMETRIC MODELING**
  - SHAPE DESCRIPTION
  - PROBLEM FORMULATION

- **AUTOMATIC MESH GENERATION**
  - INITIAL FINITE ELEMENT MODEL
  - REMESHING AS SHAPE CHANGES

- **ATTRIBUTE SPECIFICATION**
  - TRACTION, DISPLACEMENT AND TEMPERATURE BOUNDARY CONDITIONS AT GEOMETRY LEVEL

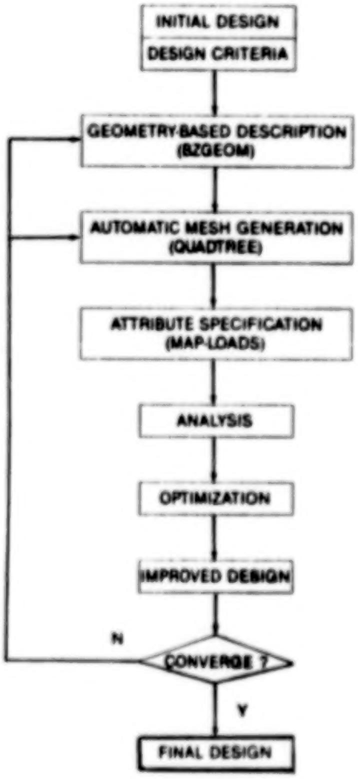
INITIAL DESIGN
DESIGN CRITERIA
GEOMETRY-BASED DESCRIPTION (BZGEOM)
AUTOMATIC MESH GENERATION (QUADTREE)
ATTRIBUTE SPECIFICATION (MAP-LOADS)
ANALYSIS
OPTIMIZATION
IMPROVED DESIGN
N
CONVERGE ?
Y
FINAL DESIGN

Figure 4

TURBINE DISC OPTIMIZATION

The DESIGN-OPT/SHAPE-OPT software was successfully employed for several practical applications including the design of rotating disc which represents a key structural component in several rotating machineries like gas turbines, steam turbines and aircraft engines. The optimization problem in this case usually consists of finding the axisymmetric shape of the disc to minimize the weight. Constraints are imposed on radial, tangential and Von Mises stresses, the disc burst speed, displacements, natural frequencies, and certain geometric considerations, etc. The disc is analyzed, in most cases, as an axisymmetric problem subjected to centrifugal and thermal loading. A uniform pressure is also applied at the rim (i.e., the top of disc) to model the centrifugal loading due to blades. Typical results are shown in Figure 5 in the form of disc shapes and weights versus optimization iterations. Finite element models, generated automatically by QUADTREE, are also illustrated. It is clear from these results that the disc shape and the corresponding mesh change substantially during the optimization process, demonstrating thereby the necessity of integrating an automatic mesh generation software into an effective and practically usable shape optimization methodology. Although the results are not shown here, it has also been noted that the same optimal design, in terms of the disc shape, weight and constraints, is usually obtained irrespective of initial designs. This observation provides some level of confidence that for the present class of problems we are able to achieve a nearly global optimal solution within the context of a given problem formulation and the solution approach. In most cases, it took less than 10 optimization iterations to converge to the optimal design.

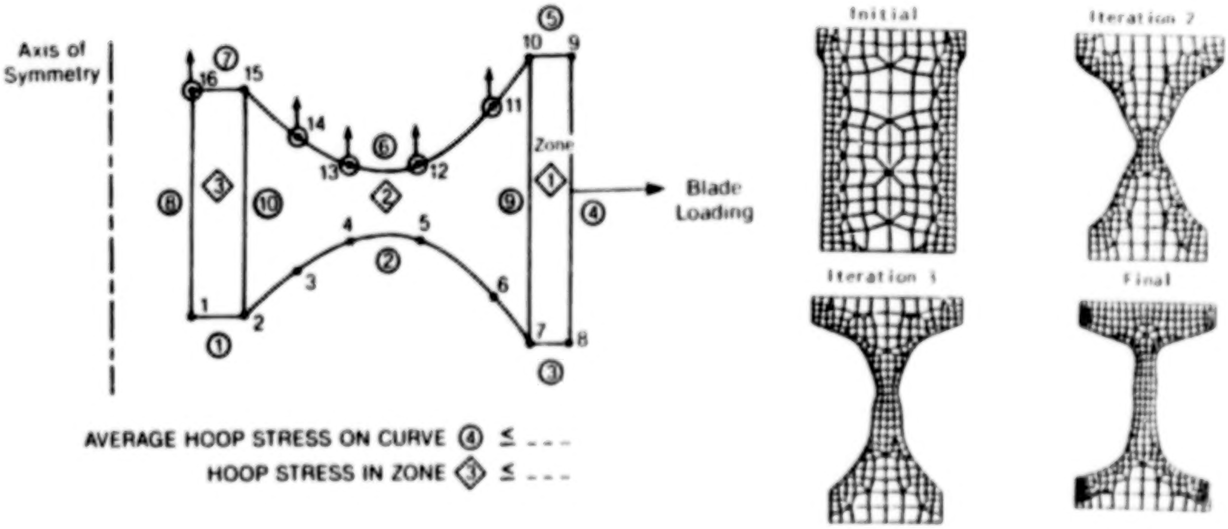

Figure 5

EFFECT OF SHAPE DESCRIPTION ON OPTIMAL RESULTS

In contrast with size optimization where the number of design variables are fixed for a given problem, the design variables for shape optimization can be specified in a number of different ways. The shape design variables are usually specified by the user at the problem formulation stage, and they remain fixed during the optimization process. A shape description involving a large number of design variables may lead to substantial increase in the computation time without adding any improvements in the final solution. A choice of too small a number of design variables, on the other hand, may not provide enough degrees of freedom for shape variations, resulting in a poor optimal design. it becomes necessary, therefore, to change the shape description during the optimization process in an interactive and dynamic manner. A strategy was developed and implemented in the SHAPE-OPT software that allows the user to specify different design models, i.e., number and locations of design variables, corresponding to different optimization iterations at the problem formulation and input file preparation stages. In other words, the user can specify n_1 design variables during the first k_1 iterations, n_2 during k_2 and n_ℓ during k_ℓ iteration stages, where $n_1, n_2, - -, n_\ell \leq n$ which is the maximum number of design variables in the overall optimization process. Several technical and software-related issues had to be addressed to implement this capability. For example, a reduction in the number of design variables necessitates change in the definition of the spline curve passing through the relevant design points. Also, the deleted design variables have to be kept updated on the newly defined curve so that any resultant discontinuities in the design and analysis models are eliminated. Further, one has to ensure that gradients with respect to deleted design variables are not computed. Some example results are shown below in Figure 6. The strategy consisted of performing several optimization runs, one keeping all the design variables throughout the optimization process and the other runs that employ different design variables at various optimization iterations. The results show that comparable optimal weights are obtained with different computation time for various strategies.

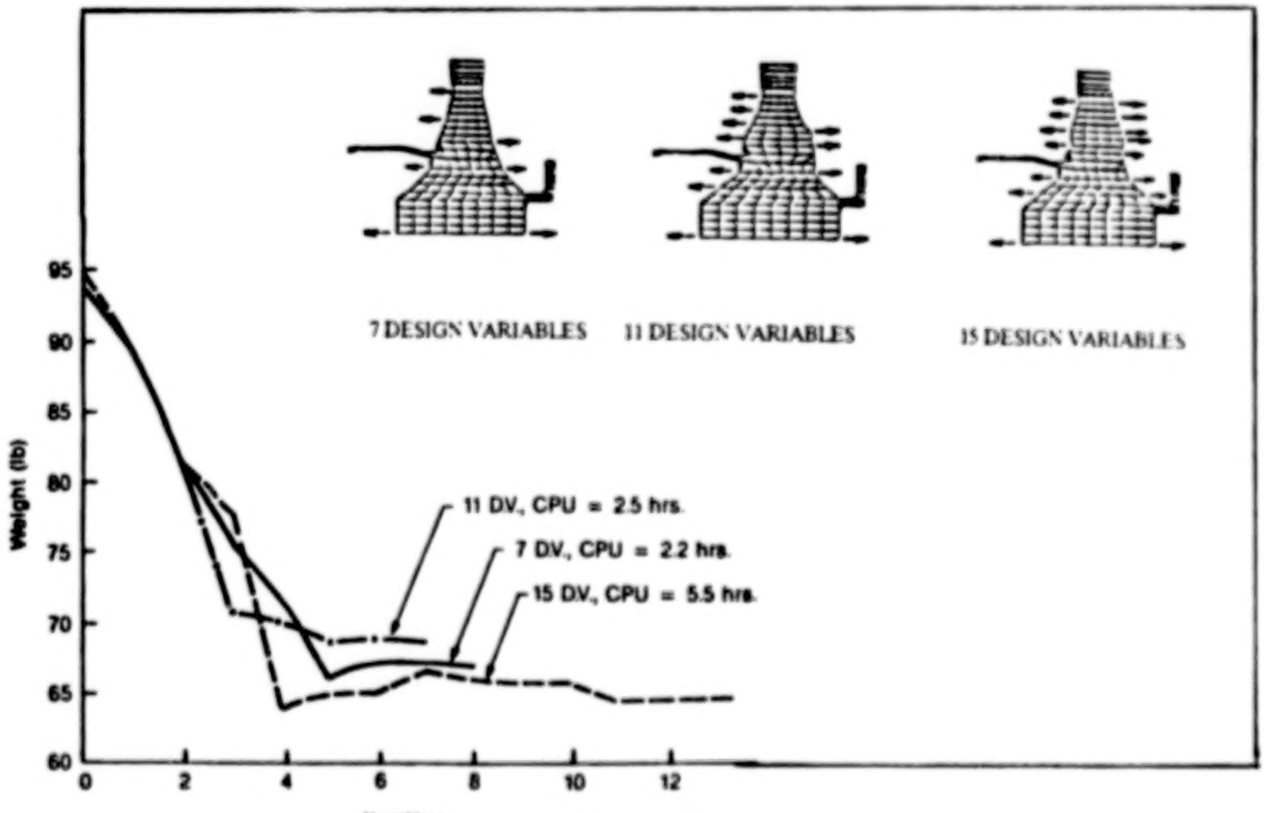

Figure 6

SHAPE OPTIMIZATION OF TURBINE BLADES

Design of turbine blades represents an ideal application of 3-D shape optimization involving multidisciplinary analysis in its real sense. The 3-D shape of a blade represents the primary design parameters, and the design objective and constraints are formulated in terms of aerodynamic performance, structural integrity requirements, aeroelastic stability margins, thermal constraints and certain other considerations as shown schematically below in Figure 7. The primary goal in almost all cases of blade design is to maximize the aerodynamic performance with secondary design objectives related to structural, aeroelastic and thermal behavior. The problem lends itself naturally into a multilevel design formulation employing decomposition models [10,11]. From a structural viewpoint, the design objective is usually to minimize the blade weight or maximize the frequency or stability margins subjected to constraints on steady state and/or vibratory stresses, frequencies and mode shapes, forced response in terms of modal participation factor, stability margins, lower and upper bounds on shape variations to maintain the aerodynamic performance, and several other considerations. In the present development, the focus so far has been placed on the structural optimization aspects of the blade design by integrating the DESIGN-OPT with in-house structural analysis and related preprocessing software packages. As one of the illustrative examples of practical interest, the shape optimization of a metallic solid blade was successfully carried out to minimize the increase in weight and maximize the range of resonance free performance so that the constraints on stresses, frequencies, forced response and shape variations are satisfied. The results obtained have clearly demonstrated the potential of numerical optimization tools for real-life complex design problems. The methodology and software system that is being developed in Reference [12] for this class of design problems is especially noteworthy.

MULTIDISCIPLINARY FORMULATION

- DESIGN PARAMETERS:
  - 3-D SHAPE, - - -
- OBJECTIVE FUNCTIONS:
  - MAXIMIZE AERO PERFORMANCE
  - MINIMIZE WEIGHT
  - MAXIMIZE FREQUENCY/STABILITY MARGINS
  - - - -
- CONSTRAINTS:
  - AERO REQUIREMENTS
  - STRESSES
  - FREQUENCY/MODE SHAPES
  - AEROELASTIC CONSTRAINTS
  - THERMAL CONSIDERATIONS
  - - - -

STRUCTURAL OPTIMIZATION

- DESIGN PARAMETERS:
  - 3-D SHAPE (MINOR VARIATIONS)
- OBJECTIVE FUNCTIONS:
  - MINIMIZE WEIGHT
  - MAXIMIZE FREQUENCY/STABILITY MARGIN
  - - - -
- CONSTRAINTS:
  - STEADY STATE/VIBRATORY STRESSES
  - FREQUENCIES/MODE SHAPES
  - FREQUENCY/STABILITY MARGINS
  - FORCED RESPONSE
  - GEOMETRY REQUIREMENTS
  - - - -

Figure 7

INTEGRATION OF AI/EXPERT SYSTEMS AND NUMERICAL OPTIMIZATION FOR ENGINEERING DESIGN

A framework has been developed for the integration of AI/expert systems concepts and numerical optimization techniques for mechanical and structural design. It is postulated that these two technologies are complementary to each other and will play a critical role in the development of a practically useful and computer-automatable methodology for engineering design. Numerical optimization methods offer a well established technology with its applicability successfully demonstrated in several fields of engineering. A large number of optimization software packages, like COPES/ADS, with a multitude of computationally efficient algorithms have also become available in recent years. These software packages have been shown to be very effective in iterative design improvements of structures and mechanical components which employ quantitative simulation models like finite element analyses. Artificial intelligence, Expert Systems (ES) and Knowledge-Based Systems (KBS), on the other hand, are based on symbolic computing and provide an extremely appealing framework for modeling non-numeric and human aspects of design. Design expertise, knowledge, experience and heuristics, etc., that are acquired through many years of strong effort and creative activities on the part of design engineers can be effectively stored in the form of knowledge data bases using AI/ES tools. In essence, the design process can be categorized in two major parts: numeric decision making and non-numeric or symbolic support systems. Numerical optimization techniques are ideal for addressing the numeric aspects, whereas the complementary symbolic or heuristics aspects are best modeled within the framework of an AI/ES concept. As illustrated below in Figure 8, both are essential ingredients of a unified, computer-automatable design methodology.

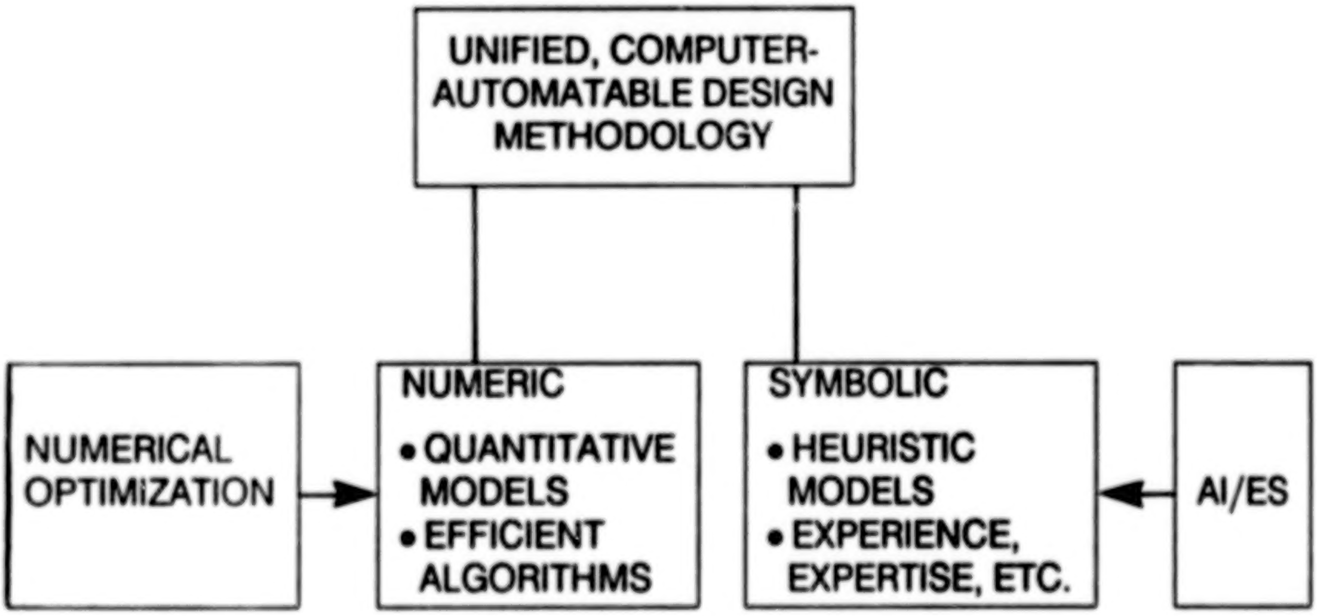

Figure 8

AN EXPERT SYSTEM ADVISOR FOR THE USAGE AND ENHANCEMENTS OF DESIGN OPTIMIZATION SOFTWARE

A pilot expert system advisor DESIGN-X is being developed for the usage and enhancements of the DESIGN-OPT software described previously. The present development environment consists of the OPS5 rule-based production system [13] COMMON LISP and the VAX machine; the system will be transferred in the near future to a SUN micro system employing KEE [14] as the ES shell. The objective of this development is to provide expert advice or assistance to the user of DESIGN-OPT at various solution stages of a given design problem: namely, problem formulation, problem solving, and solution evaluation processes (Figure 9). The problem formulation process is further subdivided into several categories such as the development of design and analysis models and the selection of numerical optimization algorithm. For example, the module related to advice on developing design models deals with issues like consistent shape description, identification of design objective and constraints, use of approximation concepts and the overall optimization strategy. Similarly, the optimization algorithm module addresses the selection of strategy, optimizer and 1-D search methods and the associated control parameters in a manner that is conceptually similar to but substantially different in details from the development reported in Reference [15]. When the optimization process terminates during execution prior to converging to the optimal solution, the problem solving assist is aimed at diagnosing the probable execution termination cause(s) and suggesting some corrective measures to the user. It can also provide on-line consultation to the user regarding changes in the optimization formulation during the software execution. The solution evaluation module is intended to assist the user in examining the quality of the final solution and at giving some expert feedback for a subsequent optimization run in case the results obtained are not satisfactory. Finally, a framework is also being developed for extending the scope of this system to another domain related to further enhancements and maintenance of the DESIGN-OPT software and is accordingly aimed at the code developers rather than the users.

PRESENT SCOPE

- PROBLEM FORMULATION
  - DESIGN MODEL
  - ANALYSIS MODEL
  - OPTIMIZATION ALGORITHM SELECTION
  - . . . .
- PROBLEM SOLVING
  - SOLUTION GUIDANCE/CONTROL
  - ERROR DIAGNOSIS/PROGNOSIS
  - . . . .
- SOLUTION EVALUATION
  - FEASIBILITY/OPTIMALITY
  - FORMULATION PHYSICS
  - 'ABNORMAL' TERMINATION
  - . . . .

EXTENSION TO A NEW DOMAIN

- SOFTWARE ENHANCEMENTS
- SOFTWARE MAINTENANCE AND SUPPORT

Figure 9

CONCLUDING REMARKS AND FUTURE DIRECTIONS

Demonstration studies which have been performed on several real-life complex design problems during the past few years have established beyond doubts that the optimization methods will play an essential role in the development of a unified design methodology of the future. From a practical viewpoint, the greatest difficulty lies in identifying various aspects of a design problem in a complete manner and in developing appropriate optimization formulations. Experience has shown that expertise-based development of optimization formulations is crucial for arriving at an acceptable optimal or final design. A straightforward mathematical programming formulation of a given design problem may lead to frustrating experience during the problem solving process if the requisite attention is not given initially at the problem definition stage. Further, it has also been observed that because of system requirements and time constraints a design engineer is most interested in finding a feasible design with a reasonable concern towards optimality of the solution. For these and many other reasons, an ES-based advisor or consultant will play an increasingly important role in practical applications of design optimization software systems. As illustrated in Figure [10] below, the present effort was initially driven by optimization applications to design problems of real-life complexity as it should be in a diversified industrial environment. Following considerable technical and software developments in subsequent years, a stage has now been reached where research, development and application efforts are being carried out in an integrated manner. Several new optimization opportunities have been identified: namely, materials processing optimization, simultaneous product and process design, and integrated conceptual and detailed design. Since most of these topics involve multidisciplinary analysis and correspondingly large-scale and complex optimization formulations, the concepts of multilevel design and decomposition model as developed by Sobieski and co-workers [10,11] will become very useful. Efforts are under way to address these new optimization applications and toward developing an integrated design methodology for industrial applications.

STRATEGY

- DRIVEN BY COMPANY APPLICATIONS

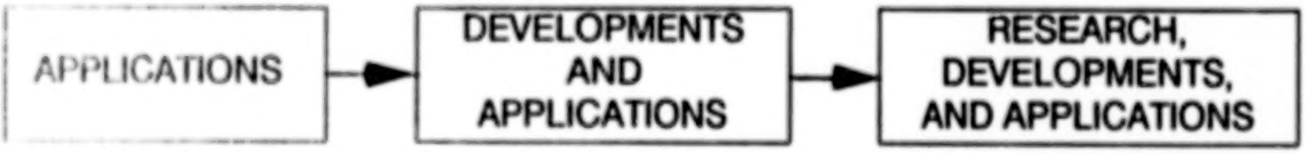

APPLICATIONS

DEVELOPMENTS AND APPLICATIONS

RESEARCH, DEVELOPMENTS, AND APPLICATIONS

Figure 10

REFERENCES

1. Vanderplaats, G. N.; and Sugimoto, H.: A General Purpose Optimization Program for Engineering Design. Int. J. Comp. Struct., Vol. 24, No. 1, 1986.
2. Kumar, V.; Lee, S. -J.; and German, M. D.: Finite Element Design Sensitivity Analysis and Its Integration with Numerical Optimization for Engineering Design. ADINA User's Conference Proceedings, Boston, MA, August 1989.
3. Botkin, M. E.: Shape Optimization of Plate and Shell Structures. AIAA J., Vol 20,. No. 3, 1988, pp. 268-273.
4. Bennett, J. E.; and Botkin, M. E.: Structural Shape Optimization with Geometric Problem Description and Adaptive Mesh Refinement. AIAA J., Vol. 23, No. 3, 1985, pp. 458-464.
5. Bennett, J. E.; and Botkin, M. E.: The Optimum Shape-Automated Structural Design. Plenum Press, New York, 1986.
6. Kumar, V.; German, M. D.; and Lee, S.-J.: A Geometry-Based 2-Dimensional Shape Optimization Methodology and a Software System with Applications. Third Int. CARS/FOF Conf. Proceed., Southfield, MI, August, 1988.
7. Shaffer, B. W.: BZANS User's Manual. GE Aircraft Engines, Lynn, MA, 1988.
8. Shephard, M. S.; and Yerry, M. A.: Approaching the Automatic Generation of Finite Element Meshes. ASME J. Comp. in Mech. Eng., 1983, pp. 49-56.
9. Graichen. C. M.; and Hathaway, A. F.: QUADTREE – A 2-D Fully Automatic Mesh Generation. GE CR&D Report, Schenectady, NY, 1988.
10. Sobieszczanski-Sobieski, Jaroslaw: A Linear Decomposition Method for Large Optimization Problems – Blueprint for Development. NASA TM-83248, February 1982.
11. Sobieszczanski-Sobieski, J.; Barthelemy, J. M.; and Giles, G.: Aerospace Engineering Design by Systematic Decomposition and Multilevel Optimization. ICAS-4.7.3.
12. Brown, K. W.; Hirschbein, M. S.; and Chamis, C. C.: Finite Element Engine Blade Structural Optimization. AIAA Paper No. 85-0645.
13. Brownston, L.; Farrell, R.; Kant, E.; and Martin, N.: Programming Expert Systems in OPS5 – An Introduction to Rule-Based Programming. Addison-Wesley, Reading, MA, 1986.
14. Intellicorp KEE™ Software Development System User's Manual. Intellicorp, Mountainview, CA, 1986.
15. Rogers, J. L.; and Barthelemy, J. M.: An Expert System for Choosing the Best Combination of Options in a General Purpose Program – Automated Design Synthesis. Presented at the 1985 ASME International Computers in Engineering Conference and Exhibition, Boston, MA, August 4-8, 1985.

OPTIMIZATION BY DECOMPOSITION: A STEP FROM HIERARCHIC TO NON-HIERARCHIC SYSTEMS

Jaroslaw Sobieszczanski-Sobieski
NASA Langley Research Center
Hampton, Virginia

INTRODUCTION AND PRESENTATION PLAN

The purpose of this presentation is to update the status report on optimization by decomposition research under way at NASA LaRC given at the predecessor meeting of this symposium in 1984. The update is focused on three developments: completion of a large scale demonstration of hierarchic decomposition applied to a transport aircraft, determination that the top-down decomposition is limited to hierarchic systems, and a proposed new algorithm for optimization by decomposition applicable to non-hierarchic systems. (Fig. 1.)

- **HIERARCHIC COMPOSITION APPLIED TO TRANSPORT AIRCRAFT.**
- **LIMITATIONS OF THE APPROACH.**
- **NON-HIERARCHIC SYSTEMS: ATTRIBUTES A SOLUTION SHOULD HAVE.**
- **A NEW ALGORITHM PROPOSED AS A SOLUTION.**
- **CONCLUSIONS.**

Figure 1

OPTIMIZATION BY LINEAR DECOMPOSITION: ITS USEFULNESS AND LIMITATIONS

Implementation and application experience with optimization by linear decomposition has been reported several times since introduction of the concept in ref.1. The concept applies to systems amenable to a hierarchic representation as shown in Fig.2a. In such applications, the general flow of information takes the analysis results from a parent to the daughters, and the optimization results and their sensitivity to the parameters received as parent output are transmitted back to the parent as seen in Fig.2b. This approach was successful in formulating structural optimization by substructuring in ref.2, and in solving a very large multidisciplinary optimization problem related to a transport aircraft design reported in ref.3 and summarized in the next three figures.

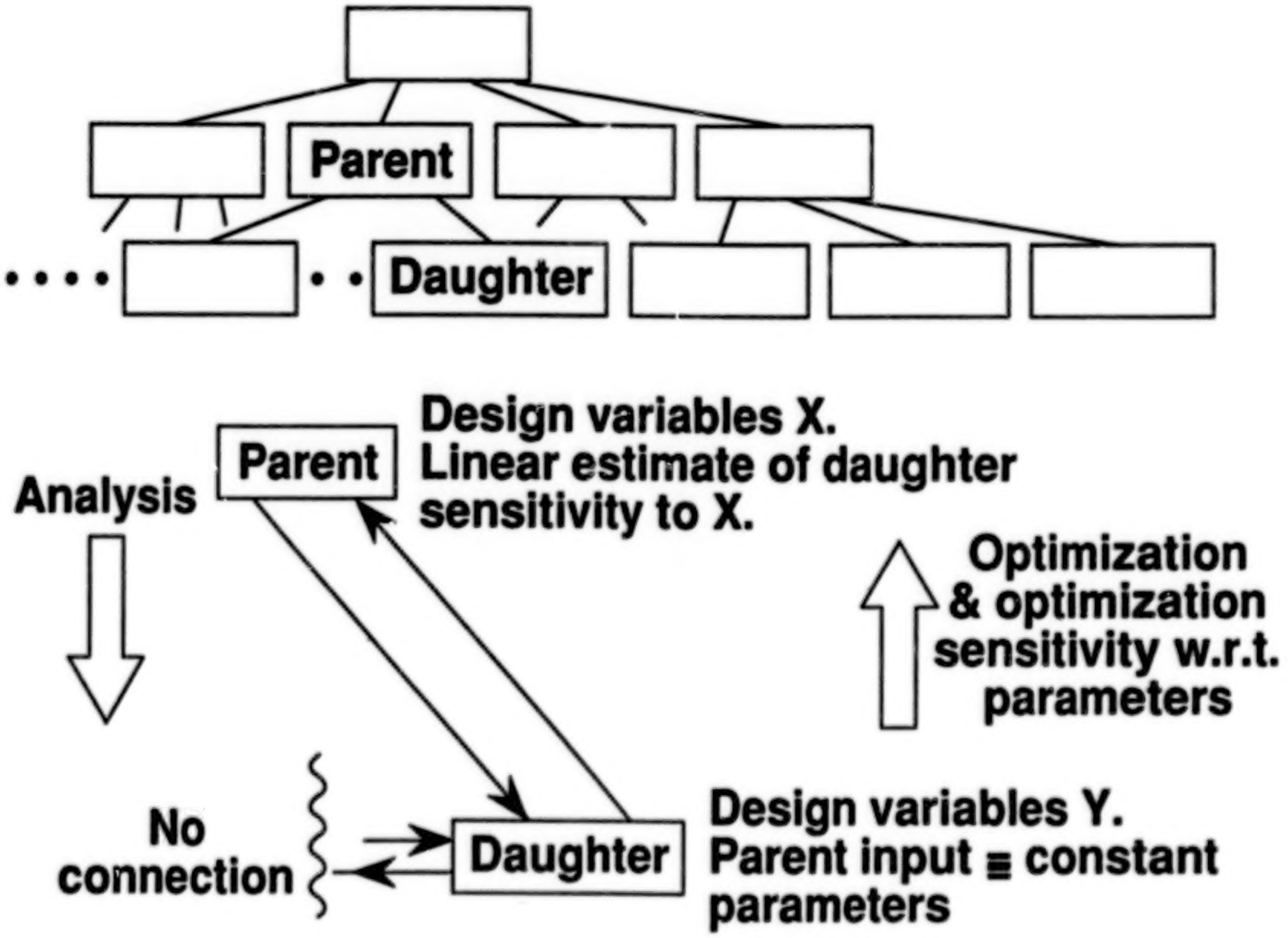
Parent
Daughter
Parent
Design variables X.
Linear estimate of daughter sensitivity to X.
Analysis
Optimization & optimization sensitivity w.r.t. parameters
No connection
Daughter
Design variables Y.
Parent input ≡ constant parameters

Figure 2

A TRANSPORT AIRCRAFT CONFIGURATION

A version of the L1011 was used as a test case in ref.3. The configuration and its finite-element model representation are shown in Fig.3. The objective function was the block fuel consumption for a particular mission profile, the constraints were drawn from structures, and aircraft performance, and the design variables were cross-sectional dimensions of stiffened wing covers, stiffness-equivalent wing cover membrane element thicknesses, and the airfoil depth-to-chord ratio at the three decomposition levels shown in the next figure. There were more than 1000 design variables, constraints, and elastic degrees of freedom in the finite-element analysis, so the problem was quite large as far as nonlinear programing optimization is concerned.

- **Typical transport (L1011) and its finite-element model**

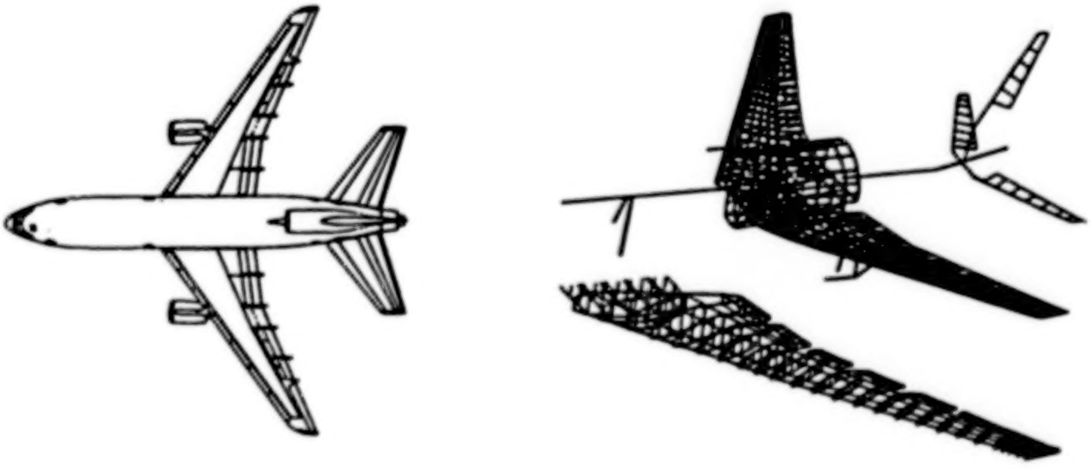

- **Objective: minimize fuel used for a given mission**
- **Large, multidisciplinary problem**
    - **1950 constraints for structures, aerodynamics, and performance**
    - **1303 design variables from detailed stringer dimensions to airfoil depth**

Figure 3

TRANSPORT AIRCRAFT LINEAR DECOMPOSITION

The objective function and system performance are represented in box 1 on the top of the hierarchy shown in Fig.4 that also displays the type of information transmitted between the levels. The mid-level consists of the wing box represented by an assembly of rods and membrane elements, the latter having orthotropic stiffnesses to account for their stringer-sheet construction. The stringer-sheet detailed dimensions were recognized as design variables at the lowest level where each wing cover panel was considered as a separate optimization problem.

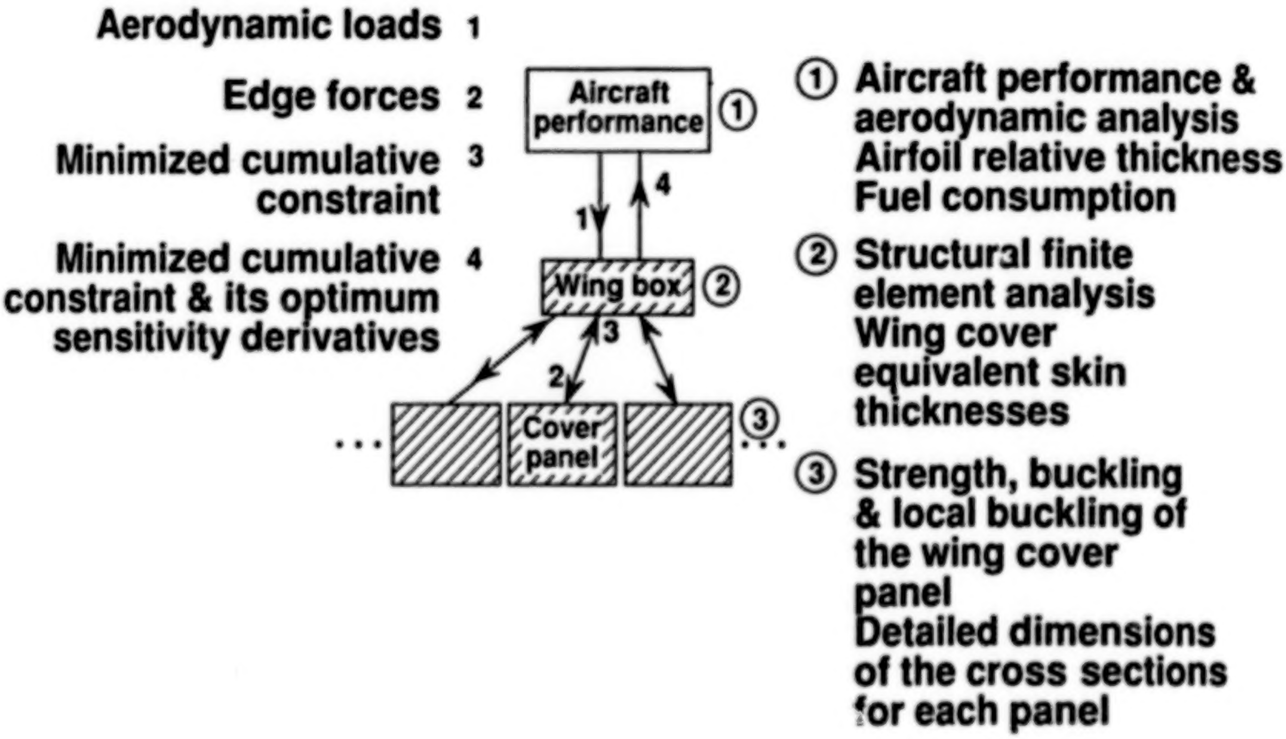
Aerodynamic loads 1
Edge forces 2
Minimized cumulative constraint 3
Minimized cumulative constraint & its optimum sensitivity derivatives 4
Aircraft performance ①
1
4
Wing box ②
3
2
Cover panel
③
① Aircraft performance & aerodynamic analysis
Airfoil relative thickness
Fuel consumption
② Structural finite element analysis
Wing cover equivalent skin thicknesses
③ Strength, buckling & local buckling of the wing cover panel
Detailed dimensions of the cross sections for each panel

Figure 4

SAMPLE OF TRANSPORT AIRCRAFT RESULTS

Test optimizations were performed from design points deliberately initialized away from the existing L1011 design in both feasible and infeasible directions. Two typical results shown in Fig.5 indicate convergence at a quite fast rate to the same results very close to the existing design. Since the subject design was well established and previously optimized by other means, the convergence to the existing design constituted a positive test of the method which demonstrated that it is possible to link mathematically a design detail at the bottom of the hierarchy to the system performance at the top in a large problem.

Several other examples of multilevel optimization are reviewed in ref.4 of this symposium.

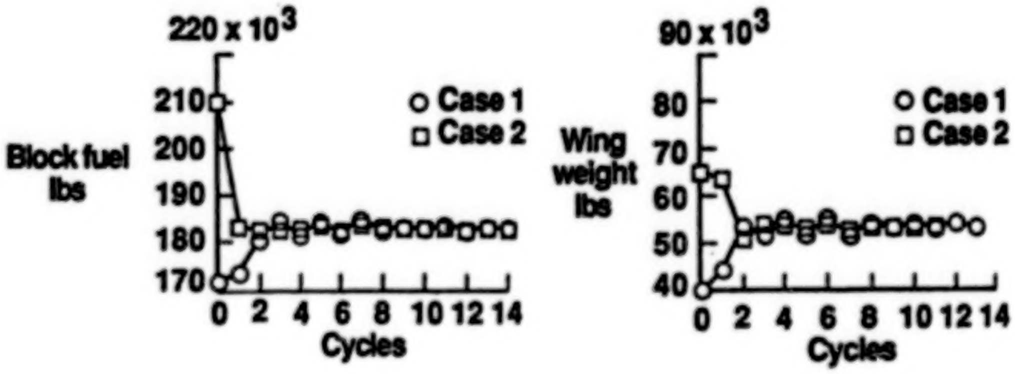

- **Fast convergence from initially infeasible and feasible designs**
- **Compared well with actual L1011 data**
- **Decomposition made it possible:**
    - **To handle more than 1000 design variables in an NLP-based optimization**
    - **To link mathematically the design detail to system performance**

Figure 5

MANY SYSTEMS ARE NOT HIERARCHIC IN NATURE

An example of a system not amenable to a hierarchic decomposition just discussed is a network system whose generic example is shown in Fig.6a. Each box labeled CA k for Contributing Analysis represents an analysis module contributing to the entire system analysis. A CA may be associated with a particular aspect of the system behavior or may represent a physical subsystem. In either case, it is treated as a black box converting input into output. The input consists of outputs from the other CA's, and of the design variables and constants prescribed externally to the system.

A specific example for a system like this is given in Fig.6b showing a schematic of an actively controlled, flexible wing described in ref.5. Although one would tend to place the PERFORMANCE at the system level, the presence of the lateral link between AERODYNAMICS and STRUCTURES and the two-way flow of information along other links preclude decomposition of this system into a top-down, hierarchic structure because one cannot limit the inputs received by a daughter to those from one parent only. Conversely, it is no longer possible to have a unique channel of influence between a daughter and the corresponding parent because part of the daughter influence may be channeled through another daughter.

Hence, another way of decomposition must be found for network systems and this inspires a non-hierarchic approach. The remainder of this paper presents a new algorithm derived from that approach. The algorithm addresses large design problems in which each CA may, typically, be tended by a group of engineers within a framework of design organization. In that setting, it is recognized that organizational and human cooperation issues are as important as the mathematical computational aspects of the problem.

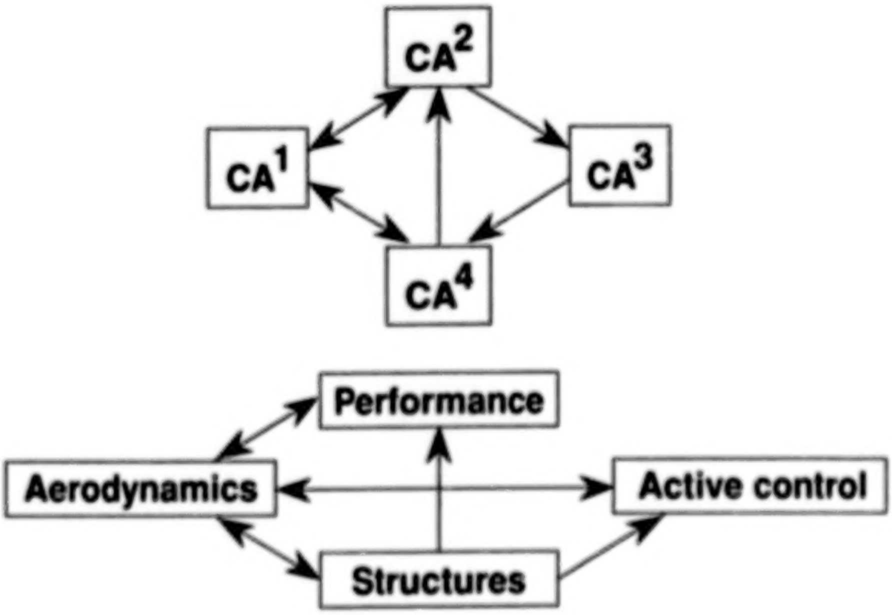

Figure 6

SYSTEM OPTIMIZATION PROBLEM DEFINITION

An optimization problem for the system presented in Fig.6 is defined in Fig.7. It calls for finding a set of design variables X that minimizes an objective function F(Y,X,P) subject to constraints g(Y,X,P). The F and the g functions are assumed to be computed within the appropriate CA's from the behavior variables Y which are the unknowns in each CA, e.g, displacements in a stiffness-based finite-element analysis. The constants are denoted by P.

If the system optimization were to be solved as a single problem, the procedure schematic might look like the one at the bottom of Fig.7.

$$\min_{X} F\,(Y, X, P), \text{ where } Y = f(X, P) \qquad (1)$$

$$\text{subject to } g_j\ (Y, X, P) \leq 0;\ j = 1, \text{NCON} \qquad (2)$$

$$g_j = \frac{\text{Demand}}{\text{Capacity}} - 1$$

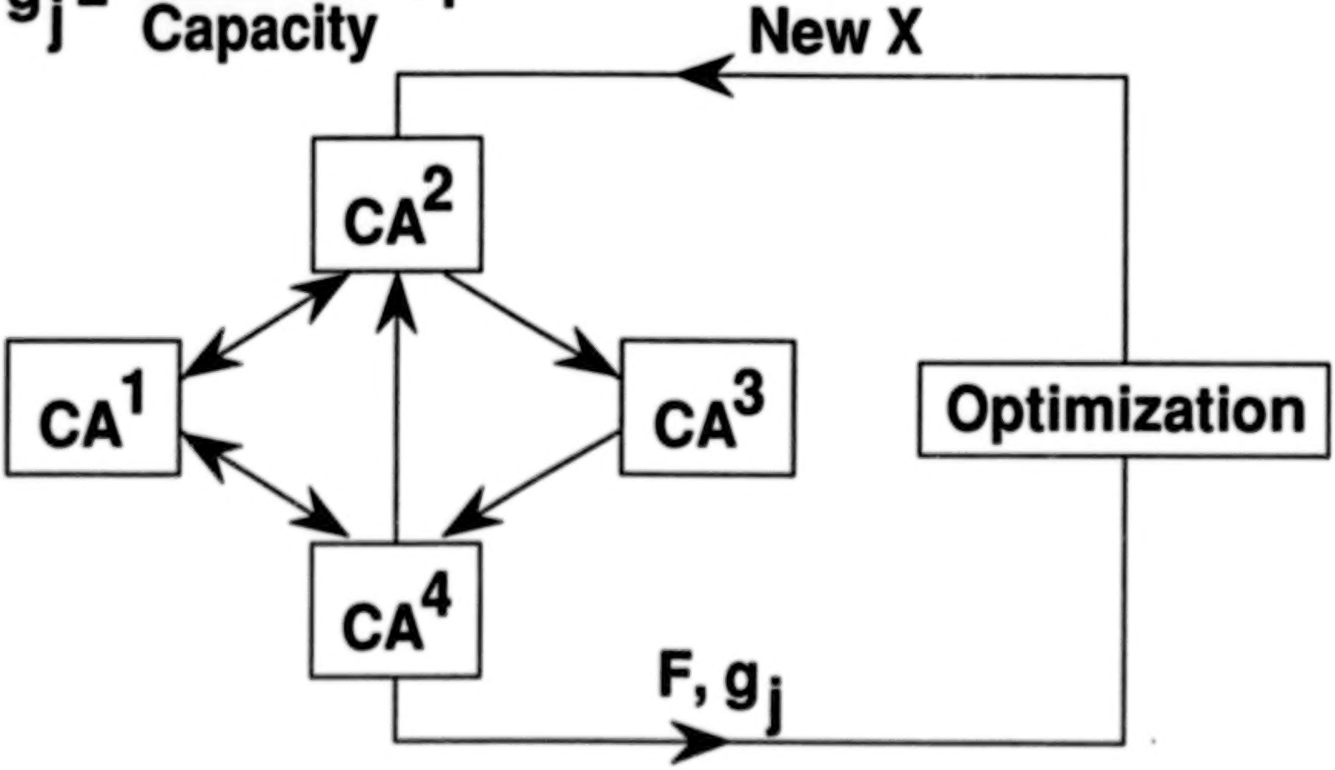

Figure 7

NEED FOR A NEW PROCEDURE FOR NETWORK SYSTEM OPTIMIZATION

For a large application, the single optimization problem approach is obviously impractical. It needs to be replaced by a procedure specifically tailored to meet the requirements of an engineering design organization it is intended for. Experience with computational support needed in industrial design processes suggests that at least the following major requirements be met. (Fig. 8.)

- **PROCEDURE SHOULD DEFINE A SYSTEM FEASIBLE IN ALL ITS PARTS AND ASPECTS, IMPROVED IN ITS PERFORMANCE OVER THE INITIAL STATE.**
- **SYSTEM ANALYSIS, SENSITIVITY ANALYSIS, AND OPTIMIZATION SHOULD BE MODULAR AND DIVIDED TO THE GREATEST EXTENT POSSIBLE INTO CLEARLY SEPARATED TASKS ASSIGNED TO SPECIALTY GROUPS THAT MAKE UP A DESIGN ORGANIZATION WHICH MAY BE GEOGRAPHICALLY DISPERSED.**
- **SYSTEM ANALYSIS REPETITIONS SHOULD BE AS FEW AS POSSIBLE.**
- **EACH GROUP SHOULD BE QUANTITATIVELY INFORMED ABOUT THE INFLUENCE THEIR DESIGN DECISIONS HAVE ON THE OTHER GROUPS' TASKS AND ON THE SYSTEM OBJECTIVES WHILE RETAINING RESPONSIBILITY FOR ITS RESULTS.**
- **SPECIALIZED METHODS IN ANALYSIS, SENSITIVITY ANALYSIS, AND OPTIMIZATION, AND USE OF OTHER SOURCES OF INFORMATION IN LIEU OF CALCULATIONS, SHOULD BE ADMISSIBLE IN EACH GROUP'S TASK.**
- **GROUPS SHOULD BE ABLE TO DO THEIR WORK CONCURRENTLY TO THE GREATEST EXTENT POSSIBLE.**
- **HUMAN JUDGMENT AND INTERVENTION SHOULD BE ACCOMMODATED AND SUPPORTED.**
- **PROCEDURE SHOULD BE OPEN-ENDED REGARDING THE SIZE OF THE ENTIRE TASK AND ADJUSTABLE TO THE DEPTH OF DETAIL CONSISTENT WITH THE DESIGN STAGE.**

Figure 8

NEW ALGORITHM DERIVES FROM SUBSPACE OPTIMIZATION METHOD

It should be possible to meet the above requirements by following an approach suggested by the well-known method of subspace optimizations (SSO). The method changes a subset of the design variable vector at a time, while holding the remainder of the vector constant. The univariate search is its ultimate implementation. However, the conventional subspace optimization technique requires repetition of the full system analysis for each subspace that may be cost-prohibitive in large systems. Also, it does not provide for concurrent execution of the separate subspace optimizations - a feature regarded as essential for applications in engineering design process. Therefore, the technique must be modified to reduce computational cost and to allow for concurrent optimizations.

The algorithm implementing the above modifications will be presented as a "walk through", with a rationale for each step given as the steps unfold, building toward a complete flowchart. (Fig. 9.)

- **CONVENTIONAL SUBSPACE OPTIMIZATION METHOD MANIPULATES ONE SUBSET OF DESIGN VARIABLES AT A TIME, HOLDING THE OTHER SUBSETS CONSTANT.**
- **UNIVARIATE SEARCH IS THE ULTIMATE OF THE ABOVE.**
- **IN THE PROPOSED ALGORITHM, SUBSPACE OPTIMIZATION METHOD IS MODIFIED TO ELIMINATE THE NEED FOR FULL ANALYSIS FOR EACH SUBSPACE, TO ALLOW CONCURRENT OPTIMIZATIONS IN SUBSPACES, AND TO MEET OTHER SPECIFIED REQUIREMENTS.**

Figure 9

SYSTEM ANALYSIS

The system optimization procedure begins with a system analysis (SA) presented in Fig.10. The superscripts identify the CA's and the corresponding partitions of Y and X. In the most general case, the system may be fully coupled, so that each CA sends its output Y to input in every other CA. However, in most practical cases, a particular CA transmits some of its Y elements to some of the other CA's. If there are two-way couplings and if the CA's involved are non-linear, the SA requires iterations for its solution. A typical example is an iteration between nonlinear aerodynamic and structural analyses to converge the aerodynamic loads and structural displacements of an elastic wing.

In most applications, the CA's are simply computer programs, but they may also represent experiments, graphs, look-up tables, or even guesstimates, in other words, a CA may be any source of information producing output in response to an input presented to it.

$$
\begin{array}{l}
CA^1((X^1, Y^2, Y^3, \ldots Y^k), Y^1) \\
CA^2((X^2, Y^1, Y^3, \ldots Y^k), Y^2) \\
CA^3((X^3, Y^1, Y^2, \ldots Y^k_{\ldots}), Y^3) \\
\vdots \\
CA^k((X^k, Y^1, Y^2, Y^3_{\ldots}), Y^k) \\
\vdots
\end{array}
$$

Figure 10

SYSTEM SENSITIVITY ANALYSIS

Following the SA, we perform a system sensitivity analysis (SSA) to compute the system sensitivity derivatives (SSD). These derivatives are defined in Fig.11, Eq.1. Each derivative is a measure of the influence of a particular design variable X on a particular behavior variable Y. It is crucially important to have these influences computed to fully account for the couplings among the CA's. This may be accomplished per ref.6, by computing for each CA the partial sensitivity derivatives of its output w.r.t. its input, the input including the Y's received from the other CA's and those X variables which are directly input into that CA. Any sensitivity analysis techniques appropriate for the nature of a particular CA may be used in this operation, including finite difference procedures, although analytical and semi-analytical methods are preferred for their efficiency and accuracy. It is important for the organization of this phase of the sensitivity analysis that the partial sensitivity derivatives may be computed concurrently for all the CA's.

The partial derivatives enter the matrix of coefficients and the right hand side vectors of a set of simultaneous, linear, algebraic equations termed Global Sensitivity Equations (GSE) in ref.6 and shown in Fig.11, Eq.2. Solution of these equations yields a vector of the system sensitivity derivatives for each design variable X represented on the right hand side. Having the derivatives of Y with respect to X available, enables one to also obtain the derivatives of the F and g functions with respect to X by simple postprocessing. These derivatives measure the first order influence of each design variable on the objective function and all constraints in the system, even though the influences may be indirect. As we will see later, this capability plays a key role in decomposing the system for optimization purposes while retaining a degree of coupling.

$$\frac{dY_i^p}{dX_j^k} \; ; \; i = 1, NY^p; \; p = 1, NSS; \; k = 1, NX^k \qquad (1)$$

$$\begin{bmatrix} I & \left[-\frac{\partial Y^p}{\partial Y^k}\right] \\ \left[-\frac{\partial Y^k}{\partial Y^p}\right] & I \end{bmatrix} \begin{Bmatrix} \frac{dY^p}{dX_i^2} \\ \frac{dY^k}{dX_i^2} \end{Bmatrix} = \begin{Bmatrix} \frac{\partial Y^p}{\partial X_i^2} \\ \frac{\partial Y^k}{\partial X_i^2} \end{Bmatrix} \ldots \qquad (2)$$

Figure 11

ORGANIZATION OF SEPARATE SUBSPACE OPTIMIZATIONS (SSO)

For optimization purposes it is necessary to partition the vector X into subsets to be used in the separate optimizations replacing the large, original problem. The intent is to have each separate optimization involve only one CA. The allocation of the X partitions (subsets) to the corresponding separate optimization problems must be unique, and may be accomplished by heuristics augmented with the sensitivity information carried by the system sensitivity derivatives. The derivatives may be used to rank the variables X in order of the degree of their influence on the constraints and contributions to the objective function computed in each CA. This information, used judiciously, should guide the allocation decisions. For instance, under that approach we might find an X variable representing the cross-sectional area of a wing spar cap as the most influential on the wing strength constraints, hence that X would be allocated to the structural optimization. On the other hand, the X governing the wing span might be found to exert a strong influence on both the wing strength and aerodynamic constraints and so, in keeping with tradition, it might be judgmentally assigned to the aerodynamic optimization. (Fig. 12.)

- **ONE CA**
- **SUBSET OF X**
- **SINGLE CUMULATIVE CONSTRAINT REPRESENTING ALL CONSTRAINTS DERIVED FROM CA.**
- **CARRIED OUT BY A GROUP OF SPECIALISTS, E.G., WING PLANFORM OPTIMIZATION - AERODYNAMICS GROUP.**

Figure 12

CUMULATIVE CONSTRAINT

The cumulative constraint represents by a single number all the g's computed from the CA associated with the SSO. The cumulative constraint is formulated as a Kreisselmeier-Steinhauser function (KS function), Eq.1, per ref.7. The derivatives of the KS function with respect to a g are obtained analytically and combined in a chain differentiation with the derivatives of the g with respect to X to yield the derivatives of the cumulative constraint with respect to X, Eq.2.

Knowing the system solution, its sensitivity to design variables, and having organized the design variables and CA's in separate optimization problems, we may now begin the optimizations. (Fig. 13.)

- **Kreisselmeier-Steinhauser function:**

$$KS = \frac{1}{\rho} \ln\left(\sum_j e^{\rho g_j}\right) \qquad (1)$$

$$\frac{\partial KS}{\partial x_i^k} = \left(\sum_j e^{\rho g_j}\right)^{-1} \left(\sum_j \left(e^{\rho g_j} \frac{\partial g_j}{\partial x_i^k}\right)\right) \qquad (2)$$

ρ = user controlled factor

Figure 13

SUBSPACE OPTIMIZATION (SSO)

The subspace optimizations are temporarily decoupled and executed concurrently - their coupling will be restored in the coordination problem. Here, we focus on one particular, k-th, SSO.

In the SSO, we want to reduce violation of the cumulative constraint of the k-th SSO at the least penalty of the system objective function increase, or, if the cumulative constraint is already satisfied, we want to reduce the system objective function as much as possible without violating that constraint. Remembering that we operate on a part of a system, we want to do the above while contributing to the reductions of the violated cumulative constraints in the other SSO's and without causing violation of the satisfied cumulative constraints in the other SSO's.

Recognizing that the cumulative constraint of the k-th SSO is going to get a similar consideration in the other, concurrently executed SSO's, we need to aim at reducing the violated cumulative constraint by only a fraction, counting on the other SSO's to reduce the remainder of the violation. By the same token, we may even allow the cumulative constraint to remain violated, provided that violation is offset by influence of the other SSO's.

Formally, all the above is expressed by a formulation shown in Fig.14. When the SSO's are concluded, the results are new X's, new values of the C's, and a new value of F.

min $F(X^k)$ subject to (1)

$$C^p \leq C^{po} s^p \left(1 - r_k^p\right) + \left(1 - s^p\right) t_k^p ; \; p = 1, NSS \qquad (2)$$

$$X_L^k \leq X^k \leq X_U^k \qquad (3)$$

- **If CA^k contributes to F indirectly, then**

$$F = F^o + \sum_i \left(dF_i/dX_i^k\right) \Delta X_i^k \qquad (4)$$

- **C^k from CA^k using $Y = Y^o + \sum_i \left(dY/dX_i^k\right) \Delta X^k$ for coupling inputs** (5)
- **C^p , $p \neq k$, from $C^p = C^{po} + \sum_i \left(dC^p/dX_i^k\right) \Delta X^k$** (6)
- **r_k^p, t_k^p are constants; variables in coordination problem**
- **s^p is a "switch"coefficient, 0 or 1**

Figure 14

COMMENTS ON SUBSPACE OPTIMIZATION FORMULATION - COEFFICIENTS r

Owing to the system sensitivity derivatives, we are in a position to account for the influence we exert on the objective function of the system while performing an SSO, even if that SSO has no direct influence on that function. By the same means, we are able to consider the effect of the decisions taken in one SSO on the constraints in the other SSO's. This cross-influence is represented by linear extrapolations and is the key feature of the proposed approach. It enables all participants in design of a complex system to work in concert toward improving the design of the entire system while remaining on the familiar grounds of their own specialty domains.

In a system, the p-th violated cumulative constraint may be satisfied not only by the X-setting decisions taken in the p-th SSO but also by such decisions taken in the other SSO's owing to the couplings among the CA's. For instance, overstress in a wing spar may be reduced partially by spar cap resizing (structural SSO) and partially by decreasing the wing aspect ratio (aerodynamic configuration SSO). To account for this, we introduce coefficients r to represent the "responsibility" assigned to the k-th SSO for reducing the violation of the cumulative constraint of the p-th SSO. For this purposes, the violated constraint value normalized to unity is divided into fractions r^p_k . The superscript identifies the constraint and the subscript points to the SSO responsible for its partial reduction. Of course, all the r^p_k fractions must add up to unity when summed over k for a given p - that requirement is built into the coordination problem (to be defined later) in which these coefficients appear as variables. For each cumulative constraint there are NSS coefficients r^p_k , so for NSS cumulative constraints we have a total of NSS^2 such coefficients. It is logical to use the sensitivity information to initialize the r coefficients making them proportional to the degree of influence exerted by the k-th SSO on the p-th cumulative constraint. That initialization is discussed in the Appendix. (Fig. 15.)

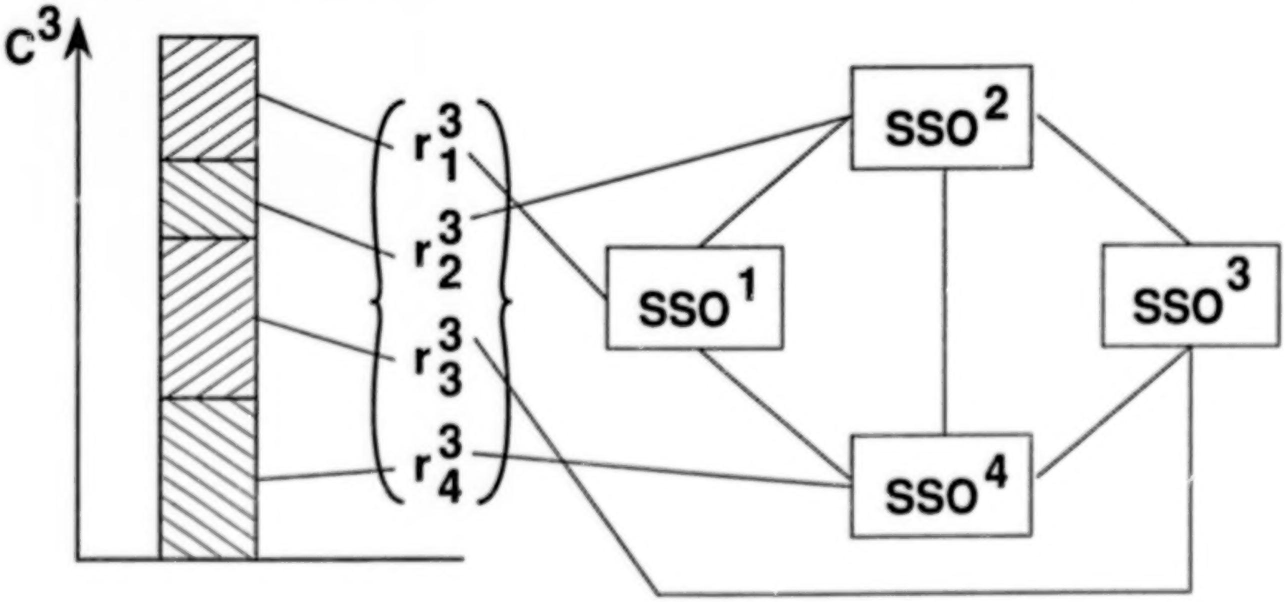

Figure 15

COMMENTS ON SUBSPACE OPTIMIZATION FORMULATION - COEFFICIENTS t.

Extending this reasoning to the case of the p-th cumulative constraint being critical for the given X, we should account for the possibility of further reducing the objective function by letting that constraint become somewhat violated in the p-th SSO, provided that the violation will be offset by oversatisfaction of that constraint in the k-th SSO. For example, should we find the wing spar stress constraint at zero (critical) in the structural SSO, we may let the stress rise above the allowable value thus reducing the spar cross-sectional area and weight, if we instruct the aerodynamic SSO to offset that violation by oversatisfying the same constraint by reducing the wing aspect ratio at the price of the induced drag increase. If the wing spar weight reduction more than offsets the induced drag increase with respect to a measure of the aircraft performance, then this is a positive trade-off the procedure ought to be able to recognize. To account for that type of trade-offs, we introduce the coefficients $t^p{}_k$ whose number equals NSS^2. For the p-th cumulative constraint, the sum of these coefficients over k must be zero, to keep the constraint in the critical, but not violated, status. This condition is enforced in the coordination problem where the coefficients t appear as variables. (Fig. 16.)

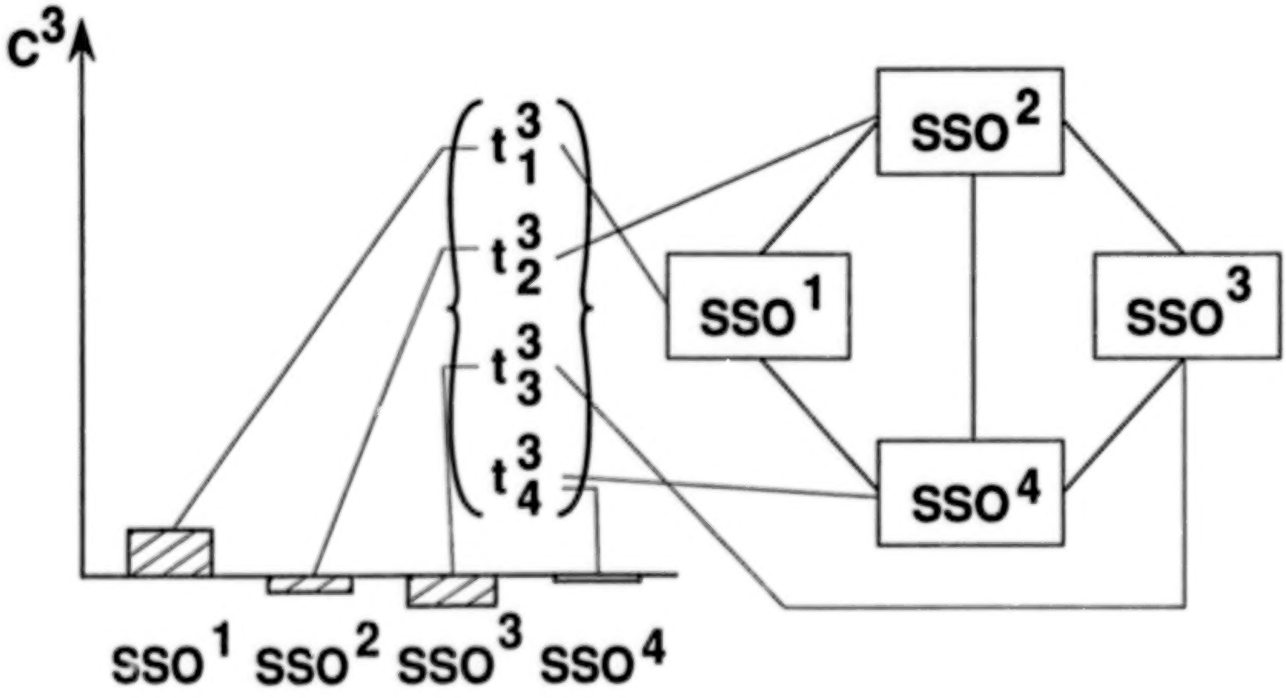

Figure 16

COMMENTS ON SUBSPACE OPTIMIZATION FORMULATION - COEFFICIENTS s

Coefficient s^p is a switch. It is set to 1 if the corresponding C^p is violated at the outset of the system optimization procedure and stays at 1 until the C^p is driven to a critical status (zero value). Then, the coefficient s^p is reset to 0 and stays at 0 until the system optimization procedure terminates. Thus, the s coefficient enables the term containing $r^p{}_k$ and disables the term containing $t^p{}_k$ while the C^p violation is in the process of being reduced and vice versa after that violation has been eliminated. There is one coefficient s^p per C^p for the total of NSS coefficients s.

In summary, Eq.2 in Fig.14 works as follows. When the p-th cumulative constraint is found violated, its value C^{po} is a positive number to be driven toward zero. This is done by dividing that number into fractions proportional to the r coefficients and by reducing each fraction toward zero independently in each separate SSO. The coefficients t set to zero and turned off by the s-switch do not interfere with that process. When the p-th cumulative constraint is reduced to zero (attains critical status), it is allowed to be violated in some SSO's and oversatisfied in other SSO's, provided that the violations and oversatisfactions are beneficial to the objective function and that they balance to zero so that the C^p critical status is preserved. This phase is controlled by the t coefficients while the r coefficients are turned off by the s-switch. (Fig. 17.)

- **$s^p = 1$, if**

  $C^p > 0$ · at the outset of the System Optimization Procedure

  · and ·

  C^p was never reduced to ≤ 0 since then

  · and ·

  $C^p > 0$ in the last SA

- **Otherwise, $s^p = 0$**

Figure 17

COMMENTS ON SUBSPACE OPTIMIZATIONS - CA AND EXTRAPOLATIONS

In the k-th SSO, the cumulative constraint C^k is evaluated from the g values obtained from the CA^k associated with that SSO while explicit form extrapolations are used to evaluate the other C^p's where p is not equal to k. That affords flexibility in choosing the ways each SSO is to be carried out - no uniformity is required at all. Optimization methods specialized for a particular discipline or a physical subsystem may be used, e.g., the optimality criteria for structural optimization. By the same token, a variety of techniques are admissible, such as the use of approximate, gradient-based analyses in the optimization loop, reciprocal variable replacements, etc. Instead of the direct extrapolation of C, one may also improve accuracy by first extrapolating the g's using their derivatives w.r.t. X and, then, substitute the new g's into the KS function to obtain a new C.

Judgmental intervention by the engineers into the optimization process is entirely acceptable too.

Regardless of the procedure, the SSO involves a CA representing the high accuracy knowledge and a set of extrapolations representing the approximate, first-order accuracy knowledge about the cross-influences on the other SSO's and on the system objective. Using an aerodynamic wing planform optimization as an example of an SSO, a group of aerodynamicists would proceed with their customary task while agreeing to include as an augmentation of that task a package of simple extrapolation formulas to inform them about the effects of their decisions on strength, control, performance, etc. (Fig. 18.)

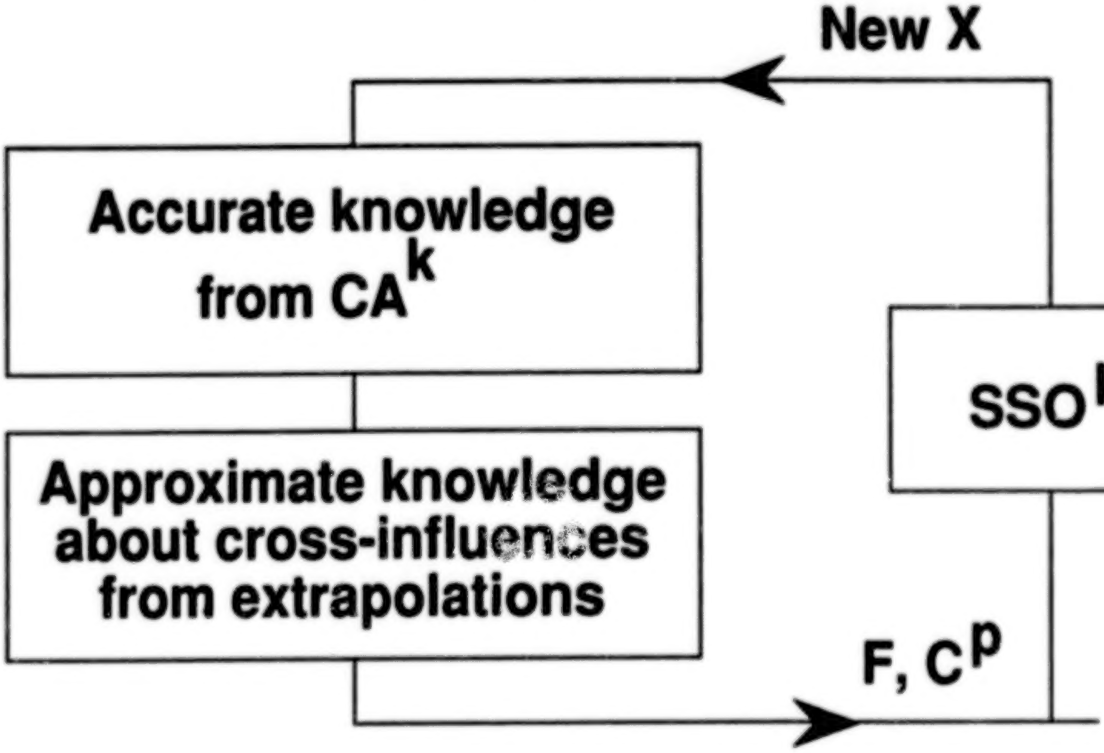
New X
Accurate knowledge from CA^k
SSO^k
Approximate knowledge about cross-influences from extrapolations
F, C^p

Figure 18

OPTIMUM SENSITIVITY ANALYSES (OSA)

The SSO's were executed with the constant coefficients r and t with unique subsets of X but with a common system objective function F. Consequently, the constrained minimum of F so obtained is a function of the constants r and t, and its derivatives with respect to r and t exist in the sense of refs. 8 and 9. Per ref.9, the derivatives are computed from the expressions shown below using the gradient information for the F and C functions. The gradient information with respect to the X's is available at the conclusion of the SSO's, provided that a gradient-guided optimizer was used in these optimizations. The gradients with respect to the r's and t's are trivial to obtain owing to the simplicity of Eq.2 in Fig.14.

Once the derivatives of F are available, the F function may be approximated in terms of r's and t's by means of a linear extrapolation shown in Fig.19. The extrapolation will be useful in formulation of a coordination problem.

- **Shorthand: $z \equiv r$ or t**
- **Lagrange multipliers λ from**

$$\lambda = -\left[\nabla_k C^T \nabla_k C\right]^{-1} \nabla_k C^T \nabla_k F \qquad (1)$$

where $\nabla_k = \frac{d(\ )}{dX^k}$; $C = \{C^p\}$;

- **Optimum sensitivity derivative of F simplifies to**

$$\frac{dF}{dz_i} = \lambda \frac{dC}{dz_i} \qquad (2)$$

because $\frac{\partial F}{\partial z_i} \equiv 0 \qquad (3)$

- **Extrapolation of F w.r.t. the z's**

$$F = F^{\circ} + \sum_i \frac{dF}{dz_i} \cdot \Delta z_i \qquad \ldots (4)$$

Figure 19

COORDINATION OPTIMIZATION PROBLEM (COP)

In the coordination problem we seek new values of the coefficients r and t, adjusted so as to further reduce the objective F. In view of the linear extrapolation of F introduced in the previous figure, the problem is a simple case of linearprogramming shown below. The constraints in Eq.2 represent the division of responsibility for the constraint violation reduction allocated to various SSO's, and the constraints in Eq.3 pertain to the constraint violation-oversatisfaction trades among the SSO's. Since the t's may be positive and negative, they would have to be expressed as differences of positive variables, if a standard form of linear programing were used to solve the problem. The move limits in Eq.5 and 6 may be needed due to nonlinearities of the original problem.

Execution of the COP follows every round of the SSO's in an iterative fashion. In the first COP execution, the r's may be initialized as suggested in the Appendix and the t's are initialized to zero. In every subsequent execution, the r's and t's are initialized to the terminal values from the previous COP execution. Judgmental intervention into the setting of the new r's and t's is quite acceptable, indeed, anticipated as a result of a teamwork among the groups responsible for the individual SSO's.

The result of the COP execution is a new set of the r's and t's to be used in the next SSO's. The adjustment of the r's and t's to the new values amounts to a reassignment of the responsibility for eliminating the constraint violations among the SSO's and to issuing a new set of instructions about trading the constraint violations-oversatisfactions among these SSO's. The expected result is a reduced value of F in the next round of SSO's. (Fig. 20.)

$$\min_{r,\,t} F\left(r_k^p, t_k^p\right)$$

$$F = F^\circ + \sum_p \sum_k \frac{dF}{dr_k} \Delta r_k^p \; \sum_p \sum_k \frac{dF}{dt_k} \Delta t_k^p ; \text{ p and k = 1, NSS} \qquad (1)$$

subject to:

$$\sum_k r_k^p = 1 \qquad (2)$$

$$\sum_k t_k^p = 0 \qquad (3)$$

$$0 \leq r_k^p \leq 1 \qquad (4)$$

$$L_{rk}^p \leq r_k^p \leq U_{rk}^p \quad (5) \qquad\qquad L_{tk}^p \leq t_k^p \leq U_{tk}^p \qquad (6)$$

Figure 20

SYSTEM OPTIMIZATION PROCEDURE - BIRD EYE VIEW

These operations form an iterative procedure shown below in a Chapin-format flowchart. The Appendix provides more detail on the r initialization, special provisions for the case of an infeasibility remaining at the conclusion of the SSO's, and the usage of the coefficients r, t, and s. (Fig. 21.)

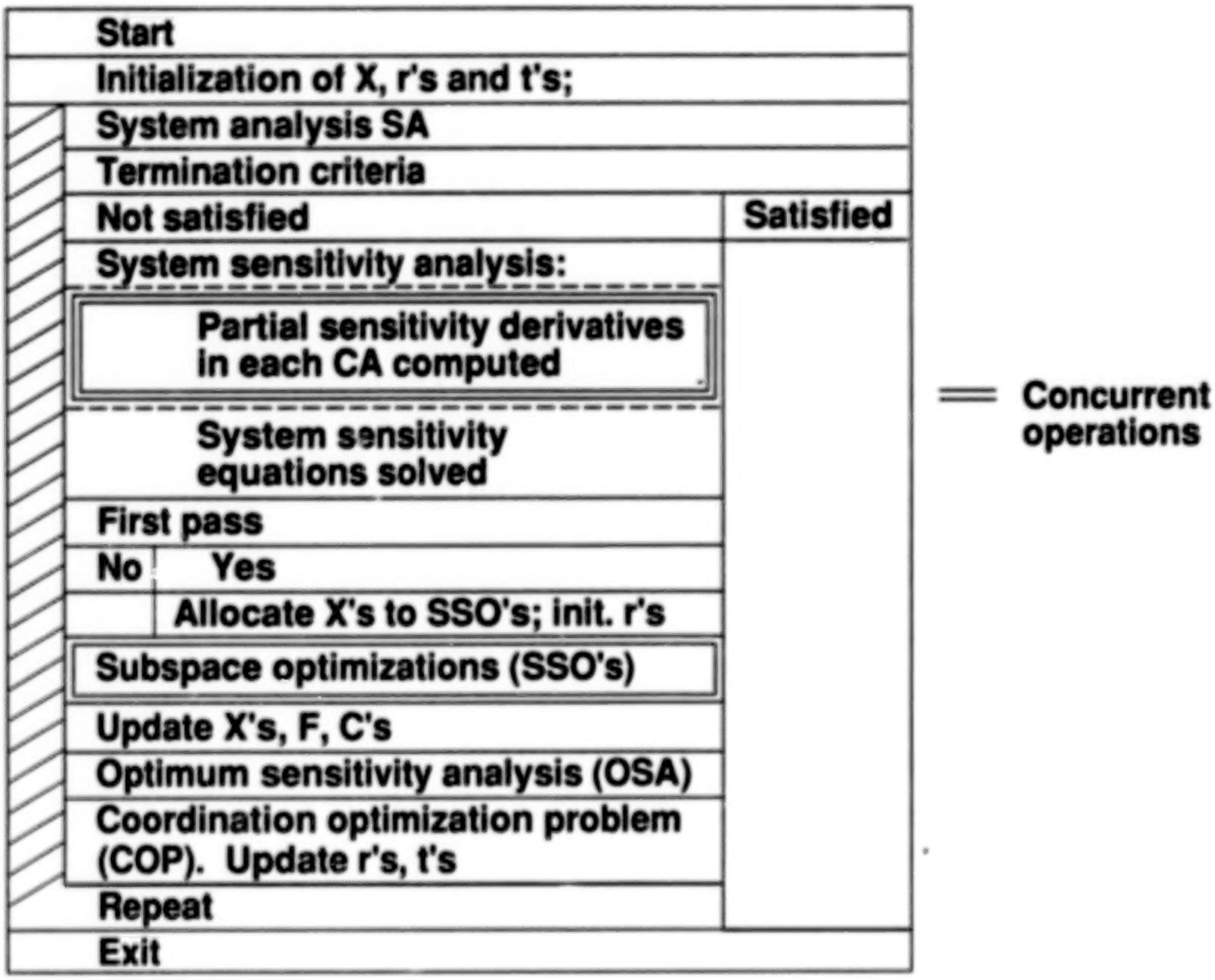
Start
Initialization of X, r's and t's;
System analysis SA
Termination criteria
Not satisfied
Satisfied
System sensitivity analysis:
Partial sensitivity derivatives in each CA computed
System sensitivity equations solved
First pass
No
Yes
Allocate X's to SSO's; init. r's
Subspace optimizations (SSO's)
Update X's, F, C's
Optimum sensitivity analysis (OSA)
Coordination optimization problem (COP). Update r's, t's
Repeat
Exit
Concurrent operations

Figure 21

DEMERITS AND MERITS

The procedure proposed has not been tested yet, but some demerit/merit remarks (demerits first to end on a positive) may be offered on the basis of experience with other decomposition-based algorithms. (Fig.22.)

- DEMERITS
  - —LINEARIZATION MAY REQUIRE NARROW MOVE LIMITS.
  - — ACTIVE CONSTRAINT SWITCHING MAY CAUSE ERRORS IN OPTIMUM SENSITIVITY DERIVATIVES.
- MERITS
  - —EFFICIENCY: NO FULL SYSTEM ANALYSIS FOR EACH SUBSPACE.
  - —COUPLINGS REDUCED TO SENSITIVITY ANALYSIS AND LP OPTIMIZATION.
  - —MODULARITY
  - —SPECIALIZED METHODS ADMISSIBLE IN SENSITIVITY AND SUBSPACE OPTIMIZATIONS.
  - —SUBSPACE OPTIMIZATIONS MAY CORRESPOND TO SPECIALTY GROUPS.
  - —GROUPS COMMUNICATION PRECISELY DEFINED.
  - —CONCURRENT SENSITIVITY ANALYSES AND SUBSPACE OPTIMIZATIONS.
  - —HUMAN JUDGMENT AND INTERVENTION ADMISSIBLE.
  - —RECURSIVITY: ANY CA MAY BE A COUPLED SYSTEM ITSELF.

Figure 22

ALTERNATIVE: LINEAR PROGRAMING WITH RESPECT TO X

An obvious alternative to this procedure is to use the system sensitivity derivatives as a basis for linearizing the entire system optimization problem with respect to X without decomposing it into the subspace optimizations (SSO's), thus eliminating the coordination optimization (COP) and the optimum sensitivity analyses (OSA) needed for it. That would reduce the flowchart to the one shown below.

This alternative is attractive for its simplicity, and the experience reported in ref.10 with a similar scheme has been encouraging. However, the alternative forces the use of approximate information across the board while the procedure proposed herein allows the optimization to access exact analysis directly and relies on the linear extrapolation only insofar as the evaluation of the coupling effects is concerned, hence, its convergence is expected to be faster. Also, the alternative loses the advantage of being able to use specialized methods and human judgment in the subspace optimizations and the managerial convenience of having these optimizations performed by the groups into which a design organization splits naturally. (Fig. 23.)

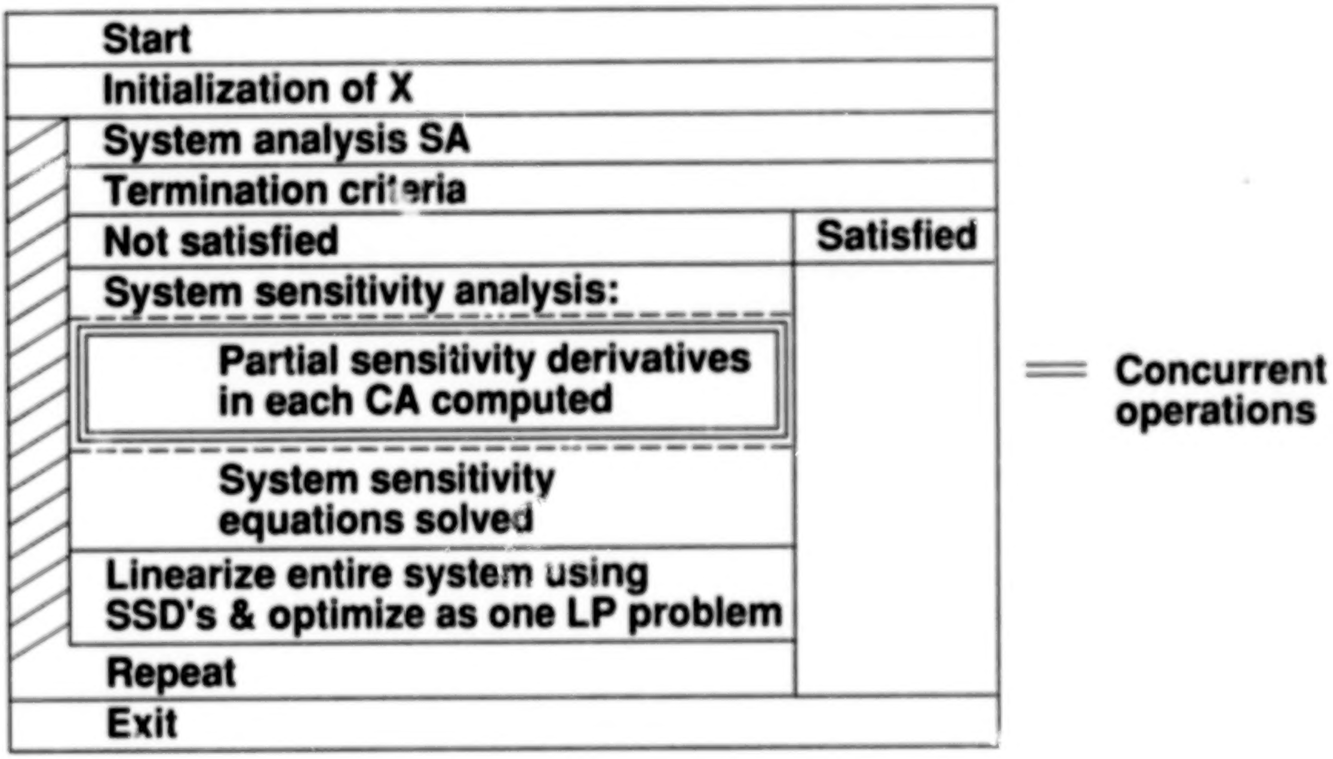
Start
Initialization of X
System analysis SA
Termination criteria
Not satisfied
Satisfied
System sensitivity analysis:
Partial sensitivity derivatives in each CA computed
System sensitivity equations solved
Linearize entire system using SSD's & optimize as one LP problem
Repeat
Exit
Concurrent operations

Figure 23

CONCLUSIONS

Optimization of a large and complex engineering system has been considered in a design organization setting that requires the work be divided among the groups of specialists representing disciplines and physical subsystems. Each group's task may be coupled to any other so that the system is laterally coupled (a network system) and its optimization problem does not lend itself to the hierarchic decomposition previously introduced in the literature.

A new, non-hierarchic decomposition is formulated for this system optimization. Its ingredients are system analysis, system sensitivity analysis, temporarily decoupled optimizations performed in the design subspaces corresponding to the disciplines and subsystems, and a coordination optimization concerned with the distribution of responsibility for the constraint satisfaction and design trades among the disciplines and subsystems. The approach amounts to a variation of the well-known method of subspace optimization modified so that the analysis of the entire system is eliminated from the subspace optimization and the subspace optimizations may be performed concurrently. It is evident that for convex problems each iteration of the procedure improves the design in terms of either reducing the constraint violations or reducing the objective function if the constraints are satisfied. However, the procedure is based, in effect, on a linearization approach to a problem that may be, in the general case, nonlinear, hence no problem independent assertions can be made regarding the procedure convergence.

No operational experience with the procedure is available as yet, hence this presentation is intended to be a blueprint for research development and it suggests a set of specifications for consideration in other developments addressing the same problem. (Fig. 24.)

- **NEW, NON-HIERARCHIC DECOMPOSITION HAS BEEN FORMULATED FOR LATERALLY COUPLED (NETWORK) SYSTEM.**
- **IT IS BASED ON SYSTEM ANALYSIS, SENSITIVITY, INTERDISCIPLINARY SHARING OF THE RESPONSIBILITY FOR CONSTRAINT SATISFACTION, AND SEPARATE, TEMPORARILY DECOUPLED, CONCURRENT OPTIMIZATIONS.**
- **THE COUPLING IS REPRESENTED IN A COORDINATION PROBLEM FORMULATED AS LINEAR PROGRAMMING.**
- **LINEARIZATION ERRORS ARE A POTENTIAL DRAWBACK.**
- **PROPOSED PROCEDURE IS RECURSIVE.**
- **IT IS COMPATIBLE WITH DIVISION OF DESIGN ORGANIZATION INTO SPECIALTY GROUPS.**
- **IT ALLOWS THE USE OF SPECIALIZED ANALYSIS AND OPTIMIZATION METHODS.**
- **PROPOSED PROCEDURE AWAITS IMPLEMENTATION AND TESTING.**

Figure 24

APPENDIX

Initialization of the r Coefficients

The coefficients may be initialized on the basis of the sensitivity information so as to assign a greater responsibility for a cumulative constraint satisfaction to those SSO's that have relatively greater influence on that constraint. From the system sensitivity analysis (SSA) we know the derivatives of the cumulative constraints in each SSO. For the k-th SSO we have

(A1) $C_i^{pk} = dC^p/dX_i^k$

The above derivatives collected for all SSO's form a matrix

(A2) $J = [C_i^{pk}]$; NXK x NSS

Consider the p-th column of the above matrix and select

(A3) $a^{pk} = \max_i (|C_i^{pk}|)$

Repeating the above for k = 1 → NSS, we assemble the a^{pk}'s in a vector normalized such that

(A4) $v^p = \{a^{pk}/\max_k (a^{pk})\}$

This vector has an element equal to a unity at the location where the maximal a^{pk} appeared and elements smaller than unity everywhere else. The vector is now scaled so that its elements add up to unity and renamed a vector of the coefficients $r^p{}_k$

(A5) $r^p{}_k = (1/\Sigma_p v^p) v^p$; p = 1 , NSS

Elements of the above vector of length NSS may be used as initial values for the $r^p{}_k$ coefficients. The total number of the r coefficients for p = 1 → NSS is NSS^2.

Failure of Finding a Feasible Design in an SSO

The procedure requires that each SSO ends with a feasible solution because the optimum sensitivity analysis that follows it is meaningful only at a constrained optimum. Because of the use of the move limits required by linearization it may not be possible to meet that requirement when beginning with an infeasible initial design.

In the above case, one possible way to circumvent the difficulty is to use a constraint relaxation technique described in ref.11. The technique temporarily relaxes the violated constraints to bring them to a critical state and thus satisfies the formalism of a constrained minimum. The relaxation is gradually removed in the subsequent iterations to yield design feasible in a true, physical sense.

Another solution readily available in the procedure itself is to reset temporarily an appropriate coefficient t to remove the offending constraint violation. That arbitrary resetting will have the same effect as the technique from ref.11 and it will cause a violation of the constraint that requires that all the tpk coefficients summed over k add up to zero in the coordination optimization problem (COP). This violation will force a resetting of the t coefficients in the process of solving the COP toward satisfying the violated cumulative constraint by a collective influence of all the SSO's that affect it.

The r, t, and s Coefficients in System Optimization Procedure

With the entire System Optimization Procedure laid out in a flowchart format, it may be illuminating to elaborate on the way the procedure is controlled by the coefficients r, t, and s.

The simplest situation occurs when a C^p is found satisfied after the first SA. Then, its s^p is set to 0 and that, in conjunction with its t^p_k 's that always are initialized to 0, makes the SSO's to treat that constraint as an ordinary inequality constraint with 0 on the right hand side. It is likely that in at least one SSO that constraint will become critical. If so, its t^p_k 's will be adjusted in the COP and the adjusted values will be used in the next SSO's. If the constraint never becomes active in any SSO, its t^p_k 's remain dormant at the initial setting of 0.

If a C^p is found critical after the first SA, its s^p is set to 0 and in the next SSO's it is treated as an inequality constraint with 0 on the right hand side. Subsequently, its t^p_k 's will be adjusted in the COP, and the adjusted values will be used in the next SSO's.

If a C^p is found violated after the first SA, its s^p is set to 1 and its r^p_k 's initial values will be used in the SSO's. Had the SSO's operated on accurate information only, the constraint would have been driven to a critical status after the first execution of the SSO's and there would be no need to adjust its r^p_k 's in the next COP. However, due to the approximation errors incurred in the SSO's one cannot rule out that a C^p predicted satisfied or critical in the SSO's may turn out to be still violated after the next execution of the SA (this may occur also due to inability of finding a feasible design, as discussed in the preceding section of this Appendix). To prepare for that eventuality two actions are taken: the Optimum Sensitivity Derivatives w.r.t. all the r and t coefficients corresponding to that constraint are computed in the next OSA, and the constraint r^p_k 's are adjusted in the subsequent COP.

If the SA in the next pass reveals that the C^p is still violated, then the adjusted values of its r^p_k 's will be used in the next SSO to further improve the constraint satisfaction. If the C^p is found satisfied, then it undergoes the treatment described above for a satisfied or critical constraint.

It is apparent from the above that the COP is never executed with a full set of NSS^2 variables r and NSS^2 variables t because the s-switch makes the r^p_k and t^p_k mutually exclusive. That reduces the dimensionality of the COP.

On the other hand, the OSA is carried out for each SSO for a full set of the r's and a full set of the t's, at least at the beginning of the procedure until all the s-switches settle in their final settings. Using the full sets of r's and t's in OSA does not pose a computational cost problem since the partial derivatives w.r.t. these coefficients are trivial to obtain.

REFERENCES

1. Sobieszczanski-Sobieski, J.: A Linear Decomposition Method for Large Optimization Problems - Blueprint for Development. NASA TM 83248, Feb. 1982.

2. Sobieszczanski-Sobieski, J., James,B. B.; and Riley,M. F.: Structural Sizing by Generalized, Multilevel Optimization, AIAA J. Vol.25, No.1, January 1987, p.139.

3. Wrenn, G. A.; and Dovi, A. R.: Multilevel Decomposition Approach to the Preliminary Sizing of a Transport Aircraft Wing; AIAA/ASME/ASCE/AHS 28th Structures, Dynamics, and Materials Conference, Monterey, Cal., April 6-8, 1987, AIAA Paper No.87-0714-CP.

4. Barthelemy, J.-F. M.: Engineering Applications of Multilevel Optimization; paper presented at Second NASA/Air Force Symposium on Recent Advances in Multidisciplinary Analysis and Optimization, Sept. 28-30, 1988, Hampton, Virginia. Proceedings published as NASA CP-3031.

5. Abdi, F. F.; Ide, H.; Shankar, V. J.; and Sobieszczanski-Sobieski, J.: Optimization for Nonlinear Aeroelastic Tailoring Criteria, paper presented at Int'l Council for Aeronautical Sc., 16th Congress, Jerusalem, Aug.-Sept., 1988.

6. Sobieszczanski-Sobieski, J.; On the Sensitivity of Complex, Internally Coupled Systems; AIAA/ASME/ASCE/AHS 29th Structures, Structural Dynamics and Materials Conference, Williamsburg, Va, April 1988; AIAA Paper No.CP-88-2378.

7. Kreisselmeier, G.; and Steinhauser, R.: Systematic Control Design by Optimizing a Vector Performance Index; International Federation of Active Control Symposium on Computer-Aided Design of Control Systems, Zurich, Switzerland, Aug. 29-31, 1979.

8. Sobieszczanski-Sobieski, J.; Barthelemy,J.-F. M.; and Riley, K. M.: Sensitivity of Optimum Solutions to Problem Parameters; AIAA J, Vol.21, Sept. 1982, pp.1291-1299.

9. Barthelemy, J.-F.M.; and Sobieszczanski-Sobieski, J.: Optimum Sensitivity Derivatives of Objective Functions in Nonlinear Programing; AIAA J, Vol.22, No.6, June 1983, pp.913-915.

10. Vanderplaats, G. N.; Yang, Y. J.; and Kim, D. S.: An Efficient Multilevel Optimization Method for Engineering Design, AIAA/ASME/ASCE/AHS 29th Structures, Structural Dynamics and Materials Conference, Williamsburg, Va, April 1988; AIAA Paper No.CP-88-2226.

11. Barthelemy, J.-F. M.; and Riley, M. F.: Improved Multilevel Optimization Approach for the Design of Complex Engineering Systems; AIAA J., Vol.26, No.3, March 1988, pp. 353-360.

OVERVIEW OF DYNAMICS INTEGRATION RESEARCH (DIR) PROGRAM AT LANGLEY RESEARCH CENTER

Goals and Progress

Steven M. Sliwa
Guidance and Control Division
Langley Research Center
Hampton, Virginia

and

Irving Abel
Structural Dynamics Division
Langley Research Center
Hampton, Virginia

This presentation and paper describes research goals and objectives for an ongoing activity at Langley Research Center. The activity is aimed principally at dynamics optimization for aircraft. The effort involves active participation by the Flight Systems, Structures, and Electronics directorates at LaRC. The Functional Integration Technology (FIT) team has been pursuing related goals since 1985. A prime goal has been the integration and optimization of vehicle dynamics through collaboration at the basic principles or equation level. Some significant technical progress has been accomplished since then and this paper and some others at this symposium capture these results. An augmentation for this activity, Dynamics Integration Research (DIR), has been proposed to NASA Headquarters and is being considered for funding in FY 90 or FY 91.

In 1984, NASA and several outside study groups (e.g., Aero 2000) identified multidisciplinary research as a key, untapped opportunity for aeronautical research. NASA Langley prepared a new initiative for pursuing this area. The overall goals and the kickoff chart are represented. If a capability existed to analytically model all the interactions and then numerical procedures were used to iterate the design variables until performance was optimized, many significant benefits would result. These include explicitly optimized configurations, all synergistic multidisciplinary interactions exploited, greater productivity in the design process and an opportunity to all designers to exercise more creativity. Truthfully, at the time, the plans did not go much deeper. An approach had not been worked out for accomplishing the research. The new initiative was not funded. Langley then put together a multidisciplinary technical team to make some recommendations on a technical approach.

AIRCRAFT SYSTEM INTEGRATION GOALS

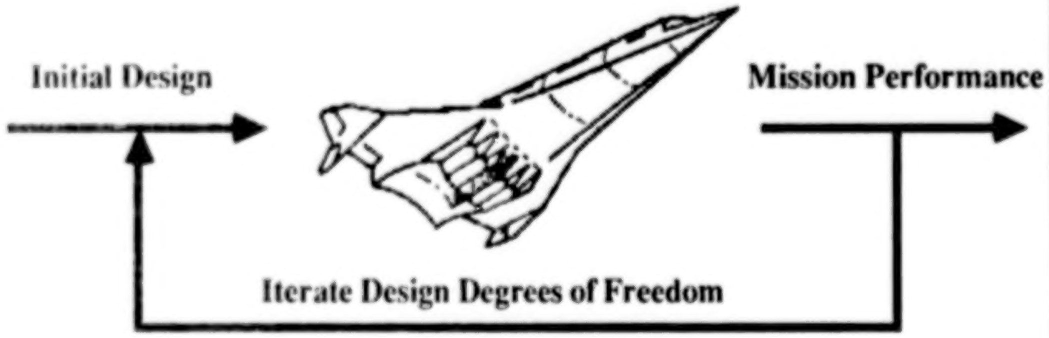

Initial Design

Mission Performance

Iterate Design Degrees of Freedom

- Explicitly Optimize Proposed Configurations
- Synergistically Exploit Multidisciplinary Interactions
- Speed Conceptual/Preliminary Design Process
- Maximize Designer's Opportunity for Creativity

The technical planning team recommended that the problem be divided and solved in two parts simultaneously. This is a standard approach for solving complex problems and decomposing the problem into simpler elements for solution. In this case, the problem is separated into dynamics integration and airframe integration. Clearly these two problem areas are not completely decoupled, and, in fact, it is anticipated that the dynamics issues can significantly impact the overall design. However, a capability to perform the integrated dynamics optimization must exist before overall system optimization is possible. Two teams were formed at LaRC to attack these problems. One is the Aircraft Configuration Integration Group (ACIG) and the other is the Functional Integration Technology (FIT) team. The latter is the subject of this paper.

AIRCRAFT SYSTEMS INTEGRATION APPROACH

SOLVE CLASSICAL MULTI-LOOP PROBLEM

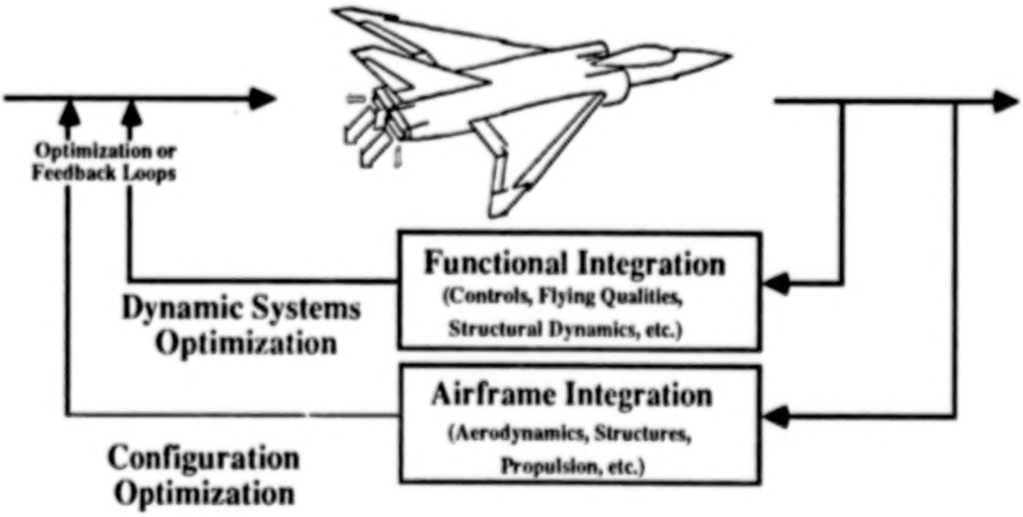

Optimization or Feedback Loops

Functional Integration
(Controls, Flying Qualities, Structural Dynamics, etc.)

Dynamic Systems Optimization

Airframe Integration
(Aerodynamics, Structures, Propulsion, etc.)

Configuration Optimization

DECOUPLE PROBLEM INTO SUBSYSTEMS

Overall aircraft system integration will require a long list of technologies and design variables to be combined and optimized. In the area of dynamics integration a subset of these issues has been selected for consideration in the research activity. Technologies being considered include flying qualities, flight path control, thrust vectored controls, structural dynamics, and aeroservoelasticity. The research goal is to develop and validate methods and tools which optimize aircraft dynamics, not just to analyze and solve problems.

MULTIDICIPLINARY DYNAMICS INTEGRATION RESEARCH

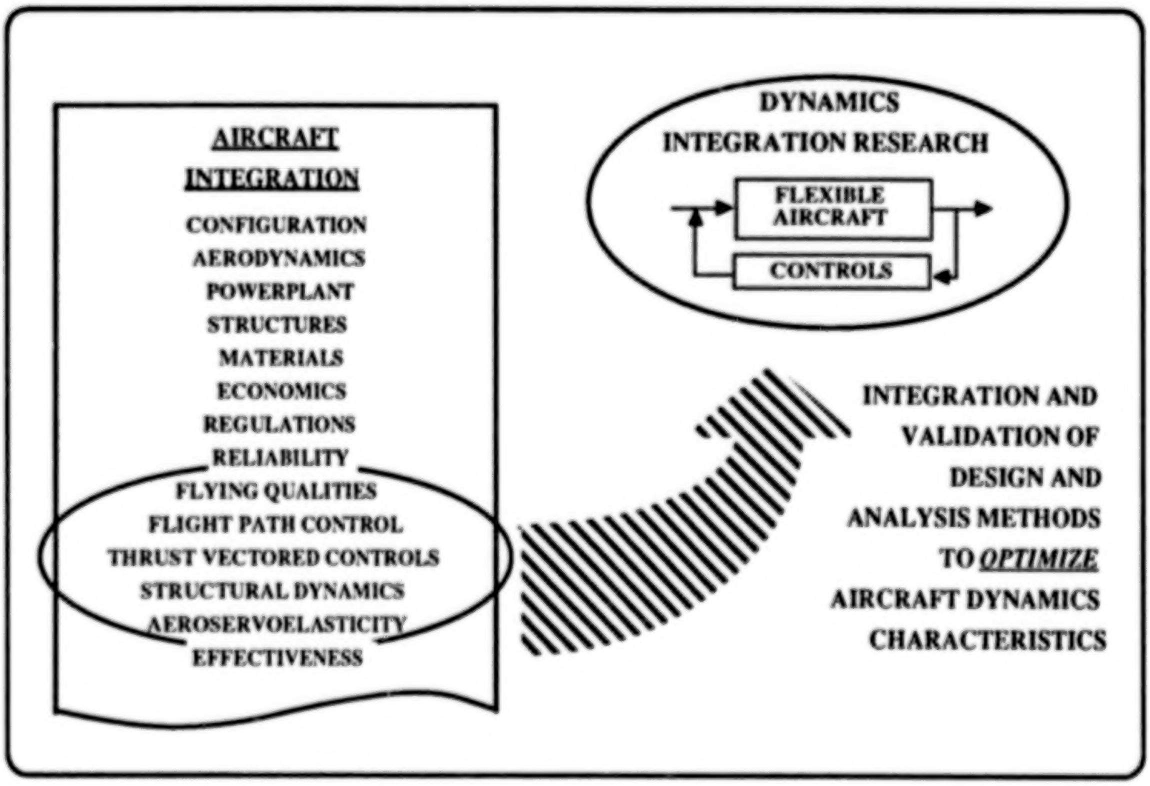

AIRCRAFT INTEGRATION

CONFIGURATION
AERODYNAMICS
POWERPLANT
STRUCTURES
MATERIALS
ECONOMICS
REGULATIONS
RELIABILITY
FLYING QUALITIES
FLIGHT PATH CONTROL
THRUST VECTORED CONTROLS
STRUCTURAL DYNAMICS
AEROSERVOELASTICITY
EFFECTIVENESS

DYNAMICS INTEGRATION RESEARCH

INTEGRATION AND VALIDATION OF DESIGN AND ANALYSIS METHODS TO *OPTIMIZE* AIRCRAFT DYNAMICS CHARACTERISTICS

Dynamics integration will be important in terms of enabling mission performance. The mission drivers below lead to the design options indicated. Taking advantage of the design options will result in aircraft characteristics that will have significant dynamics challenges to be resolved. Unstable aircraft will result from tailless configurations or reduced control surface sizes for performance and observability. Flexibility will result from minimum weight configurations which will involve coupling and unusual dynamics interactions between modes. Analysis tools will have trouble predicting these responses, many of which are strongly coupled with nonlinear phenomena. All of these challenges will have to be solved without adding to the already complex environment in which the pilot must operate the aircraft. The bottom line is that dynamics issues will play a first-order role in aircraft design.

PRESENT AND FUTURE TRENDS

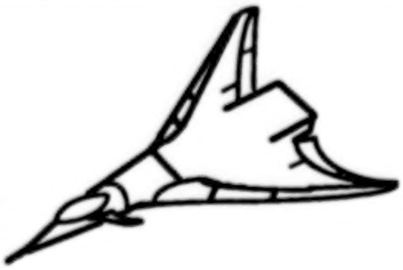

MISSION DRIVERS

- LOW OBSERVABLES
- HIGH PERFORMANCE
- EXPANDED ENVELOPES

DESIGN OPTIONS

- THRUST VECTORED CONTROLS
- LIGHTWEIGHT COMPOSITES
- NEW FLIGHT MODES
- NO TAIL SURFACES

DYNAMICS CHALLENGES

- UNSTABLE
- VERY FLEXIBLE
- UNCONVENTIONAL DYNAMICS
- STRONG COUPLING
- UNCERTAIN MODELS
- PILOTING COMPLEXITY

DYNAMICS ISSUES PLAY A FIRST ORDER ROLE IN AIRCRAFT DESIGN!

The extreme technological demands placed upon the design for dynamics issues are new. The complexity has been increasing rapidly. Past configurations were relatively rigid, stable, and characterized by conventional dynamics. In fact, past configurations were deliberately designed with weak coupling between the modes. Existing tools are now capable of predicting most of the major influences for these conventional configurations. New and future configurations will demand that significant enhancements be made in the tools and methodologies to minimize risk and maximize performance.

NEED FOR DYNAMICS INTEGRATION RESEARCH

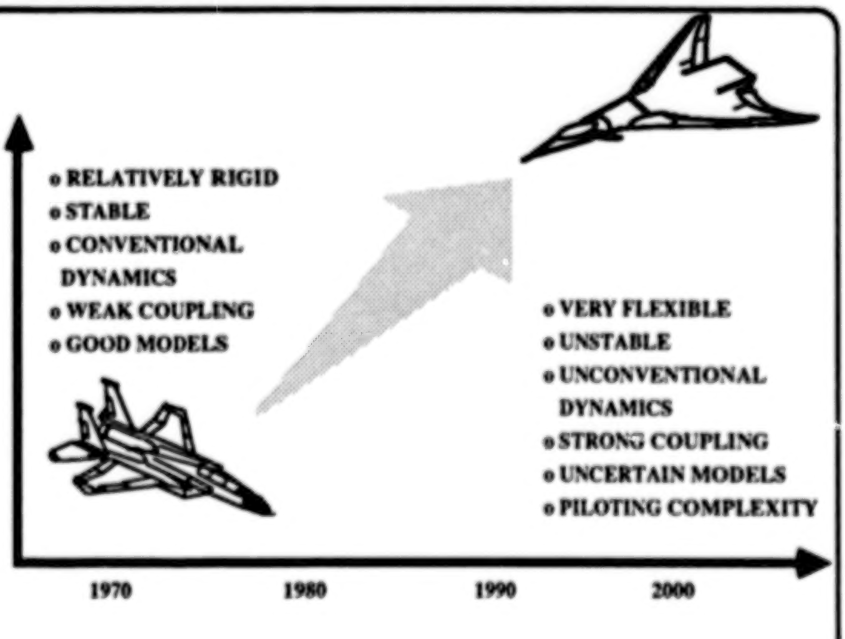

DYNAMICS INTEGRATION COMPLEXITY

- **RELATIVELY RIGID**
- **STABLE**
- **CONVENTIONAL DYNAMICS**
- **WEAK COUPLING**
- **GOOD MODELS**

- **VERY FLEXIBLE**
- **UNSTABLE**
- **UNCONVENTIONAL DYNAMICS**
- **STRONG COUPLING**
- **UNCERTAIN MODELS**
- **PILOTING COMPLEXITY**

DYNAMICS INTEGRATION CHALLENGES AND OPPORTUNITIES GROW AS ENVELOPES EXPAND

There are examples of recent aircraft configurations that have had significant dynamics problems. Each of the cases listed below had controls and structural dynamics issues that cost tens of millions of dollars each to alleviate. The F series aircraft below encountered the indicated problems after first flight, which is very late in the design process, resulting in costly delays and expensive fixes. The fixes may not even be as complete as desired since options are significantly limited at that point. A goal of LaRC's DIR program is to make sure that technologies exist to help solve as many of these problems as possible before first flight; to find optimized, multidisciplinary solutions to as many of these problems as possible; and to link these solutions to the overall configuration.

RECENT EXAMPLES OF AIRCRAFT DYNAMICS PROBLEMS

F-16

- CONTROLLER REDESIGN
- DEPARTURE PROBLEMS
- PROPULSION INTEGRATION
- FLUTTER WITH STORES

X-29A

- AEROSERVOELASTIC INTERACTIONS
- EXTREME AUGMENTATION
- SENSOR PLACEMENT
- BACK-UP MODE COMPLICATIONS

F-18

- LONG LAGS/DELAYS
- SIMULATION FIDELITY
- AILERON LIMIT CYCLE
- CONTROL SATURATION

F-15

- RUDDER OSCILLATION
- POOR PITCH DAMPING
- RUDDER LIMIT CYCLE
- STABILATOR OSCILLATION

GOAL IS TO PROVIDE VALIDATED METHODOLOGIES TO SOLVE PROBLEMS PRIOR TO FLIGHT

The chart below illustrates the complications that are pervading new aircraft configurations as typified by the previous chart. This is a plot of control authority/power versus frequency of input. Sometimes this type of chart is referred to as a Bode chart. Typical structure is for some control authority at low frequencies to improve flying qualities and stability. However, an essential goal is to "roll off" the authority at high frequency to avoid interactions with actuator and structural modes. However, unstable aircraft require more augmentation at low frequency and cannot be "rolled off" as quickly. Additionally, as an aircraft becomes more flexible, the structural modes have lower frequencies. If the control authority and structural modes have significant intersections, the probability of complicated interactions is high.

ILLUSTRATION OF GREATER DYNAMICS CHALLENGES

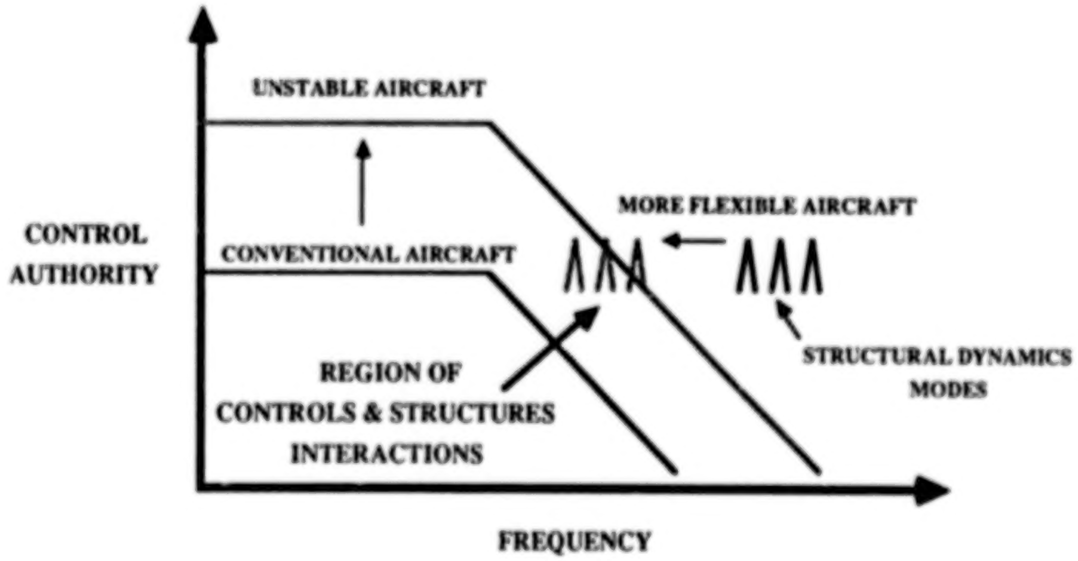

SIGNIFICANT DYNAMICS INTEGRATION CHALLENGES EXIST FOR UNSTABLE, FLEXIBLE AIRCRAFT

The research program defined by the Structures and Flight Systems directorates is depicted below. It entails methodology development and validation. Prime goals entail developing integrated modeling techniques and software tools and exploiting these to evolve design and synthesis methods. A major aspect of the proposed program is the validation of the design tools resulting from this program. Validation will occur in real-time piloted simulations and in wind tunnel tests of aeroservoelastic models in the Transonic Dynamics Tunnel. Funds are being sought to accelerate the program and to help facilitate technology transfer within the aerospace community.

TIMELY R&T BASE EFFORT TO FOCUS RESEARCH

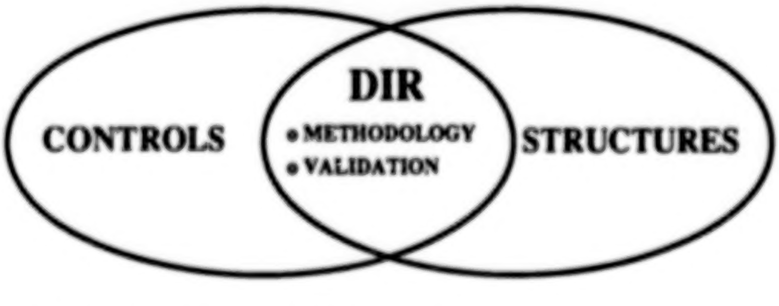

METHODOLOGY DEVELOPMENT

- o MODELING TECHNIQUES AND SOFTWARE TOOLS
- o DESIGN AND SYNTHESIS METHODS

VALIDATION ACTIVITIES

- o AEROSERVOELASTICALLY TAILORED WIND TUNNEL MODEL TESTS
- o REAL-TIME PILOTED AND BATCH SIMULATIONS

TECHNOLOGY TRANSFER

- o INDUSTRY, DoD AND UNIVERSITY PARTICIPATION

This chart represents some of the payoffs that might be accomplished if such a program is fully funded. The list includes performance benefits if a configuration is completely redesigned to exploit technologies that might result from the DIR program. Additionally, increases in reliability and effectiveness of the design tools and methods result.

DIR PAYOFFS & GOALS

VEHICLE PAYOFFS & GOALS

- o 25% INCREASE IN AIRCRAFT AGILITY
- o 15% INCREASE IN ENVELOPE VELOCITY WITH STORES
- o 30% DECREASE IN TAKE-OFF GROSS WEIGHT
- o SUPERSONIC PERFORMANCE UNCOMPROMISED DUE TO LOW-SPEED CONSTRAINTS AND FLYING QUALITIES
- o MINIMIZED NEED FOR EXPENSIVE "FIXES" AFTER FIRST FLIGHT

DISCIPLINARY PAYOFFS & GOALS

- o VALIDATED AEROSERVOELASTIC ANALYSIS AND DESIGN TOOLS
    - TAILORED WIND TUNNEL MODEL TESTS
- o INCREASED EFFECTIVENESS OF REAL-TIME SIMULATION
    - IMPROVED FIDELITY & REDUCED TIME FOR DESIGN ITERATIONS

This chart shows the prime elements of the LaRC program in Dynamics Integration Research (DIR). It includes methodology development; high-fidelity, batch simulations; validation through real-time piloted simulation; and validation of design methods through aeroservoelastic wind tunnel tests. Each of these activities is integrated and the goal is to develop and validate the tools and methods previously described.

TECHNICAL PLAN

High fidelity model

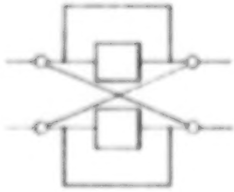

Integrated control design

Rapid simulation iteration

Experimental validation

A comparison of present design methodologies with proposed methodologies that will be enabled through the pursuit of DIR is shown below. Presently, control system design and structural design (for dynamics) are two separate and distinct functions. At some point the control system team typically delivers time histories of typical evaluation maneuvers to the structural dynamicists who analyze for structural load integrity. When the design has converged, the airplane is built and flown. Almost all recent airplanes have had significant problems with structural dynamics, controls systems, and flying qualities. Some examples were described in a previous chart. Once the airplane prototype is built and flown, many options to redesign and fix the problems no longer exist. The two basic options included redesigning the control system, which is quite expensive, and an alternative and less favorable approach, redesigning the structure (and the tooling jig, etc.). This latter option is prohibitively expensive and time-consuming. A better approach would be to allow the two teams to integrate their approaches and work with common models. In fact, if they go to simulation and generate structural loads data as well as flying qualities types of information, the cost of building and flying will be significantly reduced.

METHODOLOGIES FOR SOLVING STRUCTURAL LOADS PROBLEMS

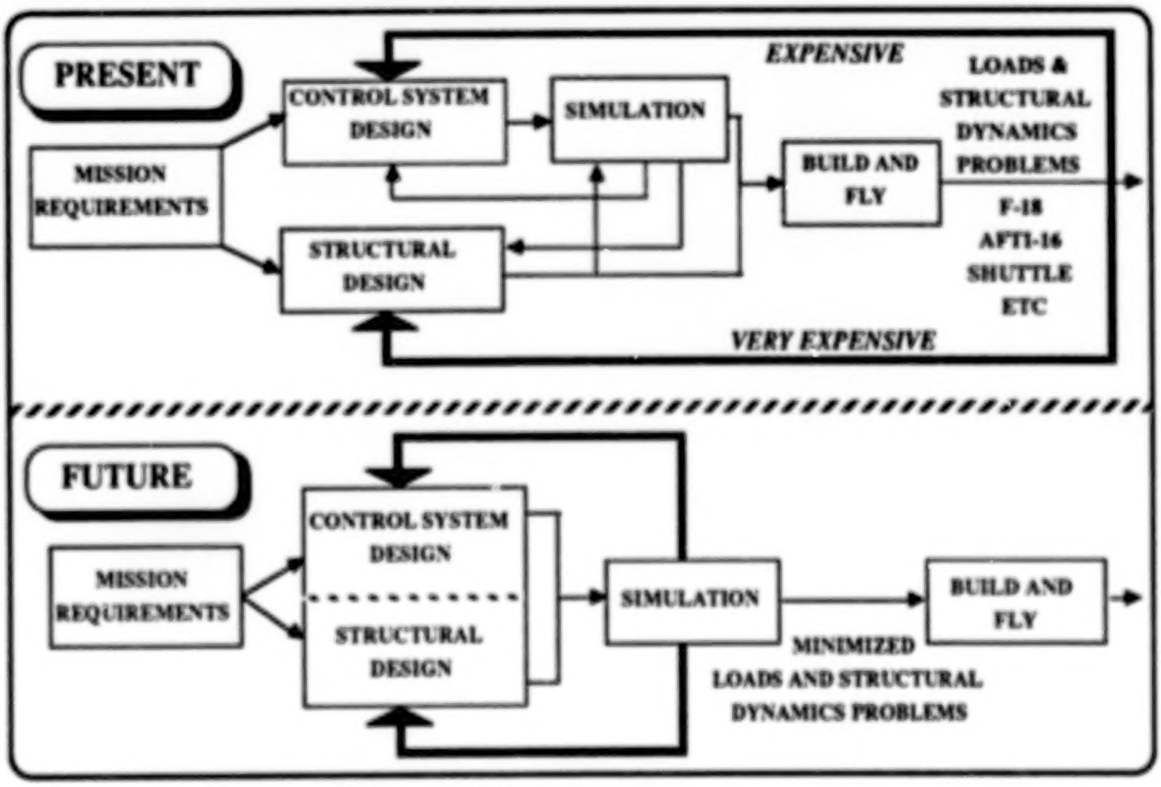

A prime goal will be to build in sufficient modeling fidelity into the real-time simulation model so that in addition to obtaining normal rigid body positions and rates, the deflections and structural loads can be estimated. It is envisioned that these loads will be displayed to test engineers while pilots maneuver their aircraft in realistic scenarios in the simulator. If loads get large or exceed nominal, the test engineer can observe changes in colors at his display and mark the data for indepth analysis. If this scenario becomes possible, test inputs will be obsolete as the pilot will be able to accurately "ring out" the configuration prior to first flight.

DEVELOPMENT OF "STRAIN-GAUGED" SIMULATIONS

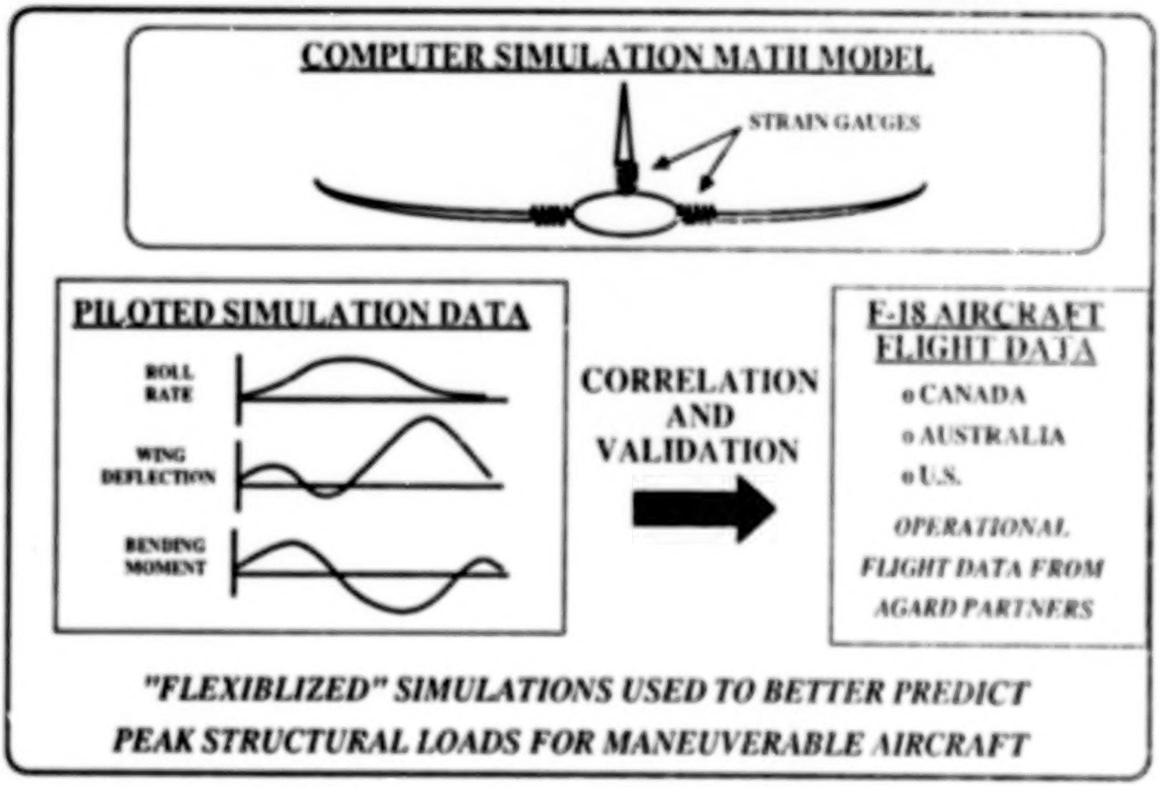

COMPUTER SIMULATION MATH MODEL

PILOTED SIMULATION DATA

CORRELATION AND VALIDATION

F-18 AIRCRAFT FLIGHT DATA

- o CANADA
- o AUSTRALIA
- o U.S.

OPERATIONAL FLIGHT DATA FROM AGARD PARTNERS

"FLEXIBLIZED" SIMULATIONS USED TO BETTER PREDICT PEAK STRUCTURAL LOADS FOR MANEUVERABLE AIRCRAFT

One accomplishment that the FIT team has contributed is a modeling methodology that constructs high-fidelity, truth models. The process has been automated significantly and involves integrating information from wind tunnels, CFD and panel, steady aerodynamic codes, unsteady aerodynamic codes and other sources into a nonlinear model. The model maintains the structure needed for nonlinear maneuvers and integrates in the structural dynamics in a rigorous way. During the model integration many terms were uncovered that are typically ignored and could be important for highly maneuverable and flexible vehicles. Tools were developed to check coordinate systems as models were transferred from one discipline to another. The result is a large parent model that is detailed enough to compute air combat maneuvers. When the parent model is trimmed, a by-product is its deflected shape. If the parent model is operated at high enough speed, it flutters. This model is too complex to be used for real-time simulation or probably with direct design tools, but such models could be extracted. The benefit is that if a common model is used for each discipline, the integration process has been fostered.

HIGH-FIDELITY, TRUTH MODEL INTEGRATES DISCIPLINES

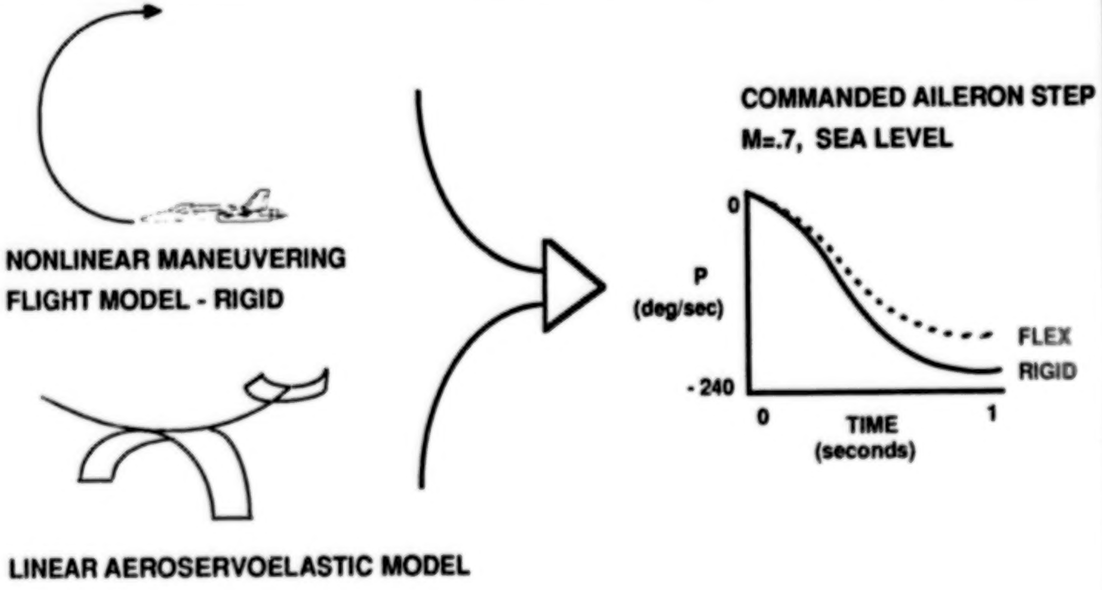

HIGH-FIDELITY OR TRUTH MODEL HAS BEEN DEVELOPED TO COUPLE AEROSERVOELASTICITY AND FLIGHT DYNAMICS

The design process can be modelled by the flow chart below. The tuning of the vehicle shape tends to occur during the configuration integration loop. The design iterations in this loop can be extremely fast. Dynamics integration normally requires real-time simulation. The effort to build and evaluate real-time simulations is normally a very time-consuming and slow process. The result is that it is difficult for information to flow from the dynamics integration loop in a timely manner to impact the configuration integration process.

CURRENT DESIGN INTEGRATION PROCESS

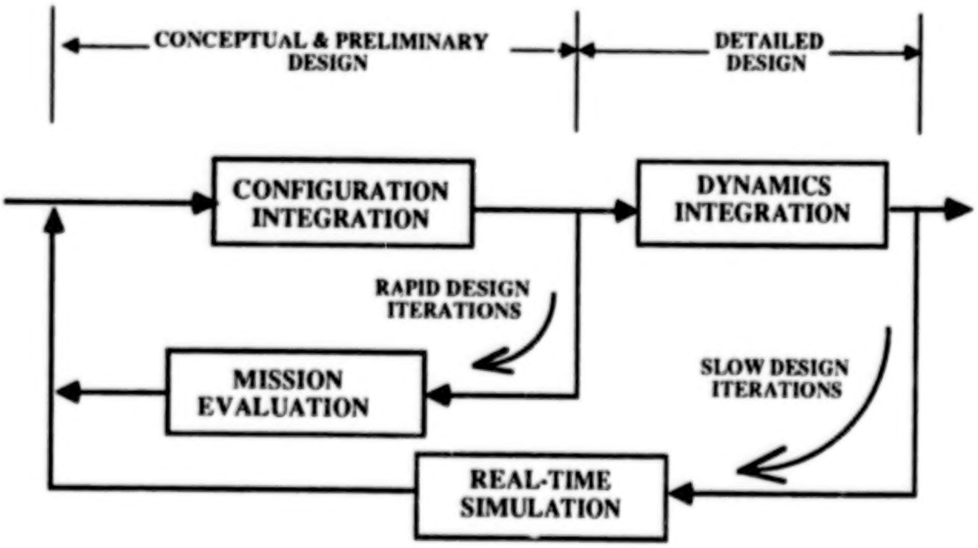

PROBLEM:

DYNAMICS INTEGRATED LATE IN DESIGN PARTIALLY DUE TO SLOWNESS OF UPDATING PILOTED, REAL-TIME SIMULATIONS

The FIT team has established a goal of trying to improve the effectiveness of real-time simulation. One aspect of improving the fidelity by including structural dynamics and aeroservoelastic effects has been discussed previously. Here the goal is to improve productivity and throughput by speeding the process of building and modifying real-time simulations. In particular, the goal is to be able to go from an updated control design to simulation within 1 day. Currently it takes on the order of a week or more to implement a new control system structure for a real-time piloted simulation. Once that goal has been achieved, then the goal will be to combine integrated control design with aeroservoelastic tailoring (in parallel, series or simultaneously). The time-frame desired will be a couple of days versus the months that it takes currently to complete a design and update the appropriate evaluation models.

SIMULATION GOALS FOR SPEEDING DESIGN ITERATIONS

INITIAL GOAL

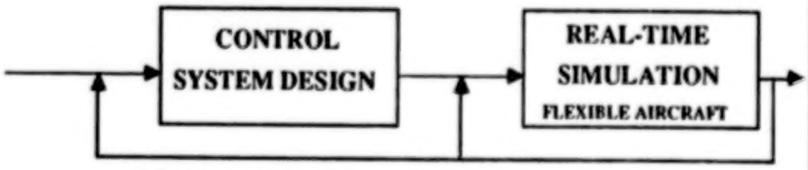

1 DAY vs. WEEKS

FUTURE GOAL

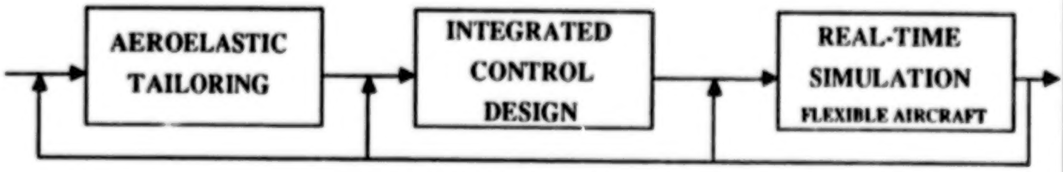
AEROELASTIC TAILORING
INTEGRATED CONTROL DESIGN
REAL-TIME SIMULATION FLEXIBLE AIRCRAFT

2 DAYS vs. MONTHS

SIMULATION EFFECTIVNESS IMPROVED THROUGH AN ORDER OF MAGNITUDE IMPROVEMENT IN TURNAROUND

Eventually the FIT and ACIG activities will merge and the ultimate goal is that the impact of configuration modifications can be evaluated. Ideally, a configuration variable could be iterated and new models generated and results from a piloted simulation flow back to the designers on the order of a week rather than in several months. If this aggressive goal can be achieved, then dynamic issues can be used to solve configuration problems and improve performance. Additionally, configuration optimization can take place with full knowledge of the impacts it may have on the dynamics of integrated systems.

FUTURE LONG-RANGE GOAL

NEW DESIGN PROCESS

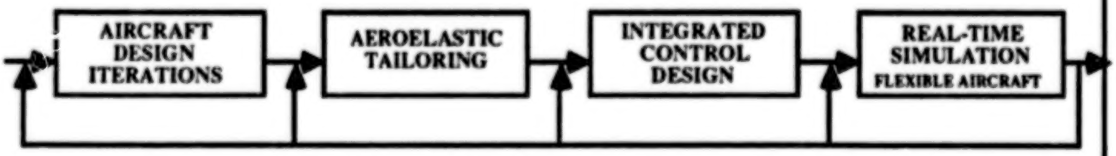

AIRCRAFT DESIGN ITERATIONS

AEROELASTIC TAILORING

INTEGRATED CONTROL DESIGN

REAL-TIME SIMULATION FLEXIBLE AIRCRAFT

1 WEEK vs. MULTIPLE MONTHS

- **ENABLE DYNAMICS ISSUES TO IMPACT CONFIGURATION THROUGHOUT DESIGN PROCESS**

Of course, many of the design interactions being discussed occur at the preliminary design level for configuration optimization. In contrast, most of the dynamic system design requires detailed design information. The key obstacle or "brick wall" that prevents such interactions is that it is very time-consuming to develop detailed models. These models either require complicated analyses or experiments, both of which take time to set up and evaluate.

PRACTICAL CONSIDERATIONS TO RAPID DESIGN ITERATIONS

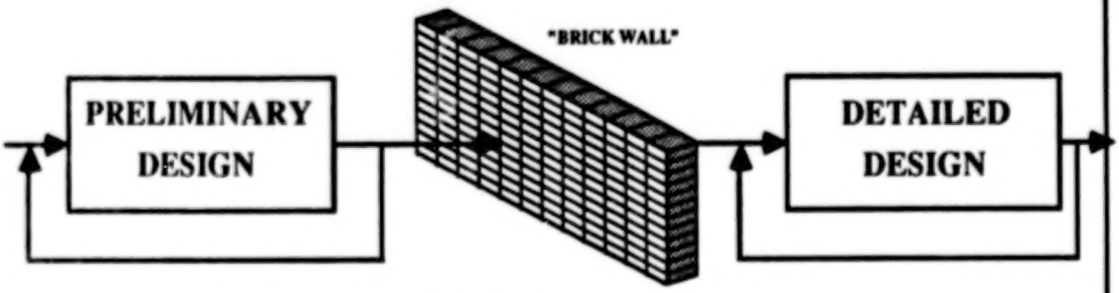

MODEL BUILDING

- **o ANALYSES**
- **o EXPERIMENTS**

DETAILED DESIGN STAGE DELAYED TO GENERATE HIGH-FIDELITY MODELS

The DIR program at LaRC recognizes the shortcomings discussed on the previous page and has developed a strategy for addressing the building of high-fidelity models. Some of the strategies include the following: develop analytical methods for computing interdisciplinary sensitivities which permit decoupled, simultaneous optimization; develop efficient model reduction techniques; pursue generalized trade studies whenever a design problem is undertaken so that the experience can be cataloged and perhaps exploited without going through the entire process for future problem, and; automate the tools in such a way as to speed the model building process.

STRATEGIES FOR IMPACTING PRELIMINARY DESIGN

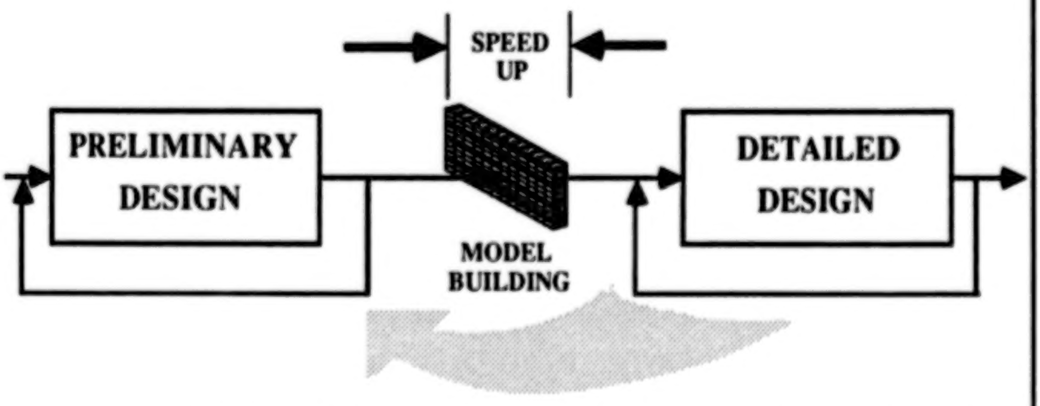

- DEVELOP INTERDISCIPLINARY SENSITIVITIES
- SOLVE MODEL REDUCTION ISSUES
- GENERALIZE DESIGN TRADES
- CAPTURE ACCELERATED DETAILED DESIGN METHODS IN PRELIMINARY DESIGN STAGE
- DEVELOP TOOLS TO SPEED MODEL BUILDING PROCESS

A summary of the key technology areas is shown. For each area a set of challenges is listed. For each challenge, an indication of the status of the available tools in terms of validation and maturity is indicated. As can be seen, at best in this multidisiciplinary focus the validation and maturity status of any particular technology area is marginal. A lot of experimental work is needed to enable designers to address these types of complicated and challenging problems. Methods cannot be integrated into design methodologies unless they have been validated to a sufficient level to permit the confident use of them for vehicle analysis and synthesis.

TECHNICAL AREAS NEEDING EXPERIMENTAL VALIDATION

AREA	CHALLENGES	STATUS
UNSTEADY AERODYNAMICS	o SEPARATED AND VORTEX FLOWS o TRANSONIC o CONTROL EFFECTIVENESS	POOR EMERGING MARGINAL
STRUCTURAL LOADS & RESPONSE	o NON-LINEAR o BUFFET	POOR MARGINAL
AEROSERVO-ELASTICITY	o HIGH GAIN CONTROLS o HIGHLY FLEXIBLE STRUCTURES	EMERGING EMERGING
CONTROL LAW DESIGN	o MULTI-CONTROL o MULTI-FUNCTION	EMERGING EMERGING
STRUCTURE/CONTROL DESIGN	o INTEGRATED STATIC/DYNAMIC AEROELASTIC TAILORING o SENSITIVITY	POOR MARGINAL

This chart shows what it means to validate methods. Various analytical schemes exist already or are under development. These sketches illustrate obtaining experimental data that corresponds directly with analytical data that has been previously computed. This comparison can then be used to investigate improvements in the analytical prediction methods (or perhaps experimental methods).

VALIDATION OF AEROSERVO-ELASTIC ANALYSIS METHODS

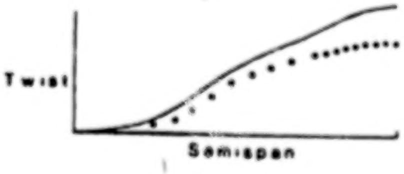

DEFORMATION OF TAILORED STRUCTURES

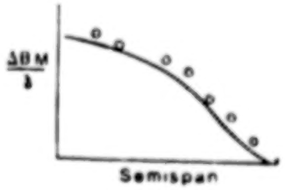

STRUCTURAL LOADS

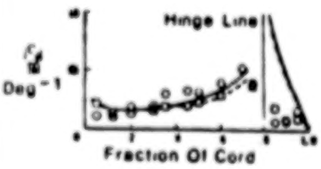

UNSTEADY AERO

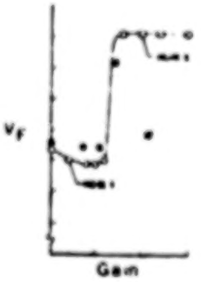

CONTROL OF AEROELASTIC RESPONSE

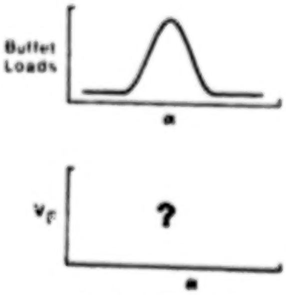

HIGH-ALPHA

BEST COPY AVAILABLE

This chart outlines the wind tunnel efforts that are planned for the full Dynamics Integration Research (DIR) program, if funded. Key areas needing validation include static and dynamic aeroservoelasticity evaluated transonically and at moderate and high angles of attack. Advanced control law synthesis will be systematically combined with advanced aeroelastic structural synthesis. The prime facility will be the Transonic Dynamics Tunnel. A new capability to evaluate unstable models is currently under way. Ideally, a rigid model should be built for studying unsteady aerodynamics and buffet problems. This could be compared with full-span and semi-span models. Initial tests will be to redesign certain structural or control law parameters of already existing models. If DIR is fully funded, the ultimate goal will be to test and compare these with a fully integrated design.

AEROSERVOELASTIC WIND TUNNEL TEST PROGRAM

o VALIDATION OF ADVANCED ANALYSIS METHODS

- STATIC AND DYNAMIC AEROSERVOELASTICITY
- TRANSONIC UNSTEADY AERO
- HIGH-ALPHA

o EVALUATE MULTIDISCIPLINARY DESIGN METHODS

- ADVANCED AEROELASTIC STRUCTURAL SYNTHESIS
- ADVANCED CONTROL LAW SYNTHESIS

o TRANSONIC DYNAMICS TUNNEL (TDT) MODELS

- UNSTABLE MODEL
- RIGID UNSTEADY AERO/BUFFET MODEL
- ACTIVE FLEXIBLE WING
- AEROELASTIC FULL-SPAN

The ongoing Active Flexible Wing (AFW) project is supported by three directorates at Langley Research Center and is a major focus of the FIT team. An advanced model with a highly aeroelastic wing and multiple leading edge and trailing edge control surfaces is a focal point for an aggressive research and testing program. The model has the capability to be free to roll. This allows the simultaneous optimization of flexible and structural modes. Multiple algorithms for combining roll control, load alleviation, and flutter suppression will be evaluated on this model.

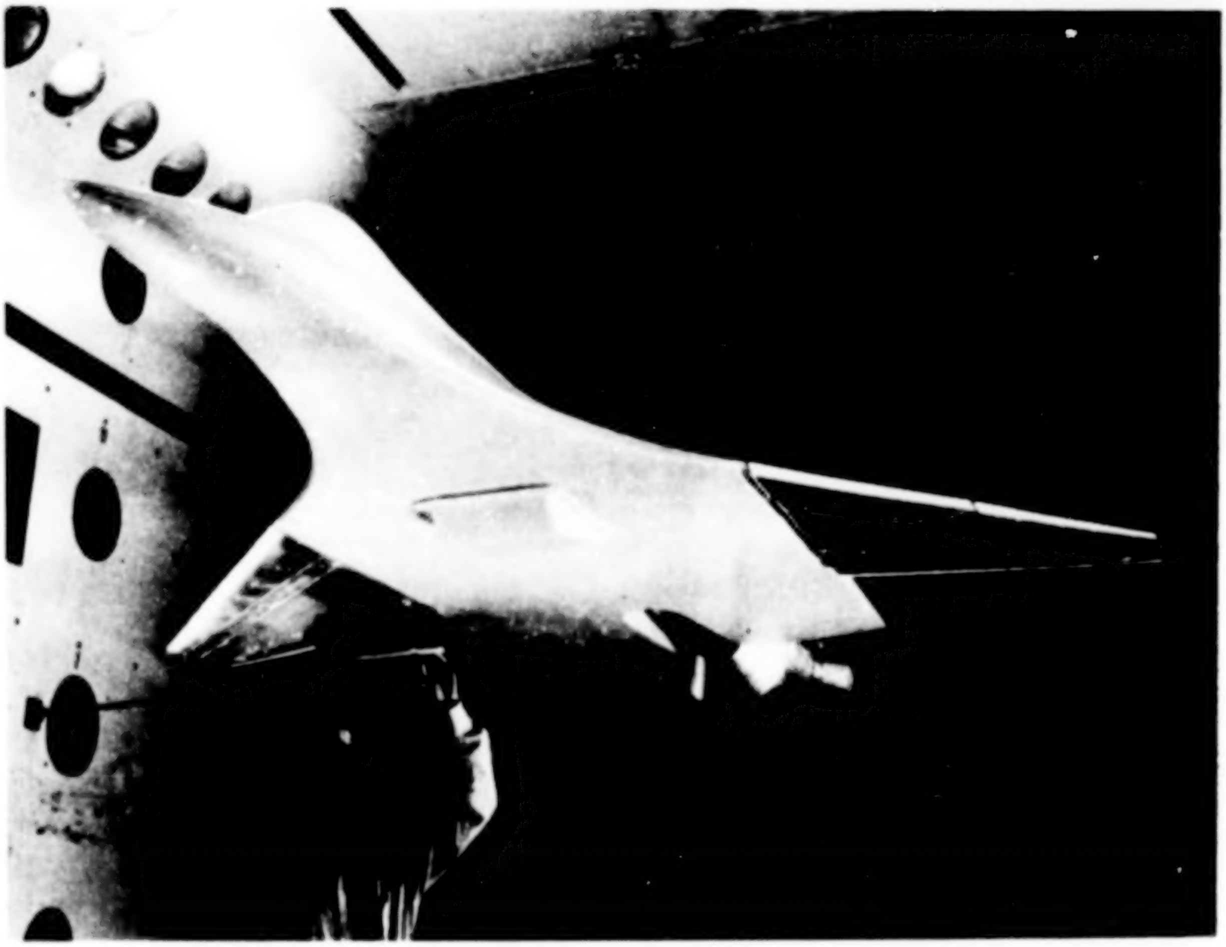

BEST COPY AVAILABLE

The Active Flexible Wing concept model has already been utilized in research experiments through two previous wind tunnel entries. The control law parameterization plot indicates that constant performance and stability may be obtained for a range of control surface deflections. Control surface deflection is a measure of the effort required by the control system to perform its function. This plot, and others like it, allow the engineer to minimize that effort by proper choice of gain factors. In a similar manner wing loads during roll maneuvers may be minimized by an alternate choice of gain factors. Additionally, relatively good agreement between analysis and experiment is indicated.

AEROSERVOELASTIC ANALYSIS VALIDATED BY WIND TUNNEL TESTS

Mach = 0.90 Dynamic pressure = 250 psf

Active flexible wing model

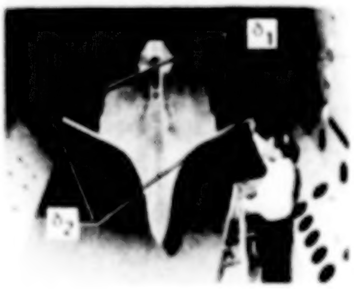

Roll rate performance

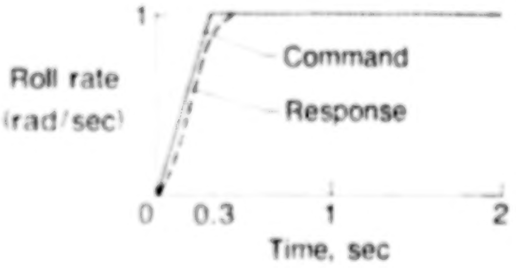

Block diagram of active roll control system

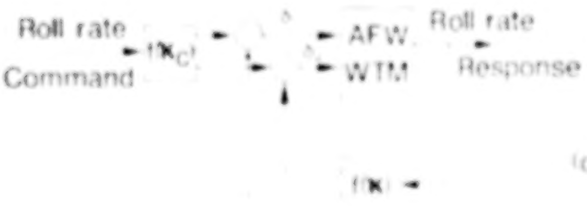

Control law parameterization

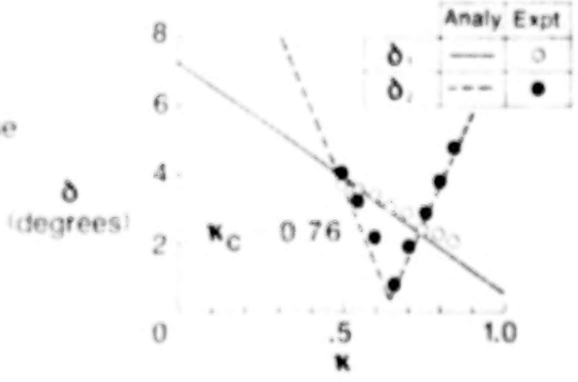

The DIR program, if funded, is envisioned as a multidisiciplinary research activity that will exploit in-house NASA research, academic research, contracted research, and system integration by the major airframers to document the benefits of synergistically combining the critical technologies. Many organizations have expressed interest in this research topic and many believe that it is important to document the benefits of early inclusion of this technology in aircraft of all classes.

COLLABORATIVE RESEARCH OPPORTUNITIES

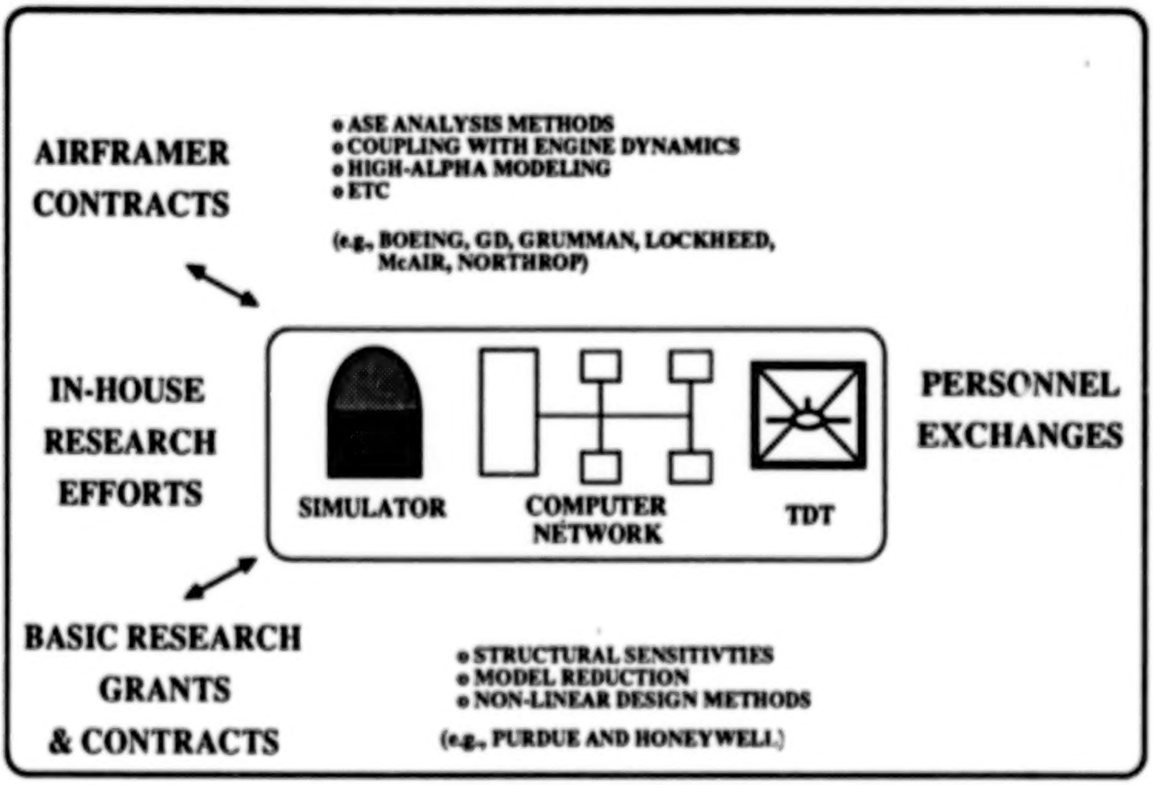

AIRFRAMER CONTRACTS

- ASE ANALYSIS METHODS
- COUPLING WITH ENGINE DYNAMICS
- HIGH-ALPHA MODELING
- ETC

(e.g., BOEING, GD, GRUMMAN, LOCKHEED, McAIR, NORTHROP)

IN-HOUSE RESEARCH EFFORTS

PERSONNEL EXCHANGES

BASIC RESEARCH GRANTS & CONTRACTS

- STRUCTURAL SENSITIVTIES
- MODEL REDUCTION
- NON-LINEAR DESIGN METHODS

(e.g., PURDUE AND HONEYWELL.)

This chart summarizes this presentation. Langley has pursued an aggressive in-house program of multidisiciplinary research combining elements of structural dynamics, aeroservoelasticity, and flight controls. Good technical progress has been made in analysis and modeling methodologies. Application to the synthesis problem is being pursued as an important part of the Active Flexible Wing project. In the event of full funding, partnerships between NASA and other parts of the aerospace community are expected.

CONCLUDING REMARKS

- LaRC HAS EMBARKED ON AN AGGRESSIVE IN-HOUSE PROGRAM TO INTEGRATE STRUCTURAL DYNAMICS, AEROSERVO- ELASTICITY, FLIGHT MECHANICS AND FLYING QUALITIES
- THERE EXISTS A TREMENDOUS OPPORTUNITY FOR SIGNIFICANT PERFORMANCE GAINS
- THE FIT TEAM HAS BEEN WORKING TOGETHER FOR 3 YEARS PLUS, HAS DEVELOPED NEW MODELING METHODOLOGIES THAT RIGOROUSLY COMBINES THE DISCIPLINES
- THE ACTIVE FLEXIBLE WING PROJECT IS A MULTIDISCIPLINARY ACTIVITY IN WHICH MEMBERS OF THE FIT TEAM ARE PARTICIPATING
- FUNDING TO ACCELERATE AND PROVIDE TEAMING ARRANGEMENTS IS BEING SOUGHT

BLANK PAGE

SESSION 2: HELICOPTERS

Chairmen: D. Anderson and R. G. Kvaternik

BLANK PAGE

AN INITIATIVE IN MULTIDISCIPLINARY OPTIMIZATION OF ROTORCRAFT

Howard M. Adelman
NASA Langley Research Center
Hampton, Virginia
and
Wayne R. Mantay
U.S. Army Aerostructures Directorate
Hampton, Virginia

INTRODUCTION

An emerging trend in the analytical design of aircraft is the integration of all appropriate disciplines in the design process (refs. 1,2). This means not only including limitations on the behavior of the design from the various disciplines, but also defining and accounting for interactions so that the disciplines influence design decisions simultaneously rather than sequentially. The integrated approach has the potential to produce a better product as well as a better, more systematic design practice. In rotorcraft design (the rotor in particular), the appropriate disciplines include aerodynamics, dynamics, structures, and acoustics. The purpose of this paper is to describe a plan for developing a helicopter rotor design optimization procedure which includes the above disciplines in an integrated manner.

Rotorcraft design is an ideal application for integrated multidisciplinary optimization. There are strong interactions among the four disciplines cited previously; indeed, certain design parameters influence all four disciplines. For example, rotor blade tip speed influences dynamics through the inertial and air loadings, structures by the centrifugal loadings, acoustics by local Mach number and air loadings, and aerodynamics through dynamic pressure and Mach number. All of these considerations are accounted for in current design practice. However, the process is sequential, not simultaneous, and often involves correcting a design late in the design schedule.

Applications of rigorous and systematic analytical design procedures to rotorcraft have been increasing, especially in the past five years. Procedures have accounted for dynamics (refs.3-9), aerodynamics (refs. 10-11), and structures (ref. 12). Generally, these applications have only considered single-discipline requirements, although in reference 5, dynamic and structural requirements were considered together, and in reference 6, dynamics and aeroelastic stability were combined. Integrated multidisciplinary applications to rotorcraft are largely nonexistent.

In early 1985, several occurrences led to an excellent opportunity at the NASA Langley Research Center to address the multidisciplinary design problem for rotorcraft. The Interdisciplinary Research Office was established and charged with the development of integrated multidisciplinary optimization methods. Nearly concurrently, the Army Aerostructures Directorate at Langley established the goal of improving rotorcraft design methodology by "discipline integration." Close cooperation between the NASA and Army organizations led to initial plans for a comprehensive, integrated analytical design capability. By 1986, a group of NASA/Army researchers had formed a committee and began detailed planning for this activity. The committee, designated IRASC (Integrated Rotorcraft Analysis Steering Committee), has now completed the bulk of the planning and has formulated the approach described in this paper.

The development of an integrated multidisciplinary design methodology for rotorcraft is a three-phased approach. In Phase 1, the disciplines of blade dynamics, blade aerodynamics, and blade structures will be closely coupled, while acoustics and airframe dynamics will be decoupled from the first three and will be accounted for by effective constraints on the other disciplines. In Phase 2, acoustics will be integrated with the first three disciplines. Finally, in Phase 3, airframe dynamics will be fully integrated with the other four disciplines. This paper deals only with the Phase 1 approach and includes: details of the optimization formulation, design variables, constraints, and objective function as well as details of discipline interactions, analysis methods, and methods for validating the procedure.

LANGLEY PARTICIPANTS IN THE ACTIVITY

The work described in this paper represents the combined efforts of a team of researchers and managers at the NASA Langley Research Center and Army Aerostructures Directorate involved in analysis and optimization of rotorcraft. Shown on the left side of figure 1 are the members of the IRASC (Integrated Rotorcraft Analysis Steering Committee). Shown on the right side of the figure are the technical contributors. This team includes experts in the areas of rotorcraft aerodynamics, dynamics and aeroelasticity, structures, and acoustics, as well as optimization and sensitivity analysis.

Integrated Rotorcraft Analysis Steering Committee (IRASC)		Technical Contributors
Wayne Mantay	Chairman	Aditi Chattopadhyay
Howard Adelman	Vice-Chairman	Ruth Martin
Ray Kvaternik		T. Sreekanta Murthy
Mark Nixon		Jocelyn Pritchard
Paul Pao		Joanne Walsh
Kevin Noonan		Matt Wilbur

Figure 1

OBJECTIVE OF THE EFFORT

Figure 2 represents the Charter of the IRASC activity. The unique features of the work are the emphasis on integrating the disciplines and explicitly accounting for the interactions among disciplines. While the team does not intend to develop new or improved analyses in any of the included disciplines, the latest developments in rotorcraft disciplinary analysis will be used. Finally, it is a goal of the team to stimulate activity in the rotorcraft (and the aircraft) community in the general area of multidisciplinary design integration and the use of formal Mathematical Programming in design work.

Develop and validate an integrated multidisciplinary design capability involving aerodynamics, dynamics, structures, and acoustics which leads to improved design practices and improved rotorcraft.

Figure 2

FUNDAMENTAL DECISION/STRATEGY

The rotorcraft optimization effort at Langley has a three-phased plan (fig. 3). The initial phase, which is well under way, will decompose the rotor design problem. This will be accomplished by driving the design through the integration of the disciplines of aerodynamics, dynamics, and structures while satisfying additional constraints imposed by airframe dynamics and rotor acoustics. The latter constraints will account for the influences of the airframe response and acoustics behavior on the overall optimization process. Phase 2 of the design plan will include rotor acoustics as a discipline inside the optimization loop; that is, integrated with aerodynamics, structures, and dynamics. Finally, in Phase 3 of the effort, all five disciplines will be fully integrated inside of an iterative design loop. This paper focuses primarily on the Phase 1 activity.

Phase 1

- **Decompose the design problem**
  - **Blade aerodynamics, dynamics, structures**
  - **Airframe analysis/modeling and acoustics**
- **Develop representation of acoustics and airframe influences on blade aerodynamic, dynamic, structural optimization**

Phase 2

- **Bring acoustics into optimization loop**

Phase 3

- **Bring airframe dynamics into optimization loop**

Figure 3

FOCUS NO. 1 - WHITE PAPER

Publication and critique of a "white paper" (fig. 4) detailing the plan for rotorcraft optimization at Langley is viewed as a prime focal point of the activity. The paper, which is presently in draft form, will present the goals of the design effort, as well as the approach and validation plan. The approach will discuss strategy, analytical methods, and discipline couplings. The validation procedure will document test problems to be used to examine the fidelity of the specific discipline tools used, as well as the overall optimization procedure. Finally, the white paper will be disseminated to industry for critique and a workshop is planned to consolidate feedback to the plan.

- Goals of the activity
- Approach and plan
  - Formulation of optimization strategy
  - Governing mathematics (varying detail)
  - Definition of interactions
  - Analysis methods (codes) to be used
  - Validation methods - test problems
- Status
  - First draft written
  - To be critiqued by industry

Figure 4

FOCUS NO. 2 - ROTOR DESIGN

A practical rotor design will be the end result of the Langley optimization effort (fig. 5). The purpose of this "fidelity check" includes not only an overall test of the methodology, but also a measure of each discipline's modeling effectiveness. The test problem for Phase 1 will contain a rotor task, mission scenario, and challenging design requirements. Simulation models describing aerodynamic, structural, and dynamic systems will be formulated to allow for key interdisciplinary couplings. Design variables, constraints, and a specific objective function will be identified. As the design activity progresses, so will the verification of individual discipline models. Finally, the optimum design will be wind tunnel tested for fidelity of the entire Phase 1 process.

- **Apply Phase 1 method to rotor design**
- **Define test problem**
  - **Rotor task and mission**
  - **Design requirements**
- **Generate math models**
  - **Aerodynamic**
  - **Dynamic**
  - **Structure**
  - **Incorporate couplings**
- **Formulate optimization problem**
  - **Objective function**
  - **Design variables**
  - **Constraints**
- **Validate design methodology**
  - **Discipline tools**
  - **Overall**

Figure 5

INTEGRATED ROTORCRAFT OPTIMIZATION DEVELOPMENT PLAN

Figure 6 depicts the general sequence of tasks that will lead to a fully integrated rotor blade aerodynamic/dynamic/structural optimization procedure which also accounts for acoustic and airframe dynamic influences. The dynamic optimization work is building on the work described in references 5, 6, and 9. The rotor aerodynamics activity has been separated into two parts. The first is aerodynamic performance optimization which is a continuation of the work described in reference 10. The second is an integration of aerodynamic loads analysis with dynamics - a procedure wherein the local airloads can be adjusted by varying the planform dimensions and twist of the blade to reduce dynamic response. A merger of the rotor performance optimization with the airload/dynamics optimization will yield a fully integrated aerodynamic/dynamic procedure. The rotor structural optimization is a continuation of the work of reference 12. A merger of all the aforementioned procedures, with the acoustic and airframe constraint interfaces, will lead to the fully integrated Phase 1 procedure. The resulting capability will be applied to a rotor test article to validate the procedures.

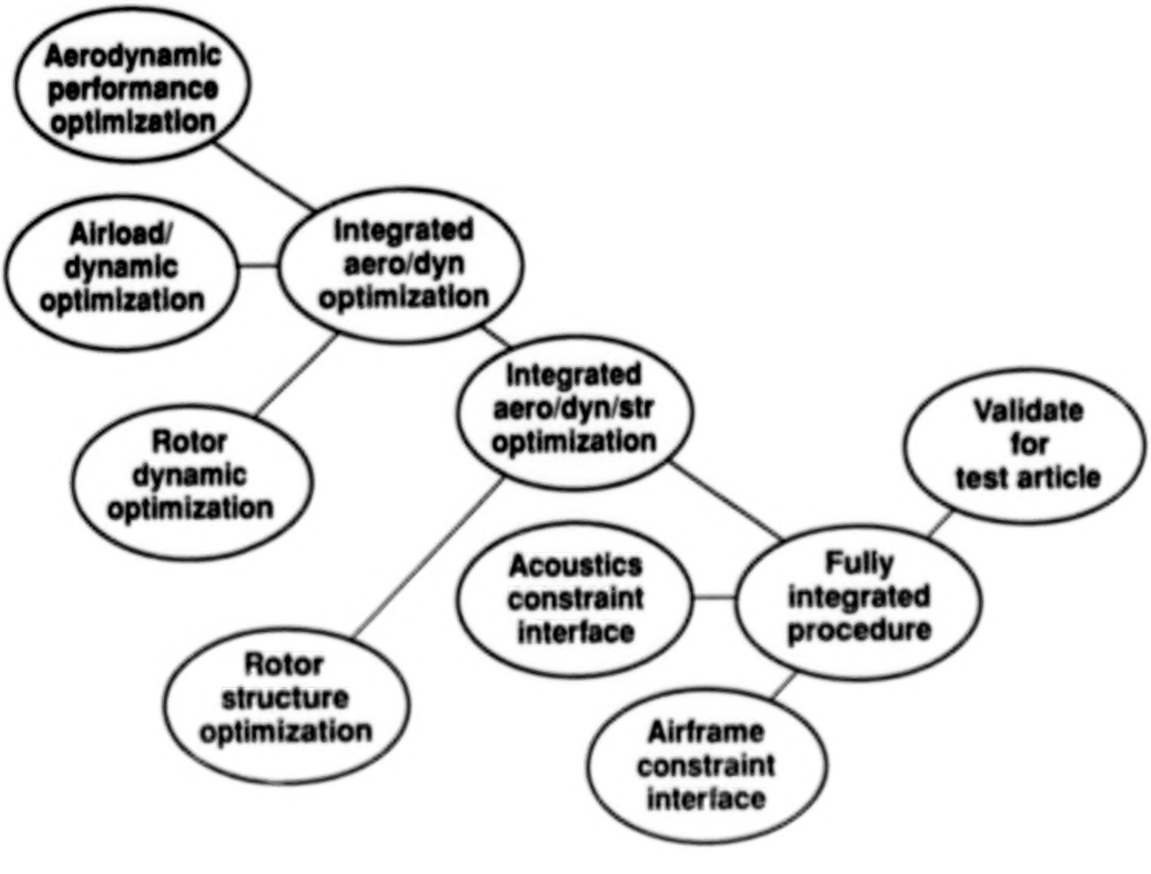
Aerodynamic performance optimization
Airload/ dynamic optimization
Integrated aero/dyn optimization
Rotor dynamic optimization
Integrated aero/dyn/str optimization
Validate for test article
Acoustics constraint interface
Fully integrated procedure
Rotor structure optimization
Airframe constraint interface

Figure 6

DEFINITION OF THE OPTIMIZATION PROBLEM

As indicated in figure 7, the next section of the paper consists of details of the integrated rotorcraft optimization problem. Included are descriptions of the following: the objective function (the quantity to be minimized for obtaining an optimum design); the design variables (dimensions and other parameters of the design); constraints (a set of behavioral or characteristic limitations required to assure acceptable and safe performance); and definitions of the interactions among the disciplines.

- **Objective function**
- **Design variables**
- **Constraints**
- **Interactions among disciplines**

Figure 7

CONTRIBUTORS TO OBJECTIVE FUNCTION

In formulating the objective function, a number of indicators (fig. 8) were considered. Basically, the indicators fell into two categories - penalty types such as weight and cost; and performance types such as vibratory loads (shears and moments); and required horsepower. It was decided, for the purpose of the Phase 1 work, to choose performance type quantities for the objective function; specifically, transmitted vertical vibratory hub shear and horsepower required at several flight conditions. Blade mass will be prevented from becoming excessive by enforcing an upper limit constraint. Cost is not explicitly accounted for in the formulation.

- **Blade mass**
- **Cost**
- **Vibratory loads**
- **Required horsepower**

Figure 8

FORM OF OBJECTIVE FUNCTION

The objective function is a linear combination of the main rotor horsepower at five flight conditions plus the transmitted vertical vibratory hub shear at a frequency of N times the blade angular speed (where N is the number of blades). As shown in figure 9, the objective function contains weighting factors K_1 through K_6 which will be assigned based on a mission criterion to be determined. The five flight conditions referred to above include hover, cruise, high speed, maneuver, and maximum range. The speed and load factor specifications for these conditions are given in the lower portion of the figure.

- **Linear combination of main rotor horsepower at five flight conditions and transmitted vertical hub shear**
- $F = K_1 HP_1 + K_2 HP_2 + K_3 HP_3 + K_4 HP_4 + K_5 HP_5 + K_6 S$

Flight condition	Description	Velocity (Kts)	Load Factor
1	Hover	0	1.0
2	Cruise	140	1.0
3	High Speed	200	1.0
4	Maneuver	120	3.5
5	Max. Range	95	1.0

Figure 9

BLADE MODEL AND DESIGN VARIABLES

Figure 10 is a depiction of the rotor blade model to be used in the Phase 1 optimization activity. Also shown in figure 10 are the design variables which are defined in figure 11. The blade model can be tapered in both chord and depth. The depth can be linearly tapered from root to tip. The chord is constant from the root to a spanwise location (referred to as the point of taper initiation) and is linearly tapered thereafter to the tip. Design variables which characterize the overall shape of the blade include the blade radius, point of taper initiation, taper ratios for chord and depth, the root chord, the blade depth at the root, the flap hinge offset, and the blade maximum twist. Tuning masses located along the blade span are characterized by the magnitude and locations. Design variables which characterize the spar box beam cross-section include the wall thicknesses at each spanwise segment and the ply thicknesses at 0° and $\pm 45^\circ$. Additional design variables include the number of rotor blades, the rotor angular speed, and the distribution of airfoils.

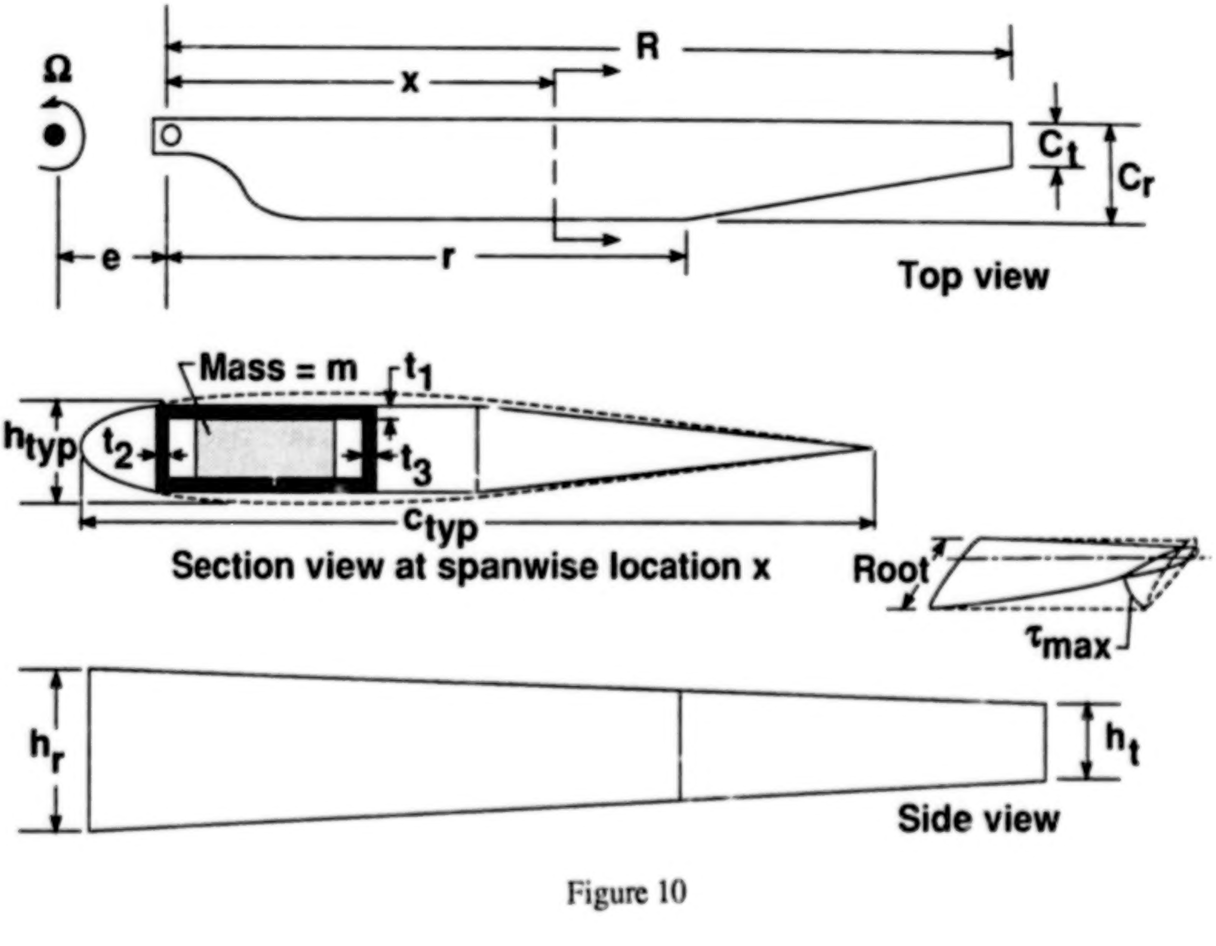

Figure 10

BLADE MODEL AND DESIGN VARIABLES (CONC.)

Description	Symbol
Tuning mass at location i	M_i
Spanwise location of i-th mass	X_i
Wing box dimensions	t_1, t_2, t_3
Ply thicknesses	t_{45}, t_o
Depth of blade at root	h_r
Ratio of blade depths at tip and root	$\lambda_h = h_r/h_t$
Maximum pre-twist of blade	$\tau \max$
Percent blade span where taper begins	r
Width of blade at root	C_r
Airfoil distribution	–
Hinge offset	e
Blade angular velocity	Ω
Number of blades on rotor	N
Blade radius	R
Ratio of root chord to tip chord	$\lambda_c = C_r/C_t$

Figure 11

CONSTRAINTS OVERVIEW

As previously described, the Phase 1 activity is based on integrating the blade aerodynamic, dynamic, and structural analyses within the optimization procedure. The acoustics and airframe dynamics analyses are decoupled from the first three disciplines and their influences are expressed in terms of constraints. Accordingly, the total set of constraints is made up of two subsets as indicated in figure 12. The first subset consists of constraints which are evaluated directly from the first three disciplinary analyses and are a direct measure of the degree of acceptability of the aerodynamic, dynamic, and structural behavior. The second subset represents indirect measures of the satisfaction of constraints on the acoustics behavior and the requirement of avoiding excessive vibratory excitation of the airframe by the rotor.

- **Aerodynamic**
- **Dynamic**
- **Structure**

Evaluated directly from analysis

- **Acoustic**
- **Airframe**

Expressed indirectly as constraints on disciplines in top group

Figure 12

SUMMARY OF CONSTRAINTS

The constraints are summarized in figures 13 and 14. The first two constraints are for aerodynamic performance and require that for all flight conditions, main rotor horsepower not exceed available horsepower and that airfoil section stall not occur at any azimuthal location. The next nine constraints address blade dynamics. The first requires that the blade natural frequencies be bounded to avoid approaching any multiples of rotor speed. The next five impose upper limits on the blade vertical and inplane loads, transmitted hub shear, and hub pitching and rolling moments. The next three dynamic constraints are an upper limit on blade response amplitude, a lower limit on blade autorotational inertia, and finally, the aeroelastic stability requirement. The structural constraints consist of upper limits on box beam stresses, blade static deflection, and blade twist deformation. The acoustic constraints are expressed as an upper bound on the tip Mach number and an upper bound on the blade thickness to limit thickness noise; and an upper bound on the gradient of the lift distribution to limit blade vortex interaction (BVI) and loading noise. The effective airframe constraints are expressed first as a separation of the fundamental blade inplane natural frequency in the fixed system from the fundamental pitching and rolling frequency of the fuselage. Second is a bounding of the blade passage frequency to avoid the proximity to any fuselage frequency. The final constraint is an upper limit on the blade mass which will avoid any designs which satisfy the constraints at the expense of large mass increases.

Constraint Description	Form of Constraint	Comments
Main rotor horsepower	$HP_i \le HP$ avail for i-th condition	For 5 flight conditions
Airfoil section stall	$C_D \le C_D \max$	Enforced at 12 azimuthal locations
Blade frequencies	$f_{il} \le f_i \le f_{iu}$	
Blade vertical load	$V_{ik} \le V\max$	
Blade inplane load	$H_{ik} \le H\max$	
Transmitted in-plane hub shear	$X_k \le X\max$ $Y_k \le Y\max$	
Hub pitching moment	$P_k \le P\max$	
Hub rolling moment	$R_k \le R\max$	
Blade response amp.	$q_k \le Q\max$	
Autorotational inertia	$\Sigma m_i r_i^2 \ge \alpha$	
Aeroelastic stability	$\mathrm{Re}(\lambda) \le -\varepsilon$	
Wing box stresses	$R \le 1$ R = Tsai - Hill criterion	

Figure 13

SUMMARY OF CONSTRAINTS (CONC.)

Constraint Description	Form of Constraint	Comments
Blade tip deflection	$w \leq w\max$	
Blade twist	$\theta \leq \theta\max$	
Blade tip Mach no.	$M \leq M\max$	Limits thickness noise
Blade thickness	$h \leq h\max$	
Blade lift distribution	$dC_l/dx \leq S\max$	Limits BVI & loading noise
Ground resonance	$\lvert\Omega - W_{l1}\rvert \leq W_{af}$	Effective airframe constraint
Rotor/Airframe frequency coupling	$f_l \leq N\Omega \leq f_u$	
Blade mass	$M \leq M$ upper	

Figure 14

ANALYSIS ASPECTS

The analytical tools (summarized in fig. 15) must provide technical fidelity in phenomena prediction, as well as connectivity between disciplines. The areas of aerodynamics, dynamics, and structures will utilize codes to predict response, as well as sensitivity information. The constraint-providing disciplines of acoustics and airframe dynamics have the analysis task of defining the impact of the design on acoustic energy and fuselage response.

The aerodynamic analysis for rotor performance prediction will include a hover momentum/strip theory code for hover and climb applications (ref. 13). The CAMRAD analysis will be used for forward flight and maneuver performance. In order to assure that the latest developments in inflow analyses are available, some modularity will be provided in the inflow modeling based on recent fidelity assessments (ref. 14).

Rotor dynamics will utilize CAMRAD for forced response calculations. Finite element modeling (ref. 15) and modal analysis (ref. 16) will form the tools for the dynamic tuning before the global analysis predicts the final blade loads, response, and rotor stability.

The structural codes involve a combination of beam analysis and laminate analysis. The beam analysis (e.g., ref. 12) is applied to the blade planform model. The laminate analysis will be applied to one or more cross-section models. The beam model consists of equivalent stiffness and masses from which displacements and forces are computed. The internal blade structure is represented by cross-section models to calculate resultant stresses associated with each beam model segment. The laminate analysis then uses these stresses to determine critical structural margins of safety.

The effectiveness of imposing Phase 1 acoustic constraints will be quantified by using the WOPWOP code (ref. 17), with appropriate motion and loading inputs from CAMRAD. Low frequency loading, thickness, and BVI noise will be generated from this analysis.

Airframe dynamics constraints for Phases 1 and 2 will result from fixed-system frequency predictions and will neglect hub motion. Phase 3 of the effort will involve finite element modeling and impedance tailoring to effect favorable rotor-body coupling in the design process.

ANALYSIS ASPECTS (CONC.)

Aerodynamic	**Hover momentum/strip theory**
	Global forward flight code
	Inflow modules
Dynamic	**Finite element modeling**
	Modal code
	Global analysis/forced response
	Eigen analysis for stability
Structure	**Beam models**
	Laminate model
Acoustic	**WOPWOP code to verify acoustic acceptability**
Airframe Dynamics	**Fixed system frequency prediction**
	Finite element models - NASTRAN

Figure 15

INTERDISCIPLINARY COUPLINGS

Phase 1 of the Langley rotorcraft optimization effort will utilize several design variables which have historically been significant drivers of disciplinary phenomena. In addition, other variables are being included to provide other unexplored design opportunities. Figure 16 shows our first attempt to quantify the interactions among the disciplines through the design variables. For example, rotor tip speed has driven past rotor designs based solely on acoustics, performance, or dynamics. This variable also influences blade structural integrity and fixed system response to transmitted loads. This provides the strong interdisciplinary coupling for tip speed shown in figure 16. There are variables, such as blade twist, which can strongly influence some disciplines, such as aerodynamics, while not perturbing others (e.g., structures) and other variables such as hinge offsets which, heretofore, have not greatly influenced conventional rotor design.

It is a significant part of the current design methodology effort to explore not only the obvious strong design variable couplings, but also to address those variables which may provide design synergism for multidisciplinary design goals. This may provide a design key for missions which have not been accomplished with today's rotorcraft.

Variable	Acoustics	Aerodyn. (Perf & Loads)	Dynamics	Structures	Fuselage Dynamics
Airfoil Dist.	S	S	W	W	W
Planform	S	S	S	S	S/W
Twist	W	S	S	W	W
Tip speed	S	S	S	S	S
Blade number	S	W	S	W	S
Stiffness	W	S	S	S	S/W
Mass dist.	W	W	S	S	S/W
Hinge offset	W	W	S/W	W	S/W

S = Strong interaction
W = Weak interaction

Figure 16

INTEGRATED AERODYNAMIC/DYNAMIC/STRUCTURAL OPTIMIZATION OF ROTOR BLADES

Figure 17 is a flow chart which explains how the integrated procedure will function. The current set of design variables (summarized in fig. 11) will be input to design variable preprocessors which will generate input tailored for each analysis. For example, box beam cross-sectional dimensions will be used to compute values of EI and GJ for use in the dynamic analysis. Each disciplinary analysis will be carried out using the preprocessed data along with the necessary input which is the product of other disciplinary analyses. For example, as the flow chart shows, the dynamic response requires airloads from the aerodynamic loads analysis. The appropriate output from each disciplinary analysis is collected in a module which computes the objective function (fig. 9) and constraints (figs. 13 and 14). The next major step is the sensitivity analysis to calculate derivatives of the objective function and constraints with respect to the design variables. At this stage, all the information is available for the optimizer module (based on the program CONMIN (ref. 18)) wherein the values of the design variables are updated. The above steps are repeated until a converged design is obtained. Convergence requires that the objective function is minimized and all constraints are satisfied.

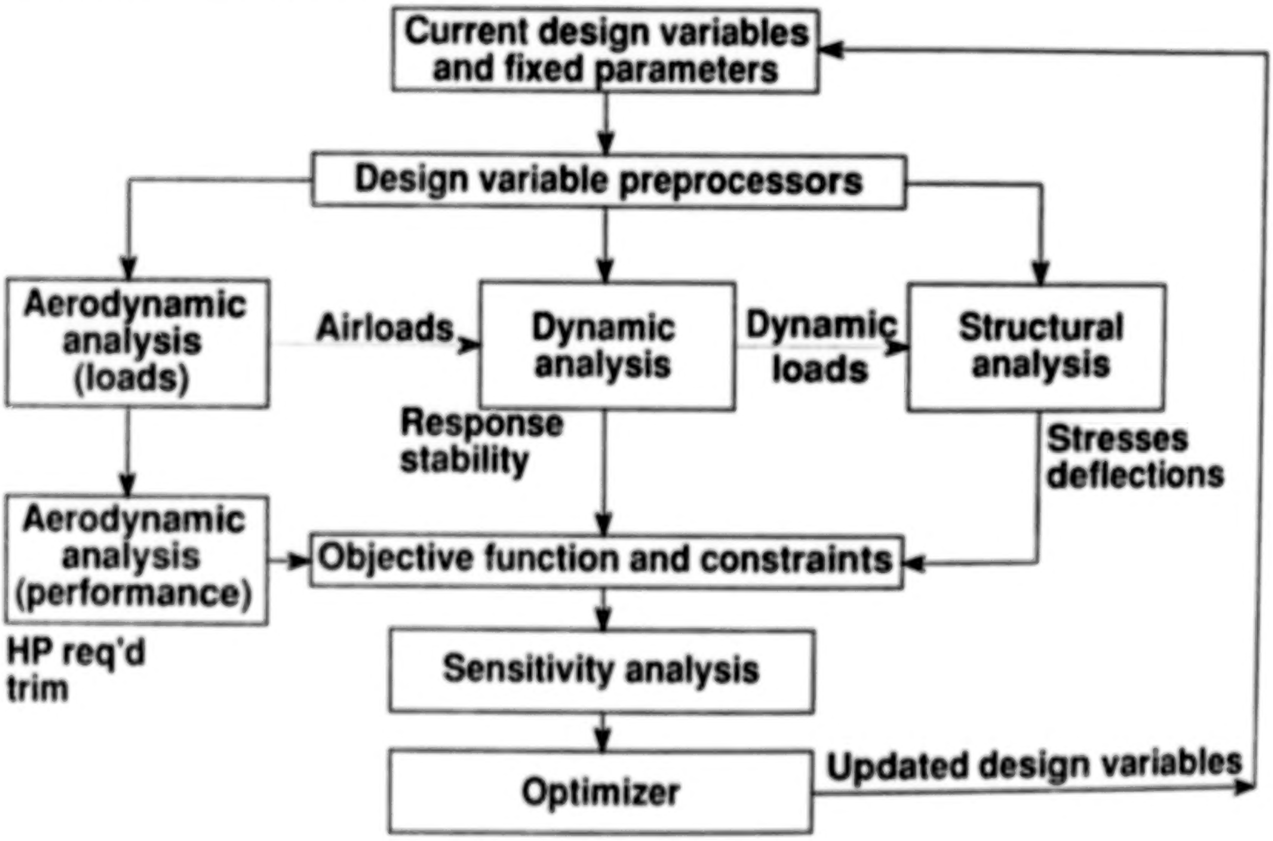
Current design variables and fixed parameters
Design variable preprocessors
Aerodynamic analysis (loads)
Airloads
Dynamic analysis
Dynamic loads
Structural analysis
Response stability
Stresses deflections
Aerodynamic analysis (performance)
HP req'd trim
Objective function and constraints
Sensitivity analysis
Optimizer
Updated design variables

Figure 17

RESULTS OBTAINED TO DATE

As indicated in figure 18, progress has been made in the areas of aerodynamic performance optimization, dynamic optimization, optimum placement of tuning masses for vibration reduction, and structural optimization. Selected results from these activities are highlighted in the next portion of the paper.

- **Aerodynamic performance optimization**
- **Dynamic optimization**
- **Optimum placement of tuning masses**
- **Structural optimization**

Figure 18

RESULTS - AERODYNAMIC PERFORMANCE OPTIMIZATION

A Mathematical Programming technique has been developed to minimize the hover horsepower for a helicopter with a specified design gross weight operating at a specified altitude and temperature (fig. 19). A conventional design approach is a two-step iterative method. The first step is design for optimum hover performance by varying taper ratio, point of taper initiation, and twist until the rotor blade configuration with the lowest hover horsepower is obtained. In the second step, this best hover design is modified by changing the root chord to meet forward flight and maneuverability requirements. The Mathematical Programming approach uses the same performance analyses as the conventional approach, but couples a general-purpose optimization program to the analyses. The conventional and Mathematical Programming approaches have been used to define the blade configuration which provides the lowest hover horsepower and satisfies forward flight and maneuverability requirements. The figure also summarizes results for the final design variable values and the main rotor horsepower required for hover from each approach. The Mathematical Programming approach produced a design with more twist, a point of taper initiation further outboard, and a smaller blade root chord than the conventional approach. The Mathematical Programming design required 25 less hover horsepower than the conventional design. Most significantly, the Mathematical Programming approach obtained results more than ten times faster than the conventional approach.

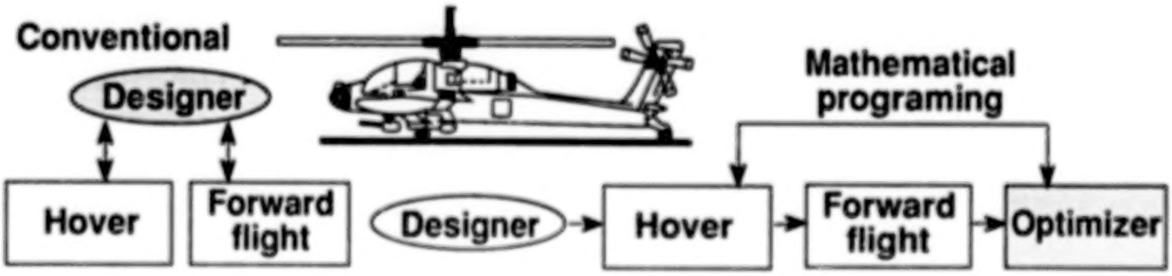

		Conventional	Mathematical programing
Objective function: Hover horsepower		1558 hp	1533 hp
Design variables	Twist, deg	-12	-15
	Percent taper	.80	.91
	Taper ratio	3.0	3.1
	Root chord, ft	2.3	1.78
Design time		5 weeks	2 days

Figure 19

RESULTS - DYNAMIC OPTIMIZATION

A rotor dynamic optimization problem is summarized in figure 20. Blade mass is the objective function. Upper and lower bound constraints are placed on the first five natural frequencies (elastic modes only) of the blades to separate them from the excitation frequencies. Also, a lower bound constraint is imposed on the blade autorotational inertia. A stress constraint is used to guard against structural failure due to blade centrifugal stress, and side constraints are imposed on the design variables to avoid impractical designs. The design variables are the box beam spar wall thicknesses, the magnitudes of tuning masses, the blade taper ratio, and the box beam height at the blade root. The program CAMRAD and CONMIN are used for the blade modal analysis and the optimization, respectively. A sensitivity analysis calculates analytical derivatives of the objective function, autorotational inertia and stress constraints, along with finite difference derivatives of the frequency constraints.

Objective function - blade mass W

$W = W_b + W_o$

W_b = box beam mass

W_o = nonstructural mass

Constraints

Frequency: $f_{i_l} \le f_i \le f_{i_u}$

$f_i \rightarrow$ first three lead-lag
first two flap

Autorotational inertia:

$$\left(\sum_{j=1}^{N} W_j r_j^2 \right) \ge \alpha$$

α: minimuim rotary inertia

Stress constraints: σ/centrifugal $\le \sigma a$

Design variables - Box beam cross-sectional dimensions
Tuning masses
Blade taper ratio

Figure 20

RESULTS - DYNAMIC OPTIMIZATION (CONCLUDED)

Optimum designs for minimum mass rotor blades have been obtained for both rectangular and tapered blades. The optimum designs are compared with an existing baseline blade denoted the 'reference' blade in figure 21. The reference blade is based on an actual flight article and is described in more detail in references 5 and 9. The figure also shows the box beam wall thickness distributions for the rectangular blade using 30 design variables (t_1, t_2, t_3 at ten spanwise locations), and for the tapered blade with 42 design variables (ten lumped masses,and h_r and λ_h are the additional design variables). Blade mass reductions of four to six percent (compared to a baseline or reference blade) have been achieved without violating the imposed constraints. The optimization process tends to shift the wall thickness distribution outboard for both designs due to the presence of the autorotational inertia constraint. The tapered design requires more outboard mass shift, but this is easily accomplished within the stress constraints.

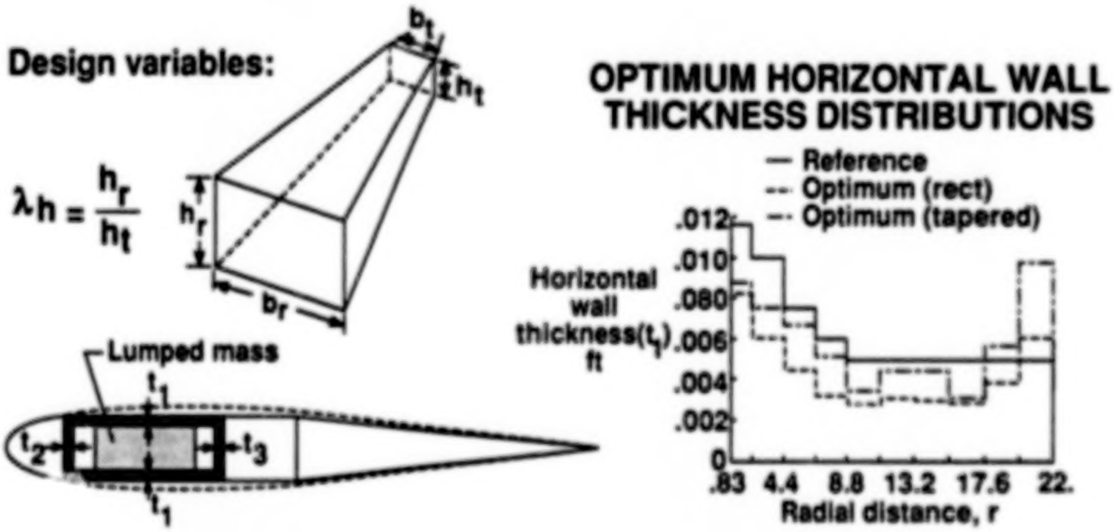

	Reference	Optimum	
		Rectangular	Tapered
Blade weight (lbs)	98.3	93.6	92.1
Percent reduction	-----	4.7	6.2

Figure 21

RESULTS - OPTIMUM PLACEMENT OF TUNING MASSES

The design problem (shown in figure 22) is to find the best combination of tuning masses and their locations to minimize blade root vertical shear without a large mass penalty. The objective function is a combination of vertical shear and the sum of the tuning masses. Constraints are placed on the frequencies to avoid resonance. The strategy employed reduces the total shear as a function of time during a revolution of the blade.

The example problem (figure 23) is a beam representation of an articulated rotor blade. The beam is 193 inches long with a hinged end condition and is modeled by ten finite elements of equal length. The model contains both structural mass and lumped (non-structural) masses. Three lumped masses are to be placed along the length of the beam. The strategy was applied to a test case of two modes responding to three harmonics of airload. The figure compares the blade vertical root shear s(t) plotted versus azimuth for the initial and final designs. The peaks on the initial curve have been reduced dramatically. For example, the oscillatory (1/2 p-p) load was reduced from 78 lbs to 0.6 lbs - nearly two orders of magnitude.

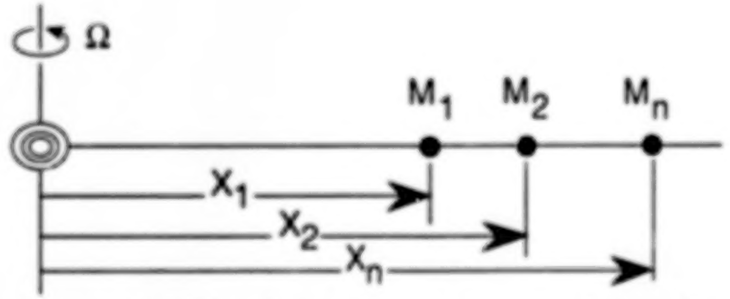

- **Design goal - Find optimum combination of masses and their locations to reduce blade root vertical shear**
- **Method - Formulate optimization procedure**
  - **Use masses and locations as design variables**
  - **Minimize -**
    - **Blade root vertical shear**
    - **Added mass**

Figure 22

RESULTS - OPTIMUM PLACEMENT OF TUNING MASSES (CONC.)

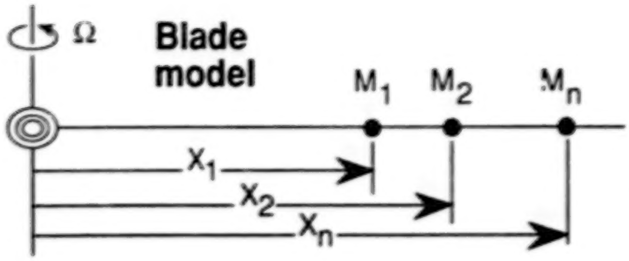

	Initial	Final
X_1 (in)	135.0	153.0
X_2 (in)	154.0	154.0
X_3 (in)	174.0	154.0
M_1 (lbm)	5.2	7.9
M_2 (lbm)	6.5	9.7
M_3 (lbm)	6.6	9.2
M_{tot} (lbm)	18.3	26.8
1/2 P-P (lbf)	78.0	0.60

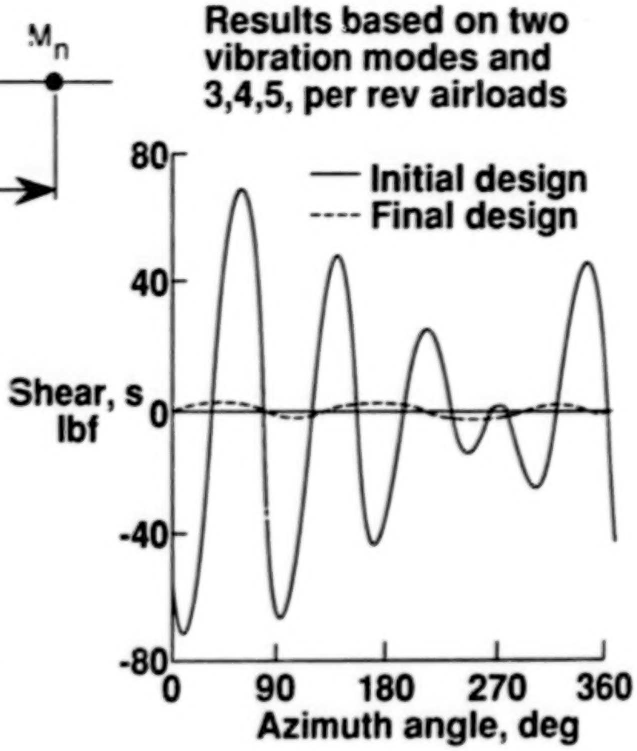

Figure 23

RESULTS - STRUCTURAL OPTIMIZATION

A blade structural optimization procedure (fig. 24) applicable to metal and composite blades has been developed in which the objective function is blade mass with constraints on stresses in the spars and in the skin, twist deformation, and autorotational inertia. The design variables are the total spar thickness and for the composite blade the percentage of ±45° plies (the remaining plies assumed to be at 0°). This procedure is described in detail in reference 12, and additional applications of the methods are also given in reference 12.

- **Objective function:** **Blade mass**
- **Constraints:** **Stress in skin and spars, twist deformation, autorotational inertia**
- **Design variables:** **Spar thicknesses, % of ±45° plies**

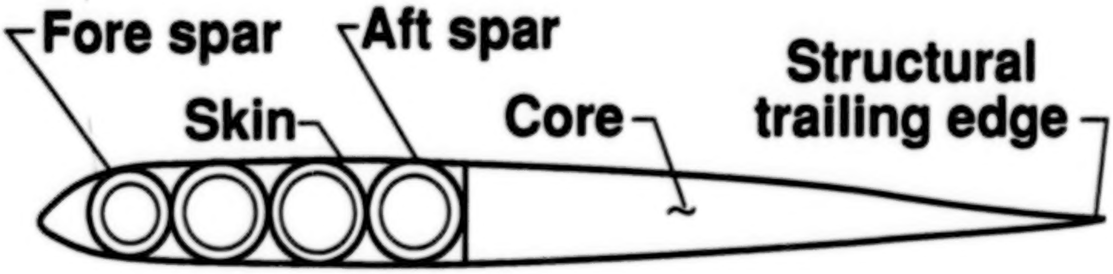

Figure 24

Two examples of rotor blade design (fig. 25) were generated using the structural design methodology. Both designs use the UH-60A Black Hawk titanium spar blade as a baseline. First, a titanium spar blade design was generated. A maximum twist deformation of 3.1 degrees was selected. The structural constraint requires that the calculated stresses not exceed the allowable material strength which is assessed using the Tsai-Hill failure criterion (ref. 12). The autorotational capability is satisfied by requiring the mass moment of inertia to be at least 19[illegible]0 in-lbs-s^2 per blade.

As shown in figure 25, the minimum metal spar thickness which satisfies all of the constraints is .130 inches and corresponds to a blade weight of 207 pounds. The actual UH-60A titanium spar is .135 inches thick and weighs 210 pounds. The new titanium spar design is only three pounds different from the actual UH-60A blade, demonstrating that the mechanics of the design methodology can produce blade designs similar to conventional design processes for the same design allowances and material. A second design was developed using a single T300/5208 graphite/epoxy D-spar. The composite design also satisfied the required constraints and the minimum weight design had a .105 inch thick spar with 20 percent of the plies oriented at ±45 degrees. The composite blade weighed 163 pounds which represents a 21.5 percent reduction over the actual UH-60A blade.

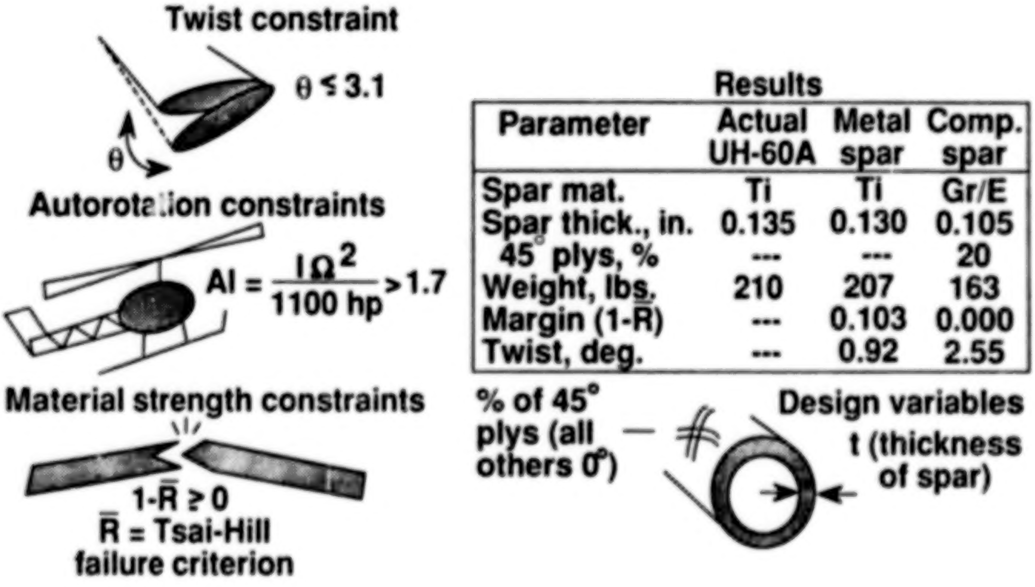
Twist constraint
$\theta \leq 3.1$
θ
Autorotation constraints
$AI = \frac{I\Omega^2}{1100\ hp} > 1.7$
Material strength constraints
$1-\bar{R} \geq 0$
$\bar{R}$ = Tsai-Hill failure criterion
% of 45° plys (all others 0°)
Design variables
t (thickness of spar)

Results

Parameter	Actual UH-60A	Metal spar	Comp. spar
Spar mat.	Ti	Ti	Gr/E
Spar thick., in.	0.135	0.130	0.105
45° plys, %	---	---	20
Weight, lbs.	210	207	163
Margin (1-$\bar{R}$)	---	0.103	0.000
Twist, deg.	---	0.92	2.55

Figure 25

VALIDATION OF PROCEDURES

The process of validating the optimization methodology (fig. 26) involves substantially more than evaluating the success of the final design. Specifically, the analyses used in optimizing the rotor during the Phase 1 effort will be examined for predictive fidelity and design technique validation. The usefulness of the basic tools involves not only accuracy of analysis, but also a reliable parametric sensitivity capability. Several opportunities are currently available to assess the fidelity of the analyses. For example, rotor performance, dynamics, and acoustics predictions need accurate inflow distributions for various flight conditions. Recent experimental efforts (e.g., ref. 19) and code validations (ref. 14) are helping to provide confidence in the available inflow models. Rotor geometric design variable sensitivity (e.g., effect of taper on performance) which was reasonably well-known for past rotor designs, is being re-examined in light of recent correlation anomalies for high-speed flight. Acoustic source mechanisms and modeling validity are also being examined (ref. 20), especially for parametric sensitivity of the acoustic energy to rotor state. Structural coupling mechanics are being exploited in new rotor designs to assess the structural tailoring benefits while satisfying structural integrity requirements (ref. 21).

Proof of the fidelity of design techniques is crucial to the overall design optimization effort. For example, aerodynamics and dynamics interact so strongly in rotor design that basic aeroelastic tailoring efforts must be validated. Such a validation effort is being undertaken at Langley, as well as other research centers (ref. 22). Also, since rotor speed is a strong driver for aeroelastic response, a program to assess variable RPM designs is under way at Langley. The object of this effort is to define the benefits and limitations of an aerodynamically and dynamically designed multi-speed rotor. In addition to design techniques, which capitalize on the strong effects of certain design variables, small variances in other blade characteristics may impede the practical operation of even conventional designs. Hence, the ability to accurately predict even these secondary phenomena is important for the design effort. For example, track-and-balance sensitivity experiments and studies are being undertaken which can lead to a practical design capability to eliminate blade-to-blade variability effects.

VALIDATION OF PROCEDURES (CONC.)

- Basic predictive tools
  - Rotor inflow fidelity
  - Acoustic source mechanisims
    - BVI
    - Loading
    - Thickness
  - Composite structural couplings
  - Parametric taper initiation studies
- Design technique validations
  - Blade dynamic tailoring
  - Variable RPM designs
  - Blade-to-blade variability effects

Figure 26

OVERALL DESIGN VALIDATION

For the overall Phase 1 validation effort (fig. 27), the Langley team has chosen a rotor task which requires maneuverability, speed, and efficiency. Specifically, the rotor mission must be accomplished with minimum power and vibration while satisfying predefined acoustic, stability, and fuselage dynamics requirements.

The assessment of the Phase 1 design methods will involve model rotor hover and wind tunnel tests. The models (a baseline and an advanced design) will be aerodynamically and dynamically scaled. Provisions for varying key design parameters are necessary to complete the validation process. In other words, the tests need to quantify not only a minima, but the gradients around it. The testing possibilities include a series of 1/5-scale model rotors, mounted on a variable drive system and tested in hover and simulated forward flight in a tunnel which can eliminate many testing "excuses" such as inappropriate Reynolds, Mach, and Froude Numbers. The Langley TDT* is the candidate facility for the major segments of the validation process.

*Transonic Dynamics Tunnel (TDT)

- **Definition of mission profile at gw/altitude/power**
  - **Maneuverability**
  - **Speed**
  - **Efficiency**
- **Minimize objective function while satisfying constraints**
- **Wind tunnel model rotors**
  - **Baseline**
  - **Advanced design with some parametric variability**
  - **Aerodynamicaly and dynamically scaled**

Figure 27

CONCLUDING REMARKS

This paper has described a joint NASA/Army initiative at the Langley Research Center to develop optimization procedures aimed at improving the rotor blade design process by integrating appropriate disciplines and accounting for important interactions among the disciplines. The activity is being guided by a Steering Committee made up of key NASA and Army researchers and managers. The committee, which has been named IRASC (Integrated Rotorcraft Analysis Steering Committee), has defined two principal foci for the activity: a "white paper" which sets forth the goals and plans of the effort; and a rotor design project which will validate the basic constituents, as well as the overall design methodology for multidisciplinary optimization.

This paper has described the optimization formulation in terms of the objective function, design variables, and constraints. Additionally, some of the analysis aspects were discussed and an initial attempt at defining the interdisciplinary couplings was described. At this writing, some significant progress has been made - principally in the areas of single discipline optimization. Results were given in the paper which represent accomplishments in rotor aerodynamic performance optimization for minimum hover horsepower, rotor dynamic optimization for vibration reduction, and rotor structural optimization for minimum weight. (Fig. 28.)

- **Defined objectives and procedures for integrated rotorcraft design**
- **Formalized Army/NASA team - Researchers and Managers**
- **Goals - Two foci**
  - **White paper to be critiqued by industry**
  - **Rotor design to validate procedures and tools**
- **Disciplinary optimization and coupling methodologies already yielding useful results**
  - **Rotor aerodynamic performance**
  - **Rotor dynamics**
  - **Rotor structure**

Figure 28

REFERENCES

1. Ashley, H.: On Making Things the Best - Aeronautical Use of Optimization. Journal of Aircraft, Vol. 19, No. 1, 1982, pp. 5-28.

2. Sobieszczanski-Sobieski, J.: Structural Optimization Challenges and Opportunities. Presented at International Conference on Modern Vehicle Design Analysis, London, England, June 1983.

3. Miura, H.: Application of Numerical Optimization Methods to Helicopter Design Problems: A Survey. NASA TM-86010, October 1984.

4. Bennett, R. L.: Application of Optimization Methods to Rotor Design Problems. Vertica, Vol. 7, No. 3, 1983, pp. 201-208.

5. Peters, D. A.; Rossow, M. P.; Korn, A.; and Ko, T.: Design of Helicopter Rotor Blades for Optimum Dynamic Characteristics. Computers and Mathematics with Applications, Vol. 12A, No. 1, 1986, pp. 85-109.

6. Friedmann, P.: Application of Modern Structural Optimization to Vibration Reduction in Rotorcraft. Vertica, Vol. 9, No. 4, 1986, pp. 363-376.

7. Friedmann, P.; and Shanthakumaran, P.: Optimum Design of Rotor Blades for Vibration Reduction in Forward Flight. Journal of American Helicopter Society, October 1984, pp. 70-80.

8. Davis, M. W.: Optimization of Helicopter Rotor Blade Design for Minimum Vibration. NASA CP-2327, Part 2, September 1984, pp. 609-625.

9. Chattopadhyay, Aditi; and Walsh, Joanne L.: Minimum Weight Design of Rotorcraft Blades with Multiple Frequency and Stress Constraints. Proceedings of the AIAA/ASME/ASCE/AHS 29th Structures, Structural Dynamics and Materials Conference, Williamsburg, VA, April 18-20, 1988. AIAA Paper No. 88-2337-CP. Also available as NASA TM-100569, March 1988.

10. Walsh, J. L.; Bingham, G. J.; and Riley, M. F.: Optimization Methods Applied to the Aerodynamic Design of Helicopter Rotor Blades. Journal of American Helicopter Society, October 1987, pp. 39-44.

11. Kumar, S.; and Bassett, D.: Rotor Performance Optimization for Future Light Helicopters. Proceedings of the 43rd Annual AHS Forum, St. Louis, MO, May 18-20, 1987.

12. Nixon, M. W.: Preliminary Structural Design of Composite Main Rotor Blades for Minimum Weight. NASA TP-2730, July 1987.

13. Gessow, Alfred; and Myers, Garry C., Jr.: Aerodynamics of the Helicopter. Frederick Unger Publishing Company, NY, 1952.

14. Berry, J. D.; Hoad, D. R.; Elliott, J. W.; and Althoff, S. L.: Helicopter Rotor Induced Velocities, Theory and Experiment. Proceedings of the AHS Specialists Meeting on Aerodynamics Acoustics, Fort Worth, TX, February 1987.

15. Whetstone, W. D.: Engineering Analysis Language Reference Manual EISI-EAL System Lend, 2091. Engineering Information Systems, July 1983. San Jose, CA

16. Lang, K. W.; and Nemat-Nasser, S.: An Approach for Estimating Vibration Characteristics of Non-uniform Rotor Blades. AIAA Journal, Vol. 17, No. 9, September 1979.

17. Brentner, K. S.: Prediction of Helicopter Rotor Discrete Frequency Noise - A Computer Program Incorporating Realistic Blade Motions and Advanced Acoustic Formulation. NASA TM-87721, October 1986.

18. Vanderplaats, G. N.: CONMIN - A Fortran Program for Constrained Function Minimization. User's Manual. NASA TMX-62282, August 1973.

19. Elliott, J. W.; Althoff, S. L.; and Sailey, R. H.: Inflow Measurement Made with a Laser Velocimeter on a Helicopter Model in Forward Flight. NASA TM-100541, April 1988.

20. Cardonna, F. X.; Lantenschlager, J. L.; and Silva, M. J.: An Experimental Study of Rotor-Vortex Interactions. AIAA Paper No. 88-0045. Presented at AIAA 26th Aerospace Sciences Meeting, Reno, Nevada, January 1988.

21. Lake, R. C.; and Nixon, M. W.: A Preliminary Investigation of Finite-Element Modeling in Analysis for Composite Rotor Blades. Proceedings of the Second International Conference on Rotorcraft Basic Research, College Park, Maryland, February 1988.

22. Weller, William H.; and Davis, Mark W.: Experimental Verification of Helicopter Blade Designs Optimized for Minimum Vibration. Proceedings of the 44th Annual Forum of the American Helicopter Society, Washington, DC, June 1988.

STRUCTURAL OPTIMIZATION OF ROTOR BLADES WITH STRAIGHT AND SWEPT TIPS SUBJECT TO AEROELASTIC CONSTRAINTS

Peretz P. Friedmann
Mechanical, Aerospace and Nuclear Engineering Department
University of California, Los Angeles, CA 90024

and

Roberto Celi
Aerospace Engineering Department
University of Maryland, College Park, MD 20742

LIST OF SYMBOLS

b	Blade semichord
C_T	Thrust coefficient
$\vec{D}$	Vector of design variables
$f(\vec{D})$	Objective function
$\nabla F(\vec{D})$	Gradient of objective function or behavior constraints
$\vec{g}(\vec{D})$	Vector of behavior constraints
h_s	Height of the single cell cross section
$[H(\vec{D}_0)]$	Hessian of objective function or behavior constraints
I_b	Mass moment of inertia of the blade in flapping
J	Mass polar moment of inertia of the rotor
ℓ	Length of the elastic portion of the blade
t_1	Thickness of the cross section
V_{zpk}	Peak-to-peak value of the 4/rev vertical hub shears, nondimensionalized through division by $2\Omega^2 I_b/\ell$
x_A	Offset between the elastic axis and the aerodynamic center, positive for aerodynamic center ahead of the elastic axis
x_I	Offset between the elastic axis and the center of gravity, positive for center of gravity ahead of the elastic axis
x_1	Distance between leading edge and internal wall in double cell cross section
x_2	Chordwise length of the cross section
γ	Blade Lock number
ζ_k	Real part of hover stability eigenvalue for the k-th mode
Λ	Tip sweep angle, positive for backward sweep
μ	Advance ratio
σ	Rotor solidity
Ω	Rotor angular velocity

1. INTRODUCTION AND PROBLEM STATEMENT

One of the most cost effective solutions to the problem of vibration in rotorcraft is to design rotor blades with an inherently low vibration level. This can be accomplished by aeroelastic tailoring the blade, using structural optimization. This implies that the blade mass and stiffness distributions and its geometry are determined in such a manner that the vibration levels at the rotor hub are minimized. Using this approach vibrations are reduced directly at their source, i.e., the rotor.

A thorough review of the literature concerning the use of optimum design techniques in dynamic problems, and particularly in helicopter rotor blade dynamic design, is presented in ref. (1). A more recent survey has been presented by Friedmann (ref. 2). These reviews reveal the existence of a very limited amount of work devoted to the structural optimization of rotor blades for vibration reduction.

In another recent survey Miura (ref. 3) states that it is not unreasonable to pursue design optimization in areas, such as helicopter vibration reduction, in which reliable prediction capabilities do not exist yet. Better optimization technology can be developed and implemented in highly modular computer codes so that new, improved analysis codes can be easily incorporated as they become available, and the optimization program can work with the best predictive capability available at any particular time.

When the mass and stiffness distributions of the blade are changed to reduce the vibration levels it is very important to be sure that no degradation of the aeroelastic stability occurs. This is even more important when tip sweep is added as a design variable because of its powerful influence on both blade response and stability (ref. 4). Prudence mandates the introduction of aeroelastic stability constraints in the optimum design process. This complicates the design problem because a fully coupled aeroelastic stability and response analysis has to be combined with the structural optimization program. Only a few studies having this capability are available (refs. 1,5,6). In refs. (1,5,6) the objective was the minimization of the 4/rev oscillatory vertical hub shears at an advance ratio μ = 0.3. The aeroelastic stability constraints required that the fundamental frequencies in flap, lag, and torsion fall between pre-assigned upper and lower bounds.

In a study by Peters *et al.* (ref. 7) two different objective functions were used to minimize blade weight in one case, and the discrepancy between desired and actual natural frequencies of the blade. A simplified forced response analysis leads the authors to conclude that the objective functions used in the study are "adequate" for vibration reduction purposes, but no comprehensive aeroelastic analysis is performed, and no stability constraints are imposed on the design.

Davis and Weller (ref. 8) used structural optimization techniques to solve four different dynamic problems, namely: (a) maximization of the in-plane structural damping of a bearingless rotor with elastomeric dampers; (b) placement of blade natural frequencies; (c) minimization of the vibratory hub shears using a simplified rotor aerodynamic model; and (d) minimization of certain rotor vibration indices. The rotor analysis codes were directly coupled to the optimization codes. No aeroelastic stability constraints were considered.

More recent work has also addressed the minimum weight design of rotor blades with frequency constraints (ref. 9) as well as the vibration reduction problem in forward flight by using optimally placed tuning masses (ref. 10) without enforcing aeroelastic response analysis to obtain the vibratory loads. Such studies are useful since they contribute towards the overall understanding of the problem; however, the possibility exists that such an approach may not produce reliable designs. A very detailed combined experimental and theoretical study (ref. 11), aimed at experimental verification of helicopter blade designs optimized for vibration reduction, indicated the need for using the dynamic loading on the blade, obtained from the aeroelastic response, in the optimization process.

A serious problem encountered in the direct coupling of a comprehensive aeroelastic stability and response code with an optimization, or nonlinear mathematical programming code is the very large computation effort required for the solution. This problem can be alleviated by constructing an *approximate*, computationally easier to solve, optimization problem (ref. 12). The approximate problems converge to the solution of the original, exact optimization problems.

One typical method of constructing the approximate problem is to expand the objective function and the behavior constraints in first or second order Taylor series in terms of the design variables, and in the neighborhood of the current design (ref. 12). This method originated in the field of static structural analysis, in which the gradient information required to construct the Taylor series expansions can be obtained at a fraction of the cost of one analysis, through implicit differentiation (ref. 13). This is difficult to achieve in helicopter aeroelastic optimization, and the gradient information has to be constructed using expensive-to-compute finite difference approximations. References (1,5,6) utilized an expensive approach based on finite differences for generating approximations to the objective function and aeroelastic constraints. The generation of the approximate problem was cumbersome and had to be carried out in an interactive manner, during the optimization process. It is also possible to construct approximate problems using derivatives, or the sensitivity of the objective function. This approach was successfully used in a recent, comprehensive optimization study by Lim and Chopra (ref. 14).

This paper has three main objectives:

1. To describe a new formulation of the structural optimization problem for a helicopter rotor blade in forward flight. The objective is the minimization of the n/rev vertical hub shears. The behavior constraints express mathematically the requirements that the blade be aeroelastically stable, that its natural frequencies fall between preassigned upper and lower bounds, and that the autorotation performance not be degraded during the aeroelastic tailoring process. A new formulation of the approximate problem allows increases in efficiency, in the complete solution of the optimum design problem, of at least one order of magnitude, compared with existing procedures.

2. To present results obtained by letting the *tip sweep angle* be one of the design variables in the optimization procedure. Tip sweep has a powerful influence on the dynamic behavior the blade, and when included in the aeroelastic tailoring process, can lead to further reductions in blade vibration levels.

3. To describe some ongoing work being carried out at UCLA on the structural optimization of rotor blades with straight and swept tips.

Finally it should be noted that a considerable amount of additional results pertaining to the first two objectives of this paper can be found in refs. (15)-(18).

2. AEROELASTIC STABILITY AND RESPONSE ANALYSIS

This section describes briefly the aeroelastic stability and response analysis and the procedure used to calculate the vertical hub shears, that is, the analysis portion of the optimum design process. The equations of motion of the straight blade are similar to those derived in ref. (19). The modeling of the swept tip is described in ref. (4). The equations describe the coupled flap-lag-torsional motion of a flexible, homogeneous, isotropic blade, modeled as a Bernoulli-Euler beam undergoing small strains and moderate deflections. Geometrically nonlinear terms are present in the structural, inertia, and aerodynamic operators, due to nonlinear beam kinematics. The inertia loads are obtained using D'Alembert's principle. Quasi-steady strip theory, with uniform inflow, is used to derive the aerodynamic loads. Stall and compressibility effects are not included. In the modeling of the swept tip the independence principle is assumed to apply, that is, the aerodynamic loads depend only on the component of the flow contained in the plane of the cross section, and radial flow effects are neglected (ref. 4).

The spatial dependence of the partial differential equations of motion of the blade is eliminated by using a Galerkin method of weighted residuals (ref. 19). This results in a finite element discretization. Cubic interpolation polynomials are used for the modeling of flap and lag bending, quadratic interpolation polynomials for the modeling of torsion. The resulting finite elements have a total of 11 degrees of freedom: displacement and slope at each end of the element, for flap and lag bending, rotation at each end of the element and at a mid-element node, for torsion. The axial degree of freedom is eliminated by making the assumption that the blade is inextensional. The partial differential equations of motion of the blade are thus transformed into a set of nonlinear, coupled, ordinary differential equations with periodic coefficients. A modal coordinate transformation is performed to reduce the number of degrees of freedom. Six rotating coupled blade normal modes are used to perform the modal coordinate transformation. The coupled modes are calculated for a root pitch angle equal to the collective pitch.

In forward flight, the equilibrium position of the blade is time dependent, and is obtained by solving a sequence of linear, periodic response problems, using quasilinearization. The stability of the system is determined using Floquet theory. A special, implicit formulation of quasilinearization (ref. 20) which reduces considerably the implementation effort is used. The algebraic expressions that define the aerodynamic loads are not expanded explicitly. They are coded separately in the computer program and combined numerically during the solution procedure. Quasilinearization is a Newton-Raphson type procedure, and the derivative matrices that are required by the algorithm are computed using finite different approximations.

The overall helicopter trim procedure used in this study is a propulsive trim procedure identical to that used in ref. (21).

The calculation of the hub loads, consisting of forces and moments, is performed using the direct force integration method. The response of the blade is obtained from the aeroelastic response calculation code; thus the hub loads are obtained from a spanwise integration of the inertia and aerodynamic loads distributed along the blade. Details on the hub loads calculations can be found in refs. 15-18.

3. FORMULATION OF THE OPTIMUM DESIGN PROBLEM

The optimization problem is cast in nonlinear mathematical programming form. Thus the objective is to minimize a function $f(\vec{D})$ of a vector $\vec{D}$ of design variables, subject to a certain number of constraints $\vec{g}(\vec{D}) \le 0$:

$$\text{minimize } f(\vec{D}) \tag{1}$$

subject to:

$$\vec{g}(\vec{D}) \le 0 \tag{2}$$

To reduce the computational requirements, the computer program performing the aeroelastic analysis is not connected directly to the optimization program. Instead, the optimization is conducted on an *approximate problem*, which reproduces the characteristics of the actual problem in a neighborhood of the current design, and which is continuously updated as the optimization progresses.

An effective method of building an approximate problem is to expand the objective function and the behavior constraints in Taylor series in terms of the design variables (ref. 9):

$$F(\vec{D}) \approx F(\vec{D}_0) + \nabla F(\vec{D}_0)\delta\vec{D} + \frac{1}{2}\,\delta\vec{D}^T[H(\vec{D}_0)]\delta\vec{D} \tag{3}$$

where $F(\vec{D})$ is taken to be any objective or constraint function, $\vec{D}_0$ is the current design, and $\nabla F(\vec{D}_0)$ and $[H(\vec{D}_0)]$ are respectively the gradient and the Hessian matrix at the current design. The Hessian matrix is the matrix of the second partial derivatives of the objective function with respect to the design variables. The perturbation vector $\delta\vec{D}$ is defined as

$$\delta\vec{D} = \vec{D} - \vec{D}_0 \tag{4}$$

The most expensive function to evaluate is the objective function. The cost of one evaluation of the objective function is two orders of magnitude higher than the total cost of evaluating the behavior constraints. No analytic expressions for the gradients are available for the objective function, and finite difference approximations are required for the construction of the derivative information in Eq. (3). Therefore, if n design variables are used in the optimization, n additional aeroelastic analyses are required to compute the gradient, and an additional n(n+1)/2 for the calculation of the Hessian, making the cost of building the Taylor series approximation to the objective function extremely high. For this reason an alternative approximation technique, introduced by Vanderplaats [22,23], was used in this study.

This alternative technique is based on the idea of approximating the gradient and the Hessian in Eq. (3), not by using small finite difference steps, but by using whatever design information is available at the time. Eq. (3) can be rewritten, in expanded form, as (refs. 22,23).

$$\begin{aligned}\Delta F = {} & \nabla F_1 \delta D_1 + \nabla F_2 \delta D_2 + \ldots + \nabla F_n \delta D_n + \tfrac{1}{2}(H_{11}\delta D_1^2 + H_{22}\delta D_2^2 + \ldots + H_{nn}\delta D_n^2) \\ & + H_{12}\delta D_1 \delta D_2 + H_{13}\delta D_1 \delta D_3 + \ldots + H_{1n}\delta D_1 \delta D_n \\ & + H_{23}\delta D_2 \delta D_3 + \ldots + H_{n-1,n}\delta D_{n-1}\delta D_n \end{aligned} \tag{5}$$

In which

$$\Delta F = F(\vec{D}) - F(\vec{D}_0) = F - F_0 \tag{6}$$

and

$$\nabla F_i = \nabla F_i(\vec{D}_0) \; ; \qquad H_{ij} = H_{ij}(\vec{D}_0) \tag{7}$$

Assume that a baseline design $\vec{D}_0$ has been analyzed to give F_0, and that other designs $\vec{D}_1, \vec{D}_2, \ldots, \vec{D}_k$ have been previously analyzed, to provide $F_1, F_2, \ldots F_k$. Let

$$\delta\vec{D}_i = \vec{D}_i - \vec{D}_0 \qquad i = 1,2,\ldots,k \tag{8}$$

and

$$\Delta F_i = F_i - F_0 \qquad i = 1,2,\ldots,k \tag{9}$$

If k designs are available, Eq. (5) can be written k times. The unknowns of the resulting linear system are ∇F_1, $\nabla F_2, \ldots, \nabla_k$, and H_{11}, $H_{12}, \ldots, H_{nn}$. If the designs are linearly independent, the system ℓ equations (5) will provide all the coefficients required for the quadratic polynomial approximation Eq. (3). If all the designs are very closely spaced, the solution to the gradient and Hessian matrix at $\vec{D}_0$. Equation (3) will then represent a truncated Taylor series expansion of F, valid in a neighborhood of $\vec{D}_0$. If the designs are dispersed in the design space, Eq. (3) will simply be a quadratic polynomial approximation, defined over a wider region of the design space.

An important characteristic of this technique is that the system of equations (5) can be written with less than ℓ equations. If at least n + 1 designs are available, the solution of the system will provide a linear portion of the approximation, Eq. (3). An approximate optimization can be conducted, based on this linear approximation. The resulting optimum is then analyzed precisely and provides an additional design: a system of n + 2 equations (5) can then be written. Its solution will provide a new approximation, Eq. (5), with all the linear terms plus one pair of quadratic terms of the symmetric Hessian matrix. The process can then be repeated, with each new approximate optimum providing an additional design point to increase the number of terms in the quadratic approximation to objective function and behavior constraints.

One iteration of the optimum design process thus consists of the following six steps:

1. Calculation of the blade properties, including natural frequencies and mode shapes;
2. Aeroelastic analysis in hover;
3. Aeroelastic analysis in forward flight, including calculation of hub loads;
4. Calculation of objective function and behavior constraints;
5. Calculation of a new approximation (linear or incomplete quadratic) to objective function and behavior constraints;
6. Solution of the approximate constrained optimization problem, using the feasible direction code CONMIN (refs. 24,25) to obtain a new, improved blade design.

The process is terminated when a feasible, optimum design has been reached, or arbitrarily, when the improvement in the design is considered "adequate".

The first n + 1 iterations of the procedure are not true optimization iterations because steps 5 and 6 above are not performed. In fact, these initial iterations are used to generate a sufficient number of designs to build at least an initial linear approximation to objective function and behavior constraints.

Side constraints are placed on the design variables to prevent them from reaching impractical values which violate practical, physical constraints. Thus all the thicknesses and distances are assumed to be nonnegative numbers.

Three different types of *behavior constraints* are placed on the design.

1. *Frequency placement constraints.* The fundamental frequencies in flap, lag and torsion are required to fall between preassigned upper and lower bounds. If ω is one of the three frequencies, and ω_L and ω_U are the preassigned lower and upper bound respectively, the frequency placement constraint is expressed mathematically in the form:

$$g(\vec{D}) = \frac{\omega^2}{\omega_U^2} - 1 \leq 0 \qquad (10)$$

$$g(\vec{D}) = 1 - \frac{\omega^2}{\omega_L^2} \leq 0 \qquad (11)$$

Equations (10) and (11), written for each of the three fundamental frequencies of the blade, provide a total of six behavior constraints. Furthermore, the frequencies are also constrained so as to be sufficiently removed from the n/rev frequencies.

2. *Aeroelastic stability constraints.* The blade is required to be aeroelastically stable in hover. No constraints are placed on the stability in forward flight because all the blade configurations considered in this optimization study are soft-in-plane blade configurations, and the effect of forward flight is usually stabilizing for this type of blades (ref. 21). The aeroelastic stability constraints are expressed mathematically in the form:

   $$g(\vec{D}) = \zeta_k \leq 0 \qquad k = 1,2,\ldots,m \qquad (12)$$

   If m modes are used to perform the modal coordinate transformation in the solution of the equations of motion, there are m constraint equations like Eq. (12), where the quantify ζ_k is the real part of the hover stability eigenvalue for the k-th mode. As indicated in the results section, in some cases more stringent aeroelastic constraints were also imposed.

3. *Autorotation constraints.* The autorotation constraint expresses the requirement that possible mass redistributions produced in the optimization process do not degrade the autorotation properties of the rotor. The most convenient autorotation constraint is one which restricts variations of the polar mass moment of inertia of the rotor (ref. 26, pp. 346-364). Therefore, the autorotation constraint is expressed mathematically in the form:

   $$g(\vec{D}) = 1 - \frac{J}{0.9J_0} \leq 0 \qquad (13)$$

   The constraint equation (13) requires that the mass polar moment of inertia J of the rotor maintain, during the optimization, at least 90% of its initial value J_0.

Therefore, *a total of thirteen behavior constraint equations* are placed on the design variables.

4. RESULTS

The basic blade configuration considered in this study is a soft-in-plane hingeless blade, shown in Figure 1, which is part of a four bladed rotor. The uncoupled fundamental lag, flap, and torsion frequencies, for zero tip sweep, are 0.732/rev, 1.125/rev, and 3.17/rev respectively. The Lock number is $\gamma = 5.5$, the thrust coefficient $C_T = 0.005$, and the rotor solidity $\sigma = 0.07$. For the swept tip configurations, the outermost 10% of the blade is swept. The blade precone angle β_p, the root offset e_1, the offset x_A between the elastic axis and the aerodynamic center, and the offset x_I between the elastic axis and the cross sectional center of gravity are all set to zero, unless specified otherwise. The modal coordinate transformation is based on the six lowest frequency, rotating, coupled modes of the blade. In all cases the six modes were one torsion, two lag, and three flap modes. The blades were modeled using 5 finite elements, with nodes at 0%, 22.5%, 45%, 67.5%, 90% and 100% of the span. Selected results are presented here. Numerous additional results can be found in refs. (15)-(18).

Two types of cross sections are considered in this study, namely a single cell, rectangular cross section, and a double cell cross section. Both cross sections are shown in Figure 2. Up to five, and up to nine independent design parameters can be specified for the single cell and the double cell cross section respectively (ref. 16). In this study the cross sectional design parameters are linked in such a way as to reduce the number of independent design parameters to two, for both the single and the double cell cross sections. The first independent design variable is the thickness t_1 of all the elements of which both cross sections are composed. The second independent design variable is the chordwise width x_2 for both cross sections. In the single cell cross section the ratio between the width x_2 and the height h_s is kept constant, with $x_2/h_s = 4.5$. In the double cell cross section the internal wall is placed halfway between the leading edge and the rear wall, so that $x_1 = x_2/2$. The outside wall of the double cell cross section has the shape of a NACA 0012 airfoil. The properties of both cross sections are presented in ref. (16).

As a preliminary to the optimization studies, the effect of tip sweep on the peak-to-peak values of the 4/rev vertical hub shears was investigated.

Figure 3 shows the peak-to-peak value V_{zpk} of the vertical hub shears as a function of the tip sweep angle Λ, for four different values of the advance ratio μ, for the soft-in-plane blade configuration. Figure 3 shows that tip sweep may or may not be beneficial for the soft-in-plane configuration, depending on the advance ratio and the tip sweep angle. At an advance ratio $\mu = 0.3$ the oscillatory loads rapidly increase with tip sweep. At $\mu = 0.4$, instead, tip sweep has a beneficial effect. Based on the results of this preliminary investigation, the advance ratio at which the 4/rev vertical hub shears are minimized was set at $\mu = 0.4$.

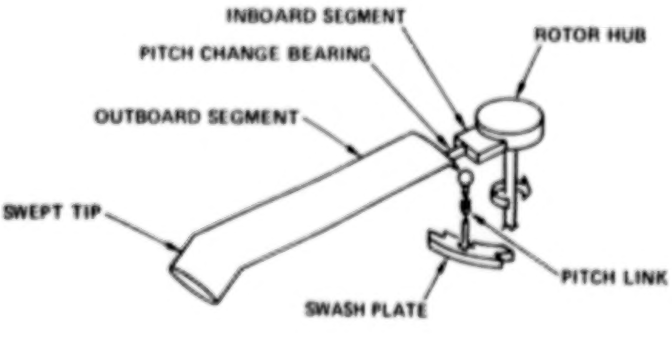

Figure 1: Swept tip hingeless rotor blade model.

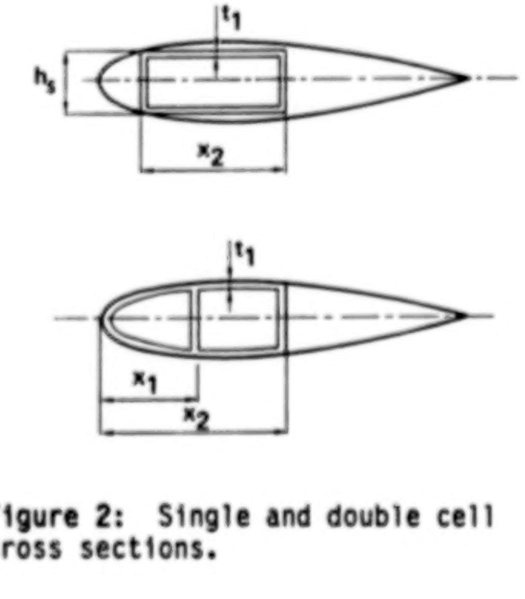

Figure 2: Single and double cell cross sections.

Three optimization studies were conducted using the general procedure outlined in the previous section, namely:

1. Optimization of a completely straight blade, having a two-cell cross section. The objective function is the peak-to-peak value of the 4/rev vertical hub shears at an advance ratio $\mu = 0.4$.

   The design variables are defined at three distinct cross sections of the blade: the root section, the tip section, and the cross section at the 67.5% span, *for a total of six independent design variables*. The 67.5% station, at which two design variables are defined, is the junction section between the third and the fourth finite element. The blade properties are assumed to vary linearly between two consecutive stations at which the design variables are specified.

2. Optimization of a completely straight blade, having a single cell cross section. As in the previous case, the objective function is the peak-to-peak value of the 4/rev vertical hub shears at an advance ratio $\mu = 0.4$.

   As in Case 1, the design variables are defined at three distinct cross sections of the blade: the root section, the tip section, and the cross section at the 67.5% span, *for a total of six independent design variables*.

   The cross section is rectangular, therefore doubly symmetric. Because leading edge masses have not been used in this particular example, the center of gravity and the aerodynamic center are located on the elastic axis of the blade - which is taken to be coincident with the pitch axis. Therefore the associated offsets are equal to zero.

3. Straight blade with a swept tip. The objective function is the peak-to-peak value of the 4/rev vertical hub shears divided by the thrust coefficient C_T, at

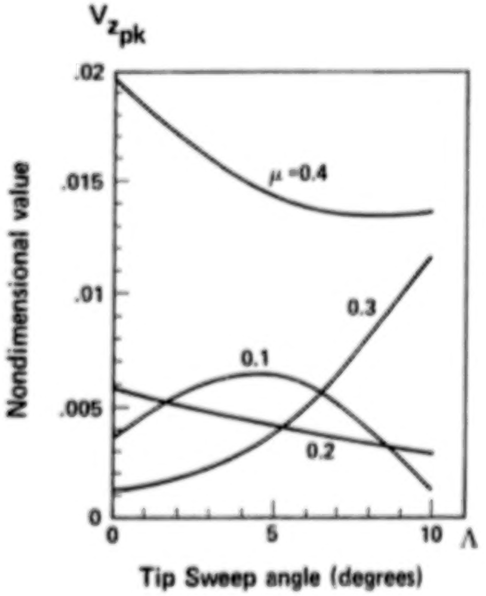

Figure 3: Effect of tip sweep on the peak-to-peak value of the vertical hub shears, soft-in-plane blade configuration.

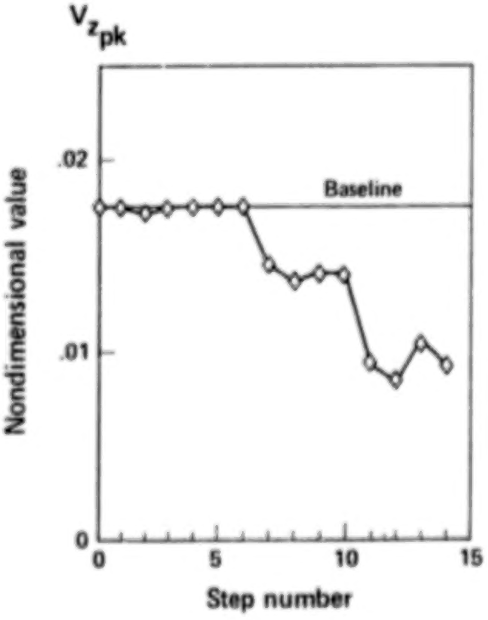

Figure 4: Case 1 - Iteration history of the objective function.

an advance ratio $\mu = 0.4$. This particular choice of objective function is an attempt to compensate for the inaccuracy of the trim program, which neglects the torsional deformation of the blade and thus overestimates the thrust that the rotor is actually capable of developing.

The outermost 10% of the blade is swept, with the sweep angle being a design variable of the optimization procedure. The cross section is rectangular, and therefore the offsets x_I and x_A are equal to zero. The cross sectional design variables are designed as in Case 2. Therefore *a total of seven design variables* is used in this case.

The initial blade configuration, for all three cases, is the baseline soft-in-plane configuration.

Optimization Case 1

The iteration history of the objective function for case 1 is shown in Fig. 4. It should be noted that for all three optimization cases, design n is defined as the design produced at the end of the optimization step n. Step 0 and the first six steps are not true optimization steps: they are required to obtain enough information to build linear approximations to the objective function and behavior constraints. Step 0 is the analysis of the baseline design. In steps 1 through 6 each of the six design variables is perturbed, one at a time. Because the perturbations were relatively small - 1% of the baseline value - the linear approximations obtained at the end of step 6 can be considered as gradients calculated using forward flight difference approximations.

Step 7 is the first true optimization step and consists of the solution of a linear optimization problem. Move limits were placed on the design variables, which could not change by more than 25% of the baseline value. The optimization continues for three additional steps (8-10). Each new proposed design is analyzed precisely and is used to improve the polynomial approximations to objective function and behavior constraints. The diagonal of the Hessian matrix is built first, as more function evaluations become available. (The term "Hessian" is used in this section with the general meaning of "matrix coefficients of the quadratic terms at the approximation"). Figure 4 shows that, after reaching a minimum at step 8, the objective function slightly oscillates.

As the constrained optimum of the approximate problem, the approximate flap damping constraint for the first flap mode was active. In most helicopter blades the first flap mode tends to be highly damped, and a precise analysis of the proposed design showed that this indeed was the case, and that the precise first flap stability constraint was satisfied. The constraint was therefore reformulated as

$$\zeta_{F1} - 0.3 < 0 \qquad (14)$$

The subsequent optimization steps were performed with this new form of the constraint, which prevents the *approximate* constraint from becoming critical. Two more steps (11 and 12) are performed with the relaxed flap constraint. The design of step 12 is a local, unconstrained minimum of the approximate problem. The corresponding blade is such that a reduction of 54.3% is achieved in the objective function, compared with the baseline configuration. The design suggested by the optimizer for step 13 is practically the same as that for step 12. A different design was instead arbitrarily selected for step 13. This design was "close" to that of step 12, and was selected for the only purpose of adding one design to the design data base and to try to improve the accuracy of the approximations in the neighborhood of design 12 -

with the design of step 13 the full diagonal of the Hessian can be built. Step 14 is the last optimization step, and it produces a value of the objective function that is slightly higher than the minimum of step 12. The optimization was arbitrarily stopped at this point. All the designs generated during the optimization were feasible. Iteration histories on the design variables are presented in refs. (15)-(17), and for conciseness are not repeated here.

Optimization Case 2

The iteration history of the *objective function* for case 2 is shown in Fig. 5. Steps 0 through 6 are not true optimization steps. These steps are required to generate enough designs to construct at least linear approximations to objective function and behavior constraints. The design at step 0 is the baseline blade design. The designs analyzed in steps 1 through 6 are obtained by changing one design variable at the time. Since the change in each variable was equal to 10% of its baseline value, the resulting linear approximations to objective functions and behavior constraints cannot be strictly considered as gradients.

The first true optimization step is step 7, which consists of a linear, constrained optimization problem. A reduction of 37.6% is achieved, compared with the baseline design. In the next step the objective function increases slightly. Because this behavior is somewhat similar to the one observed in case 1, the optimization was arbitrarily concluded as this point, and restarted *with a new set of behavior constraints.*

The aeroelastic stability constraints used in case 1, and up to this point in case 2, consist of requiring that the blade be aeroelastically stable in hover. It is prudent to require that the optimization process do not degrade too much the stability margin of the baseline design. The optimization was thus restarted from step 9 with these more stringent behavior constraints. The aeroelastic constraints of Eq. (12) are reformulated as

$$g(D) = 1 - \frac{\zeta_k}{0.95\zeta_{kB}} \leq 0 \qquad k = 1,2,\ldots,m \tag{15}$$

Equation (15) expresses the requirement that the loss of stability of a given mode should not exceed 5% of the baseline value ζ_{kB}.

The optimization is not restarted with a new calculation of an initial linear approximation. Rather, the previous designs are reused to provide the initial approximation for the new case. While designs 0 through 8 were all feasible with respect to the old set of behavior constraints, some of these designs are now feasible with respect to the tightened aeroelastic stability constraints. In particular, design 8, which becomes the initial design for the second phase of this optimization, is infeasible.

The first design produced by the optimizer with the new set of constraints is feasible with respect to the *approximate* behavior constraints. When this design is analyzed precisely, it proves to be infeasible with respect to the *exact* behavior constraints. The successive design (step 10) is feasible with respect to both the approximate and the exact behavior constraints. The next design (step 11) is again feasible with respect to the approximate, but not the exact behavior constraints. In steps 9 through 11 the objective function is constantly at a value higher than the baseline value and does not show any signs of convergence to the optimum. In other words, the optimizer does not seem to be able to produce a feasible design that improves on the baseline design, which satisfies the new constraint equations, Eq. (15).

The apparently erratic behavior of the objective function required a reconsideration of the optimization strategy which, starting from step 14, was modified, and tighter move limits were enforced, in a selective manner. This modified approach finally yields design 16 which represents a reduction in peak-to-peak value of the 4/rev vertical hub shears to 16.6% compared to the baseline value. Thus the imposition of aeroelastic constraints reduces the gains in the objective function by more than 50%.

Optimization Case 3

Figure 6 shows the iteration history of the objective function for case 3, which is the peak-to-peak value of the 4/rev vertical hub shears divided by the thrust coefficient C_T. The tightened aeroelastic constraints of Eq. (15) are enforced.

Design 0 is the baseline soft-in-plane straight blade configuration. The first seven steps are not true optimization steps. As in cases 1 and 2, they provide enough precise values of the objective function and behavior constraints to build at least a linear approximation of objective and constraints. In the designs 1 through 7 each of the seven design variables is perturbed, one at a time. Design 7 is the only swept blade design. Designs 0 through 6 are straight blade designs and are identical to the corresponding designs of case 2. Thus these designs are not reanalyzed to derive the results of Figure 3, and need not be recalculated.

Thus the optimization process of case 3 begins without the need for any precise analyses, in the sense that the eight precise analyses required to start the procedure were already available from previous parts of this study and could be directly reutilized. The ability to make use of previously analyzed designs, even if not very

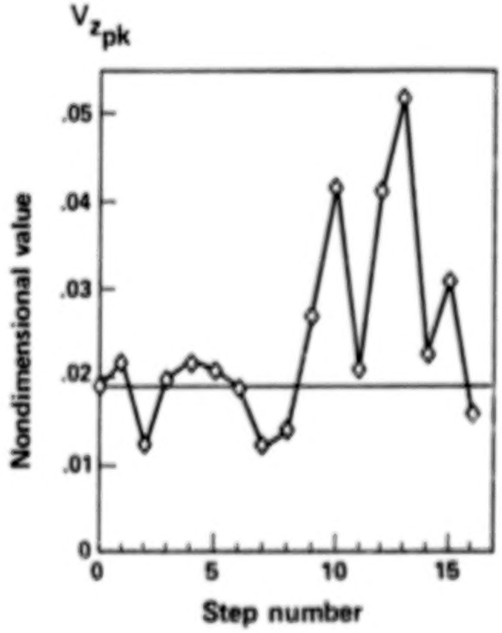

Figure 5: Case 2 - Iteration history of the objective function.

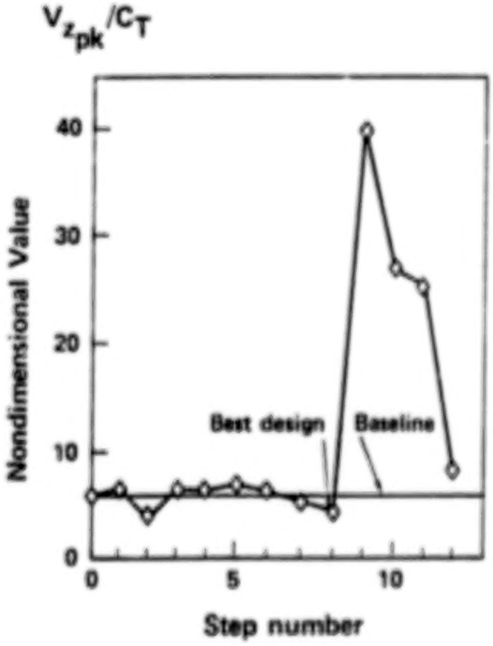

Figure 6: Case 3 - Iteration history of the objective function.

close to the expected optimum in the design space of the current problem, is one of the most important features of the optimization algorithm used in this study.

The first true optimization step, step 8, produces a design with a reduction of 27.2% of the objective function with respect to the baseline straight blade. This also corresponds to a reduction of 14.5% with respect to the best swept tip design obtained without applying formal optimization techniques, that is design 7. When analyzed precisely, the design proves feasible, with no constraints active. Compared with the final result of case 2, in which the blade is straight, the use of tip sweep as an additional design variable allows a further reduction of the objective function of almost 10%.

The next two steps (9 and 10) produce much higher values of the objective function. Starting from step 11 the "modified" strategy previously outlined is employed. The next two steps (11 and 12) provide considerable reductions of the objective function, but the best design is still design 8. The optimization is arbitrarily stopped at this point, both for cost reasons, and because the design appears to converge towards design 8.

The iteration histories of the thickness t_1, the chordwise extension of the spar, and the tip sweep angle Λ are shown in Figs. 7, 8, and 9 , respectively. The tip sweep angle corresponding to the best design is $\Lambda = 9°$.

Next, it is relevant to comment on the computational requirements encountered in this study. The results were obtained on an IBM 3090-200 computer. Each precise aeroelastic analysis required three to four iterations of quasilinearization (ref. 16). Each iteration of quasilinearization required 80-110 CPU seconds for a straight blade and 140-180 CPU seconds for a swept tip blade. Because a variable step, Adams-Bashforth technique was used to integrate the equations of motion (ref. 4), the exact CPU time required to complete an iteration of quasilinearization was problem dependent.

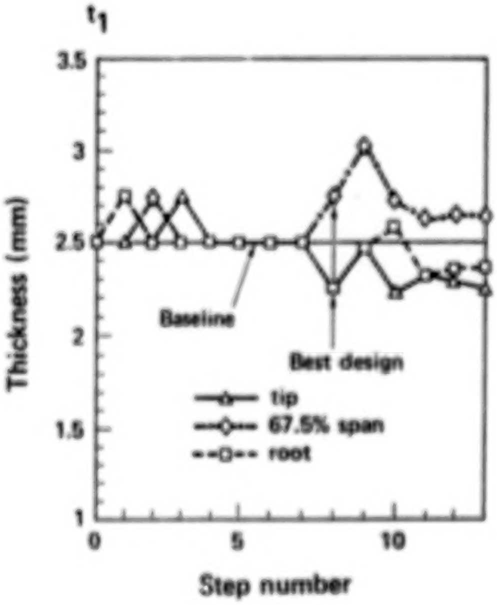

Figure 7: Case 3 - Iteration history of thickness t_1.

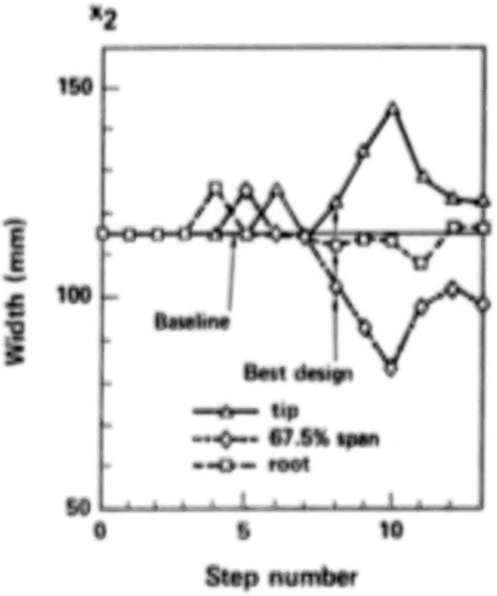

Figure 8: Case 3 - Iteration history of chordwise width x_2.

The remaining portions of a complete optimization step, namely the calculation of the cross sectional properties of the blade, the calculation of the vertical hub shears from the aeroelastic response of the blade, the derivation of the polynomial approximations to objective function and behavior constraints, and the solution of the approximate constrained optimization problem, required an average *total* 1-2 CPU seconds.

5. ONGOING EXTENSION OF THE RESEARCH ON ROTOR BLADE OPTIMIZATION WITH AEROELASTIC CONSTRAINTS

Ongoing research at UCLA is aimed at extending the work described in the previous sections in several directions. First, more efficient means of generating the approximate problem are being considered using intermediate design variables representing cross-sectional stiffness properties. Next, the structural model of the blade is being improved by replacing the isotropic structural blade model by a model which is capable of modeling a composite rotor blade with multicell cross sections. A more accurate representation of the unsteady aerodynamic loads is also being pursued. Finally alternative choices for the objective functions are also being considered so that the multidisciplinary nature of our current optimization capability is enhanced.

6. CONCLUDING REMARKS

The main conclusions obtained in the present study are summarized below. Their application to the structural optimization of a helicopter blade should be limited by the assumptions used in obtaining the numerical results presented in this study.

1. The optimum design procedure described in this study is very efficient, and can produce improved designs with a very limited number of precise analyses. The

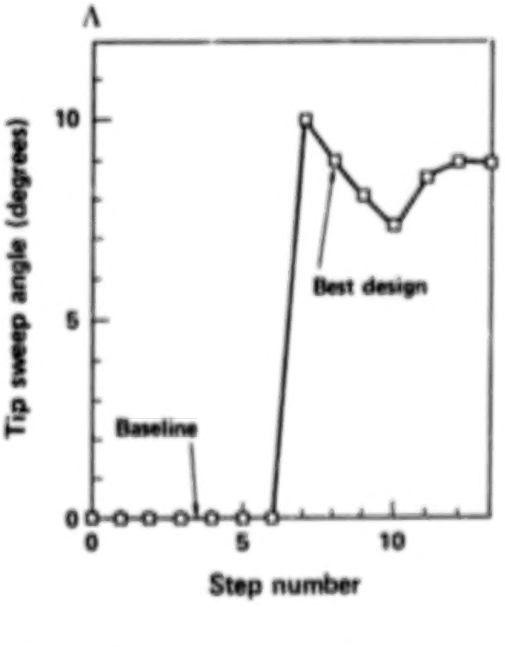

Figure 9: Iteration history of tip sweep angle Λ.

method of constructing the approximate problem is such that previously conducted aeroelastic analyses can be reused in a new optimization problem. For example, if an optimization study is preceded by a parametric study in which the effect of various combinations of blade design parameters is examined, all the aeroelastic analyses performed for the parametric study can be reutilized in the optimization study. This is not possible when the approximate problem is built from Taylor series expansions.

2. The results of the optimization are quite sensitive to the aeroelastic stability margins required of the blade. In the optimization of case 2, changing the aeroleastic stability constraints from simply requiring that the blade be stable in hover, to requiring that the stability margins be maintained during the course of the optimization, reduced the gains in n/rev vibration levels by more than 50%.

3. The introduction of tip sweep can reduce the n/rev vertical hub shears beyond the level that can be obtained by just modifying the mass and stiffness distributions of the blade.

ACKNOWLEDGMENT

This research was funded primarily by NASA grant NAG 2-226, NASA Ames Research Center, Moffett Field, CA. Funding of the continuation of this research under NASA Grant NAG 1-833, by NASA Langley Research Center, is also gratefully acknowledged.

REFERENCES

1. Shantakumaran, P., "Optimum Design of Rotor Blades for Vibration Reduction in Forward Flight," Ph.D. Dissertation, University of California, Los Angeles, CA, 1984.

2. Friedmann, P.P., "Application of Modern Structural Optimization to Vibration Reduction in Rotorcraft," *Vertica*, Vol. 9, No. 4, 1985, pp. 363-373.

3. Miura, H., "Application of Numerical Optimization Methods to Helicopter Design Problems - A Survey," *Vertica*, Vol. 9, No. 2, 1985, pp. 141-154.

4. Celi, R., and P.P. Friedmann, "Aeroelastic Modeling of Swept Tip Rotor Blades Using Finite Elements," *Journal of the American Helicopter Society*, April 1988, pp. 43-52.

5. Friedmann, P.P., and P. Shanthakumaran, "Aeroelastic Tailoring of Rotor Blades for Vibration Reduction in Forward Flight," AIAA Paper No. 83-0914, Proceedings of the AIAA/ASME/ASCE/AHS 24th Structures, Structural Dynamics and Materials Conference, Lake Tahoe, NV, Vol. 2, May 1983, pp. 344-359.

6. Friedmann, P.P., and P. Shanthakumaran, "Optimum Design of Rotor Blades for Vibration Reduction in Forward Flight," *Journal of the American Helicopter Society*, Vol. 29, No. 4, October 1984, pp. 70-80.

7. Peters, D.A., M.P. Rossow, A. Korn, and T. Ko, "Design of Helicopter Rotor Blades for Optimum Dynamic Characteristics," *Computers and Mathematics with Applications*, Vol. 12A, No. 1, 1986, pp. 85-109.

8. Davis, M.W., and Weller, W.H., "Application of Design Optimization Techniques to Rotor Dynamics Problems," Proceedings of the 42nd Annual Forum of the American Helicopter Society, Washington, DC, June 1986, pp. 27-44.

9. Chattopadhyay, A., and J. Walsh, "Minimum Weight Design of Rectangular and Tapered Helicopter Rotor Blades with Frequency Constraints," Proceedings of the Second International Conference on Rotorcraft Basic Research, College Park, MD, February 1988.

10. Pritchard, J.L., and H.M. Adelman, "Optimal Placement of Tuning Masses for Vibration Reduction in Helicopter Rotor Blades," Proceedings of the Second International Conference on Rotorcraft Basic Research, College Park, MD, February 1988.

11. Weller, W.H., and M. Davis, "Experimental Demonstration of Helicopter Blade Designs Optimized for Minimum Vibration," Proceedings 44th Annual Forum of the American Helicopter Society, Washington, DC, June 1988.

12. Schmit, L.A., Jr., and H. Miura, H., "Approximation Concepts for Efficient Structural Synthesis," NASA CR-2552, 1976.

13. Schmit, L.A., Jr., "Structural Synthesis - Its Genesis and Development," *AIAA Journal*, Vol. 18, No. 10, 1981, pp. 1249-1263.

14. Lim, J., and I. Chopra, "Aeroelastic Optimization of a Helicopter Rotor," Proceedings of the 44th Annual Forum of the American Helicopter Society," Washington, DC, June 16-19, 1988, pp. 545-558.

15. Celi, R., and P.P. Friedmann, "Efficient Structural Optimization of Rotor Blades with Straight and Swept Tips," Paper No. 3-1, Proceedings of Thirteenth European Rotorcraft Forum," Arles, France, September 8-11, 1987.

16. Celi, R., "Aeroelasticity and Structural Optimization of Helicopter Rotor Blades with Swept Tips," Ph.D. Dissertation, Mechanical, Aerospace and Nuclear Engineering Department, University of California, Los Angeles, CA, September 1987.

17. Celi, R., and P.P. Friedmann, "Structural Optimization with Aeroelastic Constraints of Rotor Blades with Straight and Swept Tips," AIAA Paper 88-2297, Proceedings AIAA/ASME/aSCE/AHS 29th Structures, Structural Dynamics and Materials Conference, Part 2, Williamsburg, VA, April 18-20, 1988, pp. 668-680.

18. Friedmann, P.P., and R. Celi, "Aeroelasticity and Structural Optimization of Rotor Blades with Swept Tips," ICAS Paper 88-5.7.4, Proceedings Sixteenth Congress of International Council of the Aeronautical Sciences, August 28-September 2, 1988, Jerusalem, Israel, pp. 1092-1108.

19. Straub, F.K., and P. Friedmann, "Application of the Finite Element Method to Rotary Wing Aeroelasticity," NASA CR-165854, February 1982.

20. Celi, R., and P.P. Friedmann, "Use of Implicit Formulation Based on Quasi-linearization for the Aeroelastic Response and Stability of Rotor Blades in Forward Flight," Proceedings of the AIAA Dynamics Specialists Conference, Monterey, CA, Part 2B, April 1987, pp. 730-742.

21. Friedmann, P., and S.B.R. Kottapalli, "Coupled Flap-Lag-Torsional Dynamics of Hingeless Rotor Blades in Forward Flight," *Journal of the American Helicopter Society*, Vol. 27, October 1982, pp. 28-36.

22. Vanderplaats, G.N., Approximation Concepts for Numerical Airfoil Optimization," NASA Technical Paper 1370, March 1979.

23. Vanderplaats, G.N., *Numerical Optimization Techniques for Engineering Design, With Applications*, McGraw-Hill Book Co., 1984, pp. 211-215.

24. Vanderplaats, G.N., and F. Moses, "Structural Optimzation by Methods of Feasible Directions," *Journal of Computers and Structures*, Vol. 3, July 1973, pp. 739-755.

25. Vanderplaats, G.N., "CONMIN - A FORTRAN Program for Constrained Function Minimization; User's Manual," NASA TM X-62,282, August 1973.

26. Prouty, R.W., *Helicopter Performance, Stability and Control*, PWS Publishers, Boston, 1986.

OPTIMIZATION OF ROTOR BLADES FOR COMBINED STRUCTURAL, PERFORMANCE, AND AEROELASTIC CHARACTERISTICS

David A. Peters
and
Y. P. Cheng
School of Aerospace Engineering
Georgia Institute of Technology
Atlanta, Georgia

ABSTRACT

This paper outlines the strategies whereby helicopter rotor blades can be optimized for combined structural, inertial, dynamic, aeroelastic, and aerodynamic performance characteristics. There are three key ingredients in the successful execution of such an interdisciplinary optimization. The first is the definition of a satisfactory performance index that combines all aspects of the problem without too many constraints. The second element is the judicious choice of computationally efficient analysis tools for the various quantitative components in both the cost functional and constraints. The third element is an effective strategy for combining the various disciplines either in parallel or sequential optimizations.

INTRODUCTION

This paper describes ongoing work in the optimization of helicopter main rotor blades. The helicopter is intrinsically interdisciplinary due to the close coupling between aerodynamics, dynamics, and the blade structural details. As a result, the optimization of a helicopter rotor involves important design considerations from many diverse engineering disciplines. In our present work, we attempt to combine several of these important effects in a unified manner. First, the blade must be designed to have natural frequencies that are removed from integer multiples of the rotor speed. This is necessary in order to ensure good dynamic characteristics. Second, the blade must be as light as possible but yet have sufficient inertia to allow autorotational landings. Third, the structure must be designed to ensure that blade stresses can be safely carried by the cross section through an adequate number of loading cycles. Fourth, this cross-sectional structure must fit within the aerodynamic envelope of the blade and be manufacturable. Fifth, that aerodynamic envelope must yield satisfactory rotor performance in hover and forward flight. Sixth, the combined structural, inertial, and aerodynamic characteristics of the blade must be aeroelastically stable with low vibrations. In the present work, we concentrate on the best methods of formulation for the above considerations such that the blade can be optimized effectively.

There has been a good deal of good work in rotor optimization through the years. Although we do not have space to do a complete survey, certain important contributions should be mentioned. In ref. 1, it is noted that efficient placement of lumped masses within the blade can lower helicopter stresses. References 2 and 3 attempt optimum placement of these masses but note that the minimum vibration solution often results either in high blade stresses or in bending-torsion flutter due to the natural migration of the torsional frequency to an integer multiple of rotor speed during the optimization process. Bielawa, ref. 4, performs a "man-in-the-loop" optimization in which aeroelastic stability is an integral part of the problem. He notes that a major hindrance to completely automated optimization is the complexity of constraints that define a realistic blade design.

In more recent work, Taylor (ref. 5) shows that optimization to low vibrations can result from efficient tailoring of mode shapes as well as from frequency placement. Reference 6 provides a combined aeroelastic and vibration optimization with complete flap-lag-torsion equations. The work shows that such an optimization is feasible, but that frequency constraints must still be applied in order to prevent migration of some modes to undesirable values. Reference 7 provides an optimum placement of dynamic frequencies based on initial designs of in-service rotor blades. Design parameters are taken to be the internal structural thicknesses of box beams and lumped masses (rather than the generic EI's, etc., used in previous work). Results show that all frequencies can be effectively placed with the use of realistic structural changes that can fit within the aerodynamic envelope. Reference 8 presents work on the optimization of rotor blades in order to have good aerodynamic performance, a consideration that is lacking in the earlier structural optimizations.

In the most recent work, refs. 9 and 10 re-examine the optimization problems of refs. 5 and 7 but with emphasis on optimization strategies and use of limited design spaces. Reference 11 provides some of the most involved aeroelastic optimization to date. This research shows the importance of obtaining analytic modal gradients in order to make the optimization procedure efficient. Finally, ref. 12 offers the first experimental verification that numerical optimization can truly result in rotor blades with lower vibrational characteristics.

In this paper, we look at the theoretical and practical problems associated with the addition of stress constraints and aerodynamic performance goals to the traditional structural and aeroelastic optimizations listed above. In traditional design methodologies in the industry, the choice of the aerodynamic blade shape (chord, thickness, twist, etc.) is the first step in the design process. This geometry is chosen based on aerodynamic performance considerations. Next, a structural design is performed in order to find an adequate structure (i.e., one that can withstand the blade fatigue loads) that can fit within the aerodynamic surfaces. Third, aeroelastic and vibrational analyses are performed to see if the blade needs to be tuned further in order to eliminate either instabilities or harmonic resonances (the latter of which would impact the stress calculations). It may very well be that a more "optimum" design could be obtained if these various individual optimizations were done in parallel rather than in series. For example, it may be that a slight compromise in blade performance (in order to accommodate additional structure) might lower vibrations to the point that a heavy vibration absorber could be eliminated, thus mitigating the performance loss. Therefore, it is important to determine how such a unified optimization might be performed.

THEORETICAL BACKGROUND

Structure

The first step in the optimization research described herein is to replace the true blade with a realistic, box-beam model that has dynamic characteristics similar to that of the true beam as well as a realistic stress distribution. Figure 1 depicts the schematic model used here. The blade chord and airfoil thickness are assumed to come from a performance analysis which could be running in parallel or in series with the structural analysis. This, then, defines a geometric area within which the box beam may be placed. The primitive design variables for the box beam are its width (b), its flange thickness (t), and its web thicknesses (s_1 and s_2). The box beam is assumed to carry all blade tension and all vertical bending. However, the secondary cell formed by the trailing-edge skin is assumed to contribute to both torsional stiffness and inplane stiffness through a skin thickness (p). Two additional primitive design parameters (a and d) allow for additional freedom in weight distribution. The parameter (a) defines the size of the tip weight, and the parameter (d) defines the width of a lumped mass internal to the box beam. These seven design parameters (along with given material properties) define the blade mass and structural properties. Naturally, they are constrained such that the pieces must fit within each other (e.g., $d<b-s_1-s_2$).

Now, these seven primitive design variables translate into eight overall structural properties. These are the two bending stiffnesses (EI_f and EI_c), the torsional stiffness and center-of-shear location (GJ and ϵ), and the mass and inertial properties of the cross-section (m, e, ρI_f, and ρI_c). However, these last two rotary inertia terms are only important in that their sum affects torsional frequency. Thus, there are seven primitive variables and seven overall structural properties. Therefore, the analyst (or optimizer) has freedom to change all structural properties in a fairly independent manner, but, on the other hand, there are severe restrictions on the space within which these changes can be made due the geometric constraints on primitive variables. Part of our research is to determine the tradeoffs between optimization with primitive variables and optimization with overall properties.

In those cases for which we optimize with primitive properties, we must first convert the overall properties of a given blade into primitive quantities. In effect, this is the problem of finding the properties such that our schematic blade (fig. 1) will have the properties of the true blade. Similarly, if one optimizes with overall quantities, then post processing must be done in order to convert those properties into primitive design variables. Thus, in either case, one must be able to translate structural properties into the corresponding primitive variables (when that is possible). In this research, we have accomplished this through a separate optimization process which finds the best fit between the properties of the schematic beam and the desired properties. It should be pointed out, however, that sometimes the desired properties cannot be exactly matched.

The reverse process, to turn primitive variables into structural properties, is rather straightforward and is outlined in ref. 7. Finally, if aerodynamic optimization is included, the blade chord and airfoil thickness (c and h) would also be variables.

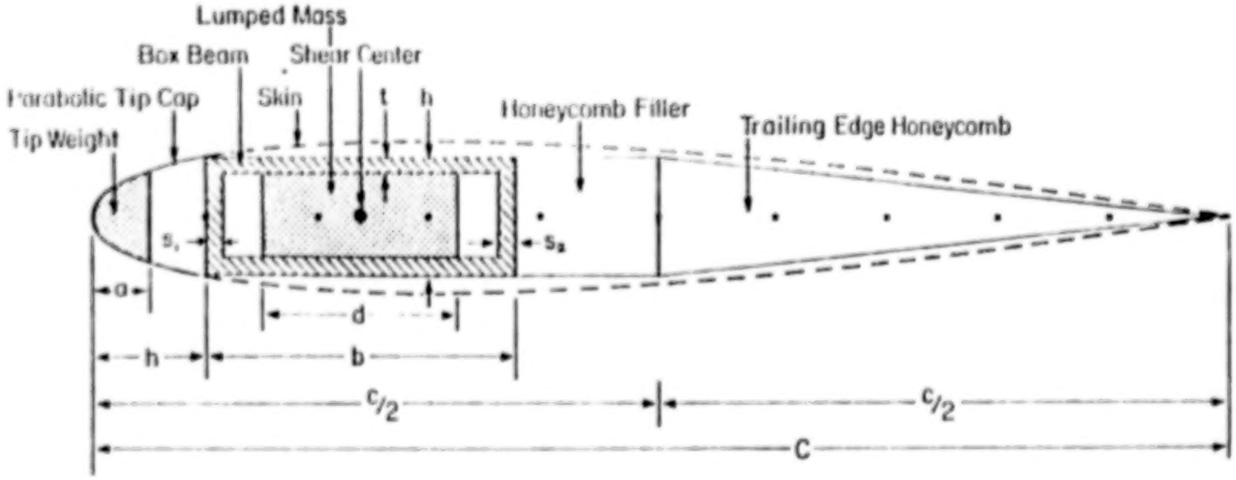

Physical properties:
t, s_1, s_2, b, a, d, c, h, p(skin thickness)

Material properties:
Density (box beam, lumped weights, & honeycomb filler)
E & G (box beam & skin)

Design variables:
t, s_1, s_2, b, a, d

Structural data:
EA, EI_f, EIc, GJ
m, ρI_f, ρI_c, e

Figure 1. Cross-Sectional Geometry

Elements of Analysis

Once the structure is defined, the next steop is to set up the analysis tools required in the optimization process. These are listed below:

1. Weight and inertias
2. Natural frequencies and modes
3. Performance and handling qualities
4. Vibrations and loads
5. Blade stresses and fatigue life
6. Aeroelastic stability

In the first category, a calculation of blade weight is necessary because blade mass not only adds its own weight to the helicopter but also results in additional weight in the control system, bearings, etc. Thus, every pound of blade weight could result in 3 pounds of structural weight, which implies less payload, more fuel, or shorter range. The mass moment of inertia is important because it must be large enough to support autorotation. For example, some companies recommend that the kinetic energy in the blade divided by hover power should be at least 2 sec. Also, the chordwise mass balance is important to vibration and to bending-torsion flutter. All three of these aspects are included in the present work.

In the second item, we find that the natural frequencies and mode shapes can also enter the optimization process. Past optimization studies have found it necessary and useful to keep blade frequencies within prescribed bounds. Figure 2 from ref. 7 shows vertical shears as a function of the second natural frequency of a teetering rotor (symmetric mode). One can see the strong coupling between frequency

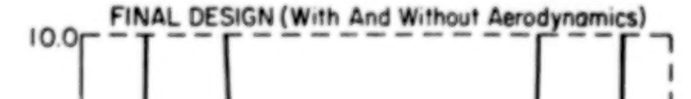

Figure 2. Effect of Frequency on Shear Stress

placement and vibrations both with and without the aerodynamic damping. This is one reason that frequency placement has always been a high priority of blade designers. Furthermore, as pointed out in refs. 5 and 12, the mode shape, itself, also has a strong influence on vibration because it affects the generalized force of each mode. In addition, poor placement of lower-frequency modes can adversely affect handling qualities; while proper placement of higher-frequency modes can improve performance. In this work, we use a subspace-iteration method to find the modes and frequencies of the structure. In the initial phase of optimization, frequency placement is part of the objective function such that frequencies begin to move within some prescribed window. Once any frequency falls within this window, however, its placement is then switched to a constraint. This process allows us to overcome problems associated with an infeasible initial guess. Table 1 summarizes the eigen analysis.

The third item deals with the performance of the aircraft. This area is very sensitive to the mission of a vehicle, and the "optimum" performance depends on the mission profile. In order to gain insight into multidisciplinary optimization without being mired in undue computations, we have chosen to optimize for the best hover performance out of ground effect. Admittedly, this is a very simple beginning; but it, nevertheless, allows for the important aerodynamic interactions which we wish to study. In particular, the blade twist, solidity, and taper ratio will enter the problem in important ways.

The next item on our analysis agenda is vibration and loads. These can enter the optimization through several paths. For example, there may be a minimum vibration requirement in which case it would enter as a constraint. On the other hand, additional vibration could require vibration attenuation devices which would add weight to the vehicle and thus degrade performance. In either case, vibratory

Table 1: Some Features of the Finite Element Program of Rotor Blade.

Elements:

1. Tapered and twisted beam elements are used.
2. Beam properties are specified at two ends of element and are varied linearly along element.
3. Lumped mass matrix with the effect of elastic offset included.
4. Stiffness terms include the following: bending, torsion, elongation, tension, kinetic energy due to inplane displacement, and "torsion-rotation" energy.

Capabilities of Program:

1. Rigid links are performed mathematically to increase efficiency of program and precision of results.
2. Discontinuity of beam properties is allowed.
3. Hinges of the blade are modeled "exactly".
4. Gradient information is calculated analytically.
5. Subspace iteration method is used to increase the efficiency of the iteration process.

airloads contribute to the fatigue of components and affect the life of blades. As with performance, we have elected to begin the optimization study with a simplified vibration analysis. Thus, in the initial stages, we are applying a given load spectrum to the blade with viscous damping added to simulate aerodynamic feedback. Obviously, this is a far cry from the detailed aeroelastic vibration analysis we plan to do later. However, it does give reasonable loads that interact with frequencies and mode shapes in a meaningful way. Therefore, it will allow a study of problems in combined optimization. It should also be noted that, since mode shapes enter the vibratory response, gradients of the modes are required in order to perform the optimization, see ref. 11.

The fifth item of analysis is that of stresses and fatigue life. Perhaps the most important goal of this present work is to incorporate this into the optimization process. In computation of stresses, we use the combined tensile stresses (due to centrifugal force) and the bending-torsion stresses due to the loading described above. These are combined in the conventional tensor way in order to find the three-dimensional "Mohr's Circle" that describes the stress state (static plus oscillatory). Fatigue life is then computed based on the methodologies described in refs. 13 and 14. In particular the infinite-fatigue-life stress is lowered by the typical "Endurance Reduction Factor" of 0.8 to obtain a "Reduced Endurance Limit." Next, a "Weighted Fatigue Approach" is used to modify the computed stresses. In this methodology, the alternating loads are multiplied by a factor of 2.0 and added to the static loads. A design is within the stress constraint if this computed maximum stress is less than the reduced endurance stress at all points within the structure. The use of stress as a constraint requires the computation of stress gradients. When primitive design variables are used in optimization, this method is straightforward, although involved. However, when the overall quantities are used, the detailed thicknesses are unknown at each iteration; and the stress computation encounters some necessary approximations. In this work, we also explore the consequences of these approximations.

The final element in the analysis is aeroelastic stability. Past work has shown this to be very important either when frequency placement is not a constraint or for hingeless and bearingless rotors. In this phase of our research, we are restricting ourselves to articulated and teetering rotors for which aeroelastic stability is not generally a problem. Thus, for the aeroelasticity portion of the analysis, we simply include a constraint that the center of mass be forward of the elastic axis of the blade at all cross sections. This prevents any classical bending-torsion flutter.

Objective Function

For the case of optimizing hover performance, it is possible to unify the entire problem into one objective function. This could be the payload (lifting force) of the rotor at a certain altitude at a given temperature. Such an objective function would be penalized by blade weight, by a reduction in rotor figure of merit, or by the added weight of vibration absorbers. To make this operational, one would have to decide on numerical values for the ratio of total mass to blade mass (taken above as 4 to 1) and on the number of pounds of isolator mass required to eliminate a certain number of pounds of 4/rev vibration at some location. Thus, the objective function would be the lifting capability at a given power minus the blade weight (multiplied by a factor to account for control-system weight to blade weight) minus the weight of vibration absorbers based on calculated vibrations. Similar objective functions could be formulated for other missions in terms of range or maneuverability.

RESULTS AND DISCUSSION

Scope of Present Results

This paper describes work in progress. However, we do have some very interesting numerical results obtained in the first phase of our work; and these results are presented here. In these first results, we have added the effect of stress constraints to the optimization, but we have not added the aerodynamic performance. Thus, the results below are for a fixed aerodynamic envelope. The initial blade design is the so-called "Hughes blade" of ref. 7 which resembles a typical McDonnell Douglas AH-64A blade in geometry but not in detailed design. The box-beam material is taken to be 6061 T6 Aluminum alloy with $35x10^3$ psi yield stress and $13x10^3$ psi endurance limit. Blade loads are considered harmonic in nature with a quadratic radial distribution. The strength of the zero harmonic is based on a given C_T, and other harmonics are given magnitudes based on the flight loads survey in ref. 15. The optimization is performed with CONMIN.

Section Properties

The first step in this optimization study was to try to match the physical data with the primitive cross-sectional variables. In the beginning work, we found that the optimizer indiscriminately placed stiffness in the box beam (rather than in the skin) which made skin thicknesses unreasonably small. Therefore, we fixed skin thickness and only allowed its modulus to vary. As a result, we could match all the physical stiffness properties with reasonable success, although the shear center seemed to end up closer to the front end of the box beam than in the data. Tables 2 and 3 outline the initial and modified procedures for this pre-optimization.

Table 2: Procedures Now Used to Determine Section Properties from Given Structural Data.

- **Step 1: Design variables:** t, s_1, s_2, or p(skin thickness)

  Objective: $w_1(EA - EA_0)^2 + w_2(EI_f - EI_{f0})^2 + w_3(EI_c - EI_{c0})^2$

  Constraints: $s_1 + s_2 < b$, $GJ < GJ_0$

  $(1-\tau_2)(EA_0) < EA < (1+\tau_1)(EA_0)$

  $(1-\tau_4)(EI_{f0}) < EI_f < (1+\tau_3)(EI_{f0})$

  $(1-\tau_6)(EI_{c0}) < EI_c < (1+\tau_5)(EI_{c0})$

- **Step 2: Solve G(skin), so that $GJ = GJ_0$**

- **Step 3: Design variables:** a, d, skin density.

  Objective: $w_1(m - m_0)^2 + w_2(\rho I_f - \rho I_{f0})^2 + w_3(\rho I_c - \rho I_{c0})^2 + w_4(e - e_0)^2$

  Constraints: $(1-\tau_2)(m_0) < m < (1+\tau_1)(m_0)$

  $(1-\tau_4)(\rho I_{f0}) < \rho I_f < (1+\tau_3)(\rho I_{f0})$

  $(1-\tau_6)(\rho I_{c0}) < \rho I_c < (1+\tau_5)(\rho I_{c0})$

  $(1-\tau_8)(e_0) < e < (1+\tau_7)(e_0)$

- Where w_i is weighting scalar, τ_i is tolerant value, $(\ )_0$ is given data, $(\ )_f$ represents quantity in flapping direction, $(\ )_c$ represents quantity in chordwise direction, and e is elastic offset.

Table 3: Proposed Procedures to Determine Section Properties from Given Structural Data.

- Step 1: Design variables: t, s_1, s_2 (Given skin thickness & Gskin))

  Objective: $w_1(EA - EA_0]^2 + w_2(EI_f - EI_{f0}]^2 + w_3(EI_c - EI_{c0}]^2 + w_4(GJ - GJ_0)$

  Constraints:

  $$s_1 + s_2 < b$$
  $$(1-\tau_2)(EA_0) < EA < (1+\tau_1)(EA_0)$$
  $$(1-\tau_4)(EI_{f0}) < EI_f < (1+\tau_3)(EI_{f0})$$
  $$(1-\tau_6)(EI_{c0}) < EI_c < (1+\tau_5)(EI_{c0})$$
  $$(1-\tau_8)(GJ_0) < GJ < (1+\tau_7)(GJ_0)$$

- Step 2: If the results from Step 1 are not acceptable, then the another skin thickness and Gskin) are selected and Step 1 is performed again. Repeated Steps 1 & 2 until reasonable data are obtained.

- Step 3: Design variables: a, d (Given skin density)

  Objective: $w_1[m - m_0]^2 + w_2[(\rho I_f + \rho I_c) - (\rho I_{f0} + \rho I_{c0})]^2 + w_3[e - e_0]^2$

  Constraints:

  $$(1-\tau_2)(m_0) < m < (1+\tau_1)(m_0)$$
  $$(1-\tau_4)(\rho I_{f0}) < \rho I_f < (1+\tau_3)(\rho I_{f0})$$
  $$(1-\tau_6)(\rho I_{c0}) < \rho I_c < (1+\tau_5)(\rho I_{c0})$$
  $$(1-\tau_8)(e_0) < e < (1+\tau_7)(e_0)$$

Next we optimized the blade for frequency placement using both the overall properties (EI, GJ, etc.) and the primitive variables (t, s, etc.). Here, we found that we could optimize the blade by either method and then restore overall properties to primitive values by the properties optimization methodology discussed above. Table 4 summarizes the three phases of this process. In the first two phases, various frequencies are brought within the desired windows by the use of frequency placement in the objective function. Then, with all frequencies within these windows, the windows become constraints and weight is minimized. Table 5 shows the result of this optimization when the structural properties (primitive variables) are used. A total of 77 iterations are required to meet all requirements. Table 6 shows the identical optimization when the physical properties (EI, etc.) are used. In this case, an optimum is reached in only 61 iterations. Thus, there is some saving in not using primitive variables. However, one has the added problem of turning these overall quantities into primitive variables in order to realize the design. Furthermore, one cannot apply stress constraints at each iteration if the internal geometry is not known. Therefore, in the work to follow, we concentrate on optimization with primitive variables.

Optimization with Stress Constraints

Next, we added stress constraints to the optimization process. In the beginning of this phase, when we only considered yield stresses, we found that the stress constraint never became active. In other words, the optimization to place frequencies never did anything so drastic to the blade that any section would reach yield stress. However, when we extended the stress constraints to include fatigue life, stresses became an important part of the analysis.

Table 4: Procedures of Optimizing the Hughes Articulated Rotor Blade.

Based on:	Structural Properties	Physical Properties
Frequency placement (I)		
Design variables:	EI_f, EI_c, m, ρI_f, ρI_c	t, s_1, s_2, a, d

Constraints

$1.0 < p(\text{flapping-1st})^* < 1.5$
$2.3 < p(\text{flapping-2nd}) < 2.75$
$0.3 < p(\text{inplane-1st}) < 0.7$
$4.23 < p(\text{torsion-1st}) < 4.7$
1.2581×10^4 (mugs-in^2) < autorotation
side constraints on design variables

Objective $[\,p(\text{flapping-3rd}) - 4.5\,]^2 + [\,p(\text{inplane-2nd}) - 6.5\,]^2 + [\,p(\text{flapping-4th}) - 7.5\,]^2$

* p = (blade natural frequency) / (rotor rotational frequency).

Based on:	Structural Properties	Physical Properties
Frequency placement (II)		
Design variables:	EI_f, EI_c, GJ, m, ρI_f, ρI_c	t, s_1, s_2, a, d

Constraints

$1.0 < p(\text{flapping-1st}) < 1.5$
$2.3 < p(\text{flapping-2nd}) < 2.7$
$4.3 < p(\text{flapping-3rd}) < 4.7$
$7.3 < p(\text{flapping-4th}) < 7.7$
$0.3 < p(\text{inplane-1st}) < 0.7$
$6.3 < p(\text{inplane-2nd}) < 6.7$

Structural Properties	Physical Properties
$4.25 < p(\text{torsion-1st}) < 4.7$	$4.3 < p(\text{torsion-1st}) < 4.7$
	$12.3 < p(\text{torsion-2nd}) < 12.7$

1.2581×10^4 (mugs-in^2) < autorotation
side constraints on design variables

Objective $(\,[\,p(\text{flapping-5th}) - 11.5\,]^2$
$+ [\,p(\text{torsion-2nd}) - 12.5\,]^2\,)$

Table 4: Procedures of Optimizing the Hughes Articulated Rotor Blade (Concluded).

Based on	Structural Properties	Physical Properties
Weight Minimization		
Design variables:	EI_f, EI_c, GJ, m, ρI_f, ρI_c	t, s_1, s_2, a, d
Constraints	$1.0 <$ p(flapping-1st) < 1.5 $2.3 <$ p(flapping-2nd) < 2.7 $4.3 <$ p(flapping-3rd) < 4.7 $7.3 <$ p(flapping-4th) < 7.7 $11.3 <$ p(flapping-5th) < 11.7 $0.3 <$ p(inplane-1st) < 0.7 $6.3 <$ p(inplane-2nd) < 6.7 $4.3 <$ p(torsion-1st) < 4.7 $12.3 <$ p(torsion-2nd) < 12.7 0. < elastic offset* 1.2581×10^4 (mugs-in²) < autorotation side constraints on design variables	
Objective	Weight of Blade	

* Except at station 75 which originally has an elastic offset equal to -.52 and has the constraint (elastic offset > -0.54).

Table 5: Optimization Results of Hughes Blade (Structural Properties as Design Variables).

	Original	Frequency Placement(I)	Frequency Placement(II)	Weight Minimization
Weight (lbs)	203.42	217.36	217.03	193.03
Autorotation	12581.	13233.	13203.	12661.
p(inplane-1st)	0.4756	0.4820	0.4820	0.4677
p(flapping-1st)	1.0293	1.0304	1.0304	1.0257
p(flapping-2nd)	2.7451	2.6143	2.6287	2.6876
p(torsion-1st)	4.2483	4.2501	4.2563	4.3058
p(flapping-3rd)	4.9035	4.5101	4.5772	4.6979
p(inplane-2nd)	6.8914	6.5029	6.5118	6.6958
p(flapping-4th)	7.9378	7.5026	7.5923	7.5558
p(flapping-5th)	12.058	10.933	11.500	11.302
p(torsion-2nd)	12.921	12.927	12.500	12.642
p(flapping-6th)	16.996	15.521	15.921	15.484
Iterations(CONMIN)	--	21	7	49

Table 6: Optimization Results of Hughes Blade (Physical Properties as Design Variables).

	Original	Frequency Placement(I)	Frequency Placement(II)	Weight Minimization
Weight (lbs)	203.42	213.86	214.55	203.15
Autorotation	12581.	12579.	12777.	12656.
p(inplane-1st)	0.4756	0.4841	0.4824	0.4708
p(flapping-1st)	1.0293	1.0310	1.0305	1.0269
p(flapping-2nd)	2.7451	2.5801	2.6049	2.6989
p(torsion-1st)	4.2483	4.3448	4.3345	4.3014
p(flapping-3rd)	4.9035	4.5049	4.5779	4.6985
p(inplane-2nd)	6.8914	6.5020	6.5186	6.6272
p(flapping-4th)	7.9378	7.4962	7.6803	7.6934
p(flapping-5th)	12.058	11.151	11.500	11.553
p(torsion-2nd)	12.921	12.580	12.684	12.380
p(flapping-6th)	16.996	15.850	16.243	16.293
Iterations(CONMIN)	--	16	7	38

Figure 3 shows the critical stresses along the blade for the original design (i.e., the schematic model of the blade with one cell in the spar). The dashed line is the static stress in hover which comes primarily from tension stress and bending moments. Notice that the moment must go to zero at the hinge and at the tip, but the tension is zero only at the tip. The solid line is the dynamic stress from our oscillatory vertical loading distribution. This loading, based on ref. 15, includes up to 8 harmonics; and the oscillatory part is doubled as per the fatigue methodology in refs. 13 and 14. The solid curve with open symbols is the reduced fatigue-life stress discussed earlier. We can see that the original blade meets the fatigue-life criterion except near the hinge.

Figure 4 shows the stress distribution on the optimized blade for which frequencies have been placed in predetermined windows but without stress constraints, as in ref. 7. One can see that the slight overstress near the hinge (r=50) still exists. However, a large overstress has developed at r=240. This is due to a lower thickness which was placed there to lower the frequencies of the 3rd flapping and 2nd torsional modes. Therefore, this previously obtained optimum has reduced fatigue life. Starting with this solution, we began a second optimization with the fatigue criteria as side constraints. Figure 5 shows the results for the newly optimized blade. We can see that the optimizer is able to maintain the frequencies within the desired windows and still satisfy the fatigue life constraints. The constraint is active near the root and at the soft section. Furthermore, although extra structural material has been added to lower stresses, this allows added mass to be removed (the autorotational constraint) so that the final design is no heavier than the one that violated the stress constraints.

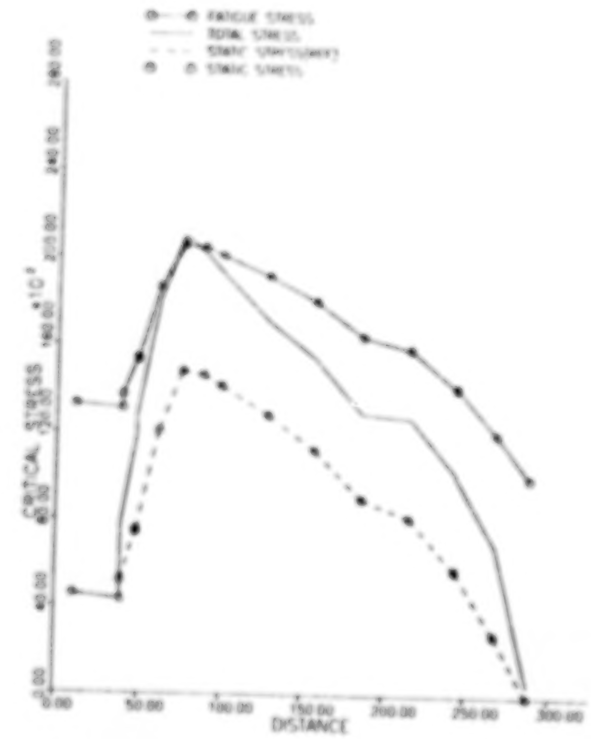

Figure 3. Stresses of Initial Design

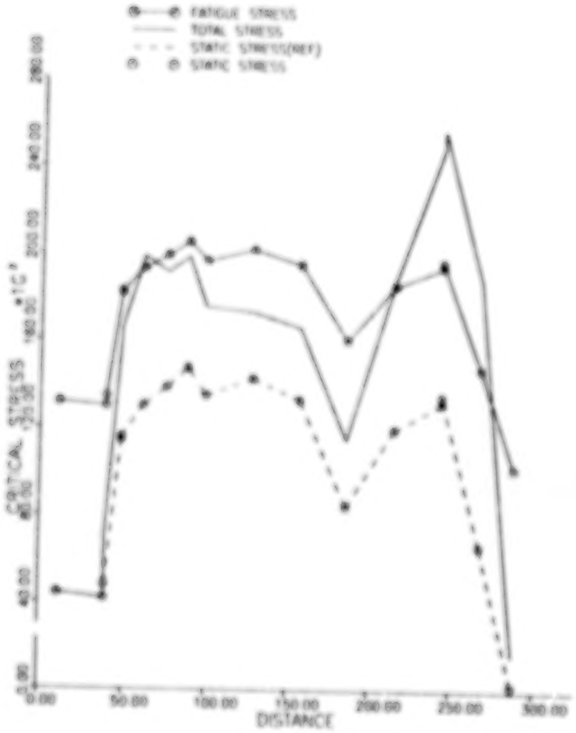

Figure 4. Stresses of Optimum Design

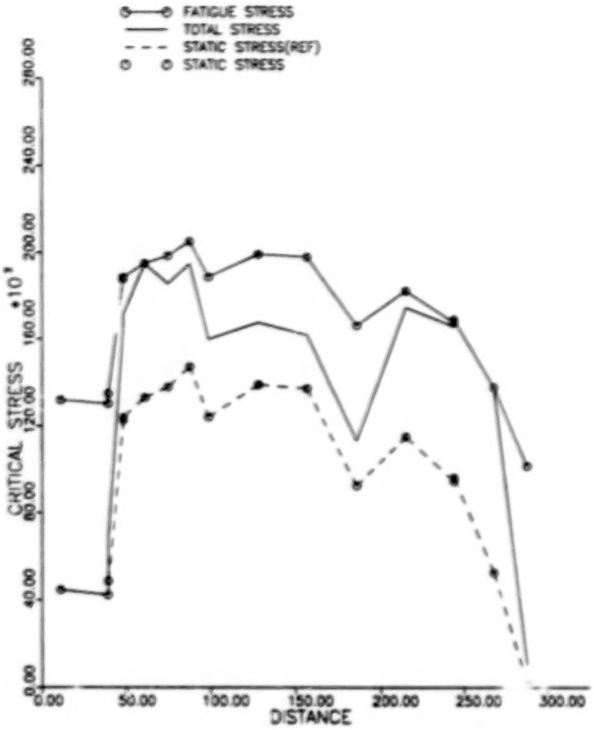

Figure 5. Stresses after Stress Constraint

Figures 6-10 show the major primitive variables (t, s_1, s_2, a, and d) before optimization (diamonds), after frequency placement (dashed line), and after application of stress constraints (solid line). Looking first at thickness, fig. 6, we see that (after frequency placement) the thickness has been drastically reduced near station 240. However, once the stress constraint is applied, this thickness is returned to its original value at the point of high stress (station 240) but not further inboard where modal curvature is highest. Therefore, there is no need to compensate for this added stiffness (which occurs primarily in GJ and EI_{yy}). One also notices that a large increase in thickness occurs at to the tip. As pointed out in ref. 7, near the tip there is no real distinction between structural mass and lumped mass because structure is ineffective. Consequently, the lumped mass added to the tip (to minimize weight for a given inertia) has been placed in box-beam mass rather than in non-structural mass, figs. 9 and 10. The decrease in web thickness with frequency placement, seen in figs. 7 and 8, does not impact the fatigue life because it occurs away from the high-stress areas. Thus, little change occurs in s_1 or s_2 after the stress constraint is applied.

It should be noted here that the addition of the stress constraints increases the computational time required to optimize by a factor of 5 to 6. The increased time is not so much in the stress computation (which is very simplified here). Rather, the computational time is expended in moving from unfeasible to feasible solutions and in calculating the complicated modal sensitivities that are needed for gradients of the stress constraints. Thus, more research must be done in these areas before more sophisticated stress and aeroelastic constraints can be applied.

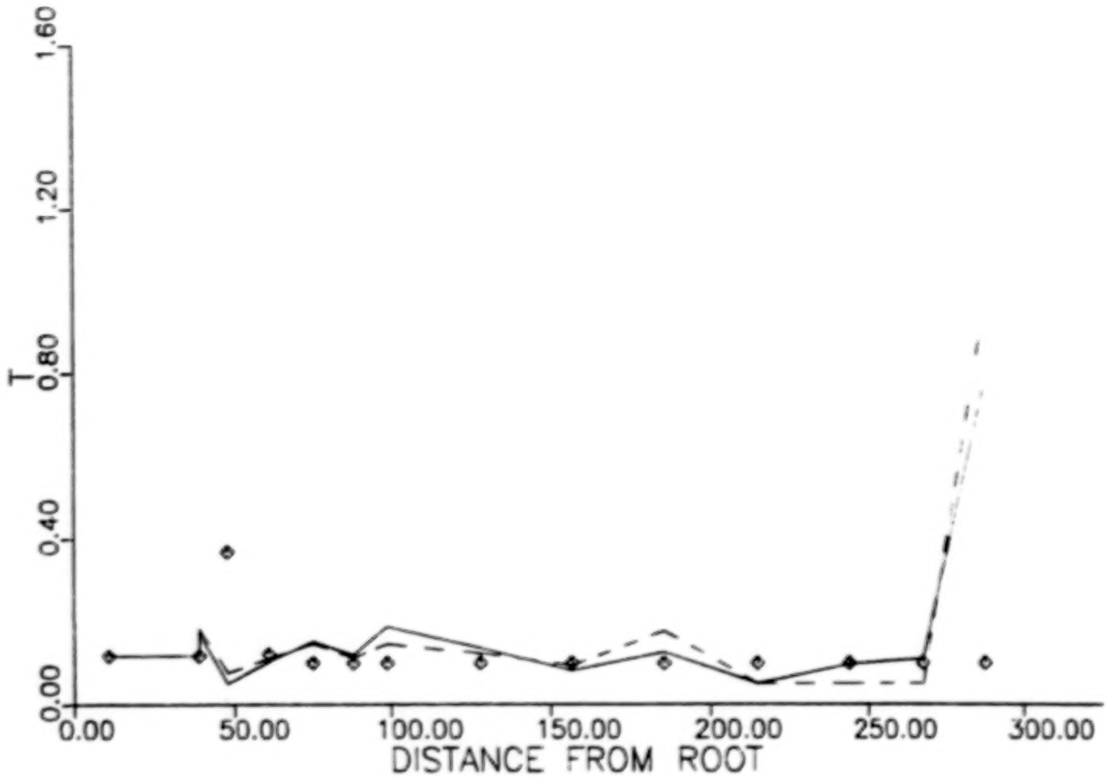

Figure 6. Flange Thickness, t

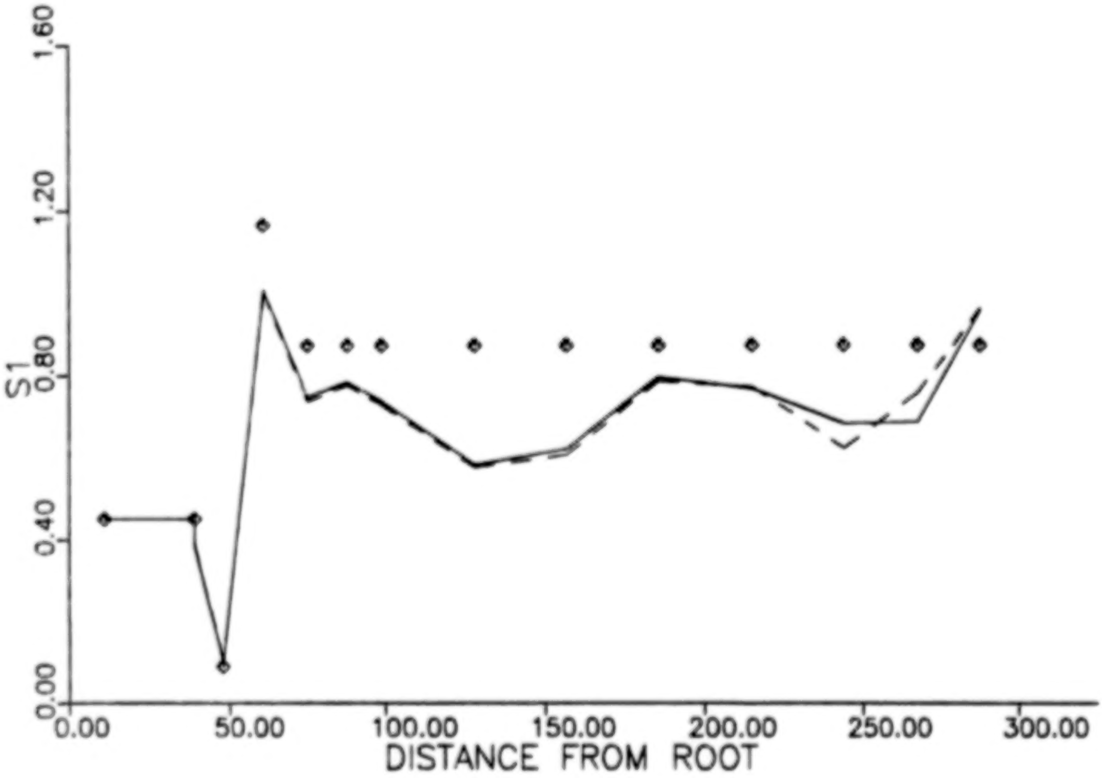

Figure 7. Webb Thickness, s_1

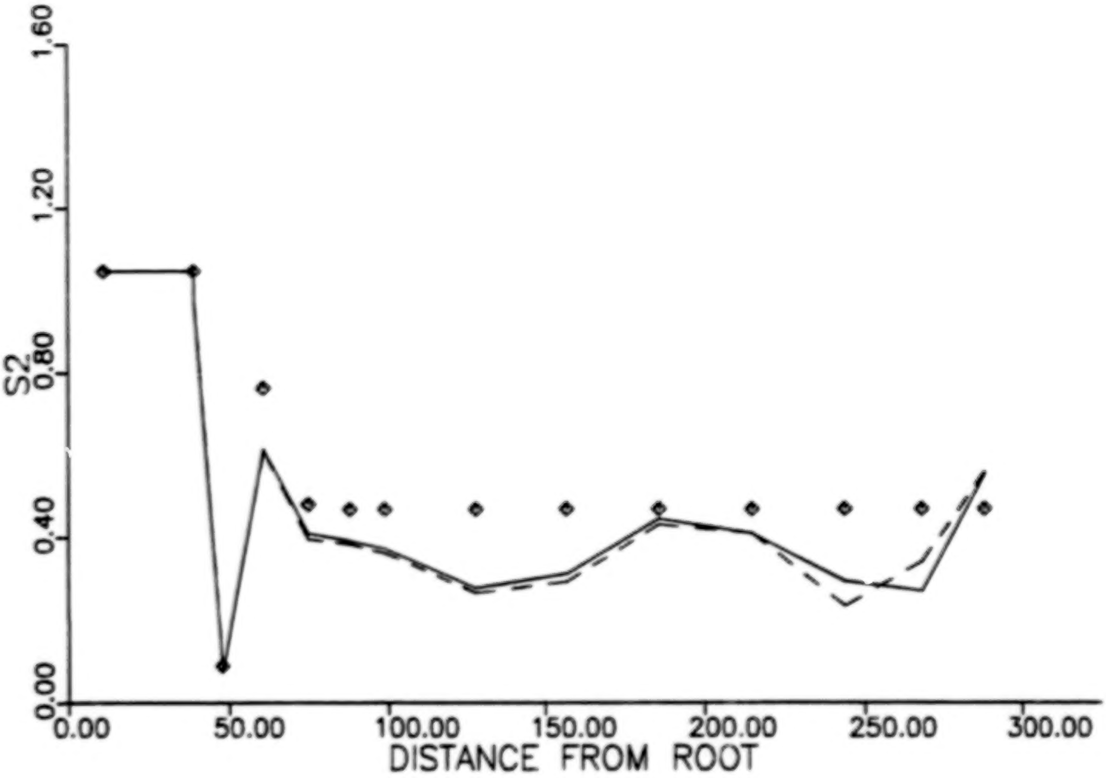

Figure 8. Webb Thickness, s_2

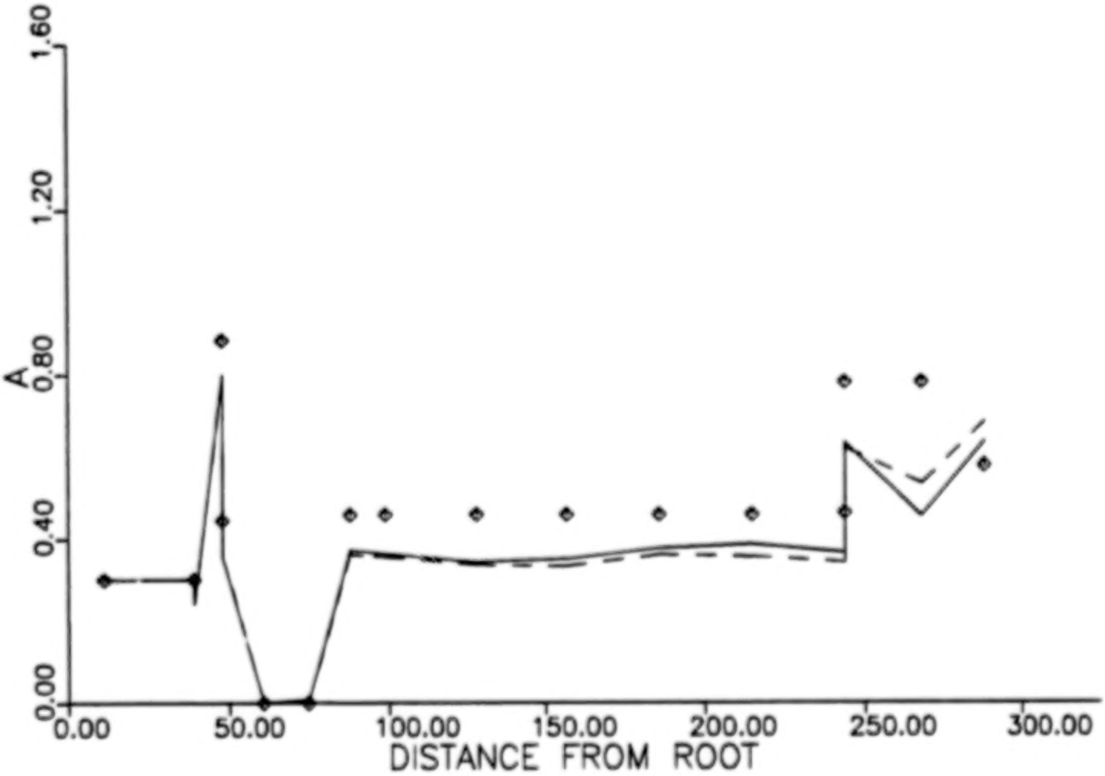

Figure 9. Tip Mass Size, a

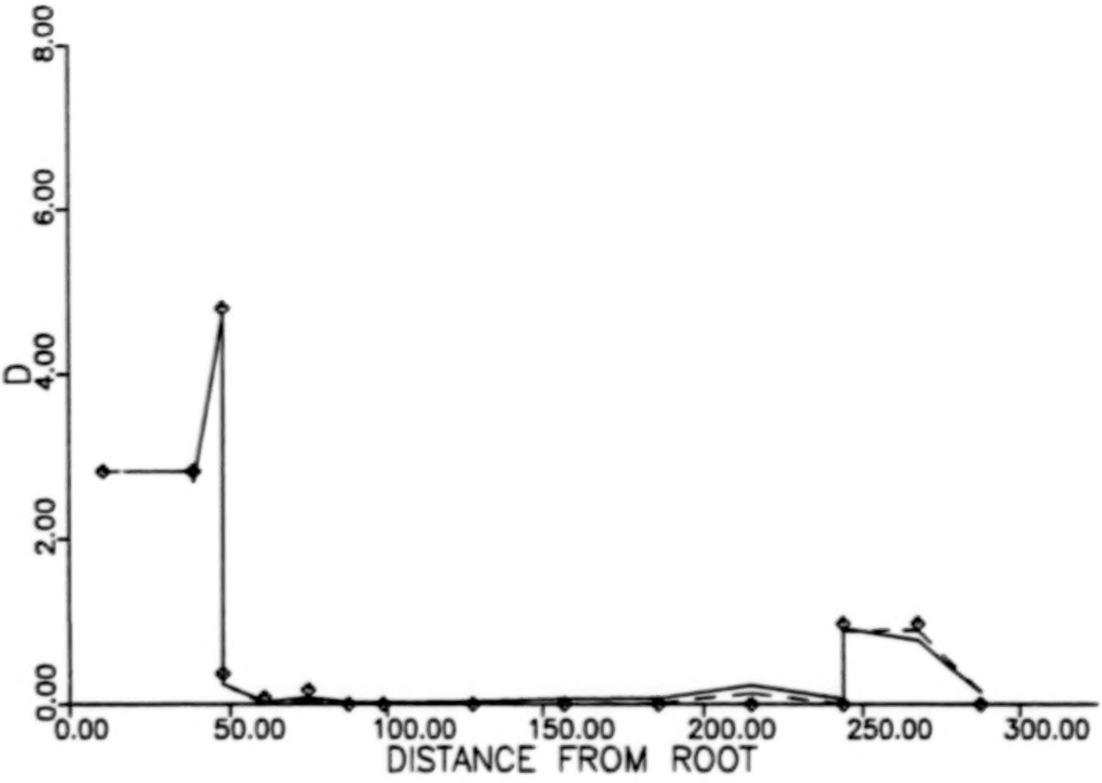

Figure 10. Internal Mass Size, d

SUMMARY AND CONCLUSIONS

In this paper, we have outlined general principles whereby multidisciplinary optimization could be performed in the design of helicopter blades. A very important part of the problem is the development of efficient computational schemes for the various components of the analysis. Results show that stress constraints based on fatigue life can be added to conventional structural optimization. However, we are still a long way from a completely integrated, automated design process.

ACKNOWLEDGMENT

This work was sponsored by the Interdisciplinary Research Office, National Aeronautics and Space Administration, Langley Research Center, Grant No. NAG-1-710, Howard Adelman, technical officer.

REFERENCES

1. Hirsch, Harold, Dutton, Robert E., and Sasumoff, Abner, "Effect of Spanwise and Chordwise Mass Distribution on Rotor Blade Cyclic Stresses," Journal of the American Helicopter Society, Vol. 1 (2), April 1956.

2. Miller, Rene H. and Ellis, Charles W., "Helicopter Blade Vibration and Flutter," Journal of the American Heliciopter Society, Vol. 1 (3), July 1956.

3. Daughaday, H., DuWaldt, F., and Gates, C., "Investigation of Helicopter Blade Flutter and Load Amplification Problems," Journal of the American Helicopter Society, Vol. 2 (3), July 1957.

4. Bielawa, Richard L., "Techniques for Stability Analysis and Design Optimization with Dynamic Constraints of Nonconservative Linear Systems," AIAA/ASME 12 SDM Conference, Anaheim, California, April 19-21, 1971, *AIAA Paper No. 71-388*.

5. Taylor, Robert B., "Helicopter Vibration Reduction by Rotor Blade Modal Shaping," Proceedings of the 38th Annual National Forum of the American Helicopter Society, Anaheim, California, May 1982.

6. Friedmann, P.P. and Shanthakumaran, P., "Optimum Design of Rotor Bades for Vibration Reduction," *Journal of the American Helicopter Society*, Vol. 29(4), October 1984, pp. 70-80.

7. Peters, David A., Rossow, Mark P., Korn, Alfred, and Ko, Timothy, "Design of Helicopter Rotor Blades for Optimum Dynamic Characteristics," *Computers and Mathematics with Applications*, Vol. 12(1), 1986, pp. 85-109.

8. Walsh, Joanne L., Bingham, Gene J., and Riley, Michael F., "Optimization Methods Applied to the Aerodynamic Design of Helicopter Rotor Blades," *Journal of the American Helicopter Society*, Vol. 32(4), October 1987, pp. 39-44.

9. Chattopadhyay, Aditi and Walsh, Joanne L., "Minimum Weight Design of Rectangular and Tapered Helicopter Rotor Blades with Frequency Constraints," Second International Conference on Rotorcraft Basic Research, University of Maryland, February 1988.

10. Pritchard, J. and Adelman, H., "Optimal Placement of Tuning Masses for Vibration Reduction in Helicopter Rotor Blades," Second International Conference on Rotorcraft Basic Research, University of Maryland, February 1988.

11. Lim, Joon W. and Chopra, Inderjit, "Aeroelastic Optimization of a Helicopter Rotor," Proceedings of the 44th Annual National Forum of the American Helicopter Society, Washington, DC, June 16-18, 1988.

12. Weller, W.H. and David, M.W., "Experimental Verification of Helicopter Blade Design Optimization for Minimum Vibration," Proceedings of the 44th Annual National Forum of the American Helicopter Society, Washington, DC, June 16-18, 1988.

13. Noback, R., "State of the Art and Statistical Aspects of Helicopter Fatigue Substantiation Procedures," *Helicopter Fatigue Life Assessment*, AGARD Conference Proceedings No. 297, also presented at the 51st Meeting of the AGARD Structures and Materials Panel, Air-in-Provence, France, September 14-19, 1980.

14. McDermott, John, "The Methodology of Fatigue Analysis and Testing - Main Rotor Blade and Hub - Hughes YAH-64 Advanced Attack Helicopter," *Helicopter Fatigue Life Assessment*, AGARD Conference Proceedings No. 297, also presented at the 51st Meeting of the AGARD Structures and Materials Panel, Air-en-Provence, France, September 14-19, 1980.

15. Esculier, J. and Bousman, W.G., "Calculated and Measured Blade Structural Response on a Full Scale Rotor," *Journal of the American Helicopter Society*, Vol. 33(1), January 1988.

TRANSONIC AIRFOIL DESIGN FOR HELICOPTER ROTOR APPLICATIONS

Ahmed A. Hassan and B. Jackson
McDonnell Douglas Helicopter Company
Mesa, Arizona

ROTOR AIRFOIL DESIGN

Despite the fact that the flow over a rotor blade is strongly influenced by locally three-dimensional and unsteady effects, practical experience has always demonstrated that substantial improvements in the aerodynamic performance can be gained by improving the steady two-dimensional characteristics of the airfoil(s) employed. The two phenomena known to have great impact on the overall rotor performance are: 1) retreating blade stall with the associated large pressure drag, and 2) compressibility effects on the advancing blade leading to shock formation and the associated wave drag and boundary-layer separation losses.

HOVER **FORWARD FLIGHT** **MANEUVERS**

GENERAL DESIGN OBJECTIVES

- MAXIMUM LIFT CAPABILITY AT LOW SPEED
- HIGH MACH DRAG DIVERGENCE
- NEAR ZERO PITCHING MOMENT
- LOW PROFILE AND COMPRESSIBILITY DRAG

ROTOR AIRFOIL DESIGN IS A MULTIPLE DESIGN POINT PROBLEM

CLASSIFICATION OF DESIGN PROBLEMS

Two design problems are identified:

ITERATIVE DIRECT METHODS [1,2]: In these methods, direct solutions are sought with an airfoil geometry that is modified in an iterative process (either by the designer or through numerical optimization utilizing a set of geometric shape functions) to minimize the differences between the computed and the prescribed target pressures.

INVERSE METHODS [3-5]: Here a target pressure distribution is prescribed and the objective is to find the airfoil geometry that would yield the specified target pressure at design conditions.

The above two inviscid procedures have also been extended to allow for viscous effects through coupling with an integral boundary-layer formulation [6,7].

DIRECT

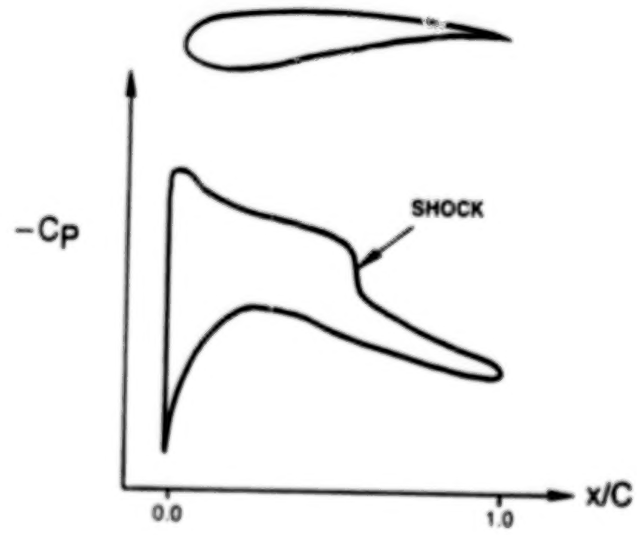

ADVANTAGES :
- FIRM CONTROL OF GEOMETRY
- RAPID CONVERGENCE RATES
- APPLICABLE FOR SHOCKED & SHOCKLESS DESIGNS

LIMITATIONS :
- ABILITY TO CONTROL AERODYNAMIC CHARACTERISTICS IS ABSENT (TRIAL AND ERROR)

INVERSE

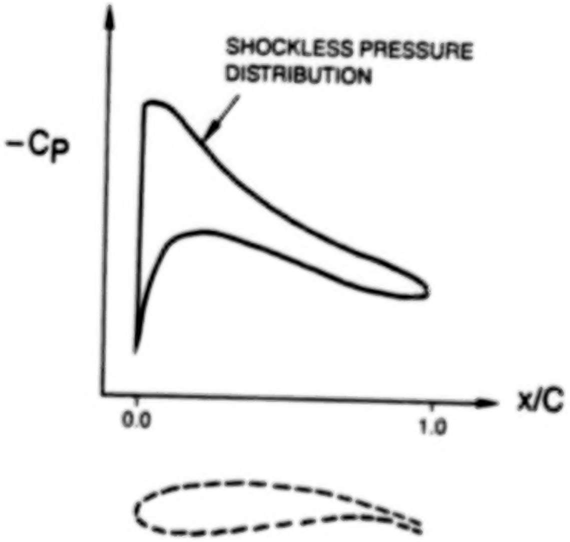

ADVANTAGES:
- BETTER CONTROL OF AERODYNAMICS

LIMITATIONS :
- LACKS CONTROL OF GEOMETRIC REGULARITY
- SLOWER CONVERGENCE RATES
- LIMITED TO SHOCK-FREE DESIGNS

ITERATIVE DIRECT PROCEDURE

Two primary design tools were utilized at McDonnell Douglas Helicopter Company in generating an airfoil designated HH-06 [8-11]. FLO-6 OPT [12-14]; a two-dimensional transonic full potential direct solver with a constrained function minimization routine and, the BAUER code [15]; a two-dimensional transonic full potential direct solver with boundary - layer corrections. In the design process, the airfoil geometry was optimized using FLO-6 OPT to meet the prescribed design objectives. The resultant profile was then evaluated (at design and off-design conditions) and further refined using the BAUER code.

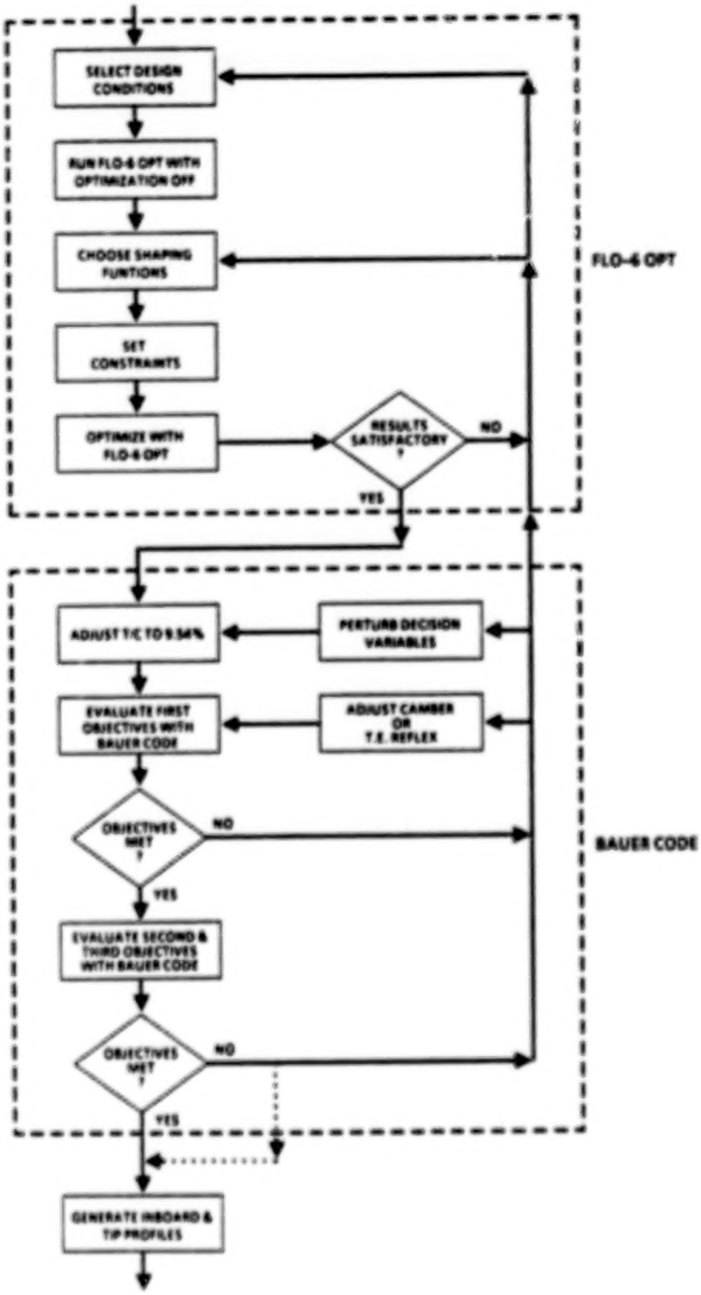
SELECT DESIGN CONDITIONS
RUN FLO-6 OPT WITH OPTIMIZATION OFF
CHOOSE SHAPING FUNTIONS
SET CONSTRAINTS
OPTIMIZE WITH FLO-6 OPT
RESULTS SATISFACTORY ?
NO
YES
FLO-6 OPT
ADJUST T/C TO 9.34%
PERTURB DECISION VARIABLES
EVALUATE FIRST OBJECTIVES WITH BAUER CODE
ADJUST CAMBER OR T.E. REFLEX
OBJECTIVES MET ?
NO
YES
BAUER CODE
EVALUATE SECOND & THIRD OBJECTIVES WITH BAUER CODE
OBJECTIVES MET ?
NO
YES
GENERATE INBOARD & TIP PROFILES

DESIGN PROCEDURE

In the design of the HH-06 airfoil, the initial profile was modified through the application of different shape functions to its upper and lower surfaces. A specific aerodynamic parameter (or object function) such as the drag coefficient is minimized through adjusting the decision variables (e.g., n, m, p, ...etc) which control the magnitude and location of the shape functions. Constraints, either geometric or aerodynamic, may be added to the minimization process. The effect of each shape function is then assessed by perturbing its decision variable and computing the change in the object function. The resulting gradient is then traced until a local minimum is found or a constraint is reached.

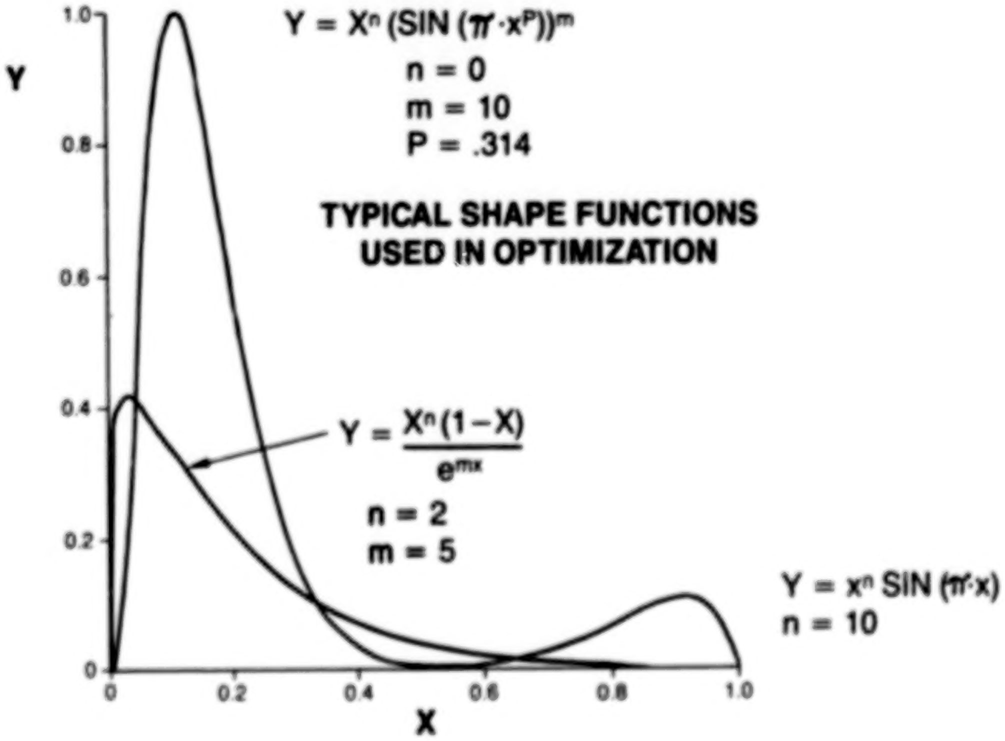

TYPICAL SHAPE FUNCTIONS USED IN OPTIMIZATION

Object function : CD @ M=0.81, Alfa=-0.5°
Geometric Constraint : 0.10 ≥ t/c ≥ 0.095
Aerodynamic constraints : |CM| ≥ 0.010 @ M=0.30, Alfa=-0.5°
|CM| ≥ 0.015 @ M=0.80, Alfa=-0.5°
ML ≤ 1.400 @ M=0.80, Alfa=-0.5°
ML ≤ 1.400 @ M=0.40, Alfa=12.5°

RESULTS OF THE ITERATIVE DIRECT PROCEDURE

In the late seventies, the National Aeronautics and Space Administration awarded two contracts (Boeing VERTOL, Lockheed Georgia) for the design of an advanced airfoil for rotorcraft applications [16,17]. A set of design objectives was defined which, when met, would ensure acceptable performance during hover and through high-speed flight. The VERTOL design later evolved to the successful VR-12 family of airfoils. In 1983 engineers at the McDonnell Douglas Helicopter Company embarked on the further refinement of the Lockheed design using the NASA set objectives as design goals.

COMPARISON OF HH-06 TEST RESULTS WITH DESIGN OBJECTIVES

	OBJECTIVE	HH-06
	$t/c = .0954$	$t/c = .09542$
First Priority:		
	1) $\lvert C_{M_o}\rvert \leq .01$ $M = .3$	$C_{M_o} = .0014$
	2) $C_{L_{max}} \geq 1.5$ $M = .4$	$C_{L_{max}} = 1.49$
	3) $M_{DD_o} \geq .81$	$M_{DD_o} = .808$
	4) $\lvert C_{M_o}\rvert \leq .015$ $M \leq .80$	$C_{M_o} = -.0055$
Second Priority:		
	5) $C_D \leq .008$ $C_L = .6,\ M = .6$	$C_D = .0094$
	6) $C_{L_{max}} \geq 1.5$ $M = .5$	$C_{L_{max}} = 1.21$
	7) $\lvert C_M\rvert \leq .02$ $C_L = 1.0,\ M = .3$	$C_M = -.0174$
	8) $C_{D_o} \leq .01$ $M = M_{DD_o} + .02$	$C_{D_o} = .0137$ $M = .828$
Third Priority:		
	9) $M_{T_o} \geq M_{DD_o}$	$M_{T_o} = .800$
	10) Gradual Stall	
	$M = .3$	MIXED
	$M = .4$	MIXED
	11) $C_{D_o} \leq .007$ $M_{DD} = M_{DD} - .1$	$C_{D_o} = .0070$ $M = .708$

M_{DD} @ $dC_D/dM = .1$

M_T @ $dC_M/dM = -.25$

BEST COPY AVAILABLE

AERODYNAMIC CHARACTERISTICS OF THE HH-06 AIRFOIL

A comparison is made between the aerodynamic characteristics of the designed HH-06 airfoil and those of other airfoils which represent state-of-the-art designs. The comparisons represent the variation in the maximum sectional lift (Clmax) at a free-stream Mach number of 0.40 versus zero-lift drag divergence Mach number. As seen, the HH-06 characteristics compare quite well with the other recently developed families of airfoils [18-21].

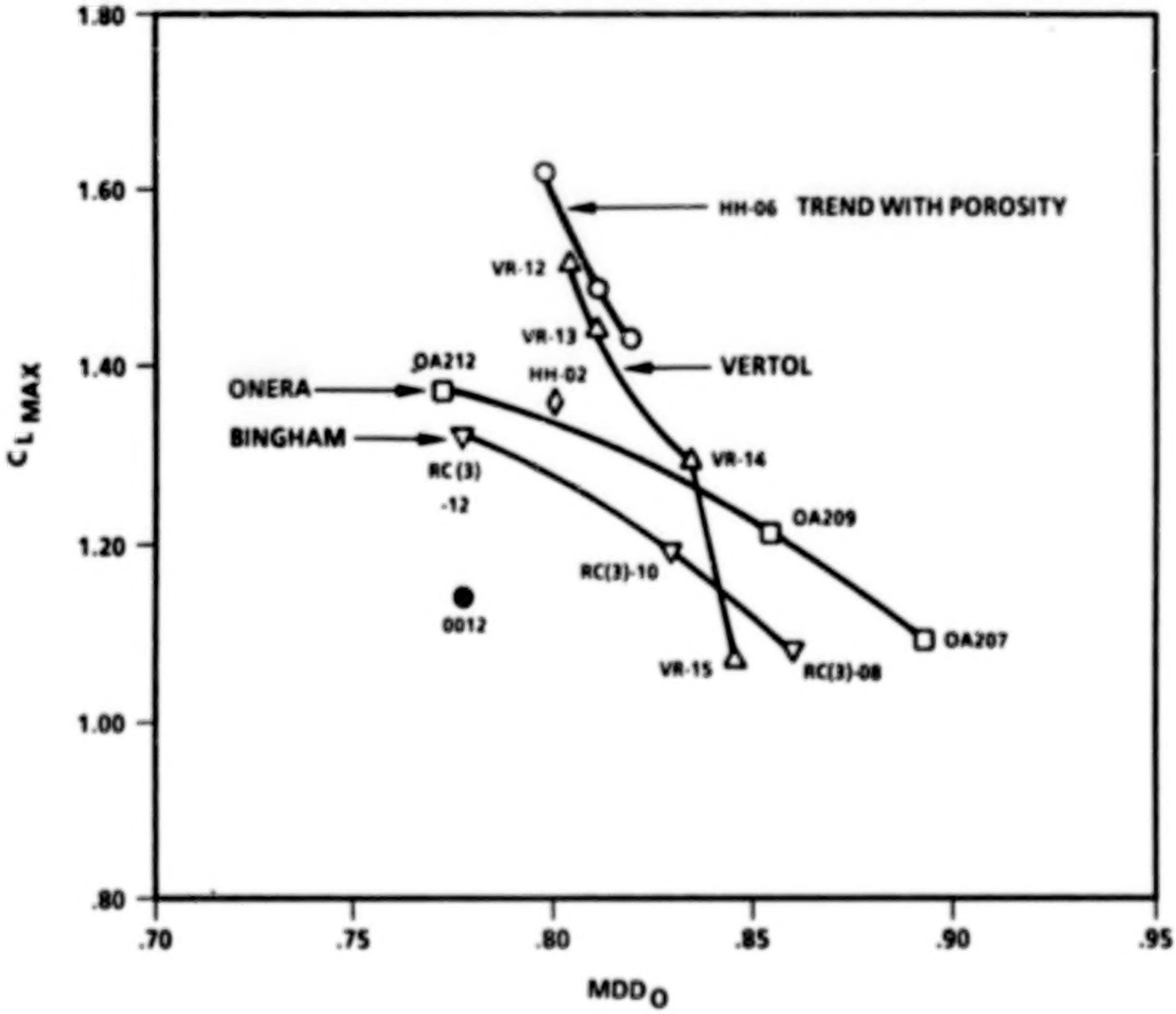

HYBRID DESIGN PROCEDURE

It is obvious that for many practical applications, structural or aerodynamic, that the most desirable design procedure is one which combines the advantages from a direct computational method with those of an inverse method. In this respect, the shortcomings of each are overcome by the strengths of the other. Such methods, commonly referred to as "***Hybrid Methods***" have been successfully applied in the design of subcritical airfoil sections for fixed wing applications [22], and in the design of supercritical cascades for turbomachinery applications [23].

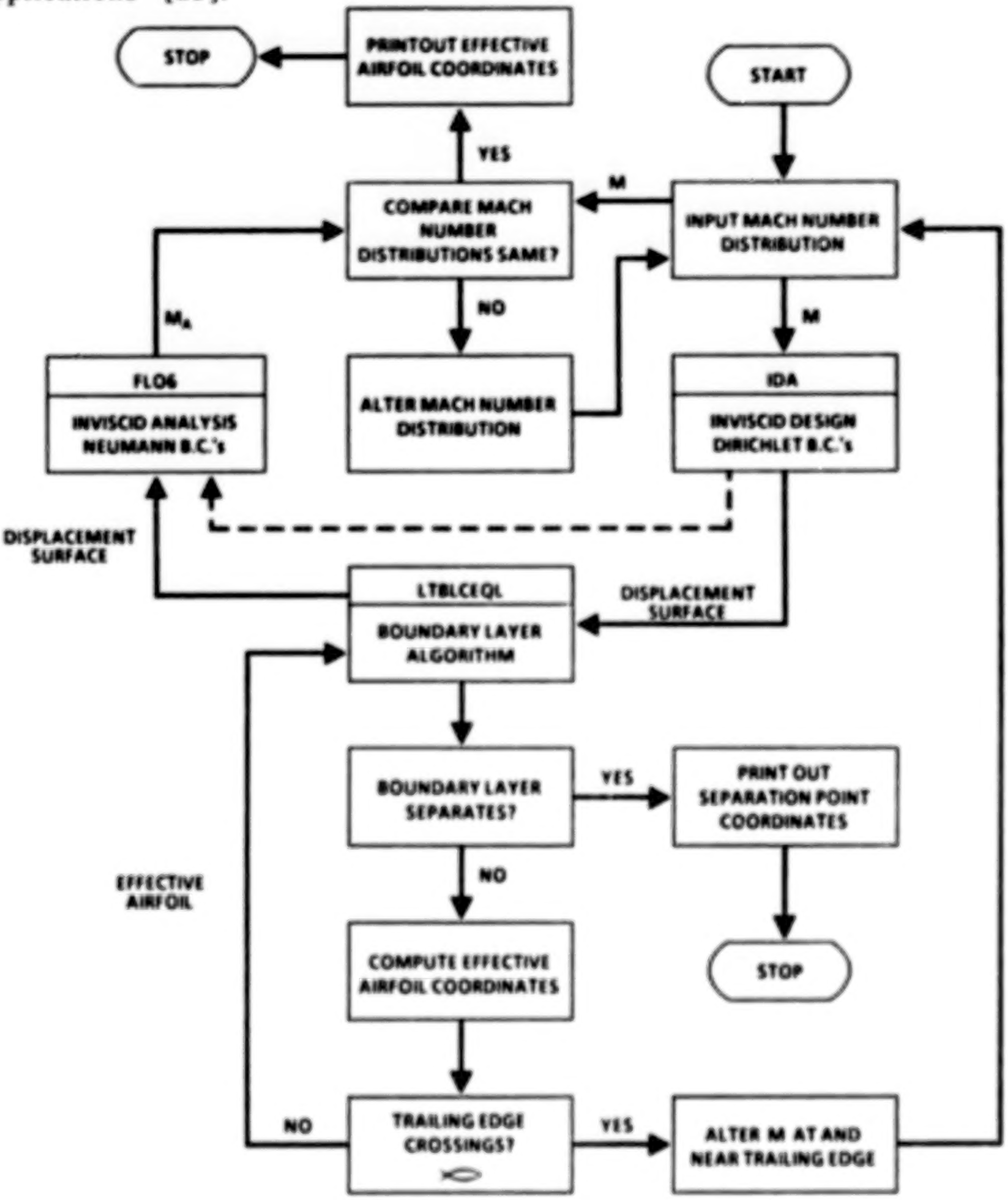
STOP
PRINTOUT EFFECTIVE AIRFOIL COORDINATES
START
YES
M
COMPARE MACH NUMBER DISTRIBUTIONS SAME?
INPUT MACH NUMBER DISTRIBUTION
NO
M_A
M
FLO6
INVISCID ANALYSIS NEUMANN B.C.'s
ALTER MACH NUMBER DISTRIBUTION
IDA
INVISCID DESIGN DIRICHLET B.C.'s
DISPLACEMENT SURFACE
LTBLCEQL
BOUNDARY LAYER ALGORITHM
DISPLACEMENT SURFACE
BOUNDARY LAYER SEPARATES?
YES
PRINT OUT SEPARATION POINT COORDINATES
NO
EFFECTIVE AIRFOIL
COMPUTE EFFECTIVE AIRFOIL COORDINATES
STOP
NO
TRAILING EDGE CROSSINGS?
YES
ALTER M AT AND NEAR TRAILING EDGE

RESULTS OF HYBRID PROCEDURE

The inverse design procedure is based on a conformal transformation of the semi-infinite, two-sheeted Riemann hodograph free-surface representation of the airfoil into the unit circle. The input to the procedure includes a prescription of a target subsonic-sonic pressure distribution (or Mach number) and the free-stream conditions. The analysis of the airfoil configuration which results from the inviscid inverse procedure at design and off-design conditions is carried out using Jameson's [24] full potential solver FLO6. To account for viscous effects, the basic approach is to calculate a boundary-layer displacement thickness and use it to correct the location of the displacement surface. That is, vector subtraction of the displacement thickness from the inviscid displacement surface yields the effective airfoil configuration.

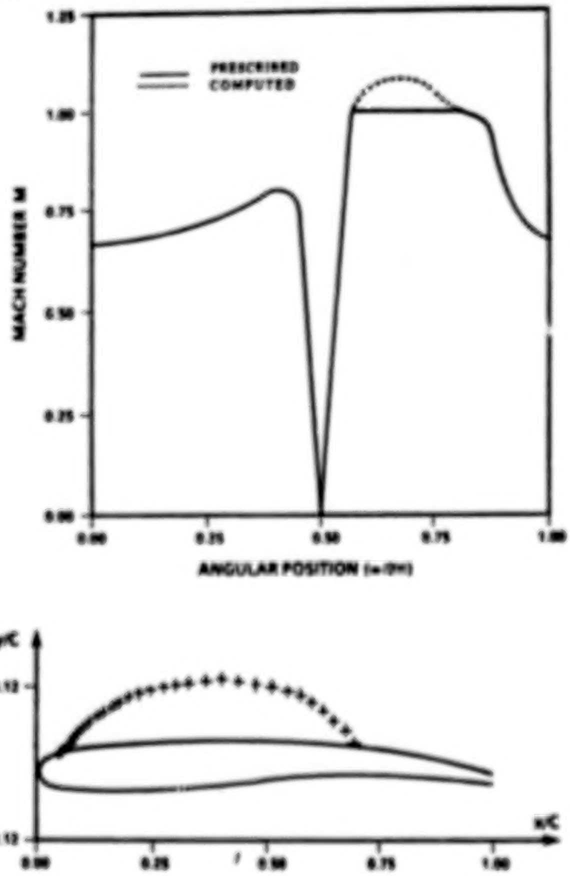

INPUT MACH NUMBER AND RESULTING AIRFOIL

	M	CL	CD	CM	ALFA
DESIGN :	0.75	0.055	0.0093	-0.065	1.30
OFF-DESIGN :	0.40	1.175	0.0124	-0.083	8.24

A PROPOSED EFFICIENT HYBRID DESIGN PROCEDURE

It is apparent that the existing structure of the hybrid design procedure could be further enhanced if a more "***GENERAL***" flow solver assumes the roles of both the existing direct (FLO6) and inverse (IDA) solvers. This in turn, eliminates the required interpolation of the computational results between the two different grid systems.

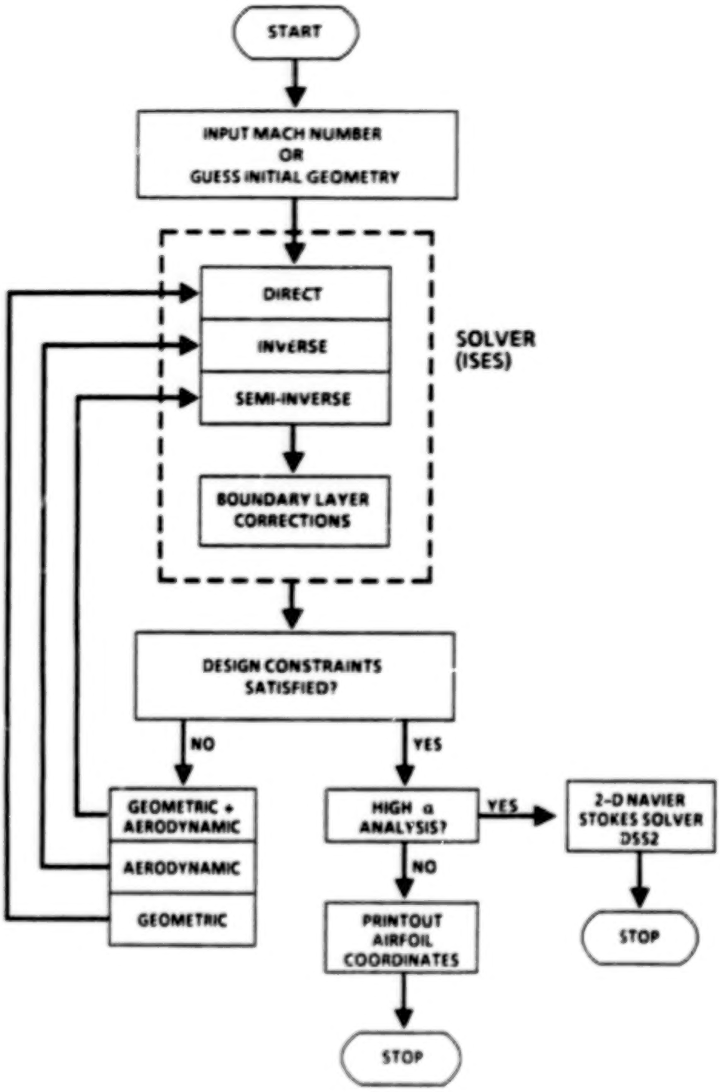

CONCLUSIONS

- OPTIMIZATION ROUTINES ARE A POWERFUL TOOL FOR FINDING SOLUTIONS TO MULTIPLE DESIGN POINT PROBLEMS

- THE OPTIMIZATION PROCESS MUST BE GUIDED BY THE JUDICIOUS CHOICE OF GEOMETRIC AND AERODYNAMIC CONSTRAINTS

- OPTIMIZATION ROUTINES SHOULD BE APPROPRIATELY COUPLED TO VISCOUS, NOT INVISCID, TRANSONIC FLOW SOLVERS

- HYBRID DESIGN PROCEDURES IN CONJUNCTION WITH OPTIMIZATION ROUTINES REPRESENT THE MOST EFFICIENT APPROACH FOR ROTOR AIRFOIL DESIGN

- UNSTEADY EFFECTS RESULTING IN THE DELAY OF LIFT AND MOMENT STALL SHOULD BE MODELED USING SIMPLE EMPIRICAL RELATIONS

- INFLIGHT OPTIMIZATION OF AERODYNAMIC LOADS (e.g., use of variable rate blowing, flaps, etc........) CAN SATISFY ANY NUMBER OF REQUIREMENTS AT DESIGN AND OFF-DESIGN CONDITIONS

REFERENCES

1. Volpe, G. and Melnik, R. E. "The Role of Constraints in the Inverse Design Problem for Transonic Airfoils," AIAA Paper 81-1233, June 1981.

2. Hicks, R. M. and Vanderplaats, G. N. "Application of Numerical Optimization to the Design of Supercritical Airfoils Without Drag Creep," SAE Paper 770440, March 1977.

3. Hassan, A. A., Sobieczky, H. and Seebass, A. R. "Subsonic Airfoils With a Given Pressure Distribution," AIAA J., Vol. 22, No. 9, pp. 1185-1191, September 1984.

4. Bauer, F., Garabedian, P. and Korn, D. "Supercritical Wing Sections III," Lecture Notes in Economics and Mathematical Systems, Springer Verlag, New York, 1977.

5. Hassan, A. A., Sobieczky, H. and Seebass, A. R. "Shock-Free Transonic Airfoils with a Given Pressure Distribution," Computer Methods in Applied Mechanics and Engineering, Vol. 58, pp. 285-304, 1986.

6. Hassan, A. A. "The Design of Shock-Free Supercritical Airfoils Including Viscous Effects," Communications In Applied Numerical Methods, Vol. 2, pp. 37-45, 1986.

7. Melnik, R. E., Mead, H. R. and Jameson, A. " A Multi-Grid Method for the Computation of Viscid/Inviscid Interactions on Airfoils," AIAA Paper 83-0234, January 1983.

8. Jackson, B. "Wind Tunnel Report for the Development of Airfoils for MDHC," McDonnell Douglas Helicopter Company Technical Report ATN 86-018, February 1986.

9. Wegryn, S. J. "BSWT 602 A Supersonic Wind Tunnel Test of Nine Two-Dimensional Airfoils," Boeing Report Number D6-52979, October 1985.

10. Brown, B. "Two-Dimensional Wind Tunnel Tests of Hughes Helicopter Inc. Airfoils HH-01, HH-02, and CR-2961 (Data Release)," Lockheed Report LR-30531 (S-434), September 1983.

11. Prouty, R. "Wind Tunnel Report of Potential HARP Airfoils," Hughes Helicopters Report 150-A-1015.

12. Vanderplaats, G. N. "CONMIN - A FORTRAN Program for Constrained Function Minimization," NASA TM-X-62282, 1973.

13. Hicks, R. and Vanderplaats, G. N. "Application of Numerical Optimization to the Design of Low Speed Airfoils," NASA TM-X-3213, March 1975.

14. Hicks, R. and Vanderplaats, G. N. "Airfoil Section Drag Reduction at Transonic Speeds by Numerical Optimization," Presented at the Society of Automotive Engineers, Business Aircraft Meeting, April 1976.

15. Bauer, F., Garabedian, P., and Korn, D. "Supercritical Wing Sections II," Lecture Notes in Economics and Mathematical Systems, Volume 108, Springer Verlag, 1975.

16. Blackwell, J. and Hinson, B. "The Aerodynamic Design of an Advanced Rotor Airfoil," NASA CR-2961, May 1977.

17. Dadone, L. "Design and Analytical Study of a Rotor Airfoil," NASA Report CR-2988, 1978.

18. Thibert, J. and Gallot, J. "Advanced Research on Helicopter Blade Airfoils," Vertica, Vol. 5, No. 3, 1981.

19. McVeigh, M. and MuHugh, F. "Recent Advances in Rotor Technology at Boeing VERTOL," Presented at the American Helicopter Society Forum, May 1982.

20. Bingham, G. and Noonan, K. "Two-Dimensional Aerodynamic Characteristics of Three Rotorcraft Airfoils at Mach Numbers from 0.35 to 0.90," NASA TP-2000, March 1982.

21. Wortmann, F. X. and Drees, J. M. "Design of Airfoils for Rotors," Presented at CAL/AVLABS Symposium on Aerodynamics of Rotary Wing and VTOL Aircraft, 1969.

22. Hassan, A. A. "A Viscous-Inviscid Coupling Method for the Design of Low Reynolds Number Aerofoil Sections," Communications In Applied Numerical Methods, Vol. 2, pp. 419-427, 1986.

23. Ives, D. C. "Inverse and Hybrid Cascade Design Methods," Proc. Int. Conf. on Inverse Design Concepts in Engineering Sciences (ICIDES), Austin, Texas, pp. 555-572, 1984.

24. Jameson, A. "Iterative Solution of Transonic Flows Over Aerofoils and Wings, Including Flows at Mach 1," Comm. Pure Appl. Math., Vol. 27, pp. 283-309, 1974.

BLANK PAGE

EFFICIENT SENSITIVITY ANALYSIS AND OPTIMIZATION OF A HELICOPTER ROTOR

J. W. Lim
and
I. Chopra

Center for Rotorcraft Education and Research
Department of Aerospace Engineering
University of Maryland
College Park, Maryland

Aeroelastic Optimization Approach

Aeroelastic optimization of a system essentially consists of the determination of the optimum values of design variables which minimize the objective function and satisfy certain aeroelastic and geometric constraints. The process of aeroelastic optimization analysis is shown in Figure 1. To carry out aeroelastic optimization effectively, one needs a reliable analysis procedure to determine steady response and stability of a rotor system in forward flight. The rotor dynamic analysis used in the present study is developed inhouse at the University of Maryland and is based on finite elements in space and time [1,2,3]. The analysis consists of two major phases: vehicle trim and rotor steady response (coupled trim analysis), and aeroelastic stability of the blade. For a reduction of helicopter vibration, the optimization process requires the sensitivity derivatives of the objective function and aeroelastic stability constraints. For this, the derivatives of steady response, hub loads and blade stability roots are calculated using a direct analytical approach. An automated optimization procedure is developed by coupling the rotor dynamic analysis, design sensitivity analysis and constrained optimization code CONMIN [4].

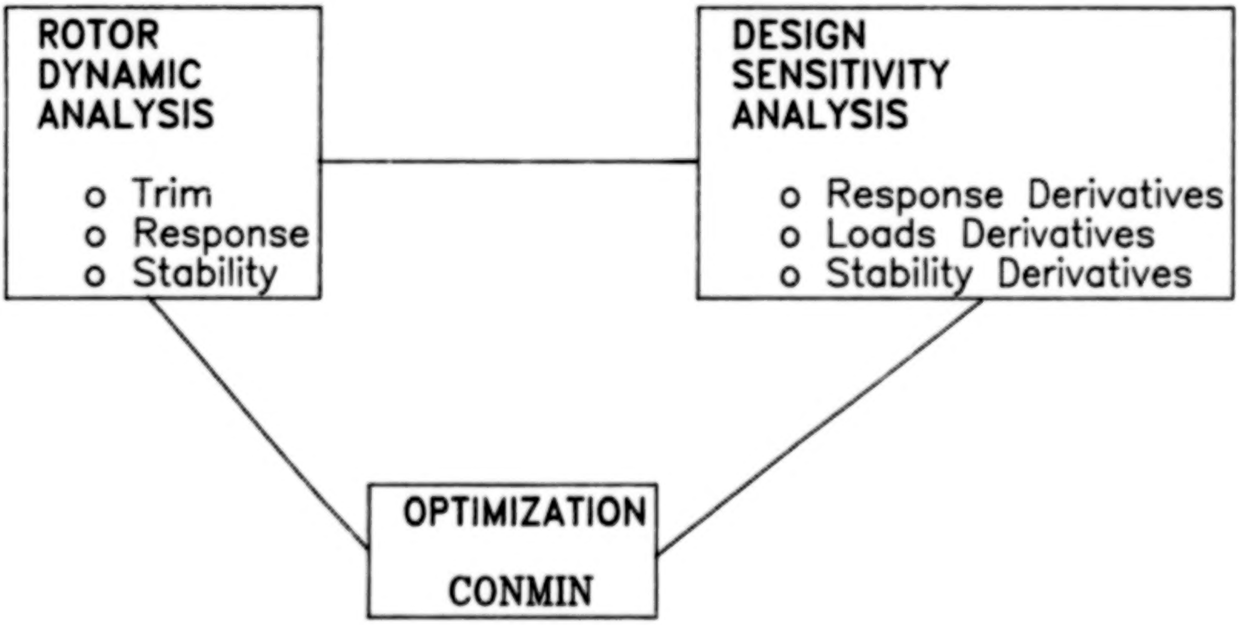

Figure 1

Coupled Trim Analysis

Coupled trim analysis in forward flight consists of calculation of vehicle trim (propulsive), blade steady response and hub loads. The vehicle trim solution determines the control settings and vehicle attitude for the prescribed flight condition. It is calculated from the overall nonlinear vehicle force and moment equilibrium equations. The blade steady response solution involves the determination of time dependent blade deflections at different azimuth locations. The blade is assumed as an elastic beam undergoing flap bending, lag bending, elastic twist and axial deflections, and is discretized into a number of beam elements. To reduce computation time, a large number of finite-element equations are transformed to a few (typically eight) normal mode equations. These nonlinear periodic equations are then solved for steady response using a finite-element method in time formulated from Hamilton's weak principle. The hub loads are obtained using a force summation approach. For the coupled trim analysis, the vehicle trim and rotor response equations are solved iteratively as one coupled solution using a modified Newton method. The converged trim and response solutions satisfy simultaneously the overall force and moment equations of the vehicle. Figure 2 shows the blade steady flap response at tip for an advance ratio of 0.3. For a completely trimmed condition, there is no unbalanced force or moment acting on the hub, and the lag and torsion responses consist primarily of 1/rev amplitudes, whereas the flap response is dominated by 2/rev amplitude.

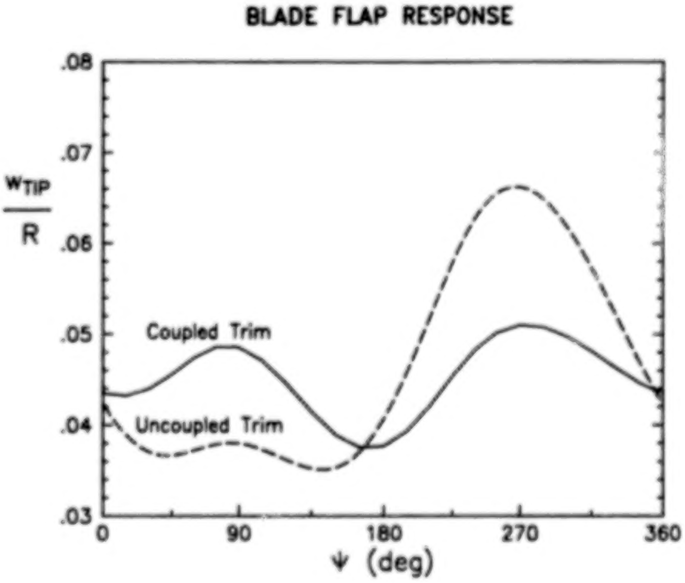

$C_T/\sigma = 0.07$, $\mu = 0.3$, $X_{CG} = 0.0$, $Y_{CG} = 0.0$, $h/R = 0.2$
$\omega_{L1}=0.70$, $\omega_{F1}=1.13$, $\omega_{T1}=4.47$

Figure 2

Design Sensitivity Analysis

A design sensitivity analysis involves calculation of sensitivity derivatives of the objective function and behavior constraints. Most of the optimization studies use finite difference approach to calculate sensitivity derivatives. This approach is easy to implement, but costly because of heavy computation time. Also, the selection of proper step size is not easy. However, a direct analytical approach is more complicated in formulation but reduces the computation time substantially. In the present study, the derivatives of blade response, hub loads and blade stability with respect to the design variables are calculated using a direct analytical approach [1,2,5]. The formulation of the derivatives of blade response including hub loads is developed as an integral part of the basic steady response analysis. The implementation of this scheme is made possible through the use of the finite-element method in time. **Figure 3 compares the sensitivity derivatives of the 4/rev vertical hub shear** with respect to the design variables at the mid span location. The numerical results for finite difference and direct analytical approaches show quite identical trends.

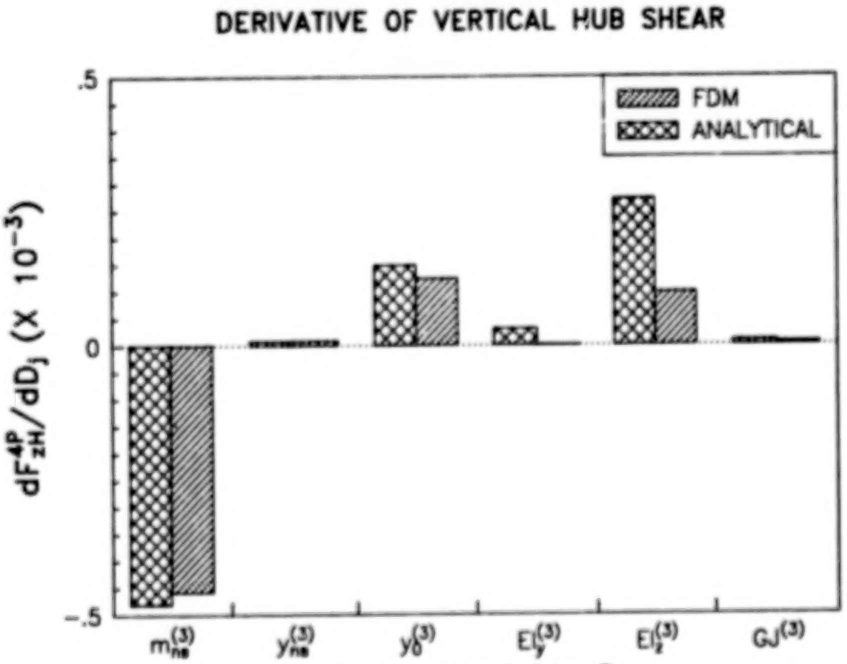

Derivative Of 4/Rev Vertical Hub Shear With Respect To Design Variables At Mid Span ; $\mu=0.3$, $c_T/\sigma=0.07$

Figure 3

CPU Time for Design Sensitivity Analysis

The stability sensitivity analysis involves the calculation of the derivatives of blade stability roots, and again constitutes an integral part of the basic stability analysis. For this, the Floquet transition matrix is extended to include the derivatives of blade stability roots. Figure 4 shows CPU time required in UNISYS-1100/90 for calculation of sensitivity derivatives of blade response, oscillatory hub loads (objective function) and blade dampings (behavior constraints) of the baseline blade using finite difference and direct analytical approaches. For five design variables, the CPU time used is 110 min for the finite difference, and 25 min for the direct analytical approach. For thirty design variables, the CPU time is increased to 560 min for the finite difference, while it is 50 min for the direct analytical approach. As the number of design variables is increased, the difference of the CPU time required becomes larger.

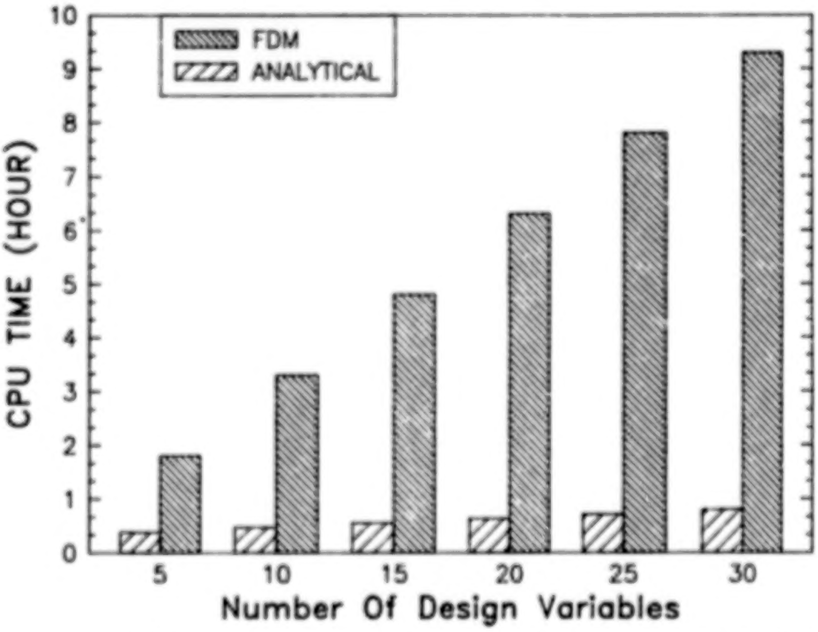

CPU Time Required In UNISYS-1100/90 For Calculation Of Derivatives Of Blade Response, Stability And Hub Loads

Figure 4

Design Variables

Figure 5 shows the blade and airfoil section. For the analysis, the blade is discretized into five beam elements of equal length, and the numerals indicate the order of beam elements. Each beam element consists of fifteen degrees of freedom, representing flap bending, lag bending, elastic twist and axial deflections. In the airfoil, the 'e.a.' denotes the elastic axis, and the m_0 is a baseline blade mass per unit length (reference), which has an offset of y_0. There can be placed an extra nonstructural mass (m_{ns}) at a chordwise location of y_{ns}. Therefore, structural design parameters can be chosen from nonstructural mass (m_{ns}), chordwise offset of nonstructural mass (y_{ns}), blade center of gravity offset (y_0), and blade flap bending stiffness (EI_y), lag bending stiffness (EI_z) and torsional stiffness (GJ). These structural parameters can have spanwise variations. Thus, the total design variables for five beam elements are

$$(6 \text{ structural parameters}) \times (5 \text{ beam elements}) = 30$$

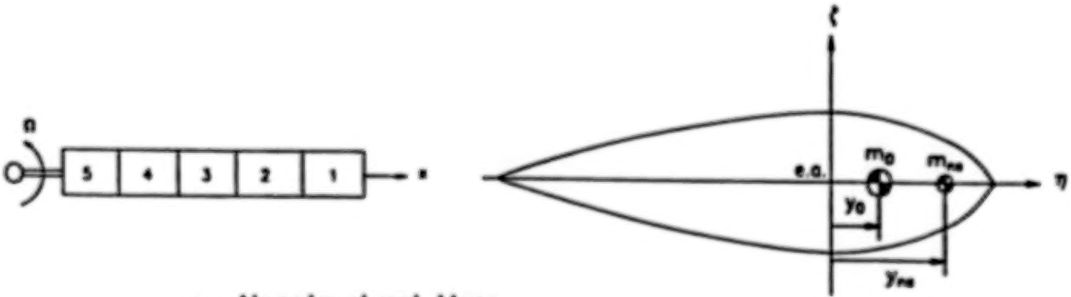

- o Nonstructural Mass
- o Chordwise Location of Nonstructural Mass
- o Chordwise Location of Blade CG
- o Blade Flap Bending Stiffness
- o Blade Lag Bending Stiffness
- o Blade Torsional Stiffness
- Spanwise Variations
- Total 30 Design Variables

Figure 5

Minimization of 4/Rev Vertical Shear Alone

Helicopter vibrations are characterized by means of oscillatory hub loads including three forces and three moments. To reduce helicopter vibrations, most of the optimization studies minimized 4/rev vertical shear alone for a four-bladed rotor, without constraining other components of oscillatory hub forces or moments. Figure 6 shows the optimization iteration history when 4/rev vertical hub shear alone is minimized. After 7 iterations, the 4/rev vertical hub shear is reduced by 75%. Other 4/rev hub loads are increased instead; an increase by 30% for longitudinal and lateral hub shears, 10% for rolling and lateral hub moments and 210% for yawing hub moment. This is due to the fact that other components of oscillatory hub loads besides 4/rev vertical hub shear are not involved in the objective function. This shows that one needs to make a careful choice of the objective function to achieve an optimum solution.

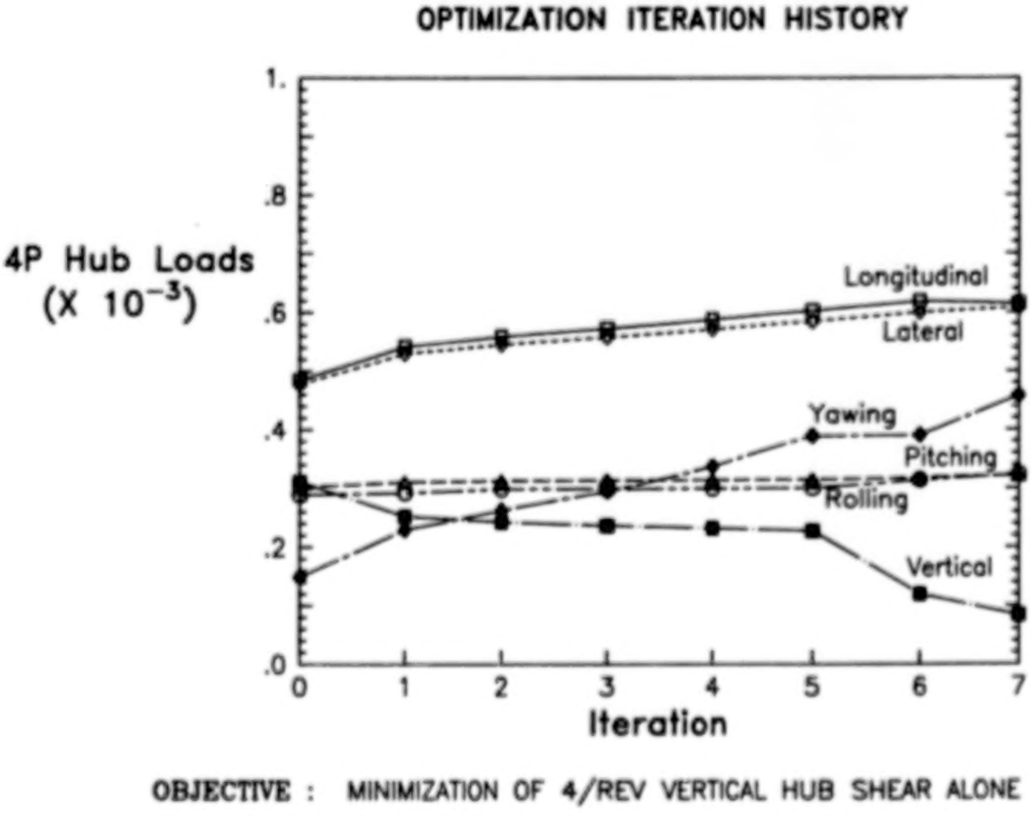

OBJECTIVE : MINIMIZATION OF 4/REV VERTICAL HUB SHEAR ALONE

Figure 6

Minimization of All Hub Forces and Moments

The objective function involves all six components of hub forces and moments in either the hub-fixed nonrotating frame or rotating frame, and is defined as a sum of hub force resultant and moment resultant. In the present study, hub loads in the nonrotating frame are used. The weighting functions are simply chosen as unity. To achieve an optimum solution, the best choice of design variables is found in Ref. [6] involving nonstructural masses and their locations (chordwise and spanwise), and spanwise distribution of blade flap bending, lag bending and torsional stiffnesses. In this case, twenty five design variables are involved. Figure 7 shows the optimization iteration history of the objective function. Each optimization iteration involves updating the search direction from the sensitivity analysis, determining the optimum move parameter by polynomial approximation in the one dimensional search and checking the convergence to terminate the optimization process. After each optimization iteration, the objective function becomes reduced. The optimum solution is obtained after 8 iterations, and a 77% reduction of the objective function is achieved.

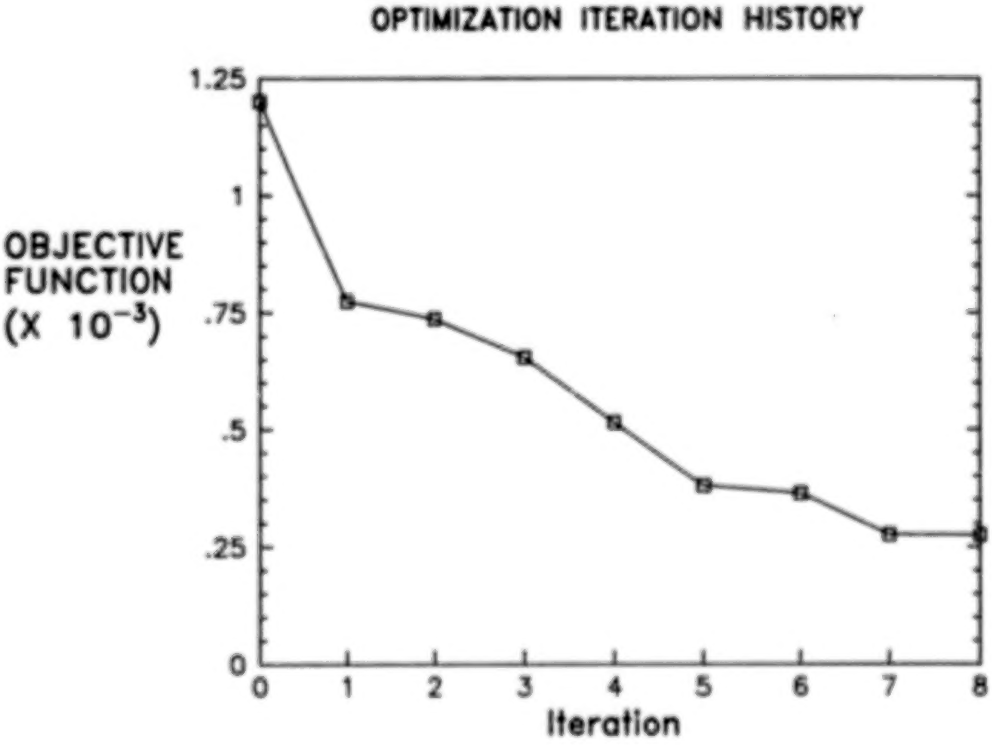

OBJECTIVE : MINIMIZATION OF ALL HUB FORCES AND MOMENTS

Figure 7

Optimum Hub Loads

Figure 8 compares optimum 4/rev hub forces and moments with the baseline values. The optimum result shows that all the 4/rev hub forces and moments are reduced from the baseline values. This is because all the components are included in the objective function, and also equal weighting function is enforced on each component. There are considerable reductions of 4/rev hub loads achieved: an 80% reduction for longitudinal and lateral hub shears, a 60% reduction for vertical hub shear, an 80% reduction for rolling and pitching hub moments and a 90% reduction for yawing hub moment. For a reduction of helicopter vibration, the objective function must, therefore, include all six components of 4/rev hub loads in conjunction with appropriate weighting functions.

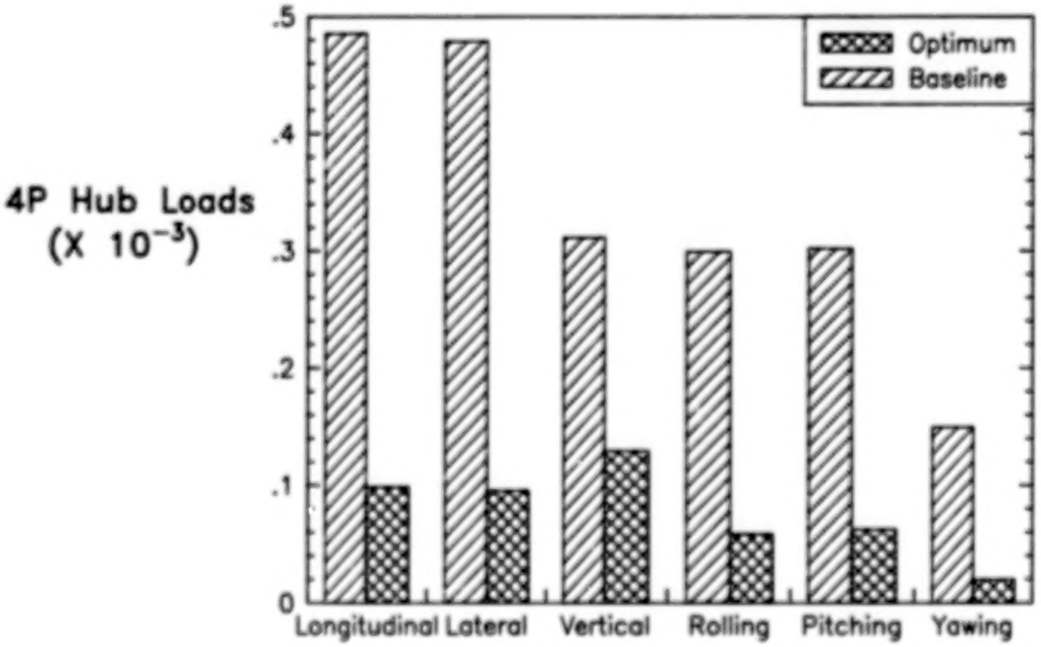

OBJECTIVE : MINIMIZATION OF ALL HUB FORCES AND MOMENTS

Figure 8

Aeroelastic Stability Constraints

For structural optimization problems, one may impose behavior constraints which must be satisfied for a feasible design. In the present optimization analysis, the aeroelastic stability of the blade in forward flight is constrained to be stable for all modes. For this, the blade damping, which is the real part of the characteristic exponent with a negative sign, is kept in the positive range. Figure 9 shows the optimization iteration history of blade damping of first lag, flap and torsion modes. For lag and flap modes, the blade damping varies smoothly at each iteration. However, for torsion mode the damping is changed abruptly between iterations 2 and 4. This may be associated with a large shift of effective c.g. offset because of nonstructural masses. All three blade modes, however, remain stable for all iterations. Thus, the design solution in the optimization process stays within the feasible design space for all iterations (unconstrained optimization process).

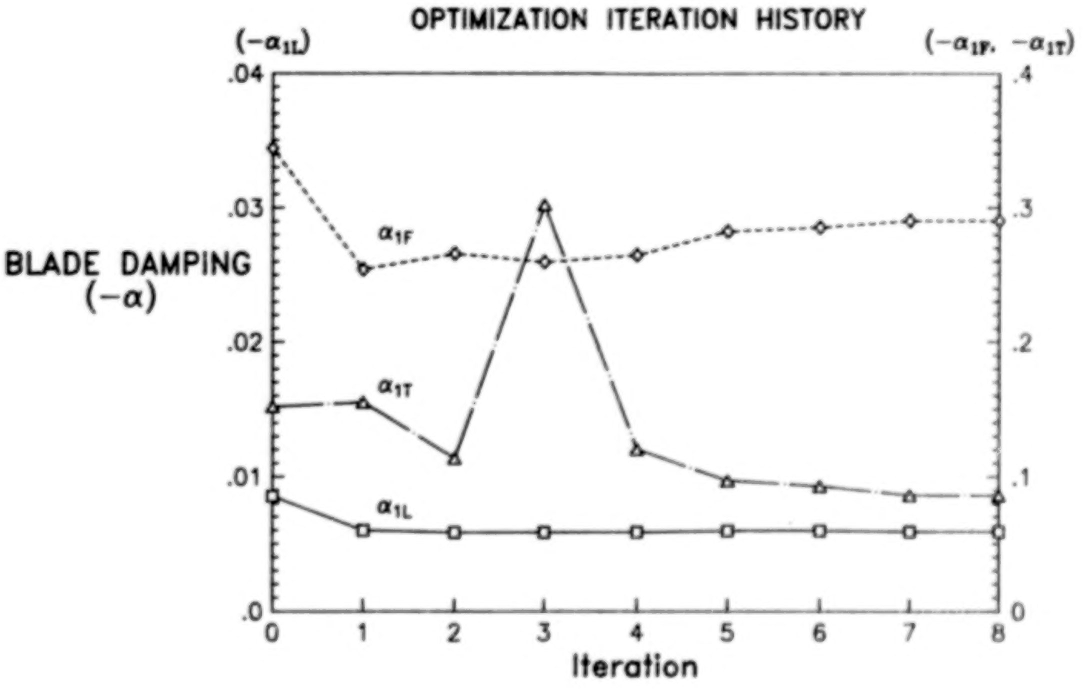

BEHAVIOR CONSTRAINTS : BLADE DAMPINGS

Figure 9

CPU Time for Optimization Analysis

Figure 10 shows the comparison of CPU time required for the optimization process on UNISYS 1100/90 using finite difference and direct analytical approaches. For finite difference approach, the CPU time is approximated based on the number of function evaluations. To achieve an optimum solution, there is about an 80% reduction in CPU time with the present approach as compared with the frequently adopted finite-difference approach. Comparing the CPU time for the sensitivity analysis, one can easily realize that this substantial reduction of CPU time results from an efficient evaluation of sensitivity derivatives of the objective function and/or constraints in the sensitivity analysis by using a direct analytical approach.

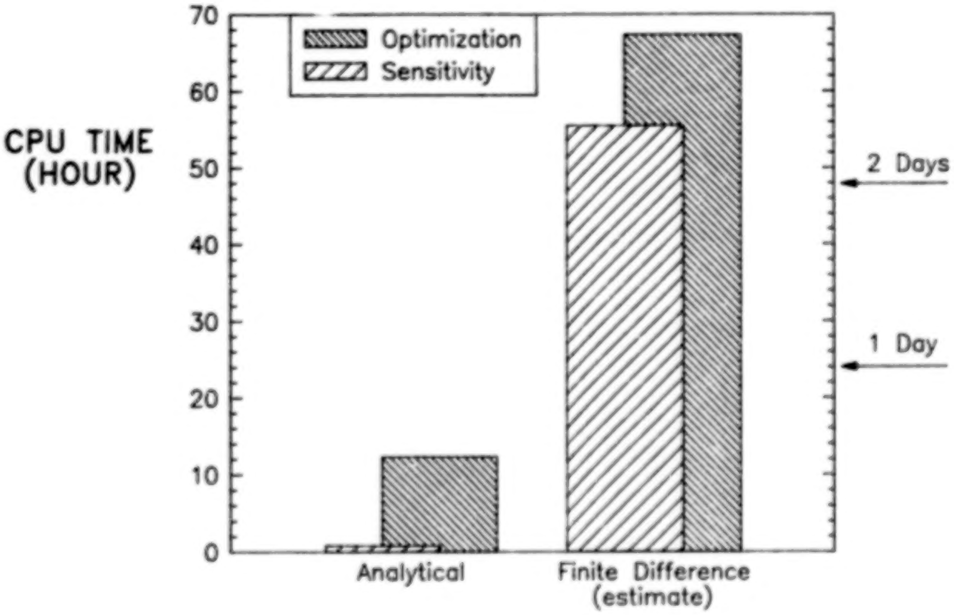

Comparison of CPU Time for Optimization Process in UNISYS 1100/90 Using Analytical and Finite Difference Approaches

Figure 10

BEST COPY AVAILABLE

Behavior Constraints -- Initially Infeasible

If the design solution stays in the feasible design space for all iterations, behavior (aeroelastic stability) constraints do not become active (see Figure 9). Here, we have investigated a case in which behavior constraints have been violated, right from the beginning for the baseline configuration. Figure 11 shows the optimization iteration history of blade damping of first lag, flap and torsion modes when 1% margin of blade damping is imposed for stability. The lag mode damping for the baseline configuration is less than 1%. In the next iteration, the design solution is moved into the feasible design space along the feasible direction by the optimizer CONMIN [4], and the blade becomes aeroelastically stable. In subsequent iterations, the blade stability is well maintained. Similar to Figure 9, the blade damping of lag and flap modes varies smoothly at each iteration, but the torsion mode damping is changed abruptly due to a large shift of effective c.g., offset resulted from the nonstructural mass placement.

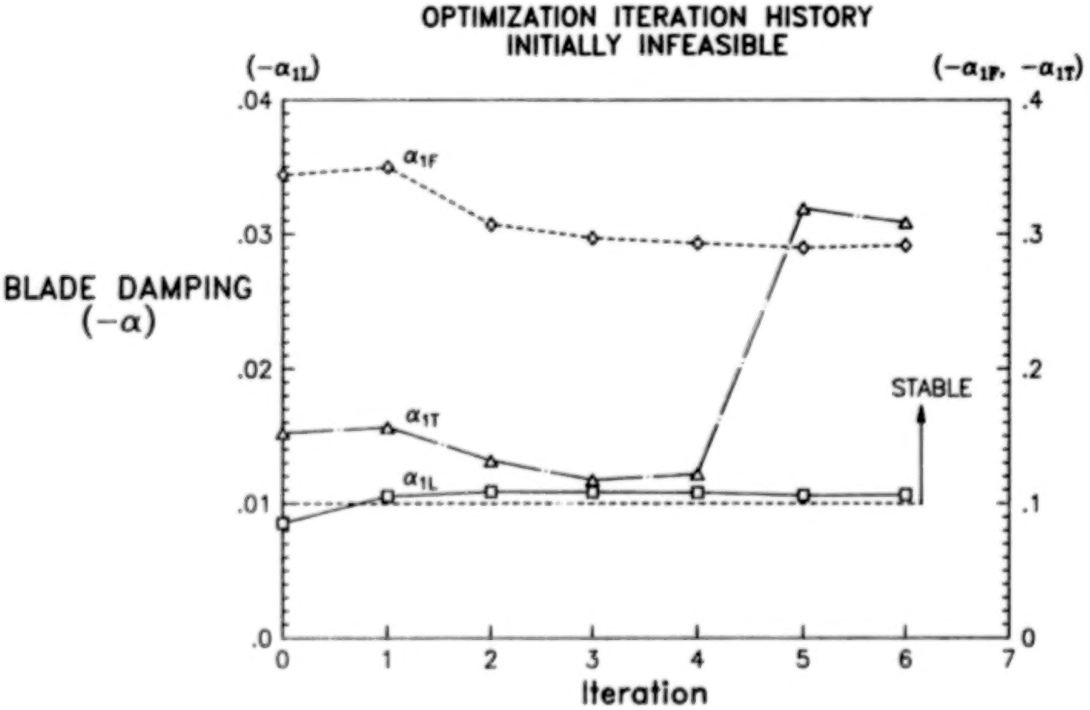

BEHAVIOR CONSTRAINTS : BLADE DAMPINGS

** 1% DAMPINGS MAINTAINED FOR STABILITY

Figure 11

Initially Infeasible Design

Figure 12 shows the optimization iteration history of the objective function for the case in which behavior (aeroelastic stability) constraint is violated by the baseline configuration. The objective function involves minimization of all six components of 4/rev hub loads for a four-bladed rotor. The design variables involve nonstructural masses and their locations (spanwise and chordwise), and spanwise distribution of blade bending stiffnesses (flap, lag and torsion), and there are total twenty five design variables. The optimizer enforces the design solution to move along the feasible direction so that no behavior constraint is violated. After first iteration, the design solution becomes feasible (see Figure 11), and the objective function is slightly increased. In subsequent iterations, the objective function becomes continually reduced. The optimum solution is obtained after six iterations, and there is about a 25% reduction of the objective function achieved. Comparing with the case of initially feasible design where no stability constraint was violated and a reduction of 77% of the objective function was achieved, the optimum for initially infeasible design is far less achieved.

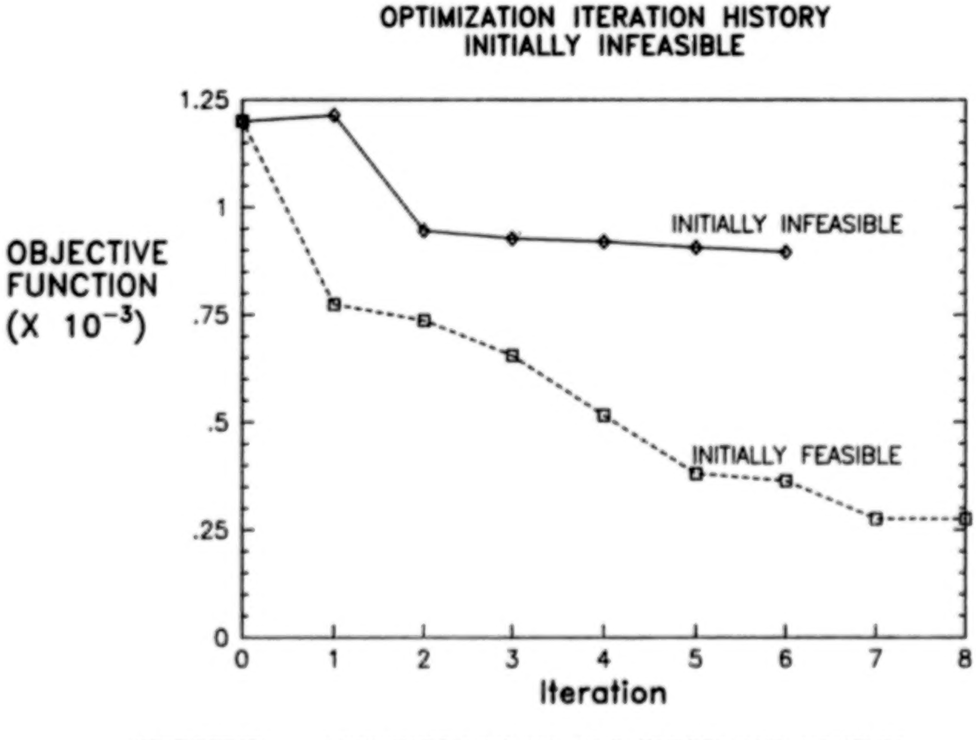

OBJECTIVE : MINIMIZATION OF ALL HUB FORCES AND MOMENTS

Figure 12

References

[1] J. W. Lim and I. Chopra,''Design Sensitivity Analysis for an Aeroelastic Optimization of Helicopter Blades,'' 28th AIAA Dynamics Specialists Conference, Monterey, CA, April 1987, Part 2B

[2] J. W. Lim, ''Aeroelastic Optimization of a Helicopter Rotor,'' Ph.D. Dissertation, University of Maryland, May 1988

[3] B. Panda and I. Chopra,''Dynamics of Composite Rotor Blades in Forward Flight,'' Special Issue in the 10th Anniversary of Vertica, 1987

[4] G. N. Vanderplaats,''CONMIN - A Fortran Program for Constrained Function Minimization,'' User's Manual, NASA TMX 62282, 1973

[5] J. W. Lim and I. Chopra,''Stability Sensitivity Analysis for Aeroelastic Optimization of a Helicopter Rotor,'' 29th AIAA SDM Conference, Williamsburg, VA, April 1988 ; Also, Appeared in The Workshop on Dynamics and Aeroelastic Stability Modeling of Rotor Systems, Florida Atlantic University, November 1987

[6] J. W. Lim and I. Chopra,''Aeroelastic Optimization of a Helicopter,'' 44th Annual Forum of American Helicopter Society, Washington, D.C., June 1988

Structural Optimization of Rotor Blades With Integrated Dynamics and Aerodynamics

Aditi Chattopadhyay
Analytical Services & Materials, Inc.
Hampton, Virginia

and

Joanne L. Walsh
National Aeronautics and Space Administration
Langley Research Center
Hampton, Virginia

INTRODUCTION

The helicopter rotor design process is highly multidisciplinary in nature and requires a merging of several technical disciplines such as dynamics, aerodynamics, structures and acoustics. In the past the conventional design process was controlled by the designer's experience and the use of trial and error methods. Today, one of the more promising approaches to the rotor blade design process is the application of structural optimization techniques. An extensive amount of work has been done in developing design optimization procedures to bring the state of the art to a very high level[1-5]. While these techniques have received wide attention in the fixed-wing field[1], they are fairly recent in the rotary wing industry[3-5]. Most of the work involving application of optimization techniques to rotor blade design has been focused on nearly independent technical disciplines with very little consideration of the coupling and interaction between the disciplines. For example, the dynamic design requirements have been considered in the optimum rotor blade design in refs. 6-10. Blade aerodynamic and structural requirements were considered in refs. 11 and 12, respectively.

The necessity of merging appropriate disciplines to obtain an integrated design procedure has been recently emerging and with improved understanding of helicopter analyses and optimization schemes, it is now possible to apply optimization techniques and include the couplings between the disciplines. In refs. 13-15 the dynamic and structural design requirements were coupled with airloads in the analysis and in refs. 16 and 17 the dynamic and aeroelastic requirements were integrated. The optimization procedure described in this paper is part of an effort at NASA Langley Research Center[18] and is aimed at integrating two technical disciplines, aerodynamics and dynamics. As a first investigation, the airloads will be included to perform coupled airload/dynamic integration of rotor blades. Later the aerodynamic performance requirements will be added to obtain an integrated aerodynamic/dynamic optimum design procedure. The procedure is no longer sequential - rather it will account for the interactions between the two disciplines simultaneously. The paper briefly describes some of the recent work done by the authors which focussed on optimum blade design with dynamic behavioral constraints and presents some of the authors' recent experiences in developing a strategy for structural optimization with integrated dynamics/aerodynamics of rotor blades.

INTEGRATED ROTORCRAFT ANALYSIS

Currently at the NASA Langley Research Center, there is an effort to integrate various technical disciplines such as dynamics, aerodynamics and structures into the rotor design process. Shown below in fig. 1 is a tentative plan of the integrated rotor analysis program. The plans are to perform independent discipline level optimizations, (e.g. rotor aerodynamic, dynamic and structural optimization as shown by the clear bubbles) by considering design variables, constraints and objective functions that affect the particular discipline considered. The next step is to couple rotor aerodynamics and dynamics to perform integrated aerodynamic/dynamic optimization. This would involve considerations of design variables and requirements of importance to each discipline, although there are certain design variables that influence all the disciplines involved. The structural design criteria are then introduced to obtain an integrated aerodynamic/dynamic/structural optimization procedure. The influence of airframe dynamics and acoustics will be accounted for through constraints in the design optimization to obtain the 'fully integrated procedure.' The final step is to validate this optimization procedure for a blade test article.

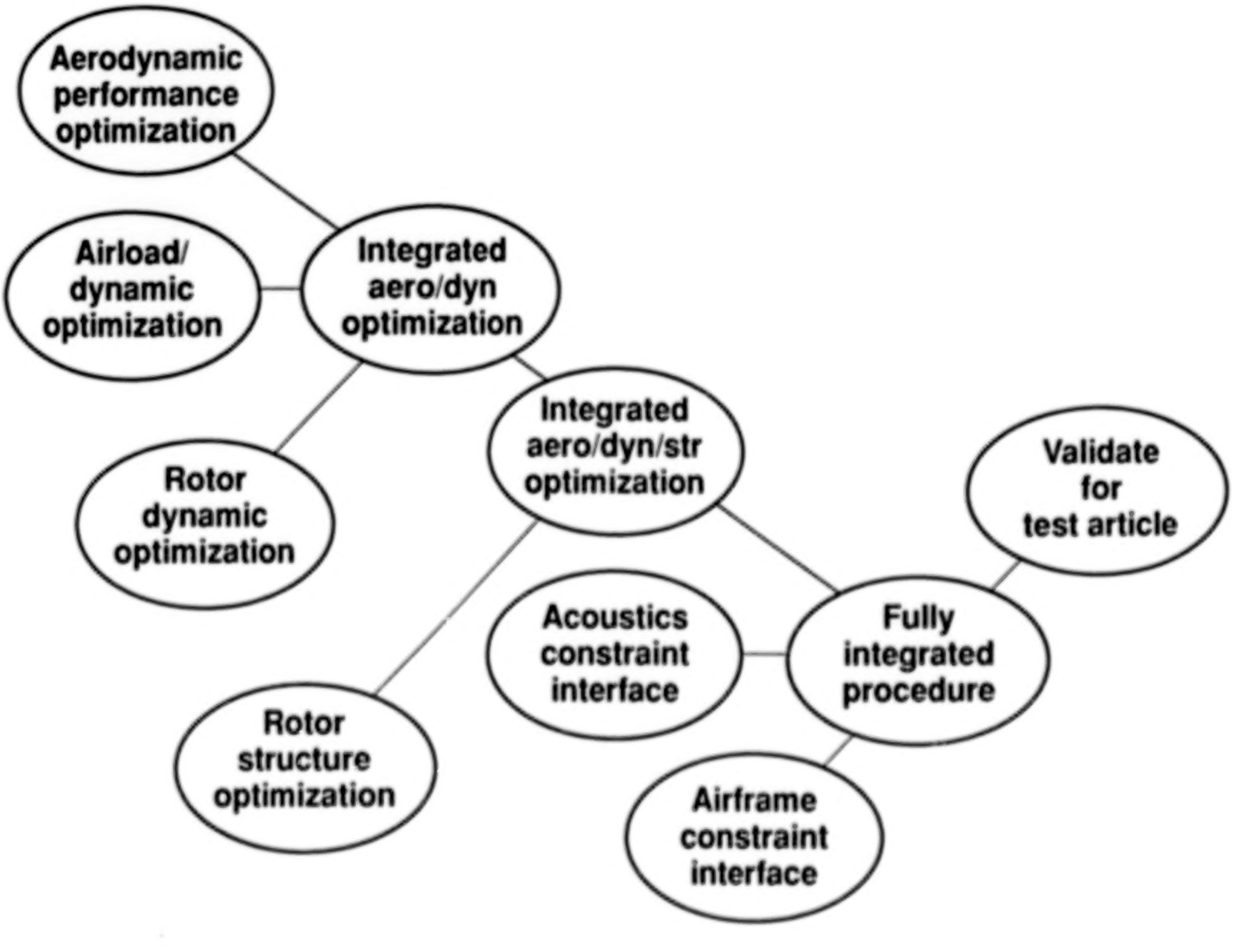
Aerodynamic performance optimization
Airload/ dynamic optimization
Integrated aero/dyn optimization
Rotor dynamic optimization
Integrated aero/dyn/str optimization
Validate for test article
Acoustics constraint interface
Fully integrated procedure
Rotor structure optimization
Airframe constraint interface

FIGURE 1

ROTOR BLADE DESIGN CONSIDERATIONS

Rotor blade design involves several considerations some of which are listed below in fig. 2. The blade design must satisfy specified strength criteria and should be damage tolerant. The rotor blade aerodynamic design process consists of proper selection of blade geometric variables such as planform, airfoils, twist, etc. to meet performance requirements[11]. Helicopter performance is usually expressed in terms of horsepower required as a function of velocity. The horsepower required to drive the main rotor for any part of a mission must be less than the available horsepower. The airfoil section stall must also be avoided, i.e. the airfoil sections must operate at section drag coefficients less than a specified value. Two other major criteria in rotor blade design have been low weight and low vibration. For a helicopter in forward flight, the nonuniform flow passing through the rotor causes oscillating airloads on the rotor blades. These loads in turn are translated into vibratory shear forces and bending moments at the hub. Therefore, vibration alleviation without weight penalty is an important criterion. The blade should also be aeroelastically stable[17,19] and finally, the noise levels generated by the rotor which are a function of local Mach number and airloads should be reduced. This paper will concentrate on the low vibration and the low blade weight aspects of the design.

- **Strength, survivability, fatigue life**
- **Aerodynamic performance**
- **Vibration**
- **Weight**
- **Aeroelastic stability**
- **Acoustics**

FIGURE 2

DYNAMIC OPTIMIZATION PROBLEM STATEMENT

As mentioned before, low vibration is an important design requirement in helicopter rotor blade design. One way of reducing the vibration level in the blade is to design the blade such that the natural frequencies are separated from multiples of the driving frequencies. Failure to consider frequency placement early in the design process can cause a significant increase in the final blade weight later if postdesign addition of nonstructural masses is required. Appropriately placing the natural frequencies can be done by a proper tailoring of the blade mass and/or stiffness distributions to meet the necessary design requirements using structural optimization. This section of the paper presents an overview of the dynamic optimization work which has been completed. The goal of the dynamic optimization problem (fig. 3) is to obtain minimum weight designs of blades with constraints on multiple coupled flap-lag natural frequencies. It is also important that the autorotational performance of the blade not be degraded during the tailoring process since the blade should have sufficient inertia to autorotate in case of an engine failure. In order to ensure a safe design, the blade centrifugal stress should be limited by an appropriate upper bound. For this study only centrifugal stress has been considered. The blade is assumed to be in vacuum in this investigation and the results of this analysis will generate a good starting point for the integrated optimization.

- **Goal - Minimize blade weight with constraints on multiple coupled natural frequencies, autorotational inertia and stress**
- **Approach - Stiffness and/or mass modifications, placement of tuning masses**
- **Assumption - Blade is in vacuum - generates good starting point for integrated optimization**

FIGURE 3

ROTOR BLADE MODEL FOR DYNAMIC OPTIMIZATION

The rotor blade model for dynamic optimization is shown below in fig. 4. The blade is articulated and has a fixed hub, a pretwist and a root spring which allows torsional motion. A box beam with unequal vertical wall thicknesses is located inside the airfoil and lumped nonstructural masses are located inside the box and distributed spanwise. This model is based on an existing blade design denoted the 'reference blade' described in refs. 8, 9, and 13. As in ref. 13, it is assumed that the box beam contributes all the blade stiffness, that is, the contributions of the skin, honeycomb, etc. to the blade flap and lag stiffnesses are neglected. The details for calculating the box beam section properties can be found in ref. 8. The properties of the box beam located inside the airfoil are as follows: $h=0.117$ ft, $b=0.463$ ft, $\rho=8.645$ slugs/ft^3, $E=2.304\times10^9$ lb/ft^2, allowable stress $\sigma_{max}=1.93\times10^7$ lb/ft^2 and factor of safety, FS=3. The blade is discretized into ten segments. Both rectangular and tapered blades are considered. For the rectangular blade, the box beam outer dimensions along the blade span remain unchanged. The design variables for the rectangular blade are the box beam wall thicknesses t_1, t_2, and t_3 and the magnitudes of the nonstructural weights located inside the box beam at ten spanwise locations. For the tapered blade it is assumed, as in refs. 8 and 9 that the box beam is tapered and the additional design variables are the box beam height at the root, h_r, and the taper ratio, λ_h, which is defined as the ratio of the box beam height at the root to the corresponding value at the tip. A linear variation of the box beam height, h, in the spanwise direction is assumed.

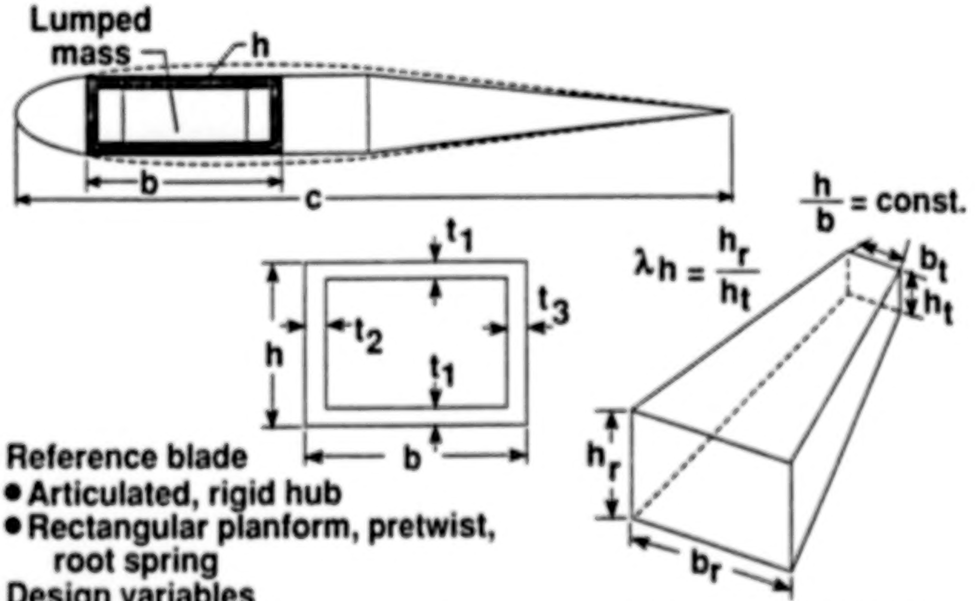

- **Reference blade**
  - **Articulated, rigid hub**
  - **Rectangular planform, pretwist, root spring**
- **Design variables**
  - **Box beam wall thicknesses, t_1, t_2, t_3 (10 spanwise positions)**
  - **Box beam outer dimension h_r**
  - **Taper ratio λ_h**
  - **Magnitudes of lumped masses (10 spanwise positions)**

FIGURE 4

FORMULATION OF DYNAMIC OPTIMIZATION PROBLEM

The purpose of the optimization procedure, as described in fig. 5 below, is to minimize the weight W of the rotor blade while constraining the natural frequencies f_k to be within specified 'windows' (upper and lower bounds). An existing blade which is being used in a production helicopter has been selected as a baseline blade and will be referred to as the 'reference blade'. A modal analysis of the reference blade showed that the frequencies of interest were not near the n per rev (critical values) values where n denotes the total number of blades. Hence it was decided to define constraints to force the frequencies of the optimum blade to be close to those of the reference blade. The concept of 'windows' has been used since the nonlinear programming method used in this work cannot handle equality constraints. These windows, denoted by f_{k_L} and f_{k_U} (for the lower bound and upper bound on frequency, respectively), are on the frequencies of the first three lead-lag dominated modes and the first two flapping dominated modes (elastic modes only). The frequency windows are carefully selected to alleviate any shear amplification problem. A prescribed lower limit α on the blade autorotational inertia AI and an upper bound σ_{max} on the blade centrifugal stress σ_k have also been used. Side constraints ϕ_{i_L} and ϕ_{i_U} (lower and upper bounds on the i^{th} design variable ϕ_i) have been imposed on the design variables to avoid impractical solutions.

- **Objective function**
  - **Minimum blade weight W**

    $W = W_b + W_o$
- **Constraints**
  - **Frequency windows on first 3 lead-lag and first 2 flapping elastic modes**

    $f_{k_L} \leq f_k \leq f_{k_U} \qquad k = 1,2,3,4,5$
  - **Lower bound on autorotational inertia**

    $AI \geq \alpha$
  - **Upper bound on centrifugal stress**

    $\sigma_k \cdot FS \leq \sigma_{max}$
  - **Bounds on design variables**

    $\phi_{i_L} \leq \phi_i \leq \phi_{i_U}$

FIGURE 5

METHODOLOGY FOR DYNAMIC OPTIMIZATION PROBLEM

The procedure described in this paper uses the program Comprehensive Analytical Model of Rotorcraft Aerodynamics and Dynamics (CAMRAD)[20]. The modal analysis portion of the program CAMRAD which uses a modified Galerkin approach[21] has been used for the dynamic optimization problem. According to ref. 22, this approach is the preferred method for computing mode shapes and frequencies of structures having large radial variations in bending stiffness. The general purpose optimization program CONMIN[23] which uses the nonlinear programming method of feasible directions has been used for the optimization. The method of solution described below (fig. 6) starts with discretizing the blade into finite segments. In the search for the optimum vector of new design variables, CONMIN requires derivatives of the objective function and constraints. The user has the option of either allowing CONMIN to calculate derivatives by using forward differences, or by supplying those derivatives to CONMIN. In the work presented in this paper, the latter approach has been used. Analytical expressions for the derivatives of the objective function and the autorotational inertia constraint have been obtained. A central difference scheme has been used for the derivatives of the frequency constraints. The initial attempt[8,9] using forward differences gave highly inaccurate derivatives.

The optimization process generally requires many evaluations of the objective function and the constraints before an optimum design is obtained. The process therefore can be very expensive if exact analyses are made for each evaluation. To reduce computational requirements, the optimization is based on the use of approximate analyses. In the present paper a piecewise linear analysis, based on first order Taylor Series expansions, is used. The approximate analyses should produce accurate characteristics of the real problem in a neighborhood of the current design which is continuously updated during optimization. The method has been found to be effective in the past (e.g., ref. 24) for providing accurate approximations.

- **Codes used**
  - **CAMRAD - Blade modal analysis (modified Galerkin approach)**
  - **CONMIN - Optimization (nonlinear programming approach - method of feasible directions)**
- **Method of solution**
  - **Discretize the blade (10 finite segments)**
  - **Compute mode shapes and frequencies**
  - **Perform sensitivity analysis**
    - **Analytical derivatives of objective function, autorotational inertia constraint and stress constraints**
    - **Central differences for frequency constraint derivatives**
- **Use approximate analysis techniques**

FIGURE 6

DYNAMIC OPTIMIZATION RESULTS FOR RECTANGULAR AND TAPERED BLADES

Results obtained by applying the dynamic optimization procedure to the design of both rectangular and tapered rotor blades are summarized here (fig. 7). The table below depicts some of the representative results for the rectangular and tapered blades. For the rectangular blade the 40 design variables are the box beam wall thicknesses (t_1, t_2, t_3) and the magnitudes of the nonstructural masses at ten spanwise locations. For the tapered blade with 42 design variables, the two additional design variables are the box beam height at the root and the taper ratio. In each table, column 1 represents the reference blade data; column 2 gives the corresponding information for the optimum design for the rectangular blade with constraints on the five frequencies, autorotational inertia and stress; and column 3 gives results for the optimum design for the tapered blade with the same set of constraints. In all cases convergence to optimum designs typically has been achieved in 8-10 cycles.

The table indicates that the optimum rectangular blade is 4.7 percent lighter than the reference blade and the optimum tapered blade is 6.2 percent lighter than the reference blade. Although the first lead-lag frequency (f_1) is at its prescribed upper bound after optimization, both frequencies are satisfactory as far as the shear amplification problem is concerned. The autorotational inertia constraint is also active (i.e. exactly satisfied) in all the cases.

	Reference blade	Optimum blade	
		Rectangular (40 design variables)	Tapered (42 design variables)
λ_h	1.0	1.0	1.49
f_1, Hz	12.285	12.408*	12.408*
f_2, Hz	16.098	16.075	16.066
f_3, Hz	20.913	21.081	20.888
f_4, Hz	34.624	34.823	34.678
f_5, Hz	35.861	35.800	35.507
Autorotational inertia(AI), lb-ft^2	517.3*	517.3*	517.3*
Blade weight, lb	98.27	93.61	92.16
Percent reduction in blade weight !	----	4.74	6.21

! From reference blade   * Active

FIGURE 7

OPTIMUM HORIZONTAL WALL THICKNESS (t_1) DISTRIBUTIONS WITH MULTIPLE FREQUENCY AND STRESS CONSTRAINTS

The optimum box beam horizontal wall thickness (t_1) distributions along the blade span are shown below in fig. 8 and are compared with the corresponding distribution of the reference blade. On the left, the optimum distribution corresponds to the rectangular blade with 40 design variables (column 2, fig. 7). On the right, the optimum distribution corresponds to the tapered blade with 42 design variables (column 3, fig. 7). In both cases the optimum blade has a larger value of t_1 than the reference blade at the blade tip. The explanation for this is as follows. The autorotational inertia can be increased with an increase in the moment arm and, therefore, the constraint on the autorotational inertia is satisfied easily if more mass is moved to the blade tip. However, the presence of the centrifugal stress constraint counteracts this tendency. Therefore, the net result is more blade mass towards the outboard region of the blade (although, not necessarily all at the tip).

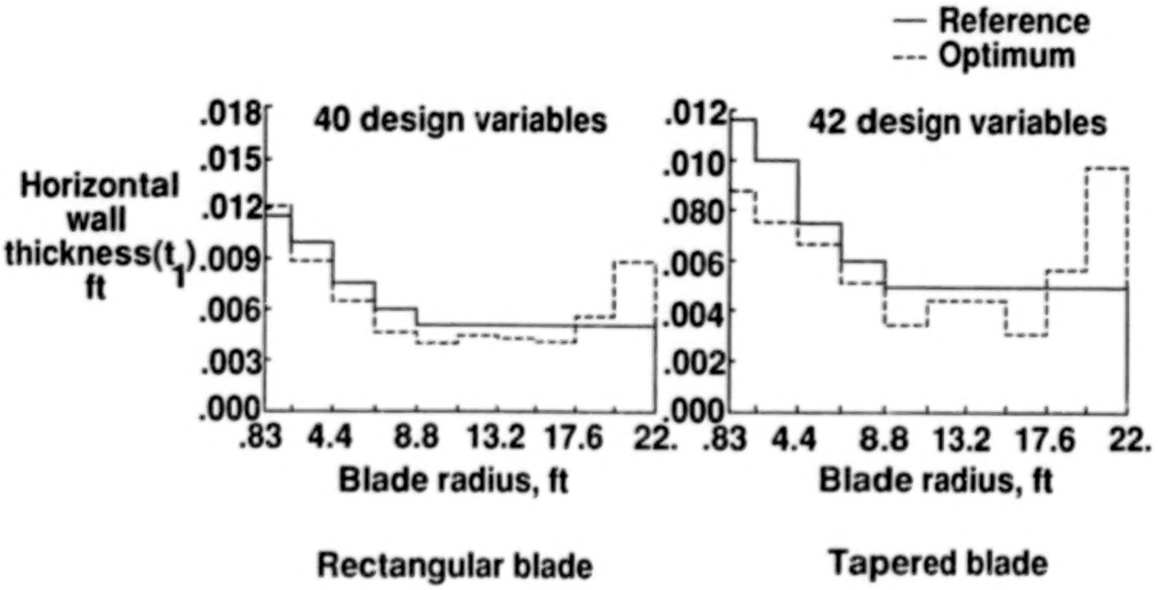

FIGURE 8

OPTIMUM VERTICAL WALL THICKNESS (t_2) DISTRIBUTIONS WITH MULTIPLE FREQUENCY AND STRESS CONSTRAINTS

The optimum box beam vertical wall thickness (t_2) distributions along the blade span are shown below in fig. 9 and are compared with the corresponding distribution of the reference blade. On the left, the optimum distribution corresponds to the rectangular blade with 40 design variables (column 2, fig. 7). On the right, the optimum distribution corresponds to the tapered blade with 42 design variables (column 3, fig. 7). In both cases the optimum blade has a larger value of t_2 than the reference blade at the blade tip due to the presence of the autorotational inertial constraint as explained in the previous chart. However, the difference in magnitude between the optimum and reference blade value at the blade tip is not as significant as it is for the horizontal wall thickness t_1. The nature of the horizontal and vertical wall thicknesses (t_1 and t_2, respectively) are also different as the former primarily affects the flapping frequency and the later affects the lead-lag frequency.

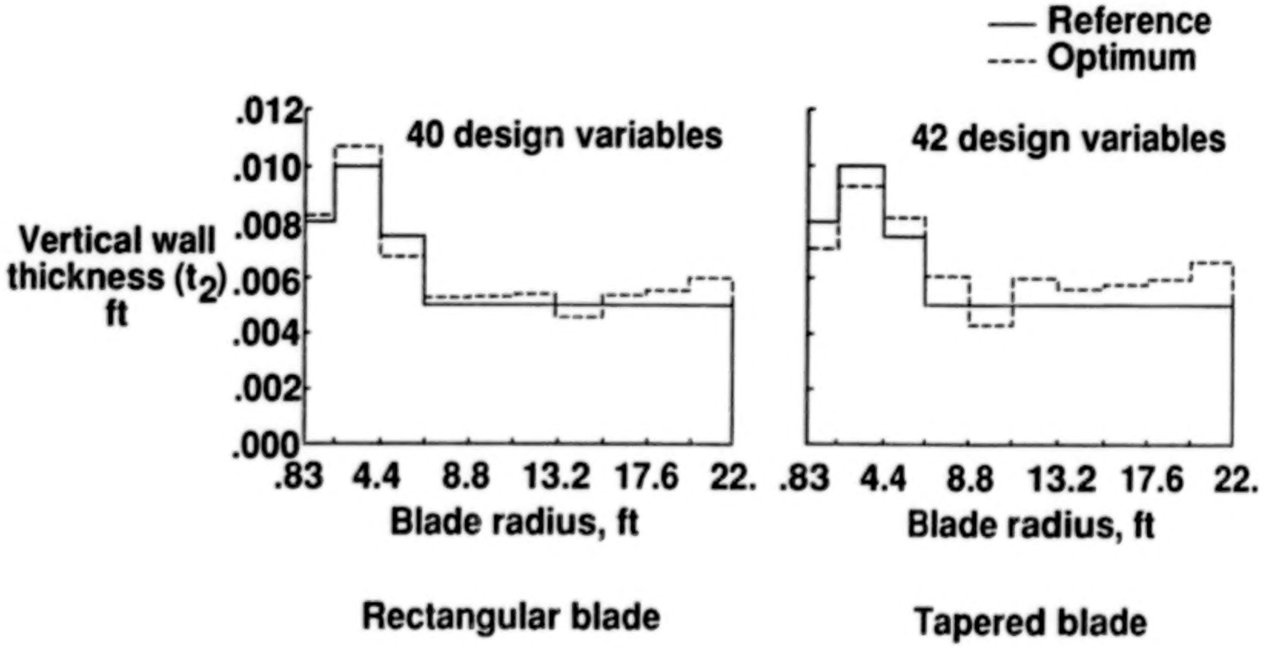

FIGURE 9

OPTIMUM NONSTRUCTURAL SEGMENT WEIGHT DISTRIBUTIONS WITH MULTIPLE FREQUENCY AND STRESS CONSTRAINTS

Shown below (fig. 10) are the optimum and the reference blade nonstructural segment weight distributions along the blade radius for both the rectangular blade with 40 design variables (column 2, fig. 7) and the tapered blade with 42 design variables (column 3, fig. 7). For the rectangular blade (left side of the figure) the optimum blade has lower nonstructural weight throughout the blade span. However, for the tapered blade (right side of the figure) the optimum blade has larger nonstructural weight toward the blade tip than the reference blade. This is because the tapered blade has reduced structural weight requirements at the blade tip. Hence, in order to satisfy the autorotational inertia constraint, the nonstructural weight at the tip must increase. Even so the total weight of the optimum blade is still lower than that of the reference blade.

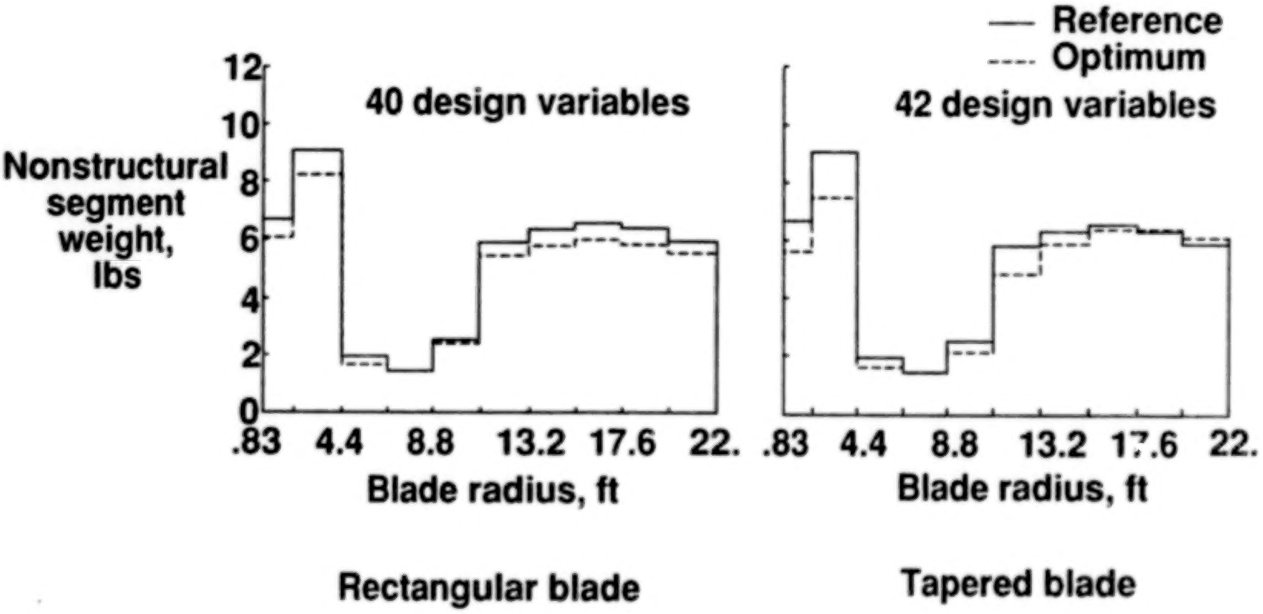

FIGURE 10

STRATEGY AND TASKS FOR STRUCTURAL OPTIMIZATION WITH INTEGRATED DYNAMICS/AERODYNAMICS

The structural optimization of helicopter rotor blades with integrated dynamics/aerodynamics involves both dynamic, aerodynamic and structural design variables, constraints and objective functions along with the blade dynamic/aerodynamic/structural analysis. Together with calculations of the associated sensitivity derivatives this can make the integrated optimization process very complicated and expensive. As a first step towards integrating dynamics and aerodynamics, it was decided to separate the aerodynamic effects into two parts: airloads and performance (fig. 11). The initial step in integrated dynamic/aerodynamic optimization will combine airloads and dynamics. The second step would involve addition of aerodynamic performance to obtain a fully integrated structural optimization procedure with dynamics/aerodynamics. The inclusion of airloads would allow calculation of hub shears and moments which enter into the objective function and/or constraints. This would allow the inclusion of blade aeroelasticity through either limits on the hub loads or the blade stability margin. The aerodynamic analysis would include trimming of the blade at each step of the design process for a specified flight condition. The trim analysis is in fact a coupled dynamic/aerodynamic/structural procedure.

The integrated design process would require the use of more than one objective function in the design formulation. This is because it is difficult to single out an objective function as the primary requirement in an engineering system as complex as the rotor blade. This leads to the necessity of using multiple objective function techniques to formulate the optimization problem. Therefore, various multiple objective function techniques are being investigated and a method called 'Global Criteria Approach'[25] is being examined.

- Dynamic/aerodynamic/structural design variables and constraints
- Include airloads first - integrated dynamic/airload optimization procedure
- Add aerodynamic performance next - fully integrated dynamic/aerodynamic optimization procedure
- Coupled trim analysis
- Several objective functions - multiple objective function handling capability required
- Evaluate 'Global Criteria' approach for multiple objective optimization

FIGURE 11

ANALYSIS COUPLINGS FOR STRUCTURAL OPTIMIZATION WITH INTEGRATED DYNAMICS/AIRLOADS

Below is a schematic diagram that shows the general flow of information between the three major analyses involved in integrated airloads/dynamic optimization. Note that the three major disciplines are internally coupled. For instance, the blade aerodynamic analysis provides the airloads and control settings which are fed into the blade dynamic analysis. The blade dynamic analysis, based on this information, provides the blade natural frequencies, mode shapes, hub shears, moments, etc. If unsteady aerodynamics is included, the dynamic and aerodynamic analyses are coupled as shown by the dotted line in fig. 12 below. The information obtained from the dynamic analysis (shears/bending moments) are fed into the structural analysis box along with the airloads from the aerodynamic analysis to perform the trim analysis. The structural analysis is also used to compute the blade centrifugal stresses which are incorporated as constraints in the optimization process.

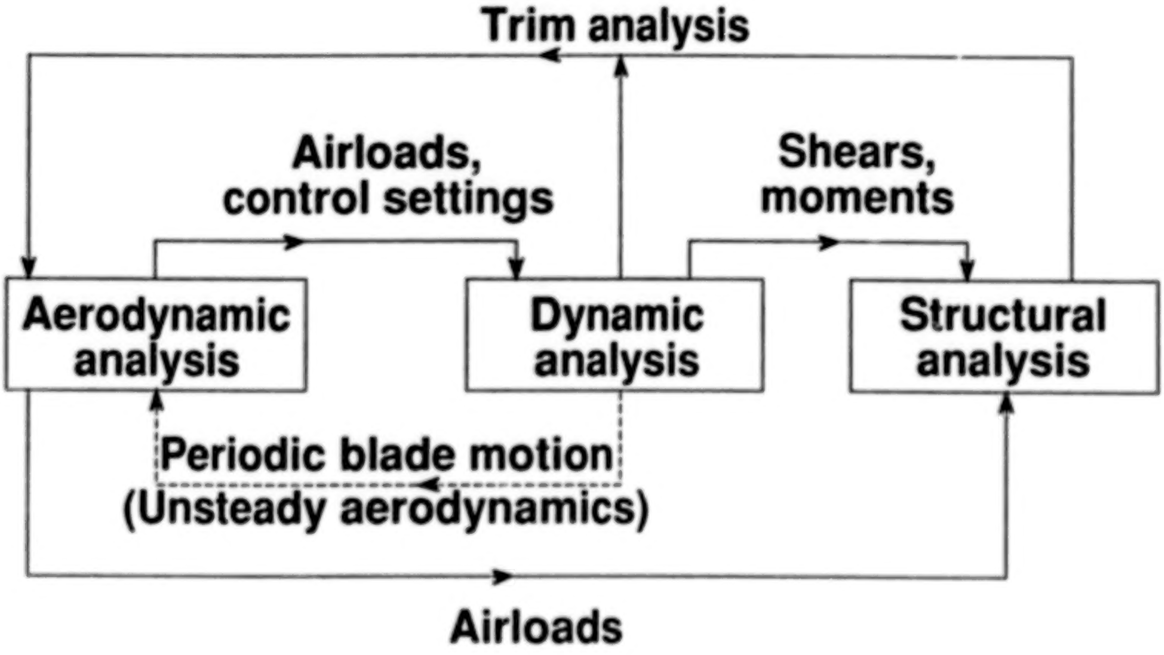

FIGURE 12

COMPUTATIONAL CONSIDERATIONS FOR STRUCTURAL OPTIMIZATION WITH INTEGRATED DYNAMICS/AIRLOADS USING CAMRAD

Some of the computational considerations involved in the structural optimization procedure with integrated dynamics/airloads is described below in fig. 13. The program CAMRAD[20] is used for the aerodynamic and dynamic analyses of the rotor blade in forward flight. The program has been found to be very reliable for analysis of helicopter rotors[8,9,26]. It uses a lifting line or blade element approach to calculate the section loading from the airfoil two-dimensional aerodynamic characteristics with corrections for yawed and three-dimensional flow effects[22]. The program also has the provision for including unsteady aerodynamics.

Each intermediate design should satisfy the trim condition. The program CAMRAD offers two broad categories of trimming - the free flight case and the wind tunnel case. In the free flight case, the entire helicopter is trimmed to force and moment equilibrium whereas in the wind tunnel case the isolated rotor is trimmed to a prescribed operating condition. It is possible to use a free flight trim option for an isolated rotor in a wind tunnel since the trim option and the degrees for freedom representing the aircraft can be specified independently. However, the wind tunnel trimming options are more typical of a rotor in a wind tunnel without consideration of the complete rotorcraft. The wind tunnel trim option is selected for this analysis since the model used in this study is a wind tunnel model of a rotor. The trim option consists of trimming the rotor lift, drag and flapping angle with collective pitch, cyclic pitch and shaft angle.

- **Aerodynamic loads (forward flight)**
  - **Lifting line theory to calculate section loading from airfoil 2-D aerodynamic characteristics**
  - **Corrections for yawed and 3-D flow effects**
- **Trim analysis**
  - **Wind tunnel trim for isolated rotor**
    - **Lift, drag and flapping angle with collective pitch, cyclic pitch and shaft angle**

FIGURE 13

FORMULATION OF THE STRUCTURAL OPTIMIZATION PROBLEM WITH INTEGRATED DYNAMICS/AIRLOADS

The optimization problem addressed here uses blade weight and blade root 4 per rev vertical shear as the objective functions to be minimized. The constraints are 'windows' on the coupled flap-lag natural frequencies to prevent them from falling into the critical ranges, a prescribed lower bound on the blade autorotational inertia and a maximum allowable upper bound on the blade stress. The design variables (fig. 14) are the blade spanwise stiffness distributions (EI's and GJ), the magnitudes of the lumped nonstructural masses distributed spanwise, the blade taper ratio and the root chord as shown below in the figure. The nonstructural masses which were used for frequency placement in the dynamics work discussed earlier will now be used for both frequency tuning as well as hub shear alleviation.

- **Objective function:** Blade weight and blade root vertical shear
- **Constraints:** Frequencies, autorotational inertia, blade stress
- **Design variables:** Stiffness and mass distributions, magnitudes of lumped/tuning masses, taper ratio, root chord

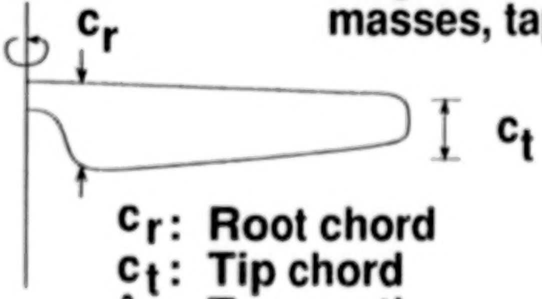

$$\lambda = \frac{c_r}{c_t}$$

c_r: Root chord
c_t: Tip chord
λ : Taper ratio

FIGURE 14

FLOW CHART OF THE STRUCTURAL OPTIMIZATION PROCEDURE WITH INTEGRATED DYNAMICS/AIRLOADS

The optimization procedure shown in the flow chart below (fig. 15) is initiated by identifying the blade preassigned parameters which are the parameters that are held fixed during optimization. The next step is to initialize the design variables and perform the internally coupled blade analysis which comprises blade aerodynamic, dynamic and structural analyses. A sensitivity analysis is part of the procedure and consists of evaluations of the derivatives of the objective function and the constraints with respect to the independent design variables. Once the sensitivity analysis is performed the approximate model is defined based on a standard approximation technique. Using CONMIN along with the approximate model updated design variable values are obtained. The process continues until convergence is achieved.

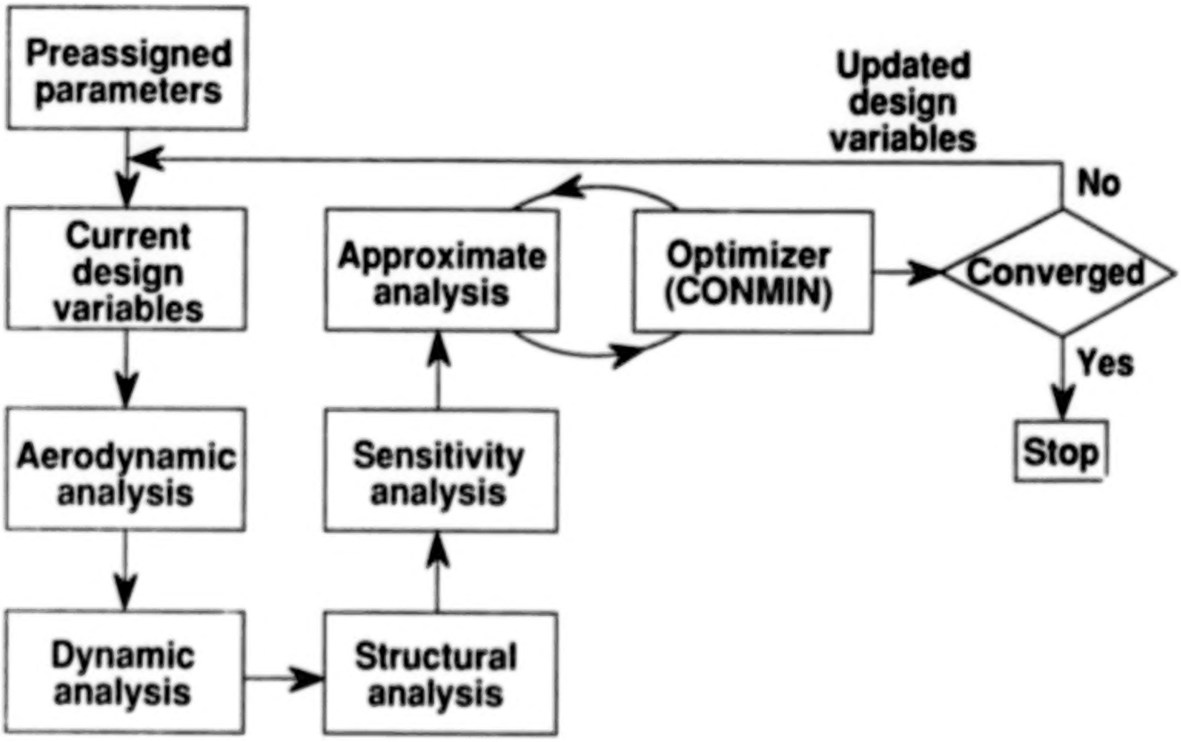

FIGURE 15

SENSITIVITY ANALYSIS

The conventional approach for performing sensitivity analysis is to calculate the derivatives either analytically or by using finite difference schemes. Since analytical expressions are seldom available and use of finite difference schemes is usually expensive and sometimes inaccurate, a new method[27] for obtaining the system sensitivity has been considered for the present work. The method enables one to calculate the sensitivity derivatives of the system solution with respect to a design variable from a set of simultaneous equations which are known as Global Sensitivity Equations (GSE). In fig. 16 the system sensitivity equations are described in terms of a coupled system consisting of the boxes A, D, and S representing aerodynamics, dynamics and structures. Each discipline box is regarded as a set of mathematical operations that solves one of the sets of governing equations on the right to produce an output denoted by Y. For example, Y_A denotes the output of the aerodynamic analysis. The coupling of the system is demonstrated in the figure below. The design variables are denoted by X. The quantities X and Y are in general vectors. Furthermore the subset of Y_A entering D may be different from the subset of Y_A entering S, although the subsets may overlap.

Using chain rule on the governing equations as in ref. 27, the system sensitivity equations are derived. The sensitivity derivatives appear as the vector of unknowns. The coefficient matrix consists of partial derivatives of the output of the various disciplinary responses with respect to each other positioned off the diagonal and identity submatrices along the diagonal. Nonzero values of these partial derivatives reflect system couplings. The right hand side vector contains the partial derivatives of the disciplinary outputs with respect to a particular design variable (e.g. X_k). The coefficient matrix needs only to be formed and factored once for a given system and then back substituted using a new right hand side vector for every new design variable. Thus the method enables the computations of derivatives of complex internally coupled systems without having to perform expensive finite difference derivatives based on the entire system analysis.

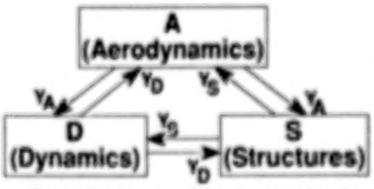

Governing equations:

$A((X, Y_D, Y_S), Y_A) = 0$

$D((X, Y_A, Y_S), Y_D) = 0$

$S((X, Y_D, Y_A), Y_S) = 0$

Coupled rotor blade analysis

Sensitivity derivatives

Global sensitivity equations:

$$\begin{bmatrix} I & -\frac{\partial Y_A}{\partial Y_D} & -\frac{\partial Y_A}{\partial Y_S} \\ -\frac{\partial Y_D}{\partial Y_A} & I & -\frac{\partial Y_D}{\partial Y_S} \\ -\frac{\partial Y_S}{\partial Y_A} & -\frac{\partial Y_S}{\partial Y_D} & I \end{bmatrix} \begin{Bmatrix} \frac{dY_A}{dX_k} \\ \frac{dY_D}{dX_k} \\ \frac{dY_S}{dX_k} \end{Bmatrix} = \begin{Bmatrix} \frac{\partial Y_A}{\partial X_k} \\ \frac{\partial Y_D}{\partial X_k} \\ \frac{\partial Y_S}{\partial X_k} \end{Bmatrix}$$

FIGURE 16

MULTIPLE OBJECTIVE FUNCTION - GLOBAL CRITERIA APPROACH

As indicated before, the current optimization procedure requires a multiple objective function approach. Several methods have been proposed for the solution of multiobjective optimization problems. However, many of these methods suffer from a need for assigning relative priorities to the individual objective functions, e.g. assigning weight factors. The optimization goal is to find the set of design variables ϕ which minimizes N objective functions $(F_1(\phi), F_2(\phi), \ldots, F_N(\phi))$ subject to a set of inequality constraints g_j $(j=1,2,\ldots,\text{NCON}$ where NCON denotes the total number of constraints). Using the Global Criteria Approach described in fig. 17, the optimum solution ϕ^* is obtained by minimizing a prescribed 'global criterion' $\hat{F}(\phi)$ which is defined as the sum of the squares of the relative deviations of the individual objective functions $F_i(\phi)$ from their respective feasible optimum values $F_i(\phi_i^*)$. The optimum solution, ϕ_i^*, to the i^{th} individual objective function is obtained by minimizing $F_i(\phi)$ subject to the constraints $g_j(\phi) \le 0$, $j=1,2,\ldots,\text{NCON}$. The optimization problem now is to minimize the composite objective function $\hat{F}(\phi)$ subject to exactly the same set of constraints as used in the individual optimizations. The method is less judgmental in the sense it imposes equal priority to each individual objective function[25].

Global Criteria Approach

- **Optimization goal**

  Minimize "N" objective functions

  $$F_1(\phi), F_2(\phi), F_3(\phi), \ldots, F_N(\phi)$$

  subject to $g_j(\phi) \le 0 \quad j = 1,2,\ldots, \text{NCON}$

- **Global criterion formulation**

  Minimize

  $$\hat{F}(\phi) = \sum_{i=1}^{N} \left\{ \frac{F_i(\phi) - F_i(\phi_i^*)}{F_i(\phi_i^*)} \right\}^2$$

  subject to $g_j(\phi) \le 0 \quad j = 1,2,\ldots, \text{NCON}$

  (ϕ_i^*) obtained from

  Minimize $F_i(\phi)$

  subject to $g_j(\phi) \le 0 \quad j = 1,2,\ldots, \text{NCON}$

FIGURE 17

FORMULATION OF STRUCTURAL OPTIMIZATION PROBLEM WITH INTEGRATED DYNAMICS/AIRLOADS USING GLOBAL CRITERIA APPROACH

Using the the Global Criteria Approach the airload/dynamic optimization problem with multiple objective functions can be formulated as shown in fig. 18. The two objective functions $F_1(\phi)$ and $F_2(\phi)$ are the blade weight W and the blade root 4 per rev vertical shear F_Z, respectively. The constraints are on the frequencies f_k, k=1,2,...6 (three lead-lag and three flapping dominated modes), the blade stress σ and the blade autorotational inertia AI. Using the Global formulation the new global objective function $F(\phi)$ is defined as the sum of the squares of the deviations of the objective functions, W and F_Z, from their respective individual optimum values W^* and F_Z^*. The optimization problem now is to minimize $F(\phi)$ subject to the original set of constraints.

Multiple objective functions: $F_1(\phi) = W$

$F_2(\phi) = F_Z$

Constraints, $g(\phi)$:

$$1 - f_k / f_{k_L} \leq 0$$

$$f_k / f_{k_U} - 1 \leq 0$$

$$\alpha - AI \leq 0$$

$$\sigma \cdot FS - \sigma_{max} \leq 0$$

Global objective function:

$$\hat{F}(\phi) = \left(\frac{W - W^*}{W^*}\right)^2 + \left(\frac{F_Z - F_Z^*}{F_Z^*}\right)^2$$

subject to $g(\phi) \leq 0$

FIGURE 18

STUDY OF GLOBAL CRITERIA APPROACH FOR WEIGHT-STRESS OPTIMIZATION (BLADE IN VACUUM)

Before attempting to solve the above integrated airload/dynamic optimization problem it was first decided to study the Global Criteria Approach for the dynamic optimization problem with the blade in vacuum and the blade weight and centrifugal stress as the two objective functions to be minimized (fig. 19). There F_1 is equal to W which is the blade weight and F_2 is equal to σ which represents the maximum centrifugal stress in the blade. The constraints are windows on the first coupled lead-lag dominated and the first flapping dominated frequencies and the blade autorotational inertia. The formulation of the test problem is shown in the figure. The new global objective function is a measure of the deviations of the individual objective functions, W and σ, from their respective optimum values W^* and σ^* and is denoted by $\hat{F}(\phi)$.

Multiple objective functions: $F_1(\phi) = W$

$F_2(\phi) = \sigma$

Constraints, $g(\phi)$:

$$1 - f_k / f_{k_L} \leq 0$$

$$f_k / f_{k_U} - 1 \leq 0$$

$$\alpha - AI \leq 0$$

Global objective function:

$$\hat{F}(\phi) = \left(\frac{W - W^*}{W^*}\right)^2 + \left(\frac{\sigma - \sigma^*}{\sigma^*}\right)^2$$

subject to $g(\phi) \leq 0$

FIGURE 19

OPTIMIZATION RESULTS FOR RECTANGULAR BLADE USING GLOBAL CRITERIA APPROACH (BLADE IN VACUUM)

Following are the optimization results for the weight-stress optimization procedure discussed in the previous chart performed with the blade in vacuum. Figure 20 presents results obtained from the single objective function compared to those obtained from the multiple objective function formulation using the Global Criteria Approach. The results are for the rectangular blade with 30 design variables (t_1, t_2 and t_3 at ten spanwise locations). Case 1 corresponds to the values obtained after optimization with blade weight as the single objective function and Case 2 refers to the values obtained after optimization with maximum centrifugal stress as the single objective function. Case 3 corresponds to the values obtained after optimization with multiple objective functions (blade weight and maximum centrifugal stress) using the Global Criteria Approach. When only the blade weight is minimized, the blade stress increases (Case 1). On the other hand when blade stress is minimized, the blade weight increases (Case 2). As shown using the Global Criteria Approach (Case 3), when considering both stress and blade weight simultaneously, the optimum results fall in between those obtained using only single objective functions. Compared to Case 1 the blade weight is slightly larger but the stress is much lower. Compared to Case 2 the blade weight is much lower and the stress is only slightly increased. The Global Criteria Approach therefore provides the 'best' compromise when two such conflicting objective functions are used.

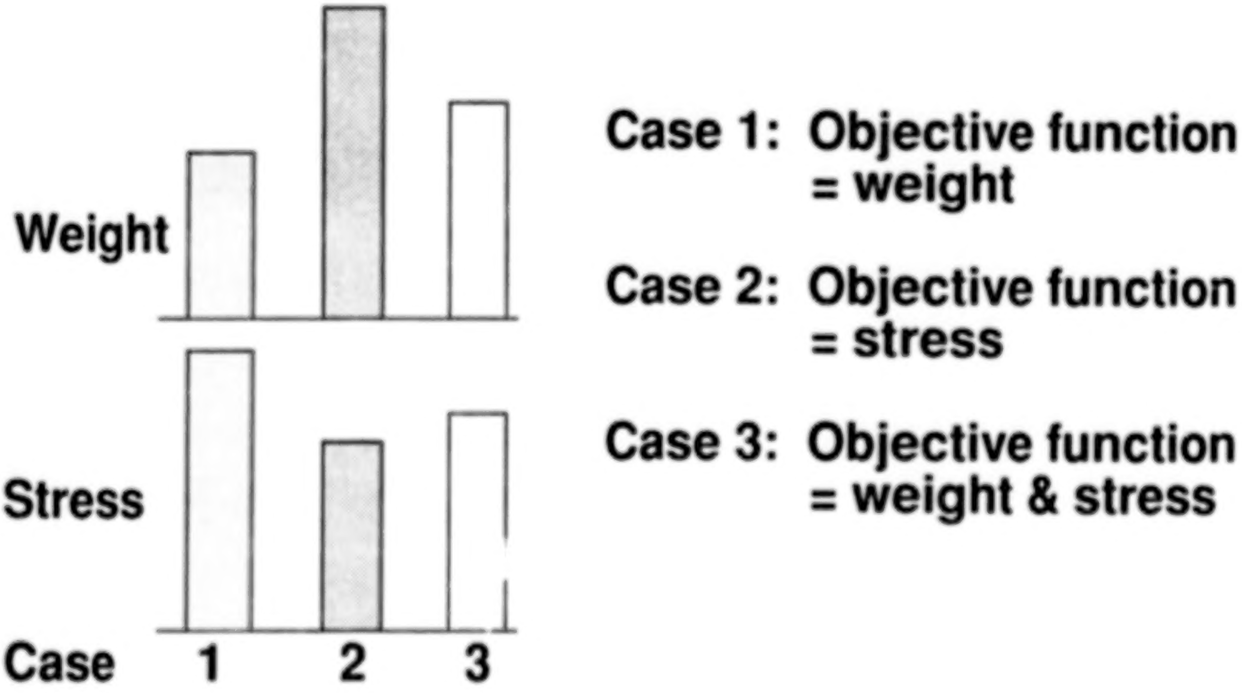

FIGURE 20

CONCLUDING REMARKS

The paper addresses the problem of structural optimization of helicopter rotor blades with integrated dynamic and aerodynamic design considerations. Results of recent optimization work on rotor blades for minimum weight with constraints on multiple coupled natural flap-lag frequencies, blade autorotational inertia and centrifugal stress has been reviewed. A strategy has been defined for the ongoing activities in the integrated dynamic/aerodynamic optimization of rotor blades. As a first step the integrated dynamic/airload optimization problem has been formulated. To calculate system sensitivity derivatives necessary for the optimization recently developed Global Sensitivity Equations (GSE) are being investigated. A need for multiple objective functions for the integrated optimization problem has been demonstrated and various techniques for solving the multiple objective function optimization are being investigated. The method called the 'Global Criteria Approach' has been applied to a test problem with the blade in vacuum and the blade weight and the centrifugal stress as the multiple objectives. The results indicate that the method is quite effective in solving optimization problems with conflicting objective functions. (Fig. 21).

- **Reviewed procedure for dynamic optimization with minimum weight objective and frequency, autorotational inertia and stress constraints**
- **Defined strategy for integrating the above with complete aerodynamic optimization**
- **Formulated integrated dynamic/airload optimization**
- **Investigating global sensitivity equations for calculating system sensitivity derivatives**
- **Described need for multiple objective functions**
- **Investigated 'Global Criteria' approach for multiple objective optimization**

FIGURE 21

REFERENCES

1. Ashley, H., "On Making Things the Best - Aeronautical Use of Optimization," AIAA J. Aircraft, Vol. 19, No. 1, 1982.

2. Sobieszczanski-Sobieski, J., "Structural Optimization Challenges and Opportunities," presented at Int. Conference on Modern Vehicle Design Analysis, London, England, June 1983.

3. Miura, H., "Application of Numerical Optimization Method to Helicopter Design Problems: A Survey," NASA TM 86010, October 1984.

4. Bennett, R. L., "Application of Optimization Methods to Rotor Design Problems," Vertica, Vol. 7, No. 3, 1983, pp. 201-208.

5. Sobieszczanski-Sobieski, J., "Recent Experiences in Multidisciplinary Analysis and Optimization," NASA CP 2327, 1984.

6. Peters, D. A., Ko, Timothy, Rossow, Mark P., "Design of Helicopter Rotor Blades for Desired Placement of Natural Frequencies," Proc. of the 39th Annual Forum of the AHS, May 9-11, 1983, St. Louis, Missouri.

7. Taylor, R. B., "Helicopter Vibration Reduction by Rotor Blade Modal Shaping", Proc. of the 38th Annual Forum of the AHS, May 4-7, 1982, Anaheim, California.

8. Chattopadhyay, Aditi and Walsh, Joanne L., "Minimum Weight Design of Rectangular and Tapered Helicopter Rotor Blades with Frequency Constraints," Proc. of the 2nd Int. Conference on Rotorcraft Basic Research, February 16-18, 1988, College Park, Maryland. Also available as NASA TM 100561, February 1988.

9. Chattopadhyay, Aditi and Walsh, Joanne L., "Minimum Weight Design of Rotorcraft Blades with Multiple Frequency and Stress Constraints," Proc. of the AIAA/ASME/ASCE/AHS 29th Structures, Structural Dynamics and Materials Conference, Williamsburg, Virginia, April 18-20, 1988. AIAA Paper No. 88-2337-CP. Also available as NASA TM 100569, March 1988.

10. Weller, W. H. and Davis M. W., "Experimental Verification of Helicopter Blade Designs Optimized for Minimum Vibration," Proc. of the 44th Annual Forum of the AHS, June 16-18, 1988, Washington, D. C.

11. Walsh, J. L., Bingham, G. J., and Riley, M. F., Optimization Methods Applied to the Aerodynamic Design of Helicopter Rotor Blades. Journal of the American Helicopter Society, Vol 32, No. 4, October 1987.

12. Nixon, M. W., "Preliminary Structural Design of Composite Main Rotor Blades for Minimum Weight," NASA TP-2730, July 1987.

13. Peters, D. A., Ko, Timothy, Korn, Alfred, and Rossow, Mark P., "Design of Helicopter Rotor Blades for Desired Placements of Natural Frequencies," Proc. of the 39th Annual Forum of the AHS, May 9-11, 1983, St. Louis, Mo.

14. Hanagud, S., Chattopadhyay, Aditi, Yillikci, Y. K., Schrage, D., and Reichert, G., "Optimum Design of a Helicopter Rotor Blade," Paper No.

12, Proc. of the 12th European Rotorcraft Forum, September 22-25, 1986, Garmisch-Partenkirchen, West Germany.

15. Peters, D. A., Rossow, Mark P., Korn, Alfred, and Ko, Timothy, "Design of Helicopter Rotor Blades for Optimum Dynamic Characteristics," Computers & Mathematics with Applications, Vol. 12A, No. 1, 1986, pp. 85-109.

16. Friedmann, P. P. and Shantakumaran, P., "Optimum Design of Rotor Blades for Vibration Reduction in Forward Flight," Proc. of the 39th Annual Forum of the AHS, May 9-11, 1983, St. Louis, Missouri.

17. Celi, R. and Friedmann, P. P., "Efficient Structural Optimization of Rotor Blades with Straight and Swept Tips," Proc. of the 13th European Rotorcraft Forum, Arles, France, September 1987. Paper No. 3-1.

18. Adelman, H. M. and Mantay, W. R., "An Initiative in Integrated Multidisciplinary Optimization of Rotorcraft," To be presented at the Second NASA/Air Force Symposium on Recent Advances in Multidisciplinary Analysis and Optimization, Hampton, Virginia, September 28-30, 1988.

19. Lim, Joon and Chopra, Inderjit, "Stability Sensitivity Analysis for the Aeroelastic Optimization of a Helicopter Rotor," Proc. of the AIAA/ASME/ASCE/AHS 29th Structures, Structural Dynamics and Materials Conference, Williamsburg, Virginia, April 18-20, 1988.

20. Johnson, W., "A Comprehensive Analytical Model of Rotorcraft Aerodynamics and Dynamics," Part II: User's Manual, NASA TM 81183, June 1980.

21. Lang, K. W., and Nemat-Nasser, S., "An Approach for Estimating Vibration Characteristics of Nonuniform Rotor Blades," AIAA Journal, Vol. 17, No. 9, September 1979.

22. Johnson, W., "A Comprehensive Analytical Model of Rotorcraft Aerodynamics and Dynamics," Part I: Analysis Development, NASA TM 81182, June 1980.

23. Vanderplaats, G. N., "CONMIN - A Fortran Program for Constrained Function Minimization," User's Manual, NASA TMX-62282, August 1973.

24. Walsh, Joanne L., "Applications of Numerical Optimization Procedures to a Structural Model of a Large Finite-Element Wing," NASA TM 87597, 1986.

25. Rao, S. S., "Multiobjective Optimization in Structural Design with Uncertain Parameters and Stochastic Processes," AIAA Journal, Vol. 22, No. 11, November 1984.

26. Callahan, C. and Bassett, D., "Application of a Comprehensive Analytical Model of Rotorcraft Aerodynamics and Dynamics (CAMRAD) to the McDonnell Douglas AH-64A Helicopter," Proc. of 43rd Annual AHS Forum, St. Louis, Missouri, May 18-20, 1987, pp. 293-355.

27. Sobieszczanski-Sobieski, J., "On the Sensitivity of Complex Internally Coupled Systems," NASA TM 100537, January 1988.

BLANK PAGE

MULTI-OBJECTIVE/LOADING OPTIMIZATION FOR ROTATING COMPOSITE FLEXBEAMS

BRIAN K. HAMILTON
JAMES R. PETERS

McDonnell Douglas Helicopter Company
Mesa, AZ

Introduction

With the evolution of advanced composites, the feasibility of designing bearingless rotor systems for high speed, demanding maneuver envelopes, and high aircraft gross weights has become a reality. These systems eliminate the need for hinges and heavily loaded bearings by incorporating a composite flexbeam structure which accommodates flapping, lead-lag, and feathering motions by bending and twisting while reacting full blade centrifugal force, Figure (1). The flight characteristics of a bearingless rotor system are largely dependent on hub design, and the principal element in this type of system is the composite flexbeam. As in any hub design, trade off studies must be performed in order to optimize performance, dynamics (stability), handling qualities, and stresses. However, since the flexbeam structure is the primary component which will determine the balance of these characteristics, its design and fabrication are not straightforward. Some of the considerations which must be addressed are as follows:

1. Flap-Lag-Torsion deformations will be accommodated through the flexbeam.
2. Effective flapping hinge offset has to be properly controlled for a balance between maneuverability and dynamic vibration.
3. Hub size must be kept at a minimum in order to reduce weight and hub drag.
4. Optimum tailoring of the pitchcase, snubber/damper and inplane flexbeam deformation must be obtained in order to maximize inplane damping.
5. The flexbeam must be able to endure peak loading from high *g* maneuvers as well as endurance flight loads.
6. Flexbeam design criteria are influenced by rotor shaft/mast/hub impedance characteristics.

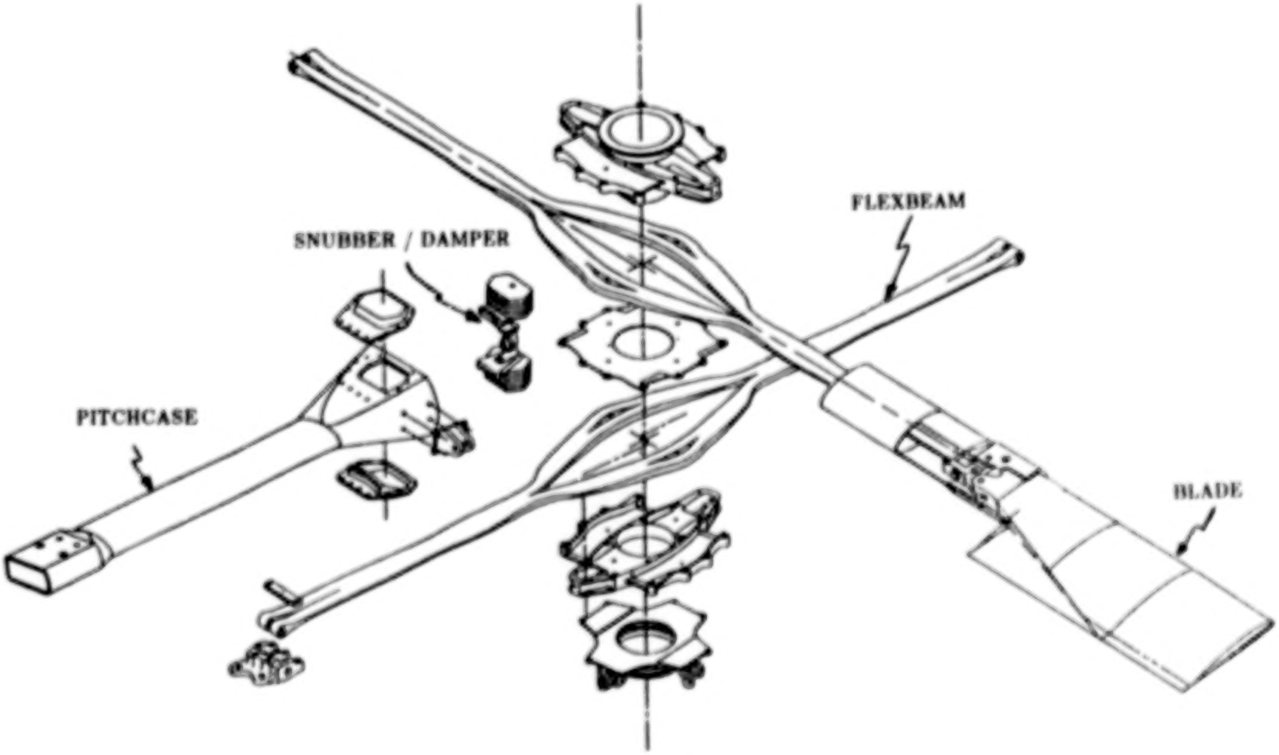

Figure (1)

Model Development

At McDonnell Douglas Helicopter Company, the previous considerations have been integrated into a mathmatical procedure for design and optimization of advanced composite bearingless rotor systems. Because of the highly coupled structural and damping requirements of the flexbeam, it was critical to include a representation of the pitchcase and snubber/damper, as well as the flexbeam, in the math model. Various alternatives can be proposed for formulation of such a problem:

1. choice of flexbeam cross section
2. choice of composite material type and configuration
3. choice of hub attachment configuration
4. choice of objective function and constraints for optimization routine
    (a) minimization of peak stresses due to flap, lag and torsion with a requirement on damper motion and hence rotor inplane damping
    (b) maximization of rotor damping with upper bound contraints on stresses

Flexbeam Cross Section

In an effort to simplify the beam design and fabrication, a comprehensive review of candidate cross sections was conducted under a company IRAD[*]program . Geometries studied ranged from rectangular, cruciform and multiple "H" closed sections to multiple element open sections and elastomericly connected rectangular cross sections.

Based on this review, a simple rectangular section was selected as the best overall configuration for the advanced flexbeam. In addition to the efficient load carrying capability, the relatively straightforward rectangular configuration offered advantages of simplified fabrication resulting in lower production costs, superior quality control, and simplified inspectability.

Composite Material Selection

The composite material selected for the advanced flexbeam was S-2 fiberglass impregnated with a 350 deg F cured "toughened resin" epoxy system. The resin system was selected based on the results of an extensive study of candidate systems conducted under other McDonnell Douglas Helicopter Company IRAD programs.

The S-2 fiberglass provides improved compressive stress margins and reduces long term enviromental degradation concerns associated with the previously selected Kevlar material.

---

[*] Internal Research and Development

Hub Attachment Configuration

Flexbeam design criteria are influenced by rotor shaft/ mast/hub impedance characteristics. A relatively soft rotor mast mount can significantly modify a flexbeam's effective flapping hinge offset and bending requirements. An inhouse analysis has indicated that a softer mount can result in an increased level of airframe vibration and the need for vibration suppression systems.

The Helicopter Advanced Rotor Program (HARP) flight test program demonstrated low vibration characteristics for the initial composite flexbeams using the McDonnell Douglas Helicopter Company rigid mast system with no active or passive vibration control equipment required. The advanced beam design approach was also based on the proven rigid mast configuration.

Objective Function and Constraints

Significant progress has been made both by industry and the goverment in the study of flexbeam design over the past ten years. McDonnell Douglas Helicopter Company has kept abreast of this work and has incorporated the lessons learned both by ourselves and other investigators into the present math model.

The primary goal in flexbeam sizing is to achieve the required rotor blade motions without exceeding the allowable stresses in the composite material. Simultaneous goals are to minimize flexbeam length, to achieve blade flap and lead-lag hinge offsets which provide suitable dynamics properties, and to obtain sufficient lead-lag motion at the snubber/damper for satisfactory dynamic response to cyclic loads. The criteria for blade motions include the maximum blade cyclic flap, lead-lag, and feathering motions seen in the flight envelope (the one hour condition), as well as endurance limit, static droop and start-up conditions.

Rotor blade flapping, lead-lag and feathering motions acting in combination with the blade and pitchcase centrifugal force cause flexbeam deformations. The flexbeam must be so designed as to allow these blade motions without exceeding the allowable stresses of the fiber composite of which it is constructed. Because blade motions have both steady and cyclic components, fatigue loads prevail and the fatigue strength of the composite material is critical for design. Therefore, the one hour and endurance limit flap, lead-lag, and torsional motions are applied to the flexbeam. The cyclic stresses which the one hour motions cause should not exceed the corresponding one hour fatigue allowables of the composite material. Similarly, cyclic stresses due to endurance limit loads should not exceed endurance limit fatigue allowables. In addition, criteria for the blade motions include static droop and start-up torque conditions. These goals, taken together, are used in sizing the flexbeam in lieu of a complete fatigue life analysis covering the full operating spectrum of the helicopter.

The objective function selected for the advanced beam was minimization of stresses due to a critical combination of flap, lead-lag and torsional deformation. In addition, a displacement constraint is imposed for adequate damper motion to satisfy the dynamic requirements.

Theoretical Background

The conventional finite element method is not applicable in the case of an elastic structure undergoing high angular motions. This is of interest because numerous structural configurations such as spinning helicopter blades, satellites, rotating flexbeams, shafts and linkages fall into this category. The analysis of these rotating structures differs from that of stationary structures due to the complexity of the accelerations which act throughout the system. In addition to the accelerations resulting from elastic structural deformations, contributions due to Coriolis and centripetal acceleration may be of significance. Also, the stiffness characteristics of the structure may be modified by the internal loads induced by the centrifugal forces. The finite element formulation given in this section includes all these effects in a uniform general formulation.

The variational principle useful for problems in dynamics is Hamilton's principle. The functional for this principle is the Lagrangian, L, defined as

$$L = T - U - V \tag{1}$$

where T is the kinetic energy, U is the strain energy, and V is the potential of the applied loads. The strain energy density may be expressed as

$$dU = \frac{1}{2}\epsilon^T \sigma dV = \frac{1}{2}\epsilon^T C \epsilon dV \tag{2}$$

where C is the material elastic matrix. The potential of the applied loads, V, may be expressed as the sum of the potential of the body forces and surface tractions as

$$V = -\int_V (\bar{X} \cdot u) dV - \int_S (\bar{T} \cdot u) dS \tag{3}$$

where $\bar{X}$ is the body force vector, u is the displacement vector, and $\bar{T}$ is the vector of surface tractions. The second integral is over the surface of the body on which the surface tractions are prescribed.

The total kinetic energy density is defined as

$$dT = \frac{1}{2}\rho V^T V dV \tag{4}$$

where ρ is the density of the material and V is the absolute velocity of a particle in the element as given by

$$V = V_{RB} + \dot{u} + \tilde{\omega} u \tag{5}$$

Here, V_{RB} is the velocity of the particle due to frame motion, $\mathbf{u}$ is the vector of elastic deformations, and ω is the angular velocity of the element coordinate system. Substitution of equation (5) into (4) gives

$$
\begin{aligned}
dT = \frac{1}{2}\rho V_{RB}^T V_{RB} dV &+ \frac{1}{2}\rho \dot{\mathbf{u}}^T \dot{\mathbf{u}} dV \\
&+ \frac{1}{2}\rho(\dot{\mathbf{u}}^T \tilde{\omega}\mathbf{u} - \mathbf{u}^T \tilde{\omega}\dot{\mathbf{u}} - \mathbf{u}^T \tilde{\omega}\tilde{\omega}\mathbf{u}) dV \\
&+ \frac{1}{2}\rho(V_{RB}^T \dot{\mathbf{u}} + \dot{\mathbf{u}}^T V_{RB} + V_{RB}^T \tilde{\omega}\mathbf{u} - \mathbf{u}^T \tilde{\omega} V_{RB}) dV
\end{aligned}
\tag{6}
$$

The first term in equation (6) is the kinetic energy due purely to frame translation. This term will be deleted since frame motion is assumed to be entirely prescribed. The second term represents the kinetic energy due to elastic deformations only. The third term is the energy due to frame rotation, and the fourth term gives the forces due to coupling between frame translation, elastic deformations and frame rotation.

Using equations (2), (3) and (6), the functional in equation (1) may be expressed in the following form:

$$
\begin{aligned}
L = \frac{1}{2}\int_V \rho \left(\dot{\mathbf{u}}^T \dot{\mathbf{u}} + \dot{\mathbf{u}}^T \tilde{\omega}\mathbf{u} - \mathbf{u}^T \tilde{\omega}\dot{\mathbf{u}} - \mathbf{u}^T \tilde{\omega}\tilde{\omega}\mathbf{u}\right) dV \\
- \frac{1}{2}\int_V \epsilon^T C \epsilon dV \\
+ \frac{1}{2}\int_V \rho(V_{RB}^T \dot{\mathbf{u}} + \dot{\mathbf{u}}^T V_{RB} + V_{RB}^T \tilde{\omega}\mathbf{u} - \mathbf{u}^T \tilde{\omega} V_{RB}) dV \\
+ \int_V \mathbf{u}^T \hat{X} dV + \int_S \mathbf{u}^T \hat{T} dS
\end{aligned}
\tag{7}
$$

The statement of Hamilton's principle is as follows: Among all possible time histories of displacement configurations which satisfy compatibility and the constraints or kinematic boundary conditions and which also satisfy conditions at times t_1 and t_2, the history which is the actual solution makes the Lagrangian functional a minimum. This principle may be expressed mathematically as

$$
\delta \int_{t_1}^{t_2} L dt = 0 \tag{8}
$$

Application to the Finite Element Method

Most problems are too complex to use energy principles to obtain the exact solution directly. The usual technique is to guess, a priori, a trial family of solutions for the unknown quantity in order to construct a variational functional. We therefore choose an approximate pattern for the trial solution and apply the energy principles to the approximate functional to obtain the equations necessary to find the approximate solution. In the theory of the finite element method for structural analysis, once the proper variational principle has been selected for the given problem, we express the functional involved in terms of approximate assumed displacement functions which satisfy the geometric boundary conditions. We then minimize the approximate functional using equation (8) to obtain a set of governing equations.

General Displacement Models

The basic philosophy of the finite element method is piecewise approximation. That is, we approximate a solution to a complicated problem by subdividing the region of interest and representing the solution within each subdivision by a relatively simple function. In the displacement method of structural analysis, the structure or body is divided into finite elements. Then, simple functions are chosen to approximate the displacements within each element. These functions are called displacement models, displacement functions, displacement fields, or displacement patterns. A polynomial is the most common form of displacement model used for two principal reasons. First, it is easy to handle the mathematics of polynomials in formulating the desired equations for various elements and in performing digital computation. In particular, the use of polynomials permits us to differentiate and integrate with relative ease. Secondly, a polynomial of arbitrary order permits a recognizable approximation to the true solution; however, for practical purposes we are limited to one of finite order. By truncating an infinite polynomial at different orders, we clearly vary the degree of approximation.

An exact solution for the displacement $u(x)$ is then approximated by various degree polynomials of the general form

$$u(x) = \alpha_1 + \alpha_2 x + \alpha_3 x^2 + \cdots + \alpha_{n+1} x^n \tag{9}$$

The greater the number of terms included in the approximation, the more closely the exact solution is represented. In equation (9), the coefficients of the polynomial, the α's, are known as generalized coordinates or generalized displacement amplitudes. The number of terms retained in the polynomial determines the shape of the displacement model, whereas the magnitudes of the generalized coordinates govern the amplitude. These amplitudes are called generalized because they are not necessarily identified with the physical displacements of the element on a one-to-one basis; rather, they are linear combinations of some of the nodal displacements and perhaps of some of the derivatives of displacements at the nodes as well. The generalized coordinates represent the minimum number of parameters necessary to specify the polynomial amplitude.

Equation (9) can be expressed in vector form as

$$u(x) = \phi^T \alpha \tag{10}$$

where

$$\phi = \{1 x x^2 x^3 \cdots x^n\}^T,$$

and

$$\alpha = \{\alpha_1 \alpha_2 \alpha_3 \cdots \alpha_{n+1}\}^T.$$

The degrees of freedom can thus be related to the generalized coordinate system by employing the displacement model. We can evaluate the generalized displacements at the nodes by substituting the nodal coordinates into the model. For example, using a model of the form given by equation (10), we may write, for a single node point

$$u(x) = \phi\alpha \tag{11}$$

where u is the vector of degrees of freedom for a single node; or, for the entire element,

$$x = \begin{Bmatrix} u(node1) \\ u(node2) \\ \cdots \\ u(nodeN_n) \end{Bmatrix} = \begin{bmatrix} \phi(node1) \\ \phi(node2) \\ \cdots \\ \phi(nodeN_n) \end{bmatrix} \alpha = A\alpha \tag{12}$$

where N_n is the total number of nodes for the element being considered, x is the vector of nodal degrees of freedom, and the notation in parentheses indicates that the dependent variables are assigned their values at the particular node. We may invert equation (12) to get

$$\alpha = A^{-1}x \tag{13}$$

where A^{-1} is a displacement transformation matrix. Note that A is a square matrix, hence, the total number of generalized coordinates equals the total number of joint and internal degrees of freedom. Equation (13) may then be used to eliminate the generalized coordinates to obtain

$$u = \phi A^{-1}x = Nx \tag{14}$$

which expresses the displacements u at any point within the element in terms of the displacements of the nodes x.

Since the derivations of the element matrices are performed in the α coordinate system, we further develop the necessary relationships in terms of the generalized α coordinates rather than the physical x coordinates.

The strains are expressed in terms of some combination of the derivatives of the displacements u. Since the generalized coordinates α are not functions of the spatial coordinates, these derivatives must be performed in terms of the matrix ϕ. If ε is the vector of the relevant strain components at an arbitrary point within the finite element, we use the strain-displacement equations and the displacement model to write

$$\varepsilon = B_\alpha \alpha \tag{15}$$

It is important to note that for geometrically nonlinear problems ε and B_α are functions of the independent space coordinates as well as functions of the generalized coordinates. Decomposing these quantities into linear and nonlinear parts, we have

$$\varepsilon = \varepsilon_l + \varepsilon_{nl} \tag{16}$$

and therefore,

$$B_\alpha = B_{\alpha_l} + B_{\alpha_{nl}} \tag{17}$$

If σ is the vector of stresses corresponding to the strains ε, we may use an appropriate matrix form of the stress strain equations and equation (15) to write the element stresses as

$$\sigma = C B_\alpha \alpha \tag{18}$$

where C is the matrix of material constants given by equation (3).

Variational Formulation of Element Matrices

As discussed above, the method used here for calculating the element matrices and load vectors is the application of Hamilton's principle. Therefore, we develop the Lagrangian given in equation (7) in terms of the α generalized coordinates and apply equation (8) to obtain the element equations in terms of the generalized coordinates and shape functions.

In order to formulate the Lagrangian in terms of the generalized coordinates, we insert equations (11), (15) and (18) into equation (7) to obtain

$$\begin{gathered}
L = \frac{1}{2} \int_V \alpha^T B_\alpha^T C B_\alpha \alpha dV \\
-\frac{1}{2} \int_V \rho \left(\dot{\alpha}^T \phi^T \phi \dot{\alpha} + \dot{\alpha}^T B_2 \alpha - \alpha^T B_2 \dot{\alpha} - \alpha^T B_1 \alpha \right) dV \\
-\frac{1}{2} \int_V \rho \left(V_{RB}^T \phi \dot{\alpha} + \dot{\alpha}^T \phi^T V_{RB} + V_{RB}^T \tilde{\omega} \phi \alpha - \alpha^T \phi^T \tilde{\omega} V_{RB} \right) dV \\
- \int_V \alpha^T \phi^T \bar{X} dV - \int_S \alpha^T \phi^T \hat{T} dS
\end{gathered} \tag{19}$$

where

$$B_1 = \phi^T \tilde{\omega} \tilde{\omega} \phi \tag{20}$$

and

$$B_2 = \phi^T \tilde{\omega} \phi \tag{21}$$

Applying the variational principle given by equation (8), we obtain

$$\begin{gathered}
\int_{t_1}^{t_2} \left(\delta\alpha^T \int_V (B_\alpha^T C B_\alpha + B_\sigma) dV \, \alpha - \delta\dot{\alpha}^T \int_V \rho \phi^T \phi dV \, \dot{\alpha} \right) dt \\
+ \int_{t_1}^{t_2} \left(-\delta\dot{\alpha}^T \int_V \rho B_2 dV \, \alpha + \delta\alpha^T \int_V \rho B_2 dV \, \dot{\alpha} \right) dt \\
+ \int_{t_1}^{t_2} \left(\delta\alpha^T \int_V \rho B_1 dV \, \alpha \right) dt \\
- \int_{t_1}^{t_2} \left(\delta\dot{\alpha}^T \int_V \rho \phi^T V_{RB} dV - \delta\alpha^T \int_V \rho \phi^T \tilde{\omega} V_{RB} dV \right) dt \\
- \int_{t_1}^{t_2} \left(\delta\alpha^T \int_V \phi^T \bar{X} dV + \delta\alpha^T \int_S \phi^T \hat{T} dS \right) dt = 0
\end{gathered} \tag{22}$$

where the matrix B_σ arises from the variation of the nonlinear part of the matrix B_α which is a function of the generalized coordinates α. The i^{th} row of the matrix B_σ is given by

$$B_{\sigma_i} = \alpha^T B^T_{\alpha_l} C \frac{\partial B_{\alpha nl_i}}{\partial \alpha_i} \tag{23}$$

for $i = 1, 2, \cdots, 12$. Integration of the terms in equation(22) by parts with respect to time gives

$$\begin{aligned} &\int_{t_1}^{t_2} \delta\alpha^T \left(\int_V \rho\phi^T \phi dV \ddot{\alpha} + \int_V 2\rho B_2 dV \dot{\alpha} \right) dt \\ &+ \int_{t_1}^{t_2} \delta\alpha^T \left(\int_V (B^T_\alpha C B_\alpha + B_\sigma + \rho \dot{B}_2 + \rho B_1) dV \alpha \right) dt \\ &+ \int_{t_1}^{t_2} \delta\alpha^T \left(\int_V (\rho\phi^T \dot{V}_{RB} + \rho\phi^T \tilde{\omega} V_{RB}) dV \right) dt \\ &- \int_{t_1}^{t_2} \delta\alpha^T \left(\int_V \phi^T \tilde{X} dV - \int_S \phi^T \tilde{T} dS \right) dt = 0 \end{aligned} \tag{24}$$

Since the variations of the generalized displacements, $\delta\alpha$, are arbitrary, the sum of the expressions in parentheses must vanish. Therefore we obtain the equations of motion for the element as

$$M^\alpha \ddot{\alpha} + C^\alpha \dot{\alpha} + K^\alpha \alpha = F^\alpha \tag{25}$$

where M^α is the consistent mass matrix defined by

$$M^\alpha = \int_V \rho\phi^T \phi dV \tag{26}$$

C^α is the damping matrix due to frame motion as given by

$$C^\alpha = 2 \int_V \rho B_2 dV \tag{27}$$

and K^α is the element stiffness matrix in terms of α coordinates as given by

$$K^\alpha = \int_V (B^T_\alpha C B_\alpha + B_\sigma) dV + \int_V \rho(B_1 + \dot{B}_2) dV \tag{28}$$

The first integral in the above equation is the stiffness due to strain energy and will be referred to as K^α_u. The second integral is the stiffness due to frame motion to be referred to as K^α_m. Recall from equation (17) that B_α is comprised of linear and nonlinear parts. Then the stiffness due to strain energy, K^α_u, may be decomposed into linear and nonlinear parts to give

$$K^\alpha_{u_l} = \int_V B^T_{\alpha_l} C B_{\alpha_l} dV \tag{29}$$

$$K^a_{\alpha_{nl}} = \int_V B^T_{\alpha_l} C B_{\alpha_{nl}} dV + \int_V B^T_{\alpha_{nl}} C B_{\alpha_l} dV$$

$$+ \int_V B_{\alpha_{nl}}{}^T C B_{\alpha_{nl}} dV + \int_V B_\sigma dV \tag{30}$$

The stiffness matrix resulting from the first three terms in equation (30) is known as the *large displacement* matrix. The stiffness matrix arising from B_σ is dependent on the stress level and is known as the *initial stress* matrix, Ref. (1).

Finally, the load vector, F^a, is defined by

$$F^a = \int_V \phi^T \tilde{X} dV + \int_S \phi^T \hat{T} dS$$

$$- \int_V (\rho \phi^T \dot{V}_{RB} + \rho \phi^T \tilde{\omega} V_{RB}) dV \tag{31}$$

Displacement Models for a Beam Element

Having formulated the expressions for the element matrices and loads in terms of the general shape functions, the next step is to choose the displacement models that will approximate the solution for the problem at hand. A flexbeam is a cantilever beam under tension. For a beam element, axial, lateral and torsional deformations are of interest. To approximate the deformation field in a flexbeam, the polynomial shape function of equation (9) is truncated to obtain the approximate representation of the true axial, bending and torsional displacements.

Linear and cubic shape functions are used to express the displacements of the beam in terms of the α generalized coordinates. For axial deformations due to axial forces, the following linear shape function is employed:

$$u_a = \alpha_1 + \alpha_2 x \tag{32}$$

This shape function satisfies rigid body motion, constant strain states conditions and the compatibility conditions.

For deformations due to bending about the y and z axes, the following cubic shape functions are used:

$$v_b = \alpha_3 + \alpha_4 x + \alpha_5 x^2 + \alpha_6 x^3 \tag{33}$$

$$w_b = \alpha_7 + \alpha_8 x + \alpha_9 x^2 + \alpha_{10} x^3 \tag{34}$$

where v_b is the displacement due to bending about the z axis and w_b is the bending displacement about the y axis. These shape functions are also compatible and complete. The compatibility conditions at the ends of the element are met on displacements as well as the slopes.

For deformations due to torsion, the following linear shape function is used

$$\theta = \alpha_{11} + \alpha_{12}x \tag{35}$$

With the above shape functions, and the general expressions for the element matrices given by equations (26) to (28) and (31), the element matrices can be easily obtained via a symbolic manipulation program such as SMP.

Having the element matrices constructed, the assembly and the solution of the equations of motion are a routine matter.

Simplification of Equations of Motion

Element matrices given by equations (26) to (30) can be further simplified for the flexbeam application. We start with equation (28), the second integral, which represents the softening effect of the frame rotation on the element stiffness matrix. This term is usually small compared to the first integral if the rotor angular velocity is not close to one of the structural natural frequencies. For flexbeam design, it is small if the rotor angular velocity is not close to the first lead-lag frequency of the nonrotating flexbeam. Neglecting this term will make the model stiffer than the real flexbeam, and hence will make the prediction of stresses more conservative.

The second set of terms which can be neglected in the flexbeam design is the first three integrals in equation (30). These integrals represent the effect of large rotations on the equilibrium equations of the flexbeam. For angles smaller than 15° this term is much smaller than the structural stiffness $K_{u_l}^{a}$ and the centrifugal stiffness B_{σ}. In a flexbeam design this term can also be neglected, resulting in more a conservative design.

Finally, the calculation of the centrifugal stiffness matrix, B_{σ}, can be simplified by noting that most of the CF force is caused by the weight of the blade and the pitchcase. Since the weight of the flexbeam is negligible compared to the weight of the blade and the pitchcase, we can assume that the CF force remains constant throughout the length of the flexbeam. The magnitude of this force can then be calculated separately and used as input to the program. This will eliminate the extra calculations otherwise needed to compute this force and hence results in saving computational time.

Equivalent Flexbeam Composite Properties

The composite properties of the flexbeam in the principal material directions can be obtained using the Halpin-Tsai equations of Ref.(2) as follows:

$$E_1 = \varsigma E_f + (1-\varsigma)E_m \tag{36}$$

$$E_2 = \frac{(1+2\varsigma)}{(1-\varsigma)}E_m \tag{37}$$

$$G_{12} = \frac{G_m[G_f + G_m + (G_f - G_m)\varsigma]}{G_f + G_m - (G_f - G_m)\varsigma} \tag{38}$$

$$\nu_{12} = \varsigma\nu_f + \nu_m(1-\varsigma) \tag{39}$$

where

E_1 = composite Young's modulus in fiber direction

E_2 = composite Young's modulus pependicular to the fiber direction

G_{12} = composite shear modulus

ν_{12} = composite Poisson's ratio

E_f , E_m = Young's moduli of fiber and matrix, respectively

G_f , G_m = shear moduli of fiber and matrix, respectively

ν_f , ν_m = Poissons's ratio of fiber and matrix, respectively

ς = fiber volume fraction

Rigid Constraint Element

For bearingless rotor flexbeam design, a pitchcase model is required. One might attempt to use a stiff beam element for the pitchcase model; however, a stiff beam will result in an ill-conditioned stiffness matrix. Since a kinematic constraint involves a relationship between degrees of freedom, the correct approach is that of employing a multipoint constraint.

For large angular motion constraints between the degrees of freedom of an element, ideally a nonlinear constraint relationship is required. However, in flexbeam design, the angular rotations of flexbeam and pitchcase are small, and hence a linear constraint is sufficient.

To derive the rigid constraint element which will be used to represent the pitchcase, consider two node points A and B, which are connected by a rigid link. The rotational degrees of freedom of nodes A and B are θ_A and θ_B, respectively. Similarly, the displacement degrees of freedom are u_A and u_B. Assuming a rigid member between the two nodes, the displacements and rotations of node B can then be expressed in terms of the displacements and rotations of node A as

$$u_B = u_A + \theta_A \times r^{BA} \tag{40}$$

and

$$\theta_A = \theta_B \tag{41}$$

where r^{BA} is a vector from node A to node B the magnitude of which is the length of the rigid member. Writing the vector cross product in matrix form, we obtain

$$\begin{bmatrix} u_1 \\ u_2 \\ u_3 \\ \theta_1 \\ \theta_2 \\ \theta_3 \end{bmatrix}_B = \begin{bmatrix} 1 & 0 & 0 & 0 & L_z & L_y \\ 0 & 1 & 0 & -L_z & 0 & L_x \\ 0 & 0 & 1 & L_y & -L_x & 0 \\ 0 & 0 & 0 & 1 & 0 & 0 \\ 0 & 0 & 0 & 0 & 1 & 0 \\ 0 & 0 & 0 & 0 & 0 & 1 \end{bmatrix} \begin{bmatrix} u_1 \\ u_2 \\ u_3 \\ \theta_1 \\ \theta_2 \\ \theta_3 \end{bmatrix}_A \tag{42}$$

This, then, is the constraint equation relating the degrees of freedom of the outboard end of the flexbeam to the degrees of freedom of the snubber/damper element.

HUBFLEX Mathematical Model

Using the mathematical formulations presented earlier, a finite element computer program called HUBFLEX was developed. This computer program is tailored specifically for the analysis of flexbeams with rectangular cross sections.

HUBFLEX is a finite element analysis model for a cantilevered beam under centrifugal force. The model permits rapid calculation of spanwise load and stress distributions for a specific geometry flexbeam with specified material properties, centrifugal force, and modal deflections. The analysis has been validated against two- and three-dimensional NASTRAN models of equivalent beams, and has shown excellent correlation. Spanwise stress distributions can be calculated with HUBFLEX in less than 10 seconds CPU time on a Digital Equipment Corporation VAX 11/785. Substantial economies in the study of new designs are thus realized.

Analytically, HUBFLEX treats the flexbeam as fixed at the inboard end of the rotor mast. At the outboard end, radial tension, bending moments, shears, and torque are applied. The beam is a statically indeterminate structure in that the elastic/cross sectional properties influence the load distribution. When any section of the beam is modified, a complete iteration is required to determine the new load and stress distribution along the beam.

The HUBFLEX model utilizes the stiffness matrix method presented earlier to solve for flexbeam load distributions. Tension beam effects are modeled using centrifugal stiffening terms in each element, B_σ in equation (28). The effect of the pitchcase redundant load path is modeled by a rigid element, equation (42), attached to the flexbeam at the outboard end and attached to the flexbeam at the inboard end by a snubber/damper of given stiffnesses in the flapwise and chordwise directions. In the chordwise direction, the spring stiffness corresponds to the stiffness of the damper pads. In flap, the spring rate is equal to the stiffness of the snubber corrected for the pitchcase flapwise flexibility. The pitchcase is rigidly attached to the flexbeam at its outboard end. Inputs to the program include section element definition, flexbeam geometry, material properties, applied loads, and the desired deflections/rotations at the blade attachment point. The input forces and moments represent those applied to the flexbeam by the blade spanwise moment and shear distributions. The shear to moment ratios at the blade attachment have a powerful influence on the flexbeam deflected shape and are determined separately in an iterative procedure. They are continually updated as the configuration evolves. The spanwise load and stress distribution results include the effect of combined loadings associated with the relative phasing of the flap, chord, and torsion motions. As with the shear to moment ratios, the phasing has a powerful influence on the final results especially for the critical shear loads due to combined normal bending and feathering. The phasing relationships were defined using an aeroelastic analysis (DART) and were verified by the HARP flight test results.

HUBFLEX/ADS Computer Program

The HUBFLEX finite element model was initially used to study flexbeam geometries that were established by engineering judgment. Because of the indeterminate nature of the problem and the millions of possible geometry variations which could be developed, engineering judgment was deemed inadequate to quickly define an optimum (lowest stresses) configuration. In addition, an optimum configuration for one specific flight condition, such as cruise flight, was significantly different from a configuration which would produce minimum stresses in a maneuver condition. To address this problem an optimization routine called ADS (Automated Design Synthesis), Ref. (3), was added to the HUBFLEX analysis program. The routine permitted holding certain parameters of the design fixed or within specified bounds while freeing other variables to achieve a minimum stress distribution along the length of the beam. A further enhancement was added by providing for the weighted optimization of several flight conditions simultaneously. A block diagram of the optimization procedure is provided in Figure (2).

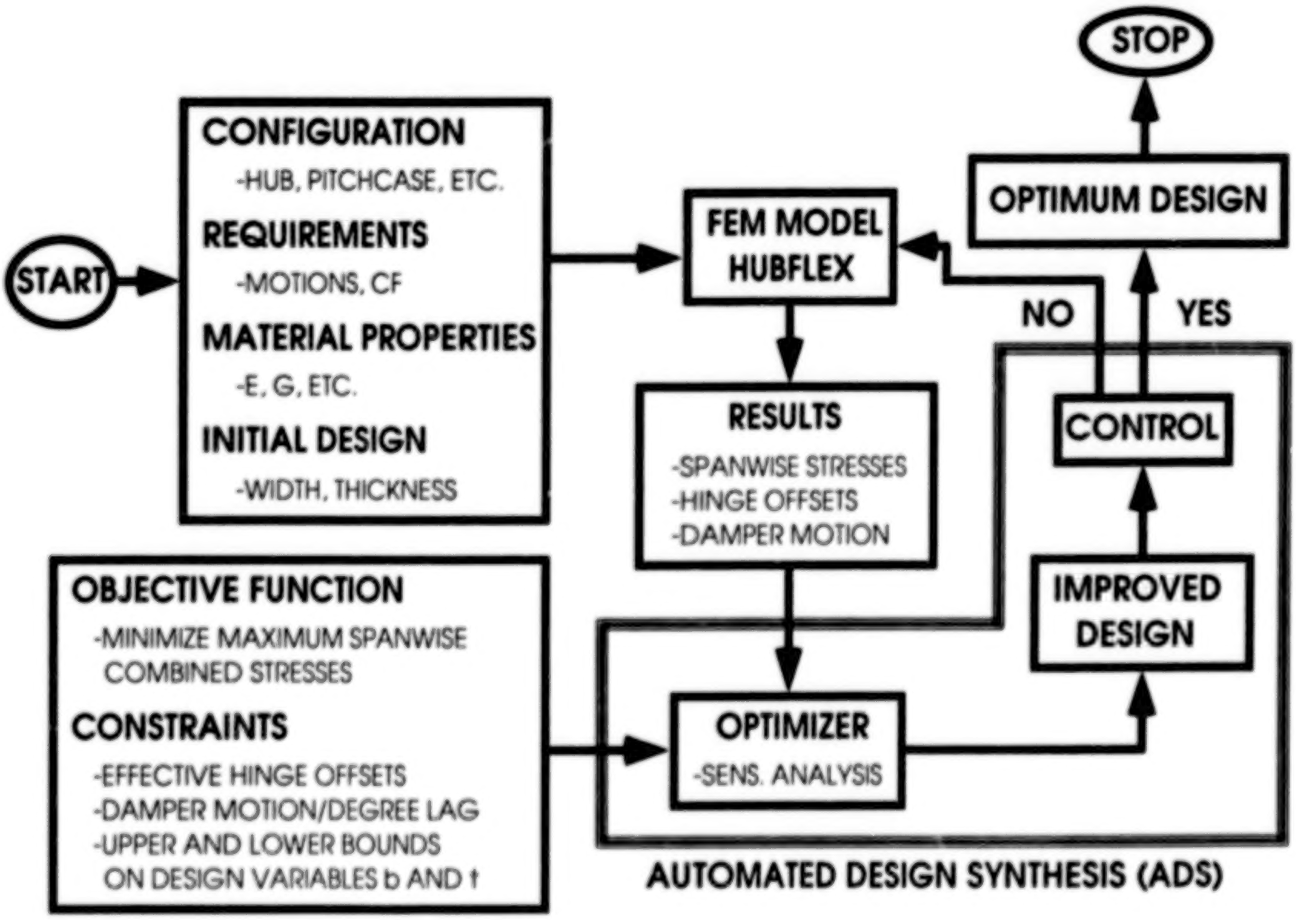

Figure (2)

In practice, the optimization program was used to minimize the maximum stresses (normal and shear) caused by maximum maneuver and endurance motions. Design variables were the dimensions of the beam element, with upper and lower bounds established for manufacturing feasibility. The required damper motion per degree lag motion was selected as a constraint in the optimization process.

The results of this work led to the highly tailored design configurations established for three different flexbeams for three different helicopters. These are, ACH (Advanced Composite Hub), advanced HARP and most recently, the MDX* flexbeam. The advanced HARP flexbeam was designed in less than a week (the old HARP flexbeam took more than 6 months), while it took only half a day to design a flexbeam for the MDX main rotor. The reduction of design time from one week for advanced HARP to half a day for the MDX flexbeam was purely due to postprocessing of the optimization results. The postprocessing of the advanced HARP flexbeam results was carried out by hand and relied upon engineering judgment, while the postproccessing of the MDX flexbeam optimization results was done by computer and hence human factors and consequently excessive time was removed completely from the optimization process.

In general, it was found that the endurance level flight condition dictated the geometry of the outer portion of the beam where high cycle shear stresses were most critical. The low-cycle high g maneuver condition dictated the beam geometry of the inboard end due to high normal stresses.

Among the three optimized flexbeams, the advanced HARP is the only one which has been fabricated and successfully tested in fatigue as well as in the Duits Nederlandse Windtunnel (DNW).

Optimization Results

The finite element optimization program HUBFLEX/ ADS was used to optimize the advanced HARP flexbeam. The composite material selected for the advanced beam was S2-Glass fiber and the matrix was Epoxy. The maximum combined normal and/or shear stresses for the one hour flight condition as well as endurance were selected as the objective function. To achieve at least 3% critical damping, a damper motion of 0.1 inch per degree lag was required. Therefore a lower constraint was put on the damper motion. In addition to this active constraint, to insure the continuity of fibers, a set of constraints was put on the beam cross sectional area variation over the length of the beam such that the area was required to either decrease or remain constant, but was not allowed to increase from inboard to outboard. In addition to these constraints, lower and upper constraints were imposed on the dimensions of the beam element, based on manufacturing requirements.

---

* McDonnell Douglas (X)

The HUBFLEX/ADS computer program was used to optimize the advanced beam based on the above optimization statement. A comparison between the initial design and the optimum design for the advanced beam is shown in Table(1). As can be seen in this table, it took more than 6 months to design the old flexbeam with unacceptable stresses. However with the HUBFLEX/ADS program, an acceptable configuration was obtained in a week, with acceptable stresses. The damper motion per degree lag, the hinge offsets in flap and lag directions, and the corresponding first frequencies for both the old and the advanced beams are acceptable as shown in the table. The alternating angles for which the old and the advanced beams were designed are also shown in the table.

A three-dimensional view of the advanced beam is shown in Figure (3). As seen in the figure, the variations of width and thickness are such that the geometric area of the beam section is always decreasing or is constant. This particular requirement insures the continuity of the fibers.

Table(1)

PARAMETER	"OLD" HARP	NEW HARP
Time to design configuration	6 mo.	1 wk.
Normalized max combined normal stresses	1.70	1.04
Normalized max combined shear stresses	0.96	1.03
Damper motion per deg. lag	0.18	0.16
$\frac{e_F}{R} \times 100$	5.3	4.2
$\frac{e_L}{R} \times 100$	24.8	15.6
$\frac{\omega_F}{\Omega}$	1.06	1.04
$\frac{\omega_L}{\Omega}$	0.61	0.50
β	6.8	6.8
ζ	2.0	2.0
θ	11.5	11.5

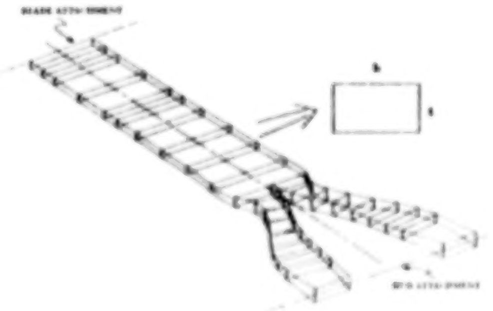

Figure (3)

HUBFLEX/NASTRAN Comparison

In the development stage, the HUBFLEX program was validated against 2-dimensional and 3-dimensional equivalent beam NASTRAN models and showed excellent correlation.

For the advanced HARP program, an additional level of verification was obtained by creating a 3-dimensional nonlinear anisotropic solid element NASTRAN model of the detailed flexbeam structure. The model was constructed using 3048 8-noded (octahedron) and 8 6-noded (hexahedron) solid elements incorporating over 12,000 degrees of freedom, Figure (4). The snubber damper centering bearing was rigidly attached to the flexbeam using constraint equations. The chordwise and flapwise damper stiffnesses were represented by elastic springs and attached to a rigid element pitchcase. The inboard end of the flexbeam was rigidly constrained. The outboard blade attachment location was multipoint constrained to allow loads and the pitchcase attachment to be applied at a single centerline grid point.

The detailed nonlinear model was run for flap, lead-lag and feathering one hour flight motions using MSC/NASTRAN's geometric nonlinear solution 64 (whose algorithm is an extension of the differential stiffness approach, Ref (4)). The CF loading was applied in the linear elastic step and then combined with the corresponding flap, lead-lag and feathering loading in the following differential stiffness step. The combined loading was then taken through one additional nonlinear interation for an improved solution. Computation time for each run amounted to 8 hours of CPU time running on a VAX 11/785.

The primary loading condition of interest was lead-lag where the HUBFLEX program approximates the chordwise stiffness of the split leg/shear web section of the flexbeam by an equivalent 'I' beam moment of inertia.

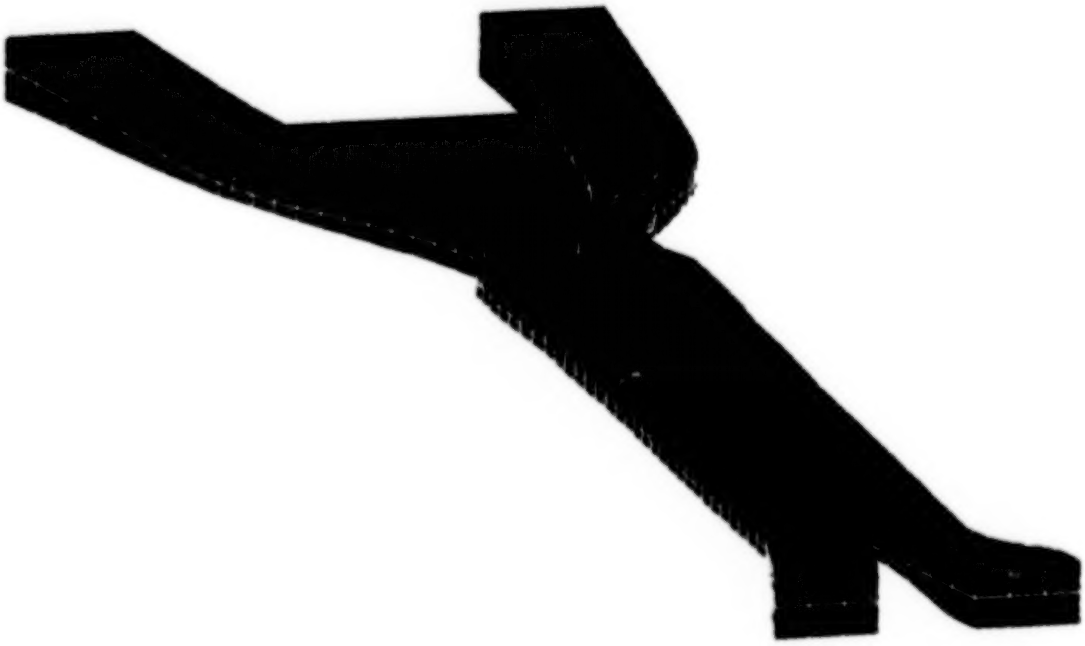

Figure (4)

In order to compare with the HUBFLEX output of spanwise displacements, a set of grid points on the centerline of the flexbeam was selected to represent the overall deformation. For the comparison of spanwise normal stress distributions, element stress peak values obtained within the corresponding cross section location were used.

Correlation of chordwise loading indicated that the HUBFLEX chordwise stiffness approximation produced a stiffer beam resulting in conservative peak stress values that were approximately 10 percent higher than those of the detailed solid element model. A comparison of the chordwise displacement and spanwise stress distribution is provided in Figures (5) and (6).

For the trivial flapwise and feathering loading cases, correlation was excellent as expected. Peak stress values were typically 3 to 5 percent higher for the HUBFLEX model. Figures (7) and (8) demonstrate this correlation for the flapwise loading case.

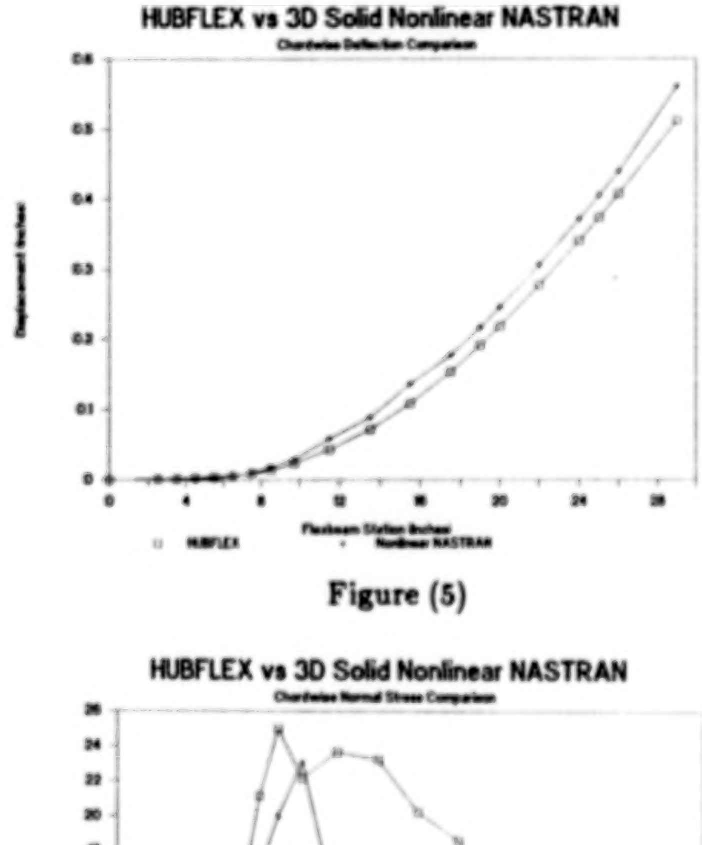

Figure (5)

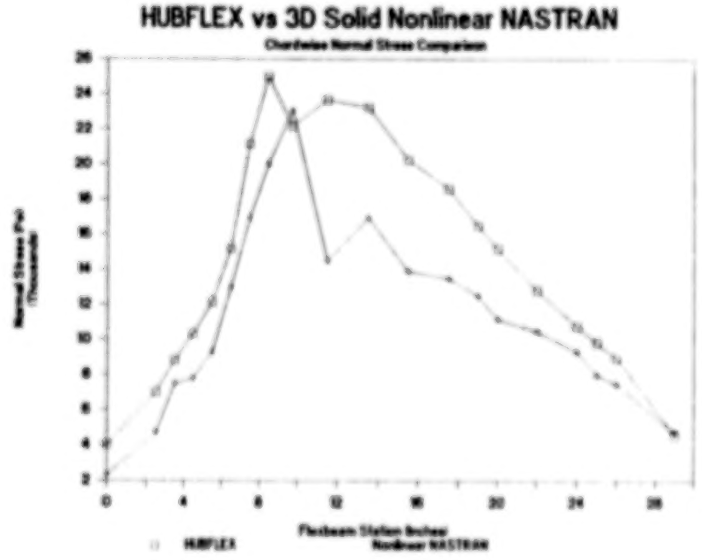

Figure (6)

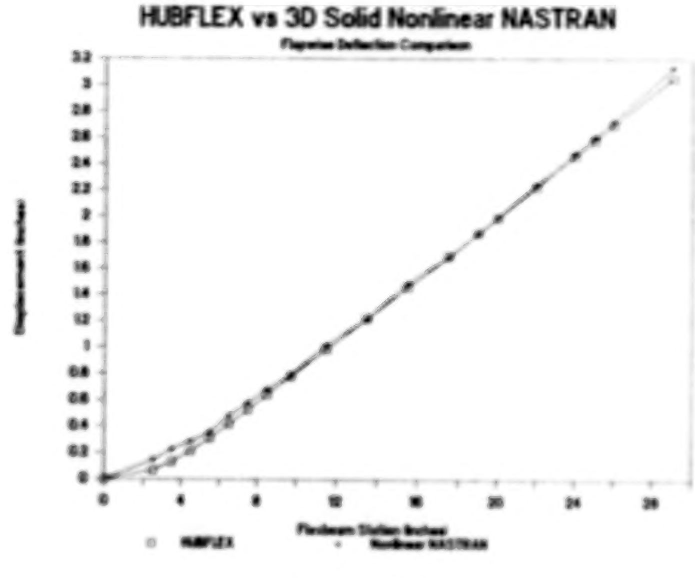

Figure (7)

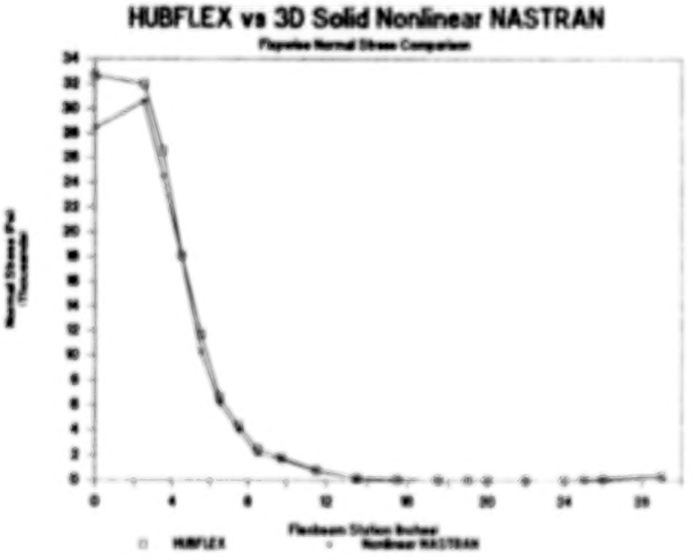

Figure (8)

Conclusions

1. Pitchcase and snubber damper representations are required in the flexbeam model for proper sizing resulting from dynamic requirements.
2. Optimization is necessary for flexbeam design. It reduces the design iteration time and results in an improved design.
3. Inclusion of multiple flight conditions and their corresponding fatigue allowables is necessary for the optimization procedure.
4. A simplified beam model is adequate for flexbeam sizing. The simplified model gives excellent accuracy (compared to a detailed 3D nonlinear NASTRAN analysis) with a significant reduction in computational time.
5. HUBFLEX's rapid computation capability enables design parameters to be easily modified and implemented.

References

1. Zienkiewicz, O.C., "*The Finite Element Method*", 3rd Edition, McGraw Hill Book Co., New York, 1982.
2. Jones, R.M., "*Mechanics of Composite Materials*", McGraw Hill Book Co., New York, 1973.
3. Vanderplaats, G.N., "*ADS - A Fortran Program for Automated Design Synthesis*", Version 1.00 , NASA Contract Report 172460, Langley Research Center, Hampton, Virginia, 1984.
4. MSC/NASTRAN Application Manual, Macneal- Schwendler Corporation, March 1981.

SESSION 3: ARTIFICAL INTELLIGENCE

Chairmen: K. H. Abbott and P. Hajela

BLANK PAGE

New Directions for Artificial Intelligence (AI) Methods in Optimum Design

Prabhat Hajela
Aerospace Engineering, Mechanics, & Engineering Science
University of Florida, Gainesville, Florida

Abstract

Developments and applications of AI methods in the design of structural systems is reviewed. Principal shortcomings in the current approach are emphasized, and the need for some degree of formalism in the development environment for such design tools is underscored. Emphasis is placed on efforts to integrate algorithmic computations in expert systems.

Knowledge-Based Systems for Structural Design

Generating an optimum structure is a multistage process, generally initiated with the definition of a structural model to transmit applied loads to the support points. This definition is not necessarily unique and falls in the category of topology assignment problems that are discussed in later sections. Once the topology is known, a finite element analysis is typically invoked, requiring a suitable discretization of the model. This discretized model is used for repetitive analysis in optimum design, a process that is computationally demanding, and very often necessitates the generation of a discrete design model with fewer degrees of freedom. Creation of a design model that is distinct from an analysis model is also often necessary for improving efficiency of optimization algorithms. In addition to creating efficient analysis and design models, the choice of suitable optimization algorithms and algorithm parameters for the problem under consideration, selection of design variables and constraints for the problem, and monitoring as well as enhancing the efficiency of the algorithm, are important steps, requiring insight that is available to few experts in the field.

The need to disseminate such information to a larger user community prompted the development of a prototype expert system OPSYN, configured as an online consultant to provide interactive assistance in the task of finite element modeling, optimum design modeling, and in the selection of optimization strategies for structural design. In addition to a knowledge base and an inference engine with an explanation facility, the system is also equipped with a knowledge-acquisition facility, an input-output facility that includes a knowledge-base editor and a graphical display capability.

The rules for finite element modeling include information pertaining to location of nodes, node numbering, mesh generation, mesh refinement, element selection, and guidelines to eliminate element distortion. The rules for optimum design modeling include concepts pertinent to selection of design variables, constraints, approximation techniques, and strategies for sensitivity analysis. A third set of rules to enhance optimization performance primarily assists the user in selecting optimization strategies for the design problem. This includes rules for both unconstrained and constrained optimization problems, and rules for algorithm switching in the event that the initial selection is unsatisfactory. Additional details about this implementation are available in References [1-3]. A schematic illustrating the framework of this implementation is shown in Figure 1.

Knowledge acquisition and representation are important issues in expert system development and are addressed in a novel manner in the OPSYN system. Misrepresentation of information is a frequent dilemma, particularly when text alone is used for communication. This limitation was overcome by adding a graphical display of both rules and actions in addition to the textual format. A CAD-based knowledge acquisition system embracing the protocol analysis approach [4], was also developed for this system. Automated knowledge acquisition and analysis to generate new rules are key features of this system.

OPSYN is in the general category of consultative type systems for structural analysis and design modeling (other notable systems include SACON [5], ESSDAN [6] and ADEPT [7]). Such systems facilitate in the dissemination of large amounts of documennted and experiential knowledge in this domain to a larger user community. The goals or objectives of the work are well understood, and hence a backward reasoning strategy is naturally applicable. The suitability of such an approach in design, which is essentially a generative process, is questionable. This issue is a principal focus of the present work. The design problem under consideration may be stated as follows: given a design domain, a set of distributed or applied loads, and a set of support points, generate a structural configuration that is optimal with respect to the stated objectives and design constraints.

The traditional design approach starts with a chosen initial configuration and successively refines this design to obtain an optimum with reference to a set of prescribed constraints. Despite the success in using this approach, it has a limitation in that the final outcome is strongly linked to the initial model abstraction process. Human designers are quite adroit at finding a promising configuration and developing it into a feasible design. The present paper deals with the development and evaluation of strategies to facilitate the automated search for alternative preliminary design configurations, with the goal of spanning the space of conceptually distinct plausible designs.

The preliminary structural layout problem has received some attention but with no emphasis on optimality of the final design. References [8] and [9] report initial efforts in the development of expert systems for preliminary form design of structural machine parts. The general approach adopted in this study was one in which the structure was decomposed into primitive components. Previously catalogued case studies were used to build the structural form, starting at the primitive level and incrementally adding degrees of complexity. The study also emphasized the need for algorithmic processing in such activity. Nevill and his co-workers [10,11] and Brown [12] also recognize the importance of the preliminary synthesis problem. The research activity in this group has resulted in the development of an automated preliminary design system MOSAIC, currently implemented for 2-D mechanical and structural systems. In this system, point loads are stabilized by connecting them to predefined supports, using structural elements that satisfy other established goals. The thrust of this work is in generating a sequence of promising initial designs, but with no focus on optimality.

The developments described above are drawn from the discipline of structural design. Numerous efforts along similar lines are reported in the chemical, electrical and mechanical engineering domains. These efforts have been somewhat disjointed in form, each devoting significant development effort in building a framework that was considered by its developer as novel and necessary for the application at hand. Other than the fact that such systems have common components in the form of a knowledge base and an inference facility, there is very little adherence to a set of common development guidelines. This unproductive approach results, in most instances, in marginal contributions towards advancing design practice in that domain and is largely responsible for the growing skepticism about the expert system field in general.

There exists no general agreement on what is regarded as a good model for engineering design practice. In fact, definitions of what design entails are varied, with every practitioner having a different philosophical viewpoint. Recent efforts have focussed at attempting to establish some formalism in knowledge-based design [13,14]. Not surprisingly, the principal concepts of such proposals have been part of the optimum design literature that is traditionally not associated with heuristic methods. Subsequent sections of this paper attempt to develop a framework that is based on one such model of design, largely in the context of optimum structural synthesis.

A General Framework for Automated Structural Design

Tong [13] presents an elaborate description of the principal components of knowledge-based problem solving systems. The framework for automated structural design systems discussed in this section incorporates some of these ideas, and extends them to the structural design domain. At the very outset, it is important to recognize the levels at which the automated design process can be organized. Tong classifies these as the knowledge level, the function level, and the program level. The present paper describes the attributes of each of these levels of organization, using the task of optimum structural synthesis (both conceptual and refined) as the design domain. A typical relational arrangement of these levels of organization is shown in Figure 2.

Knowledge Level

This level constitutes a rigorous and detailed description of the design domain. Applicable theories for analysis in the domain should be accessible at this level, as should criterion or rules that define acceptable solutions. There is scope for a significant amount of organization at this level. The types of design applications envisaged for such systems would very seldom generate designs that bear no resemblance to their predecessors. It is therefore possible to classify previous feasible solutions based on salient characteristics and the design constraints to which they conform. This step provides a general nomenclature and classification of types of design constraints, of problems that can be solved, and of possible solution strategies.

As stated in earlier discussions, optimum design of structural systems starts with the process of proposing a structural configuration to transmit a set of prescribed loads to given supports. Once an initial model is obtained, it can be refined to yield an optimum. To limit the scope of the present paper, this discussion will be confined to the problem of optimal generation of structural topology. The domains that must be considered in this exercise include geometric modeling, structural analysis, and optimization methodology. The problem is further simplified by restricting load deflection analysis to the linear region. The tools to analyze the structure or parts of the structure must be accessible at the knowledge level. In the implementation under study, a finite element analysis program EAL [15] and several independent analysis modules provide this capability. Also available at this stage are simplistic tools to implement and analyze geometrical layouts of structures for feasibility. Finally, access to gradient and non-gradient based optimization methods is made available at this level [16,17].

In creating a taxonomy of design requirements for the problem under consideration, it is also important to identify any salient characteristics that result from an imposition of such requirements. Structural design requirements may be classified on the basis of strength, stiffness, elastic stability, degree of redundancy, types of support conditions, dynamic behavior, and a requirement of least weight or least complexity in manufacturability. Clearly, each of these requirements has an influence on the design that distinguishes it from designs dominated by other requirements. As an example, a structure that is governed by structural stability requirements will have elements that can withstand compression (not cables or chains) and further, such elements will typically have aspect ratio and stiffness properties that would reduce elastic instabilities. A structure governed by bending stiffness requirements would have large bending moments of inertia in preferred directions. It is possible that two or more requirements result in similar characteristics, and these must be accounted for in the taxonomy. In as far as possible, however, it is advantageous to distinguish one requirement with one observed characteristic. Failing this, the classification must clearly indicate the relative contribution of a requirement to a salient characteristic.

The class of problems that can be solved is determined by the scope of information in the knowledge level. To further augment the usefulness of a taxonomy based on design requirements, a definition of possible solutions (obtained in previous work) that may be in a primitive or refined form and satisfy the requirements, is proposed in the present work. The stabilization of point loads to supports may be handled by a truss structure. Axial force elements or their combinations resulting in simple truss units are provided at the knowledge level to use for the desired task. These primitive forms may have to be varied to meet current design specifications, an example of which is provided by a manufacturability requirement limiting the length of any one member by lower and upper bounds. These refinements would be introduced at the function level of the design process. In a similar manner, design requirements that require the transmittal of distributed loads to supports, or point and/or distributed loads to a single support, must do so by a beam element or a combination of beam elements. Primitive seed designs to implement this are available at the knowledge level.

There are two additional points about domain knowledge at this level that are very essential to the design process. First, knowledge must be available to judge a proposed solution as an acceptable design. This essentially involves both structural and topological analysis to assess feasibility. The other requirement, and one that is not so easy to satisfy, is the evaluation of the domain theory to see if it contains sufficient knowledge to both generate and recognize a solution to the problem. This has been termed as "epistemological adequacy" by McCarthy [18].

Function Level

The actual task of design implementation is relegated to the function level, as it is desirable to keep all strategies pertinent to the design problem separate from the knowledge level. The design specifications handed down from the knowledge level are attempted to be satisfied at the function level. All problem independent strategies which assist the design process, are confined to this stage. These generic problem solving operators are explained here in context of the structural design problem. A controller must be formulated at this level to direct the flow of the design from one process operator to another. Although designs can be generated by considering all requirements simultaneously, this methodology is not considered appropriate for the task at hand. Design is, more naturally, a process of refinement in steps to satisfy local goals and to keep track of how the current design step is likely to influence the global design. Some of these approaches are similar to methods of multilevel decomposition represented in recent studies [19,20].

The process of refinement in steps is initiated by a decomposition of the problem into smaller, more tractable, and preferably, single goal problems. The underlying principle in such a refinement is that the solution space is more likely to be unique in the presence of a higher degree of specification detail. The approach is one where a set of refinement operators are invoked by the controller to add greater detail in either the specifications or to the initial design (Figure 3). These two approaches for refinement have their accompanying ramifications, and are discussed in the following paragraphs. The design of a portal framework of beam elements to carry point forces and moments (Figure 4) is used to illustrate these concepts. The choice of the beam cross section must be made between an I-section, an open C-section, and a hollow circular section. The support points are defined and a choice of pin or clamped supports is available.

Refinement in specifications requires that the design specifications be arranged by a priority derived from their relative importance. For the sake of illustration the design specifications for the portal framework are ordered as follows:

a) The structure must be such that all loads have a load path to all supports.
b) The structure must not allow static displacements larger than specified values at points of load application.
c) The components (beam elements) must not be overstressed beyond elastic limits.
d) Local buckling or crimping in structural elements is disallowed.

The first requirement is of a topological nature and is handled by accessing domain knowledge available at the knowledge level. A controller would invoke an element generating program to generate beam elements that would meet this specification without attention to any other requirements. The next set of specifications would require assignment of cross sectional properties (cross sectional areas and moments of inertia) to the beam elements. No attention is paid at this level to the specificity of cross sections involved. The controller can either look for existing designs at the knowledge level or proceed with a generate-and-test strategy to implement the requirement. The next two requirements similarly dictate selection of particular types of cross sections based on the load conditions and also require detailed sizing of these cross sections for the problem at hand.

A design obtained by this approach is likely to vary with different ordering of design specifications. This difficulty can be alleviated to some extent by requiring that each design specification be only partly satisfied as it is considered. This is akin to maintaining a constant buffer in the constraint activity and tightening all constraints after each specification has made a contribution to the design.

A second approach of refinement is one where the system design specification is decomposed into design specifications for components of the system. This type of refinement can actually be embedded into the one described above, wherein each design specification is further decomposed into component specifications. The underlying philosophy in this approach is one that assumes elimination of a large number of possible solutions with increasing detail in specifications. This hierarchical decomposition is described in terms of the portal frame problem as follows.

A design with all previous specifications and an additional requirement of minimum weight must be obtained. While all conditions cannot be transferred to the component level, the structural generation problem can be viewed as designing each component separately for whatever specifications are applicable. Beam element A is sized for each of the applicable specifications. Its length is determined by distance from load P_1 to the support point S_1. Similarly, the cross sectional type and the corresponding section dimensions are obtained from strength and local buckling considerations. At the component level, however, sufficient detail is not available to see if component level design satisfies the specification of the global structural stiffness. A recommended procedure at this level is to determine the sensitivity of global structural stiffness to local component variables, and to use this information when an assemblage of the components is done.

In addition to processors that implement strategy, testing operators comprise an important component of the function level. The controller is faced with the formidable task of directing execution of generators and testers in an efficient sequence. Clearly, if a generated concept fails an acceptability test, several remedial measures are available for implementation. The simplest entails a backtracking to the last decision, and revising that decision with the failure as a constraint. As an example, if a square cross section was selected for a beam element to satisfy stiffness and strength requirements and was later found unfit from a manufacturablity standpoint, one would simply backtrack to the decision of choosing a cross section with the additional manufacturability constraint. Another frequently used approach, and described by Tong [13] as "pruning", is especially applicable if specification decomposition allows construction of tree-like deduction paths. Here, failure of a partial design can result in eliminating several possibilities from the search space.

Finally, the controller must have the option of modifying the design rules, particularly if it assists in realizing the design specifications. The acceptability tests can themselves be relaxed to admit designs. Examples of this include relaxation of manufacturability requirements to admit non circular cross sections. Likewise, allowable values of stress or displacements can be modified to pass the acceptability test. This concept is particularly powerful, if critical satisfaction of constraints in partial designs is consciously avoided. Yet another option available at this stage is to extend the design without replacing the current design. This translates into adding features which work with an existing design to enable it to pass the acceptability requirements.

Program Level

The foregoing discussion details the requirements and assigned tasks of the knowledge and function level. The mechanics of implementing all the design steps, including programming procedures, production rules, and database management systems is relegated to the program level. No problem solving knowledge is available at this level - it simply implements and manages instructions passed in from the other levels.

Particular attention must be directed at the database management capabilities of such a system. Significant amounts of data are generated and must be managed for a design system to work efficiently. This is even more crucial as large amounts of algorithmically generated numerical data must be stored and post-processed to use meaningfully in the iterative process. Two levels of data management are planned in the current system. The global data base is at the core of such a system and records information for long term usage. Problem and subproblem related databases are extracted from the main system and are local to the knowledge level. This provides a convenient blackboard for constraint posting and propagation as the design is taken through a process of incremental refinement (Figure 5).

The inference facility is another important feature at this level. In the structural design problem that is currently under implementation, a rule-based, C Language Integrated Production Systems (CLIPS) [21] is being used. This utility can be invoked from within a FORTRAN program, making available a convenient link between algorithmic and heuristic processing of information.

Optimal Topology Assignment

The basic goals of an optimal topology generation system within the framework of a problem solving system described in previous sections is outlined here for completeness. A set of load conditions and support points are defined in a design space.

The design space also consists of obstacles and prohibited zones in which no portion of a structural assembly may be placed. An optimal, minimum weight structural topology is to be generated to transfer the applied loads to the supports, satisfying requirements of allowable stress in structural members, displacements at load points, and limits on component and system static stability.

The types of structural elements that may be used in the structural synthesis are limited to axial force members (tension only, and tension/compression), flexural beam elements, and membrane elements (triangular and quadrilateral). In addition to these primitive elements, assembly of axial force elements (tension/compression) in a triangular truss is also available as a master element.

The topology generator is first invoked to construct a series of structural assemblies that stabilize the applied loads. This is an incremental process which attempts to meet the problem specifications in one of two ways. The first approach looks at each load sequentially, assessing its geometric orientation with respect to the supports, and selects an appropriate element to provide partial stability. At any step of the generation, a branching can be introduced to implement more than one acceptable alternative. A second approach divides the structural domain into four quadrants, and a structure is generated in each quadrant to account for loads in that region. The substructures are then connected by acceptable least weight elements. At this stage of the problem, the only active problem specifications are those related to the geometry of the load distribution and the applicable element types.

A sequence of refinements is made to these configurational possibilities, with each step accounting for one design specification from an ordered list. Such an approach assumes that a set of alternate designs optimized in this manner are better suited to identifying the most promising configuration for detailed design. A second approach that is planned for implementation in the proposed study uses the topology generator to seed the design space with possible alternatives. An optimal topology is then obtained by a combination of the most favorable characteristics of the seed designs. The generate and test approach outlined above relies to a large extent on algorithmic processing and efficient handling of numerical data. The three tier organization of the problem solving system described in preceding sections is ideally suited to this complex task. Additional details of the implementation will be presented in [22].

Closing Remarks

The present paper presents the framework of a knowledge-based system for structural design. The process of design of a structural system includes the initial structural geometry definition followed by successive refinement of this initial configuration to obtain an optimum. The system described for this task is distinct from previous systems in this domain. The latter were largely restricted to consultative tasks. The use of decomposition principles to make the design problem more tractable is very similar to multilevel decomposition techniques proposed in automated optimum synthesis of structures. A formalism in the organization of such systems is considered very important if significant advances in problem solving capabilities are to be realized. Finally, the role of integrating algorithmic and heuristic processing of databases is considered vital for the success of such systems.

Acknowledgments

The author gratefully acknowledges his discussions with doctoral student N. Sangameshwaran during the preparation of this paper.

References

1. J.L. Chen and P. Hajela, "FEMOD: A Consultative Expert System for Finite Element Modeling", proceedings of the AIAA/ASME/ASCE/AHS SDM Conference, April 6-8, 1987, Monterey, California. Computers and Structures, Vol. 29, No. 1, 1988.

2. J.L. Chen and P. Hajela, "A Rule Based Approach to Optimum Design Modeling", Computer Applications in Structural Engineering, (ed. D.R. Jenkins) ASCE, New York, pp. 66-81, 1987.

3. P. Hajela and J.L. Chen, "CAD Interfaces in the Development of Expert Systems for Optimum Structural Design", Proceedings of the Second International Conference in Computational Engineering Science, Atlanta, Georgia, April 1988, Computational Mechanics, Springer Verlag, April 1988.

4. A. Hart, "Knowledge Elicitation: Issues and Methods", Computer Aided Design, Vol. 17, No. 9, November 1985, pp. 455-462.

5. J. Bennett, L. Creart, R. Englemore and R. Melosh, "SACON: A Knowledge Based Consultant for Structural Analysis", Technical Report STAN-CS-78-699, Stanford University, Stanford, California, 1978.

6. S.C.-Y. Liu, "A Consultative Expert System for Finite Element Modeling of Strip Drawing", presented at XIII North American Research Conference, University of California at Berkeley, May 1985.

7. R.H. Holt and U.V.L. Narayana, "Adding Intelligence to Finite Element Modeling", Expert Systems in Government

Symposium (eds. K.N. Karna, K. Parsaye and B.G. Silverman), IEEE, New York, 1986, pp. 326-337.

8. J.J. Shah, "Development of a Knowledge Base for an Expert System for Design of Structural Parts", Proceedings of the ASME International Computers in Engineering Conference, 1985.

9. J.J. Shah, "Deziner - An Expert System for Conceptual Form Design of Structural Parts", Proceedings of the ASME International Computers in Engineering Conference, 1986.

10. G.E. Nevill, L.A. Jackson, and J.H. Clinton, "Automated Hierarchical Planning for Structural Design", proceedings of the ASME International Computers in Engineering Conference, San Francisco, California, August 1988.

11. G.E. Nevill, and G.H. Paul, "Knowledge Based Spatial Reasoning for Designing Structural Configurations", proceedings of the 1987 ASME International Computers in Engineering Conference, New York, Vol. 1, pp. 155-160.

12. J.P. Brown, "Managing Interacting Design Subproblems in Incremental Preliminary Design", M.S. Thesis, Department of Aerospace Engineering, Mechanics and Engineering Science,University of Florida, August 1988.

13. C. Tong, "Toward an Engineering Science of Knowledge-Based Design", Artificial Intelligence in Engineering, Vol. 2, No. 3, 1987, pp. 133-166.

14. C. Tong, "KBSDE: An Environment for Developing Knowledge-Based Design Tools", proceedings of Knowledge Compilation Workshop, Oregon State University, September 1986.

15. D. Whetstone, "SPAR - Reference Manual", NASA CR-145098-1, February 1977.

16. P. Hajela, "Genetic Search - An Approach to the Nonconvex Optimization Problem", in review for presentation at the 30th AIAA/ASME/ASCE/AHS/ASC SDM Conference, Mobile, Alabama, April 1989.

17. G.N. Vanderplaats, " An Efficient Feasible Direction Algorithm for Design Synthesis ", AIAA Journal, Vol. 22, No. 11, October 1984, pp. 1633-1640.

18. J. McCarthy and P. Hayes, "Some Philosophical Problems from the Standpoint of Artificial Intelligence", Readings In Artificial Intelligence, Nilsson, 1981.

19. J.E. Sobieski, A Linear Decomposition Method for Larger Optimization Problems - Blueprint for Development, NASA TM-83248, 1982.

20. J.E. Sobieski, B.B. James, and A. Dovi, "Structural Optimization by Multilevel Decomposition", AIAA Journal, Vol., 23, No. 11, 1983, pp.1775-1782.

21. CLIPS Reference Manual, JSC-22948, NASA Johnson Space Center, April 1988.

22. P. Hajela and N. Sangameshwaran, "A Coupled Algorithmic and Heuristic Approach for Optimum Structural Topology Generation", in review for International Conference in Computer Aided Optimum Design of Structures, 20-23 June 1989, Southampton, England.

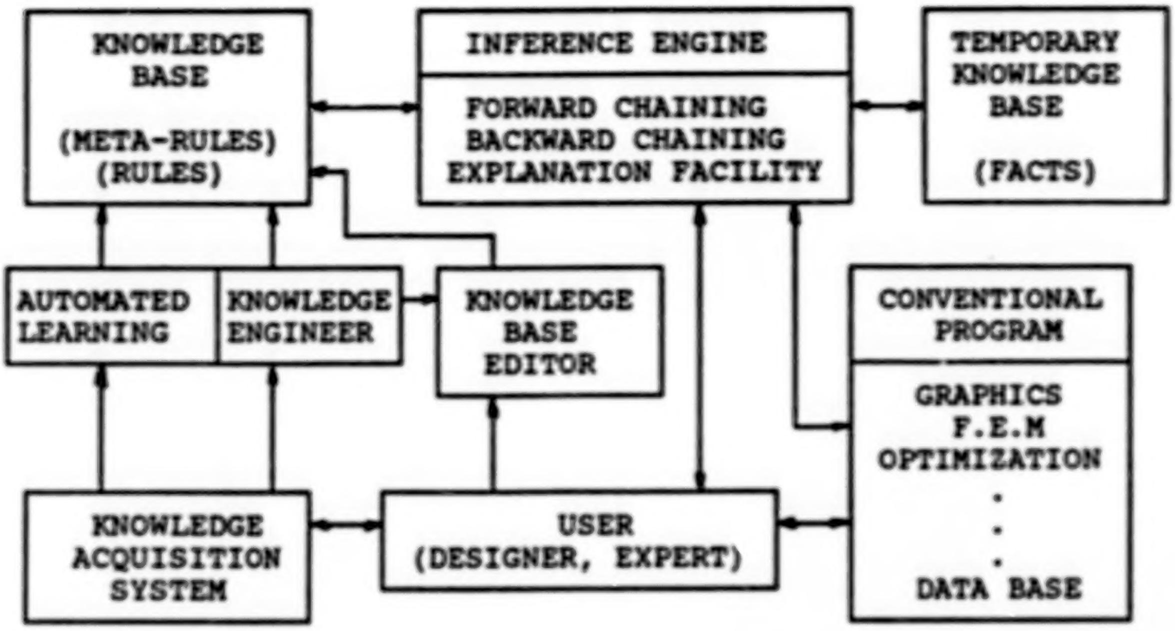

Figure 1. Architecture of the OPSYN system

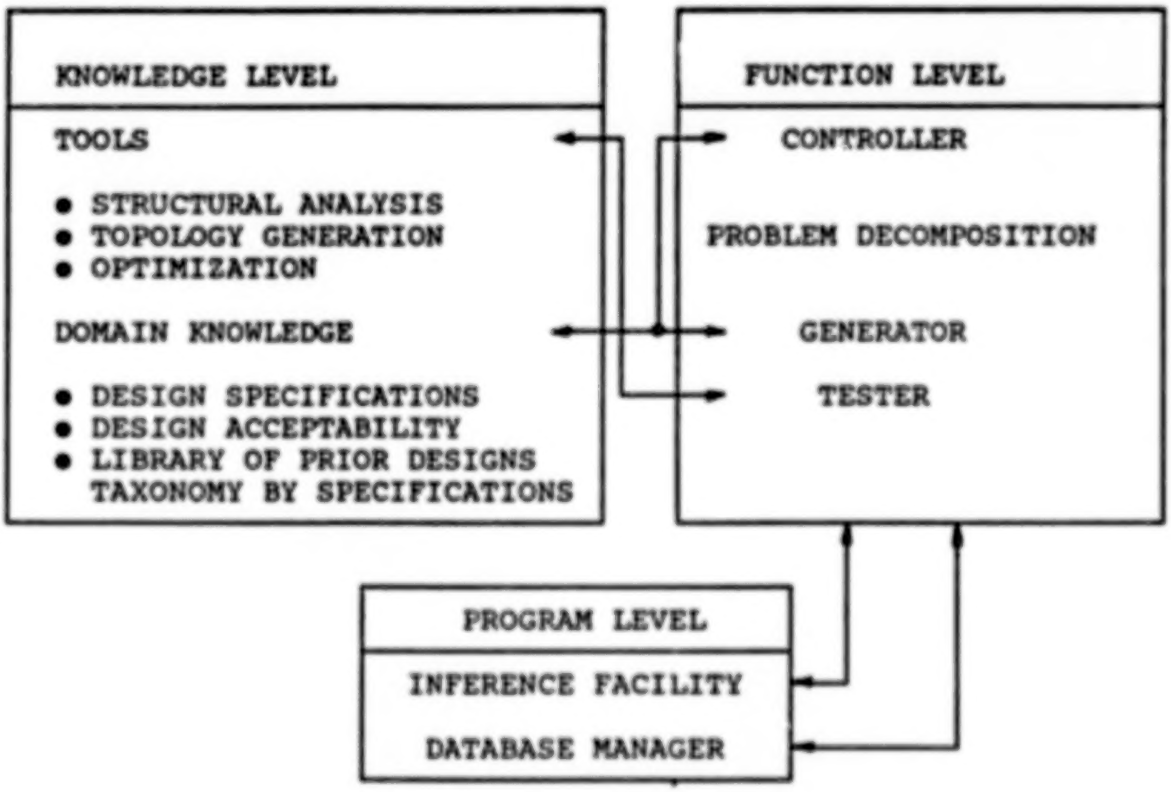

Figure 2. Organization/Subdivsion of tasks in a typical problem solving system.

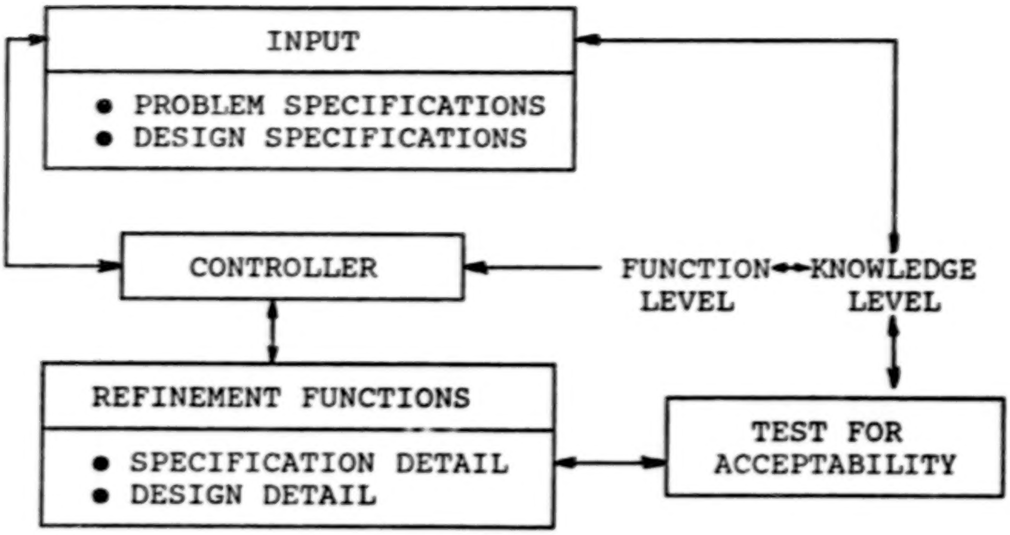

Figure 3. Schematic of a refinement operator

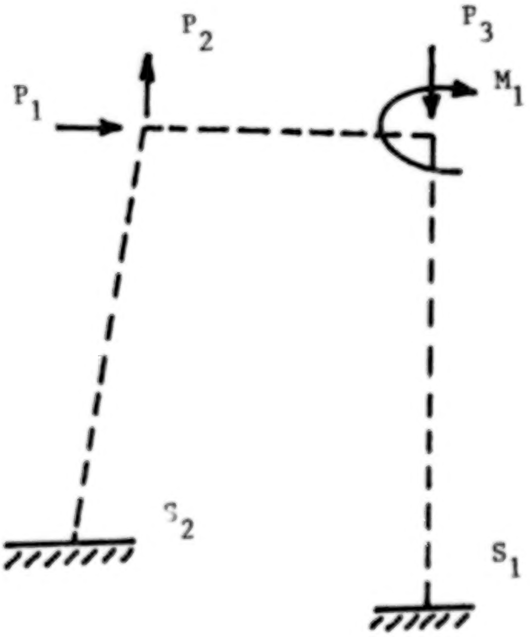

Figure 4. The portal framework problem.

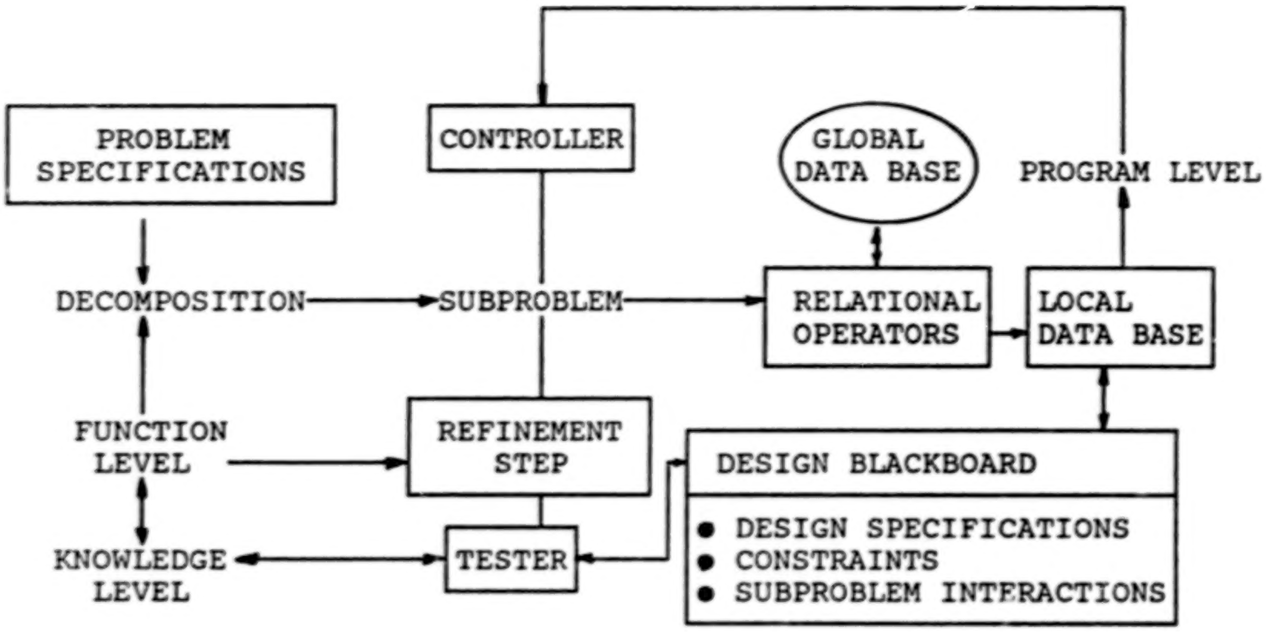

Figure 5. Significance of database management in problem solving systems.

DEVELOPMENT OF A MICRO-COMPUTER BASED INTEGRATED DESIGN SYSTEM FOR HIGH ALTITUDE LONG ENDURANCE AIRCRAFT*

by

David W. Hall** & J. Edward Rogan***

ABSTRACT

In recent years, increasing attention has been given in the aerospace industry to integration of aircraft design disciplines. This approach has been applied theoretically to sailplane design and to solar powered high altitude long endurance (HALE) aircraft design. More recently, it has been applied to the design of microwave powered aircraft. These studies describe attempts to arrive at integrated designs of one class of aircraft using then-existing state-of-the-art computer capabilities. No attempt was made in any of these cases, though, to use new programming techniques derived from Artificial Intelligence (AI) research to develop more flexible systems for the conceptual design of HALE aircraft.

The purpose of this study was to investigate the feasibility of developing a general parametric sizing capability for micro-computers using integrated design methodology implementing an existing HALE methodology as a test case. The methodology described here incorporates some detailed calculations, many qualitative rules-of-thumb and constraints which are not easily quantified except by the accumulation of design experience. In this regard, the resultant software which will be developed in future efforts will be a knowledge-based system for the conceptual design of HALE aircraft.

---

[*] This work was sponsored as a Phase I SBIR by the NASA/Ames Research Center, Advanced Plans & Programs Office

[**] David Hall Consulting, AIAA member

[***] The Georgia Institute of Technology, School of Aerospace Engineering, AIAA member

INTRODUCTION

Advances in computing technology have made it possible to create a new kind of design tool. Current generation CAD/CAE/CAM systems are based on an idea of the computer as a "number cruncher"---computations are thought of as manipulations of numbers. This approach has led to an emphasis on geometry representation and numerical techniques in engineering computing. Viewed in this way, computers *aid* design, but are essentially external to the design process.

An alternative view of the computer has been around since Alan Turing's epoch-making work in the 1930's: the view of computing as manipulation of *symbols,* (which might include numbers among other things). The great beauty of Turing's work is in the intimate connection between the scientific definition of what a computer is (it's called a Turing Machine) and aspects of mathematics as a *language* that are among the most important scientific discoveries of this century (Kurt Gödel's completeness and incompleteness theorems).

What does any of this have to do with design or aircraft? After all, designers are notoriously,and admittedly, innocent of mathematics[1]. However, designers, like everyone else, use a language of symbols to solve problems. The idea of a symbolic **programming language for (aerospace) design,** clearly delineated and with most of the main pieces present, is the primary innovation of the work described in this paper.

The application, if not the development, of a programming language for design must be graphical since designers think graphically. A symbolic "design programming language" must provide the designer with the means to describe design concepts and manipulate them in a convenient, but disciplined, manner. Certainly, the language must provide the capability to describe (1) the air vehicle itself ("What it is"), (2) the *functional decomposition* ("What it does") and (3) various approximate theories, analyses and models which collectively describe "How it works".

What does it mean to execute or "run" (the word "interpret", in its everyday sense, rather than in the specialized computing sense, is probably most accurate) computer programs written in such a language? Interpretation of a computer program involves defining contexts (environments) in which names (variables, attributes) are *bound* (assigned, set) to values (which may be numbers or other symbols)[2]. Procedures, in which the named variables appear as parameters, are then evaluated in the environments. On the other hand, execution of an air vehicle design process involves exploring how alternative design ideas fit together by preparing engineering drawings and performing analyses. The process of making an engineering drawing is a decision-making process that results not only in the design specification, but in the designer's *understanding* of how the final concept works and why design decisions were made the way they were. It is this understanding that allows the designer to conscientiously "sign off" that the design is correct in the designer's professional opinion.

The design programming language to be described in this report allows designers to use computers to *do* design, rather than to *aid* design. This means that interpretation of computer programs written in the design programming language must support the design decision-making process. Designers must be able to use computer programs written in the "programming language for design" to gain a technical understanding of the way the aircraft will work and might fail, and to develop and communicate their rationales for design decisions.

Background

A programming language for design is a "knowledge-based system" in the sense that the basic architecture (knowledge-base, inference engine, problem state or context) and the techniques used for structuring and interpreting computer programs (inheritance, constraint propagation, objects/modularity/state, data and procedure abstraction, and metalinguistic abstraction) are basically the same. However, a "programming language for design" is far from being an "expert" system. The idea of an expert system is that once knowledge has been extracted from the expert (or experts), the computer program is able to reach conclusions that can be logically inferred from the rule base with only minimal human intervention. The implication is that novices would then be able to tackle many of the problems that can nowadays only be solved by experts. In contrast, the programming language for design is a tool specifically for use *by* expert aircraft designers. The intention is to accomplish the kinds of productivity gains for aircraft designers that word processing provides for authors and secretaries, or that symbolic mathematics programs (e.g., MACSYMA or SMP) provide for mathematicians and other scientists.

An example is a *decision-oriented* (rather than drafting oriented) user interface for preparing aircraft three-views. An important insight resulting from the research is that *a fundamentally wrong turn is being taken with the introduction of three-dimensional geometry in the very early phases of conceptual design in that the* ***decision-support*** *aspects of the three-view drawing have been overlooked in favor of the* ***product defintion*** *advantages of three-dimensional surfaced geometric models.* The three-view drawing is a classic example of the suppression of non-essential detail (required to implement a 3-D model) in order to emphasize critical design aspects: placement of landing gear, pilot visibility, wing planform shape, static stability, propulsion integration, etc. The three-view should properly be used to make these design decisions. Three-dimensional surface definition should then be developed by *interpreting* the three-view drawing. Procedures for interpreting three-views would be implemented using the computer programming language for design.

Successful implementation of the integrated design system for micro-computers will accelerate the use of computers to *do* design, increasing product quality and reducing the length of the development cycle by allowing designers to look at a broader range of design concepts. Additional benefits obtain if the use of a computer programming language for design is carried forward into preliminary design, detailed design, production, and support phases of the system life cycle. Here, the ability of computers to manage complexity and detail would be invaluable. The idea that a product decision history, represented by a portion of the computer programs for the design, could be carried onboard each "tail number" and used to assess the impact of maintenance actions and for configuration control has considerable appeal for long-life, high-value systems such as aircraft and reusable spacecraft.

The advantages of a computer programming language for design are clear. The question remains, "How can a design computing language be implemented?". The answer to this question begins with an assessment of some alternative approaches to applying advanced computing technology to design, comparing and contrasting them with our technical approach. From this discussion will emerge key issues that must be addressed to establish proof-of-concept for the design computing language. These issues then provide a backdrop for the technical discussions, results and conclusions which follow.

Alternative Approaches

The design computing language being developed at DHC, (called "***windFrame***") is one of several design tools that could justifiably be said to represent the next generation. These alternative approaches are in various stages of maturity, ranging from research projects to small, new-start CAD companies and new directions being taken by established CAD vendors. One of the first projects to break ground in design computing languages was the **Paper Airplane** project at the Massachusetts Institute of Technology [3]. Paper Airplane contributed the idea that constraint propagation could be used in conjunction with a symbolic representation of design "attributes" and relationships among those attributes to free the designer from the tendency of FORTRAN synthesis programs to have "hard-wired" design decision paths. Newton's method was applied in a single variable to solve the constraints in the "backward" direction. Paper Airplane, written in the LISP programming language, was envisioned primarily as a tool for conceptual design.

Rubber Airplane, currently being developed by Mark Kolb at M.I.T., was started as a result of a technical exchange between Dr. Elias and Randy Smith, then (December 1985) at The Lockheed-Georgia Company [4]. Smith had been working on a FORTRAN code for parametric geometry and 3-D surface definition, called GRADE. In his Rubber Airplane work, sponsored by the NASA/Ames Advanced Plans and Programs Office, Kolb continues to apply a constraint propagation technique based on the successful Paper Airplane ideas (Rubber Airplane is written in Common LISP). However, Rubber Airplane provides *components,* which are similar (from a design point of view) to the components defined in GRADE (except that the designer has much more flexibility). Rubber Airplane also provides *design links* between components. Paper Airplane was originally developed on a VAX using Franz Lisp. Rubber Airplane is being implemented on Texas Instruments Explorer workstations, although it also runs on Symbolics LISP Machines.

At about the same time Elias was starting work on Paper Airplane, Larry Rosenfeld was developing a parametric geometry modeller that eventually evolved into the **ICAD** system[5]. The details of how ICAD works are rather closely guarded; however, it can be noted that the system provides an advanced parametric surface definition capability and demand-driven propagation of symbolic and numeric constraints. Constraint propagation does not appear to be as powerful as those in Paper Airplane and Rubber Airplane because it works only in one direction. An often-cited problem with ICAD is that the user/designer interacts with the system primarily by programming in a LISP-like design programming language, the ICAD Language. A feature of ICAD that is important for comparison with ***windFrame*** is the structure of the design concept representation: the design is represented as a hierarchical tree of *parts,* linked by relationships that are not given any special structure. Early versions of ICAD ran primarily on Symbolics LISP Machines, but the product is becoming available on other workstations with fast LISP software.

Dr. Gene Bouchard's work at The Lockheed Aeronautical Systems Company should also be mentioned[6]. Details of the system are proprietary, except that the system is LISP-based, runs on the Symbolics, and provides a valuable graphical programming user interface. Bouchard has focused on providing designers with a quick turnaround trade study capability. Parametric surface definition capability is planned for the system but has not yet been implemented.

Intergraph Corporation made the decision about four years ago to implement their Non-Uniform-Rational-B-Spline (NURBS) package using object-oriented techniques in the C programming language. This has provided them with a significant fallout design programming language capability, although the system is primarily oriented toward geometry definition, rather than design decision-making[7].

The Cognition system attracted considerable attention when it first appeared, offering an attractive object-oriented drawing interface linked with on-line standard handbooks[8]. Constraint propagation was provided through the solution of relatively large multi-dimensional Newton-Raphson methods. The Cognition system was written in MainSail, a LISP-like object-oriented language.

windFrame was conceived to explore areas of design computing languages that were not being emphasized by any of these products or projects. These areas were

1) Apply optimization as a constraint propagation technique and use decomposition and parameter passing to limit the extent of constraint propagation.
2) Base the organization of the language around Systems Engineering discipline, especially *explicit description of design function* .
3) Focus on aircraft design and develop the system through walkthroughs of a proven aircraft design methodology, working closely with an experienced aircraft designer.
4) Develop a system that would run on a relatively inexpensive micro-computer and plan to place the system in the public domain.
5) Base the development of the language on the user interface.
6) Design the computer programming language so that it could be used throughout the life cycle of an aircraft.
7) Focus on design decision-making.
8) Use approximation techniques to provide interactive explanation and "What if?" analysis as part of the constraint propagation.

Issues that have been addressed to date include:

- Is object-oriented programming the "best" way to implement a design language? If not, what replaces or complements it?
- What "objects" (or their equivalents) are needed to organize the language around Systems Engineering disciplines?
- How can Dr. Sobieski's (NASA/Langley Research Center Interdisciplinary Research Office) decomposition techniques be extended to apply to discrete parameters?
- How can constraint propagation problems be formulated as optimization problems?

- Is there a suitable programming environment to support high productivity user-interface-oriented programming on the Macintosh? Can critical capabilities for the design language be demonstrated in such a programming environment?

- What would one experienced aircraft designer want the user interface to look like?

- If the system were available in the public domain, what kinds of users would be interested?[9]

DESIGN OF THE *windFrame* LANGUAGE

Considerable emphasis has been placed on the design of the *windFrame* language itself. The success of this effort can be judged by the fact that the results seem somewhat obvious in hindsight. However, *details of the structure of the language strongly influence how it will be used.* The difficulty of identifying a good set of basic elements for the language can be seen in the wide disparity of choices of these elements in the alternative next generation design tools discussed above. The technical approach taken in this effort has been to select an initial set of basic elements based on ref. 10, and then to evaluate this choice of elements by a "walkthrough" of an existing design methodology in close association with an experienced aircraft designer. Alternative computer programming techniques for implementing the basic *windFrame* language elements were then investigated.

The *Architecture and Integration Requirements for an ULCE Design Environment* study[10] represents one step in the direction of bridging the gap between systems engineering discipline and traditional airplane design practice[11]. This study took a dramatically different approach to the integration of downstream concerns (such as supportability and producibility) into early design decision-making. Specifically, the study took a fundamental look at the *subtext* of what designers do; that is, the things designers do without thinking about them. This aspect of the study is also highly relevant to the design of the *windFrame* language. From this point of view, the design process is not static, but highly dependent on the technical content of the design concepts and on the nature of the requirements. The ref. 10 study also highlighted the decision-making aspects of design, as opposed to the generation of product definition data. One of the conclusions of this study was that the architecture of Unified Life Cycle Engineering *as a process* must include

1) the generation of design alternatives,

2) planning of the decision-making process based on the technical content of these alternatives, and

3) execution of the design decision-making process (Figure 1).

The intermediate planning step thus involves "design of the design process", and is therefore a "meta-design process". Development of design deliverable data items, such as engineering drawings, was viewed as an output of the decision-making process. *Parametric* definition of concepts to be specified by these deliverable engineering drawings was to be established as part of the original description of the design alternative.

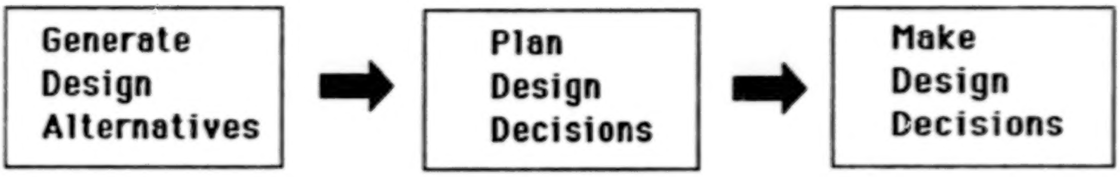

FIGURE 1. ULCE (META) DESIGN PROCESS ARCHITECTURE.

Advances in computing technology were an early motivating force for the USAF Project Forecast II Unified Life Cycle Engineering (ULCE) initiative. The ref. 10 concept was based in part on the use of a parametric design description and specification language for capturing design alternatives in step 1 (Generate Design Alternatives) of the ULCE process. The study was performed by an interdisciplinary team including engineers from preliminary design, supportability, and producibility, as well as design technology. As a result, the need for a systems engineering approach, and specifically for an *explicit description of system function* as a part of the design language was made very clear. Explicit description of function allows an interdisciplinary design team to organize various theories, models, and analytical tools representing different views of how a single system function is performed. This organization is essential for engineers of different technical backgrounds to be able to recognize how these different views interact to make the system work or fail.

The *windFrame* language was specifically developed to address these needs. Basic elements of the *windFrame* language are a precursor to the *system hierarchy*, called the "multiHierarchy", an explicit description of the *functional decomposition* (functionDecomp). The designer defines *theories and models* (theories&Models) at the intersection of the multiHierarchy (which describes alternative system implementations), and the functionDecomp. The theories and models define how the system concept elements associated with specific alternative implementations work to accomplish a given function. Explicit representation of system function allows more than one view of (and associated theories and models for) that function. In casual terms, the functionDecomp provides "hooks on which to hang different ways of looking at the same thing." Similarly, explicit representation of theories and models in the *windFrame* language allows multiple levels of approximation and alternative ways of predicting closely related phenomena, essential in applied aerodynamics (e.g. closed-form approximations, lifting-line, panel, and flowfield methods). The fourth and final basic element of the *windFrame* language is the *design decision* (designDecisions).

One way of thinking about how such a next-generation design environment might be used is that the designer defines the system, performs engineering analyses, and makes design decisions using computer programs that function as integrated "executive", "user interface", and "database" software. Integrating the executive, user interface, and database makes it possible for the software to represent the *state* of the design process, thus such a tool might be viewed as capturing the "design-in-process" (Figure 2).

Evidently, development of a computer program performing all three of these functions is a highly complex software engineering problem, even for a specific domain area such as aircraft design. In this area, our technical approach has been to apply programming techniques such as inheritance; constraint propagation; data and procedure abstraction; modularity, objects, and state; and metalinguistic abstraction[2].

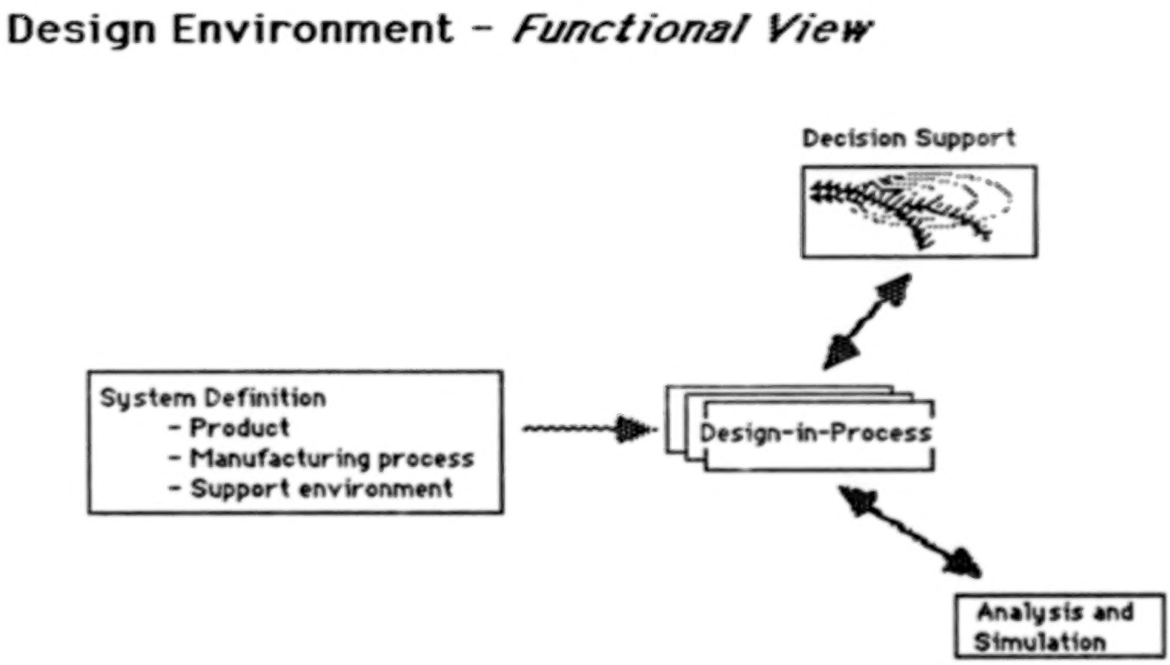

FIGURE 2. DESIGN-IN-PROCESS.

Work began using the MacScheme programming language on the Macintosh SE[12]. The idea was to implement the basic elements of the *windFrame* language using block structure and **make-environment** for modularity. However, this approach was unsatisfactory, primarily because the resulting design computing language was already highly "LISP-like" at the earliest phases of development. Our development philosophy has been, and continues to be, to develop a tool that designers will want to use through intermediate steps that designers would also want to use. Thus far, the LISP programming language has failed to gain wide acceptance among airplane designers, in spite of its obvious advantages. Preliminary experimentation with HyperCard established that (1) the basic *windFrame* elements could be implemented using HyperTalk, (2) instantiation, inheritance, and constraint propagation could be supported, and (3) the resulting design language was *highly* graphical and accessible to aircraft designers. The discussion and results in this report are based on the HyperCard approach.

The *windFrame* language, based on HyperTalk, allows designers to write computer programs using a highly graphical, user-interface oriented programming environment. These programs define design concepts (in terms of "what the concept is", "what it does" and "how it works"). The programs are "object-like" in that they represent prototype design concepts which can be *instantiated*. Based on the technical content of these descriptions, the designer writes more computer programs which manage the user interface for decision support and control instantiation of the design concept "objects". These designDecision programs are also "written" in the highly graphical, user-interface oriented style encouraged and even enforced by HyperCard. Writing the designDecision computer programs will be partially or completely automated once a basic set of decision tools has been established. The design process is then an interactive execution of the design decision programs.

The idea of controlling constraint propagation, instantiation, and inferencing through interactive *designDecision* object-like elements of the *windFrame* language is original with this study and is one of the key innovations of the David Hall Consulting technical approach. The way designDecision elements will work is probably best explained by the following examples. The first example looks at the impact of designDecision-making on the precursor to the system hierarchy (*multiHierarchy*). This example clearly shows how the multiHierarchy evolves into a system hierarchy as a result of executing the design decisions. It should be emphasized that this process is mapped directly into the *windFrame* design language. The second example illustrates how one type of interactive decision support interface for a designDecision might look. This example also clarifies the role of design- Decisions in managing instantiation of design concept "objects".

A discussion of the impact of design decisions on the *multiHierarchy* must be introduced with some additional background on the basic structure of the *multiHierarchy*. Recall that the *multiHierarcy* is used to define "what the system is". In the *windFrame* langage, the system definition is made up of *conceptElements*. For example, the high altitude long endurance aircraft itself would be a conceptElement in *windFrame*. "*conceptElements*" have *attributes* associated with them. Continuing the high altitude long endurance aircraft example, *attributes* associated with the **aircraft** *conceptElement* would include **takeoff gross weight**, **configuration**, **propulsion**, and so on. In specifying a value for an attribute, the designer can choose from among several *alternatives*. *Alternatives* for the **configuration** *attribute* of a high altitude long endurance aircraft might include **pusher**, **joined-wing**, **canard**, **three-surface**, and **conventional tailplane** (Figure 3).

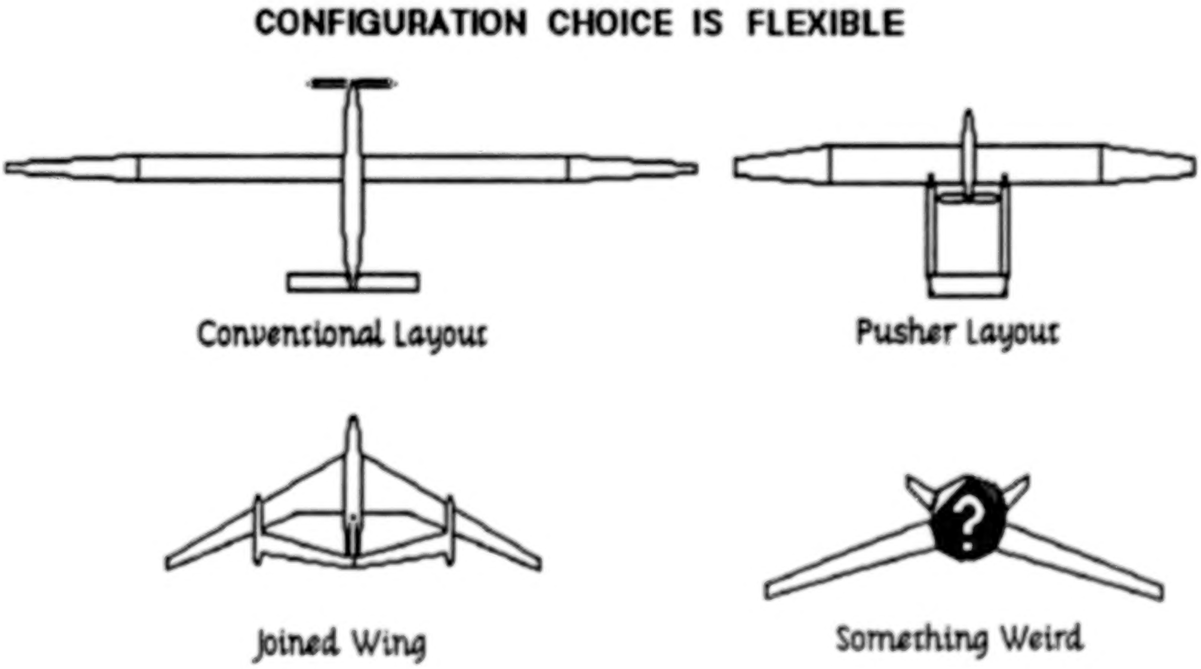

FIGURE 3. *ALTERNATIVES FOR* *CONFIGURATION* *ATTRIBUTE.*

Alternatives for the **takeoff gross weight** *attribute* could be described as "positive dimensioned real numbers". Writing software procedures to handle "positive dimensioned real numbers" (e.g. converting units, finding non-dimensional combinations of parameters, math functions) is completely straightforward, so it makes sense to say that **takeoff gross weight** is completely specified (as an *attribute in windFrame* ---of course no value has been selected for it yet) by saying that it is a "positive dimensioned real number". Not so with the **configuration** *attribute*, which seems to need further description.

How should the *multiHierarchy* description be carried forward for attributes such as **configuration**? The approach taken in *windFrame* is to recognize that the distinctions between *alternatives* for complicated *attributes* (like **configuration**) arise from the fact that different concepts are associated with each alternative. For example, the **canard** *alternative* includes a **canard** *conceptElement* (as does the **three-surface** *alternative*), while the **conventional tailplane** *alternative* does not. *windFrame* thus tackles specification of complicated design ideas through a *conceptElement-attribute-alternative-conceptElement* tree structure, the *multiHierarchy* which is shown in Figures 4 through 9.

The *multiHierarchy* evolves into a classical systems engineering tool, the "system hierarchy"[11]. The designer uses the object-like *designDecision* elements of the *windFrame* language to select among alternative design concepts. The *designDecision* elements of *windFrame* manage the partial instantiation of design alternatives needed to apply the engineering analysis procedures contained in the '*theories & Models*. The *designDecision* elements of *windFrame* collectively provide the designer with interactive control over constraint propagation, while keeping track of intermediate results and partially defined alternative configurations and accumulating approximations to design goals, requirements, and constraints as surfaces that delimit the design space. This information is used in *windFrame* to provide interactive explanation-oriented constraint propagation.

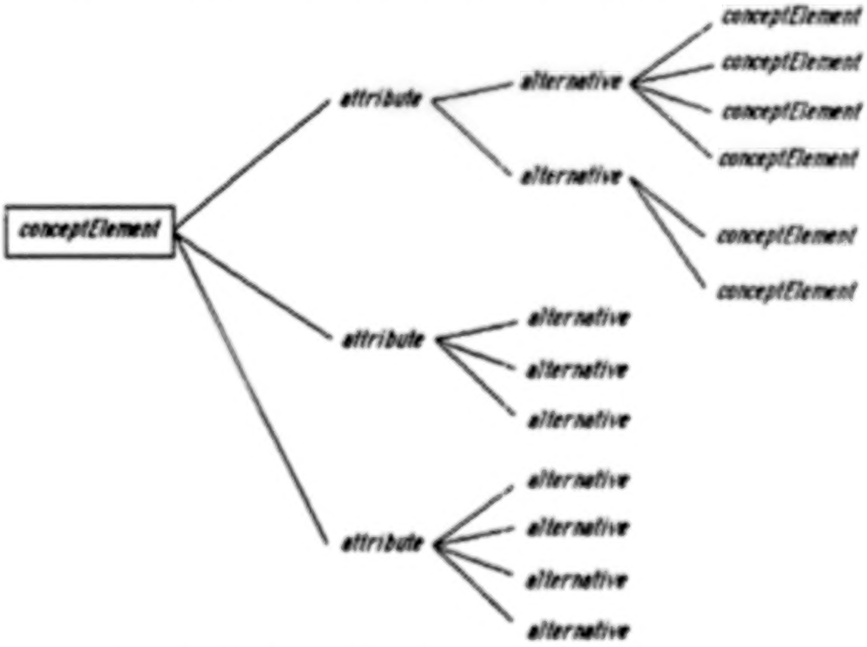

FIGURE 4. *MULTIHIERARCHY* TREE STRUCTURE.

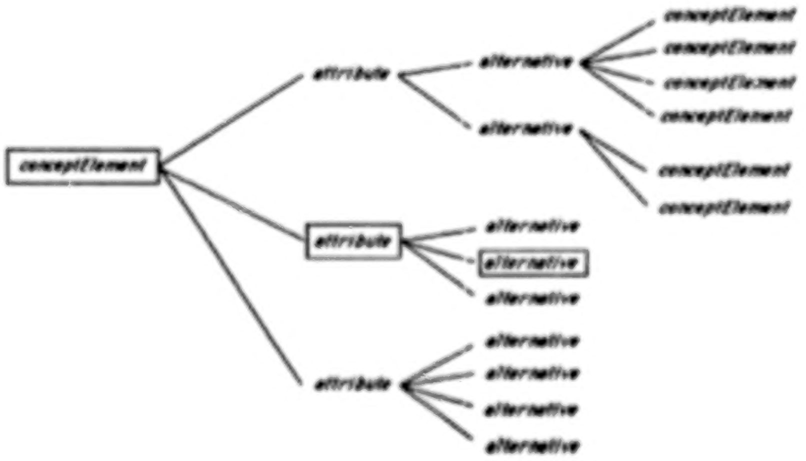

FIGURE 5. *DESIGNDECISIONS* BIND *ATTRIBUTES* TO *ALTERNATIVES*.

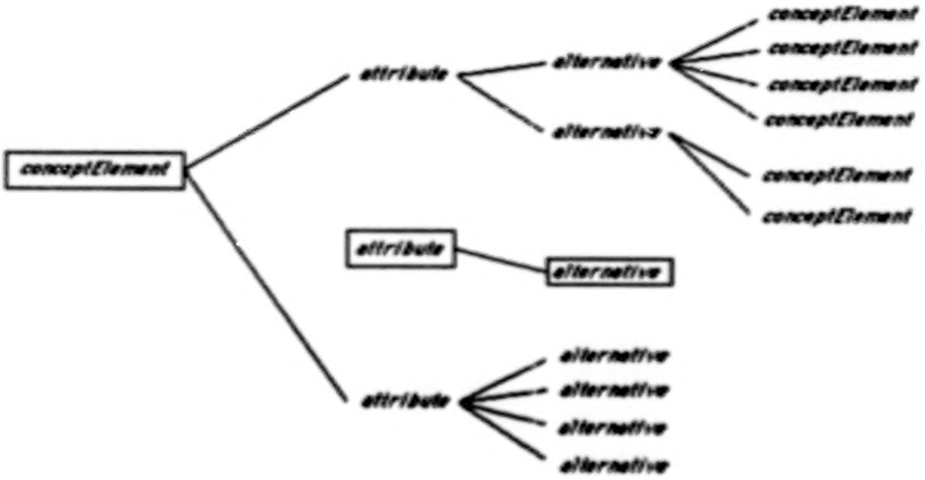

FIGURE 6. "*ATTRIBUTES* THAT ARE COMPLETELY SPECIFIED . . ."

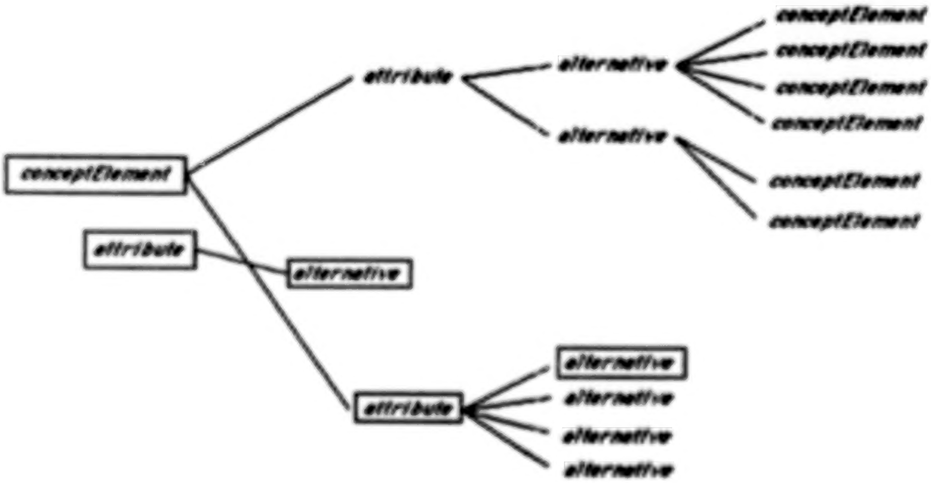

FIGURE 7. ". . . BECOME PART OF THE *CONCEPTELEMENT* SPECIFICATION."

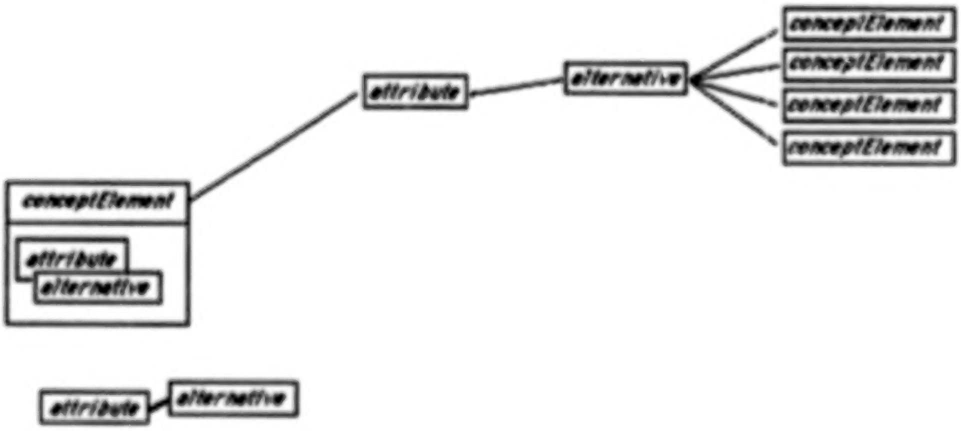

FIGURE 8. "*ATTRIBUTES* THAT FAN OUT TO ANOTHER LEVEL OF *CONCEPTELEMENTS* . . ."

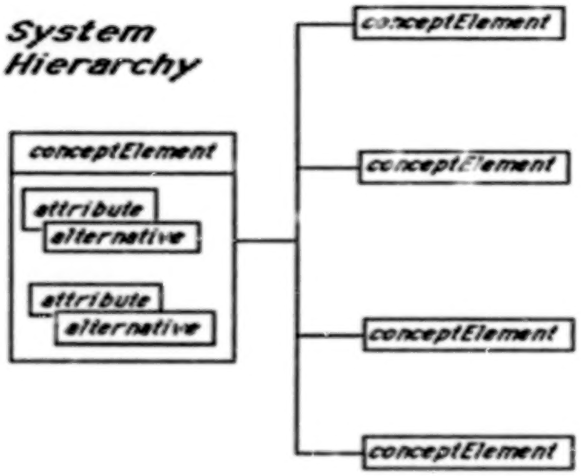

FIGURE 9. " . . . DEFINE THE NEXT LEVEL OF THE SYSTEM HIERARCHY."

One of the results of the design decision-making process supported by *windFrame* is the (aircraft) system specification. Development of the system specification is controlled by the designer through the *designDecisions*. Looked at from the point of view of the *multiHierarchy* as it evolves into the system hierarchy, *designDecisions* bind *attributes* to one of their *alternatives* (Figure 5).

Attributes that are completely specified by this binding (e.g., once a "positive dimensioned real number" has been chosen for **takeoff gross weight**, no additional specification is needed) become part of of the *conceptElement* specification (Figures 6 and 7). Attributes which fan out to another level of *conceptElements* (Figure 8) define the next level of the system hierarchy (Figure 9). An important aspect of the design of the *windFrame* language is that the subtle distinction is clearly made between specifying levels of the system hierarchy through the design decision-making process and specifying levels of design alternatives (by creating a multiHierarchy down to some level of description). This aspect of *windFrame* gives the design language enough expressive power to capture "levels of approximation" which are needed for various *theories&Models*. In fact, the level of approximation of a *theory/Model* is essentially the amount of depth in the multiHierarchy that must be instantiated in order to apply that *theory/Model*.

designDecision elements of the *windFrame* language are used to partially instantiate "object-like" pieces of the design concepts described by the *multiHierarchy* and *theories&Models* . Only those *attributes* of the design concept needed to perform an evaluation of the concept against design goals, criteria, and requirements are bound to *alternative* values. This binding is made in a context (in the sense of interpretation of a computer program discussed above) that is managed by the *designDecision* element. This context is exploratory. Not all the partially instantiated designs in this context will meet requirements. Some of them may be inconsistent or infeasible.

One type of *windFrame* interface that is used by the designer to control this instantiation and evaluation process has the appearance of a set of one-dimensional, two-dimensional, carpet, or other types of plots used for presenting aircraft design and performance information. Another interface, appropriate for discrete, qualitatively different alternatives, is a "trade table" [11]. Both of these classes of decision support tools are familiar to designers. There are limitations to the use of these classical decision support interfaces, however. Their succesful use depends on the designer's ability to set up a design decision process that will rapidly converge on a satisfactory design solution. One of the risks inherent in the integration of new technology is that coming up with a good design process is basically the same problem as coming up with a good design.

The development of the *windFrame* language will make it practical to provide designers with some tools for "designing the design process". The technical approach is to use local optimization and parameter passing to formulate the design process as a network of interrelated decisions. Initial sensitivity and examination of design alternatives are applied to identify sequences of design decisions that have good convergence. As the design space is explored, approximation techniques can be used to build models of complex interactions between design attributes and requirements. The process comes full circle when these approximations are plotted and trade tables are made up using the "classical" decision interfaces. An "explanation" process, using both the "classical" decision interfaces and the design space approximations, can be used by the designer to "design a new design process"---at the same time the designer is designing a new type of aircraft.

The second example illustrating the role of *designDecisions* in *windFrame* is closely linked with these ideas. A prototype decision support interface for exploring the design space would consist of a collection of x-y plots of one attribute against another (Figure 10). For example, the attributes could be **wing loading** and **power loading**. (The values shown in Figure 10 are screen coordinates at the location of the "design instance"). Within allowable limits on *alternative* values for **wing loading** and **power loading**, any point on the plot corresponds to a partial specification of a design. Of course, this information, along with appropriate *theories&Models* may be sufficient to evaluate these design alternatives (e.g., against FAR 23.67). Using the mouse with appropriate pull-down menus and/or HyperCard "buttons", the designer can 1) create an interface to access a partial instantiation of a design alternative in the context of this *designDecision* , 2) interpret computer programs to create the partial instance itself, and 3) evaluate the partial instance using appropriate *theories&Models*. Results of these evaluations can be accumulated in the *designDecision* context and used as the basis to construct design space approximations.

The decision support interface in this example (Figure 10) is based on a technique for constructing multidimensional quadratic splines based on systematic evaluation of design alternatives. The simplex pattern referred to in Figure 10 (drawSimplex---top "button" on right hand side of screen and moveSimplex) is a pattern used in Experimental Design. A simplex is made up of the minimum number of points in n-dimensional space required to construct a first-order (linear) model. A "zero-dimensional" simplex is a point, a one-dimensional simplex is a line (two endpoints), a two-dimensional simplex is a triangle (three corner-points), a three dimensional simplex is a tetrahedron (four corner-points), and so on. The n+1 points in the simplex must be arranged so that substituting the points $x^1, \ldots, x^{n+1}$ (these points are n-dimensional vectors) into the linear model results in n+1 independent equations:

$$a_0 + a_1 x^1{}_1 + \cdots\cdots a_n x^1{}_n = F(x^1)$$

$$\vdots$$

$$a_0 + a_1 x^{n+1}{}_1 + \cdots\cdots a_n x^{n+1}{}_n = F(x^{n+1})$$

The equations can be inverted to give a unique solution for the coefficients a_i of a linear approximation to an unknown math function F(x). The technique uses the idea that exploration of a design space usually involves evaluating designs on adjacent simplices. If the first derivatives of F are continuous across the boundaries between these adjacent simplices, then a second-order spline approximation to F can be found that fits the design points within each simplex and is continuous across the simplex boundaries. For a pattern of two simplices in two-dimensional (x_1, x_2) space, with the common boundary at $x_1=0$, the spline equations are

$a_1 = b_1$
$a_{12} = b_{12}$
$a_{22} = b_{22}$
$a_2 = b_2$
$a_0 = b_0$

This gives 5 equations for the 8 unknowns in the two quadratic approximations (one on each simplex):

$$Q_1 = a_0 + a_1x_1 + a_2x_2 + a_{11}x_1^2 + a_{12}x_1x_2 + a_{22}x_2^2$$

$$Q_2 = b_0 + b_1x_1 + b_2x_2 + b_{11}x_1^2 + b_{12}x_1x_2 + b_{22}x_2^2$$

The remaining 3 equations can be used to fit the spline near some design alternatives within the simplex boundary that are of interest. These approximation techniques are more qualitative than quantitative, in the sense that they are used by the designer to guide exploration of the design space and to dynamically estimate stability and convergence characteristics of a design process plan.

An alternative approach, accomplishing the same thing but based on different assumptions, can be derived from the ideas of Fleury [13]. Fleury applies the idea of diminishing returns to conclude that a general parameter optimization problem can be cast (at least locally) in the form:

objective: minimize $w = w_1x_1 + \cdots\cdots + w_nx_n$

constraints: $a^1{}_1(x_1)^{-1} + \cdots\cdots\cdots + a^1{}_n(x_n)^{-1} + a^1{}_0 \geq 0$

A design variable y_i may have to be transformed to $x_i = (y_i)^{-1}$ depending on the local slopes of the constraints and the objective function to ensure that the "law of diminishing returns" can be applied. Fleury has also come up with some ingenious heuristics to extend the approach to discrete design parameters.

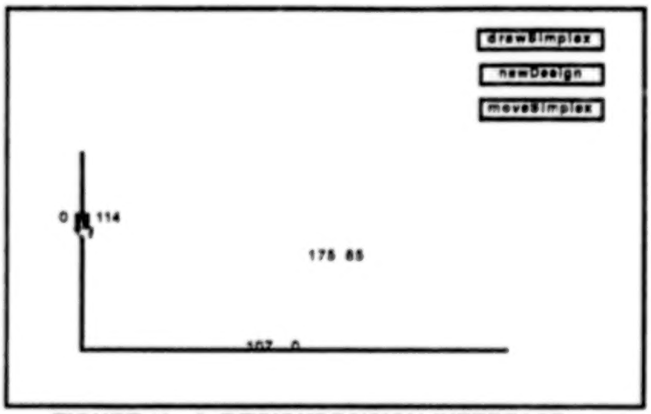

FIGURE 10. A *DESIGNDECISION* INTERFACE.

WALK-THROUGH IMPLEMENTATION OF A HALE DESIGN

Users will have made several system-level choices prior to reaching the aircraft-related portion of the interface which starts with the chart presented in Figure 11 below. This figure is a depiction of the relationship of historical aircraft categories to one another. Users may choose an aircraft category by clicking on any ellipsoidal area. Under each ellipse is an invisible button which is programmed to take users to the branch of the interface designated specifically for the one particular case. Users may then enter more detailed information about the specific aircraft they wish to investigate. Or, they may wish to investigate several alternatives within one class of aircraft such as high altitude long endurance (HALE). Figure 12 presents several choices within the HALE class. Users must make a decision which will again branch the interface. HALE design considerations for each powertrain vary enough from one another to warrant this further branch.

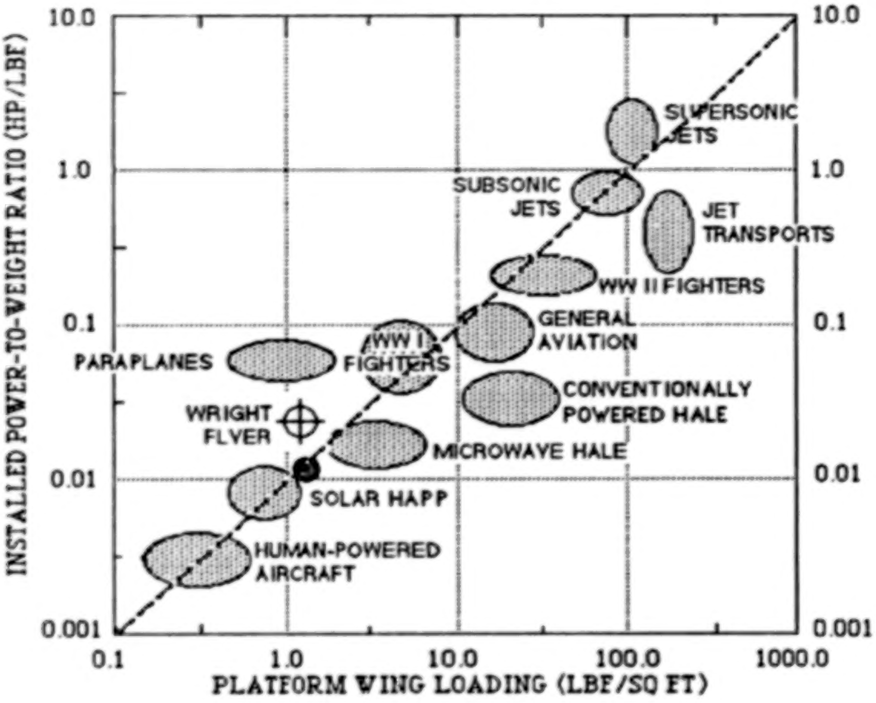

FIGURE 11. HISTORICAL AIRCRAFT CATEGORIES.

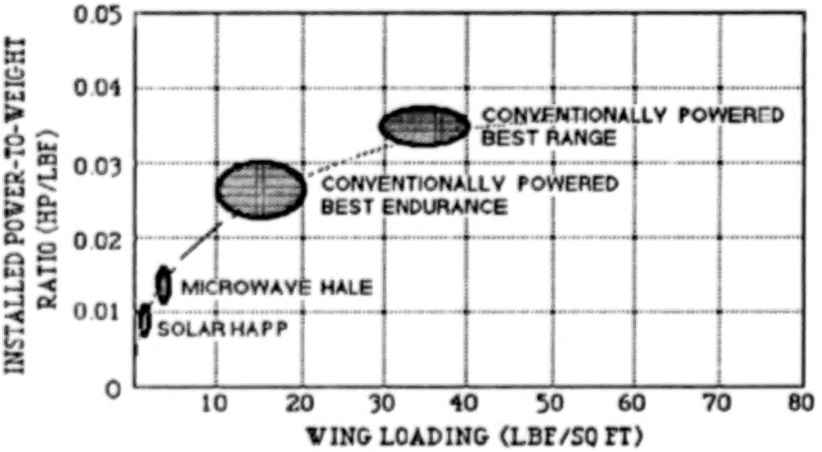

FIGURE 12. HISTORICAL HALE AIRCRAFT CATEGORIES.

Once users have determined which category and sub-category to investigate, they may start entering information about the specific aircraft they wish to model.

As an example, Figure 13 shows how a generic HALE mission profile may be described. This schematic has invisible HyperCard fields adjacent to each mission leg label which users may tab through when entering data. Tabbing is clockwise and returns users to the field in which they started. To exit, users have choices of returning to a previous screen or going to the next by clicking on the "Done" button. Returning to a previous screen voids entries and going to the next screen accepts them.

At this point, users have choices of investigating point designs or doing parametric analyses. Parametric analyses start with defining ranges of design parameters to be investigated by using an entry screen similar to that shown in Figure 14.

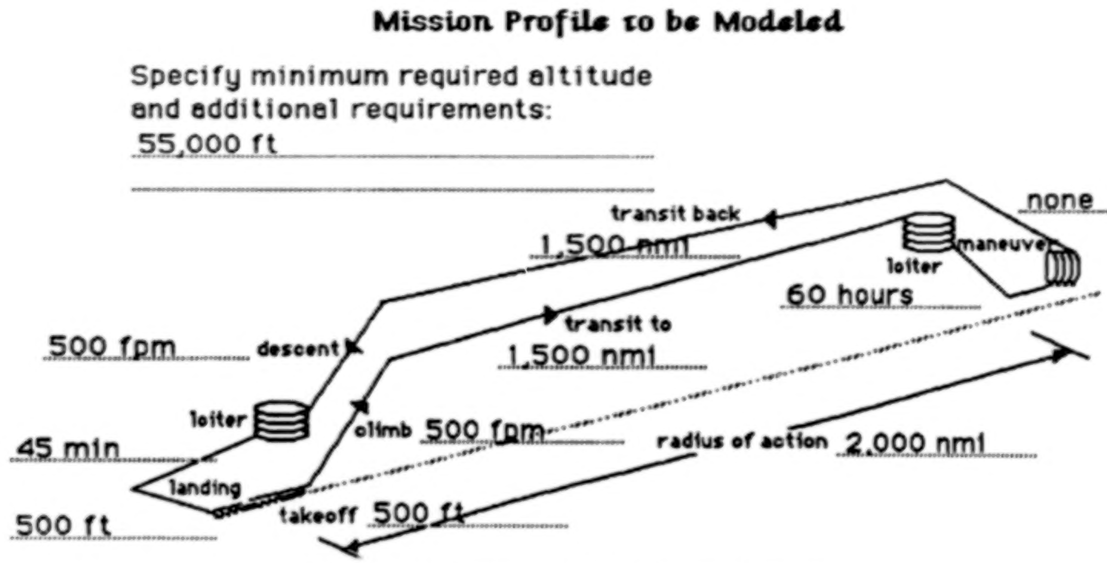
Mission Profile to be Modeled

Specify minimum required altitude
and additional requirements:
55,000 ft

FIGURE 13. TYPICAL HALE MISSION PROFILE.

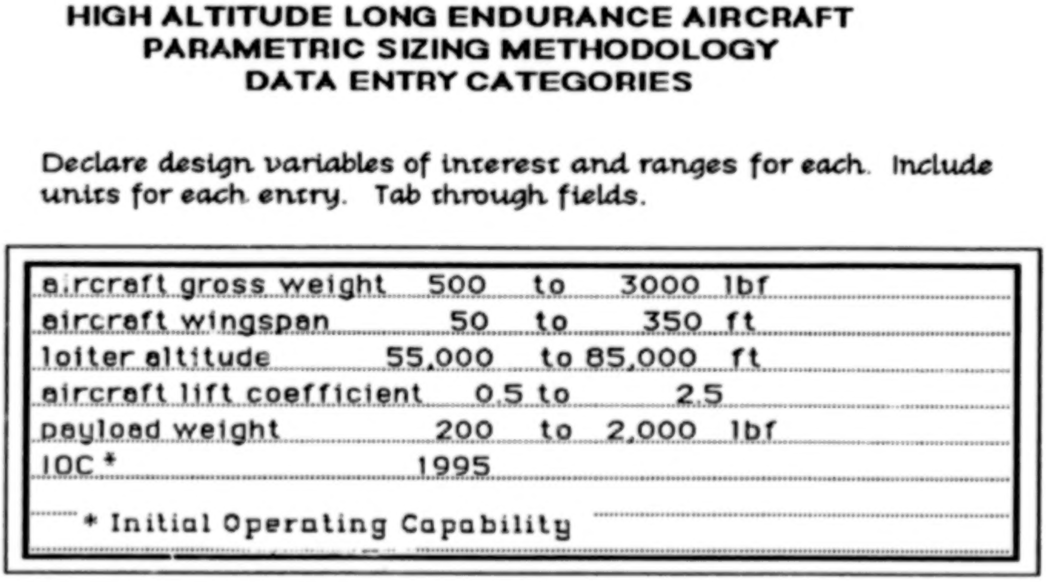
**HIGH ALTITUDE LONG ENDURANCE AIRCRAFT
PARAMETRIC SIZING METHODOLOGY
DATA ENTRY CATEGORIES**

Declare design variables of interest and ranges for each. Include units for each entry. Tab through fields.

aircraft gross weight 500 to 3000 lbf
aircraft wingspan 50 to 350 ft
loiter altitude 55,000 to 85,000 ft
aircraft lift coefficient 0.5 to 2.5
payload weight 200 to 2,000 lbf
IOC * 1995

* Initial Operating Capability

FIGURE 14. PARAMETRIC DATA ENTRY SCREEN.

Output may be presented in several formats, one of which is presented in simplified form in Figure 15 below. At times, users may want to examine the effect of changes in propulsion cycle on figures of merit for their chosen mission. Endurance is an obvious figure of merit with which to examine the effect of propulsion cycle choice. Numeric and symbolic data may be manipulated to provide curves which identify domains of endurance for which each propulsion cycle is best suited. Ideally, users would be able to click on any point on these curves and examine calculated design parameters in more detail.

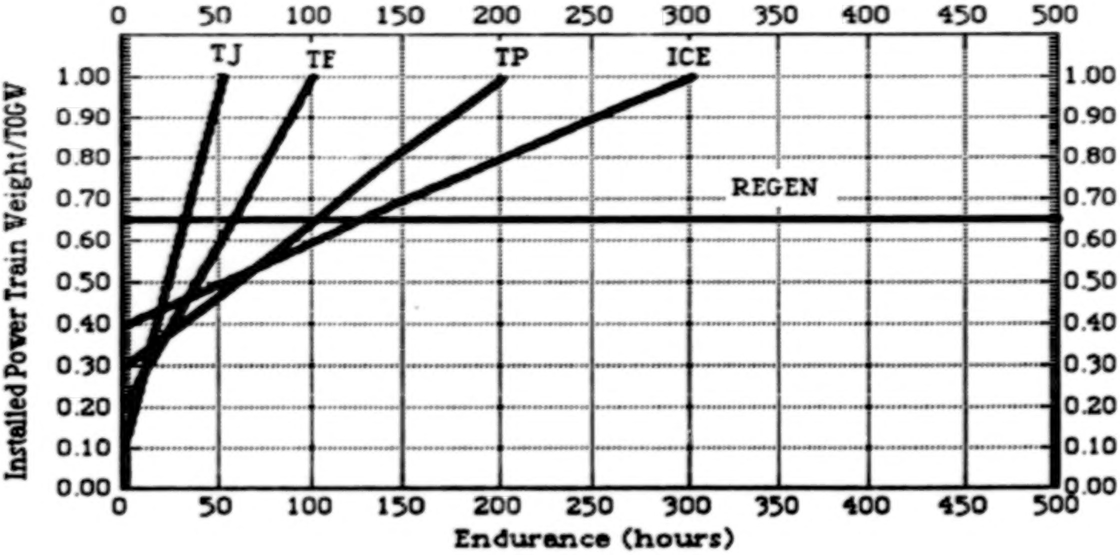

FIGURE 15. EFFECT OF ENGINE CYCLE CHOICE ON ONE DESIGN PARAMETER.

A more useful format, perhaps, for these investigations of domains of design points which satisfy a given set of conditions is a parametric plot such as Figure 16 below which is one of several parametric plots created during a feasibility study of a microwave powered HALE aircraft [14]. This plot would be the result of calculations done after users have made branching choices inside the interface. The choices in this case would be regeneratively powered HALE from Figure 11, microwave powered HALE from Figure 12, and an alternative mission profile screen than Figure 12 since microwave HALE mission tracks tend to be more or less circular when viewed from above. Figure 17 below presents a generic microwave HALE mission data entry screen to act as an additional branch to Figure 13.

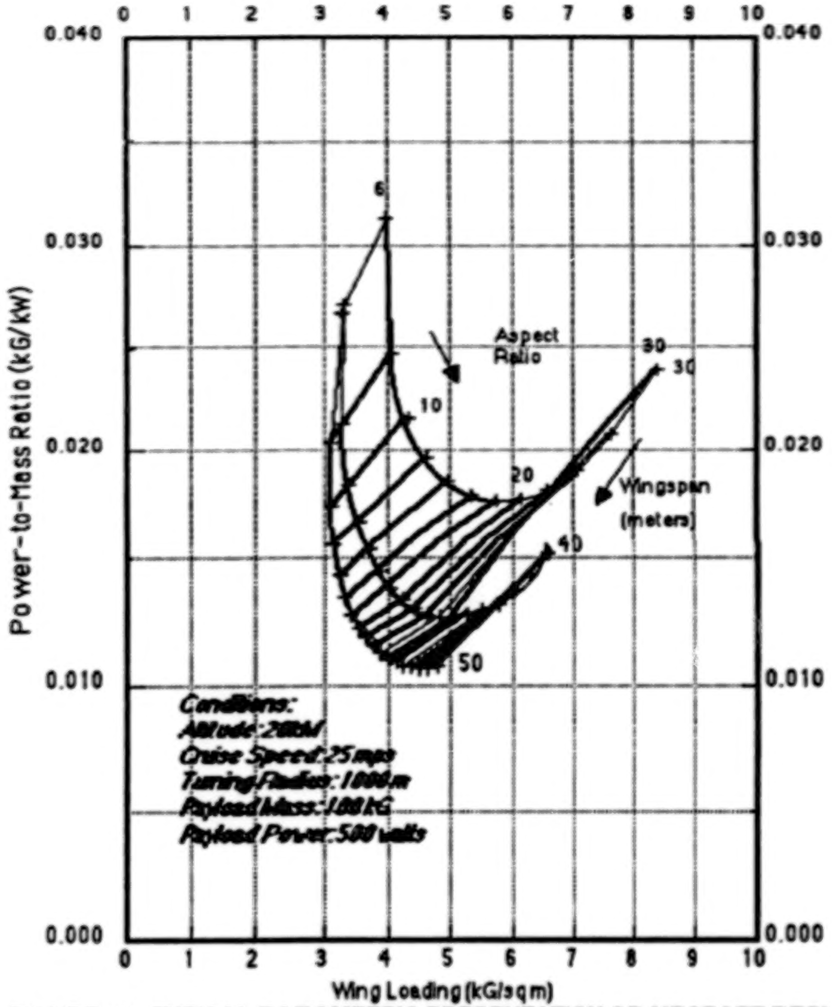

FIGURE 16. TYPICAL PARAMETRIC PRESENTATION OF AIRCRAFT DESIGN DATA.

For a solar powered HALE, an additional mission description screen (Figure 18) branch from Figure 13. Users would identify the part of the world over which a solar HALE would fly by clicking on the general area and HyperTalk would record mouse position at the click. Mouse position could then be converted to latitude and longitude by the card script. Given altitude and time of year, insolation could

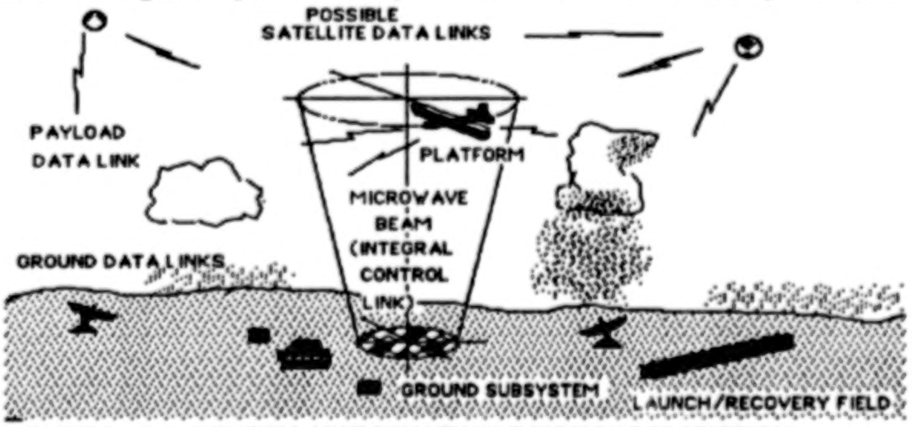

FIGURE 17. A GENERIC MICROWAVE HALE MISSION DESCRIPTION.

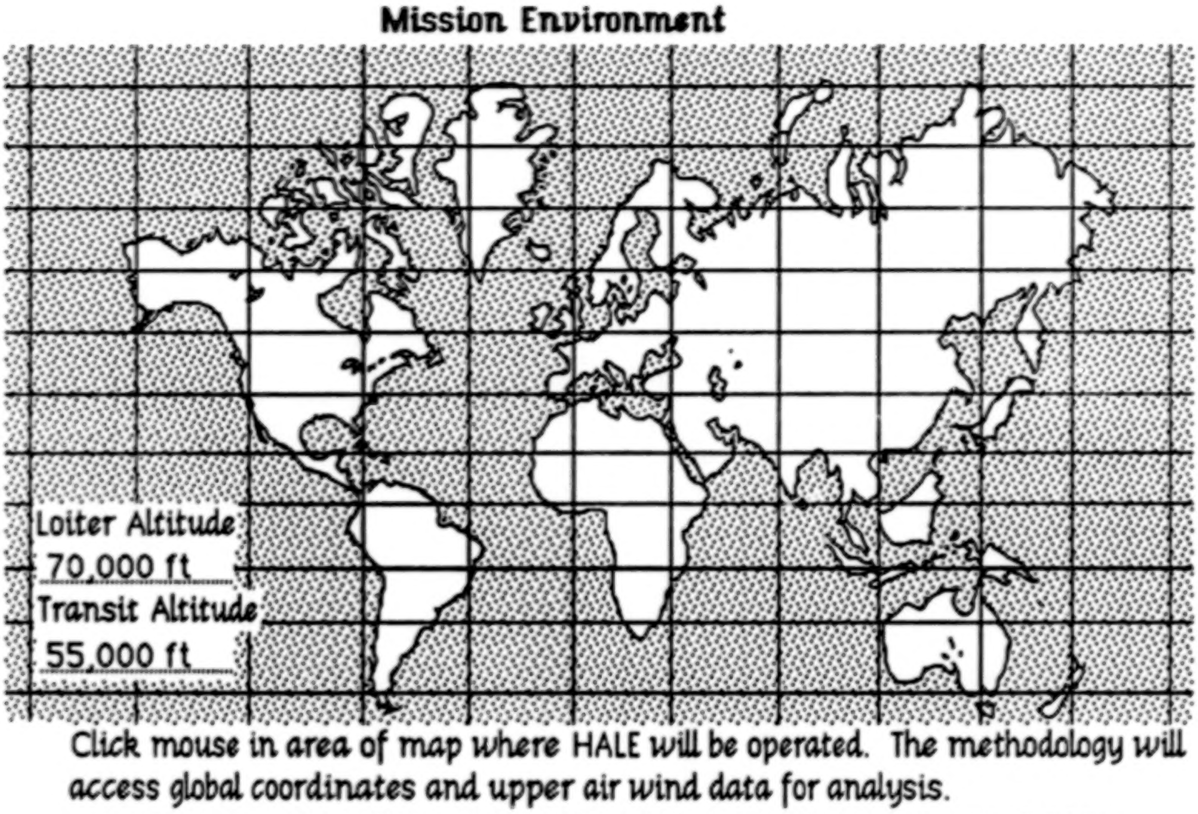

Loiter Altitude: 70,000 ft

Transit Altitude: 55,000 ft

Click mouse in area of map where HALE will be operated. The methodology will access global coordinates and upper air wind data for analysis.

FIGURE 18. BRANCH SCREEN FROM FIGURE 13 FOR SOLAR POWERED HALE AIRCRAFT.

easily be computed using methods similar to those presented in ref. 15. Following mission data entry, the interface could define payload dimensions and constraints with a screen similar to Figure 19. The interface would then deal with the airframe by branching from a screen similar to Figure 3 to Figure 20 to describe the structural concept.

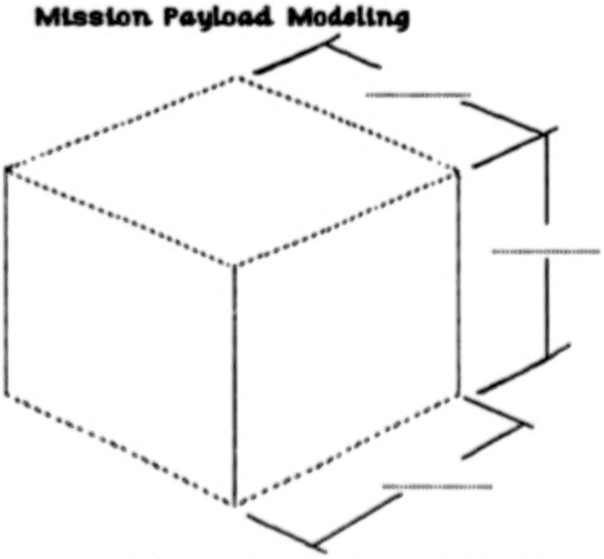

FIGURE 19. PAYLOAD SPECIFICATION.

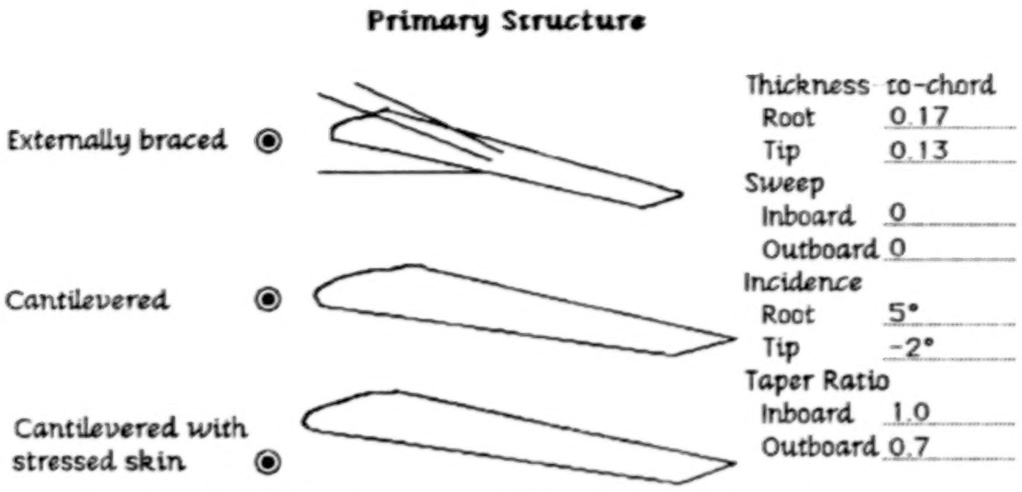

Thickness to-chord
Root 0.17
Tip 0.13
Sweep
Inboard 0
Outboard 0
Incidence
Root 5°
Tip -2°
Taper Ratio
Inboard 1.0
Outboard 0.7

FIGURE 20. PRIMARY STRUCTURE SPECIFICATION FOR WINGS.

IMPLEMENTING THE DESIGN METHODOLOGY IN *windFrame*

Two critical questions arise concerning implementation of the high altitude long endurance aircraft design methodology using *windFrame* . How do the design tasks outlined in the walkthrough map onto the basic elements of the *windFrame* computer programming language for aircraft design? How would some of the critical pieces of the *windFrame* design interface be implemented in HyperCard? These implementation issues are addressed in this section.

The power loading and wing loading relationships shown in Figures 11 and 12 represent a theoretical relationship between these parameters which all reasonable aircraft must satisfy, at least approximately. The existence of such a relationship suggests that this part of the design methdology should be implemented using the *theories&Models* elements of *windFrame.*

Several interesting issues arise at this point. Recall that the *theories&Models* elements of *windFrame* are conceptually at the intersection between system functions and alternative design concepts. Yet, the wing loading/power loading plots are intended to identify classes of aircraft. The designer is supposed to choose the class of aircraft that is most appropriate for the mission. From this point of view, the Figure 11 and Figure 12 interfaces are *designDecisions.* The *attributes* to be chosen are *ranges* of wing-loading and power loading. Can a convenient *conceptElement* be identified in association with these *attributes* ? An **aircraft** *conceptElement* seems a likely choice. The *function* element should probably be **perform mission** (Figure 13). The **perform mission** *function* will have some *functionAttributes* associated with it, specifying ranges, altitudes, maneuvers and speeds. At the level of the **historical aircraft categories** *designDecision* , the level of approximation employed in a *theory/Model* describing how a given alternative (one of the aircraft categories) performs the **perform mission** function is that gust loads, maneuver requirements and loads, maximum speeds, payload/range/endurance requirements, structural and fuel weight fractions associated with the mission determine an approximate relationship between the relative size of the propulsion system (power loading) and the magnitude of the aerodynamic forces and moments generated by the aircraft (wing loading).

This example indicates that the basic elements of the *windFrame* language provide an excellent way to implement the walkthrough design process in HyperCard. However, the high altitude long endurance aircraft design methodology as it has been developed so far does not make full use of the expressive power of *windFrame* , at least for the **historical aircraft categories** *designDecision* being considered here. The value of this expressive power can be seen if we consider a slightly different use for the same *windFrame* language elements. What if the designer wanted to assess the impact of a new structural material or design concept, a new set of design criteria for gust loads, or a different approach to flying a certain mission? The same *windFrame conceptElements, theories&Models,* and *designDecisions* could be used to determine where the new concept falls on the **historical aircraft categories** plot. This information could help to assess whether an existing class of aircraft might be able to play a new role, or to identify that a totally new class of aircraft is needed.

RESULTS AND CONCLUSIONS

Significant progress toward the development of *windFrame* has been achieved. A carefully thought-out design for the computer programming language has been developed. This design was developed through walkthrough implementations of an existing high altitude long endurance aircraft design methodology. Used with this methodology, *windFrame* provides a convenient way to integrate traditional aircraft design practice with systems engineering discipline. *windFrame* has also been designed to provide support for "metaDesign", a process in which new technologies and evolving requirements are rapidly integrated into design concepts by "designing the design process" concurrently with the design of the aircraft.

Design decision-making is the primary emphasis for the design approach embodied in the *windFrame* computer programming language for design. The highly graphics/user interface-oriented programming style supported by HyperCard is a particularly compatible approach. Key elements of the decision support interface have been prototyped in HyperTalk and integrated with designer interface prototypes developed as part of the walkthrough implementation. Together, these HyperCard computer programs provide a prototype of the *windFrame* language which can be used for concept demonstration. Interested readers may wish to obtain references 16 through 18. These references are HyperCard stacks containing demonstrations of user interfaces and other aspects of the prototype *windFrame* design language. They are available through David Hall Consulting or NASA/Ames Research Center Advanced Plans and Programs Office.

REFERENCES

1. Stinton, Darrol P., The Design of the Aeroplane, Van Nostrand ReinholdCompany, New York, 1983.

2. Abelson, Harold & Sussman, Gerald & Julie, Structure and Interpretation of Computer Programs, The MIT Press, McGraw-Hill Book Company, Cambridge, Massachusetts, 1985.

3. Elias, Antonio L., "Knowledge Engineering of the Aircraft Design Process", Chapter 6 in Knowledge Based Problem Solving, Kowalic, J.S., ed., Prentice-Hall, Englewood Cliffs, New Jersey, 1985.

4. Kolb, M.A., "A Flexible Aid for Conceptual Design based on Constraint Propagation and Component-modelling", AIAA-88-4427 ,AIAA/AHS/ASEE Aircraft Design, Systems, and Operations Meeting, Sept. '88

5. Rosenfeld, L., "Intelligent CAD Systems - CAEDM for the 90's", 6th National Conference on University Programs in Computer-Aided Engineering, Design, and Manufacturing, June 1988, Atlanta, Georgia.

6. Bouchard, E.E, "Applications of AI Technology to Aeronautical Systems Design", 6th National Conference on University Programs in Computer-Aided Engineering, Design, and Manufacturing, June 1988, Atlanta, Georgia.

7. Floyd, Bryan, "Synergistic Information Systems", 6th National Conference on University Programs in Computer-Aided Engineering, Design, and Manufacturing, June 1988, Atlanta, Georgia.

8. Steinke, G., "Engineering by the Book . . . And On-Line", Mechanical Engineering, November 1985.

9. Anonymous, Apple Macintosh HyperCard User's Guide, Apple Computer, Inc., Cupertino, California, 1987.

10. Brei, M.L., et al., Architecture and Integration Requirements for an ULCE Design Environment, IDA Paper P-2063, Institute for Defense Analyses, Alexandria,Virginia, April 1988.

11. Anonymous, Systems Engineering Management Guide, Defense System Management College, Contract MDA 903-82-C-0339, Lockheed Missiles andSpace Company, Inc., October 1983.

12. Anonymous, MacScheme Reference Manual, Semantic Microsystems, Inc., Beaverton, Oregon, 1986.

13. Fleury, C., and Schmit, L.,"Discrete-Continuous Variable Synthesis Using Dual Methods", AIAA Journal, v. 16, no. 12, December 1980.

14. Bouquet, Donald L., Hall, David W. and McElveen, R. Parker,II, "Feasibility Study of a Carbon Dioxide Observation Platform System", NASA/MArshall Space Flight Center Contractor Report, 1987.

15. Hall, D.W., Fortenbach, C.D., Dimiceli, E.V. and Parks, R.W., "Feasibility of Solar Powered Aircraft and Associated PowerTrains", NASA/Langley Research Center C ontractor Report 3699, 1982.

16. Hall, D.W., "A Guided Tour of Our Developing HALE Methodology", HyperCard stack, David Hall Consulting, Sunnyvale, CA, March 1988.

17. Hall, D.W., "Development of an Integrated Design System for High Altitude Long Endurance Aircraft for Microcomputer Systems", HyperCard stack, David Hall Consulting, Sunnyvale, CA, March 1988.

18. Hall, D.W. and Rogan, J.E., "Development of an Integrated Design System for High Altitude Long Endurance Aircraft for Microcomputer Systems", HyperCard stack, David Hall Consulting, Sunnyvale, CA, June 1988.

DEMONSTRATION OF DECOMPOSITION AND OPTIMIZATION IN THE DESIGN OF EXPERIMENTAL SPACE SYSTEMS

Sharon L. Padula
NASA Langley Research Center
Hampton, VA

Chris A. Sandridge
Virginia Polytechnic Institute and State University
Blacksburg, VA

Raphael T. Haftka
Virginia Polytechnic Institute and State University
Blacksburg, VA

Joanne L. Walsh
NASA Langley Research Center
Hampton, VA

INTRODUCTION

Effective design strategies for a class of systems which may be termed Experimental Space Systems (ESS) are needed. These systems, which include large space antenna and observatories, space platforms, earth satellites and deep space explorers, have special characteristics which make them particularly difficult to design. This paper will argue that these same characteristics encourage the use of advanced computer-aided optimization and planning techniques.

The broad goal of this research is to develop optimization strategies for the design of ESS. These strategies would account for the possibly conflicting requirements of mission life, safety, scientific payoffs, initial system cost, launch limitations and maintenance costs. The strategies must also preserve the coupling between disciplines or between subsystems. For instance, the strategies must recognize that changes in the structural design influence the selection of materials and the design of the control system. This research is unique because it focuses on optimization of multidisciplinary system design problems and because it emphasizes automated decomposition of these system design problems.

The specific purpose of the present paper is to describe a computer-aided planning and scheduling technique. This technique provides the designer with a way to map the flow of data between multidisciplinary analyses. The technique is important because it enables the designer to decompose the system design problem into a number of smaller subproblems. The planning and scheduling technique is demonstrated by its application to a specific preliminary design problem.

CHARACTERISTICS OF EXPERIMENTAL SPACE SYSTEM DESIGN

Experimental space systems have special characteristics which make them difficult to design. Many of these characteristics are a function of the unique environment in which ESS operate. Space-based hardware must perform flawlessly in microgravity, yet must withstand ground-based handling and high launch loads. Exposed to unusual temperature and radiation extremes, they must continue to operate for extended periods of time without servicing. These unique operating conditions call for special mechanisms, built with unusually small tolerances to manufacturing errors. Often, the ESS must be constructed from exotic materials and must be designed to meet weight and packaging constraints.

The design of ESS is further complicated by the fact that these are often "one-of-a-kind" projects. Space satellites and probes are designed to answer questions about our universe. If the original mission is a success, then it need not be repeated. If the mission fails to operate or returns unexplained results, then the system must be redesigned.

Designing "one-of-a-kind" projects is essentially different from the usual task of improving an existing product to meet new specifications. First, there is no body of collected information to consult and there is limited expertise acquired from related experiences. Thus, the designer has less confidence in his intuitive design decisions. Building and testing of prototype designs might supply some of this missing information but this is not always possible. Prototypes are very expensive and hard to justify for a "one-of-a-kind" mission. Moreover, if prototypes are constructed, testing them on the ground to predict their operation in space is problematic if not impossible.

The effect of these characteristics of ESS is an emphasis on analytic prediction of performance and a need for more systematic methods of design.

UNIQUE OPERATING CONDITIONS REQUIRE:

- **Special mechanisms**
- **Exotic materials**
- **Extreme precision**
- **Low structural weight**

"ONE-OF-A-KIND" PROJECTS IMPLY:

- **No collected body of information**
- **Few "rules of thumb"**
- **Prototypes hard to justify**
- **No standardized test procedures**

OPTIMIZATION AS A DESIGN TOOL

There are many reasons to believe that optimization will have an expanded roll in future ESS design. First, it is necessary to rely on analytic prediction of the system behavior. Thus, integration of existing optimization and analysis codes should be practical. Second, ESS design involves many interrelated subsystems, many independent design variables and extremely stringent constraints. Thus, formal optimization may be the only practical way to find a feasible design. Finally, ESS designs are costly to manufacture and launch. A design which can be improved via optimization may result in substantial savings.

There are problems with the use of optimization in ESS. The most obvious problem is that optimization requires repeated execution of the system analysis codes. Often these codes require large amounts of computer resources for even a single execution. Another problem is that the performance of optimization codes often degrades as the number of design variables grows. A final problem is that optimization techniques work best when a single goal can be unambiguously defined. There is no accepted way to deal with the multiple conflicting goals which are required by the current state of the art in ESS design.

Optimization, including mathematical programming and optimal control, has been successfully employed in past experimental space system projects [1-3]. However, for the most part, optimization is used to refine some component of a nearly completed design.

Current optimization research involves extending the use of optimization to the preliminary design of an overall system [4-7]. Formulating the problem correctly is the most difficult part of system optimization. Unfortunately, tricks which facilitate optimization of one problem do not automatically apply to the next one.

AFFIRMATIVE	NEGATIVE
Analytical models exist	**Enormous compute times**
Feasible designs not obvious	**Numerous design variables**
Substantial savings possible	**Multiple conflicting goals**

THE COFS EXPERIMENT

A specific example of an experimental space system is used to illustrate the points to be made in this paper. Control of Flexible Structures (COFS) was a project initiated by NASA Langley to develop validated technology for the control of future large space structures [8,9]. The COFS I Mast Flight System (MFS) is a truss structure, attached to the shuttle, used to study techniques for system identification and active control. It must be designed to maximize the value of scientific data collected while minimizing cost and weight of the structure. Moreover, the system must be safe and reliable to operate and must withstand adverse conditions during launch and deployment.

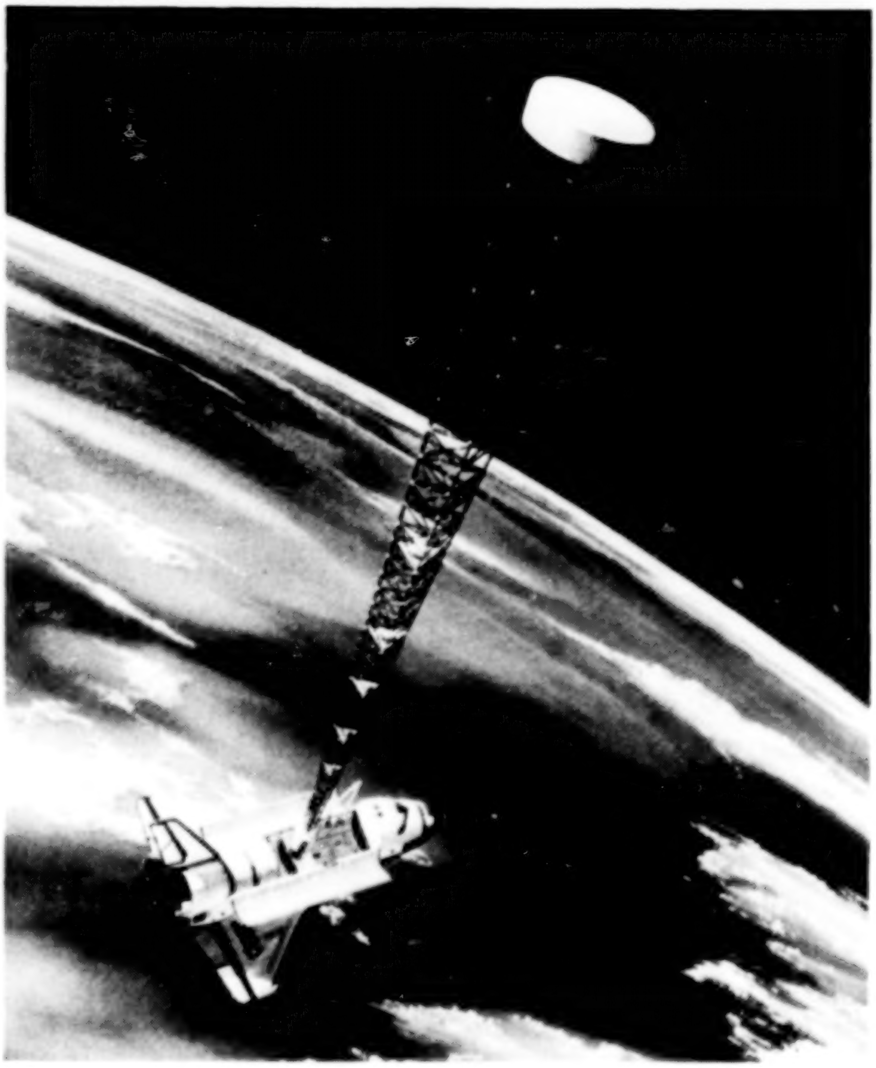

MULTILEVEL DECOMPOSITION

One promising technique for optimizing a multi-objective system such as the COFS I Mast Flight System is called multilevel decomposition [10]. This technique divides the total system optimization problem into subproblems, each with its own objective and with a reduced number of design variables. For instance, the COFS I problem might be divided into 3 subproblems. The first is to design the structure for minimum weight, the second is to design the control system minimizing a composite objective based on cost and control effort and the last is to design the placement of sensors and the application of dynamic loads to increase the value of the scientific data collected. All of these subproblems must be coordinated so that the final design is feasible and so that the cost of the project is minimized.

Several techniques for solving multilevel problems exist. At least one technique has been tested for a complicated system with a great number of design variables and has proved to be quite effective [11].

The present techniques for multilevel optimization do not include a strategy for decomposing a given system into subproblems. Merely drawing the figure below is insufficient. It is necessary to identify the design variables, analysis steps and constraints which are associated with each subproblem. A first step toward automatic decomposition is described in reference 12. This technique uses the sensitivity derivatives of the multiple objectives to decompose the system. Reference 12 describes an application where each of the objectives is nominally a function of each design variable and where each objective is computationally similar. The present research emphasizes system design problems having many dissimilar objectives, each of which is a function of some subset of all design variables.

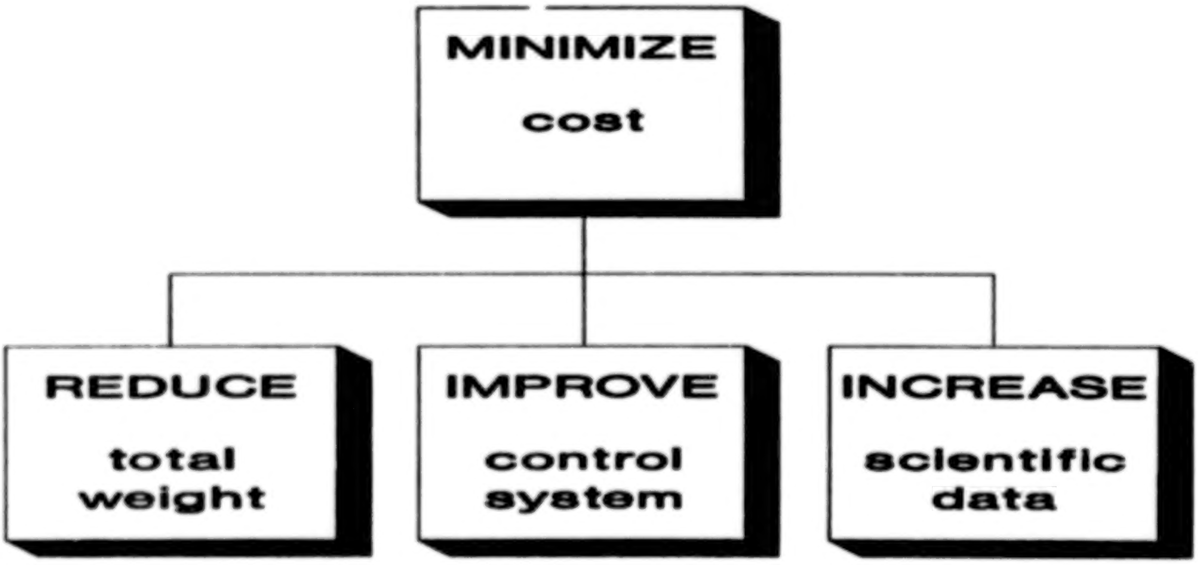

PLANNING AND SCHEDULING (P&S) TECHNIQUE

This paper explores the use of automatic planning and scheduling (P&S) techniques to assist in the decomposition. These techniques were originally developed as project management tools [13]. They can reorder a set of tasks so that all prerequisites are available when a given task is begun. The input to the P&S computer program is a list of tasks with their prerequisites. The output can be a network graph such as the one in the figure.

In the network graph below, notice that task 2 must be completed before task 4 can begin. This is indicated by the circle at the intersection of lines which exit horizontally from the box marked 2 and enter vertically the box marked 4. Indirectly, task 2 is also a prerequisite to task 5 because task 4 must precede 5 and 2 must precede 4.

A slightly unusual feature of this particular network is the feedback path from task 7 to task 4. This indicates that tasks 4,5,6 and 7 are their own prerequisites. Such a set of tasks is called a circuit. Some P&S programs can identify circuits and temporarily replace them with a single task so that the network graph can be completed. The presence of circuits in a network graph alerts the project manager that this set of tasks may have to be repeated several times before the results are satisfactory.

A planning and scheduling computer program which can handle circuits may be a useful decomposition tool. If the tasks in this network are thought of as design variables and constraints then circuits can be interpreted as optimization loops. This idea will be illustrated using the COFS I MFS example.

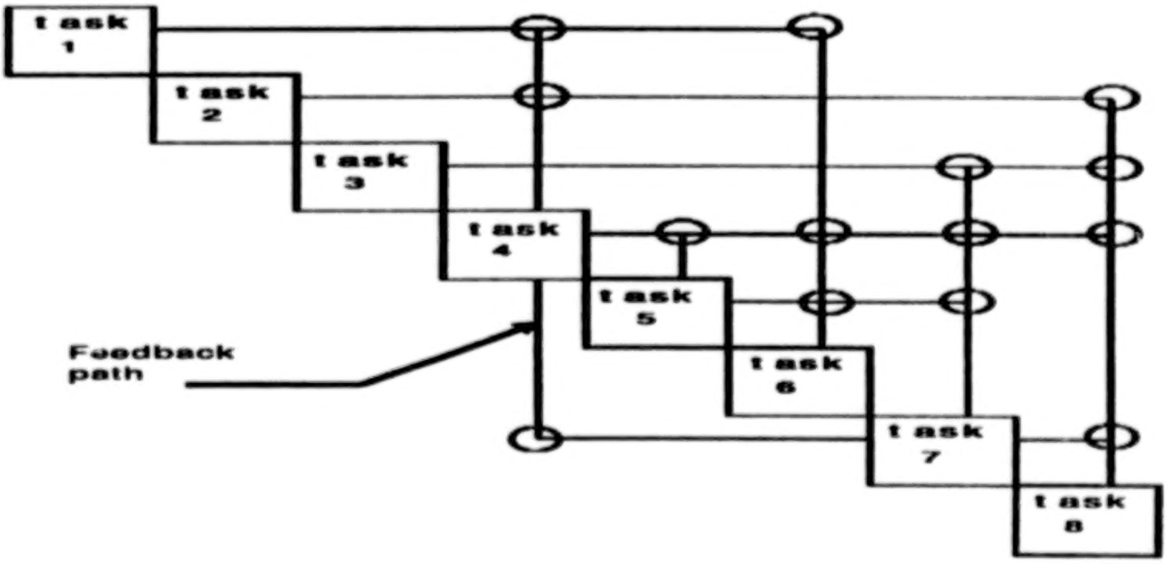

COFS I MINI-EXAMPLE

First, consider a much simplified version of the COFS I experiment. Assume that the problem is to design a space truss for testing system identification techniques. The ultimate objective is to reduce the cost of the system. Other objectives are to design a structure that can carry the required loads and which is challenging to test based on its closely spaced vibrational frequencies.

minimize:

SYSTEM COST

subject to:

(1) STRUCTURE FEASIBLE

(2) SYSTEM I.D. INTERESTING

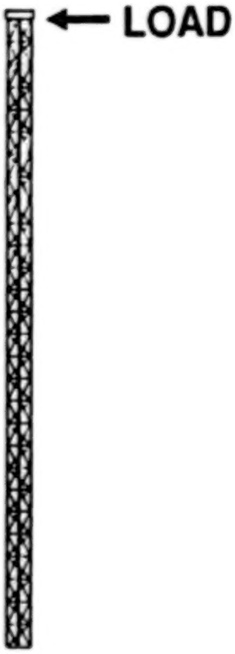

P&S STEP 1. LIST DESIGN VARIABLES

In order to apply planning and scheduling to the COFS I problem, first the design variables (v_i) must be identified. There are many possible design variables, but the length of one bay of the truss and the number of bays in the MFS are certainly important. Other possibilities are the diameter and thickness of truss elements and the number and location of sensors. Notice that some of the variables mentioned are scalars while others, such as the location of all sensors, are arrays. This is done to condense the amount of information processed by the planning and scheduling program. It will not be a problem if all the elements in the array are updated and used as a group.

symbol	meaning
v1	length of bay
v2	number of bays
v3	number of sensors
v4	truss element sizes
...	...

P&S STEP 2. LIST BEHAVIOR VARIABLES

The next step is to identify important quantities which are calculated from known values of the design variables. For the purpose of this paper, these calculated quantities will be termed behavior variables (b_i). Examples are the bending stiffness of the beam and the extra weight associated with the joints between elements. For instance, the symbol b3 is used to represent the results of an eigenvalue analysis routine. That is, b3 represents all of the mode shapes and vibration frequencies of the MFS.

symbol	meaning
b1	bending stiffness
b2	extra weight of joints
b3	mode shapes & frequencies
...	...

P&S STEP 3. LIST GOALS AND CONSTRAINTS

The next step in applying planning and scheduling is to quantify all known constraint functions (g_i). The COFS I experiment has constraints on the total weight of the system and on the vibration frequencies of the MFS and of the individual truss elements.

symbol	meaning
g1	total wt < allowable
g2	member freq. >> mast freq.
g3	fundamental freq. near target
g4	closely spaced frequencies
...	...

P&S STEP 4. PREPARE INPUT

The final step is to prepare the input to the planning and scheduling program. For each design variable, behavior variable and constraint function, there is a separate line in the input file. This line contains a symbol, an alphanumeric name and a list of dependencies. For example, the last line in the figure shows the symbol g4 is associated with the name COUPLING and that the value of this constraint function depends on b3. In physical terms, this means that there is a test to determine if two vibration frequencies are close together. Thus, the value of this constraint only depends on the values of all vibration frequencies.

The list of dependencies for constraints like g4 (COUPLING) or behavior variables like b3 (MODES) is simply a list of the design variables and behavior variables needed to evaluate that function. The meaning of dependencies in the case of a design variable such as v1 (LONGL) may not be as obvious. However, the task of selecting a new value for a design variable such as the length of a longeron is influenced by the values of one or more constraint functions. If any constraint is violated then the optimizer will adjust the value of v1.

symbol	name	depends on
v1	LONGL	g1,g2,g3,g4,g10
...	...	...
b3	MODES	v1,v3,b1,b4
...	...	...
g4	COUPLING	b3
...	...	...

COFS I NETWORK GRAPH

This figure shows the network graph for the simplified COFS I problem. The planning and scheduling program identified three circuits in the network. These circuits correspond to three optimization subproblems:

1) determine the structural sizing for minimum weight,

2) determine dynamic excitation strategy for safe testing of the MFS, and

3) determine the best placement of the sensors for identification of mode shapes and frequencies.

This example is relatively simple. However, it illustrates a decomposition technique which can be applied to much more complicated experimental space system designs where the decomposition is not at all obvious.

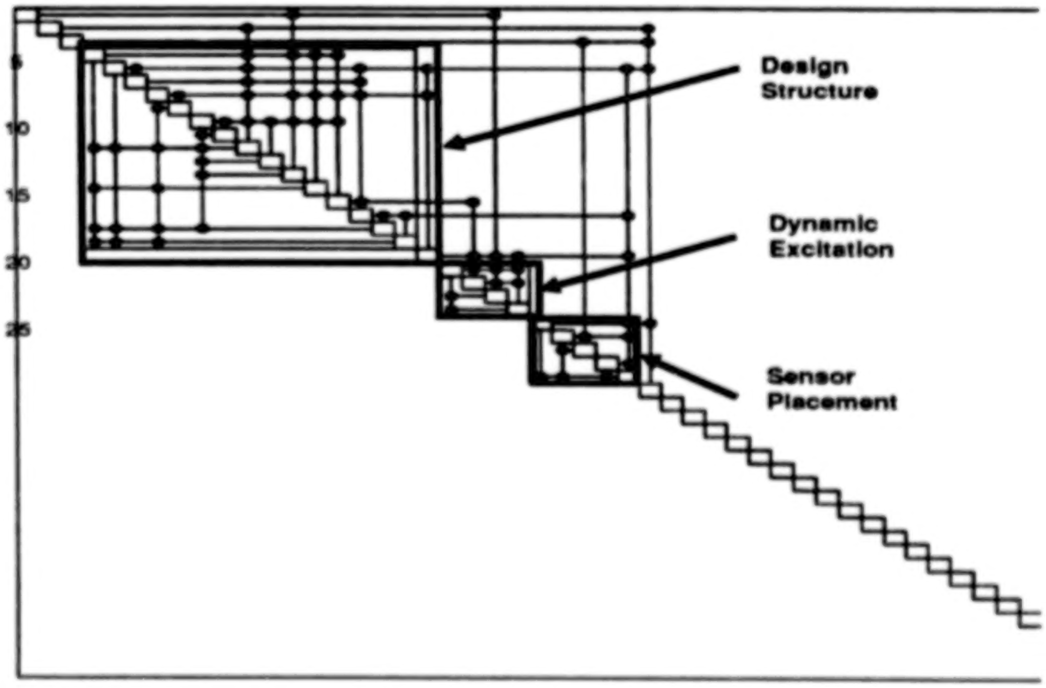

UPDATE THE INPUT

The beauty of the planning and scheduling technique is evident when the design problem requires updating. The effect of new variables and constraints can be examined by simply adding them to the P&S input file.

For example, consider modifying the simple COFS I problem above to account for a number of actuators attached to the COFS I MFS. These actuators are used for dynamic excitation of the MFS.

The figure illustrates the addition of two design variables and one constraint to the P&S input file. The design variables control the number and location (L_A), and the mass (M_A) of actuators. One of these variables, the mass, is marked "no-input". This means that the mass of each actuator is initialized along with other system level variables and is not changed by any optimization subproblem. One constraint which evaluates the effectiveness of actuator placement (CONTROL) is also added.

Besides adding new lines to the input file, the designer must check whether any of the existing variables depend on those added. In the present example, the actuators have a significant mass and therefore they will effect the calculation of mode shapes and vibration frequencies. Notice that v11 (L_A) and v12 (M_A) have been added to the list of dependencies of behavior variable b3 (MODES).

symbol	name	depends on
v1	LONGL	g1,g2,g3,g4,g10
v11	*L_A*	*g11,g14*
v12	*M_A*	*no-input*
...	...	...
b3	MODES	v1,v3,b1,b4,*v11,v12*
...	...	...
g4	COUPLING	b3
...	...	...
g14	*CONTROL*	*v11,v12,b3*

MODIFIED NETWORK GRAPH

The network graph produced for the updated COFS I design problem is shown here. Notice that the P&S program identified just a single large circuit. This suggests that either the COFS I design must be solved as a single large optimization problem, or that the input file must be revised to permit decomposition.

Careful examination of the network graph reveals that there are just two feedback paths which prevent this network from decomposing the way the last one did. These feedback paths begin at the shaded box associated with the power requirement (POW_REQ) constraints. At least one of these feedbacks can be easily removed. Notice that POW_REQ is connected to both L_A and L_S tasks. This expresses the fact that the total power required by the system is influenced by the number of actuators and by the number of sensors. However, actuators require orders of magnitude of more power than do passive sensors. Thus, the design will not be greatly effected if both connections between POW_REQ and L_S tasks are removed. The other long feedback path expresses the correct assumption that the location of actuators is an important design variable in both the structures subproblem and in the dynamic excitation subproblem. One solution is to let the structures subproblem decide the value of this variable and force the dynamics subproblem to adjust other variables to compensate.

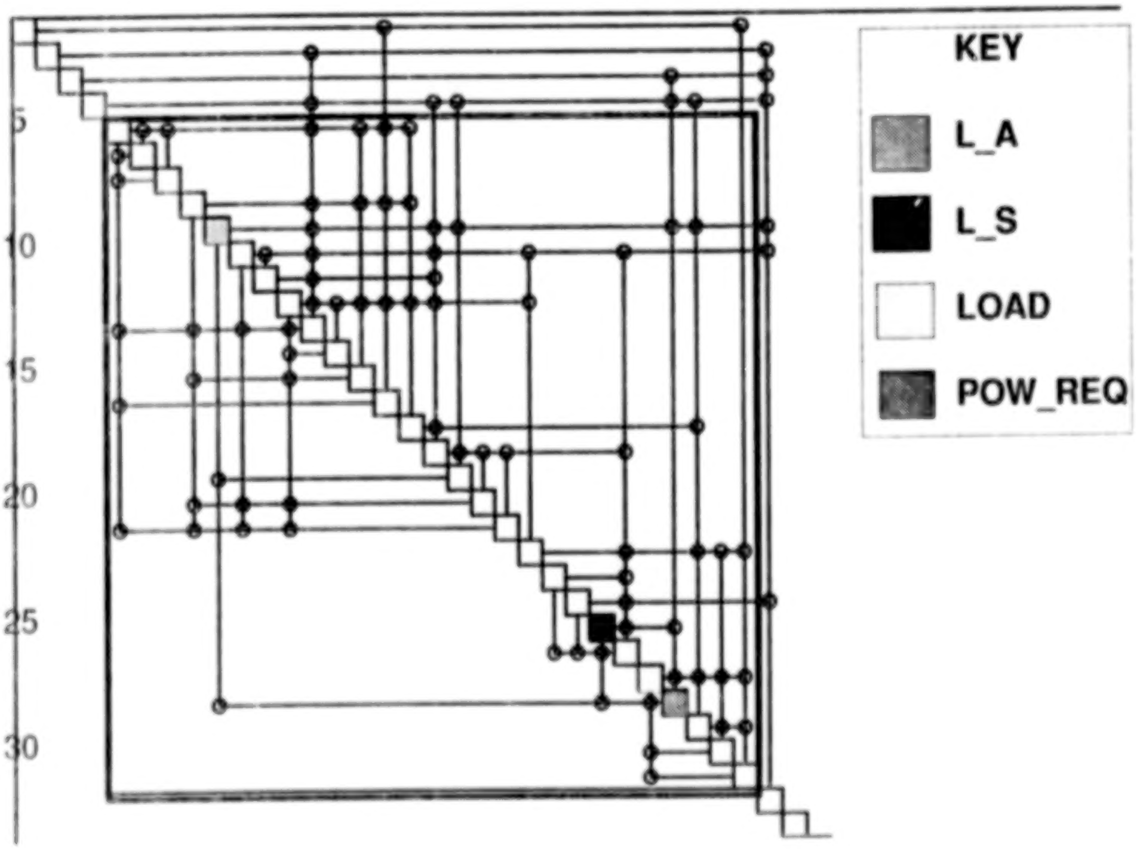

FINAL COFS I NETWORK

By gradually refining the P&S input and by adding design variables and constraints to represent the design of a control system, a final network chart was produced. This network has 6 major circuits: actuator placement, sensor placement, structures and materials design, dynamic excitation specification and a two step controls design. These are identified on the figure.

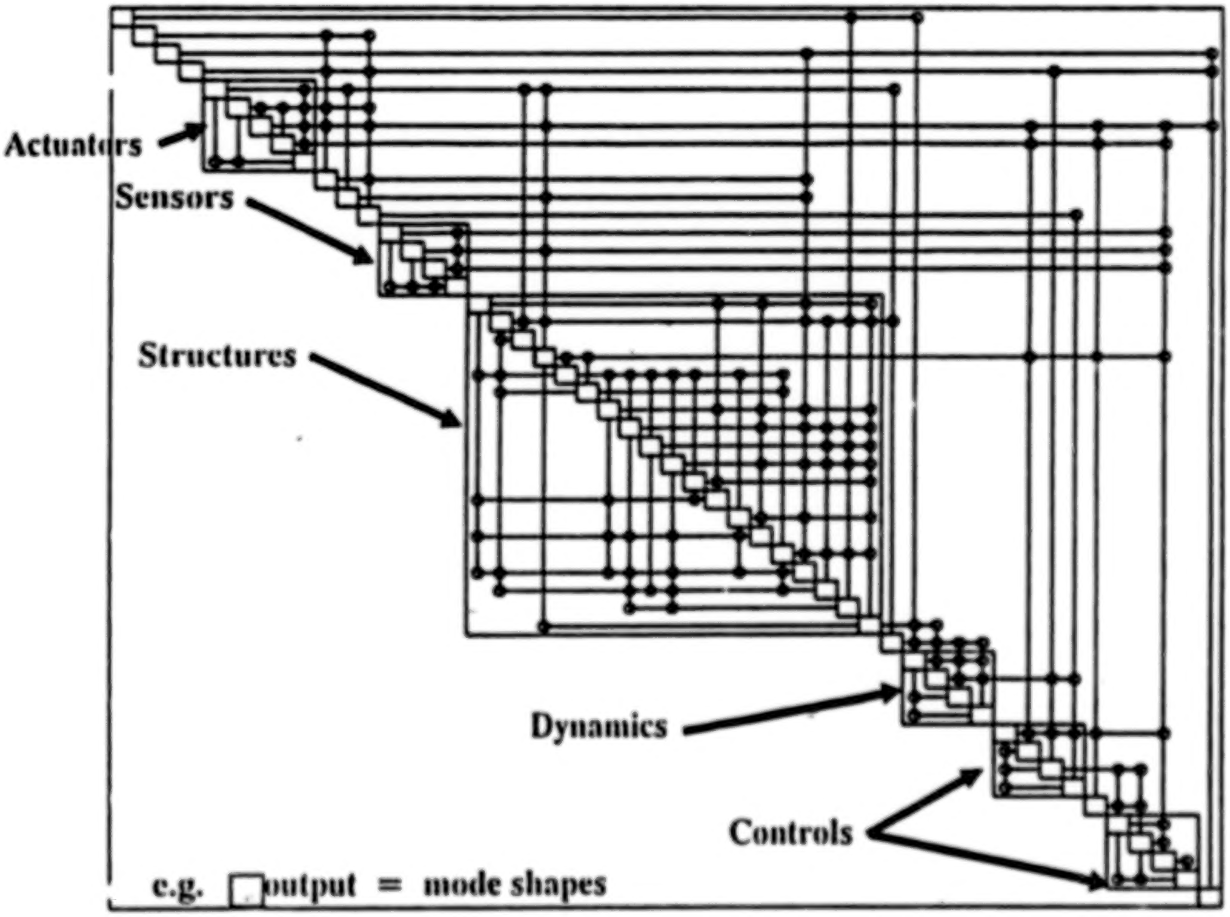

COFS I MULTI-OBJECTIVE OPTIMIZATION PROBLEM

The multi-objective optimization for designing the COFS I MFS is defined by the network graph on the preceding page. The graph indicates which analysis steps must be performed in what order and identifies the flow of data from one step to another. The actual integration of computer codes will be much easier given the wealth of information contained in the P&S network graph.

The plan which emerges for solving the COFS I design problem is summarized by this flow chart. First, system level variables are initialized. These include the mass of an actuator, the target weight of the system, the power provided to the system and the maximum buckling load allowed for any truss element. Next, actuators and sensors are located along the length of the MFS. This can be accomplished manually or using a knowledge-based system similar to that of reference 14. This is followed by a standard optimization to size the structural elements for minimum weight and another optimization to prescribe safe amounts of dynamic excitation. The final step is to design the control algorithm. At the end of the process, the system design is evaluated. If the design is acceptable and no further improvement is likely, then the process terminates. Otherwise, the system level variables can be adjusted and the process repeated. Methods for adjusting the system level variables are explained in reference 15 which contains several options for calculating the sensitivity of the subproblem outputs to changes in the values of the system level variables.

COFS I SYSTEM DESIGN

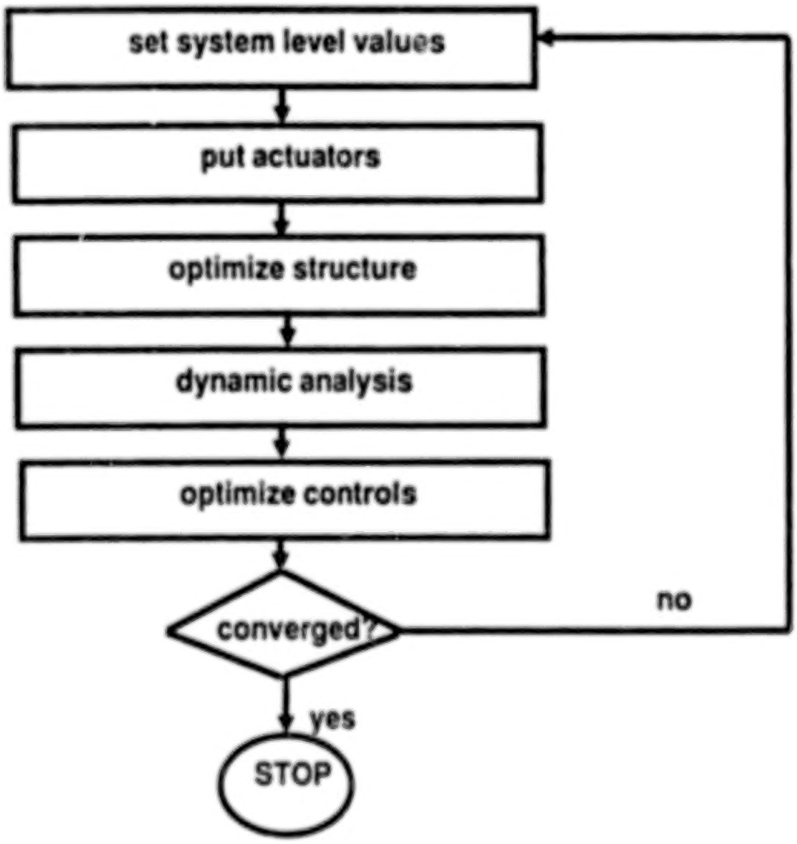

CRITIQUE OF PLANNING AND SCHEDULING

One purpose of the present study is to evaluate the usefulness of automatic planning and scheduling as a tool for decomposition of complicated systems design problems. By applying the technique to the COFS I design, it is seen that P&S is especially helpful in revealing the subtle interaction between disciplines so that the design problem can be decomposed into smaller subproblems. A second benefit of P&S is that it condenses a huge amount of information into a single chart. This chart is easy to store and to update as new information becomes available. More importantly, the network chart provides a "strawman" for experts from different disciplines to discuss.

On the other hand, planning and scheduling does require an investment of time to prepare and refine the inputs. This investment may not be justified for a rather simple problem or for a problem whose decomposition is well understood. Rather, planning and scheduling is proposed as a tool for systematically unraveling a new design problem where the interaction between disciplines is still hazy. As illustrated by the COFS I example, the process of decomposing a new design problem requires engineering judgment. The list of variables and constraints do not appear by magic. Identifying a reasonable set of independent design variables is by no means an easy task. However, this must be done eventually, and the planning and scheduling technique offers a systematic way to attack the problem early in the design cycle.

Reveals interaction between disciplines

Stores and updates info in convenient form

Facilitates communication between experts

Calls for initial investment of time

Requires engineering judgment to complete the decomposition

REFERENCES

1. Sobieski, J. (compiler): Recent Experiences in Multidisciplinary Analysis and Optimization. NASA CR-2327, September 1984.

2. Grandhi, R. V. and Venkayya, V. B.: Structural Optimization with Frequency Constraints. AIAA Paper No. 87-0787, AIAA/ASME/ASCE/AHS 28th Structures, Structural Dynamics and Materials Conference, Monterey,CA, April 1987.

3. Walsh, J. L.: Optimization Procedure to Control the Coupling of Vibration Modes in Flexible Space Structures. AIAA Paper No. 87-0826, AIAA/ASME/ASCE/AHS 28th Structures, Structural Dynamics and Materials Conference, Monterey,CA, April 1987.

4. Barthelemy, J.-F. M.: Development of a Multilevel Optimization Approach to the Design of Modern Engineering Systems. NASA CR-17218, August 1983.

5. Padula, S. L. and Sobieszczanski-Sobieski, J.: A Computer Simulator for Development of Engineering System Design Methodologies. NASA TM-89109, February 1987.

6. Vanderplaats, G. N., Yang, Y. J. and Kim, D. S.: An Efficient Multilevel Optimization Method for Engineering Design. AIAA Paper No. 88-2226, AIAA/ASME/ASCE/AHS 29th Structures, Structural Dynamics and Materials Conference, Williamsburg, VA, April 1988.

7. Mistree, F., Marinopolous, S., Jackson, D. and Shupe, J.: The Design of Aircraft using the Decision Support Problem Technique. NASA CR-4134, April 1988.

8. Wright, R. L. (compiler): NASA/DOD Control/Structures Interaction Technology 1986. NASA CR-2447, November 1986.

9. Ryan, Robert S., and Scofield, Harold N. (editors): Structural Dynamics and Control Interaction of Flexible Structures. NASA CP-2467, April 1987.

10. Sobieszczanski-Sobieski, J.: A Linear Decomposition Method for Large Optimization Problems - A Blueprint for Development, NASA TM-83248, Feb. 1982.

11. Wrenn, G.A., and Dovi, A. R.: Multilevel/ Multidisciplinary Optimization Scheme for Sizing a Transport Aircraft Wing, AIAA Paper No. 87- 0714-CP, AIAA/ASME/ASCE/AHS 28th Structures, Structural Dynamics and Materials Conference, Monterey, CA, April 1987.

12. Bandler, John W. and Zhang, Qi-Jun: An Automatic Decomposition Approach to Optimization of Large Microwave Systems. IEEE Transactions on Microwave Theory and Techniques, Vol. MTT-35, December 1987, pp. 1231-1239.

13. Steward, D. V.: Systems Analysis and Management: Structure, Strategy and Design. Petrocelli Books, Inc., New York, NY, 1981.

14. Rogers, J. L., Feyock, S., and Sobieszczanski-Sobieski, J.: STRUTEX - A Prototype Knowledge-Based System for Initially Configuring a Structure to Support Point Loads in Two Dimensions. NASA TM-100613, April 1988.

15. Sobieszczanski-Sobieski, J.: On the Sensitivity of Complex, Internally Coupled Systems. AIAA Paper No. 88-2226, AIAA/ASME/ASCE/AHS 29th Structures, Structural Dynamics and Materials Conference, Williamsburg, VA, April 1988. (also available as NASA TM-100537)

STRUTEX
A PROTOTYPE KNOWLEDGE-BASED SYSTEM FOR INITIALLY CONFIGURING A STRUCTURE TO SUPPORT POINT LOADS IN TWO DIMENSIONS

James L. Rogers
NASA Langley Research Center
Hampton, Virginia

Jaroslaw Sobieszczanski-Sobieski
NASA Langley Research Center
Hampton, Virginia

INTRODUCTION

Engineers and managers are always concerned about reducing the costs and time involved in completing a design project. Therefore, many hours of research have been devoted to speed and sensitivity improvements in the area of structural analysis. Additional research effort has been applied to the improvement of optimization algorithms. From a numerical standpoint, these areas are nearing a point of diminishing returns when using conventional computer hardware. However, one area which shows a potential for reducing design cost and time, but has had little research, is the determining and refining of an initial configuration before beginning the analysis and optimization process (figure 1). One reason is because this is a problem that is not easily solved numerically, but one that seems to require using heuristics from experienced designers.

Only recently have engineers begun making use of Artificial Intelligence (AI) tools in the area of conceptual design (refs. 1,2). To continue filling this void in the design process, a prototype knowledge-based system, called STRUTEX (ref. 3), has been developed to initially configure a structure to support point loads in two dimensions. This prototype was developed for testing the application of AI tools to conceptual design as opposed to being a testbed for new methods for improving structural analysis and optimization. This system combines numerical and symbolic processing by the computer with interactive problem solving aided by the vision of the user.

This paper describes how the system is constructed to interact with the user. Of special interest is the information flow between the knowledge base and the data base under control of the algorithmic main program. Examples of computed and refined structures are presented during the explanation of the system.

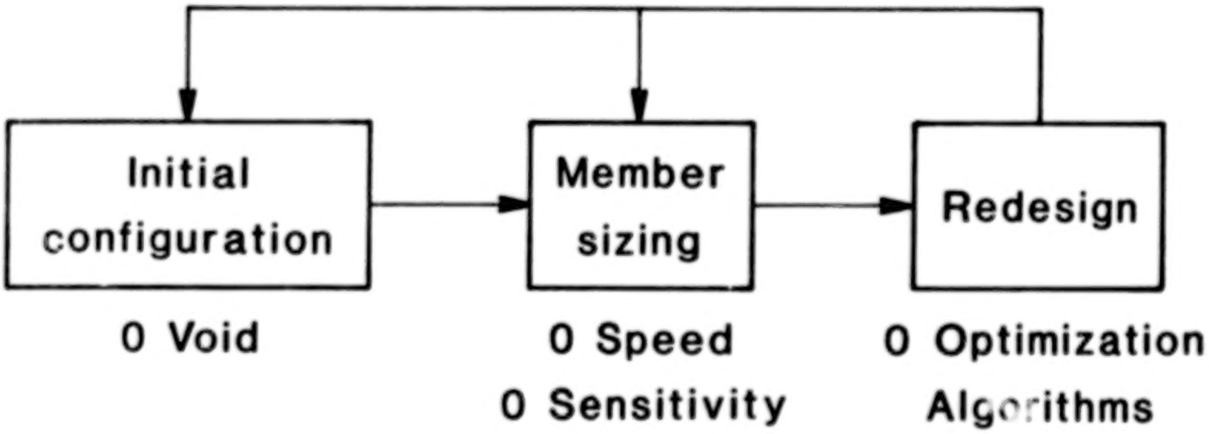

Figure 1

COMPONENTS OF THE SYSTEM

The main driver program for STRUTEX is written entirely in FORTRAN. Other components were added by linking existing software - DI-3000 (ref. 4) for the graphics, RIM (Relational Information Management, ref. 5) for the relational data base management, and CLIPS (C Language Production System, ref. 6) for the inference engine - to the main driver program. The data for RIM and the knowledge base (rules) for CLIPS are maintained in different files separated from STRUTEX. EAL (Engineering Analysis Language, ref. 7) for the structural analysis, and CONMIN (Constraint Minimization, ref. 8) for the optimization are coupled in PROSSS (Programming System for Structural Synthesis, ref. 9) to perform the analysis and optimization (figure 2).

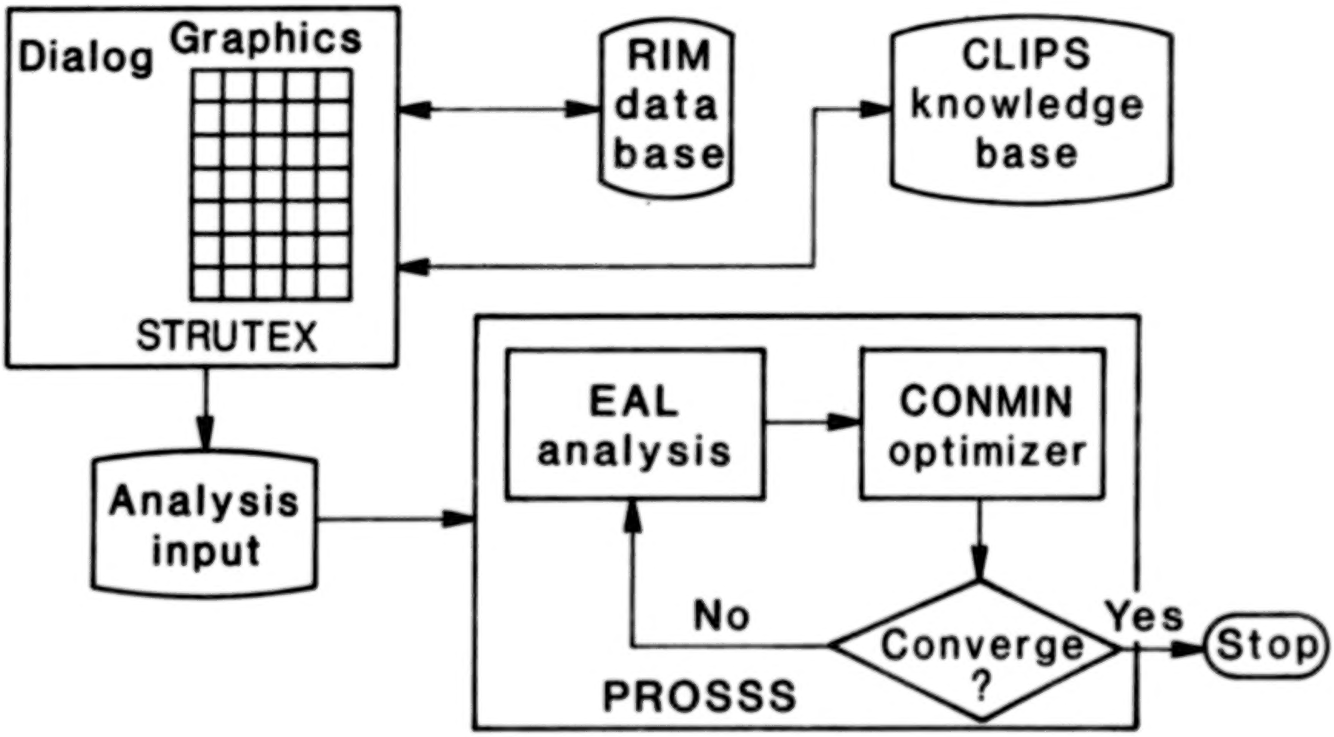

Figure 2

A PRODUCTION RULE KNOWLEDGE BASE/INFERENCE ENGINE

CLIPS is a knowledge-based system tool developed at NASA Johnson Space Center. It is written in C, performs forward chaining based on the Rete pattern matching algorithm, and has a FORTRAN interface. The knowledge base is composed of rules which are defined by the "defrule" construct. A rule states specific actions, the Right-hand side (RHS), that are to be taken if certain conditions, the Left-hand side (LHS) are met. An "=>" separates the LHS and the RHS. If, and only if, all of the conditions on the LHS are satisfied, then the actions on the RHS are performed sequentially. Each rule must contain at least one condition and one action.

Pieces of information represented by facts, the basic form of data in CLIPS, are contained in a facts-list. A fact can contain a number, a word, or a string. Facts are asserted into the facts-list before execution by the "deffacts" construct or by an assert command in the calling program, or during execution as the action caused by executing a rule. A rule executes based on the existence or non-existence of facts in the facts-list. For example, the rule for selecting a string as the type of support is shown in figure 3. It is read: If the location of the support surface is above the load and the load is a gravity type of load, then the support type is a string. This rule will execute when the two facts (SURFLC ABOVE) and (PLOADT GL) are asserted from STRUTEX and placed into the facts list. The actions, based upon a match on the two facts (conditions), are to return to STRUTEX via the KBANS1 parameter the fact that the support is a string, and to assert the fact that the support is a string into the facts-list. The KBANS1 parameter, discussed below in more detail, is the name of the subroutine in STRUTEX. In this example, only the parameters SUPPORT and STRING are needed. The 0.0 is a dummy parameter.

Currently there are only thirteen rules in the knowledge base. There are three rules for determining the type of support, beam, truss, or string. The rules for choosing the beam or truss are more complex than that of the string and use an explicit "or" coupled with three or four explicit "and"s. Another rule in the knowledge base explains the choice of support type when executed. The remainder of the rules determine whether or not bracing is required and the type of bracing that is required in a truss. Other rules determine if there are any angles formed which are not within a given range. If so, a recommendation is made to correct the problem. The action parts of the bracing rules are more complex than those of the rules for choosing the type of support. Some of the bracing actions are based on mathematical computations within the rule, while others have choices of actions within a single rule with the choice being determined by the facts.

The inference engine in CLIPS applies the knowledge (rules) to the data (facts). Pattern matching occurs on the LHS. The basic execution cycle begins by examining the knowledge base to see if the conditions of any rules have been met. All rules with currently met conditions are pushed onto the "agenda" which is essentially a pushdown stack. Once the agenda is complete the top rule is selected and the RHS is executed. As a result of these actions, new rules can be placed on the agenda and rules on the agenda may be removed. This cycle is repeated until all rules that can execute have done so.

```
(defrule string
  (SURFLC ABOVE)
  (PLOADT GL) =>
     (assert (SUPPORT STRING))
     (KBANS1 SUPPORT STRING 0.0))
```

Figure 3

FLOW OF DATA BETWEEN THE KNOWLEDGE BASE AND THE DATA BASE

Data base systems typically have little knowledge, much data, and rely on fast secondary storage techniques. Knowledge-based systems, on the other hand, have much knowledge, little data, and work within main memory. If knowledge-based systems are to be integrated into the design process, new methods must be developed so that they can handle the large amounts of data typically created during a design project.

There are three approaches (figure 4) in current long-term research efforts which are trying to determine the best way to couple these two types of systems into a single system with the best features of both (refs. 10,11,12). One approach is to begin with an existing data base system and add knowledge base features to it. A second approach is to begin with an existing knowledge-based system and add data base features to it. The third approach, and probably the most promising, is to start from scratch and develop a completely new system combining the best features of both data and knowledge-based systems. The best short-term solution appears to be taking an existing knowledge-based system and an existing data base system and loosely coupling them with an interface such as the one used by Feyock (ref. 13). This is the approach taken with STRUTEX using CLIPS.

The rules for STRUTEX are very simple and could probably have just as easily been incorporated into the main driver program with IF-THEN statements. However, one of the objectives of this project was to investigate methods for passing data between a data base and a knowledge base. Therefore the knowledge base and the data base are maintained in different files separate from the main program. The interface is made through STRUTEX by linking a RIM interface library and the CLIPS knowledge base interface library with STRUTEX. If data is needed from the knowledge base, a rule or rules must be executed. If the data is not available within STRUTEX, it is retrieved from the data base by calling RIM interface subroutines. That data is then asserted into the knowledge base again using interface subroutines. Data is returned from the knowledge base to STRUTEX which, in turn, stores the data in the RIM data base if it is necessary.

STRUTEX has three subroutines which interface with CLIPS by calling subroutines in the CLIPS FORTRAN interface library. Subroutine KBXEC initializes CLIPS, loads the rule base, and is called by other subroutines to assert facts into the knowledge base and execute the inference engine. Once all of the rules on the CLIPS agenda have been executed, control is returned to this subroutine which allows STRUTEX to continue processing. The other two routines, KBANS1 and KBANS2, receive data from CLIPS after the appropriate rule (or rules) has been executed. These two subroutines are called as an action in CLIPS. KBANS1 has three parameters, two alphanumeric and one numeric, while KBANS2 has three numeric parameters. The data returned from CLIPS are stored in these parameters for later use in other subroutines in STRUTEX.

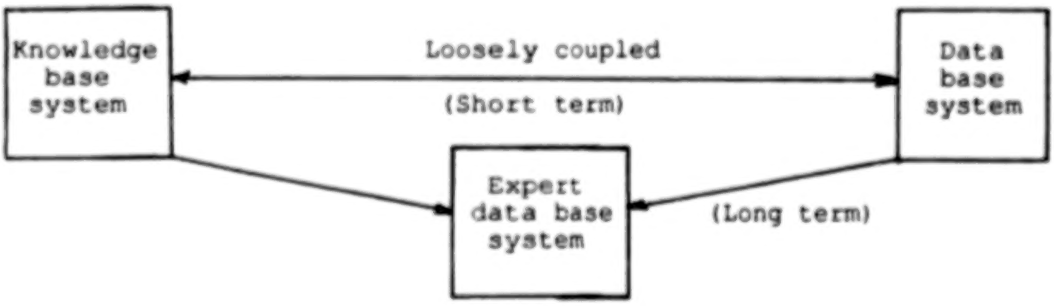

Figure 4

USER INTERACTION WITH STRUTEX

When STRUTEX begins execution, the user first answers questions about the loads. The number of load points is the first input. The next input is the type of load which can be a gravity load, vertical load, sideways load, or a combination of gravity or vertical and sideways. This is followed by an iterative process through the load points where the user inputs the vertical and horizontal magnitudes of each load and then uses the mouse to locate the load point on the graphics window. Since no units are required by STRUTEX, the user must determine the correct units for the distances and loads.

The second stage of user input concerns the support surface. The user inputs where the support surface is in relation to the load points - above, below,or to the side. The user then uses the mouse to place the midpoint of the support surface on the graph. The distance from the support surface to the first load is input without units. The distances from the remaining loads to the support surface are computed. The user inputs whether or not the support surface is a point. If it is not, then the length of the support surface is input, again with no units.

The final piece of data that is needed before the system can determine the type of support is whether it is important for the support to be inexpensive or lightweight. Once these data are known, facts are asserted into the knowledge base and the inference engine executes the rules. The type of support is returned from the rules and stored into the data base. The choice and explanation of that choice are displayed on the dialog screen as shown in figure 5.

```
An explanation from STRUTEX

************************************

 A truss is the choice for a support.

************************************

 Reasons:
  The support surface location is to
       the side of the loads.
  The support surface is not a point.
  The support must be lightweight.
```

Figure 5

A TRUSS WITH A SINGLE LOAD POINT

If the choice is a truss and there is only one load point, a triangular structure is drawn (figure 6a). The system then determines whether or not bracing is needed by checking the ratio of the forces in the members against the length of the members. The forces are computed from an equation representing static equilibrium of the loaded point. **Facts are asserted** into the knowledge base. The inference engine executes the rules and the choice is returned to the main program. If bracing is needed, the two side members are divided, and either a "Z" brace (figure 6b) if Delta is greater than 40 degrees or a "V" brace (figure 6c) if Delta is less than or equal to 40 degrees is chosen by the knowledge base. An input file is created for the analysis program and the program ends.

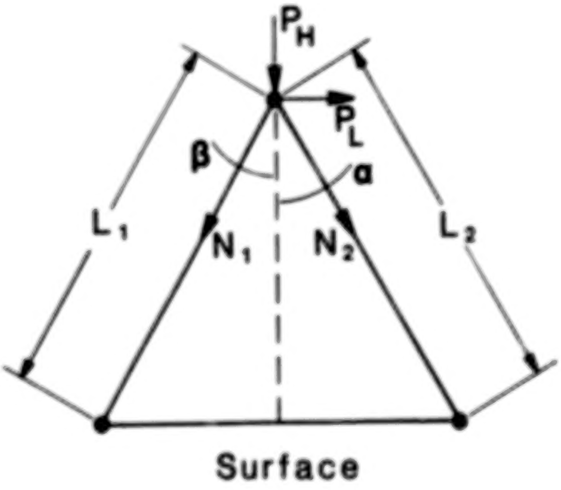

Figure 6a

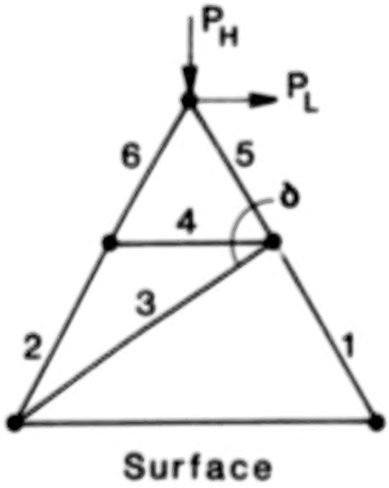

Figure 6b

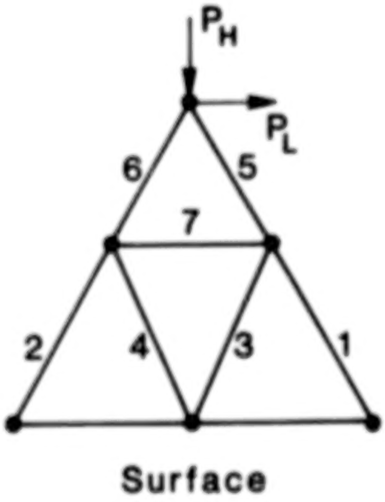

Figure 6c

BEST COPY AVAILABLE

A TRUSS WITH MULTIPLE LOAD POINTS

If the choice is a truss and there is more than one load point, then the user must build the truss guided by recommendations from the system. The user begins with the load points and the support surface. A recommendation is made to first connect all the load points forming triangles whenever possible, but not connect the load points to the support surface. Members are added by placing the mouse on the end points. Once this has been completed, there is a second recommendation for the user to connect the load points to the support surface without having a new member intersect an existing member. (The reason for using two recommendations to build the truss is discussed below.) Figure 7 displays the structure at this point in the design.

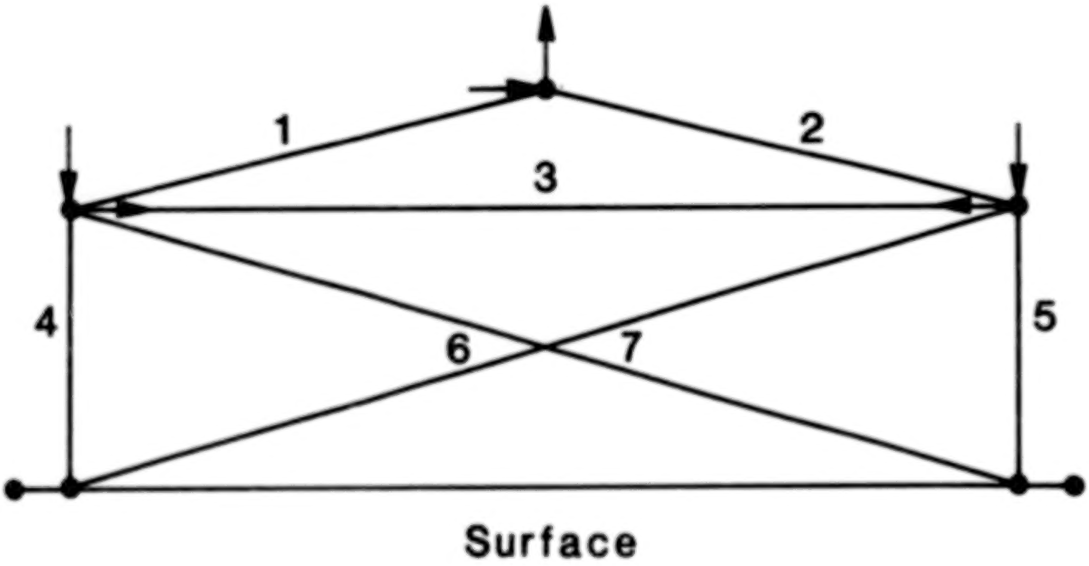

Figure 7

A RECOMMENDATION FOR IMPROVING THE MODEL BASED ON TRIANGLES

After this step is complete, the system determines all the triangles formed by the members and checks their angles. If the knowledge base determines that there are angles in the model outside a given range, a recommendation is made to correct the problem. The limiting values for the angles are judgmental and can be changed based on the experience of the user. An example of such a recommendation based on the angles is shown in figure 8.

A recommendation from STRUTEX

```
******RECOMMENDATIONS******

The following triangles contain angles that
are less than 15 degrees, therefore
a modification may be required.

TRIANGLE         ANGLE        OPPOSITE MEMBER
 1 2 3            13.7               1
 1 2 3            12.4               2

                 N1
                 /\
                /  \
           N2/      \N3

If two external members form the angle
then to expand the angle
   (1) Remove the two members N1-N2 and N1-N3
       that form the angle.
   (2) Add two new members N1-N4 and N1-N5
       to form a larger angle.
   (3) Add a new member to connect N4 and N5.
   (4) Add two members to connect
       N2-N4 and N3-N5.

                 N1
                 /\
                /  \
           N4/____\N5
             |      |
           N2|      |N3

If this recommendation can be implemented in
more than one way, choose the way that will
contract the structure rather than expand it.

*********************************************
The following triangles contain angles that
are greater than 120 degrees; therefore,
a modification may be required, such as
adding a new member to divide the angle
into two smaller angles.

TRIANGLE         ANGLE        OPPOSITE MEMBER
 1 2 3            154.               3
*********************************************
```

Figure 8

IMPROVED MODEL

The user then removes all members which contribute to the problem and adds new members to satisfy the recommendation. If the user desires, the angles in the model can again be checked for problems. This is repeated until the user is satisfied (figure 9). The input file for the structural analysis program is written and the program ends.

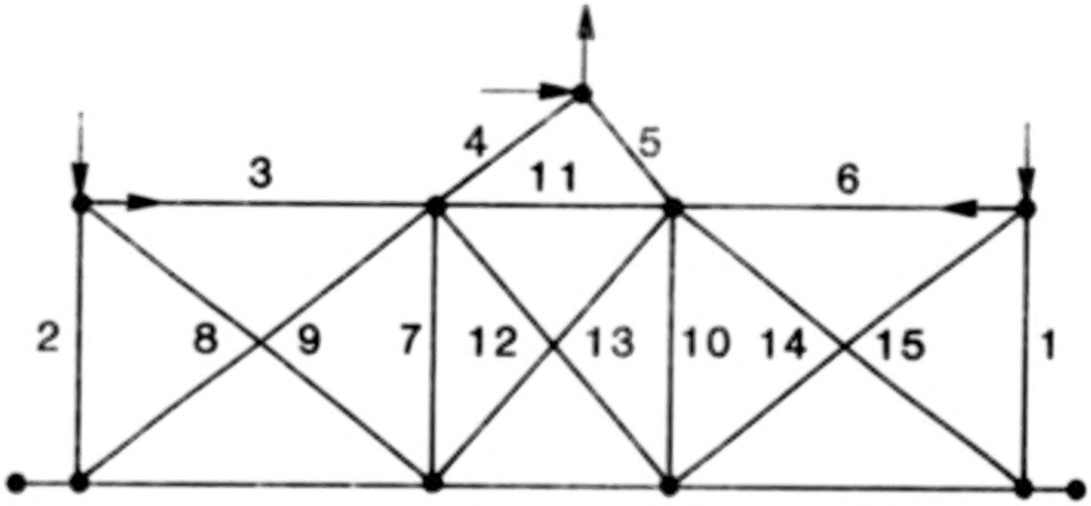

Surface

Figure 9

MODIFYING THE BRACING OF A TRUSS

For the truss with multiple load points, there are two recommendations instead of one to allow the knowledge base to determine the bracing required between two members connecting a load point to the support surface. When two members connecting a load point to the support surface form a quadrilateral, the knowledge base is given the lengths of the two members. If the two lengths are the same, an "X" bracing is added. If the two lengths are different, a brace is added from the bottom of the longer member to the top of the shorter member (figure 10).

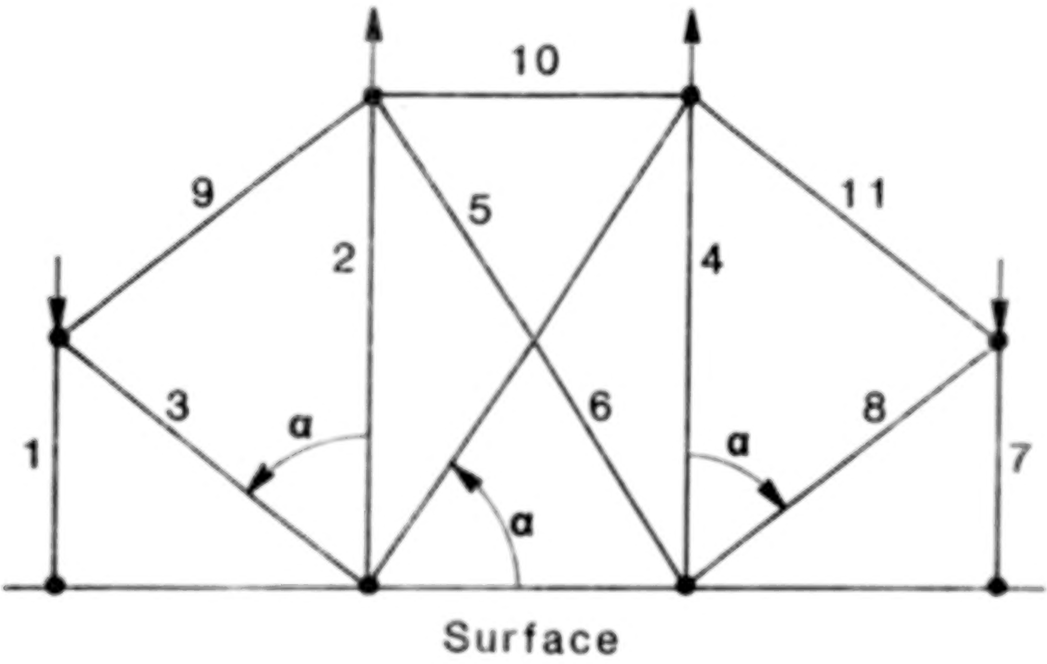

Figure 10

A RECOMMENDATION FOR IMPROVING THE BRACING

The angle, Alpha, made by the two members is passed to the knowledge base, and a recommendation is made if the angle is not within the proper range. An example of such a recommendation is shown in figure 11.

A recommendation from STRUTEX

```
******RECOMMENDATIONS******

Because the angles made by the diagonals
and the support surface are greater than 75 degrees
(Angle = 76.), it is recommended that
members 5 and 6 be removed and that
members 2 and 4 be divided in two and
reconnected with an X bracing.

Because the angle made by the diagonal
and the support surface is greater than 75 degrees
(Angle = 77.5), it is recommended that
member 3 be removed and that member 2
be divided in two and connected to the ends
of member 1.

Because the angle made by the diagonal
and the support surface is greater than 75 degrees
(Angle = 77.5), it is recommended that
member 8 be removed and that member 4
be divided in two and connected to the ends
of member 7.

************************************************
```

Figure 11

A TRUSS WITH IMPROVED BRACING

The truss in figure 12 reflects the refinements made from this recommendation. It is possible, especially in a very complex truss, that this recommendation might come out in addition to the recommendation about the triangles.

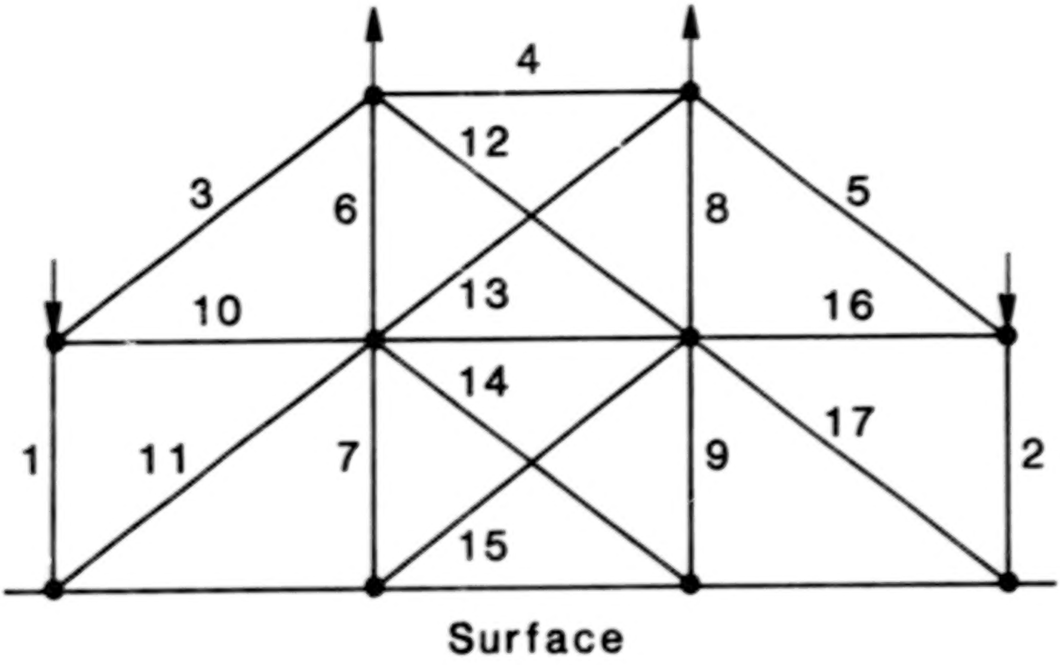

Figure 12

CONCLUSIONS

A prototype knowledge-based system has been developed to initially configure a structure to support point loads in two dimensions. There were two primary objectives for this project. The first objective was to investigate methods for passing data between a data base and a knowledge base. This was accomplished by integrating an inference engine into the system and determining the effects on the flow of data between the knowledge base and the data base. No significant problems were encountered in integrating the inference engine.

The second objective was to determine if an initial conceptual model could be improved by using symbolic processing instead of numeric processing. By applying the knowledge base, significant improvements were made to the trusses shown in the examples. If more rules were added to the knowledge base then more improvements could be made to the model.

REFERENCES

1. MacCallum, K. J.; Duffy, A.; and Green, S.: "An Intelligent Concept Design Assistant." Proceedings of the IFIP W.G.5.2 Working Conference on Design Theory in CAD, 1985, pp.233-249.

2. Shah, J.: "Development of a Knowledge Base for an Expert System for the Design of Structural Parts." Proceedings of the 1985 29thComputers in Engineering Conference, 1985, Vol. 2, pp. 131-136.

3. Rogers, J., Feyock, S. and Sobieszczanski-Sobieski, J.: STRUTEX A Prototype Knowledge Based System for Initially Configuring a Structure to Support Point Loads in Two Dimensions. "Artificial Intelligence in Engineering: Design", Computational Mechanics Publications, Southampton, PP. 315-335.

4. DI-3000 User's Guide, Precision Visuals Inc. Document Number DI3817, Release Number 4, March 1984.

5. Erickson, W. J.: "User Guide: Relational Information Management (RIM)", Report Number D6-IPAD-70023-M, Boeing Commercial Airplane Company, Seattle Washington, 1981.

6. Riley, G.; Culbert, C.; and Savely, R. T.: "CLIPS: An Expert System Tool for Delivery and Training." Proceedings of the Third Conference on AI for Space Applications, November 1987.

7. Whetstone, W. D.: "EISI-EAL: Engineering Analysis Language", Proceedings of the Second Conference on Computing in Civil Engineering, ASCE, 1980, PP. 276-285.

8. Vanderplaats, G. N.: CONMIN _ A FORTRAN Program for Constrained Function Minimization. User's Manual. NASA TM X-62282, 1973.

9. Rogers, J. L., Jr.; Sobieski-Sobieszczanski, J.; Bhat, R. "An Implementation of the Programming Structural Synthesis System (PROSSS)", NASA TM 83180, December 1981.

10. Ceri, S.; Gottlob, G.; and Wiederhold, G.: "Interfacing Relational Databases and Prolog Efficiently." Proceedings of the First International Conference on Expert Database Systems, April 1-4, 1986, pp.141-153.

11. Nguyen,G.T.: "Prototypes and Database Samples for Expert Database Systems." Proceedings of the First International Conference on Expert Database Systems, April 1-4, 1986, pp.3-14.

12. van Biema, M.; Miranker, D. P.; and Stolfo, S.J.:" The Do-Loop Considered Harmful in Production System Programming." Proceedings of the First International Conference on Expert Database Systems, April 1-4, 1986, pp. 125-138.

13. Feyock, S.; and Rogers, J. L.: "Embedded AI for Structural Optimization". Presented at the International Conference on Computational Engineering Science, April 10-14, 1988, Atlanta, GA.

BLANK PAGE

TRUSS: AN INTELLIGENT DESIGN SYSTEM FOR AIRCRAFT WINGS

Preston R. Bates* and
Daniel P. Schrage
Georgia Institute of Technology
Atlanta, GA

---

*Graduate Research Assistant

Abstract

Competitive leadership in the international marketplace, superiority in national defense, excellence in productivity, and safety of both private and public systems are all national defense goals which are dependent on superior engineering design. In recent years, it has become more evident that early design decisions are critical, and when only based on performance often result in products which are too expensive, hard to manufacture, or unsupportable. Better use of computer-aided design tools and information-based technologies is required to produce better quality U.S. products. This paper outlines a program to explore the use of knowledge based expert systems coupled with numerical optimization, database management techniques, and designer interface methods in a networked design environment to improve and assess design changes due to changing emphasis or requirements. The initial structural design of a tiltrotor aircraft wing is used as a representative example to demonstrate the approach being followed.

Introduction

As it becomes more evident that the early stages of design of complex products are where critical life cycle decisions are made, there is increasing pressure to obtain more knowledge and address more requirements early. For advanced aeronautical vehicles, this requirement growth is depicted in Figure 1. The relationship between design freedom and knowledge is illustrated in Figure 2. The obvious goal is to steepen the knowledge curve early to take advantage of the design freedom.

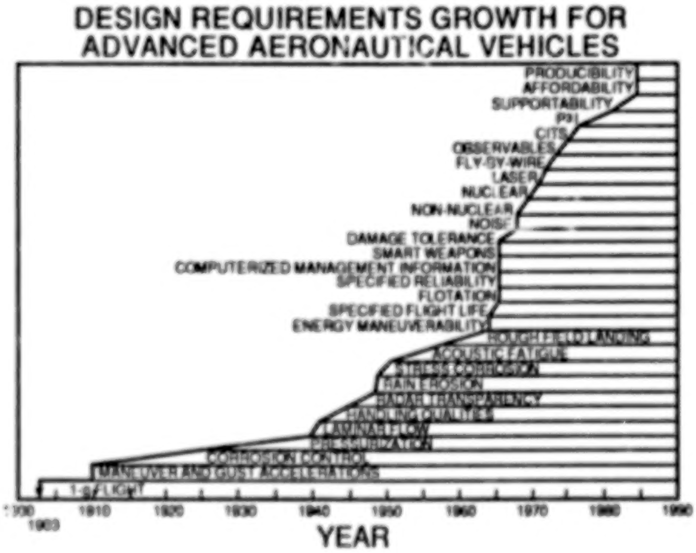

Figure 1

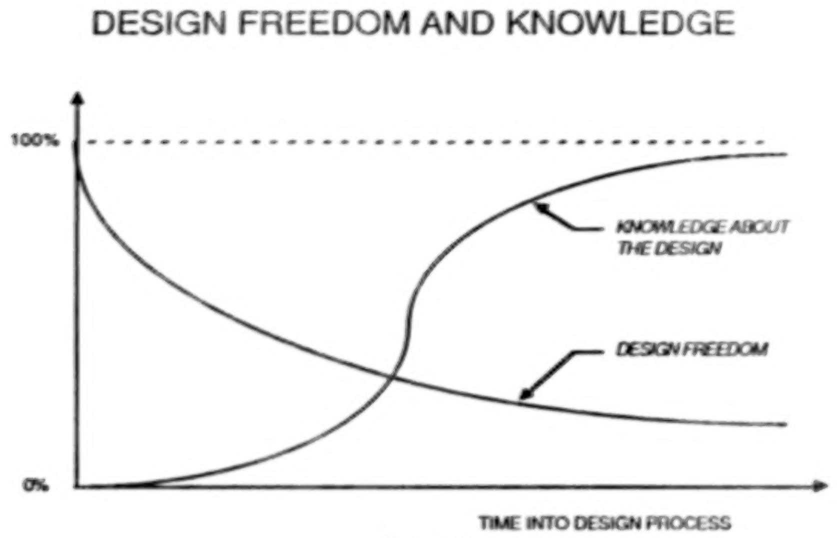

Figure 2

While this approach has received much emphasis, and terms like "design for producibility" and "design for supportability" have become popular, the implementation has been far harder to achieve. One reason is that few design engineers know how to interpret producibility, supportability, etc. requirements, and few manufacturing engineers and logisticians know much about design. There is a movement to correct this deficiency as discussed in References 1 and 2, and DoD programs have been established such as Unified Life Cycle Engineering (ULCE), Reliability and Maintainability in Computer Aided Design (RAMCAD), and Concurrent Engineering.

Necessary research areas have also been identified in Reference 3. Two major sub-areas of design theory and methodology have been identified along with three supporting disciplines whose development is critical to the future growth of the design field. The two major sub-areas are: Conceptual Design and Innovation, and Quantitative and Systematic Methods. The three major supporting disciplines are: Intelligent and Knowledge-Based Systems, Information Integration and Management, and Human Interface Aspects in Design. At the Georgia Institute of Technology, the School of Aerospace Engineering recognized the need for these research areas and supporting disciplines several years ago and has initiated a Laboratory for Information Technology in Engineering (LITE) to address them.

The LITE Program

LITE is a multidiscipline, multi-school effort whose key players stem from the Schools of Aerospace, Mechanical, and Industrial Engineering, as well as the Artificial Intelligence Branch of the Georgia Tech Research Institute (GTRI). The approach taken by the LITE program is to place design information and knowledge at the center of an integrated design process (Figure 3). The LITE philosophy is built upon three key aspects to improve the design process. Primarily investigated by the aerospace school, the first aspect is design decision-making and analysis, addressing synthesis, parametric design, and the use of artificial intelligence (AI) technology in them. Second is information integration and management through the application of shared databases (relational and object-oriented) that fulfill the unique requirements of engineering CAD systems, explored chiefly by the mechanical engineering school. Examined principally by the industrial engineering school, the third is human interface aspects in design, which studies the overall impact of integrated design technology upon individual designers and their organizations.

The LITE design study will focus on issues relative to tiltrotor aircraft like Bell Helicopter's very successful XV-15 shown in Figure 4. Over the past two years, Georgia Tech has been developing the necessary tiltrotor expertise, the design analysis tools, and the interfaces with the tiltrotor industry and government. The V-22 "Osprey" is in full-scale engineering development and will eventually provide approximately 1100 aircraft for the Marine Corps, Navy, Air Force, and Army. In addition, NASA, the FAA, Airport Authorities, and industry are all investigating the use of commercial tilt rotors to relieve airport congestion and improve regional airline productivity. The Europeans have also initiated their own commercial tiltrotor development program, known as EUROFAR, providing the element of foreign competition as well.

INTEGRATED DESIGN PROCESS

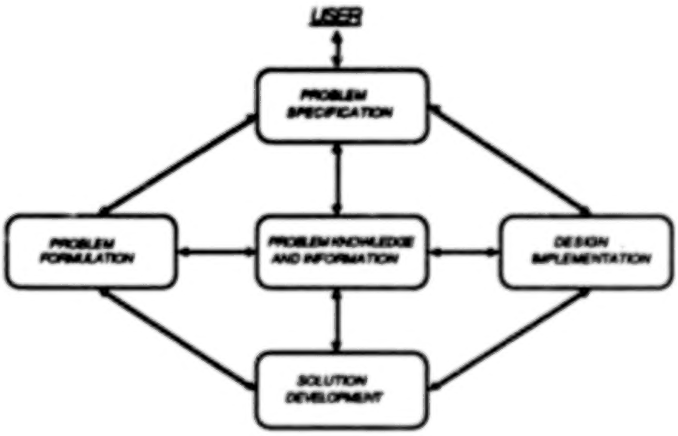

Figure 3

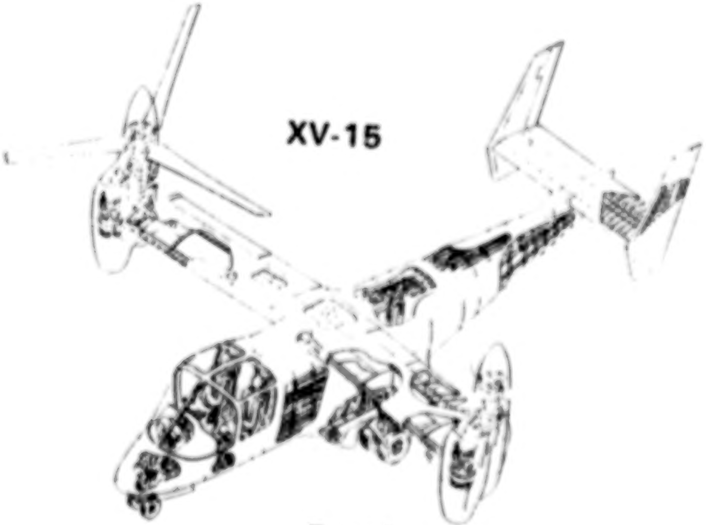

Figure 4

Specifically addressed is the structural design of the tiltrotor wing, a sufficiently intricate aircraft subsystem encompassing a wide variety of functional criteria, aeroelastic, manufacturing, and supportability issues. It presents a complexity that requires a hierarchical problem breakdown into multiple levels of the tilt rotor system, e.g. aircraft, wing, wing box, spar, spar cap. Additionally, it provides a framework to analyze how aircraft design requirements and parameters are related in civilian vs. military vs. research missions. For example, commercial designs are driven by producibility, such as minimum cost per seat-mile, compared to low cost and risk for a research aircraft. In a military application, the design is strongly impacted by operations and support issues including structural inspection and tracking, battle damage repair, and the need to operate in austere or shipboard environments.

The typical wing structural design process consists of the conceptual, preliminary, and detail design phases. At the conceptual level, general parameters related to the entire aircraft are specified. Definition of wing area, thickness to chord ratio, span, sweep, and fuel volume requirements result in geometric constraints governing the internal wing structure. During preliminary design, attempts are made to find the best way to "put the bones in the meat" of the aircraft by laying out major structural components that satisfy these constraints. At this stage, trade-off studies, coupled with mathematical analysis and optimization, are performed on the various structural configurations. Consideration of producibility, maintainability, and supportability are crucial at this level. Finally, at the detail phase, the wing subcomponents (panels, ribs, spars, etc.) are considered individually, resulting in shop drawings for their manufacture.

TRUSS (Tilt Rotor Unified Structural design System) is the present focus of LITE that incorporates in its development all of the research areas and supporting disciplines discussed so far. TRUSS is an integrated design system that attempts to automate the basic wing structural design process shown in Figure 5. From the figure it is easy to see that opportunity for automation exists by applying state of the art technologies in artificial intelligence, database management techniques, interactive geometric modelling, finite element analysis, and optimization techniques. Such a project requires a team effort, and at present there are five graduate students from the participating schools concentrating on these individual areas.

TRUSS will generate potential structural configurations commonly incorporated by industry, optimize them on a first level to meet geometric and other constraints, and finally evaluate the feasible concepts according to some common criteria, such as minimum cost or weight. Subsequently, detail design can begin at the subcomponent level. Shown in Figure 6 is an example structural decomposition of a tiltrotor aircraft. During the integration of the aircraft, only one structure from each area (fuselage, wing, etc.) may be chosen. One particular goal of TRUSS is to effectively track the reasons and decisions for these choices, at least at the wing level. Such decision tracking provides potential payoffs in product cost and time to design, and would be applicable to other areas of the aircraft as well.

WING STRUCTURAL DESIGN PROCESS

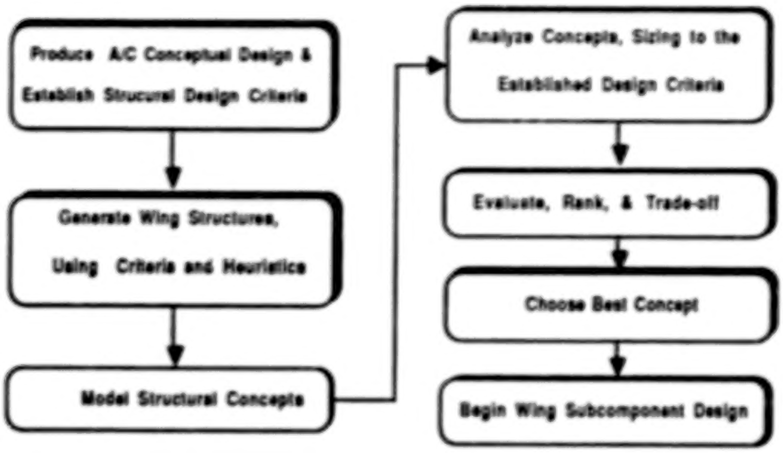
Produce A/C Conceptual Design &
Establish Strucural Design Criteria
Generate Wing Structures,
Using Criteria and Heuristics
Model Structural Concepts
Analyze Concepts, Sizing to the
Established Design Criteria
Evaluate, Rank, & Trade-off
Choose Best Concept
Begin Wing Subcomponent Design

Figure 5

STRUCTURAL DECOMPOSITION

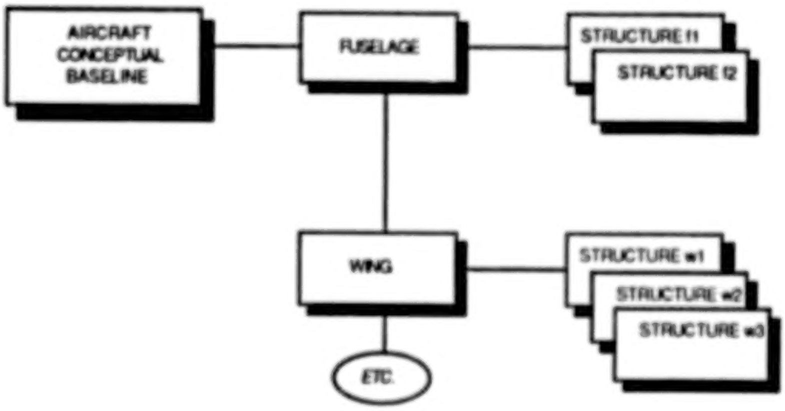

__Effective Decision Tracking Will Provide Improvements In:__

- PRODUCT COST
- TIME TO DESIGN
- APPLICATIONS TO OTHER SYSTEMS

Figure 6

BEST COPY AVAILABLE

Description of TRUSS

The issues and details of TRUSS and its various components will now be discussed in some depth. The status of their development and researchers involved will be described. Finally, an overview of the long term research objectives will be presented.

System Architecture

The architecture chosen for the system is an executive-centered concept shown in Figure 7. The executive acts as the prime communicator between all other parts of the system, including the user, and is responsible for the correct order of execution and data flow between them. Reference 4 describes a successful application of this quasi-procedural approach in detail. Individual procedural modules written in various traditional languages are linked together at runtime in an appropriate order that permits computation of a requested design variable. Part of the executive known as the computational path generator uses information on the required inputs and outputs of the available procedural modules, performs a heuristic search of a tree structure relating the design variables, and decides on the order of the routines to be executed.

This layout offers a lot of flexibility when an upgraded program is substituted into the system, requiring only one new interface to the executive. As a result, new modules can easily be added to the executive as the level of required design detail increases. From a database standpoint, multiple databases may be connected to the executive, utilizing the best features of both relational and object-centered management techniques.

TRUSS ARCHITECTURE

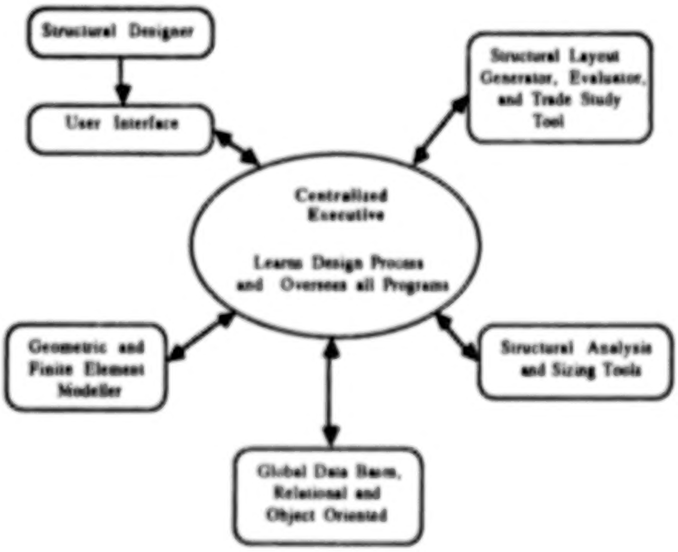
Structural Designer
User Interface
Structural Layout Generator, Evaluator, and Trade Study Tool
Centralized Executive
Learns Design Process and Oversees all Programs
Geometric and Finite Element Modeller
Structural Analysis and Sizing Tools
Global Data Base, Relational and Object Oriented

Figure 7

There are, however, some disadvantages of this architecture. Placing all of the responsibility on the executive slows down the transfer of information and requires more working memory, resulting in longer computing times. Some solutions to this include highly efficient database management procedures and the use of parallel processing. To quicken the research, LITE members will prototype TRUSS modules separately on different computers, resolving their own errors before trying to integrate the whole system.

The executive centered system was selected over a global database centered concept. Although a central database architecture may provide for faster computing time, its inherent dependency on specific software requires specialized interfaces between the database and other modules. When improved software is inserted into this system, multiple interfaces must be developed, causing increased system downtime and costs.

Problem Definition

Figure 8 presents the tiltrotor wing problem scope addressed by TRUSS. On the topmost levels, all aircraft wings are members of broadly defined groups. Tiltrotor wings are located under the V/STOL transport category. Further classification breaks down into mission application, functional discipline (structures, aerodynamics, aeroelasticity, flight controls, power train, etc.), and major structural materials. Next is the subsystem level (wing box, leading edge, fixed trailing edge, etc.), and finally the component level where actual pieces of structure, such as skin, ribs, and spars, can be found. These may even be further broken down into their components as well, such as web, chord, stiffener, etc. It is beyond the scope of TRUSS to address the entire problem space, so one of the branches in the hierarchy will be chosen as the initial design task. When all of the TRUSS participants have agreed upon the proper problem definition, module prototyping will begin. For example, initial development work might be identified by the shaded boxes, which indicate the material selection and structural analysis of the wing box spar in a commercial aircraft.

Proper design of TRUSS requires a detailed understanding of the tiltrotor wing structural design process, as well as a knowledge of the proper analysis tools and available design technologies. Figure 9 represents a design network of the required tasks, forms of data, and task interactions encountered in the design sequence. Once these have been identified, LITE team members construct a flowchart which places design tools, current or required, in their proper places in the sequence (Figure 10). Also represented on the flowchart are the state-of-the-art technologies required for design automation, such as artificial intelligence, interactive graphics facilities, and optimization. Such a view of the design process is not cast in concrete, and must be continuously re-examined and updated. In this manner, the causes of problems in the current design process can be pinpointed and reasonable solutions for improvements made. Interfacing issues among the different design tasks may also be identified. Once finalized into a valid form, such a flowchart can be programmed as a script into the centralized executive of TRUSS which would oversee all data interactions between the modules and the user.

TILTROTOR WING PROBLEM SCOPE

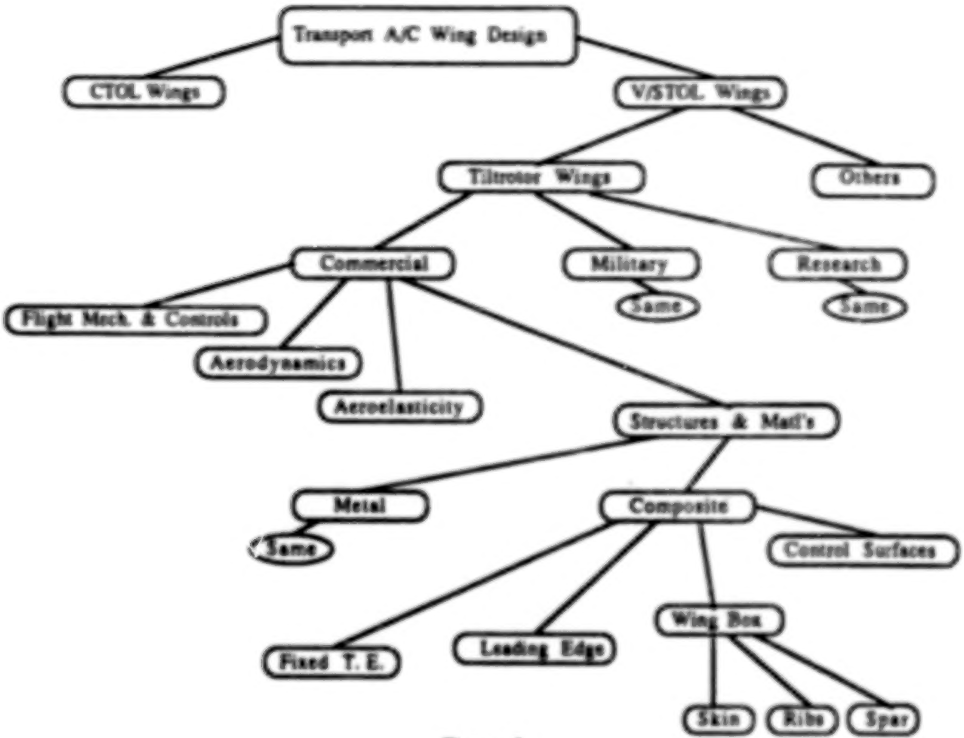

Figure 8

DESIGN NETWORK

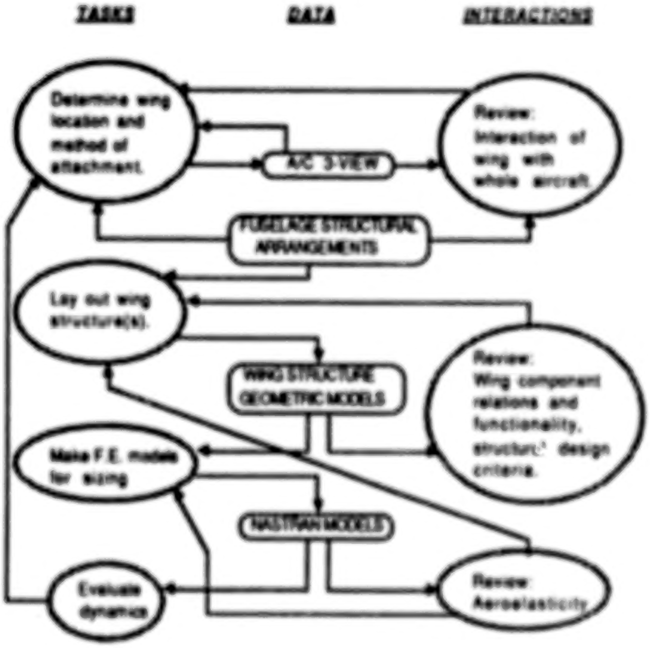
TASKS
DATA
INTERACTIONS
Determine wing location and method of attachment.
A/C 3-VIEW
Review: Interaction of wing with whole aircraft.
FUSELAGE STRUCTURAL ARRANGEMENTS
Lay out wing structure(s).
WING STRUCTURE GEOMETRIC MODELS
Review: Wing component relations and functionality, structural design criteria.
Make F.E. models for sizing
NASTRAN MODELS
Evaluate dynamics
Review: Aeroelasticity

Figure 9

TILTROTOR WING STRUCTURAL DESIGN PROCESS

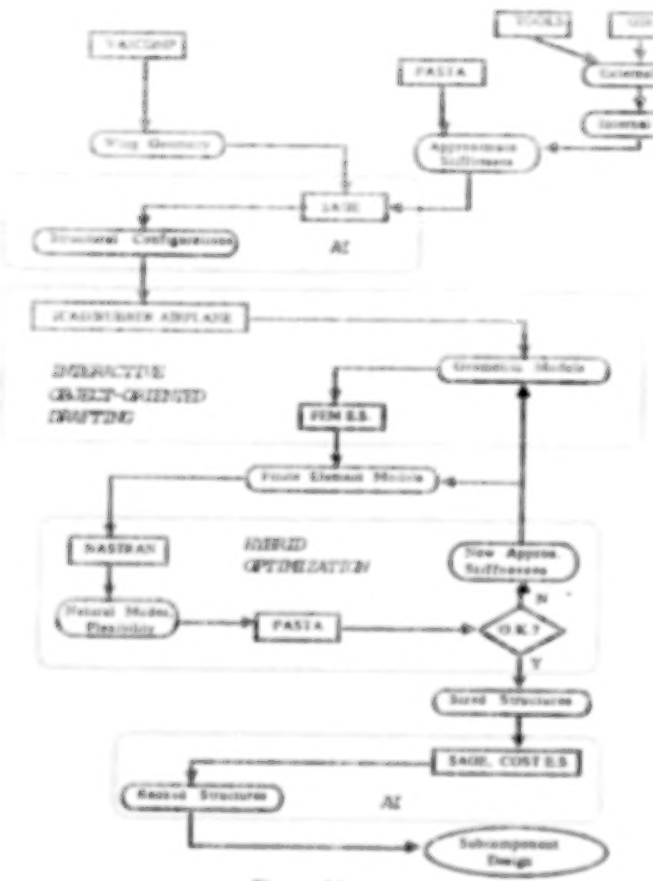

Figure 10

User Needs and Interface

One of the most important modules of the TRUSS system is the user interface. A poor interface results in a poor system. Representative designers from industry will play a key role in the development of this module by evaluating prototype interfaces and offering suggestions and requirements for improvements. A number of user needs have already been identified.

First, the system must be able to support the needs of a number of different departments within an organization. For instance, structural design reviews, marketing reviews, manufacturing consultations, and a variety of other management/administrative tasks are crucial to design decision support. While satisfying the structural designer's needs for adequate technical depth, the system should also provide broader information for upper level organizational requirements within the framework of project time and cost constraints.

Next, the system should have the ability to learn from interactive sessions with the user by remembering exactly how the user created the structural design. As a result, when minor modifications to the design must be made, the user need only change a couple of parametric values and the system automatically updates the design. This is also known as parameter-based design vs. geometry-based. Boeing

Commercial Airplane Company has successfully incorporated this feature on their wing configuration design system, CDCS, Reference 5. Still recognizing the advantages of geometric design, TRUSS will also have a drafting facility.

Finally, the system should present information to the designer in the most effective way for him to use the design data. This entails the use of user defined pop-up windows and access to the rule base, knowledge base, and databases. A sample user interface concept for TRUSS that reflects these criteria is shown by Figure 11.

TRUSS USER INTERFACE

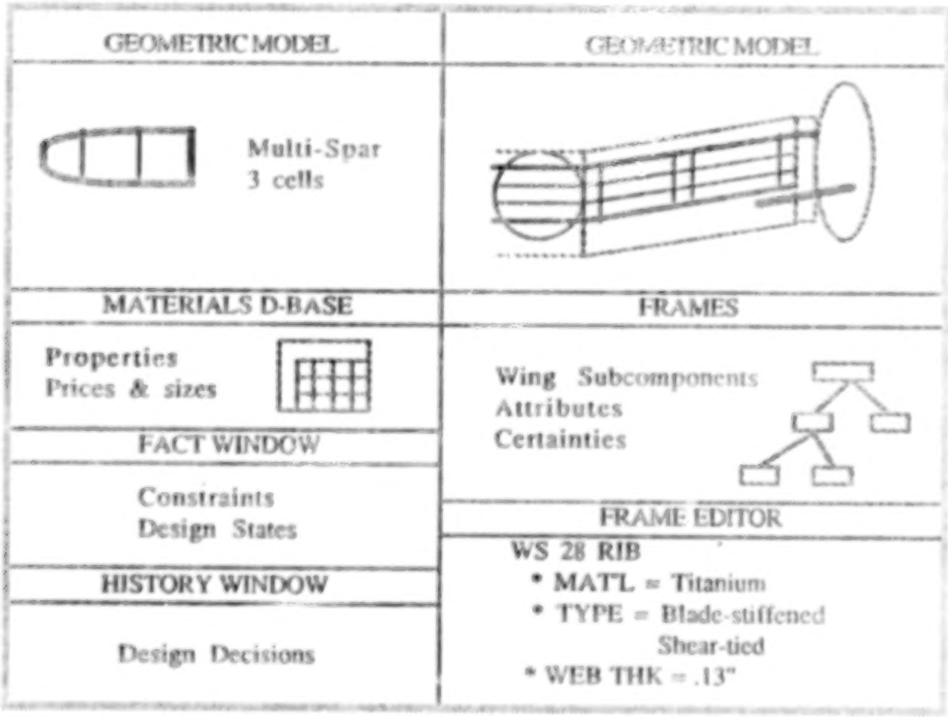

Figure 11

Database Issues

Databases are imperative to the proposed design system. They must serve as the repository for all information describing different design versions, and all design decisions up to any given time. All other TRUSS modules are dependent on this information to perform their required tasks. Specific data applications include material specifications and properties, geometric modelling data, meta-level and parametric descriptions of feasible structural configurations, sensitivity data, and machining specifications.

Reference 6 provides some detailed issues about the function of the database in TRUSS, some of which are discussed in the following paragraphs. Currently, one LITE team member is focusing his research specifically on the implementation of these items.

Modeling of complex design objects: Engineering CAD databases have requirements above and beyond those used for business applications. Engineering design problems involve large systems with complex interactions among their subsystems and components. So the need arises for more advanced modelling techniques. The use of object-oriented databases with sophisticated data structures such as semantic networks, in addition to traditional relational structures, is required for these modelling tasks.

Version/alternative control: There is seldom any single solution to a design problem, with the possibility of several optimal solutions existing that all satisfy the product requirements and constraints. Hence arises the need for the storage and arrangement of data specific to these different versions or alternatives, which may be called upon by other application programs.

View/configuration management: A system like TRUSS involves many users with different needs for design data. Even the separate modules of the system have different requirements for the same data. These differing 'views' of the design object must be supported. On one hand is an administrative view of the data where a project manager might be interested only in a few key parameters, such as system cost or production time estimates. On the other hand, the design engineer may need to know very detailed information like individual structural component weights, their raw material types, and associated costs.

Dynamic schema definition: A database schema defines the objects modelled in the database and their binding relationships. For multiple views, these schemas must be flexible for modification and extension, preferably without reloading the data base or recompiling the schemas, thus working dynamically with the system.

Concurrent control: A unified design system involves the communication among several of its modules, and among several users in a networked workstation environment. The ability to control the data of several parallel processing applications is desired from the database manager to ensure data integrity along with faster computing times. In AI terminology, such a 'blackboard' displays and modifies all data between separate application programs acting in parallel.

Partial integrity and constraints: Design of a particular object is done in an iterative fashion. While many types of design have a preferred sequence of activities that take place, the database system should not impose constraints on this sequence. It may be necessary to allow and manage inconsistent database states.

Management utilities: These include the basic tasks of data backup, recovery, security, operational accounting and performance statistics, and off-line storage and data archival.

Hardware and Software

Significant chokepoints arise in the current design process whenever hardware or software incompatibilities exist. Reference 7 tells that such days for engineers are coming to an end. Apollo Computer, Inc. has developed a set of products which create a heterogenous networked computer environment using the best features of different hardware. The requirements of TRUSS point toward the use of this type of design environment. To address this issue, LITE members are compiling a comprehensive listing of available programs used by industry and government organizations, the hardware they run on, and the language the source code is written in. Especially challenging is the marriage of traditional programs used in a "number crunching" environment to new AI tools and machines. The wide variety of such combinations is shown in Figure 12. The proper choice of hardware and software combinations is a primary goal of the TRUSS system planning, approach, and methodology currently in progress.

Discipline	Acronym	Description	Hardware
Integrated Design Tools Hardware	ICAD	Knowledge Based CAD System	Symbolics (LISP)
	INTERGRAPH	Knowledge Based CAD System	Intergraph
Expert System Tools	GEST	Generic Expert System Tool	Symbolics VAX 8600 (LISP)
Data Base Mgt Systems	RIM	Relational Data Base	VAX
	VBASE	Object Oriented Data Base	Computer Vision, Ontologic
	ORACLE	Object Oriented Data Base	IBM PC
Optimization	OPT	Reduced Gradient Method	VAX, CYBER (FORTRAN)
	SPARS	Multispar Box Optimization Program	
	FASTOP	Flutter and Strength Optimization Program	
Vehicle Synthesis	GASP	General Aviation Sizing Program	VAX
	VASCOMP II	Tiltrotor Sizing and Performance	VAX, CYBER
	HESCOMP	Helicopter Sizing and Performance	VAX, CYBER
	VSPEP	Vehicle Sizing & Perf Evaluation Program	
	AVID	Aerospace Vehicle Interactive Program	
	CDS	Configuration Development System	
	SWEEP	Structural Weight Estimation Program	
	NAPSAP	Naval Airship Program for Sizing & Perf	
Stability & Ctl	GTR	Generalized Tiltrotor Program	VAX (FORTRAN)
	MIMFOOF		
Aeroelastic Stability	PASTA	Proprotor Aeroelastic Stability Program	VAX (FORTRAN)
Structural Analysis	NASTRAN	NASA Structural Analysis Program	IBM (FORTRAN)
	ACCESS III	Structural Analysis and Optimization	VAX
	APAS III	Automated Program for A/C Structure	
	MARC		
Geometric Modelling	GEMPACK	Aircraft Geometry Generator	
	HESCAD	Helicopter Geometry Modeller	VAX (FORTRAN)
Finite Element Modelling	SACON	Expert System for MARC Analyzer	
Mission Analysis	GMAS	Goddard Mission Analysis System	
Aerodynamics	DYLOFLEX	Dynamic Loads of Flexible Airplanes	
	CLMAX	Prediction of Aerodynamic Characteristics	
	USSAERO	Aerodynamic Panel Loads Program	

Figure 12

Program Overview

An overview of the TRUSS program development plan is illustrated in Figure 13. The entire program is expected to run three-and-one-half years to final prototype demonstration. Major tasks consist of planning, system module development and integration, and frequent demonstrations to industry and government participants. Project planning will be fully addressed by the end of this year, with attention shifting to individual module management for the following years. TRUSS modules consist of the executive, relational and object-centered databases, user interface, geometric modelling facility, finite element modeller expert system, cost expert system, and SAGE (Structural Arrangement Generator and Evaluator). Currently in development, SAGE is an expert system responsible for structural concept synthesis and trade-off analyses, and will be discussed in more detail. All modules will be developed along parallel timelines, and integrated when they have reached sufficient maturity. It should be pointed out that at this time, participants for all of the modules have not been identified, but are expected to be within the next few months. Demonstrations include presentations on system concept formulation, computer demonstrations of TRUSS modules and their integration, module user validations, and finally a complete system validation.

Focus for LITE Research:
Tilt Rotor Unified Structural Design System

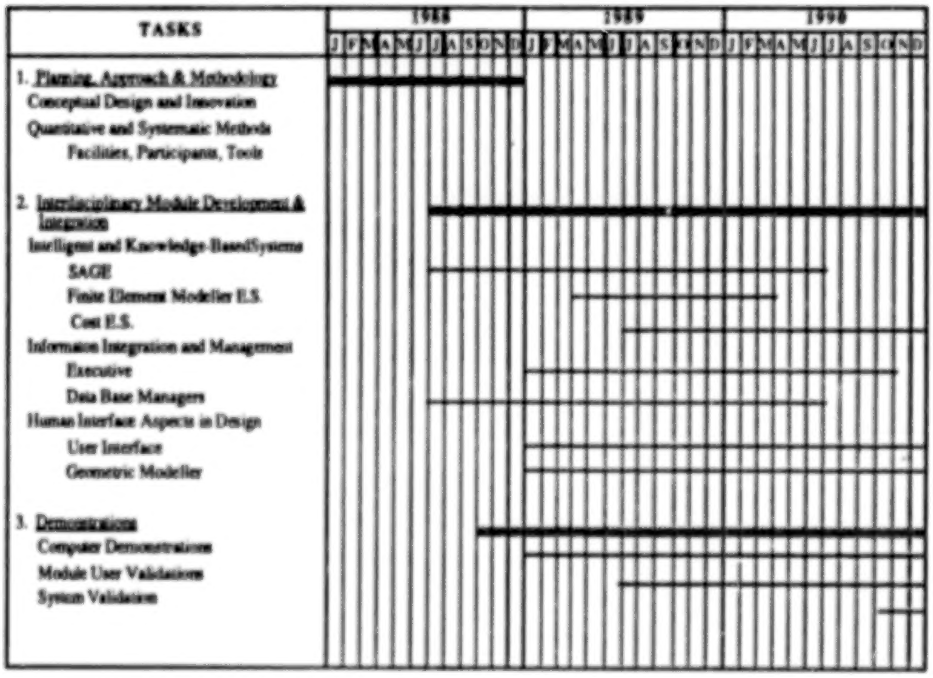

Figure 13

Description of SAGE

A man is referred to as a sage when he is known for his breadth of knowledge, wisdom, experience, and sound judgment. There is hardly a more appropriate acronym for the TRUSS module responsible for structural synthesis and trade-offs, an expert system called SAGE (Structural Arrangement Generator and Evaluator). Whereas there presently exist a number of excellent programs to analyze, size, and optimize structures, the next logical step in an automated design system is to capture the human design knowledge and expertise required to actually create and subjectively compare them.

Overview

Figure 14 shows a relational diagram for SAGE. Inputs to SAGE, in the form of structural design criteria, originate from the user and other conceptual analysis tools. They are directed by the executive, which stores them in appropriate databases. Wing geometry, fuel system specifications, weight and balance data, initial sizing criteria, and material specifications are some examples of these inputs. Using this information, the expert system may begin to configure a structural arrangement that satisfies most or all criteria. For example, the torque box cross sectional area for a two spar configuration can be roughly computed from torsional stiffness requirements and wing geometry. Then, the box problem may be decomposed into various design tasks, such as the front spar, rear spar, ribs, upper panel, and lower panel. These components may be synthesized individually, while keeping track of their functionality and interrelationships as a whole unit. Next, the structures for the box are sized via the executive using a variety of required modellers and analysis packages. Numerical and hybrid optimization techniques are employed to provide the structures with an equal basis for comparison. After all potential structures are sized, they may be evaluated heuristically with respect to level of reliability, maintainability, supportability, cost, and risk. Analytical methods in these areas are employed when possible. The results are feasible structures that have been automatically compared and appropriately ranked from best to worst concept. These may in turn be presented to the user in tabular or graphical form, from which detailed design may begin.

SAGE RELATIONAL DIAGRAM

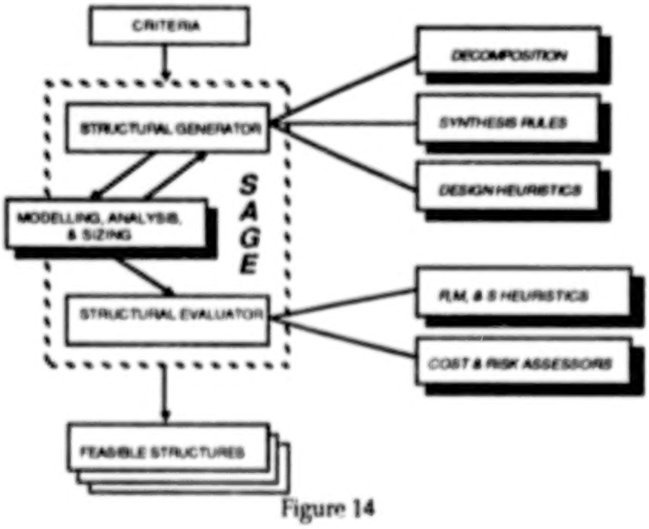

Figure 14

Reference 8 points out that the benefit of such automation is a reduction in the bottlenecks present in the current design process that arise from the unnecessary transfer of design information via humans. By efficiently closing the gaps in information exchange between humans and computers, using AI technology, much of the untimely engineering procedures present in complex system design that result in cost and time overruns can be remedied. With computers performing the more repetitive information tasks, human engineers will have the freedom to concentrate on more complex design problems.

From an academic standpoint, the development of SAGE is beneficial to research by providing a testbed for studying many fundamental design issues that can be applied not only to aircraft, but other complex transportation systems as well. Such issues include the nature of design, the sociocultural context of design, modelling the design process, design problem formulation, and the environment for design. Reference 9 discusses these in more detail.

One ongoing project of LITE similar to SAGE is MISSION (Reference 10), a knowledge-based system that explores the application of artificial intelligence to aircraft concept selection. The program selects one or more present technology aircraft to perform a given mission specified by the user. In addition, the system estimates initial sizing and performance characteristics for the different solution aircraft. MISSION currently has 23 different aircraft in its knowledge base, ranging from conventional fixed wing (supersonic and subsonic) configurations to conventional helicopters to hybrids like tiltrotors and vectored thrust concepts (Figure 15). The system is useful by providing the designer with a tool for rapid parametric studies of several entirely different aircraft types, and several different mission variations. More importantly for the development of SAGE, it serves as a useful testbed to new LITE members for understanding some of the issues involved in knowledge-based design systems, and gathering some proficiency in the use of an expert system building tool.

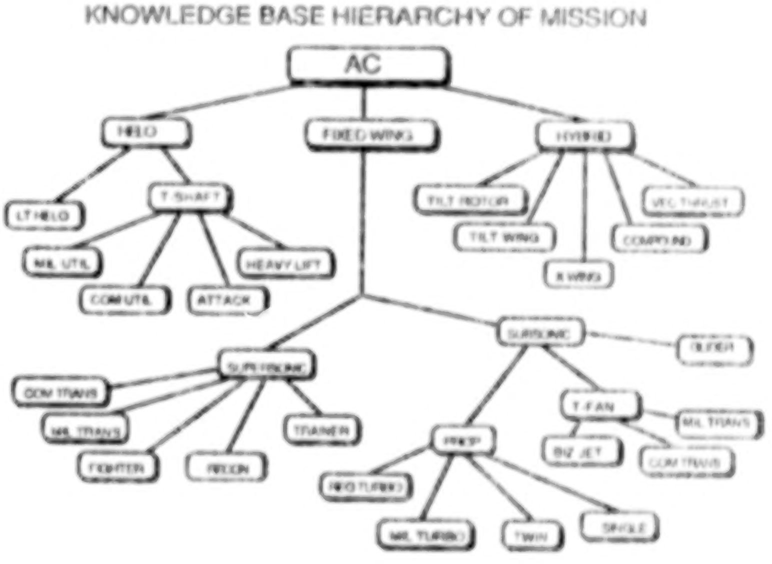

Figure 15

BEST COPY AVAILABLE

Expert System Tool

MISSION was developed using the Generic Expert System Tool (GEST), a product of the Georgia Tech Research Institute. Because of its features, availability, and hardware compatability, GEST was chosen for the development of SAGE. The software currently runs on all Symbolics, Texas Instruments TI Explorer, MicroVax II workstations, and VAX 8600 computers, providing a large variety of hardware to prototype the system and test integration with other modules of TRUSS. SAGE is being developed on the Explorer.

From Reference 11, GEST offers several advantageous features which make it one of the most comprehensive tools available today. Summarized in Figure 16, it has four knowledge representation schemes, including a production rule scheme which can generate hypotheses, deduce conclusions, and make additions and deletions to the design state. The inference engine supports three gears in all chaining modes: single steps through the rule base, continuous single rule firings, and continuous multiple firings. In addition, dynamic rule set modification and two levels of an explanation facility for the end-user alleviate the debugging task. Such features make GEST a robust tool that will expedite the development of SAGE.

GEST FEATURES

TOPIC	FEATURES	TOPIC	FEATURES
Knowledge Representation Schemes	FACTS FRAMES FUNCTIONS PRODUCTION RULE SCHEME	Inference Engine	FWD CHAIN BACKWARD BOTH 3 GEARS
Production Rule Scheme	HYPOTHESES CONCLUSIONS CHANGE DESIGN STATE	Rule Set Modification	EDITING CONFLICT DEPENDENCE SIMILARITY
Rule Conflict Resolution	COMPLEXITY RECENCY ANTECEDENT CONSEQUENT	Explanation Facility	PROGRAMMER USER
Evidential Reasoning	BAYESIAN SENSORY CERTAINTY FACTORS		

Figure 16

Architecture

Figure 17 shows the basic architecture of SAGE. First is the interface to the TRUSS executive, through which all data coming into or out of SAGE will pass. Next is the design state, or working memory, where pertinent design criteria, descriptions of candidate structural arrangements, and other local data reside. The remaining knowledge and rule bases are tied directly to the design state and to each other. The knowledge base contains domain specific knowledge for tiltrotor wings, required to understand the design state and act upon it. This includes a hierarchical breakdown of various structural arrangements used today (Figure 18), as well as knowledge of fasteners, basic pieces of structure, and how parts are related. The rule base drives the rest of the expert system, dynamically changing the design state, and making additions to the knowledge base as the design progresses.

Several categories of the rule base have been identified. When partial descriptions of the design criteria exist, a set of criteria rules attempts to complete them based on several sources, such as Federal Aviation Regulations. SAGE relies on the user to complete the criteria when it cannot. Procedural attachments are used to regulate any calls to outside programs that are needed to determine additional information for constraint generation and sizing.

Synthesis rules configure the major pieces of substructure in the system, such as the torque box and fixed trailing edge, and make sure that the interactions between them are accounted for. They will guide the configuration development in accordance with the structural design criteria. Shown in Figure 19, these rules model the design procedures used in industry today, which draw from a variety of sources such as company philosophy, FAR's, design manuals, and methods of manufacturing, maintenance, and support.

Evaluation rules will construct trade-off matrices that will be used to rank various choices of materials and structural concepts. After the structural concepts are optimally sized, they must be ranked according to some objective function, which may be cost, weight, level of maintainability, etc., or combinations thereof. SAGE will possess the knowledge required to evaluate the concepts both numerically and subjectively, presenting its results to the user for verification before the detailed design of structural subcomponents begins.

SAGE ARCHITECTURE

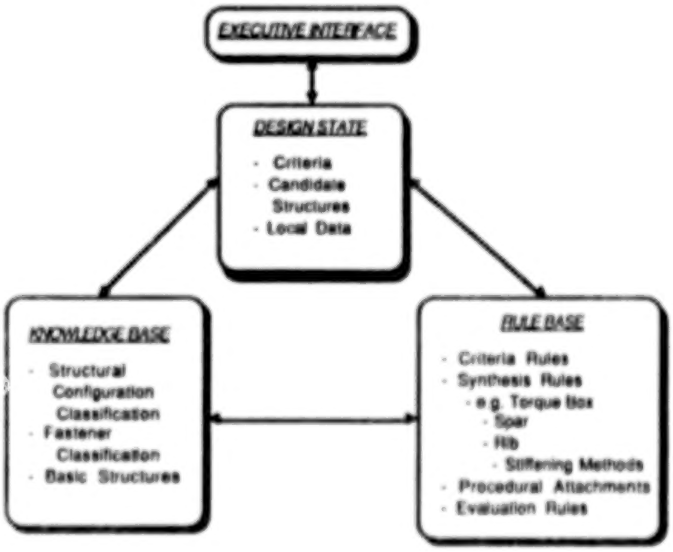

Figure 17

BEST COPY AVAILABLE

SAGE KNOWLEDGE BASE

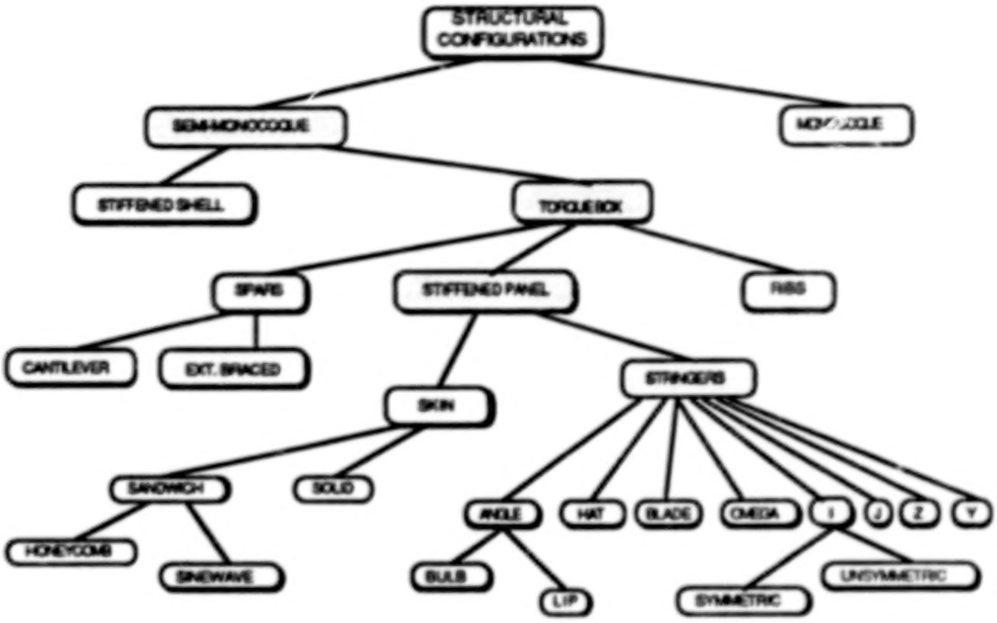

Figure 18

SYNTHESIS RULES

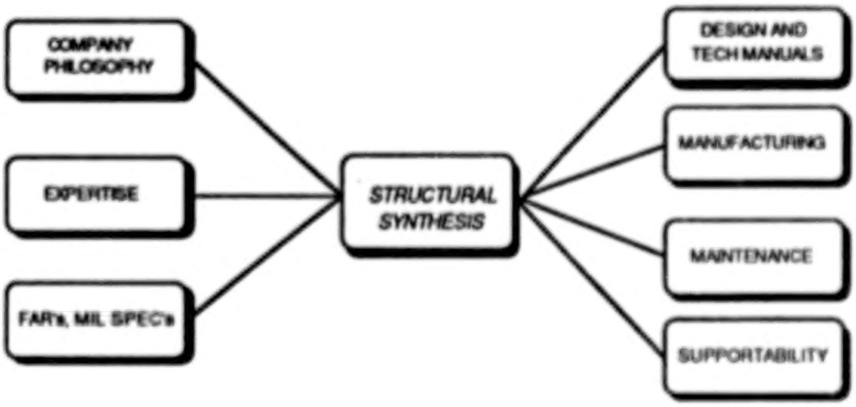

Figure 19

Timeline

The project schedule for SAGE is shown in figure 20. By the start of 1989, the problem scope will be narrowed to a specific task and formalized for all TRUSS participants. A three month phase of prototyping will commence, resulting in a basic working model of the expert system, which includes final rule and knowledge base prototypes, as well as local data management schemes. The majority of the remaining time will be spent on rule base modification and enhancement, accomplished by personal interviews with experts and development testing. User validation and completion of the prototype is expected in the first quarter of 1990.

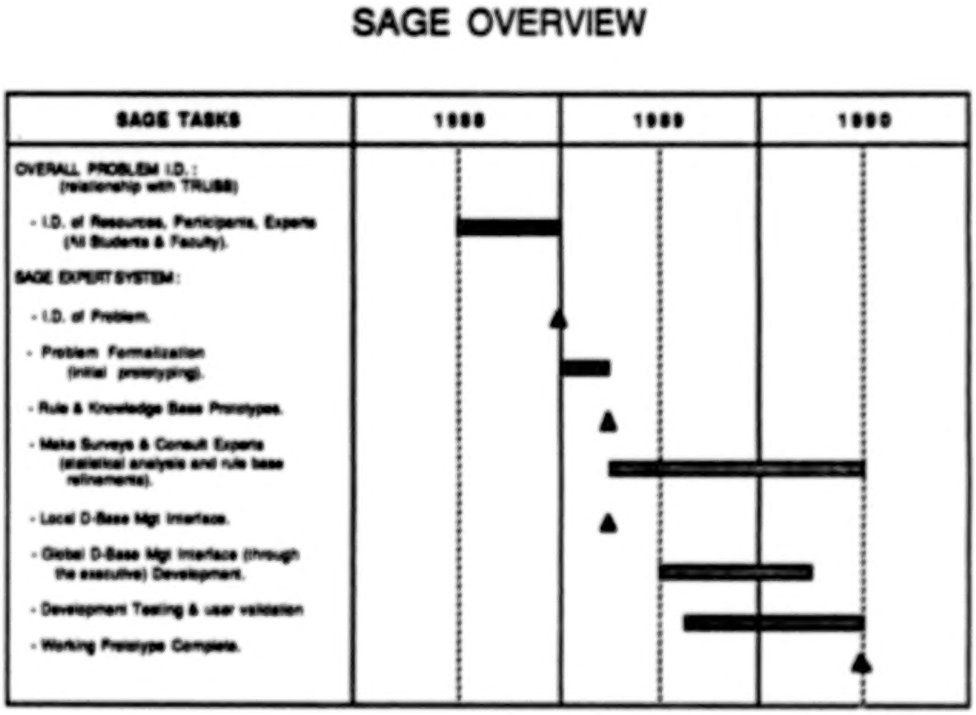

Figure 20

Example

This paper concludes with an example of how SAGE configures a wing structure. The first step is the examination of the overall wing characteristics. Figure 21 shows some typical specifications, giving the number of engines per wing, fuselage location, desired fuel system type, etc. SAGE searches its knowledge base for possible material types and makes selections based on their weight properties and compatibility with corrosion, for instance. Next, SAGE begins to arrange the basic pieces of tiltrotor wing structure: spars, ribs, panels, stringers, drive shafts, gearboxes, conversion spindle, pylon downstop, and so on. As it does so, analyses of lines of penetration check redundant load paths for damage tolerance. First level weights analysis ensures that the wing c.g. is within acceptable limits. Basic analysis of stiffness checks the aeroelastic stability merits of the pattern, and SAGE intelligently stiffens the structure with additional elements if necessary. Figure 22 shows how manufacturing methods are also considered by identifying necessary element spacing, as well as manufacturing access holes and closeouts.

All of this is done by combining the different pieces of structure in an intelligent manner, checking all of their feasible permutations. By doing so, the design space of a very large number of structural concepts is narrowed to a few in a systematic way.

When this process is finished, several versions of structural arrangements will exist and be specified like the one in Figure 21. These structures must now be modelled and sized. Geometric modelling and finite-element codes take the data from SAGE. These data include physical descriptions of the structural concepts, (honeycomb spars, integral hat-stiffened skin, etc.), geometric locations (fuselage station, wing station, relative geometries, etc.), and initial sizing data for the structural elements. From this point, other expert systems for finite-element modelling or drafting can use the data for their purposes. As the structures are sized, SAGE monitors the weights data, and makes adjustments to the structure if necessary. Iteration is required, and it may be found that some structures cannot be sized to meet the weight and stiffness requirements. SAGE flags these concepts and notifies the user, asking him to reject them or make changes to the design criteria.

Once the structures have been successfully sized, they are heuristically and numerically evaluated for levels of maintainability, reliability, supportability, cost, and risk. They are finally ranked and presented to the user tabularly and graphically as shown in Figure 23.

STRUCTURAL ARRANGEMENT GENERATION

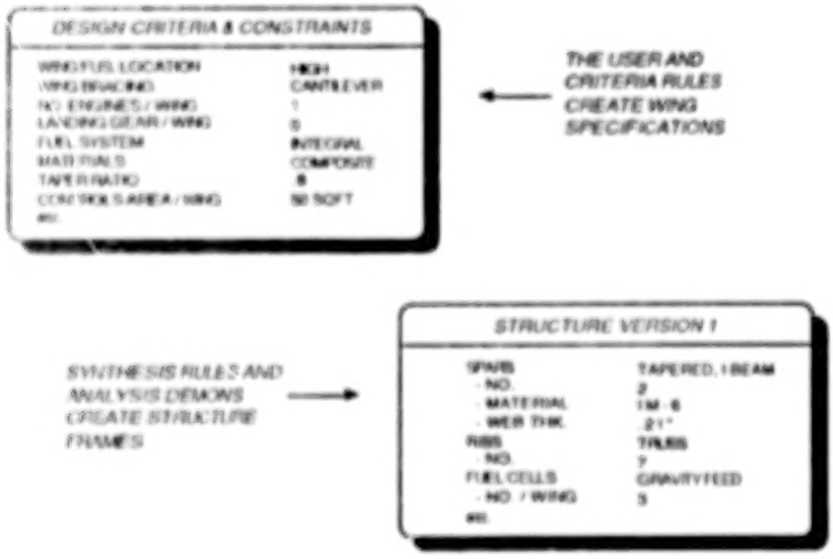

Figure 21

EXAMPLE

SYNTHESIS
RULE 100 : IF FUEL TANK SEALING IS INTEGRAL
THEN RIB SPACING IS AT LEAST 25 INCHES

EXPLANATION : In order to provide proper room for the assemblers to put sealant around ribs, spars, and other structural components comprising the fuel cell, a minimum of 25 inches between ribs is required.

Figure 22

TRUSS SYSTEM OUTPUT

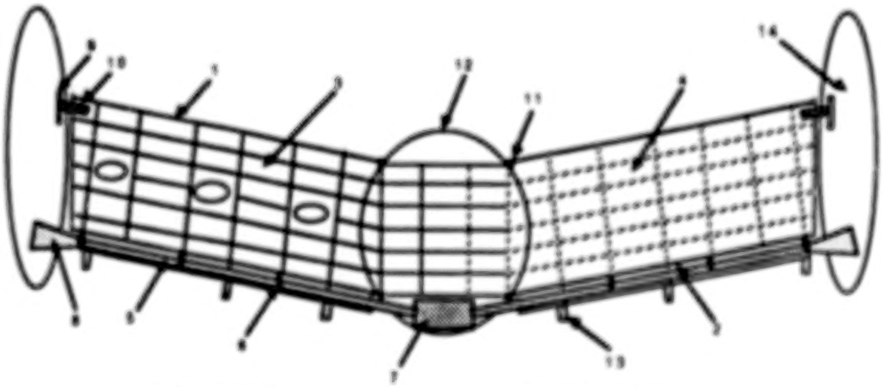

1. Front Beam Assy
2. Rear Beam Assy
3. Lower Panel
4. Upper Panel
5. Drive Shaft
6. Drive Support Bearing
7. Center Gear Box
8. Conversion Spindle
9. Conversion Actuator
10. Conversion Actuator Spindle
11. Pin Fittings (4)
12. Fuselage Attachment Ring
13. Flaperon Hinge Fitting
14. Engine

Figure 23

Summary and Conclusions

This paper has reviewed TRUSS, an integrated design system that incorporates and addresses design issues currently persued by academia, government, and industry. While the program described is quite ambitious, it is the only way the proper focus can be given to this complex integration problem. The program will invoke faculty from several schools, as well as numerous graduate students. Close cooperation with industry is essential to obtain the required knowledge expertise. When the necessary hardware, software, and manpower are in place, significant research progress can rapidly be made in the field of complex systems design.

References

1. Johnson, V., "Minimizing Life Cycle Cost for Subsonic Commercial Aircraft," AIAA Paper 88-4402, 1988.

2. Kemp, A., "Effective Integration of Supportability Design Criteria into Computer Aided Design for the Conceptual Design Phase," AIAA Paper 88-4473, 1988.

3. "Goals and Priorities for Research in Engineering Design, a Report to the Design Research Community," The American Society of Mechanical Engineers, United Engineering Center, 345 East 47th St., New York, NY 10017.

4. Kroo, I., Takai, M., "A Quasi-Procedural, Knowledge-Based System for Aircraft Design," AIAA Paper 88-4428, 1988.

5. Britton, C., Jenkinson, W., "A Computer Aided Design System for Airplane Configuration," Computer Applications in Aircraft Design & Operation, Computational Mechanics Publications, Springer-Verlag, Berlin, Heidelberg, New York, London, Paris, Tokyo, 1987.

6. Staley, S., Anderson, D., "Functional Specification for CAD Databases," Computer-Aided Design Journal, 1986.

7. Dawson, C., "1993: A Vision of the Design Center," AIAA Paper 88-4451, 1988.

8. Hedenfels, R., "Integrated, Computer-Aided Design of Aircraft," Aircraft Design Integration & Optimization, Vol. I, AGARD Conference Proceedings No. 147, 1973.

9. Rouse, W., Boff, K., System Design, Behavioral Perspectives on Designers, Tools, & Organizations, Elsivier Science Publishing Co., Inc., New York, 1987.

10. Schrage, D., Bates, P., "The Configurator and Conceptual Design for Rotary Wing Aircraft," AIAA Paper 87-2891, 1987.

11. Gilmore, J., Ho, D., Howard, C., "GEST - The Generic Expert System Tool," Proceedings of the SPIE Applications of AI III, Vol. 635, 1986.

BLANK PAGE

Real-Time Application of Knowledge-Based Systems

Randal W. Brumbaugh
PRC System Services
Aerospace Technologies Division

Eugene L. Duke
NASA Ames Research Center
Dryden Flight Research Facility
Edwards, California

The Rapid Prototyping Facility (RPF): A Real-Time Application of Knowledge-Based Systems.

At the Dryden Flight Research Facility of the NASA Ames Research Center, the Aircraft Automation Group is engaged in research aimed at applying expert systems technology in a real-time flight test environment. NASA and PRC researchers have developed a facility which allows an expert system prototype to be rapidly and safely demonstrated with a test aircraft. Applications range from monitoring and displays to outer loop aircraft control.

This presentation is intended to document the facility development and architecture, demonstrate its utility by presenting a typical application, and detail recent accomplishments and future goals.

Rapid Prototyping Facility: Concept

The development of a knowledge-based or expert system generally includes an early implementation of a prototype system. This prototype system provides a means of assessing concept feasibility, examining knowledge representation and inference strategies and provides a demonstration to gain support for a larger, more complete program.

The value of prototyping the major components of a knowledge-based system early in the development cycle is that many problems or potential problems can be discovered. Addressing these problems at an early stage is generally less costly and time-consuming than later modification.

The facility discussed here provides a flexible, general-purpose capability for prototyping flight systems which contain a combination of knowledge-based and algorithmic components. The user has a wide choice of processors, tools and resources, including the Ames-Dryden real-time simulation facility and research aircraft, through the Remotely Augmented Vehicle (RAV) system.

A developer with a concept for a knowledge-based flight system may select resources and distribute applications to rapidly develop a prototype system. The facility then allows easy transition to simulation verification and validation, and possible flight test of the concept.

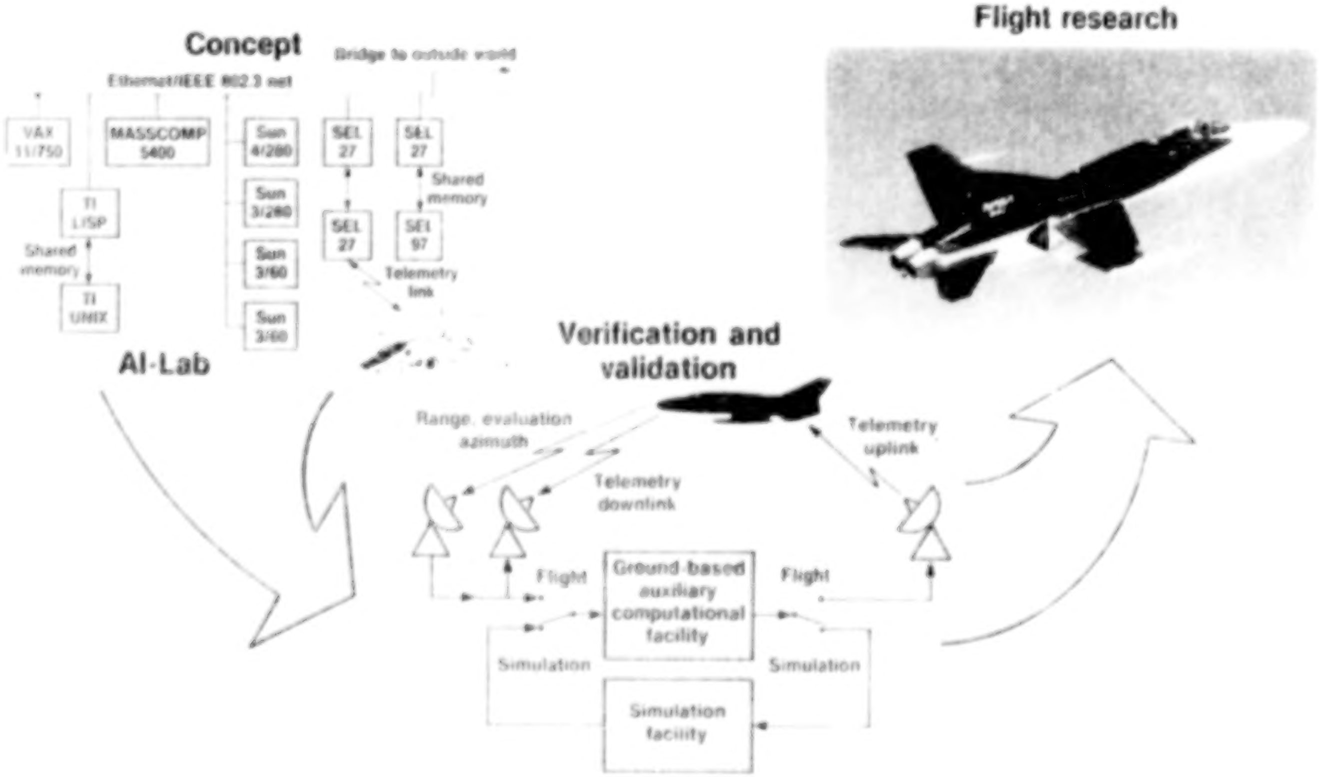

Components: The Remotely Augmented Vehicle (RAV) System

The rapid prototyping facility is an extension of the Ames-Dryden RAV system capability. The main elements of this facility, shown in the figure, are

1. A specially modified aircraft
2. An auxiliary computational facility
3. A high fidelity simulator

Each element serves a unique function in providing a path for rapid system transition from simulation to flight. It is this transition capability that provides the power of the facility to a prototype system developer.

The aircraft used requires two main modifications. The first is the addition of sensors and a high quality instrumentation and telemetry downlink system. The second is the integration of a telemetry uplink system into the onboard systems. Uplinked data may be routed to the flight control system for closed loop control, or to an onboard display system if displays are desired. Once so configured, the aircraft requires no further modifications; changes are performed by altering the auxiliary computational facility.

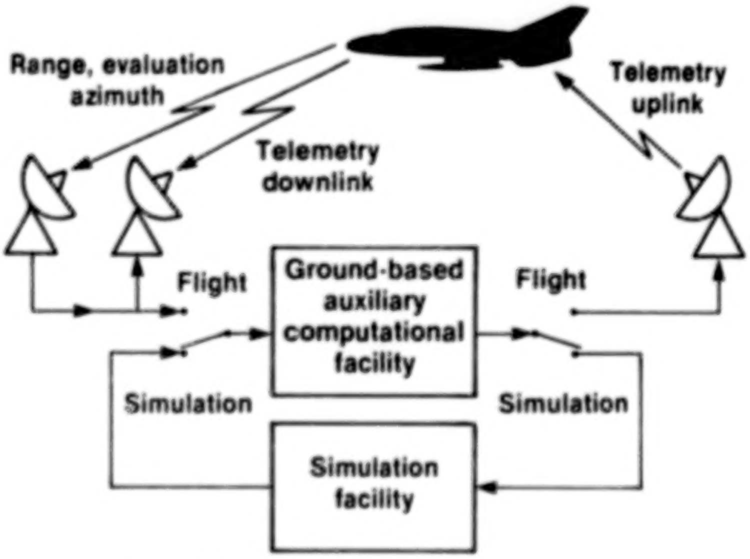

- **Specially modified aircraft**
- **Simulation facility**
- **Auxiliary computational facility**
  - **–Numeric and symbolic processors**
  - **–Duplication of flight systems in simulation facility**

Components: The Remotely Augmented Vehicle (RAV) System

When the telemetry links are operating, the aircraft systems essentially become a node in a distributed processing system which includes a suite of ground based computational facilities. These may include systems for handling TM links, for displaying, recording, or processing data in real-time, or for performing specialized tasks such as knowledge - based control or monitoring. This allows processors which cannot be physically located onboard the vehicle due to limitations in space, ruggedization or cooling, to act nearly identically to an onboard computer.

As an alternative to the flight system, the aircraft may be replaced by the simulation system. The simulation facility provides modelling of the aircraft so that systems may be verified prior to flight operation. It is a key feature, and a requirement for safety, that the interface between the simulation and the actual aircraft TM links be identical. In this way, a concept tested in the simulator is provided a path to flight test experience (see previous figure).

How Fast is "Real Time" ?

Any system which must provide a response in a given time interval can be said to be a "real-time" system. The length of the time interval varies greatly, depending on the system and application. It may even differ between components of a single system. A display processor will typically have a slower response criterion than an aircraft flight control system, although both are parts of a larger system. Some systems also have requirements such as a constant frame time, or connection to a regular clock interrupt.

The rapid prototyping facility provides for real-time response at several levels. Interactive systems must provide response at human speeds. Typically this applies to editors, compilers, and display systems. Outer-loop systems provide control of system state trajectory, and inner-loop systems are required for system stability. A trajectory guidance controller is an example of outer-loop control; a flight control system provides inner-loop functions.

The final measure of a real-time system is that it respond "in-time." The developer using the RPF chooses from computing resources and tools with different capabilities. Efficient distribution of processing is key to meeting response time specifications, but redistribution of processes is not difficult.

Real-Time Applications Within Rapid-Prototyping Facility

What does real-time mean?

- Interactive
    - Response at human speeds (1.0–0.1Hz)
- Outer-loop systems
    - Response required to control system trajectory (25–1Hz for aerospace systems)
- Inner-loop systems
    - Response required to stabilize dynamic system (1000–25Hz for aerospace systems)
- In-time
    - Response provided in time required

Goals for rapid-prototyping facility

- In-time responses for tasks up to 25Hz

Flexibility through Standardization

The wide selection and flexibility of the resources available in the RPF is a result of the use of standard interfaces which are widely recognized and supported by nearly all manufacturers. Expanding or altering the network of computers is a quick and simple procedure. The use of standards also provides access to the resources available to users of the central facility computers, which contain a variety of printers, plotters and disk storage devices.

The computers are linked through a network based on a thick Ethernet/IEEE 802.3 cable. The DOD standard TCP/IP protocol is used throughout for communication. Standard utilities for virtual terminal emulation (telnet) and file transfer (ftp) are available to users during development. Executing processes transfer data in single precision IEEE 754 floating point format. Many processors support this format directly; others require a simple conversion routine to change the data to their local floating point format.

Communication Standards in AI-Lab

Process layer User data buffers	**ANSI/IEEE Standard 745-1985** **IEEE Standard for Binary Floating Point Arithmetic**
Host-to-host layer TCP	**Transmission Control Protocol MIL-STD-1778** **Connection Oriented Transport Control Specification**
Internet layer IP	**Internet Protocol MIL-STD-1777** **Protocol for Providing the Connectionless Mode Network Service**
Network access layer IEEE 802	**IEEE 802.2 Logical Link Control** **IEEE 802.3 CSMA/CD Media Access Control Protocol for Bus Topology**

Current Architecture

The computer systems in the RPF are divided into two groups. The first is the computer systems of the Aircraft Automation group; the other is the systems of the Ames-Dryden Simulation/ RAV facility.

The simulation/RAV computers are shown on the right side of the figure. These are very high speed FORTRAN processors. The systems shown are typical. The facility contains several systems used for development, simulation and RAV. Each system contains two computers connected by a high-speed shared memory link. These systems provide simulation, cockpit interfaces and displays, connection to hardware-in-the-loop simulation components and RAV linkage.

The majority of the remaining computers are general purpose UNIX - based workstations with high resolution graphics interfaces. These provide general purpose computing and development resources. Several languages and tools are available to users including C, FORTRAN and CLIPS.

The VAX 11/750 is used primarily for its disk storage and tape facilities. It also hosts several tools for expert system development including C, FORTRAN, Common LISP, OPS5 and CLIPS.

The TI Explorer LX is a multi-processor system designed for applications requiring close integration of symbolic and numeric computing. The primary processor is a symbolic processing architecture with LISP, ART and a graphics interface. It communicates through shared memory or data streams with a conventional processor running applications under the UNIX operating system.

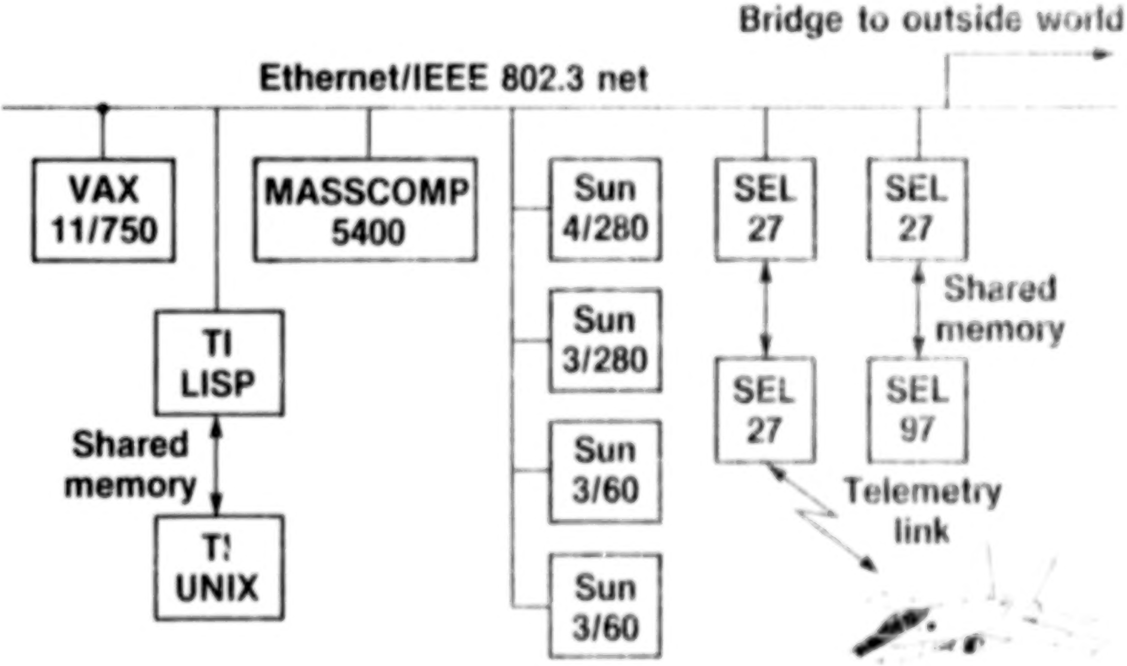

BEST COPY AVAILABLE

An Application: The Automated Flight Test Management System (ATMS)

The ATMS system, developed by Sparta, Inc., is designed as the premier application for the rapid prototyping facility. This system demonstrates many of the capabilities of the RPF for use in planning, monitoring and control tasks involving several cooperating resources. It includes expert systems, numerical algorithms, graphics, simulation, control, monitoring and use of RAV capability.

The ATMS aids engineers in a flight test environment by using expert system technology to optimize flight maneuver lists to fit time and range constraints. It is designed to aid both in pre-flight planning and in in-flight execution and monitoring. It is designed to benefit flight test engineers, researchers and pilots so that the best data possible is obtained at minimum cost and time.

- **Flight test planning**
  - **Program planning**
  - **Block planning**
  - **Preflight planning**
- **Flight test trajectory control**
- **Flight test maneuver monitor**
- **In-flight re-planner**

ATMS: Final System

The final ATMS system implementation will provide full flight planning, monitoring and control capabilities. The system uses knowledge of a flight project's goals, priorities and needs to formulate a plan for blocks of flights, individual flights, and finally chooses lists of maneuvers for each flight. The maneuvers for a specific flight are ordered to optimize use of available time, range, space and fuel.

After the FTE and system have defined a flight card containing an ordered list of maneuvers to be performed during the flight, the flight can be simulated either with a 3 degree-of-freedom simulation, or a more correct 6 degree-of-freedom simulation.

During the flight, the selected maneuvers can be flown by a research pilot or by a flight test trajectory controller through the RAV link. As each maneuver is performed, the monitor function checks data to be sure that it is of acceptable quality for research requirements. It also monitors constraints such as range boundaries and restrictions and aircraft structural limits to be sure they are not violated.

If a maneuver is stopped or unacceptable, the ATMS recommends a course of action: drop the maneuver, repeat it, or reschedule during a subsequent flight. Based on interaction with the FTE, a new plan can then be formulated in-flight.

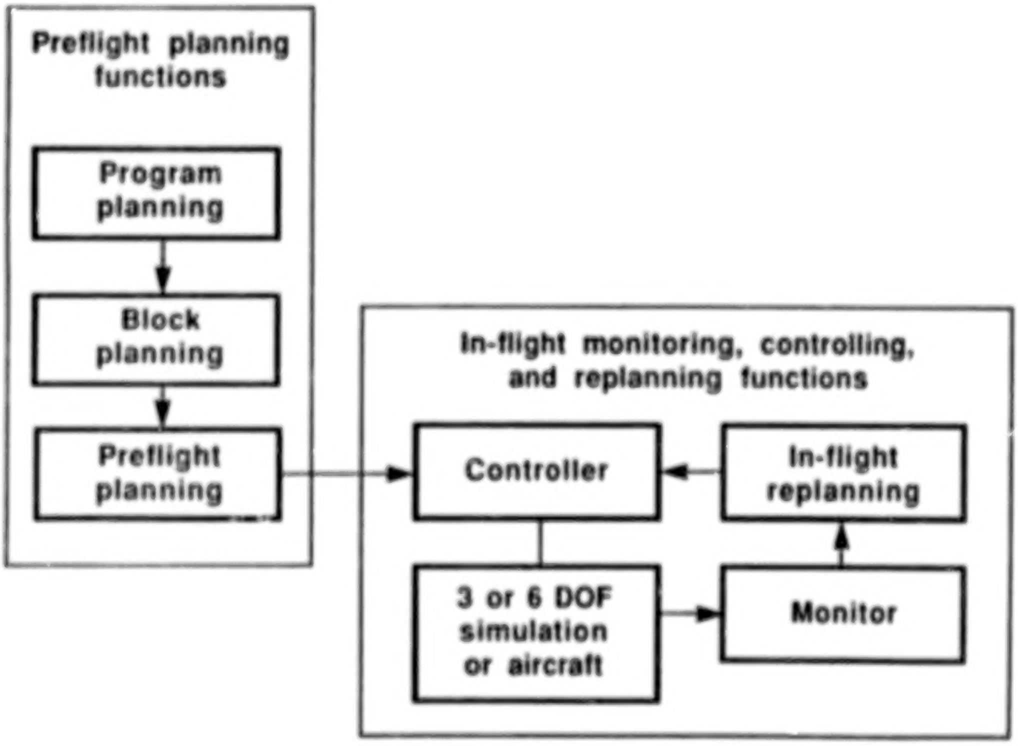
Preflight planning functions
Program planning
Block planning
Preflight planning
In-flight monitoring, controlling, and replanning functions
Controller
In-flight replanning
3 or 6 DOF simulation or aircraft
Monitor

ATMS: Current Functions

The current ATMS system (Phase I) implements a carefully selected subset of the final system design. The parts selected for implementation are designed to demonstrate distribution of processing, real-time control in a simulation environment, and limited planning and monitoring capability. This system was presented in a demonstration in June, 1988.

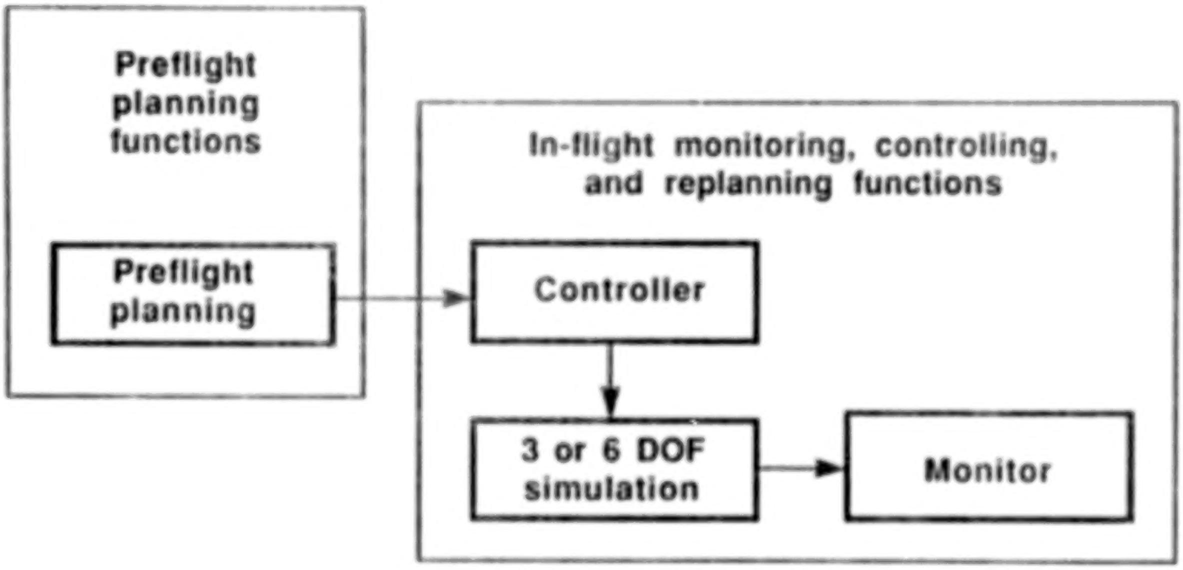
Preflight planning functions
Preflight planning
In-flight monitoring, controlling, and replanning functions
Controller
3 or 6 DOF simulation
Monitor

BEST COPY AVAILABLE

ATMS: Workstation Configuration

The following three figures depict three different configurations of the ATMS, showing how tasks are distributed among the processors. The configurations progress from planning to validation to flight test.

The first shows how tasks are partitioned for the flight test engineer workstation. This system allows the FTE to enter maneuvers, simulate maneuvers to estimate time, space and fuel used, and suggests an order for flight. The simulations are performed in a local workstation rather than the simulation facility to avoid scheduling time on the simulation computers until a more refined flight plan has been constructed.

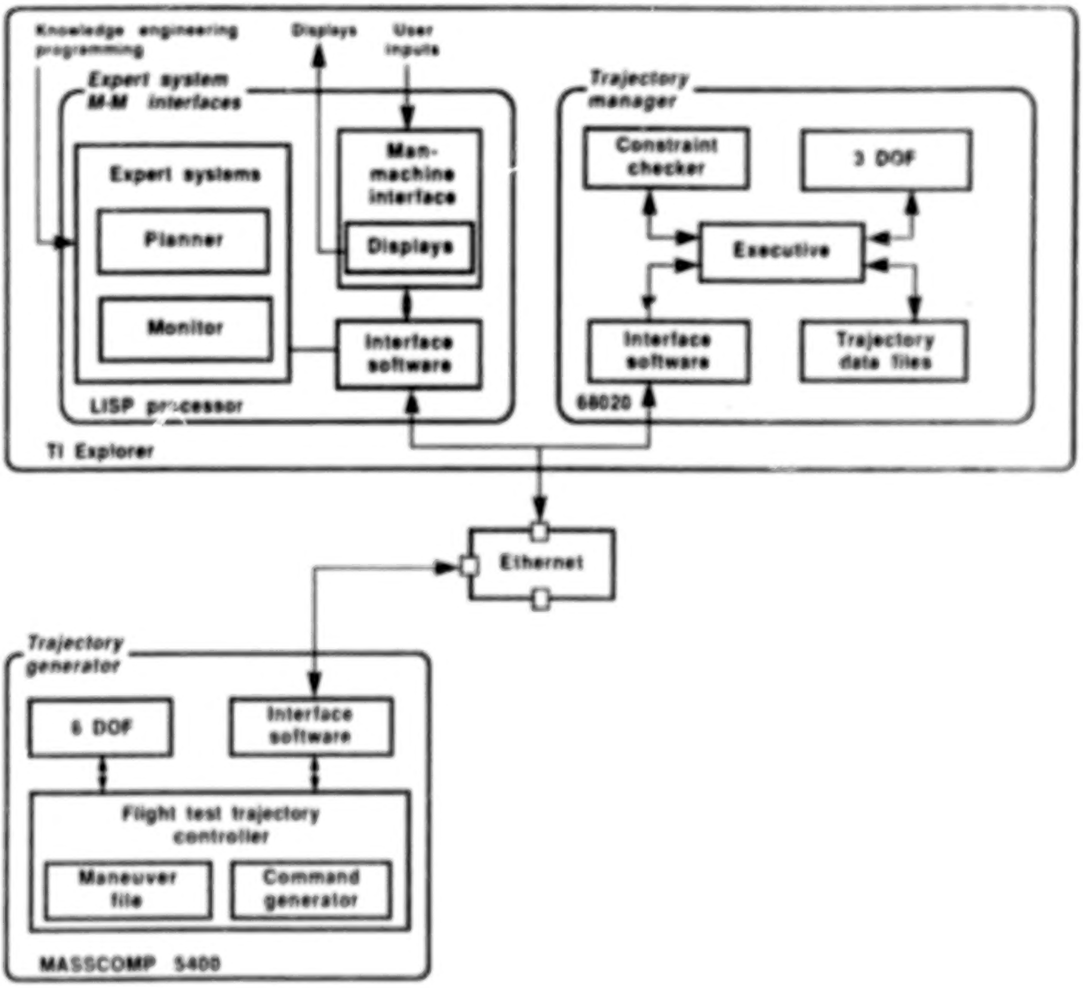

[illegible] Flight Configuration

[illegible] satisfied that the flight card is acceptable, the flight is conducted. The [illegible] can monitor data and range constraints, perform maneuvers, or both. The aircraft with RAV links is inserted in place of the simulation computers.

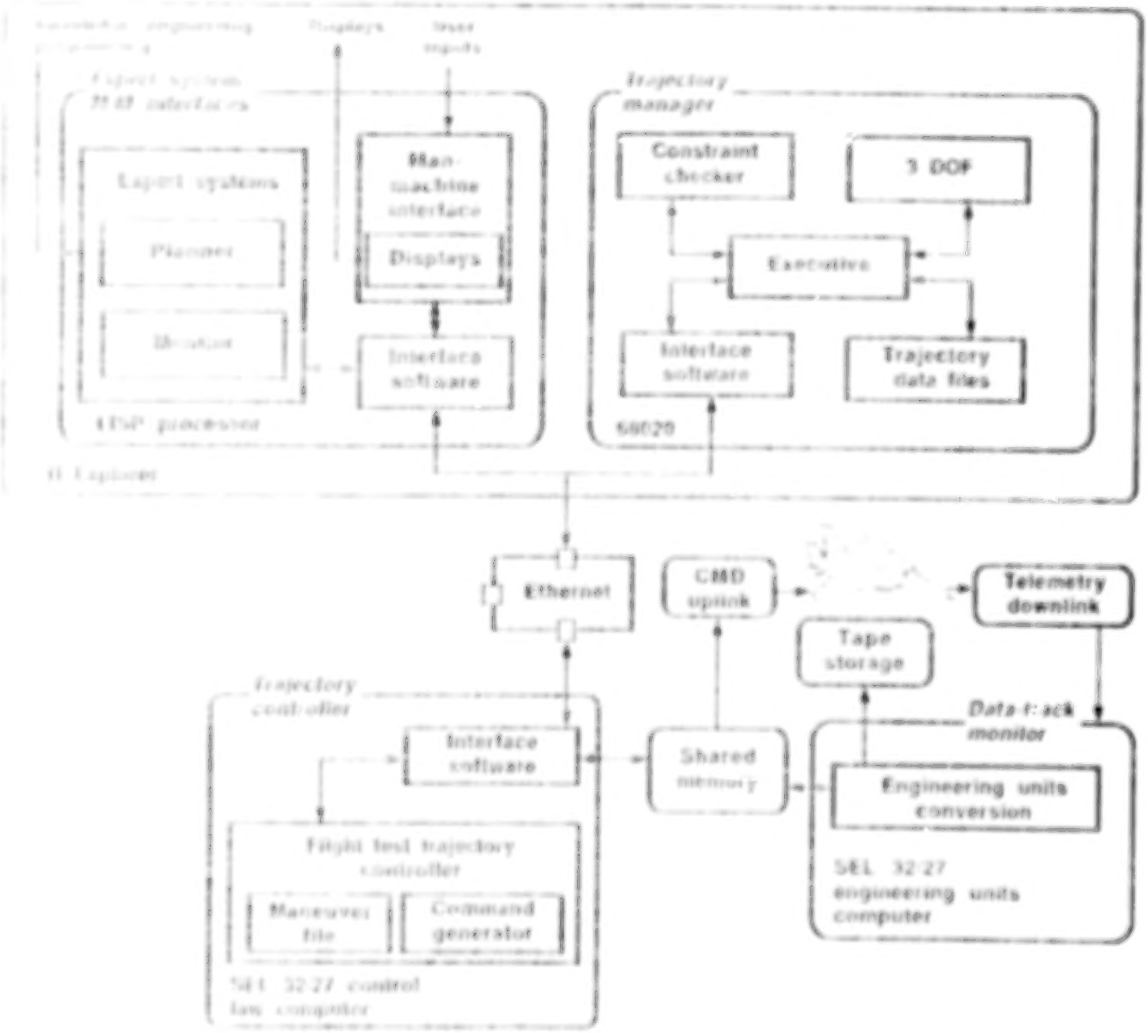

ATMS: Validation Configuration

The simulation validation system adds the Ames-Dryden real-time simulation facility computers and cockpits in place of the workstation. In this mode, the FTE can preview the flight with a research pilot, or obtain very accurate information about the fuel and range requirements.

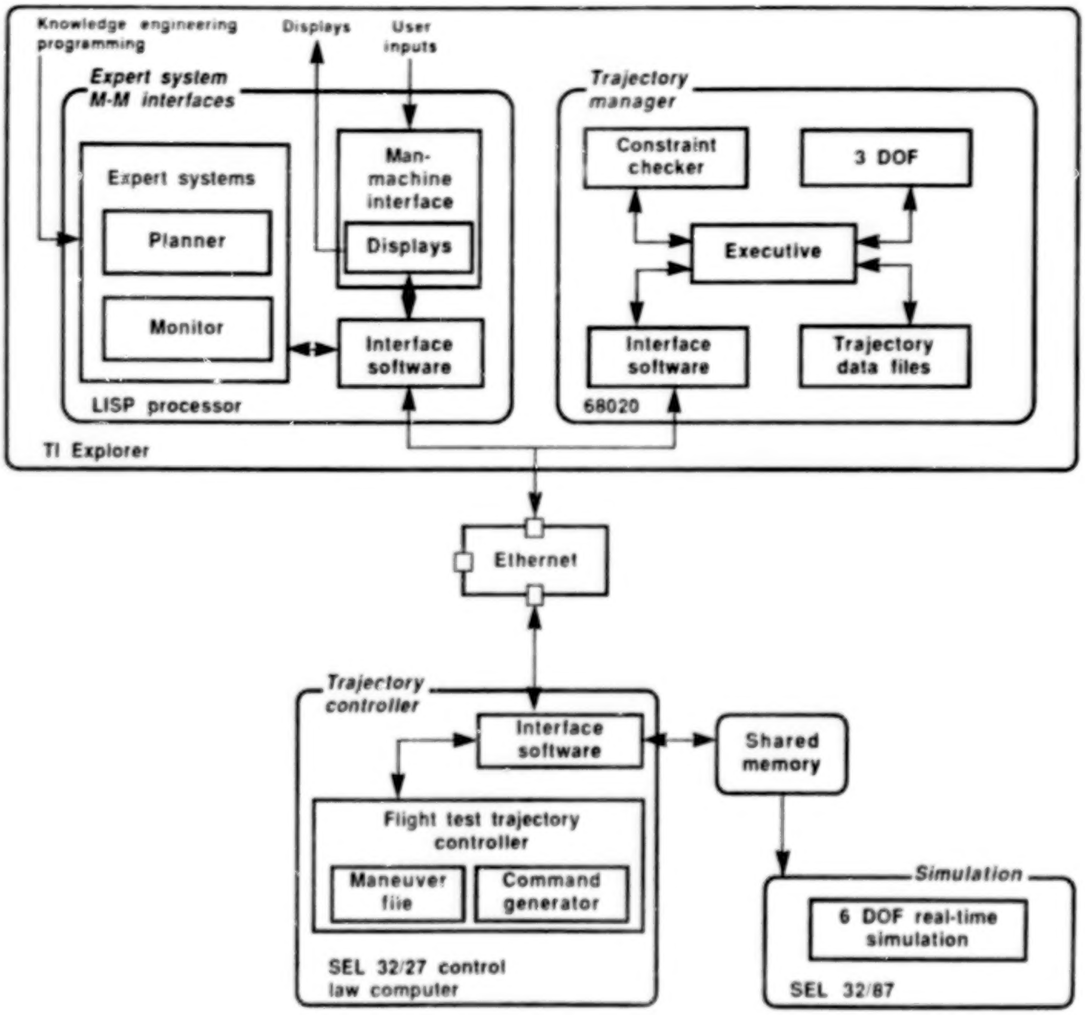

Status of the Rapid Prototyping Facility

The Rapid Prototyping Facility was developed to meet a need for a facility which allows flight systems concepts to be prototyped in a manner which allows for real-time flight test experience with a prototype system. This need was focused during the development and demonstration of the expert system flight status monitor (ESFSM). The ESFSM was a prototype system developed on a LISP machine, but lack of a method for progressive testing and problem identification led to an impractical system.

The RPF concept was developed, and the ATMS designed to exercise its capabilities. The ATMS Phase I demonstration provided a practical vehicle for testing the RPF, as well as a useful tool. ATMS Phase II development continues.

A dedicated F-18 is expected to be assigned for facility use in late 1988, with RAV modifications.

A knowledge-based autopilot is being developed using the RPF. This is a system which provides elementary autopilot functions and is intended as a vehicle for testing expert system verification and validation methods.

An expert system propulsion monitor is being prototyped. This system provides real-time assistance to an engineer monitoring a propulsion system during a flight.

- **Demonstration of expert system flight status monitor (10/86)**
- **Demonstration of Phase I ATMS (6/88)**
- **F-18 identified for facility (expected by 10/88)**
- **KBS autopilot**
- **Engine monitor**

BLANK PAGE

THE DESIGNER OF THE 90'S: A LIVE DEMONSTRATION

Tommy L. Green
Basil M. Jordan, Jr.
Timothy L. Oglesby

LTV Aircraft Products Group
Military Aircraft Division

THE DESIGNER OF THE 90'S: A LIVE DEMONSTRATION

A LOOK BACK

Whenever we attempt to look forward to anticipate changes that need to be made, we must first look back to see where we have been, for our experience, our history, and our culture should, and does, affect our vision of the future. Certainly, this principle applies in the area of aerospace design, and it is with this principle in mind that we take a few brief moments to look backward to see what we have learned that can be applied to the future.

When Orville Wright climbed into the seat of his power driven, heavier than air machine on that fateful day in December of 1903 at Kitty Hawk, North Carolina, he represented the ultimate in intimate involvement in the design process. The Wrights conceived the design; they worked out the details of the design; they analyzed the design both structurally and aerodynamically; they determined how the design could be built; they tested the design; and they ultimately flew the design. They knew all there was to know about that machine.

With that beginning, the era of flight began, and yet the knowledge required to fly had only been scratched. In a larger sense, that flight began an era of aerodynamic reason and understanding that probably reached its zenith in the late 40's and early 50's. There was so much to be learned that no one person could learn it all. Theoretical understanding was progressing at such a rapid pace that the average engineer had to begin specializing in particular disciplines so that he could remain cognizant in at least some part of the industry. As a result, aerospace engineering organizations were developed that recognized that need, and the aerospace specialist was born. This was both required and right.

The 1950's brought with it a new innovation that made even more sophisticated analyses possible. The advent of the computer opened up opportunities to analyze configurations and structures previously thought impractical. With it, the need for a new, more highly specialized engineer was created: the Engineer/Programmer. The tool became a technology in itself, and the Engineer/Programmer developed large, complicated analysis systems capable of analyzing structures of almost any complexity, limited only by "cpu power." These systems developed by the Engineer/Programmer in themselves bred another specialist, the applications user, who made it his full-time job to understand and execute these mammoth systems. This, too, was required and right.

HERE WE ARE

The 1960's and 1970's continued this trend of increased specialization as computer power and affordability dramatically increased so that today we are an aerospace engineering society that for the most part is made up of individuals who are experts in localized disciplines. What we lack are significant numbers of design engineers who can embody all the disciplines into a single design. As a matter of fact, the highly sophisticated computer solution techniques are rapidly making the young engineer ignorant of very worthwhile "back-of-the-envelope" solutions. Furthermore, engineers in general are becoming insecure of all but the most sophisticated solutions.

The ramifications of such a situation are significant. First of all, the numbers of functional specialists are staggering: conceptual designers, detail designers, stress analysts, fatigue analysts, aeroelasticians, dynamicists, mass properties engineers, materials and property experts, vibroacousticians, aerodynamicists, propulsion analysts, reliability experts, maintainability experts, producibility engineers, static test engineers, dynamic test engineers, flight test engineers, ad infinitum. That in itself is not necessarily bad, but in the design process as it is practiced in most aerospace companies today, the designer upon completion of his concept will shuffle out the design to all the different disciplines for them to weave their magic. What comes back to him is a series of usually late, conflicting requirements that puts the designer into the mode of iterating the requirements between the different disciplines to come out with a design that meets everyone's requirements. Unfortunately the requirements of some functional disciplines are not included since members of those teams are in such short supply they cannot cover all the bases. When everything is working perfectly, however, the system is tedious; time consumption is odious; and the design is hardly integrated. Furthermore, the design may be unproducible.

A LOOK AHEAD

Somehow, a less costly and higher quality design must be produced that encompasses all aspects of design including producibility. Producibility is singled out here because historically design engineering has emphasized configuring and sizing the aircraft so that it can meet its defined mission. How it will be built is someone else's problem. We see this as a serious flaw in the system. In addition, the other "ilities", ie., reliability and maintainability, must have their proper places in the initial phases of the design. And finally, the iteration time with all the different disciplines must be drastically reduced.

We have decided in the Military Aircraft Division of LTV Aircraft Products Group that to solve this problem, we must return more responsibility to the designer. That is, we want the designer to have the ability and the responsibility to design in the different disciplines himself without having to depend on analysts to do it for him. We want the analysts to act as specialists who work in the role of facilitator, consultant, and final analysis and checkoff.

In short, the designer will become the integration specialist with enough knowledge to at least preliminarily include all the design considerations in the design. In large measure, the only limitations to his ability to finally design in the different disciplines might be final definition of loads as defined by the customer. On the other hand, he will not be expected to perform major analyses such as finite elements, for example

Finally, we expect significant cost reductions using this approach, and we must provide a mechanism by which we can ensure that the improvements are reflected in the bids to the customer. Otherwise, we will use the additional time to further "fine tune" our design. Therefore, we must provide estimating tools that automatically include the productivity improvements that are provided.

THE DILEMMA

Certainly, we have defined a concept that sounds good, but how do we make it happen? The designer, as he reads this, probably feels like the poor guy in Figure 1. We are telling him he has the responsibility to be cognizant of all elements of design engineering and to personally include those elements in the design. He knows though, as we do, that no one engineer is likely to possess all this knowledge, and yet we believe that centralizing the design of a part in the hands of a single designer is the only way to get a truly integrated design and a resulting cost reduction.

"YOU MUST BE KIDDING!"

Figure 1

THE SOLUTION

The expert knowledge provided to him by individuals in the past must now be provided to him automatedly at his design work station as tools that he can use when he needs them. These tools must be computerized and must be provided in terminology that he can understand. Specifically, they must not be provided to him using terminology that the specialist uses but instead must be provided to him using terminology that he uses. The tools must be easy and convenient to use, and they must be integrated with his own design tools.

The expert system programming languages available now on the market provide us the opportunity to accomplish these goals. At LTV we are using these languages to capture the knowledge of our experts and, in turn, to provide that knowledge in an easy to understand way to our designers. In this way, we are capturing the thought processes of our experts and are coupling those thought processes with appropriate analysis tools so that the designer always has immediate access to the expert. Furthermore, our Engineering memory will never be lost as we shall always be updating these expert systems as design techniques change. This, by the way, becomes one of the main responsibilities of the specialist in this new design environment.

Realizing that multiple expert systems will be required for the designer to have access for all the different disciplines, we want to share data between those systems. This drives us, of course, to integrated data bases, and the development of those data bases becomes an integral part of the overall system. Furthermore, the different expert systems will be providing conflicting data requirements to the designer, thereby necessitating the need for an expert manager who will help him negotiate the conflicts. This is shown schematically in Figure 2 and represents probably our biggest challenge.

Finally, these tools must be brought to the designer in an easy-to-access manner that will encourage him to use them. In our way of thinking, this means that the same graphics terminal must be capable of delivering both the design tools and the design graphics. In addition, the terminal should be capable of accessing multiple computers simultaneously since the tools might be resident on a different machine than the design graphics machine.

EXPERT SYSTEMS IN THE DESIGN PROCESS

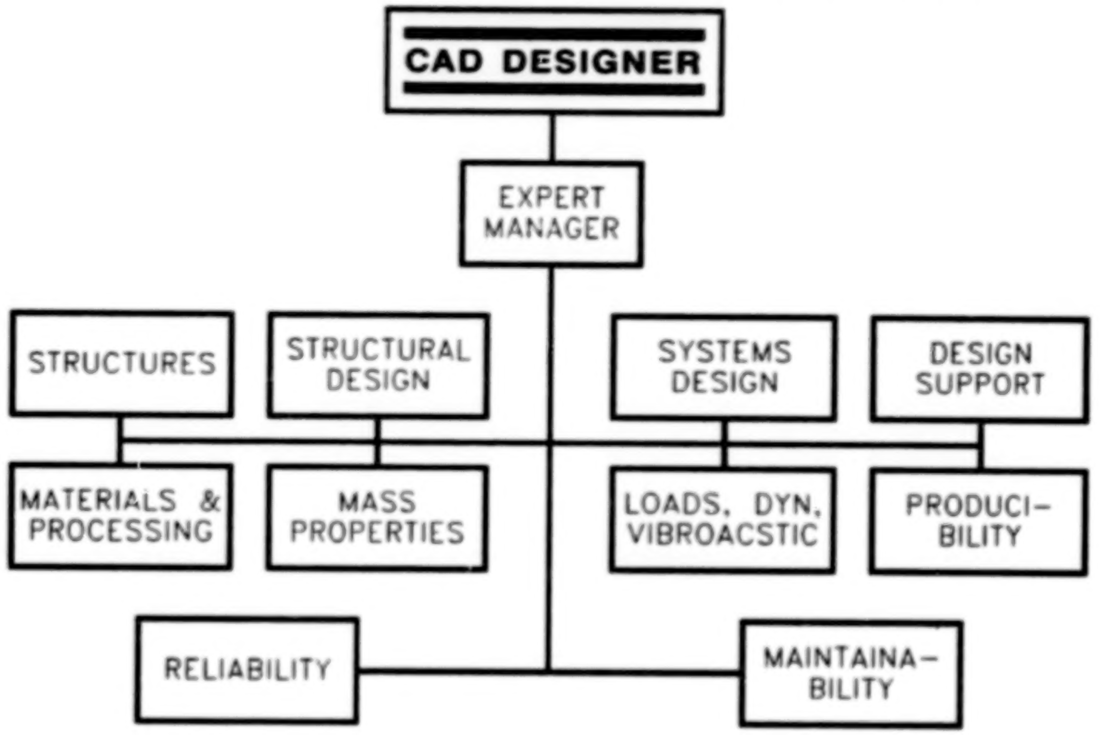

Figure 2

THE CULTURE

It should be apparent by now that we are not talking about automating the way we currently design our product. Instead, we are talking about changing the design process, putting more responsibility in the hands of a single designer. We are talking about culture changes. These kinds of changes are sometimes painful and sometimes involve turf battles. The team effort, where everyone is working together, must be emphasized. Willingness to change must be encouraged at every level. The analyst must be willing to accept that his role will be more one of providing the tools to the designer. Design teams must be co-located where communication is a standard and not an exception. Ultimately, this realization must be carried beyond the portals of Engineering to include manufacturing and quality technologies so that some day we'll be able to almost close that circle as it is shown in Figure 3.

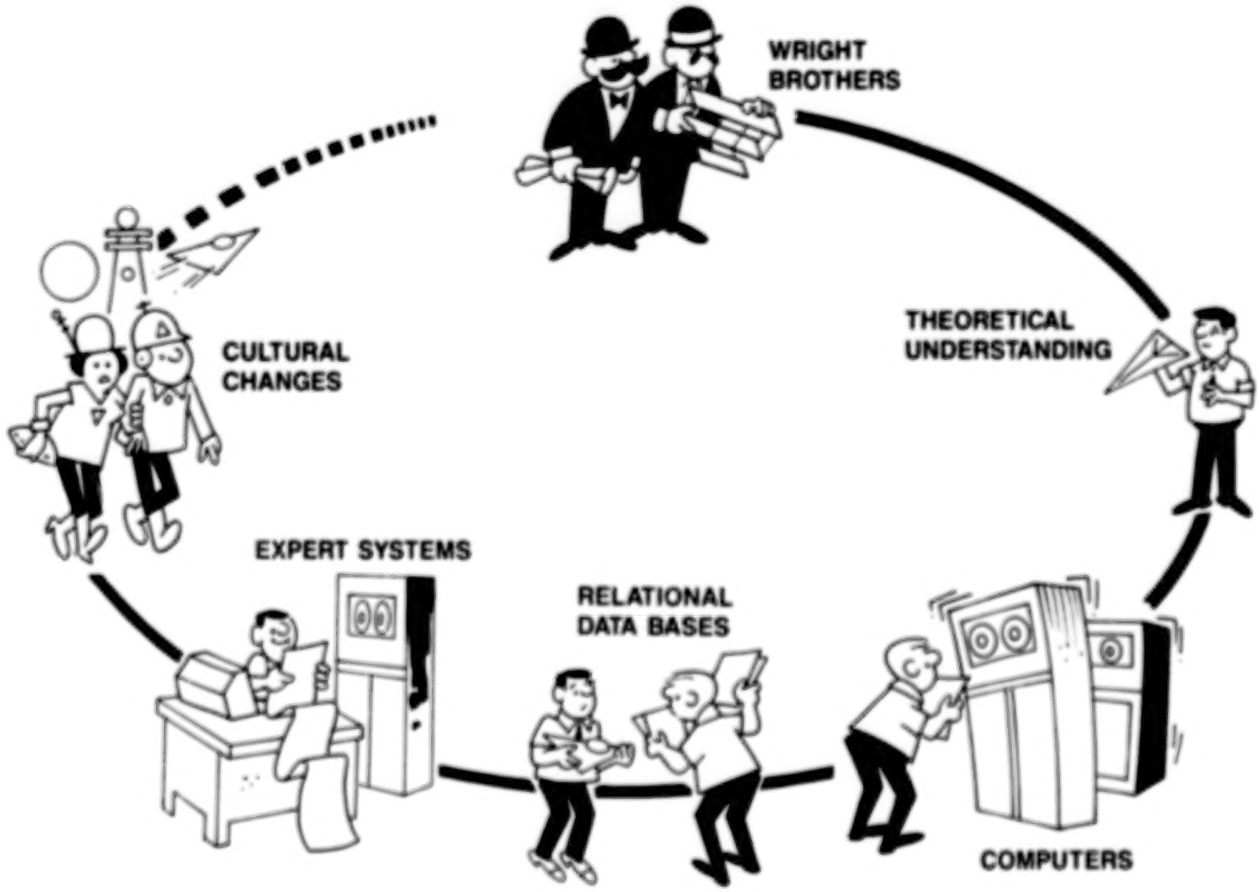

Figure 3

THE LTV AIRCRAFT PRODUCTS GROUP EXPERIENCE

The remainder of this paper details our experiences in developing the tools to meet the goals previously described. We started from scratch with a new organization, Computer Integrated Engineering (CIE), in April of 1986, and we obviously have a long way to go. We believe, however, we have glimpsed the future, and this paper is our first attempt to share that with the rest of the industry.

The Medium

The design tools that we are currently constructing are targeted to be utilized by the designer concurrently with the design graphics environment. As a result, we had to find a way to deliver tools to assist the design process at the design graphics workstation. One assumption we made is that Engineering will continue for the next several years to use IBM mainframe based design graphics packages until graphics workstations themselves become powerful enough and software mature enough to perform design graphics tasks locally in a cost effective manner. This seems reasonable since most major aerospace companies currently use IBM mainframe based design graphics packages for production work. CADAM, marketed by CADAM Incorporated, and NCAD/NCAL, which is a proprietary product of the Northrop Corporation, are the design graphics software packages currently in production usage by LTV APG Engineering for 2-D drafting and 3-D respectively.

The first approach we investigated as a solution to the problem of simultaneously delivering CIE tools and design graphics was that of utilizing the IBM 5080 equivalent graphics terminal which is the normal device used to display the design graphics. We hoped that this terminal could concurrently display the CIE tools with the design graphics. Although a simultaneous 3270 text window is supported on the IBM 5080 in addition to the high performance graphics capability utilized by the design graphics, access to the graphics capability of the 5080 device is restricted to a single software package at a time. Virtually all our tools require graphics display capability. The final conclusion was that the IBM 5080 equivalent terminal itself could be used only if the design graphics package was exited, the CIE tool was executed to completion, and the design graphics package was re-entered. This was deemed as an unacceptable limit on the interactivity between the design graphics and the CIE tools.

Another approach we considered was the provision of each designer with an independent graphics terminal for execution of CIE tools. This would provide the designer with two independent graphics display screens and two separate keyboards for entry into each system. This approach was deemed highly undesirable due to the loss of integration between the design graphics and the tools. Providing separate screens and keyboards not only consumes extra physical space, but is much more difficult for the designer to operate than a single screen and keyboard functioning in an integrated environment.

A third approach investigated was utilization of an engineering workstation that could emulate an IBM 5080 graphics terminal in software. This approach has the added advantage that workstations have powerful windowing tools that allow for the development of systems with extremely responsive user interfaces. There are several such products currently on the market; however, they all have the common problem that software emulation of an IBM 5080 is a compute intensive task which typically cannot be performed even half as fast as a hardware implementation without an unreasonably high investment in the workstation platform. Since our goal is to increase the productivity of the designer, provision of a slower design graphics terminal is hardly progress.

A unique product was found that combines a hardware implementation of an IBM 5080 equivalent graphics terminal and a workstation. At the time we originally discovered it, this product, called a CommSet 1080, was still under development as a joint effort by Spectragraphics Corporation and Digital Equipment Corporation (DEC). We obtained an evaluation machine and tested it with great success. This product consists of a standard DEC Color VAXstation 2000 and a standard Spectragraphics 1080GX. DEC VAX computers are already in use in many places within LTV. The VAXstation 2000 has the capability to run, within the constraints of VT220 or Tektronix 4014 terminal emulation, any software developed for any VAX computer within LTV without modification. The other half of the CommSet 1080 product is the Spectragraphics 1080GX. This device was already in use in several locations within LTV as an IBM 5080-002A equivalent terminal. The CommSet 1080 provides the user with a complete engineering workstation which can simultaneously display and use information from several different sources. One window on the workstation can be a design graphics terminal session utilizing the IBM 5080 equivalent capability implemented in hardware by Spectragraphics. Provision of a workstation for the designer allows the majority of the CIE tools to run locally on the workstation, providing excellent response time to the designer. The CPU power of each workstation is roughly equivalent to that of a DEC VAX 11/780. Since the workstation is directly connected to the network, it can easily exchange information with or provide terminal sessions to host VAX systems or IBM mainframes. We demonstrated the feasibility of this approach utilizing the vendor evaluation equipment to implement a preliminary sizing application developed for Structural Design. The windowing capability of the workstation has allowed the designer exactly the desired capability to simultaneously display and manipulate information from the design as well as from CIE tools that can be run locally on the workstation. The CommSet 1080 makes it possible to provide a full performance IBM 5080 equivalent graphics terminal in a workstation windowing environment.

We have concluded, therefore, that the requirements we had for delivering the tools to the designer can be met. Currently, the CommSet 1080 meets those requirements, and we are sure that more vendors will be entering this market. In the environment we have defined, simultaneous accessibility to multiple software applications on multiple hardware platforms is an absolute must, and the technology is now available to support that need.

The Tools

Having defined a philosophy and identified a medium to implement that philosophy, all that remains is to present those tools we are currently developing for the designer. The intent of all these tools is to give the designer the capability to perform more of the design himself and to design in from the beginning reliability, maintainability, and producibility considerations.

The principle tool used by the designer in the development of "drawings" is software designed to provide him with the capability to draw. Hence, the theory of design is left to the designer's experience and intuition. Even though some graphics software offers application and analysis programs to assist the designer with his tasks, these programs are usually benign in that they offer virtually no instruction or reasoning as to their use or application.

The tools being developed are designed to assist the designer in making the correct decision for a given set of circumstances. A very large portion of the time used to develop a piece of software is devoted to being certain the user interface is understandable by the user. In most of our cases, when an analysis or application is accessed by the designer, the logic for its use is part of the program. All software applying the "expert system" technology provides, as an integral part of the code, the set of rules required to obtain that particular solution. In addition, the source of all rules, be they logical or heuristic, are provided as a matter of course. Tools currently under development are summarized as follows.

PRELIMINARY SIZING: This series of programs offers preliminary sizing based on Tension-field and Shear resistant analysis of beams with flat shear webs, lug stress analysis, and joint loads analysis. Even though the term preliminary is used to describe the analysis, the methodology is as valid as the loads that are being supplied. The program emulates the way in which the analysis procedure is applied within LTV, but for the most part is an exact parity of procedures described in numerous sources. However, instead of providing the designer with raw code, the program is prefaced with a description of the code, a definition by question and answer sessions to assure understanding, and an exclamation of the output.

MATERIALS DATA BASE: Physical and mechanical data are assembled as common reference for any program that might require materials type information. Our materials data base has been limited to those materials most commonly used by our organization. Those include aluminums: 2xxx series, 5xxx series for cryogenics, 6xxx series for welding, and several 7xxx series for structural applications; titaniums, Ti6-4 and Ti10-2-3; steels to include stainless, high nickel, and inconel; composites to include fiberglass, kevlar, graphite, bismaldeide, and polyimide. Mechanical data for composites such as areal weight, resin content, density, and fiber volumes are readily available to the user be they a person doing a query or a program seeking specific information. Similar types of data are stored for metals such that rapid accurate access is possible. Other attributes of the data include the applicable material and/or process specifications cross-referenced to LTV specifications, the Military specifications, and the vendor specifications. The intent of this software is to supply needed data to the users in a very timely manner, but just as important is the need to provide the same information to all users; i.e., standardization.

STANDARDS PARTS DATA BASE: Similar to the MATERIALS DATA BASE, the principle intent is assurance that the part being referenced by the designer is a part that is a standard (whenever possible) for our company. Our data base thus far is limited to fasteners, simple fittings, and simple brackets. The key to the base is establishing the calls that will make the part unique. For instance, querying a base for all fasteners that have hex heads would produce several hundred types (which is in most cases unacceptable to the user); on the other hand, if the query said "give me a list of all fasteners that have HEX heads, have SHEAR strengths greater than 6000 lbs, but less than 7000 lbs, must be workable in a 900 deg. F environment", then the list would be greatly reduced, and a selection could be easily made that would still be from a list of standard parts. Using standard parts obviously reduces both design and manufacturing activity costs.

RELIABILITY EXPERT SYSTEM: An expert system using the backward chaining approach is used to select fasteners to be used for metal to metal, metal to composite, or composite to composite mechanically fastened joints.

Fasteners as related to structural reliability, account for about 60% of the aircraft structural maintenance items. The software uses a commercially available expert system shell, a relational data base, and an internally developed knowledge base (about 250 rules), the latter being unique to LTV. This system when applied will eliminate most of the problems associated with improper selection of fasteners. Some of the criteria used for selecting fasteners include: type of joint-single or double shear; fastener configuration-single or multi row; application-safety of flight, primary or secondary structure; location on vehicle-internal, in ducts, on the surface, fuel cells; type of installation-wet or dry, blind or open.; acoustic environment and others as would apply to the successful selection of fasteners. The expert system allows us to provide to the designer the knowledge base of our company and the industry at a point in the design process when it is most needed. By using this type of system, we are able to retain the knowledge that much more experienced personnel have observed. As these more experienced personnel retire or are promoted into managerial positions, their knowledge is retained.

MAINTAINABILITY EXPERT SYSTEM: Unlike the RELIABILITY function, MAINTAINABILITY is primarily interested in the time required to remove, repair, and replace a particular item. Their function depends almost entirely on the final configuration of the vehicle and, as a result, their ability to assess the maintenance factors only occurs near the end of the design phase. However, many examples, specifications, and requirements exist in journals, design handbooks, and technical orders. The challenge for the maintainability engineer is to move that information to the designer at a stage when the design can effectively be changed and in a form that is useful to the designer. This expert system through a series of calls and a combination of question and answer sessions allows the designer, using the Hypertext technique, to "leaf" through large volumes of information and find the bit of information that is specifically applicable to his component.

COST AND PRODUCIBILITY EXPERT SYSTEM: With cost a very prime consideration in any design, this module, CAPES, is one of the more important tools available to the designer. The concept employed is to provide the designer with the capability of choosing the least expensive method of manufacturing a particular part; i.e., should the part be a forging, bar, extrusion, plate, or composite. Each selection is dependent on the available manufacturing equipment, the availability of material, type of material, and if the part is a standard. This software is customized for LTV and must be constantly upgraded to reflect new manufacturing techniques and processes. Our ultimate goal in developing this particular application is to elevate manufacturing design considerations to the same level as configuration design considerations.

ACOUSTICS EXPERT SYSTEM: Acoustic design analysis is a difficult technology that historically is best performed by an expert in the field. The acoustics expert system attempts to capture the knowledge that has been stored by the expert and present that knowledge in an easy-to-understand manner to the designer. In this system, basic structural elements such as stiffened beams (metal or non-metal) or sandwich panels subjected to noise emitted from turbofan, turbojet (w or w/o afterburner), wakes/cavities, or unducted fans can be analyzed to determine the effects of acoustics or to size the structure to withstand the environment. The program provides the designer or project manager guidance as to the severity of the acoustic environment and helps in the design of a particular part if the software indicates a potential problem.

SCHEDULING SYSTEM: Numerous scheduling systems, more commonly called PROJECT/PROGRAM MANAGEMENT SYSTEMS, are available on the market. We are acquiring and modifying one of these systems to meet our specific requirements. Primarily, we are changing the input/output screens to use our "words" or "meanings". These systems are designed to provide real-time scheduling as opposed to hand-developed manually supported schedules that usually are only valid the minute they are prepared. To effectively provide information necessary to assess the progress of a project, information to the drawing level coupled to any organization that supplies data must be available. For the lead designer or lead supervisor to effectively manage, he must have intermediate check points within the drawing schedule that allow him to determine progress. More importantly, PROJECT MANAGEMENT SYSTEMS provide the designer, the lead person, the supervisor, project or program manager the capability of doing "what if" studies in real-time, thereby allowing the person to manage (as opposed to reacting). Similarly, the designers (or the person who is doing the task) must have and understand the activities they are tasked to do and when they are tasked to do them, and what happens when they do not. Even though this software will more than pay for itself just satisfying a need within the design community, it can be and will be a lot more than that. Along with the Drawing Tracking System described below, it will unite Engineering and Manufacturing into a more cohesive unit, giving Manufacturing insight into what Engineering is doing and Engineering insight into how its decisions affect Manufacturing. To compete in today's marketplace, integration of all technologies is mandatory, and integrated scheduling is a big part of that.

DRAWING TRACKING SYSTEM: With any project that requires even a few drawings, specifications, or procedures, the requirement to maintain configuration control of the product, to know where and when the data is being used, and to provide visibility to the users of "things to come" is of the utmost importance to the effectiveness of the project and the company. Our drawing tracking system is being devised to provide control at the earliest possible time of the activity. Specifically, when the designer determines from his schedule that a drawing of the part should begin, he provides the parameters that make the drawing unique (e.g., the part is a forging to be machined that is the cap of a spar which is the front spar of the vertical tail which is part of the aircraft). The same scheme used for the Work Breakdown Structure for the vehicle will be used to collect charges necessary to prepare the drawing and all supporting data necessary to build the part. All phases of the DRAWING TRACKING SYSTEM are electronic in nature such that designation, sign-off, release, traceability, accessibility, availability, and maintainability of individual deliverable items are simple and effective.

ENGINEERING EXPERT: Integration of these tools presently remains at the discretion of the designer. As we continue to develop design tools, the need for an ENGINEERING EXPERT will become more important. In those cases where the functional requirements conflict, the designer must be provided assistance in making decisions. As previously stated, this represents probably our biggest challenge, but it is a challenge that must be addressed.

THE CONCLUSION

The United States Aerospace industry is on the verge of a new plateau, and that plateau can be summarized in one word, INTEGRATION: integration of manufacturing and engineering, integration of data bases, integration of scheduling, and, we believe, integration of all design functions within a single discipline. We believe that to compete in an international market, this will be essential. We have attempted in this paper to express our logic for that conclusion, and we at LTV are working diligently to employ that belief in our design process. We hope that the paper has been helpful in stimulating your own thinking, and we welcome any comments that you might have on this subject.

BLANK PAGE

SESSION 4: AEROELASTIC TAILORING

Chairmen: B. A. Rommel and T. A. Weisshar

BLANK PAGE

STRUCTURAL TAILORING OF COUNTER ROTATION PROPFANS

NAS3-23941

K. W. BROWN
PRATT & WHITNEY AIRCRAFT
EAST HARTFORD, CT

AND

D. A. HOPKINS
NASA LEWIS RESEARCH CENTER
CLEVELAND, OHIO

THE STAT PROGRAM PREVIOUSLY APPLIED ONLY TO SINGLE ROTATION PROPFANS

The STAT program (refs 1 and 2) was designed for the optimization of single rotation, tractor propfan designs. New propfan designs, however, generally consist of two counter rotating propfan rotors.

STAT is constructed to contain two levels of analysis. An interior loop, consisting of accurate, efficient approximate analyses, is used to perform the primary propfan optimization. Once an optimum design has been obtained, a series of refined analyses are conducted. These analyses, while too computer time expensive for the optimization loop, are of sufficient accuracy to validate the optimized design. Should the design prove to be unacceptable, provisions are made for recalibration of the approximate analyses, for subsequent reoptimization.

- OPTIMIZATIONS ARE PERFORMED USING APPROXIMATE ANALYSES
- REFINED ANALYSES ARE USED TO RECALIBRATE APPROXIMATE SOLUTIONS

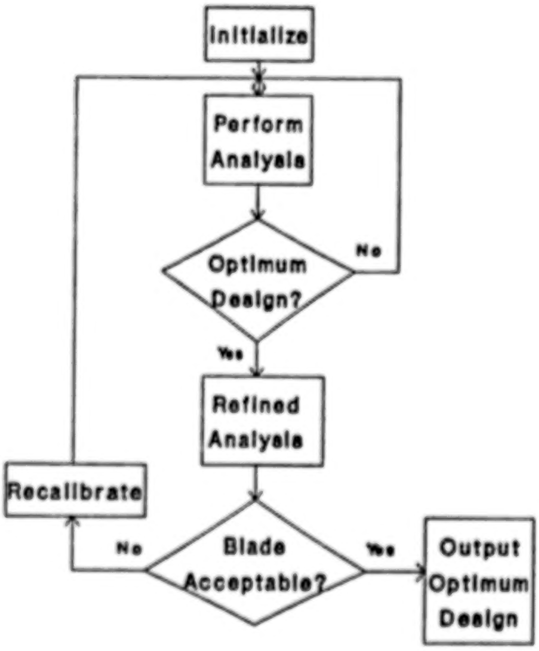

THE STAT APPROXIMATE OPTIMIZATION SYSTEM IS HIGHLY MODULAR

The STAT system has been constructed such that all analysis packages are highly modular. As appropriate, new analytical capabilities may quickly be installed into the STAT system. This tactic has proved valuable in the process of upgrading STAT for counter rotation propfans.

STAT execution is controlled by an executive module. The ADS optimization package (ref 3) is utilized to select a new geometry for evaluation. Each candidate design is analyzed to determine its efficiency and acoustic emissions characteristics. Structural response, including stress and vibrations, are determined using a large deflection finite-element analysis. Flutter and 1-P forced response analyses are performed using the modal outputs from the finite-element analysis.

- EXECUTIVE SYSTEM CONTROLS MODULE EXECUTION, DATA STORAGE
- ANALYSIS PACKAGES ARE EASILY REPLACED
- OPTIMIZER SELECTS THE NEW CONFIGURATION FOR ANALYSIS

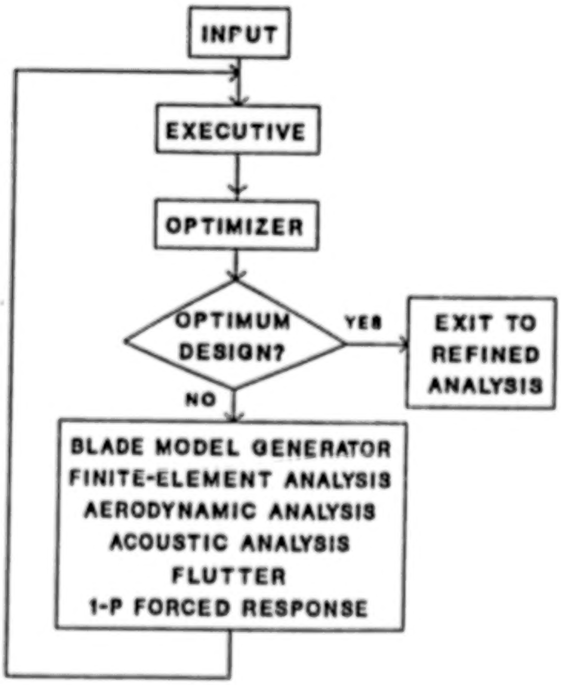

STAT HAS BEEN ENHANCED TO OPTIMIZE COUNTER ROTATION PROPFANS

To provide for the capability to optimize counter rotation propfans, many of the STAT modules required significant upgrading. The capability to input data for a rear rotor was added to STAT, while preserving the single-stage optimization capability. Counter rotation capabilities were added to the STAT aerodynamic analysis. A second finite-element analysis was added to account for the rear rotor. The acoustics analysis was upgraded from a regression analysis to a closed-form analytical procedure. The STAT objective function was enhanced to properly evaluate the cost of counter rotation propfan configurations.

- INPUTS - TWO BLADES
- AERODYNAMICS - ANALYSIS FOR TWO-STAGE ROTOR
- FINITE-ELEMENT ANALYSIS - TWO SEPARATE ANALYSES ARE CONDUCTED
- ACOUSTICS - IMPROVED ANALYSIS
- OBJECTIVE FUNCTION - ENHANCED FOR TWO-STAGE ROTOR

SEVERAL DESIGN VARIABLES AND CONSTRAINTS HAVE BEEN ADDED TO STAT

The original version of STAT allowed for significant variation of the original propfan design. This capability has been maintained in the new version of STAT, with, additionally, a full complement of design variables for the rear rotor, as well as rotor-to-rotor design variables, including blade count, rotor spacing, and rotor rotation speed.

A full set of design constraints is available for the rear rotor, including stress, resonance, flutter, and forced response limits. Additionally, n-P forced response limits have been added, along with axial clashing, total power, and rotor torque split constraints.

- ADDED DESIGN VARIABLES:
  - REAR ROTOR BLADE DEFINITION
  - BLADE COUNT
  - ROTOR SPACING
  - ROTOR ROTATION SPEED
- ADDED CONSTRAINTS:
  - n-P FORCED RESPONSE
  - AXIAL CLASHING
  - TOTAL POWER
  - TORQUE SPLIT

STAT IS USING A FULL-SCALE CRP VERIFICATION CASE

As verification of the STAT counter rotation optimization capability, the CRP-X1 counter rotation propfan model blade (NAS3-24222) has been selected. Available wind tunnel test data will provide an excellent opportunity to compare the STAT approximate analyses with actual test results.

The CRP-X1, scaled to full size, with spar-shell construction, will provide an excellent optimization vehicle to test the capability of STAT.

- TEST CASE BENEFITS FROM CRP-X1 SCALE MODEL TEST EXPERIENCE
- STAT VERIFICATION IS STUDYING A FULL-SIZE CRP
- LAP TYPE OF SPAR-SHELL CONSTRUCTION IS EMPLOYED

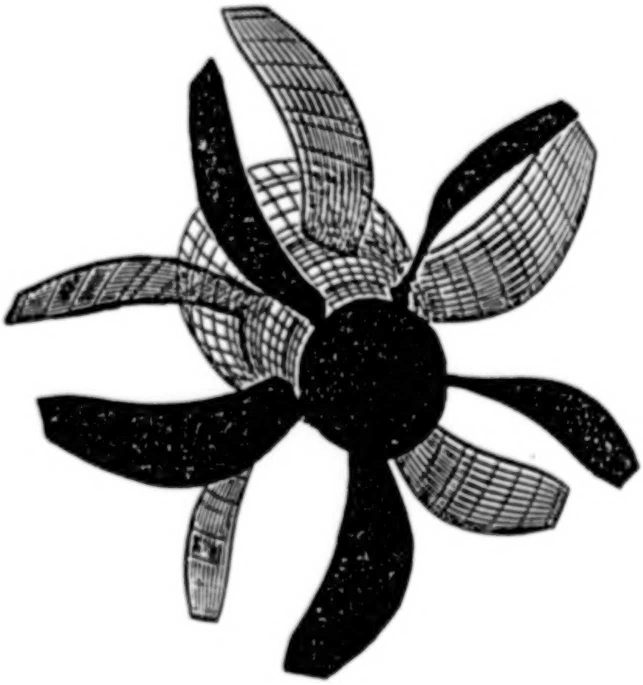

CR-STAT VERIFICATION:
CRP-X1 SCALE-MODEL PROPFAN

STAT approximate analysis results have been compared with detailed finite-element analysis and with available wind tunnel test data for the CRP-X1 solid metal scale-model propfan.

Very good at-speed frequency correlations are noted between both finite-element analyses and data taken from test. Comparisons of maximum radial stress between the two finite-element analyses also show a very good agreement.

- BASELINE CALIBRATION - WIND TUNNEL DATA FROM CRP-X1 SCALE-MODEL PROPFAN

		STAT	REFINED	TEST
• MAX STRESS, KSI		43	42	
• NATURAL FREQUENCY, CPS	f1:	217	215	200
	f2:	488	470	440
	f3:	624	675	680

CRP-X1 APPROXIMATE STRESS DISTRIBUTIONS AGREE WITH REFINED ANALYSIS

Comparisons of radial stress distributions for the camber side of the front blade of the CRP-X1 show that the approximate STAT finite-element analysis is quite accurate for both stress values and stress distributions. Similar comparisons are noted for other steady stress components.

BESTRAN ANALYSIS

FRONT BLADE
7650 RPM, Steady Stress ksi
Cruise Camber Side (Spanwise)

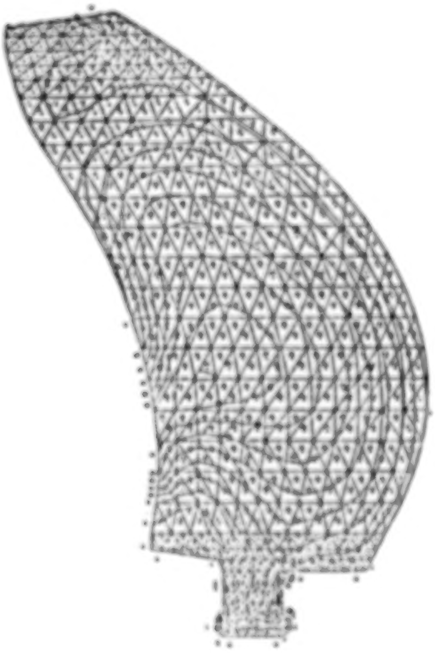

STAT APPROXIMATE ANALYSIS

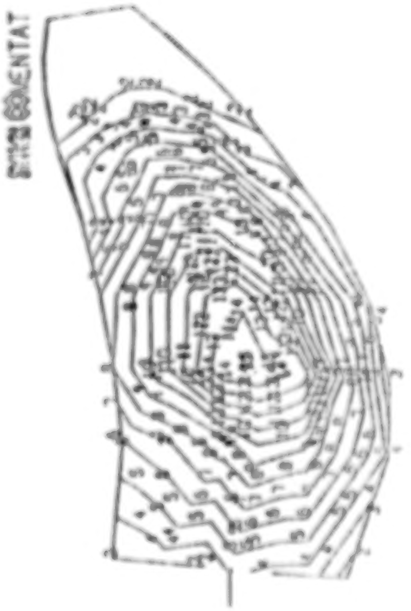

FIRST BENDING MODE SHAPES AGREE BETWEEN APPROXIMATE AND DETAILED ANALYSIS

First mode eigenvector comparisons between refined BESTRAN analysis and approximate STAT analysis show very good agreement. Mode shape differences, particularly differences in angular orientation of equi-deflection lines, have been shown important to the STAT flutter stability prediction.

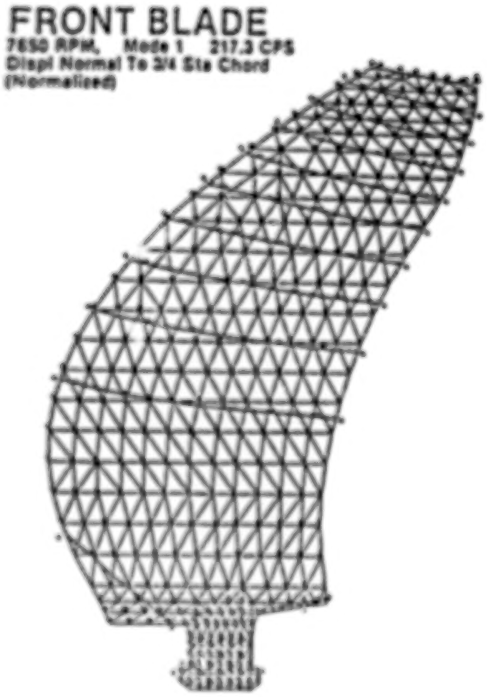

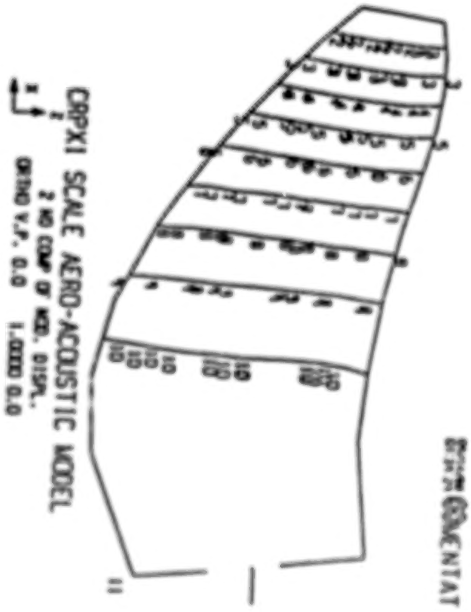

SECOND BENDING MODE SHAPES AGREE BETWEEN APPROXIMATE AND DETAILED ANALYSIS

For the second bending mode, very good frequency and mode shape correlations are also noted.

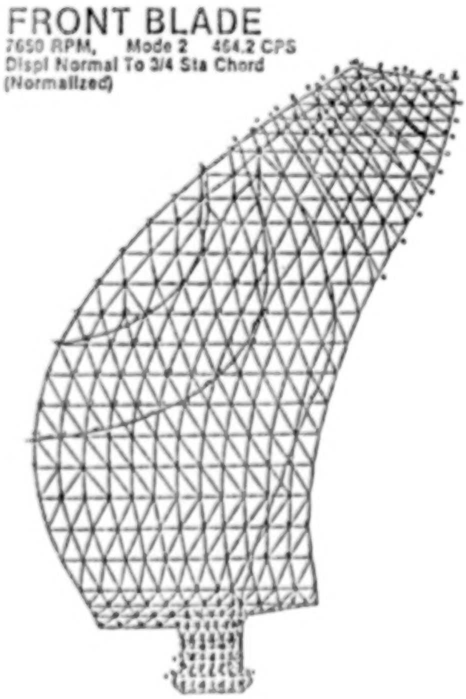

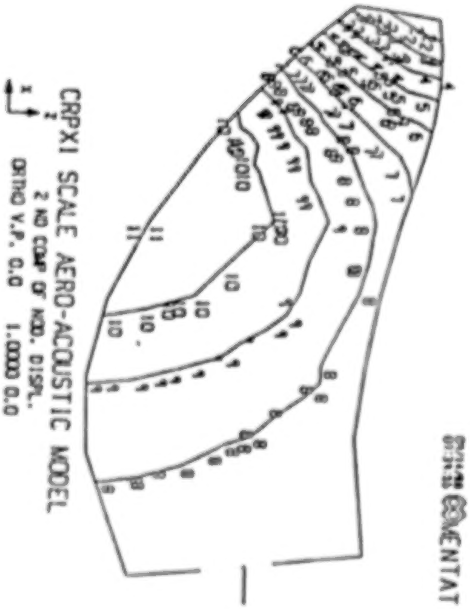

FIRST TORSION MODE SHAPES AGREE BETWEEN APPROXIMATE AND DETAILED ANALYSIS

Very good correlations are also noted for the first torsion mode. For higher modes, larger differences occur. However, for approximate optimizations, the STAT analysis gives a dependable level of accuracy.

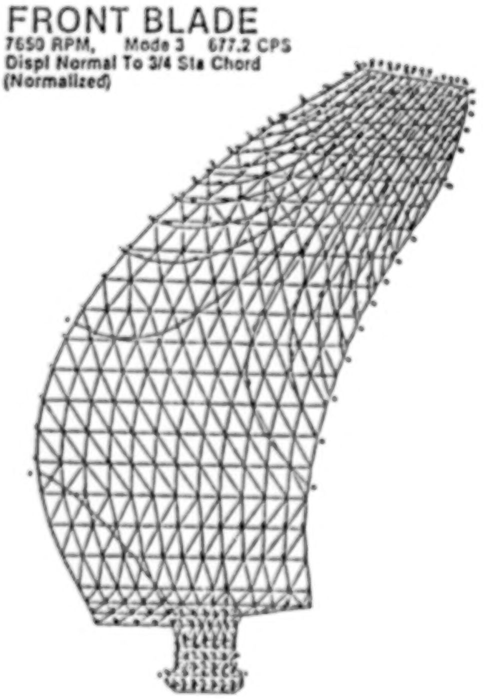

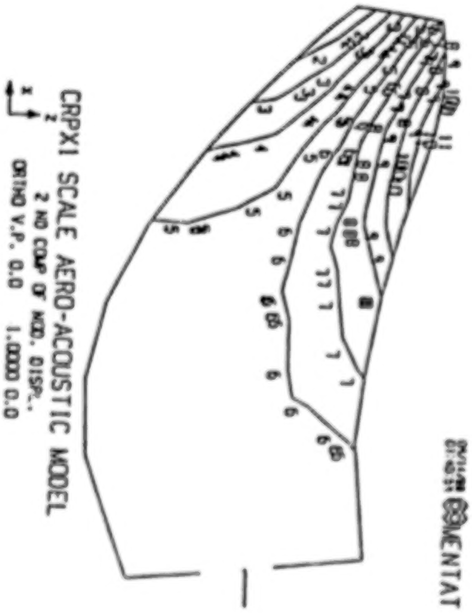

A FULL-SIZE CRP
OPTIMIZATION IS IN PROGRESS

The geometry of the CRP-X1 counter rotation propfan has been expanded to a 12-foot diameter, full-size rotor. A metal spar, fiberglass shell construction has been employed for this full-size CRP optimization. Several bugs in the system have been removed, and we are currently nearly ready to run this full scale counter rotation propfan optimization.

- CRP-X1 GEOMETRY HAS BEEN SCALED TO FULL SIZE
- SPAR-SHELL COMPOSITE CONSTRUCTION WILL BE EMPLOYED
- THE OPTIMIZATION IS NEARLY READY TO RUN

BEST COPY AVAILABLE

CONCLUSIONS

In conclusion, the STAT program has been enhanced for the tailoring of counter rotation propfans. Due to the modular nature of STAT's construction, this enhancement was possible by enhancing only the separate analysis modules, with only minor system modifications required.

The new STAT approximate analyses have shown excellent correlations with available CRP test data. A full-scale CRP optimization is currently being performed.

- STAT'S MODULAR FORM ALLOWED CONVERSION TO CRP OPTIMIZATION
- STAT APPROXIMATE ANALYSES GIVE GOOD CORRELATION WITH BOTH DETAILED ANALYSIS AND TEST
- WE WILL SOON HAVE CRP OPTIMIZATION RESULTS

REFERENCES

1. Brown, K. W.; Harvey, P. R.; and Chamis, C. C.: Structural Tailoring of Advanced Turboprops. AIAA/ASME/ASCE/AHS 28th Structures, Structural Dynamics, and Materials Conference, Monterey, Ca., April, 1987.

2. Brown, K. W.: Structural Tailoring of Advanced Turboprops (STAT). NASA CR 180861, 1988.

3. Vanderplaats, G. N.; Sugimoto, H.; and Sprague, C. M.: ADS-1: A New General Purpose Optimization Program. AIAA 24th Structures, Structural Dynamics, and Materials Conference, Lake Tahoe, Nevada, May, 1983.

COMPOSITE SIZING AND PLY ORIENTATION FOR STIFFNESS REQUIREMENTS USING A LARGE FINITE ELEMENT STRUCTURAL MODEL

N. A. Radovcich and D. P. Gentile
Lockheed Aeronautical Systems Company
Burbank, California 91520

SUMMARY

A NASTRAN bulk dataset preprocessor was developed to facilitate the integration of filamentary composite laminate properties into composite structural resizing for stiffness requirements. The NASCOMP system generates delta stiffness and delta mass matrices for input to the flutter derivative program. The flutter baseline analysis, derivative calculations, and stiffness and mass matrix updates are controlled by engineer defined processes under an operating system called CBUS. A multi-layered design variable grid system permits high fidelity resizing without excessive computer cost.

The NASCOMP system uses ply layup drawings for basic input. The aeroelastic resizing for stiffness capability was used during an actual design exercise.

INTRODUCTION

Design of efficient structures is a classic problem for high performance and fuel efficient aircraft. This is highlighted by the continuing search for more efficient materials to be used in the design process. Current aircraft designs are focusing on composites.

Aircraft designs require structural sizings which satisfy aeroelastic requirements within the airplane flight envelope. The more successful designs achieve this with lowest possible structural weight.

It is not uncommon to separate the structure sizing process into two phases: (1) sizing for strength, fatigue, and buckling, and (2) sizing for flutter, deflection constraints, tailoring for loads alleviation, and aircraft flexible stability derivatives requirements. The latter are grouped together as design for stiffness, and the structural sizing increment over the strength sized structure is known as the stiffness weight increment. While tailoring the structure characteristics to reduce loads is not the same as satisfying flutter requirements, the methodology and approach are the same. However, stiffness weight increment loses some of its meaning.

Current aircraft designs incorporate aircraft structural arrangements for fuselage, wing, canards, vertical and horizontal surfaces, which often preclude adequate structural representation by the more traditional EI/GJ based models used in dynamic analyses. Consequently, dynamic analyses require more complex structural modeling details which were once reserved only for stress analyses.

One major problem with the finite element approach is the timely availability of a strength sized design early in the design process. First, the fabrication of the finite element model is a labor intensive process. Second, the sizing of the finite element model requires first rigid loads and then flexible loads. This procedure produces at least two sizings. If the sizing is not automated, then the strength sized model may not be available for stiffness design.

The issue of generating a finite element model which is strength sized is being addressed by Lockheed in an Independent Research and Development Project called Preliminary Aeroelastic Design of Structures or PADS. PADS generates the Finite Element Model (FEM), the loads, strength sizings, stiffness sizing, and performs all related analyses.

The PADS strength sizing capability, however, relies heavily on existing computer programs which size cover panels for buckling, fatigue, and stress. These programs are for metallic structures. Currently, there is no comparable automated panel sizing capability for composites.

Recently, the design process changed and fell somewhere between the PADS environment where the FEM is not available and the configuration is changing, and the production design environment where the strength-sized model is available and the configuration is frozen. In this new environment, strength-sized models were made available while the configuration was changing.

Vehicle level structural sizing for aeroelastic requirements is contingent on either using the same mathematical structural model for the stress, loads, and flutter, or translating/interpreting/migrating structural sizing properties between different models. If the decision is made to use one structural model, which because of model size limitations must be more a stiffness model and less a stress model, the issue then is how to manage and use a large FEM (15,000 to 30,000 degrees of freedom) for designing to stiffness requirements.

Four major issues involved in conditioning a large composite finite element model for use in stiffness design are (1) the translation of high level engineering composite specifications into equivalent smeared element property values, (2) the automatic generation of the NASTRAN bulk data deck based on the high level inputs by the engineer, (3) the efficient computation of delta stiffness matrices due to changes in design variables as specified by the engineer, (4) the generation of delta weight data associated with the change in design variable.

A major development thrust was made in translating high level engineering data inputs into processes which generate delta weight and stiffness matrices. The approach uses existing programs, such as NASTRAN, and builds necessary pre and postprocessors to generate the bulk data and prepare the weight and stiffness data for use in the structural resizing. The process involved more than 20 separate programs. The functional description and the criteria for designing some of these pre- and postprocessors are described in the following paragraphs.

BUILDING ON EXISTING CAPABILITY

PADS demonstrated in References 1, 2, and 3 the feasibility of integrating diverse programs into engineering defined processes under the control of macros to size finite elements for static and dynamic gust loads, taxi loads, strength, buckling, flutter, and deflection constraints.

There are two key elements in PADS. The first element is the operating system called CBUS (Continuous Batch User System). CBUS permits the user to define engineering processes using existing computer programs. CBUS then integrates different computer programs without the need to change original functions or original user access methods. Figure 1 shows CBUS as a tree from which computer programs are hung and organized under a shell. The processes are defined in a macro-like shell, which permits nesting, branching, sub-and-super process definitions. Within CBUS is a powerful ALTER capability for real-time modification of macros which contain process definitions as well as data blocks.

The second element of PADS is the integration of static and dynamic loads, stress, structure modeling, weight, flutter, and computer programming disciplines in real-time working environment. While significant levels of automation and integration of engineering processes were accomplished under PADS, demonstration of individual discipline control within an integrated working environment was more significant.

The PADS technical capabilities which transferred directly to the current project were the generation of grid transformations between any paired coordinate systems, the generation of the delta-k matrices which relate changes in structural stiffness due to changes in design variables, the specification of user macros for flutter analyses, and data management functions. CBUS gives the engineer the capability to define complex processes in terms of modular subprocesses. Basic subprocess macros are the building blocks to form other macro functions. As the macros are developed, a collection of engineering processes become available to use at an expert-system-like level. Macros define standard but flexible solution procedures.

CBUS macros relieve the engineer from remembering and performing countless details required when executing computer programs one at a time. Relieved of the repetitive tedium, the engineer focuses his energy and expertise on the definition of processes, the management of the design flow, and, most importantly, the interpretation of the computer studies for timely inputs into the design process. Figure 2 shows the typical user on top of a pyramid constructed from user defined macros which are executed through CBUS to access computer programs and databases installed on a typical computer facility. The final cornerstone, however, is the willingness of members on the team to learn the system and to develop their own macros and tailor them to satisfy current requirements. The smaller footprint on top of the pyramid gives the engineer more time to work out the problem physics and requires less time to master the mechanics of getting analyses out of the computer.

MAPPING PHYSICAL TO MODEL PARAMETERS

In a top-down approach, the engineer modifies the structural model characteristics by specifying the changes to the structural physical parameters. Going from composite skin layup drawings to FEM material property values should require only the layup definitions and not modeling judgments to match FEM areas with ply area definitions.

Likewise, the data generated using the structural model must give the direction to move the design in terms of the structural physical parameters rather than model variables.

The goal then was to develop a preprocessor where the inputs consist of structural physical parameters and the output is the FEM model parameters, such as anisotropic values for NASTRAN *QUAD and *TRIA elements.

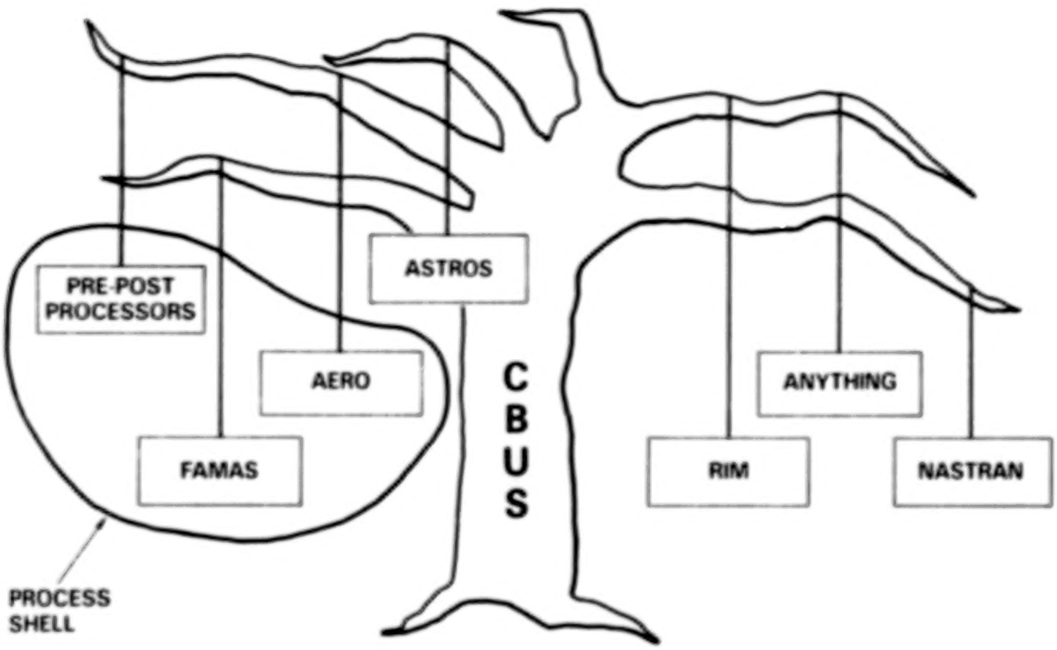

Figure 1. CBUS as an Integrating System

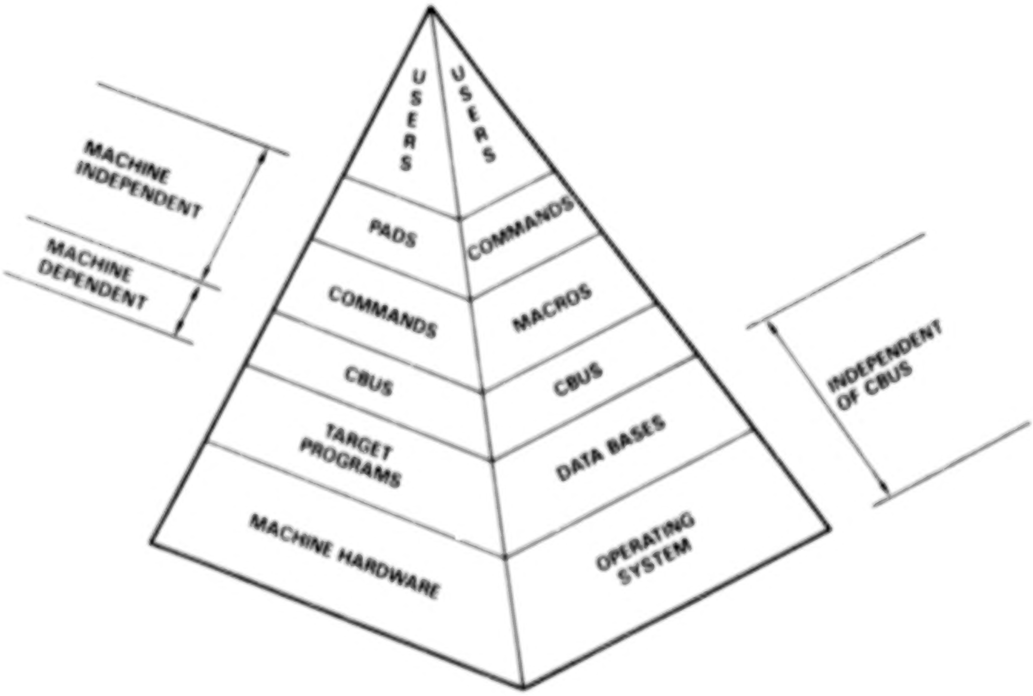

Figure 2. CBUS/PADS System Architecture

The end product is a change in structural stiffness for a change in a design variable, which is defined in terms of the structure physical parameters. While the formulation of delta stiffnesses is just a special application of mapping of physical parameters to model parameters, the mechanization details are critical relative to defining computer resource requirements.

So far, the mapping of physical parameters to model parameters has focused on the sizing specification. There are geometric mappings from the physical to the model which are used to optimize a design. The general category of shape optimization has been limited to t/c variations.

The formulation of the FEM property values directly from structural physical parameters is necessary not only for the baseline structure but also for perturbations of the baseline configuration.

In summary, the mapping of physical parameters to FEM model parameters must

- Use as input the ply layup drawings
- Map ply level changes directly into the FEM.
- Map ply level changes directly into the FEM for definition of delta stiffness and mass matrices.
- Accommodate FEM models in excess of 20,000 degrees of freedom.
- Map t/c changes to the FEM geometry.
- Accommodate automation.
- Accommodate the integration of strength sizing in the future.

AEROELASTIC STRUCTURAL SIZING OVERVIEW

Structural sizing for aeroelastic requirements involves a number of disciplines; namely, flutter, dynamic and static loads, stress, and stability and control. One way to move the design to best satisfy each discipline requirement is to generate structural sizing derivatives relative to the goals of each discipline. Even when the weighting of one discipline goal against the other for purposes of reaching a best design is known, the overall process in the academic sense is extremely complex. The issue becomes manageable, however, in practical designs when the engineer recognizes the loosely coupled interactions between one or more of these disciplines.

The need to generate strength-related derivatives are eliminated by allowing the internal loads within the structure to remain fixed while the individual structural elements are sized for those loads. Once the new sizing has been generated, new flexible loads are computed and new internal loads are then derived. Structural sizing which is compatible with internal loads converges within three loads/strength sizing cycles. Once the structure has been sized for flexible loads, the impact of the structural design on flutter margins and control effectiveness is established. Aeroelastic tailoring to reduce the loads can also be evaluated at this time.

Structural resizing for flutter is the extension of the baseline flutter analysis and the associated sensitivity studies. During the baseline flutter analyses, there are investigations into what kind of parameter variations will affect flutter margins. The more common are Mach number, fuel condition, and aerodynamic factors. Flutter margin sensitivities to actuator stiffness, control surface aerodynamics, and lifting surface gross stiffness variations produce data for identifying the existence of any major flutter margin role players.

Figure 3 summarizes the analysis parameter variations performed under baseline configuration flutter analyses and under aeroelastic optimization.

Strong interrelationships between baseline flutter analyses and the sizing of the structural components to achieve flutter margin goals is evident in Figure 4. The figure names specific outputs from the baseline flutter analyses which are critical to the optimization process.

The traditional velocity-frequency-damping, Figure 5, (VFG plots) are the mainstay of flutter analyses. The airplane aeroelastic deflections, Figure 6, computed where eigenvalue damping is equal to zero graphically describe the dominant motions for the flutter mode.

At the flutter point, energy input to the structure from the aerodynamics is balanced by the energy dissipation from structural damping and the aerodynamic damping on a per cycle basis. The energy distribution is plotted on the flutter vector plot planform. The energy distribution vector is summed over different segments of the airplane. Figure 7 shows a typical bar plot and clearly illustrates the horizontal

BASELINE CONFIGURATION FLUTTER ANALYSES

- STRESS FINITE ELEMENT MODEL
- ANALYSIS PARAMETER VARIATIONS
  - MACH NUMBER
  - FUEL – ZERO TO MAXIMUM TAKEOFF
  - CONTROL SURFACE ACTUATOR STIFFNESS
  - LIFTING SURFACE STIFFNESS
  - HORIZONTAL STABILIZER t/c
  - TAIL BOOM STIFFNESS
  - ENGINE SUPPORT STIFFNESS
  - CONTROL SURFACE AERODYNAMICS DERIVATIVES
- MODIFICATION OF UNSTEADY AERODYNAMICS
  - WINDTUNNEL DATA
  - CFD COMPUTER RUNS
    - QUADPAN AND TEAM CODE

AEROELASTIC OPTIMIZATION

- STRESS FINITE ELEMENT MODEL
- COMPOSITE STRUCTURE RESIZING
  - COVERS – THICKNESS IN EACH PLY DIRECTION
  - SPAR THICKNESS
  - RIB THICKNESS
  - MANUFACTURING CONSTRAINTS
- AEROELASTIC TAILORING

Figure 3. Flutter Analysis and Resizing for Flutter

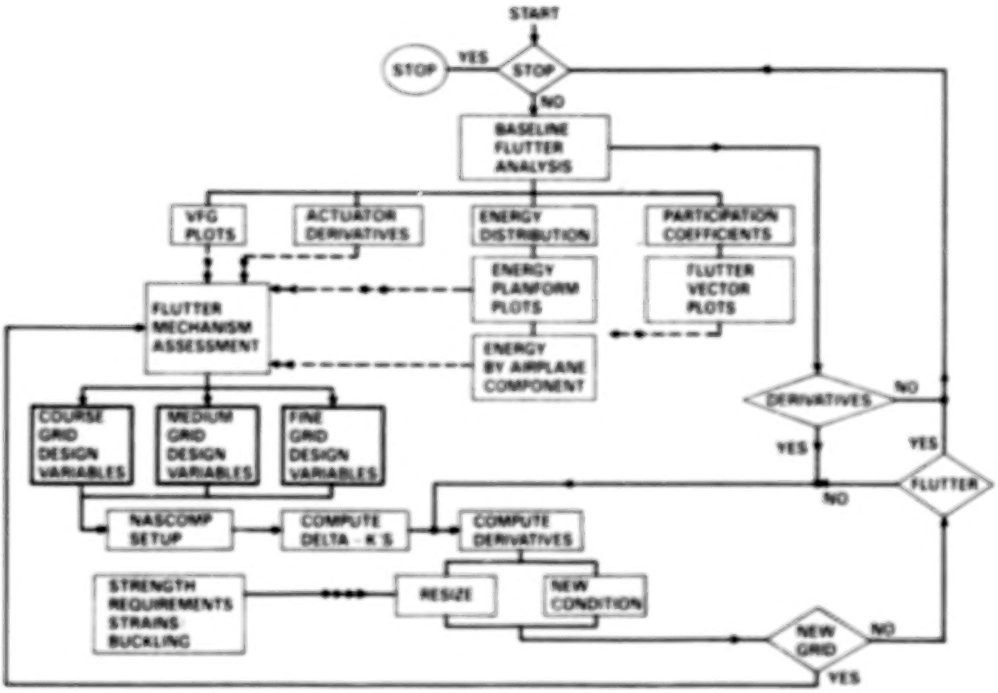
START
STOP
YES
STOP
NO
BASELINE FLUTTER ANALYSIS
VFG PLOTS
ACTUATOR DERIVATIVES
ENERGY DISTRIBUTION
PARTICIPATION COEFFICIENTS
ENERGY PLANFORM PLOTS
FLUTTER VECTOR PLOTS
FLUTTER MECHANISM ASSESSMENT
ENERGY BY AIRPLANE COMPONENT
DERIVATIVES
NO
YES
YES
FLUTTER
NO
COURSE GRID DESIGN VARIABLES
MEDIUM GRID DESIGN VARIABLES
FINE GRID DESIGN VARIABLES
NASCOMP SETUP
COMPUTE DELTA - K'S
COMPUTE DERIVATIVES
STRENGTH REQUIREMENTS STRAINS BUCKLING
RESIZE
NEW CONDITION
NEW GRID
NO
YES

Figure 4. Baseline Flutter/Resizing Functional Flow Chart

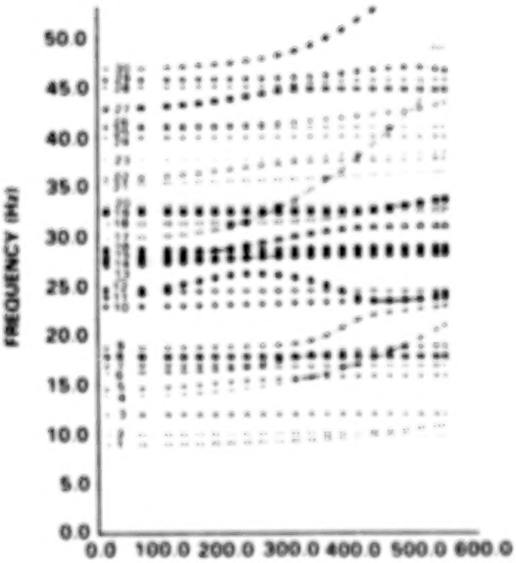

Figure 5A. Frequency Versus Airplane Velocity (Typical)

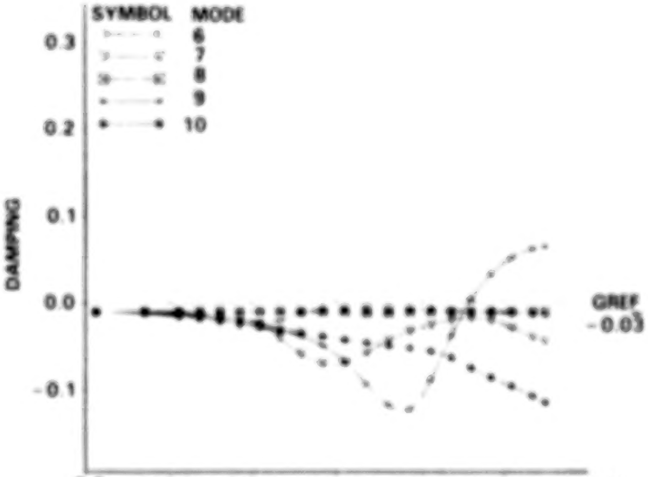

Figure 5B. Damping Versus Airplane Velocity (Typical)

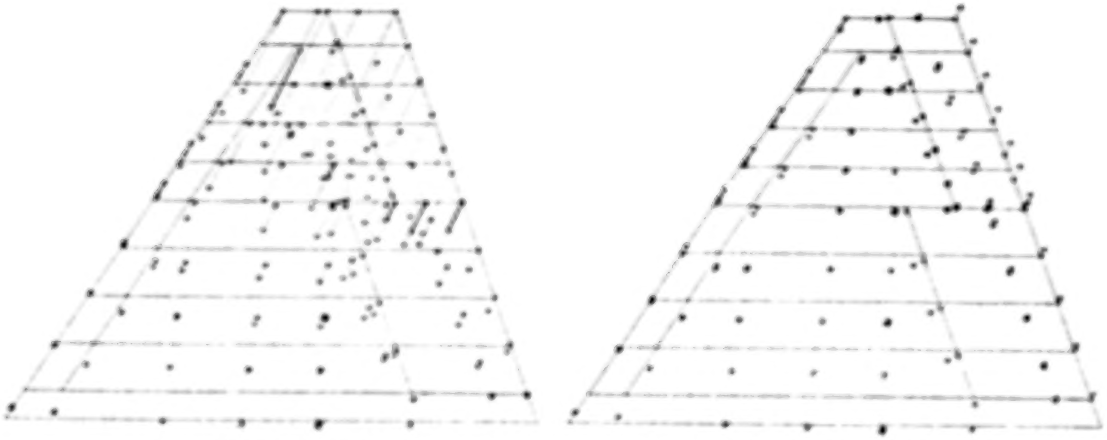

REAL PART **IMAGINARY PART**

Figure 6. Airplane Deflection at Flutter Point

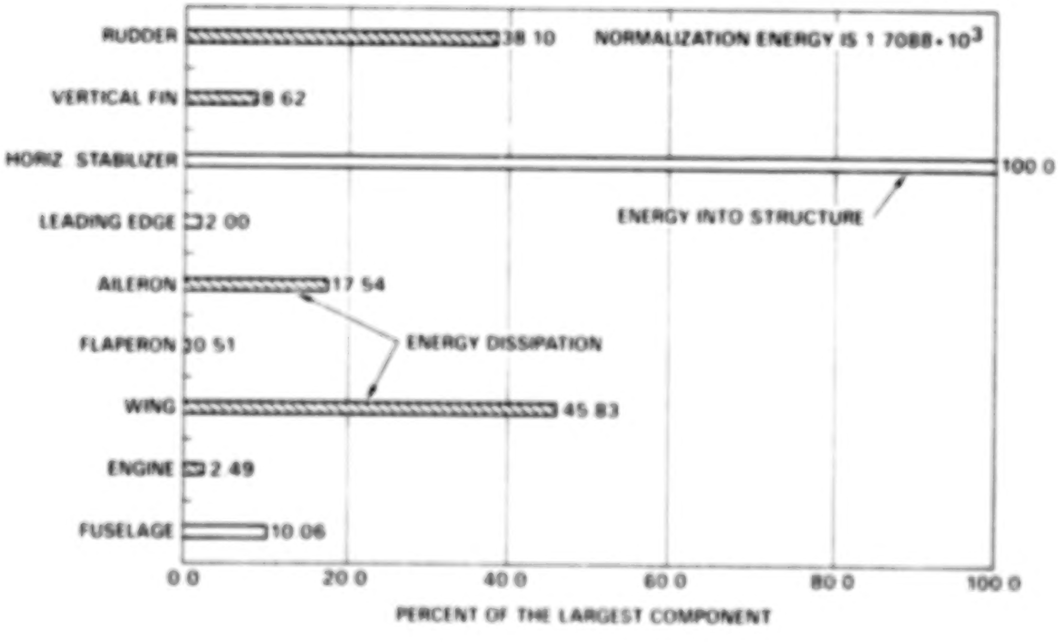

Figure 7. Airplane Component Aerodynamic Energy Distributions

stabilizer surface pumping energy into the structure and the rudder and wing removing energy from the structure.

The final source of information which may aid in establishing the flutter mechanism is the actuator flutter velocity bar plots. Figure 8 shows the stabilizer actuator as the more effective in increasing the flutter speed.

Similar plots are available for increasing the damping at the top of hump modes.

Flutter derivatives are especially helpful in establishing the flutter mechanism of deficient flutter modes. In Figure 4, this point in the aeroelastic resizing path is labelled "flutter mechanism assessment." The process is now ready to consider the definition of design variables to compute flutter derivatives.

Generally, a first definition of design variables will cover the complete airplane. The coarse grid variables are only in terms of total thickness increases and not ply level thicknesses. The medium grid design variables cover the complete surface which has been targeted for resizing. The medium grid includes ply level thickness and ply orientations. The medium design variables isolate that part of the structure which will be further subdivided to form fine grid design variables. The identification of three levels of grids for design variables is a trade-off of computer costs against resizing fidelity. Typically, the fine grid design variables cover 40 percent of the surface to be resized. The ratio of finite elements to design variables is three or less.

After the set of design variables are defined, the next task is to generate delta K's and delta M's through the NASCOMP process. Once the delta matrices are available,

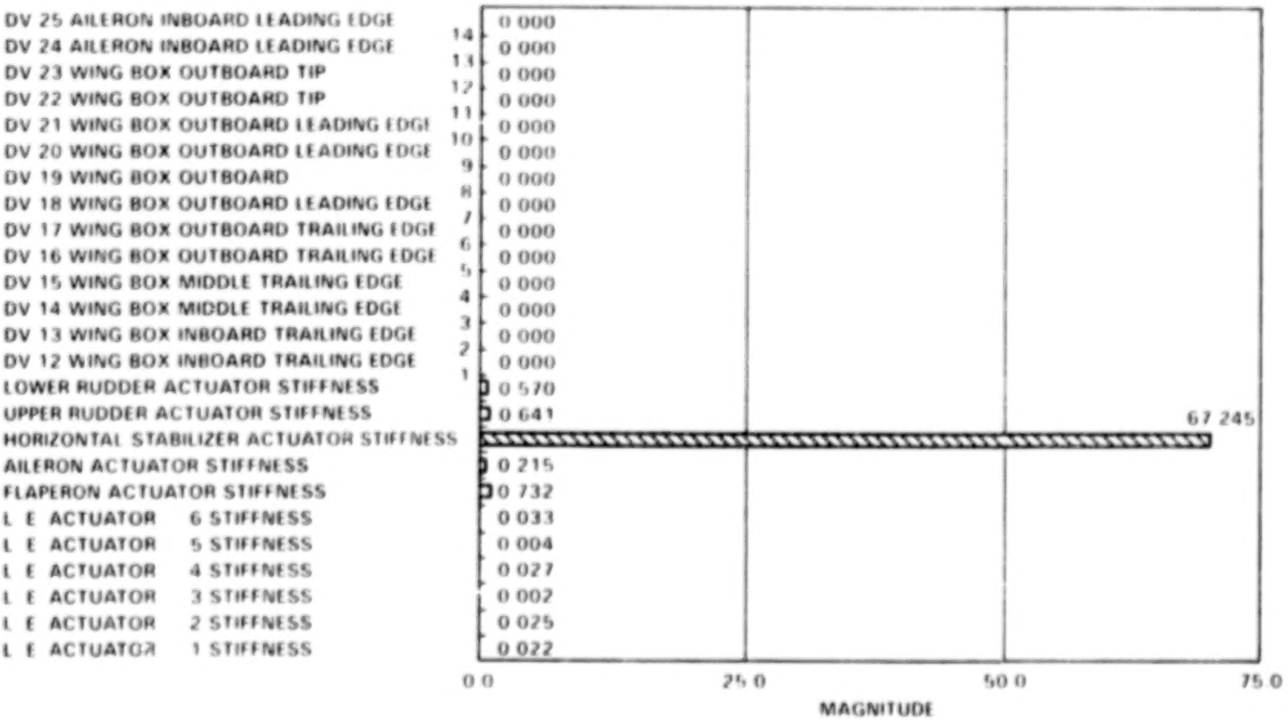

Figure 8. Flutter Speed Derivatives

the flutter velocity or top of the hump damping derivatives are computed for flutter deficient modes. Then either new grids are defined or structural resizing is performed.

NASCOMP PREPROCESSOR SYSTEM

NASCOMP is a collection of preprocessing programs designed to facilitate the integration of filamentary composite laminate properties into a NASTRAN finite element model (FEM). It is also used extensively to prepare the FEM for the generation of incremented stiffness matrices based on ply-level design variables. An incremented stiffness matrix, $[K + \Delta K]$, is a matrix that differs from a basic matrix, $[K]$, in that it is computed for a structural design in which one design variable is modified by a small amount. As a result, the derivative of $[K]$ with respect to the design variable can be approximated by a finite difference quotient.

The excessive time required for the generation of a new NASTRAN bulk data deck for each composite structure design iteration is a hindrance to the flutter optimization process. A preprocessor designed to make the desired modifications, with minimal, user-friendly instructions, greatly facilitates the optimization process as well as eliminating any error-prone hand editing of the bulk data.

The NASCOMP Preprocessor System consists of eight independent FORTRAN programs, each with a specific function, plus COMAIN, an existing program created by the Composite Development Center.

Figure 9 summarizes the input and process definition of NASCOMP.

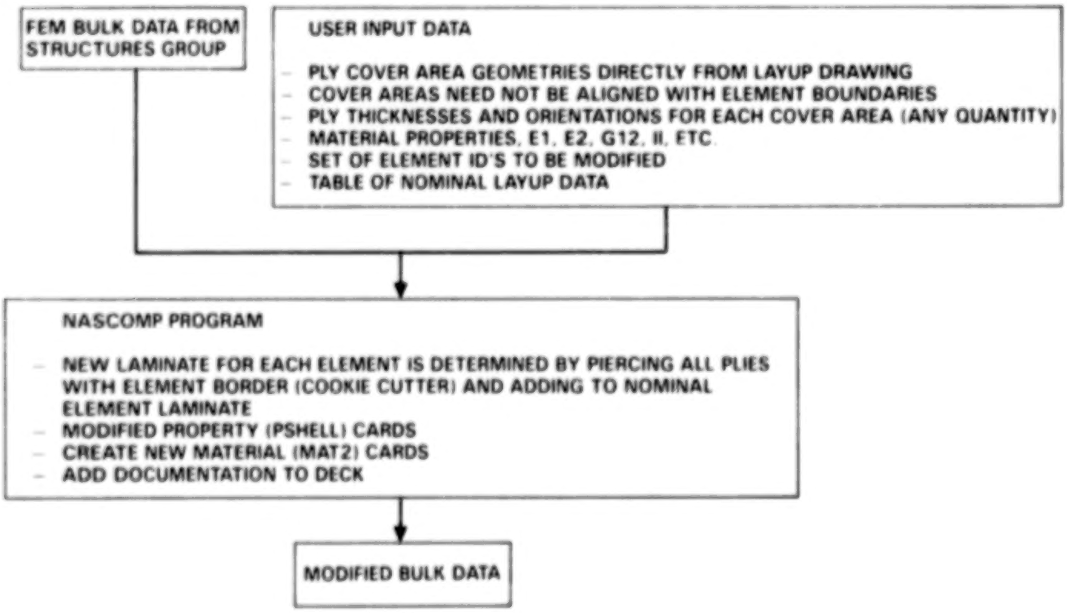
FEM BULK DATA FROM STRUCTURES GROUP
USER INPUT DATA
– PLY COVER AREA GEOMETRIES DIRECTLY FROM LAYUP DRAWING
– COVER AREAS NEED NOT BE ALIGNED WITH ELEMENT BOUNDARIES
– PLY THICKNESSES AND ORIENTATIONS FOR EACH COVER AREA (ANY QUANTITY)
– MATERIAL PROPERTIES, E1, E2, G12, ν, ETC.
– SET OF ELEMENT ID'S TO BE MODIFIED
– TABLE OF NOMINAL LAYUP DATA
NASCOMP PROGRAM
– NEW LAMINATE FOR EACH ELEMENT IS DETERMINED BY PIERCING ALL PLIES WITH ELEMENT BORDER (COOKIE CUTTER) AND ADDING TO NOMINAL ELEMENT LAMINATE
– MODIFIED PROPERTY (PSHELL) CARDS
– CREATE NEW MATERIAL (MAT2) CARDS
– ADD DOCUMENTATION TO DECK
MODIFIED BULK DATA

Figure 9. NASCOMP Input and Process Definition

PARTIT - This program simply reads the user input file and separates it into the datablocks required by the other programs. Each datablock is written to a temporary dataset which is passed along to the proper program. All user input is entered through PARTIT.

ELMSRT - This program scans the bulk data deck, extracts all necessary data pertaining to a selected set of elements, and outputs it to a single file. The inputs to the program include the types of elements to scan for and the ID ranges. The output is a table containing, for each element scanned, the element ID, the element type (CQUAD4, CTRIA3, etc.), the grid IDs and coordinates making up the element, and the property card (PSHELL, PROD, etc.) ID. By having all the necessary data in a single, concise file, multiple scans of the bulk data are avoided.

INTSCT - Also known as the "cookie-cutter," this program finds the intersections between ply cover areas and the elements contained in the table formed in ELMSRT. The inputs are the cover area definitions; i.e., the coordinates of the vertices, and the ply thicknesses and orientations. Figure 10 illustrates typical ply layups over the FEM grid points. The number of cover areas and the number of plies are unlimited. Any number of plies, with any orientation, can be applied to a given area. When computing the intersection, the three cases which must be considered are (1) the element lies completely inside the area; (2) the element is fully outside the area; and (3) the element is partially inside the area. If the element is completely inside the area, the full ply thickness is applied to the element. If the element is fully outside the area, then, obviously, nothing is applied to the element. If the element

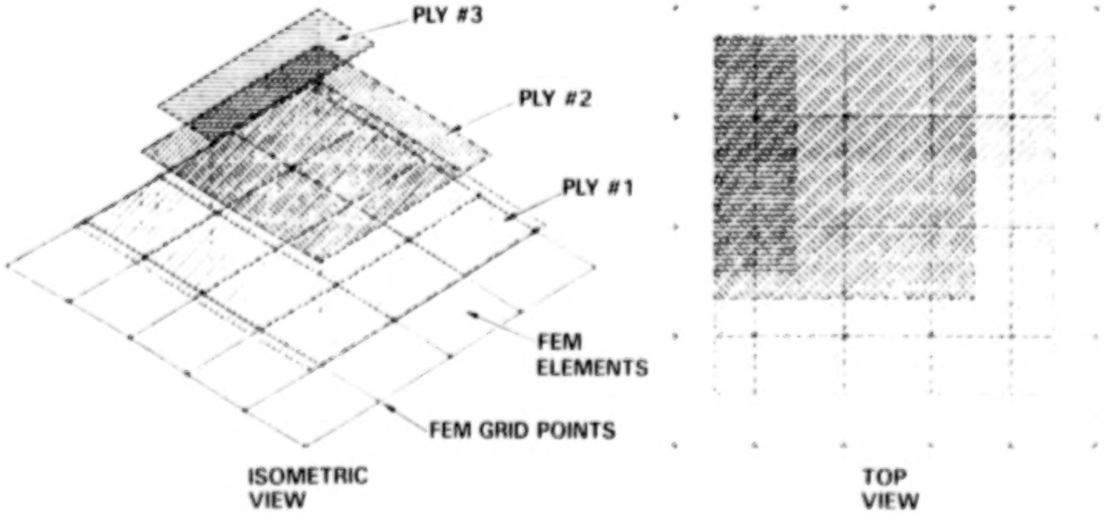

Figure 10. Ply Layups Over FEM Grid Points

is partially inside the area then a portion of the ply thickness (proportional to the ratio of intersected area to the element area) is applied to the element. The output file is a table which contains, for each element, all of the applied ply thicknesses and orientations. Elements which have no intersections with any of the areas are not listed.

BASBLK - This program takes the element ply table from INTSCT and, for each element listed in the table, adds the layup data corresponding to the nominal sizing found in the FEM. This nominal sizing data is usually obtained from the Structures Group. To compute the new element stiffness properties, the entire laminate, including both baseline data and increments, must be reconstructed. The output format is the same as the input.

COLECT - The file which is output in BASBLK, in general, contains many ply thickness/orientation entries for each element. COLECT combines all thicknesses with equal orientation angles for every element in the input table. These combined plies, or layers, are then redistributed according to a rudimentary stacking sequence specified by the user. Since several elements (e.g., adjacent) may consist of identical laminates, a filtering process is performed to separate the unique laminates. The output is a series of complete laminates, each of which is unique, and a table which relates the element IDs to these laminates.

COMPRE - This program prepares the laminate data for input to COMAIN.

COMAIN - This program, developed by the Composite Development Center, uses classical lamination theory to compute the laminate stiffness matrices for membrane, bending, and membrane-bending coupling loading conditions for thin, laminated, anisotropic plates of unit width. These matrices are usually referred to as the A, D, and B matrices respectively. They are defined below.

$$\left\{\begin{array}{l} Nx \\ Ny \\ Nxy \\ \hline Mx \\ My \\ Mxy \end{array}\right\} = \left[\begin{array}{ccc|ccc} a11 & a12 & a13 & b11 & b12 & b13 \\ a21 & a22 & a23 & b21 & b22 & b33 \\ a31 & a32 & a33 & b31 & b32 & b33 \\ \hline b11 & b12 & b13 & d11 & d12 & d13 \\ b21 & b22 & b23 & d21 & d22 & d33 \\ b31 & b32 & b33 & d31 & d32 & d33 \end{array}\right] \left\{\begin{array}{l} \epsilon x \\ \epsilon x \\ \gamma xy \\ \hline \kappa x \\ \kappa y \\ \kappa xy \end{array}\right\}$$

where:

Nx (ϵx) = normal force (strain) along laminate x-direction;

Ny (ϵy) = normal force (strain) along laminate y-direction;

Nxy (γxy) = in-plane shear force (strain);

Mz (κx) = bending moment (curvature) along axis normal to laminate x-z plane;

My (κy) = bending moment (curvature) along axis normal to laminate y-z plane;

Mxy (κxy) = twisting moment (curvature) along laminate x or y axis.

or

$$\begin{Bmatrix} N \\ - \\ M \end{Bmatrix} = \left[\begin{array}{c|c} A & B \\ \hline B & D \end{array}\right] \begin{Bmatrix} \epsilon \\ - \\ \kappa \end{Bmatrix}$$

COMPOS - The A, B, and D matrices, as well as the laminate thickness is extracted from the COMAIN output and passed along to the next step.

BDDWRT - This program modifies the bulk data to reflect the new elemental laminates. The element shell property (PSHELL) cards are modified or optionally replaced with new ones. The laminate thickness as well as the new material card IDs are entered on the PSHELL card. The A, B, and D matrices are normalized to the laminate thickness, T, to form the material moduli:

$$G_{membrane} = [A] / T$$

$$G_{bending} = [D] /(T^3/12) = [D] / I$$

$$G_{coupling} = [B] / T^2$$

The user can specify which of the moduli will be utilized for the elements; e.g., membrane only, membrane and bending, etc. All new material property (MAT2) cards are created, one or more for each laminate. The non-modulus entries on the MAT2 cards, such as density, thermal expansion coefficients, etc., are specified by the user. The new bulk data is written out including an echo of all user input data.

EDITING LARGER NASTRAN BULK DATA SETS

BULKEDIT is a general-purpose utility program designed to make changes to an existing bulk data deck. It has a wide range of capabilities including the ability to

- Replace one or more fields on selected ranges of cards with new data
- On selected ranges of cards, extract a numerical value from a certain field, modify it, and return it to the field
- Comment the cards out
- Add cards

The program performs these functions, in a fraction of the time, with minimal user input and eliminates the errors introduced by hand editing. The process is instantly repeatable; if an updated model is obtained, the changes/additions can be incorporated in seconds. BULKEDIT input/output is shown in Figure 11.

Example: A sensitivity study may require the rotation of the material property orientation axis (direction of 0-degree plies) on a range of 1000 skin elements by 10 degrees, the input cards are

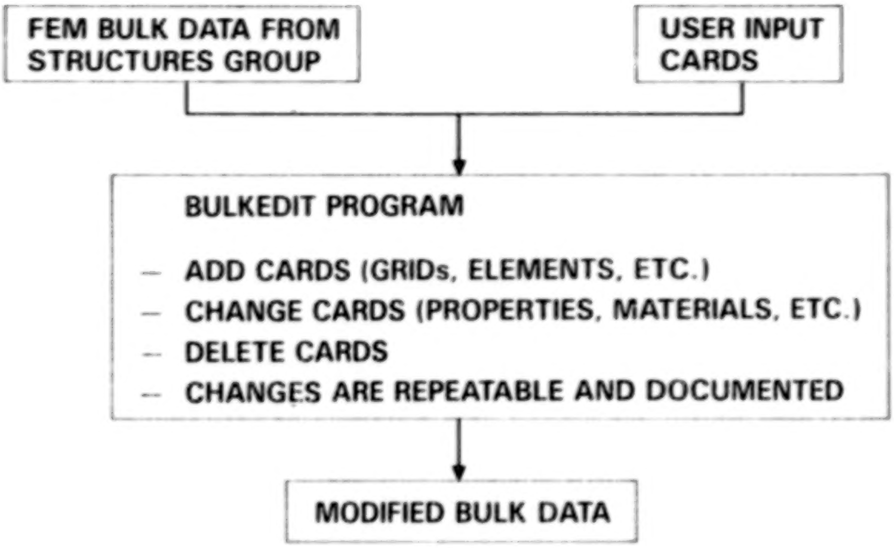
FEM BULK DATA FROM STRUCTURES GROUP
USER INPUT CARDS
BULKEDIT PROGRAM
– ADD CARDS (GRIDs, ELEMENTS, ETC.)
– CHANGE CARDS (PROPERTIES, MATERIALS, ETC.)
– DELETE CARDS
– CHANGES ARE REPEATABLE AND DOCUMENTED
MODIFIED BULK DATA

Figure 11. BULKEDIT Program

```
CQUAD4    +                                                     10.0
60001   60500
61001   61500
END
```

Field 8 (columns 57-64) on the CQUAD4 card contain the axis specification. Program BULKEDIT will add 10.0 to the quantity in field 8 on all CQUAD4 cards found with element numbers in the ranges from 60001 through 60500 and 61001 through 61500. The "+" operator in field 2 (column 9) can optionally be a "*" to multiply by 10.0 or a "#" to replace with 10.0.

Additional cases requiring different rotation angles could be completed with the change of one card.

DELTA MASS MATRICES

Delta mass matrices, corresponding to a small change in the structural model, for each design variable are required to compute the flutter speed derivatives. Program DVMASS was written to generate these matrices. A convenient output table from NASTRAN lists, among other things, the areas, A, of all plate/web elements and the lengths, L, of all rod/bar elements. This table, combined with a design variable specification table, are input to DVMASS. For each design variable, DVMASS computes the delta mass of each designated element ($\Delta m = \rho A \Delta t$ for shells and webs and $\Delta m = \rho L \Delta A$ for rods and bars) and the geometry of the element centroid. The program outputs are one delta mass matrix per design variable and a single matrix containing the centroid geometry of all elements involved. The geometry matrix is used to generate the transformation matrices needed to produce the delta mass matrices in terms of the structural degrees-of-freedom.

The design variable specification table shown below defines the input to the program.

```
$ DV   ELEM ID       INCR.  DENS   PART  MIN   DELK  DELW
$ #    RANGE(S)      THK           #     THK   MAT#  MAT#
$
$      0 DEGREE PLIES, VERTICAL FIN SECTION IA
  1    60001 60009   .005   .060   40.00 .006  3801  2801
+      60101 60109
$ ± 45 DEGREE PLIES, VERTICAL FIN SECTION IB
  2    60010 60019   .007   .100   40.00 .006  3802  2802
+      60110 60119
$    90 DEGREE PLIES, VERTICAL FIN SECTION IB
  2    60010 60019   .007   .100   40.00 .006  3803  2803
+      60110 60119
$
etc.
```

Besides being convenient for documentation, the table contains all input necessary to generate the delta mass and stiffness matrices.

The DVMASS program flow is shown in Figure 12.

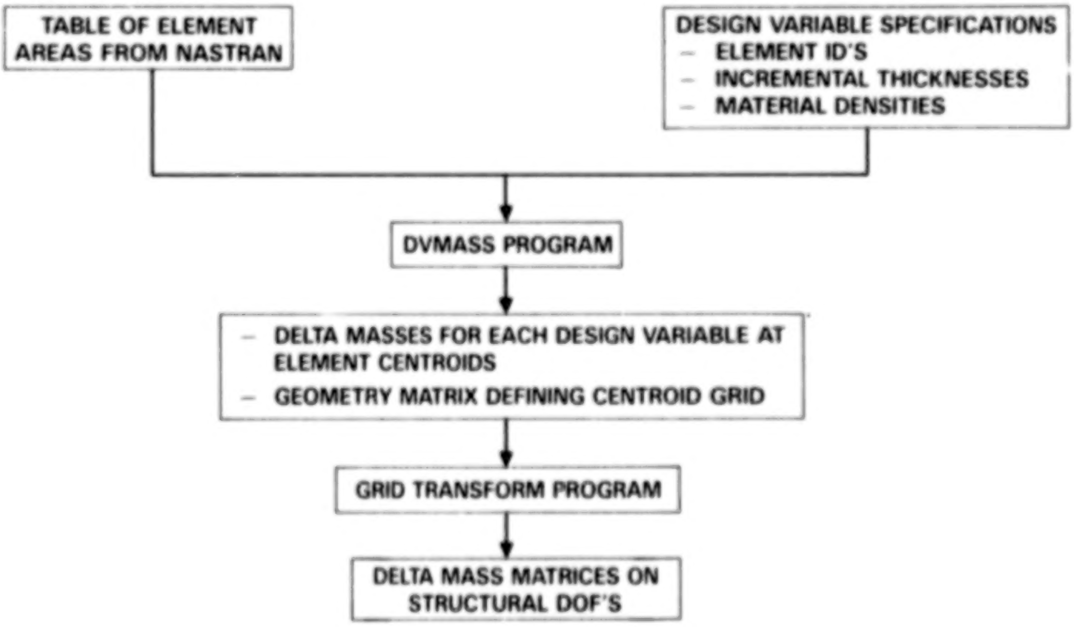
TABLE OF ELEMENT AREAS FROM NASTRAN
DESIGN VARIABLE SPECIFICATIONS
– ELEMENT ID'S
– INCREMENTAL THICKNESSES
– MATERIAL DENSITIES
DVMASS PROGRAM
– DELTA MASSES FOR EACH DESIGN VARIABLE AT ELEMENT CENTROIDS
– GEOMETRY MATRIX DEFINING CENTROID GRID
GRID TRANSFORM PROGRAM
DELTA MASS MATRICES ON STRUCTURAL DOF'S

Figure 12. Delta Mass Generation

DELTA STIFFNESS MATRICES

The computation of the delta stiffness matrices, ΔK_i, requires the submittal of a NASTRAN job for each design variable. In addition, for each design variable, the bulk data must be altered to reflect a small increment to the structural sizing. When a large number of design variables (80-100) are in use, the data management aspect of the process is quite unwieldy. Using CBUS, a macro was developed to allow the complete ΔK generation process to be executed automatically. Referring to Figure 13, the bulk data from the current resizing step is the only input to the macro. The macro contains all of the data required to run both NASCOMP and BULKEDIT for each design variable. NASCOMP is executed when ply-level ΔK's are to be computed and BULKEDIT is executed for other design variables, e.g., metal spar thickness. After the bulk data has been modified, the macro generates first the NASTRAN executive and case control decks then the Job Control Language (JCL) and finally submits the NASTRAN job for execution. All subsequent design variables are processed similarly. The spawned NASTRAN jobs will run independently of the "mother" process, considerably reducing the turnaround time.

The method in which the ΔK matrices are computed by NASTRAN was tailored to reduce the run time (=cost). The delta stiffness is first computed on a superelement basis and then reduced using the existing Guyan transformation matrix. For small increments, this technique produced results that agreed very well with the results obtained by updating the Guyan transformation matrix.

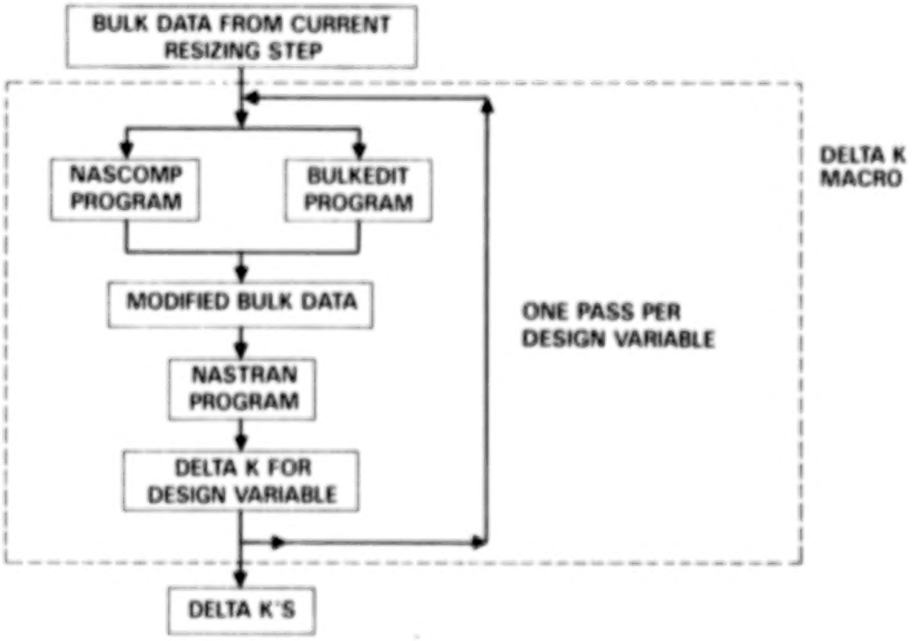
BULK DATA FROM CURRENT RESIZING STEP
NASCOMP PROGRAM
BULKEDIT PROGRAM
DELTA K MACRO
MODIFIED BULK DATA
ONE PASS PER DESIGN VARIABLE
NASTRAN PROGRAM
DELTA K FOR DESIGN VARIABLE
DELTA K'S

Figure 13. Delta Stiffness Generation

FLUTTER SPEED DERIVATIVES

The delta stiffness matrices, ΔK, and the corresponding delta mass matrices, ΔM, one for each design variable, are used to compute the flutter derivatives (Figure 14). At the present time, there is the capability to compute derivatives for two types of modes, at the flutter crossing and at the top of the hump mode. The derivatives at the flutter crossing, the point where the mode in neutrally stable are

$\frac{\delta V}{\delta m_i}$ - The derivative of the flutter crossing speed with respect to the design variable i. [KEAS/lb]

$\frac{\delta f}{\delta m_i}$ - The derivative of the flutter crossing frequency with respect to the design variable i. [Hz/lb]

The derivatives at the top of the hump mode, the point of minimum damping, are

$\frac{\delta V}{\delta m_i}$ - The derivative of the top of the hump speed with respect to the design variable i. [KEAS/lb]

$\frac{\delta g}{\delta m_i}$ - The derivative of the damping value at the top of the hump with respect to the design variable i. [percent damping/lb]

Computing the flutter derivatives has traditionally been a two step process: perform a flutter analysis to get the frequency and damping versus speed data (VFG plots); then manually select the critical modes and compute the derivatives.

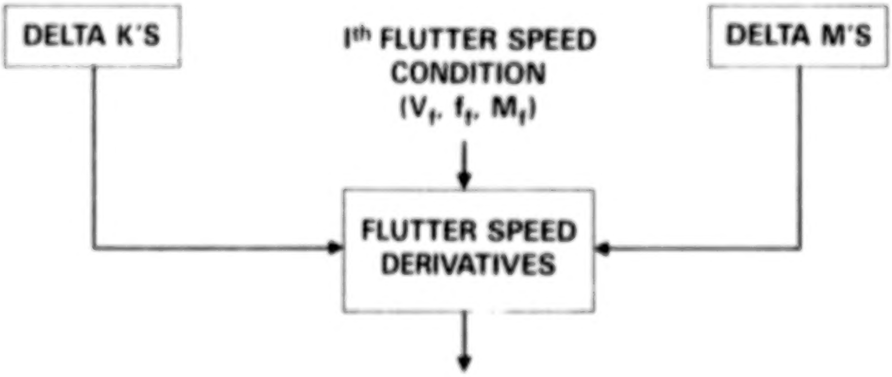

Figure 14. Flutter Speed Derivatives

Recently, a program has been developed that will process the flutter output and select the critical modes based on user-specified parameters. Speed range, frequency range, minimum damping, and which, if any, modes to exclude (if known a priori) are among the inputs. The program selects all modes which satisfy these criteria. This program was integrated into the flutter analysis stream using CBUS, and it is now possible to do the flutter analysis and get the derivatives with one job submittal.

STRUCTURAL RESIZING PROGRAM

The Structural Resizing Program computes the sizing increment based on either a specified weight increment or flutter speed increment. The effectiveness of each of the derivatives is assumed to diminish linearly as weight is added to the structure; i.e., they are fully effective for zero added weight and are completely ineffective at some predetermined weight increment, DWO. Figure 15 illustrates the declining effectiveness concept. The program computes the sizing increment, DWI, based on the most efficient use of the derivatives. If a weight increment is specified, the resulting weight distribution gives the largest velocity increment. If a velocity increment is specified, the resulting weight increment is minimum. The process is illustrated in Figure 16.

Manufacturing constraints dictate whether the resulting laminates are acceptable - laminate thickness must correspond to an integral number of finite-thickness laminate. In addition, laminate symmetry and balance must be considered.

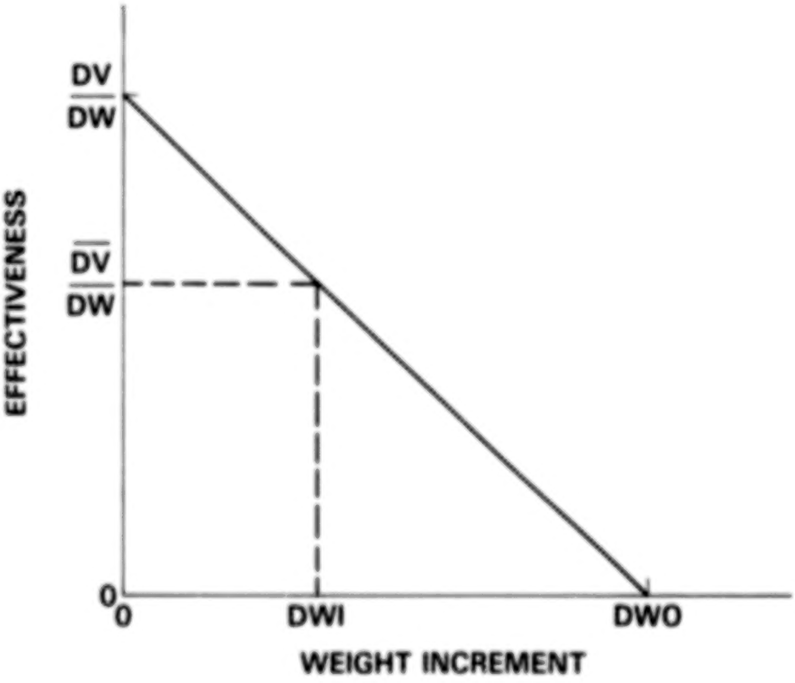

Figure 15. Derivative Effectiveness Model

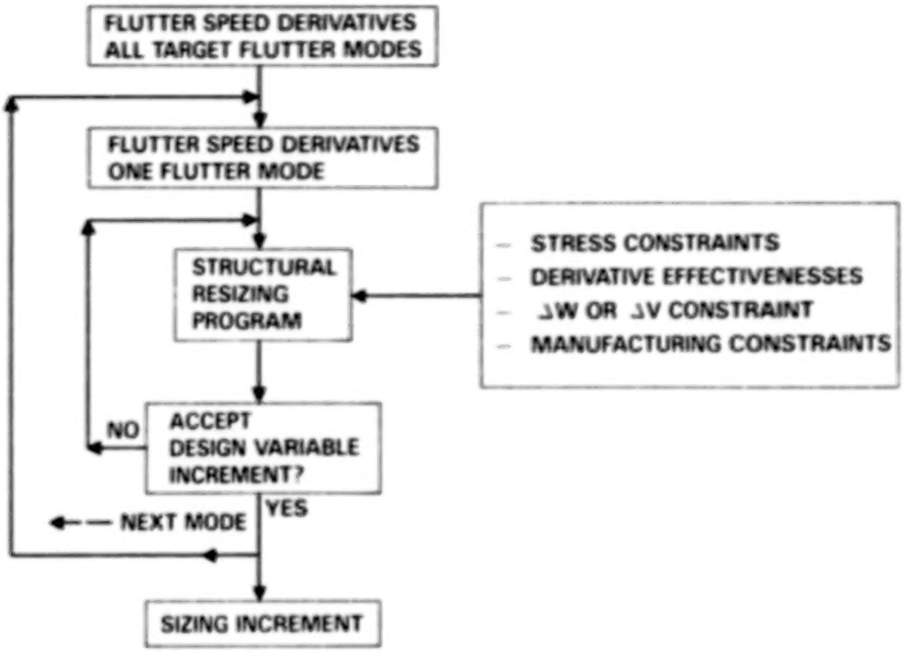
FLUTTER SPEED DERIVATIVES ALL TARGET FLUTTER MODES
FLUTTER SPEED DERIVATIVES ONE FLUTTER MODE
STRUCTURAL RESIZING PROGRAM
– STRESS CONSTRAINTS
– DERIVATIVE EFFECTIVENESSES
– ΔW OR ΔV CONSTRAINT
– MANUFACTURING CONSTRAINTS
NO
ACCEPT DESIGN VARIABLE INCREMENT?
YES
NEXT MODE
SIZING INCREMENT

Figure 16. Structural Resizing Program

UPDATED MASS AND STIFFNESS MATRICES

After the resize increment has been determined using the resizing program, the new stiffness and mass matrices are generated. The resize program outputs the incremental thicknesses to be applied to each design variable. These increments are then input to the stiffness update macro (see Figure 17). The macro generates all of the necessary control cards for the BULKEDIT program and the NASCOMP programs. Similar to the Delta K generation process, the update macro modifies the bulk data as required and spawns a single batch job. The bulk data is saved for use in generating a new set of ΔKs. The first step of the job is the execution of NASTRAN to compute the updated stiffness matrix. The second step is a FAMAS program that will generate the updated mass matrix. The mass matrix is computed by adding an incremental mass matrix to the nominal mass matrix. The incremental mass matrix is calculated using multiples of the delta mass matrices (Δm's) based on the resizing increment.

EXAMPLES AND RESULTS

Dual Rudder Vertical Stabilizer

The initial design of the dual rudder vertical stabilizer was strength sized for loads. The design, however, was deficient in flutter margin requirements by more than 100 KEAS. The structural resizing for stiffness goal was to hold the weight constant, keep the strain margins at or below the initial design levels and raise the flutter

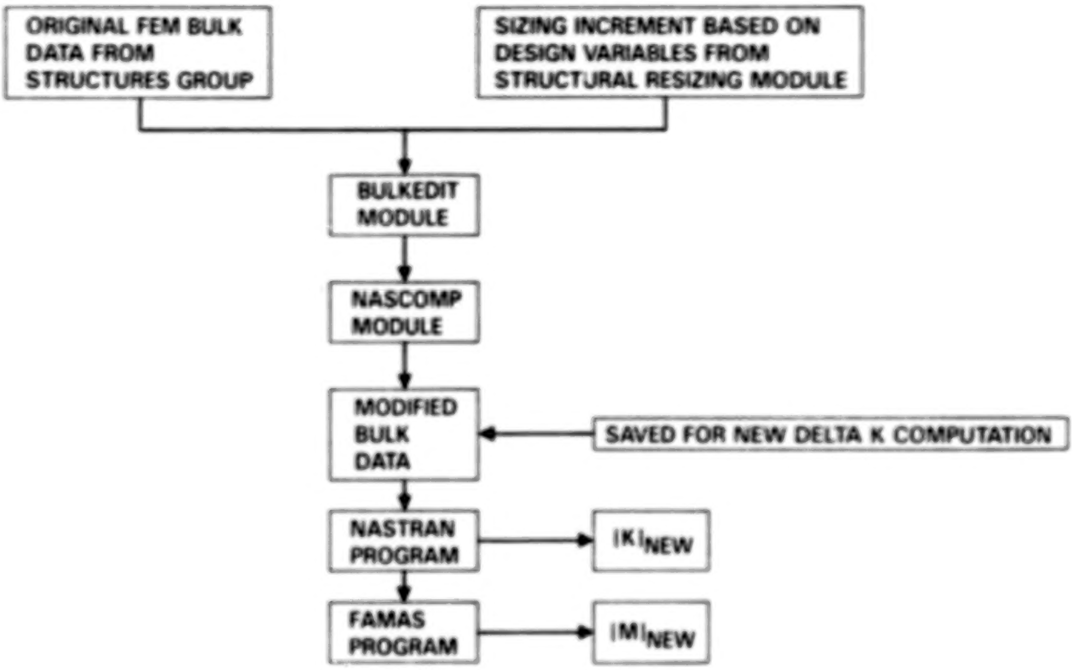
ORIGINAL FEM BULK DATA FROM STRUCTURES GROUP
SIZING INCREMENT BASED ON DESIGN VARIABLES FROM STRUCTURAL RESIZING MODULE
BULKEDIT MODULE
NASCOMP MODULE
MODIFIED BULK DATA
SAVED FOR NEW DELTA K COMPUTATION
NASTRAN PROGRAM
$[K]_{NEW}$
FAMAS PROGRAM
$[M]_{NEW}$

Figure 17. Mass and Stiffness Matrices Update

speed by 100 KEAS. This was a cantilevered case and the computer time was not a significant factor.

The derivatives for the baseline case indicated that the structure needed to be stiffened at the leading edges and the upper 1/3 of the fin structure. The move vector,which satisfied minimum and maximum thickness requirements, redistributed the material from the mid-center section out to the leading edge support structure. After three resizings, the flutter margin deficiency was removed; the critical strain values were reduced by 20 percent; the weight addition was zero.

Horizontal Stabilizer

This was the initial attempt at sizing a composite structure which was not cantilevered. While the design variables were relatively large, structural resizing produced an interesting result.

This case required the addition of material to the structure to satisfy the flutter requirements. However, with ply orientations of the material as design variables, the weight increase could be substantially reduced. The optimum ply orientation, Figure 18, for the tailored structure was an offset of the bending axes relative to the torsion axes. A check of the buckling requirements indicated that the tailored ply orientation was better. Figure 19 shows a weight savings of 70 pounds at the actuator design point.

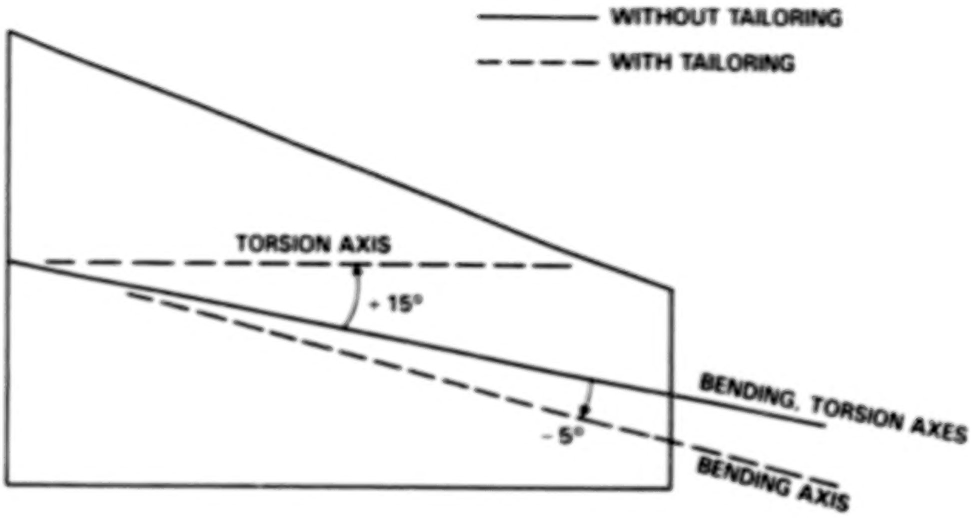

Figure 18. Optimization of Horizontal Stabilizer Ply Direction For Improved Flutter Characteristics

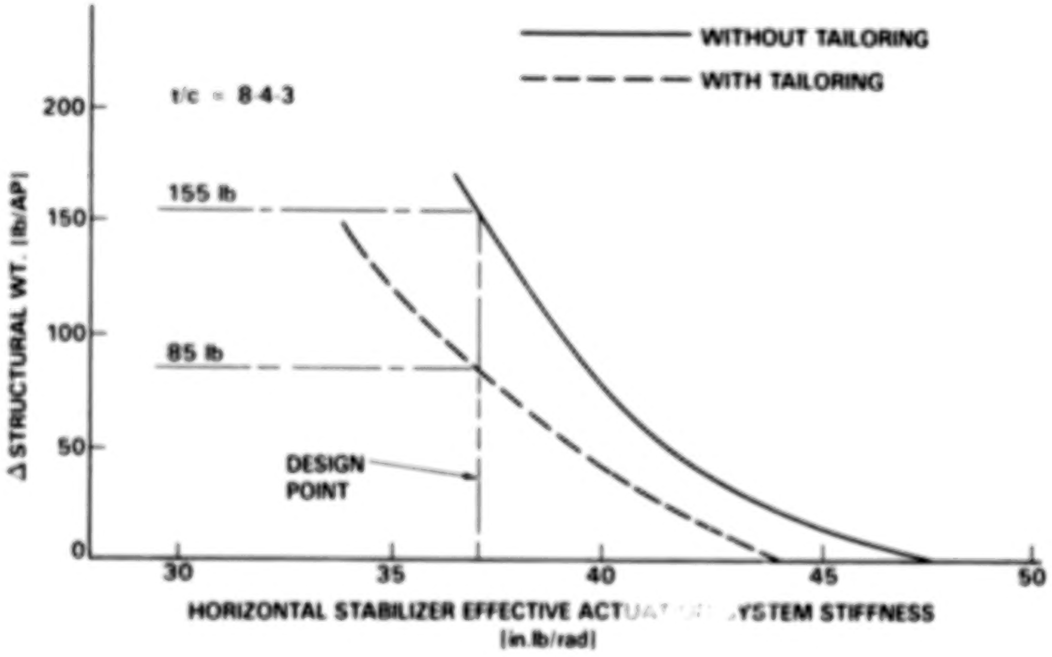

Figure 19. Horizontal Stabilizer Effective Actuation System Stiffness

Whole Airplane - Coarse-Medium-Fine Grid Example

The airplane design showed flutter deficiencies primarily at one subsonic and one supersonic speed. Both symmetric and antisymmetric boundary conditions were involved. There was principally one critical weight condition. First, design variables were constructed using total thicknesses for the wing, vertical and horizontal stabilizers. The flutter derivatives clearly demonstrated that wing design variables were not important to increasing the flutter speed of any of the deficient flutter modes. The medium design variable grid was defined for the control surface which the coarse grid design variable derivatives showed to be the prime candidate for resolving the flutter deficiency.

Results from the medium grid model further narrowed the candidate structure for resizing to 40 percent of the original control surface. A fine grid design variable derivatives were computed. Figure 20 shows sections of the control surface where the flutter derivatives were significantly higher than the surrounding structure. The figure shows flutter derivatives for ±45 plies. The structure was resized with a goal of increasing flutter speed margin by 40 KEAS. This goal was achieved with a weight increment of less than 2 pounds per surface.

FINAL OBSERVATIONS AND RECOMMENDATIONS

The full impact of the overall capability is difficult to assess in a meaningful way. Table 1 lists the steps used in the structural resizing for stiffness along with the computer setup times for each step. The major bottleneck is the significant

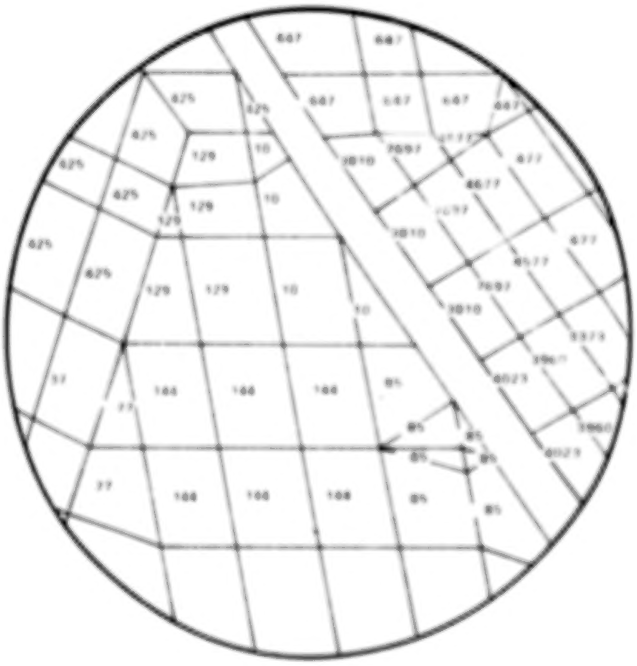

Figure 20. Normalized Flutter Velocity Derivatives (KEAS/LB) for ± Plys

TABLE 1. DESIGN TO STIFFNESS TABLE SUMMARY

GENERAL MODEL STATISTICS

NASTRAN Gset DOF → 24000
Aset DOF → 400
VIBRATION DOF → 370
FLUTTER DOF → 50

DESIGN VARIABLES → 80 TO 100

STEP	TASK	SOFTWARE	CONDITIONS	OUTPUTS	SETUP TIMES	CPU TIMES
1	FLUTTER BASELINE	FLUTTER MACRO CONTROLLED BY 30 FREE FORMATTED INPUTS TITLES VEL RANGE MACH, FUEL, DERIVATIVES	4 MACH NUMBERS 5 FUEL CONDITIONS SYM AND ANTISYM	VFG, VECTOR PLOTS, ENERGY PLOTS, 80 FLUTTER DERIVATIVES	4 MINUTES FOR SETUP PER RUN	80 CPU MINUTES (IBM 3081) PER RUN
2	SENSITIVITY STUDIES	FLUTTER MACRO SAME AS STEP 1	SAME AS STEP 1	ACTUATOR STIFFNESS, AERODYNAMIC FACTOR, CONTROL SURF H.M., A.C. SHIFT, CANTILEVERED ANALYSIS, MODE TRACKING	6 MINUTES FOR SETUP PER RUN	10 TO 50 CPU MINUTES DEPENDS ON THE TASK PER RUN
3	DESIGN VARIABLE DEFINITIONS	SIMPLE BATCH PROGRAMS FOR PLOTTING FEM GRID, ELEMENTS PREPARATION OF INPUT DATA FOR NASCOMP, DELTA MASS, ETC. PROGRAMS CADAM	COARSE WHOLE AIRPLANE GRID MEDIUM SURFACE GRID FINE SURFACE GRID 80 TO 100 DESIGN VARIABLES FOR EACH GRID		2 PERSON DAYS PER GRID	LESS THAN 20 MINUTES TOTAL

TABLE 1. DESIGN TO STIFFNESS TABLE SUMMARY (Continued)

STEP	TASK	SOFTWARE	CONDITIONS	OUTPUTS	SETUP TIMES	CPU TIMES
4	DELTA MASS MATRICES	DVMASS BATCH PROGRAM	DATA FROM STEP 3	OUTPUTS 80 TO 100 DELTA MASS MATRICES	30 MINUTES SETUP	LESS THAN 5 MINUTES TOTAL
5	DELTA STIFFNESS MATRICES	DELTAK MACRO (UNDER CBUS) IS A MOTHER JOB WHICH GENERATES 80 TO 100 NASTRAN JOBS	DATA FROM STEP 3	OUTPUTS 80 TO 100 DELTA STIFFNESS MATRICES	60 MINUTES SETUP	400 TO 500 CPU MINUTES TOTAL
6	FLUTTER DERIVATIVES	FLUTTER MACRO	SAME AS STEP 1 OPTION COMPUTED WHEN FLUTTER POINTS OR TOP OF HUMP MODES APPEAR	FLUTTER VELOCITY DERIVATIVES MODAL DAMPING DERIVATIVES	PART OF STEP 1 OR 3 MINUTES	12 MINUTES FOR FIRST FLUTTER FLUTTER MODE/HUMP THEN 3 MINUTES FOR EACH ADDITIONAL
7	RESIZE STRUCTURE	BATCH/INTERACTIVE PROGRAMS	OPTIONS TO SET: DERIVATIVE EFFECTIVENESS FACTORS, ACTIVE/INACTIVE DESIGN VARIABLES, MULTIPLE CONDITIONS, WEIGHT ON/OFF, VELOCITY/OR WEIGHT TARGET INCREMENTS	DESIGN VARIABLES INCREMENTS	30 MINUTES	LESS THAN 2 MINUTES
8	UPDATE STIFFNESS MATRIX MASS MATRIX	UPDATE MACRO SIMILAR TO DELTAK MACRO EXCEPT SUBMITS ONE NASTRAN JOB	USES OUTPUT FROM STEP 7	UPDATED STIFFNESS MATRIX UPDATED MASS MATRIX	30 MINUTES	30 MINUTES

computer resource requirements. For example, in step 5, the process setup time for the engineer is 60 minutes while the compute time for 100 NASTRAN jobs is more than 6 CPU hours. Even more leverage of CPU to setup time is possible when submitting standard flutter analyses where four minutes of setup time results in using 80 CPU minutes of computer resources.

The benefits of running analysis and optimization processes under CBUS are repeatability, low engineering setup hours, user defined levels of automation, flexibility, user defined process definition, and more visibility of the design process.

The benefits of using one FEM for stress, loads, and flutter are common basis for specifying requirements, the maintenance of one structural model, and improved analysis integrity between disciplines.

While the FEM model may not meet the full requirements for detailed stress analysis, and while the FEM may be too detailed for stiffness analyses and design requirements, the authors conclude that the benefits far outpace the limitations and that strength sizing and loads generation should be integrated to provide interdisciplinary aeroelastic design capability at a complete vehicle level.

REFERENCES

1. Radovcich, N. A., "Preliminary Aeroelastic Design of Structures (PADS) Methods Development and Application," presented at the 56th AGARD Structures and Materials Panel Meeting, London, United Kingdom, April 1983.

2. Radovcich, N. A., "Some Experiences in Aircraft Aeroelastic Design Using Preliminary Aeroelastic Design of Structures (PADS)," presented at NASA Symposium on Recent Experiences in Multidisciplinary Analysis and Optimization, NASA Langley, April 24-26, 1984.

3. Radovcich, N. A., et al., "Study For the Optimization of a Transport Aircraft Wing For Maximum Fuel Efficiency," NASA CR-172551, January 1985.

BLANK PAGE

AEROELASTIC TAILORING AND INTEGRATED WING DESIGN

Mike Love and Jon Bohlmann

GENERAL DYNAMICS
Fort Worth Division

Copyright © 1988 by General Dynamics Corporation. All rights reserved. Published by the National Aeronautics and Space Administration, with permission.

PREVIEW

Aeroelastic Tailoring is a design process which is multidisciplinary in nature. Aeroelasticity fundamentally involves interactions between aerodynamics and structures, in addition to the relationship between flexibility and controls (aeroservoelasticity). The use of composite materials and their directional stiffness properties allows a designer to tailor the structure to meet his design goals. Shirk, Hertz and Weisshaar have defined aeroelastic tailoring in an excellent survey paper on the subject [Ref. 1]:

> Aeroelastic tailoring is the embodiment of directional stiffness into an aircraft design to control aeroelastic deformation, static or dynamic, in such a fashion as to affect the aerodynamic and structural performance of that aircraft in a beneficial way.

The key, as with any design process, is to affect the aircraft to gain performance benefits, such as reduced weight, greater roll power, reduced loads, etc. This presentation will demonstrate the use of aeroelastic tailoring in the integrated design environment by discussing fundamental concepts, giving design examples, and portraying its implementation in design.

"AEROELASTIC TAILORING is the embodiment of directional stiffness into an aircraft structural design to control aeroelastic deformation, static or dynamic, in such a fashion as to affect the aerodynamic and structural performance of that aircraft in a BENEFICIAL WAY." (Shirk, Hertz, and Weisshaar, 1984)

CONCEPTS

EXAMPLES

IMPLEMENTATION

AEROELASTIC TAILORING: AN EMBEDDED PROCESS OF PRELIMINARY DESIGN

Current design trends are recognizing "aeroelasticity as a primary design parameter affecting structural optimization, vehicle aerodynamic stability, control effectiveness, and overall performance" [Ref. 2]. Because of its multidisciplinary nature, aeroelastic tailoring is clearly a process embedded in preliminary design. The objective of maximizing performance is reached subject to certain requirements that the overall configuration must meet. These include mission performance, stability and control, and structural integrity. Aeroelastic tailoring, by its nature of using lightweight, directional composite materials, can oftentimes allow the designer to meet or exceed these maneuver requirements. For example, a composite wing skin may be designed such that the structural stiffness is oriented to give a greater flutter speed. The wing may also be tailored to aeroelastically induce negative twist to reduce maneuver drag. The design objective of aeroelastic tailoring varies according to the specified requirements and goals.

Another important consideration is that flexibility significantly affects the design. Since aeroelastic tailoring impacts aerodynamics, structures, controls, and design loads, its use demands communication and an integration of the design goals. Indeed, aeroelastic tailoring is unworkable outside of an integrated, multidisciplinary design process.

- PRELIMINARY DESIGN OBJECTIVE

  OPTIMIZE CONFIGURATION PERFORMANCE SUBJECT TO SET MANEUVER REQUIREMENTS

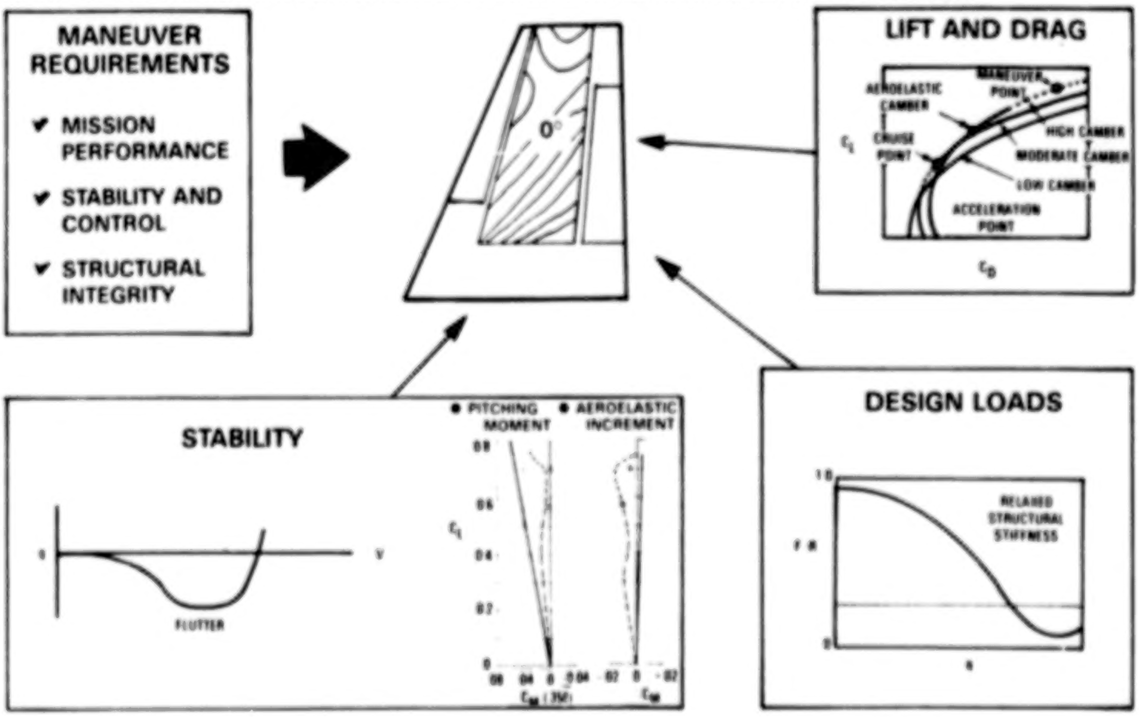

TAILORING CONCEPTS - MANIPULATE TWIST AXIS

There are two fundamental concepts in visualizing how aeroelastic tailoring utilizes composite's directional stiffness to meet design goals. One concept is to design a "washout" composite laminate, which is one where the stiffness is essentially directed most toward the front spar of a wing. This makes the trailing part of the wing less stiff such that under positive vertical load the trailing edge deflects more than the leading edge, giving a negative aeroelastic twist. This negative twist obviously reduces aerodynamic loads. The opposite of washout is "washin," a washin laminate directing stiffness toward the rear spar, giving a positive twist under positive vertical load. A washin design thus increases aerodynamic loads. A washout or washin laminate may also be thought of in terms of the location of the wing's reference twist axis relative to a "nontailored" (metallic) wing, as shown in the figure below. Whether a designer would be most interested in a predominantly washout design or washin design depends to a large extent on the configuration. A swept-forward wing may incorporate a washout design to prohibit wing divergence, while an aft-swept wing may employ some washin concepts to improve lifting surface effectiveness (e.g., a vertical tail).

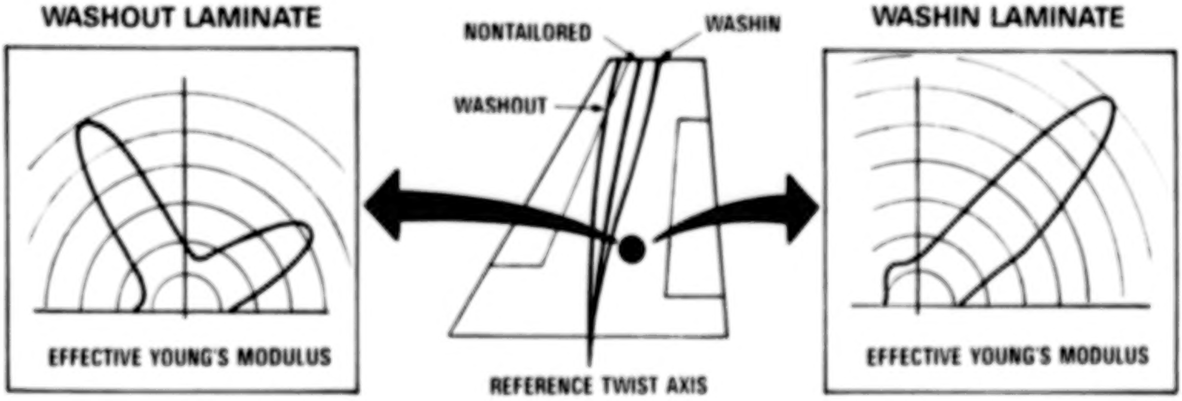

CONCEPT EFFECTIVENESS IS CONFIGURATION DEPENDENT

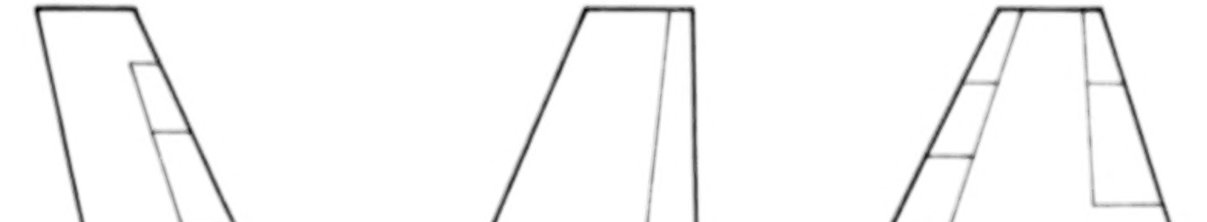

OPTIMIZATION METHODS ARE KEY TO DESIGN STUDIES

It is obviously not sufficient for the designer to merely determine how to use aeroelastic tailoring in a fundamental sense. The makeup of the composite wing skin must be determined more exactly, along with assessing its interactions with such issues as, for example, wing planform shape. As stated by McCullers [Ref. 3], the design of a composite laminate "requires the determination of the number of plies and the orientation of each ply for the material(s) selected, which increases the magnitude and complexity of the design problem. Therefore, although optimization techniques are very useful in metal design problems, they are almost essential for the efficient design of composite structures." Computational methods using optimization algorithms allow one to design a tailored structure to determine structural feasibility and predict the weight required for a given geometric and controls configuration. These two issues are primary tasks of structural design in the preliminary design process. The variance in flexibility achievable in composites necessitates a converged structural design in order to establish valid parametric trades of planform, wing design, controls, and tailoring concepts.

- **CONVERGED PRELIMINARY STRUCTURAL DESIGNS**

✓ STRUCTURAL FEASIBILITY
  - STRENGTH
  - FLUTTER
  - CONTROL

✓ WEIGHT PREDICTION
  - ANALYSIS DETAILS
  - LAMINATE REQUIREMENTS
  - DESIGN DETAILS

- **PARAMETRIC GEOMETRIC TRADE STUDIES**

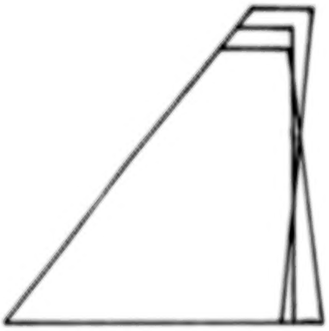

PLANFORM

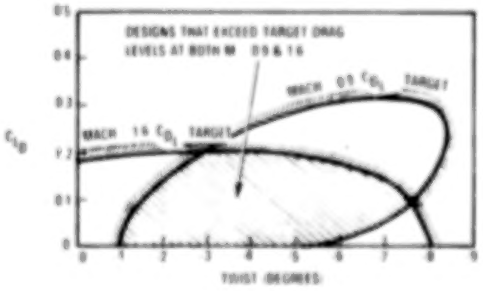

WING DESIGN

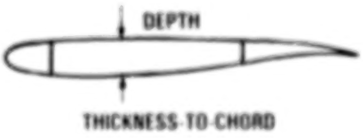

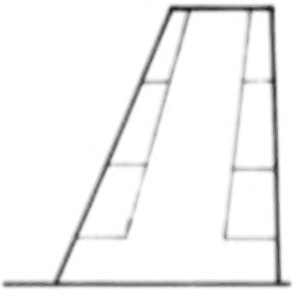

CONTROL SURFACE

TSO - A DESIGN INTEGRATION TOOL TO ADDRESS FEASIBILITY ISSUES

One particular structural optimization tool suited for aeroelastic tailoring studies is TSO, the Wing Aeroelastic Synthesis Procedure [Ref.4]. This code was developed at General Dynamics under Air Force contract in the early 1970's. TSO has been used extensively over the years to explore the use of composites in designing structural box skins of lifting surfaces. TSO applications have given much understanding in realizing practicalities of aeroelastic tailoring.

TSO incorporates a Rayleigh-Ritz equivalent plate technique for the structural model. Linear steady and unsteady aerodynamic codes are used to predict design loads. TSO's nonlinear programming algorithm allows the user to design a structural skin subject to a number of constraints. The design variables include thickness distributions of the composite layers and their fiber orientation angles. Design constraints typically consist of strength, flutter, and the effectiveness of a flaperon to produce rolling moment. TSO's computational efficiency allows the consideration of many design options, and provides an integrated, multidisciplinary tool to address design feasibilities. It is still a preliminary design tool, however, such that it serves as a precursor to finite element model analyses.

- **MULTIDISCIPLINARY TOOL**
  - STRENGTH
  - FLUTTER
  - STEADY AERO
  - NLP OPTIMIZATION
- **PRECURSOR TO FINITE ELEMENT METHODS**
  - SIMPLE MODEL
  - MULTI-MANEUVER SIMULATION
- **YEARS OF CALIBRATED USE**
  - "REAL WORLD" UNDERSTANDING
  - PRACTICAL DESIGNS

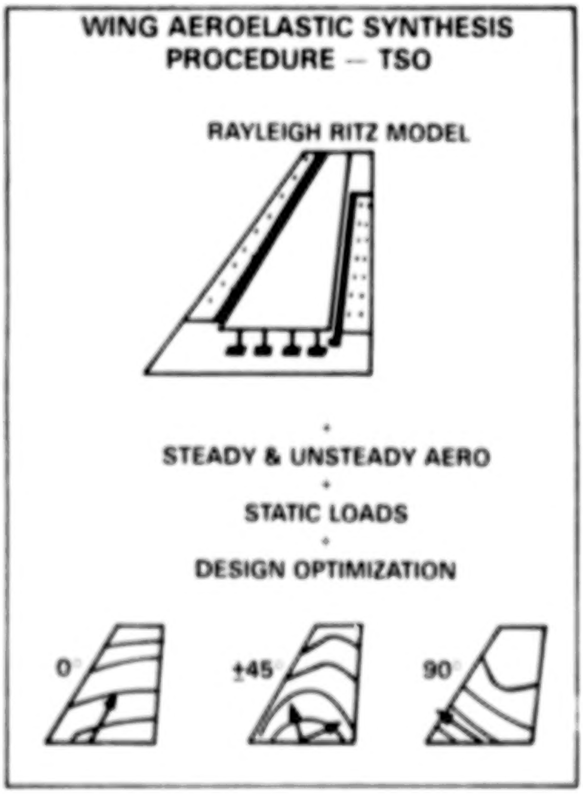

WEIGHT PREDICTION ADDRESSED THROUGH EXPERIENCE

Despite TSO's ability to aeroelastically tailor the skin of a wing or other lifting surfaces for a set of design requirements, it lacks the structural detail of finite element methods. This means that TSO cannot adequately address such design details as buckling or bolted joints. Damage tolerance and manufacturing provide other considerations that affect the makeup of a composite laminate. Such details can have a direct impact on the aeroelastic tailored design produced by TSO. Hence, previous design experience is incorporated into TSO through the use of strain limits, laminate ply percentages, shape functions and min and max gage thicknesses. Bolted joint details and low velocity impact considerations, for example, may be addressed by limiting fiber strains relative to fracture criteria. An envelope of acceptable laminate ply percentages is generally developed to account for ply stacking sequence effects in the sense of potential fracture mechanisms. Constraints have been formulated in TSO's penalty function scheme to address this issue. Weight for design details such as fasteners, sealants, and understructure are estimated through historical data. Buckling must be dealt with on the finite element level of analysis, and its impact to structural design is not to be taken lightly.

- **ANALYSIS DETAILS**

BOLTED JOINTS (STRAIN LIMITS)

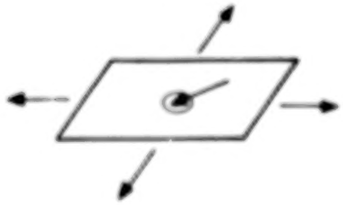

BUCKLING (?)

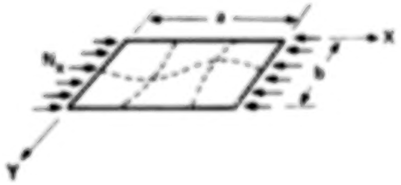

- **LAMINATE REQUIREMENTS**
  - ✔ **DAMAGE TOLERANCE**
    - STRAIN LIMITS
    - PERCENTAGE CONSTRAINTS
  - ✔ **MANUFACTURING**
    - SHAPE FUNCTIONS
    - THICKNESS CONSTRAINTS

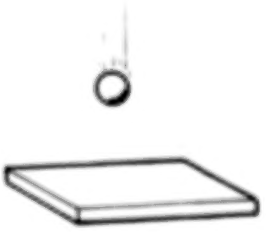

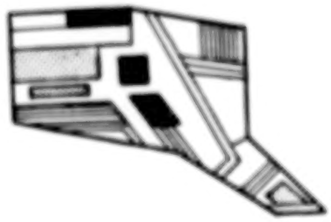

- **DESIGN DETAILS (FASTENERS, SEALANT, ETC.)**

WASHIN DESIGN INFLUENCED BY MATERIAL PROPERTIES

Let us turn now to three examples that demonstrate design sensitivities derived from implementing aeroelastic tailoring. The results in these examples were taken from TSO design studies of typical fighter aircraft configurations.

This first example is that of a vertical tail with a rudder control surface. The purpose of the study is to determine the effectiveness of various materials on the structural weight for a design criteria of strength, flutter, and primarily for rudder yaw effectiveness. The driving variable in the study was the lamina longitudinal stiffness which is governed by fiber stiffness. A washin laminate design is required to provide the necessary rudder effectiveness at a minimum weight. The graph illustrates a savings in structural weight for an increase in fiber stiffness. Also, the laminate becomes less directional (less washin) with the increase in stiffness. Since increased washin tendencies generally give better rudder effectiveness, the benefits of the greater stiffness are a trade between structural weight and rudder effectiveness. The designer could opt to waive the weight savings associated with a higher stiffness material and reinvest the weight to increase rudder effectiveness. Perhaps another trade might result in the necessity for the lower modulus material versus the requirements for aircraft control.

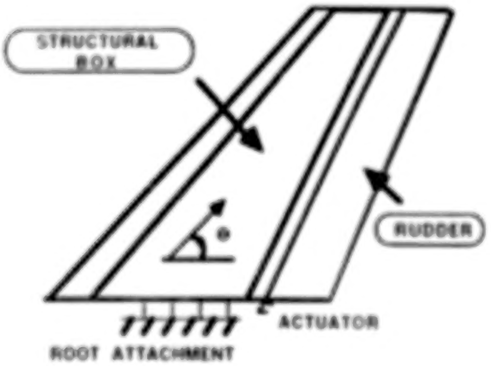

- VERTICAL TAIL (MIN. WEIGHT)
  - Rudder Effectiveness
  - Flutter
  - Strength

- FIBER STIFFNESS
  - Stiffness Increase Gives a Less Washin Laminate
  - Implied Effectiveness and Weight Benefits

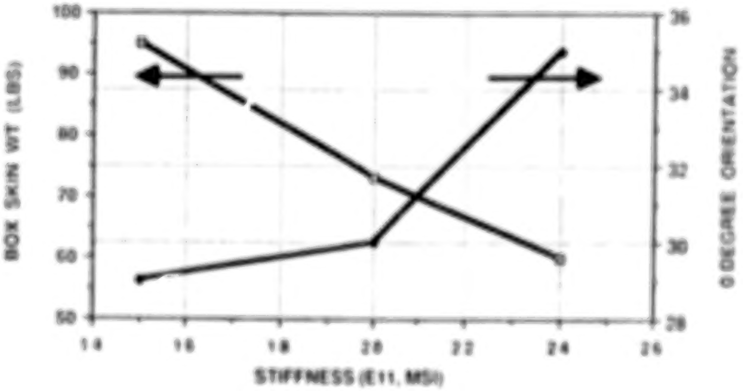

THICKNESS-TO-CHORD RATIO: STIFFNESS DESIGN VS STRENGTH DESIGN

This second example demonstrates the effect of lifting surface depth, and was derived to provide data for a trade between structural weight and supersonic wave drag. The lifting surface depth was varied through the selection of various t/c's. The box details of understructure and fasteners were estimated from historical data and are added to the box skin weight. The surface had been designed for minimum weight, control surface effectiveness, flutter, and strength. The data provides the designer with knowledge of the strength versus stiffness design. Certainly increasing box depth adds stiffness to the structure, such that the wing skin need not add as much stiffness to meet the flutter and control surface effectiveness requirements. Hence, the skin weight decreases with increasing t/c. Eventually a t/c will be reached where the box depth alone provides enough stiffness, leaving the wing skin to be designed only by strength considerations. At this point the skin is said to be strength designed, as opposed to a skin designed primarily for stiffness. It can be observed that as the box gets sufficiently deep, the added understructure weight begins to override the weight savings seen by the box skin.

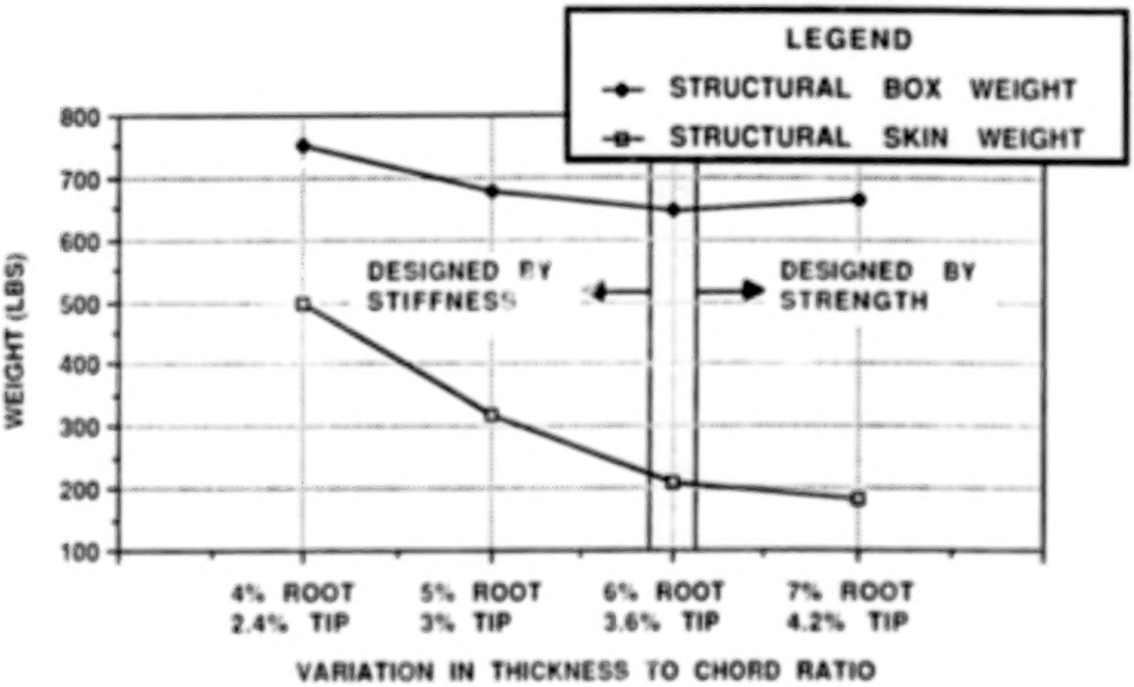

MULTIDISCIPLINARY DESIGN CONSIDERATION - FIGHTER PERFORMANCE

The final example illustrates an age old design trade of span for turning performance and weight required to achieve structural integrity. This TSO study examined the structural skin weight derived to satisfy three levels of criteria for three planforms. The first criteria consisted of the weight required to satisfy only strength requirements ("strength sized"). The second criteria added flutter and flaperon roll moment effectiveness (flex-to-rigid ratio) to the strength criteria ("aeroelastic sized"). The final criteria added a twist objective to provide aeroelastic washout for reduced lift-induced drag ("drag sized"). The planforms differed only in span. Design loads included 9g symmetric and 5.86g asymmetric maneuvers. The data indicates that a severe weight penalty exists for meeting the flutter and roll requirements, while the increase in span also facilitates the aeroelastic twist.

Associated with the structural related data is the trade with aerodynamic performance. Shown in the second graph are the associated weight of the structure designed to twist and the lift-induced drag coefficient at a Mach 0.9, 10,000 ft, 9g maneuver. The chart clearly shows a trade-off between weight and drag. This demonstrates the necessity of integrating the design process to determine how such trade-offs affect vehicle performance. The weight/drag trade-off could be evaluated through how it affects turn rate, since turn rate is directly related to the specific excess power Ps, which considers both weight and drag.

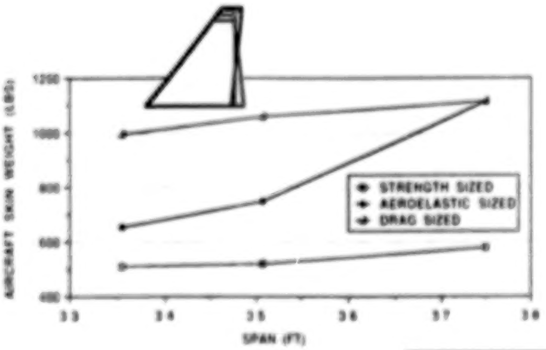

- SPAN TRADE
  - Constant Area and Sweep
  - Symmetric & Asymmetric Maneuvers
  - 3 Design Concepts

- SUSTAINED PERFORMANCE
  - Δ Weight
  - Δ Drag-Due-to-Lift
  - Δ Turn Rate

$$P_s = \frac{V\ (T-D)}{W}$$

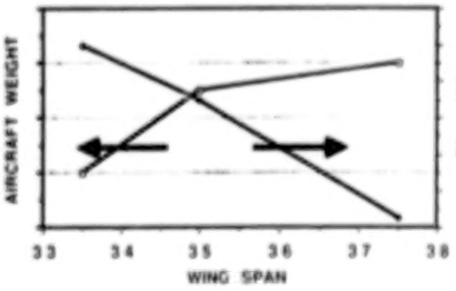

OPTIMAL DESIGN - A RESULT OF SIMULATION

The previous examples demonstrated the need to integrate the design process while being able to simulate the impacts of various design options on the aeroelastic performance of the vehicle. Many factors enter the picture to adequately address multidisciplinary and integrated issues during optimization. As a result, it is important to be able to computationally simulate many multidisciplinary influences as accurately as possible so that sensitivity data may be generated. The figure below cites several examples of important design considerations. The underlying reason for considering these implications during design is that optimization techniques will exploit weaknesses in the computational simulation. For example, if the structure is preliminarily designed to only symmetric loads, significant redesign will be required later since asymmetric loads stress the wing in critical areas as well.

- WING DESIGN
  - ✓ Camber Enhances Steady Aeroelastic Deflections
  - ✓ Twist Reduces Steady Aeroelastic Deflections
- CONTROLS CONFIGURATION
  - ✓ Upwash and Downwash Within Entire Vehicle
  - ✓ Control Surface Blending for Optimal Maneuver
- LOADS
  - ✓ Symmetric and Asymmetric Applied Loads
  - ✓ Internal Loads (Equilibrium, Fuel Pressure, etc.)
- MODELS
  - ✓ Aerodynamics - Mesh Size
  - ✓ Structures - Accurate Idealization
  - ✓ Design - Manufacturing and Performance

BOTTOM LINE - Optimization Techniques Exploit Simulation Weaknesses

OPTIMIZATION AND ANALYSIS INTEGRATION

The question remains as to implementing aeroelastic tailoring into detailed levels of multidisciplinary considerations. The figure below presents a sketch of the integrated aeroelastic design procedure currently employed at General Dynamics.

Aeroelastic tailoring through the TSO procedure is the first step past preliminary configuration definition. As TSO skin designs are passed into finite element models for more detailed analyses, TSO parametric studies continue to determine a wide range of aeroelastic influences, such as with the three examples discussed above. Such studies are valuable since, for example, the initial wing configuration is generally conceived assuming a rigid structure. Information constantly flows through the various computational procedures as "what-if" questions are raised. The analysis results give accurate indications of the integrated aeroelastic performance of the model. The results may be fed back to aerodynamic and stability & control to refine drag estimates and stability margins based upon the flexibilized data, which in turn may be used to re-estimate combat performance.

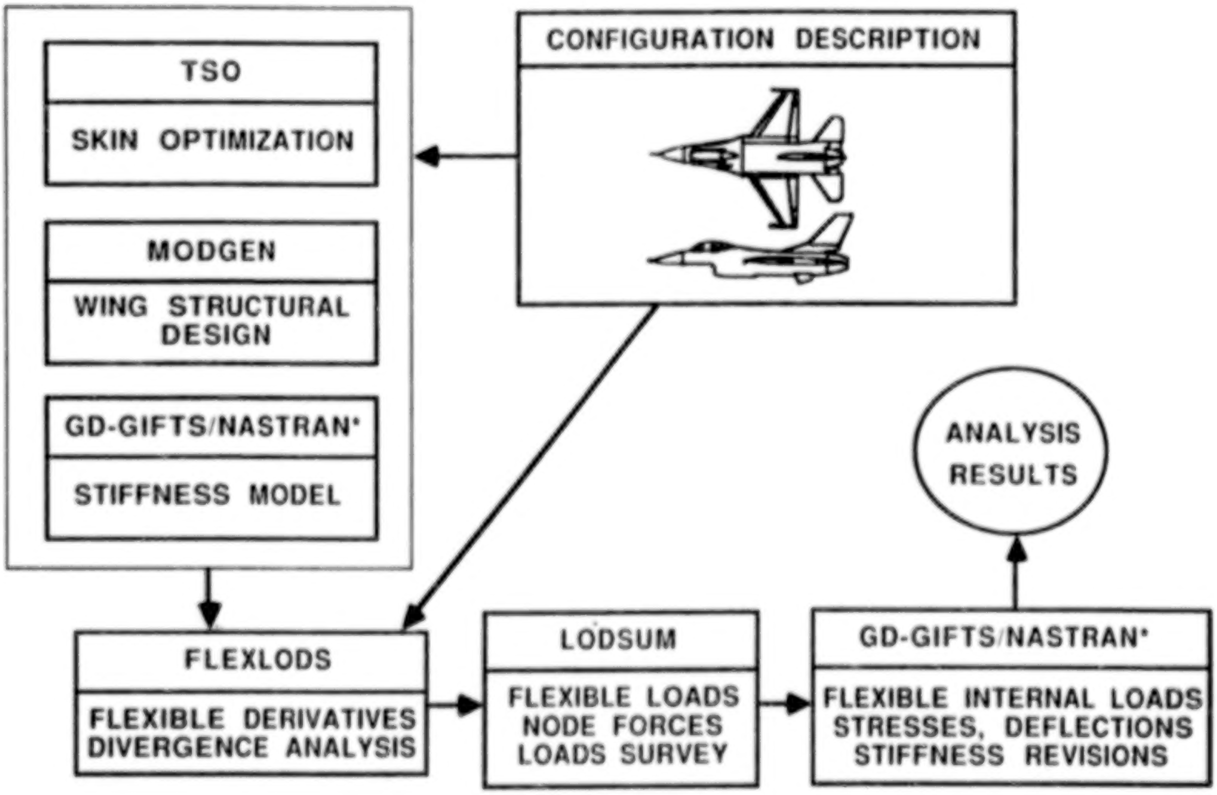

* NASTRAN is a registered trademark of NASA.

LESSONS LEARNED IMPLEMENTING TSO

In summary, much has been learned from TSO over the years in determining aeroelastic tailoring's place in the integrated design process. Indeed, it has become apparent that aeroelastic tailoring is and should be deeply embedded in design. Aeroelastic tailoring can have tremendous effects on the design loads, and design loads affect every aspect of the design process. While optimization enables the evaluation of design sensitivities, valid computational simulations are required to make these sensitivities valid. Aircraft maneuvers simulated must adequately cover the plane's intended flight envelope, realistic design criteria must be included, and models among the various disciplines must be calibrated among themselves and with any hard-core (e.g., wind tunnel) data available. The information gained and benefits derived from aeroelastic tailoring provide a focal point for the various disciplines to become involved and communicate with one another to reach the best design possible.

- AEROELASTIC TAILORING IS AN EMBEDDED PROCESS OF DESIGN
- OPTIMIZATION ENABLES EVALUATION OF DESIGN SENSITIVITIES
- VALID SENSITIVITIES ARE DERIVED FROM VALID SIMULATIONS
  - ✓ Aircraft Maneuvers Must Be Broad Spectrum
  - ✓ Design Criteria Must Be Accounted For
  - ✓ Discipline Models Must Be Calibrated
- AEROELASTIC TAILORING APPLICATIONS INTEGRATE WING DESIGN
  - ✓ Multiple Disciplines are Involved
  - ✓ Communication is Required

REFERENCES

1. Shirk, M.H., Hertz, T.J., and Weisshaar, T.A., "Aeroelastic Tailoring - Theory, Practice, and Promise," Journal of Aircraft, Vol. 23, No. 1, January 1986, pp. 6-18.

2. Wilson, E.G., Jr., "Static Aeroelasticity in the Design of Modern Fighters," AGARD Report No. 725: "Static Aeroelasticity in Combat Aircraft," January 1986.

3. McCullers, L.A., "Automated Design of Advanced Composite Structures," Proceedings of the ASME Structural Optimization Symposium, AMD-Vol. 7, November 1974, pp. 119-133.

4. McCullers, L.A., and Lynch, R.W., "Dynamic Characteristics of Advanced Filamentary Composite Structures, Volume II - Aeroelastic Synthesis Procedure Development," AFFDL-TR-73-111, September 1974.

INTEGRATED AERODYNAMIC-STRUCTURAL DESIGN OF A FORWARD-SWEPT TRANSPORT WING

R. T. Haftka, B. Grossman, P. J. Kao, D. M. Polen
Department of Aerospace and Ocean Engineering
Virginia Polytechnic Institute and State University
Blacksburg, Virginia

and

J. Sobieszczanski-Sobieski
Interdisciplinary Research Office
NASA Langley Research Center
Hampton, Virginia

OVERALL GOALS

The introduction of composite materials is having a profound effect on aircraft design. Since these materials permit the designer to tailor material properties to improve structural, aerodynamic and acoustic performance, they require an integrated multidisciplinary design process. Furthermore, because of the complexity of the design process numerical optimization methods are required.

The utilization of integrated multidisciplinary design procedures for improving aircraft design is not currently feasible because of software coordination problems and the enormous computational burden. Even with the expected rapid growth of supercomputers and parallel architectures, these tasks will not be practical without the development of efficient methods for cross-disciplinary sensitivities and efficient optimization procedures.

The present research is part of an on-going effort which is focused on the processes of simultaneous aerodynamic and structural wing design as a prototype for design integration. A sequence of integrated wing design procedures has been developed in order to investigate various aspects of the design process.

- ○ NEED
    - *composite materials*
    - *aircraft complexity*
- ○ PAY-OFF
    - *better designs*
- ○ DIFFICULTIES
    - *computational cost*
    - *software coordination*

PREVIOUS RESEARCH EFFORTS

In their initial efforts, the authors considered the integrated design of a high aspect-ratio sailplane wing. The sailplane mission was used to illustrate the advantages of including aerodynamic and structural interactions in the design process, by optimizing for circling flight in a thermal current followed by cross-country cruise. Furthermore, the simplicity of the sailplane wing planform and structural design allowed for the use of rudimentary analysis methods, (lifting-line and beam theory). The simplicity of these analyses made it feasible to calculate all the sensitivity derivatives of the aerodynamic shape and structural sizes, along with all the cross-sensitivity derivatives, directly, without any further approximation, at each step of the numerically optimized design process. The results, reported in Ref. 1, demonstrated that integrating the structural and aerodynamic design processes leads to wing designs superior to those obtained by the traditional sequential approach.

The next step of the integrated wing design procedure study again involved the sailplane wing design, but with analysis methods which are representative of methods used for low-speed aircraft wing designs. The utilization of a vortex-lattice method and a structural finite-element method, while providing for a more exact analysis and allowing for more general wing shapes, introduced the need for more design variables and constraints, and were significantly more expensive to use in the design process. In Ref. 2, it was shown that by incorporating perturbation methods for cross-sensitivity calculations and approximate optimization procedures, an estimated 10 hours of IBM 3084 CPU time for a complete integrated design, was reduced to less than ten minutes. Most of the remaining computational cost was associated with the calculation of derivatives of the aerodynamic influence coefficient matrix and the structural flexibility matrix.

○ Demonstrated benefits of integrated design using rudimentary analysis methods for sailplane design

○ Reduced computational costs by approximate optimization

○ Computational costs remain high due to sensitivity derivatives of aerodynamic and flexibility matrices

PRESENT OBJECTIVE

The present paper represents the third step of this study. The objective here is to develop an integrated wing design procedure for a subsonic transport aircraft. We still use vortex-lattice aerodynamics (so that we are restricted to subsonic speeds) and finite-element structural analysis. Even with basic aerodynamic design variables, (planform shape and twist distribution), the increased complexity of an integrated transport design over the previous sailplane wing design requires further computational reductions. We consider two approaches for reducing the computational burden of multidisciplinary optimization:

i. the development of efficient methods for cross-sensitivity calculation; and
ii. the use of approximate optimization procedures.

The sensitivity calculation is based on a modular sensitivity method (Ref. 3) for computing sensitivity derivatives of a system via partial derivatives of the output with respect to input and to design variables of each component of the system. This modular approach, corresponds to the abstraction of a system as an assembly of interacting *black boxes*. This method was developed for calculating system sensitivity without modifying disciplinary black-box software packages, Ref. 4. It allows for the calculation of sensitivity derivatives of a system with a higher accuracy and, in most cases, at a lower cost than with conventional finite differencing. The system sensitivity derivatives may be used to guide a formal optimization and a Newton's method solution of the coupled interdisciplinary equations describing the system behavior. Within this framework, we show that the sensitivities can be computed without the expensive calculation of the derivatives of the aerodynamic influence coefficient matrix, and the derivatives of the structural flexibility matrix.

Furthermore, the same process enables the determination of the sensitivity of the aeroelastic divergence dynamic pressure without the determination of the derivatives of the aerodynamic influence coefficient matrix and flexibility matrix. This feature should be useful, not only in problems of complete integrated aircraft design, but also in aeroelastic tailoring applications.

○ Develop an integrated design procedure for a transport aircraft

○ Utilize a modular sensitivity analysis

○ Reduce computational costs

WING DESIGN VARIABLES

We consider the optimum design of an aircraft wing. The objective function can be the structural weight of the wing, an aerodynamic performance index such as the lift-to-drag ratio, L/D or a combination thereof. In the present study we minimize the structural weight of the wing. The design variables associated with the aerodynamic design include the planform shape parameters defined on the figure below, and the twist schedule along the span.

For the present, preliminary study of integrated structural-aerodynamic design, we assume the airfoil shape to be supplied, along with known section characteristics. The design variables associated with the structural design are the structural sizes including panel thicknesses and spar-cap cross-sectional areas. The finite-element model of the wing is shown schematically in the figure below. Additionally, composite material ply orientations in the cover panels are used as design variables.

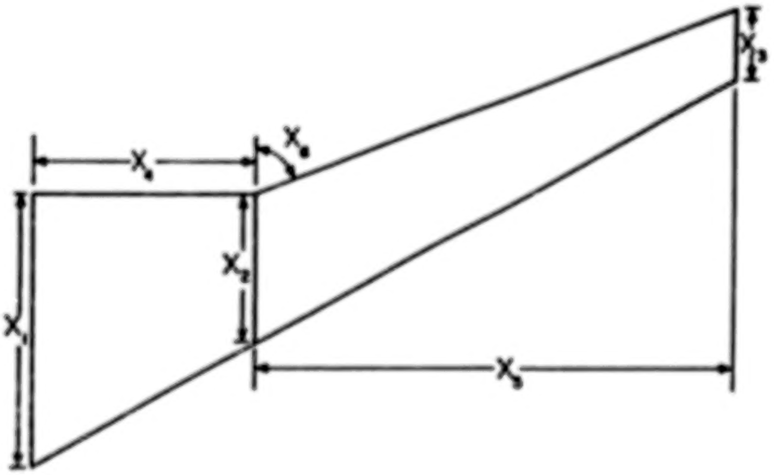

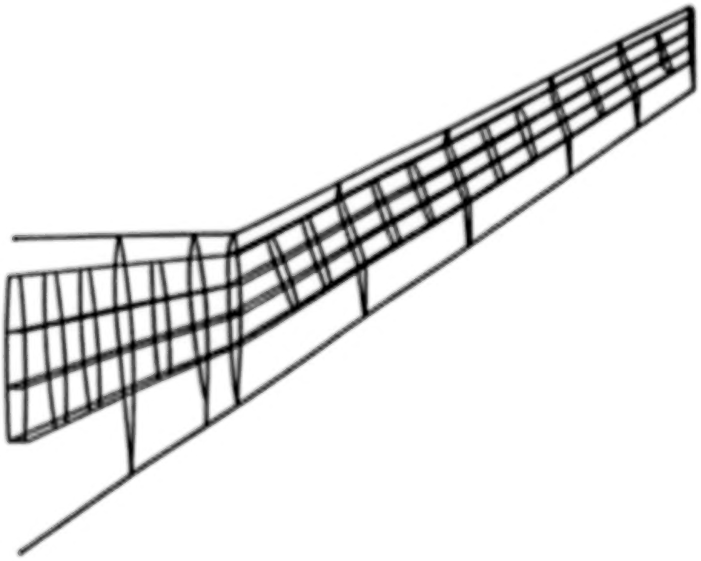

INTEGRATED DESIGN PROBLEM

Constraints are placed on the magnitudes of stresses and strains in the structure, on the aeroelastic divergence speed, and on aerodynamic performance measures and stall conditions. Additional geometric constraints are imposed on the planform shape design variables to prevent unreasonable geometries.

The aerodynamic and structural response is calculated from a coupled set of equations discussed below. Aerodynamic performance is calculated at the cruise condition, while the limits on stresses and strain are applied for a high-*g* pull-up maneuver.

○ OBJECTIVE FUNCTION

minimize wing weight

○ DESIGN VARIABLES

- *planform shape parameters*
- *panel thickness, spar cap areas*
- *ply orientation*

○ CONSTRAINTS

- *stress, strain*
- *divergence speed*
- *performance, planform shape*

AEROELASTIC FORMULATION

The aeroelastic analysis of the wing is simplified by making several assumptions. We assume that the effect of the aerodynamics on structural deformations can be approximated by lumping the aerodynamic forces at n_l structural grid points (called here the load set), and including only the vertical components of the loads. The vector of vertical aerodynamic loads is denoted as F_a. We assume that the overall aircraft response affects the wing only through the root angle of attack α. Finally, we assume that the effect of structural deformations on the aerodynamic response can be approximated in terms of the vector of vertical displacements θ at the load set.

The vertical aerodynamic loads at the load set, F_a, are determined from an aerodynamic analysis procedure. For low speed wing designs, we utilize a vortex lattice method (e.g., Ref. 5) to compute the lift and the induced drag. The wing is discretized into panels, with each panel containing an element of a horseshoe vortex of strength γ_j. By enforcing flow tangency at each panel, a vector of circulation strengths Γ may be computed from eq. (1), below, where p is a vector of design parameters and V is a matrix of influence coefficients. The aerodynamic forces are computed from a local application of the Kutta-Joukowski theorem, and compressibility effects are included through a Göthert transformation. The profile drag for each wing section is calculated from the measured airfoil drag polar. The load vector F_a is then obtained as eq. (2). Altogether we combine equations (1) and (2) as eq. (3), below. The angle of attack is obtained from the overall vertical equilibrium of the aircraft as eq. (4), where N is a summation vector, n is the load factor and W is the weight of the aircraft.

- *aerodynamic equations*

$$V(p,\theta)\Gamma = C(p,\alpha,\theta) \tag{1}$$

$$F_a = F_a(p,\alpha,\theta,\Gamma) \tag{2}$$

$$F_a = f_1(p,\alpha,\theta) \tag{3}$$

- *vertical equilibrium equation*

$$f_2(p,F_a) = \frac{1}{2}nW - N^T F_a = 0 \tag{4}$$

STRUCTURAL ANALYSIS

The vertical displacements at the load set are calculated by finite-element analysis using a modification of the WIDOWAC program (Ref. 6). First the nodal displacement vector U is calculated by solving eq. (5), where K is the stiffness matrix, T is a Boolean matrix which expands F_a to the full set of structural degrees of freedom, and F_I is the gravitational and inertia load vector. Strains and stresses are then calculated from the displacement vector U. The vertical displacements at the load set θ are extracted from U as eq. (6). Equations (5) and (6) can be combined as eq. (7).

- *structural equations*

$$K(p)U = TF_a + nF_I(p) \tag{5}$$

$$\theta = T^T U \tag{6}$$

$$\theta = f_3(p, F_a) \tag{7}$$

BEST COPY AVAILABLE

SOLUTION PROCEDURE

Equations (3), (4) and (7) are a set of nonlinear coupled equations for the vector of vertical aerodynamic loads, F_a, the wing root angle of attack, α and the vector of vertical displacements, θ. For the analysis problem, the vector of design parameters, p, is given. Reference 3 presented a modular sensitivity analysis of such coupled interdisciplinary equations. The modular approach permits treating the individual discipline analysis procedures as *black boxes* that do not need to be changed in the integration procedure. Here we employ a similar approach for the sensitivity analysis below, with f_1 representing an *aerodynamic black box* and f_3 a *structural black box*. We also use the same approach for the solution of the system via Newton's method.

Given an initial estimate for the solution F_a^0, α^0, θ^0 we use Newton's method to improve that estimate. The iterative process may be written as eq. (8), where ΔY, Δf and J are defined in eqs. (9), (10), and (11). The Jacobian is given in terms of the dynamic pressure q, the incremental aerodynamic force vector, qR, the aerodynamic influence coefficient matrix, qA and the flexibility matrix S. The incremental aerodynamic force vector is defined such that its component qr_i represents the change in F_{ai} due to a unit change in α, and the aerodynamic influence coefficient matrix, is defined such that its component qa_{ij} represents the change in F_{ai} due to unit change in θ_j. Similarly, the flexibility matrix, is such that s_{ij} is the change in θ_i due to a unit change in F_{aj}.

- *solution by Newton's method*

$$J\Delta Y = \Delta f \tag{8}$$

where

$$\Delta Y = \begin{Bmatrix} \Delta F_a \\ \Delta\alpha \\ \Delta\theta \end{Bmatrix} \tag{9}$$

$$\Delta f = \begin{Bmatrix} f_1(p,\alpha^0,\theta^0) - F_a^0 \\ f_2(p,F_a^0) \\ f_3(p,F_a^0) - \theta^0 \end{Bmatrix} \tag{10}$$

$$J = \begin{bmatrix} I & -\partial f_1/\partial\alpha & -\partial f_1/\partial\theta \\ -\partial f_2/\partial F_a & 0 & 0 \\ -\partial f_3/\partial F_a & 0 & I \end{bmatrix} = \begin{bmatrix} I & -qR & -qA \\ N^T & 0 & 0 \\ -S & 0 & I \end{bmatrix} \tag{11}$$

SOLUTION PROCEDURE (continued)

Partial solution of equation (8) yields the following three equations for the increments $\Delta\theta$, $\Delta\alpha$ and ΔF_a, shown below as eqs. (12), (13) and (14). We start with a rigid wing approximation and execute a single Newton iteration to approximate the flexible wing response.

$$(I - qSA^x)\Delta\theta = SB\Delta f_1 + \frac{SR}{N^T R}\Delta f_2 + \Delta f_3 \qquad (12)$$

$$\Delta\alpha = \frac{\Delta f_2 - N^T\Delta f_1 - qN^T A\Delta\theta}{qN^T R} \qquad (13)$$

$$\Delta F_a = \Delta f_1 + qR\Delta\alpha + qA\Delta\theta \qquad (14)$$

where

$$B \equiv I - \frac{RN^T}{N^T R} \qquad (15)$$

$$A^x \equiv AB \qquad (16)$$

- *initial conditions*

$$F_{ar} = f_1(p,0,0) + q\alpha_r R \qquad (17)$$

$$\alpha_r = \frac{\frac{1}{2}nW - N^T f_1(p,0,0)}{qN^T R} \qquad (18)$$

SENSITIVITY ANALYSIS (modular approach)

As just stated, it is common practice to follow this procedure and use a single Newton's iteration in the analysis of a flexible wing. Then for a design problem, where derivatives with respect to a design parameter p are required, equations (12), (13) and (14) are differentiated with respect to p (e.g., Ref. 2). This approach requires the calculation of derivatives of the matrices A and S which can be very costly. Here, instead, we follow Ref. 3 and differentiate equations (3), (4) and (7) with respect to p to obtain eq. (19), where a prime denotes differentiation with respect to p and where Y' and f' are defined in eqs. (20) and (21). The Jacobian J appearing in equation (19) is the identical matrix utilized in the analysis in equation (11). Equation (19) can be partially solved to yield the sensitivities shown in eqs. (22), (23) and (24).

This approach does not require any derivatives of A and S but only partial derivatives of f_1, f_2 and f_3. For example, f_1' denotes the derivative of F_a with respect to a design variable when α and θ are fixed.

- *modular sensitivity*

$$JY' = f' \tag{19}$$

where

$$Y' = [\,F_a' \quad \alpha' \quad \theta'\,]^T \tag{20}$$

$$f' = [\,f_1' \quad f_2' \quad f_3'\,]^T \tag{21}$$

- *partial solution*

$$(I - qSA^{z})\theta' = SBf_1' + \frac{SR}{N^TR}f_2' + f_3' \tag{22}$$

$$\alpha' = \frac{f_2' - N^Tf_1' - qN^TA\theta'}{qN^TR} \tag{23}$$

$$F_a' = f_1' + qR\alpha' + qA\theta' \tag{24}$$

SENSITIVITY ANALYSIS (traditional approach)

By contrast, the more traditional approach (e.g., Ref. 2) to the derivative calculation is obtained by differentiating the aeroelastic analysis equations, such as eqs. (12) to (14) with respect to p as shown in eq. (25). This complicated expression can be shown to be equivalent to eq. (22). However, the traditional approach which employs eq. (25) requires the expensive calculation of the derivatives of the aerodynamic influence coefficient matrix, A' and the derivatives of the flexibility matrix S'.

$$\begin{aligned}(I - qSA^x)\Delta\theta' = {} & qS'A^x\Delta\theta + qSA'B\Delta\theta + qSAB'\Delta\theta \\ & + S'B\Delta f_1 + SB'\Delta f_1 + SB\Delta f_1' \\ & + \frac{S'R}{N^TR}\Delta f_2 + S(\frac{R}{N^TR})'\Delta f_2 + \frac{SR}{N^TR}\Delta f_2' \\ & + \Delta f_3' \end{aligned} \tag{25}$$

AEROELASTIC DIVERGENCE

The aeroelastic divergence instability is calculated at a fixed angle of attack, because it is assumed that the pilot does not react fast enough to change the angle of attack as the wing diverges. The instability is characterized by a homogeneous solution to eq. (8), that is given in eq. (26). Equation (26) is an eigenvalue problem for q. The lowest eigenvalue is the divergence dynamic pressure q_D. Equation (26) can be reduced to a standard linear eigenproblem by substituting for $\Delta\theta$ in terms of ΔF_a to obtain eq. (27). We denote the solution of eq. (26) as $[F_{aD}, \theta_D]^T$ and note that the same eigenvalue problem has also a left eigenvector $[F_{aL}, \theta_L]^T$.

- *eigenvalue problem*

$$\begin{bmatrix} I & -qA \\ -S & I \end{bmatrix} \begin{Bmatrix} \Delta F_a \\ \Delta\theta \end{Bmatrix} = 0 \tag{26}$$

$$(AS - \frac{1}{q}I)\Delta F_a = 0 \tag{27}$$

- *right and left eigenvectors*

$$\begin{bmatrix} I & -q_D A \\ -S & I \end{bmatrix} \begin{Bmatrix} F_{aD} \\ \theta_D \end{Bmatrix} = 0 \tag{28}$$

$$[F_{aL}^T, \theta_L^T] \begin{bmatrix} I & -q_D A \\ -S & I \end{bmatrix} = 0 \tag{29}$$

DIVERGENCE SENSITIVITY

To find the derivative of the divergence dynamic pressure q_D with respect to a design parameter p, we differentiate eq. (28) at $q = q_D$ with respect to p and obtain eq. (30). We premultiply eq. (28) by the left eigenvector, $[F_{aL}^T, \theta_L^T]$, defined by eq. (29) and obtain eqs. (31) and (32). Equation (32) contains derivatives of A and S with respect to p which we have managed to avoid before. However, the corresponding terms can be simplified. Using the definition of S, eq. (11), we note the relationship in eq. (33).

To see how $S'F_{aD}$ can be calculated without obtaining S' consider a more generic case. Let f be a function of a vector X, and let D be another vector. Let X_0 be a particular choice for X, then eq. (34) provides us with a way of calculating the product $\partial f/\partial X(X_0)$ times D without calculating the individual components of $\partial f/\partial X$. Therefore, to calculate $S'F_{aD}$ we start by calculating the derivative of f_3 to a perturbation in F_a in the form of F_{aD} (because we use linear structural analysis this is the response of the structure to F_{aD}). Then we calculate the derivative of this response with respect to p assuming that F_{aD} is fixed. The term $A'\theta_D$ in eq. (32) is treated in a similar way.

- *to find* q'_D

$$\begin{bmatrix} I & -q_D A \\ -S & I \end{bmatrix} \begin{Bmatrix} F'_{aD} \\ \theta'_D \end{Bmatrix} + \begin{bmatrix} 0 & -(q_D A)' \\ -S' & 0 \end{bmatrix} \begin{Bmatrix} F_{aD} \\ \theta_D \end{Bmatrix} = 0 \tag{30}$$

- *obtain*

$$[F_{aL}^T, \theta_L^T] \begin{bmatrix} 0 & -(q_D A)' \\ -S' & 0 \end{bmatrix} \begin{Bmatrix} F_{aD} \\ \theta_D \end{Bmatrix} = 0 \tag{31}$$

or

$$q'_D = -\frac{q_D F_{aL}^T A' \theta_D + \theta_L^T S' F_{aD}}{F_{aL}^T A \theta_D} \tag{32}$$

- *to efficiently find* $S'F_{aD}$

$$S'F_{aD} = \frac{\partial}{\partial p}\left(\frac{\partial f_3}{\partial F_a}\right) F_{aD} \tag{33}$$

with

$$\frac{\partial f}{\partial X}(X_0)D = \lim_{\epsilon \to 0} \frac{1}{\epsilon}\left[f(X_0 + \epsilon D) - f(X_0)\right] = \lim_{\epsilon \to 0} \frac{d}{d\epsilon} f(X_0 + \epsilon D) \tag{34}$$

APPROXIMATE OPTIMIZATION PROBLEM

The optimization problem addressed in this paper is to minimize the structural weight W of the wing subject to aerodynamic, performance and structural constraints. It can be written as eq. (35), where g_1, g_2 and g_3 denote aerodynamic, performance, and structural constraints, respectively. The vector of circulation strengths Γ is calculated from eq. (1) and the nodal displacement vector, U, is calculated from eq. (5).

Even with the more efficient sensitivity analysis, a fully coupled structural-aerodynamic analysis and sensitivity is quite expensive. Thus, it is not feasible to optimize the design problem by directly connecting an optimization algorithm with the analysis procedure. Instead, a sequential approximate optimization algorithm is considered to be the best approach (e.g., Ref. 7). This approach replaces the original objective function and constraints with approximations based upon nominal values and derivatives at an initial point. Move limits are used to prevent the design from moving outside the bound of validity of the approximations.

The approximate optimization problem is based on a linear approximation of the aerodynamic and structural constraints about a candidate design point p_0. That is, the approximate constraints g_{1a} and g_{3a} are given in eq. (36), where $\Delta p = p - p_0$. The performance constraints are typically quite nonlinear and inexpensive to calculate, so they are calculated exactly from the linear approximation to the aerodynamic solution. The approximate optimization problem is given then in eq. (37), where E represents a vector of move limits imposed to guarantee the quality of the approximation.

- *optimization problem*

$$\begin{aligned} \textit{minimize} \quad W(p) \quad \textit{such that} \quad & g_1(\Gamma, p) \geq 0 \\ & g_2(\Gamma, \alpha, p) \geq 0 \\ & g_3(U, p) \geq 0 \end{aligned} \tag{35}$$

- *approximate constraints*

$$\begin{aligned} g_{1a}(p) &= g_1(p_0) + g_1'(p_0)\Delta p \\ g_{3a}(p) &= g_3(p_0) + g_3'(p_0)\Delta p \end{aligned} \tag{36}$$

- *approximate optimization problem*

$$\begin{aligned} \textit{minimize} \quad W(p) \quad \textit{such that} \quad & g_{1a}(p) \geq 0 \\ & g_2(\Gamma_a, \alpha_a, p) \geq 0 \\ & g_{3a}(p) \geq 0 \\ & \|\Delta p\| \leq E \end{aligned} \tag{37}$$

APPROXIMATE OPTIMIZATION PROCEDURE

The approximate optimization problem is solved sequentially as shown in the flowchart below, until the change in the design is smaller than a specified tolerance or the improvement in the objective function is smaller than another tolerance. After an optimum is found, a new approximation is constructed there, and the process is repeated until convergence is achieved. The optimizer used is the NEWSUMT-A program, Ref. 8, which is based on an extended interior penalty function procedure, and allows for various levels of constraint and objective function approximations.

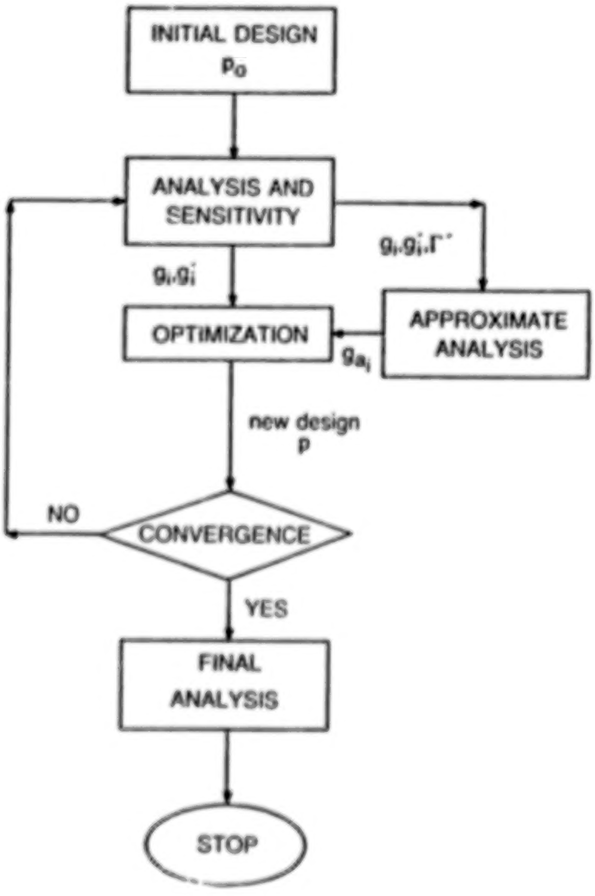

SENSITIVITY TIMING COMPARISONS

This figure presents a comparison of derivatives of vertical displacements and divergence dynamic pressure with respect to one structural design variable using the modular approach and the direct approach. We see that the values are very close.

For structural design variables, the modular approach is also shown to save 32% in CPU time. Larger savings are anticipated for aerodynamic variables, because these entail the more costly calculation of the aerodynamic influence coefficient matrix and its derivatives.

○ Sensitivity comparison of vertical displacements to skin thickness

modular approach	*direct approach*
9.2006574E-06	9.2006600E-06
-7.9199166E-06	-7.9186167E-06
-4.0682905E-06	-4.0674891E-06
-4.4964883E-06	-4.4956877E-06

○ Sensitivity comparison of divergence dynamic pressure to skin thickness

modular approach	*direct approach*
1.7295838E-03	1.7340794E-03

○ CPU comparison for 1 design variable

- *modular approach : 6.53 sec.*
- *direct approach : 9.59 sec.*

CONCLUDING REMARKS

This paper focused on the processes of simultaneous aerodynamic and structural wing design as a prototype for design integration. The research concentrated on the major difficulty associated with multidisciplinary design optimization processes, their enormous computational costs. Methods were presented for reducing this computational burden through the development of efficient methods for cross-sensitivity calculations and the implementation of approximate optimization procedures. Utilizing a *modular sensitivity analysis* approach, we showed that the sensitivities can be computed without the expensive calculation of the derivatives of the aerodynamic influence coefficient matrix, and the derivatives of the structural flexibility matrix. The same process was used to efficiently evaluate the sensitivities of the wing divergence constraint, which should be particularly useful, not only in problems of complete integrated aircraft design, but also in aeroelastic tailoring applications.

○ Modular approach applied to integrated design

○ Improved divergence sensitivity

○ Computational efficiency of the modular approach

ACKNOWLEDGMENT

The Virginia Polytechnic Institute portion of this research was funded by the NASA Langley Research Center under grant NAG-1-603 and by the National Science Foundation under grant DMC-8615336.

REFERENCES

1. Grossman, B., Strauch, G. J., Eppard, W. M., Gurdal, Z. and Haftka, R. T., "Integrated Aerodynamic-Structural Design of a Sailplane Wing", *AIAA Paper No. 86-2623*, Oct. 1986.
2. Haftka, R. T., Grossman, B., Eppard, W. M. and Kao, P. J., "Efficient Optimization of Integrated Aerodynamic-Structural Design", *Proceedings of 2nd Intl. Conf. on Inverse Design Concepts and Optimization in Engineering Sciences*, Oct. 1987, pp. 369-386.
3. Sobieszczanski-Sobieski, J., "On the Sensitivity of Complex, Internally Coupled Systems", *AIAA Paper No. 88-2378*, presented at the *AIAA/ ASME/ ASCE/ AHS 29th Structures, Structural Dynamics and Materials Conference*, Apr. 1988.
4. Steward, D. V., *Systems Analysis and Management*, P. B. I., publishers, 1981.
5. Bertin, J. J. and Smith, M. L., *Aerodynamics for Engineers*, Prentice Hall Inc., 1979.
6. Haftka, R. T. and Starnes, J. H. Jr., "WIDOWAC: Wing Design Optimization with Aeroelastic Constraints-Program Manual", *NASA TM X-3071*, 1974.
7. Schmit, L. A. and Farshi, B., "Some Approximation Concepts for Structural Synthesis", *AIAA J.*, **12**, 1974, pp. 692-699.
8. Grandhi, R. V., Thareja, R. and Haftka, R. T., "NEWSUMT-A: A General Purpose Program for Constrained Optimization Using Constraint Approximations", *ASME J. Mech., Trans. & Automation in Design*, **107**, 1985, pp. 94-99.

BLANK PAGE

STATIC AEROELASTIC ANALYSIS AND TAILORING OF MISSILE CONTROL FINS

S. C. McIntosh, Jr.
McIntosh Structural Dynamics, Inc.
Mountain View, California

M. F. E. Dillenius
Nielsen Engineering & Research, Inc.
Mountain View, California

PROBLEM DEFINITION

This paper describes a new concept for enhancing the design of control fins for supersonic tactical missiles. The concept makes use of aeroelastic tailoring to create fin designs (for given planforms) that limit the variations in hinge moments that can occur during maneuvers involving high load factors and high angles of attack. It combines supersonic nonlinear aerodynamic load calculations with finite-element structural modeling, static and dynamic structural analysis, and optimization.

The problem definition is illustrated in figure 1. The fin is at least partly made up of a composite material. The layup is fixed, and the orientations of the material principal axes are allowed to vary; these are the design variables. The objective is the magnitude of the difference between the chordwise location of the center of pressure and its desired location, calculated for a given flight condition. Three types of constraints can be imposed -- upper bounds on static displacements for a given set of load conditions, lower bounds on specified natural frequencies, and upper bounds on the critical flutter damping parameter at a given set of flight speeds and altitudes. The idea is to seek designs that reduce variations in hinge moments that would otherwise occur. The block diagram at the left in figure 1 describes the operation of the computer program that accomplishes these tasks. There is an option for a single analysis in addition to the optimization. Additional details concerning this work may be found in reference 1.

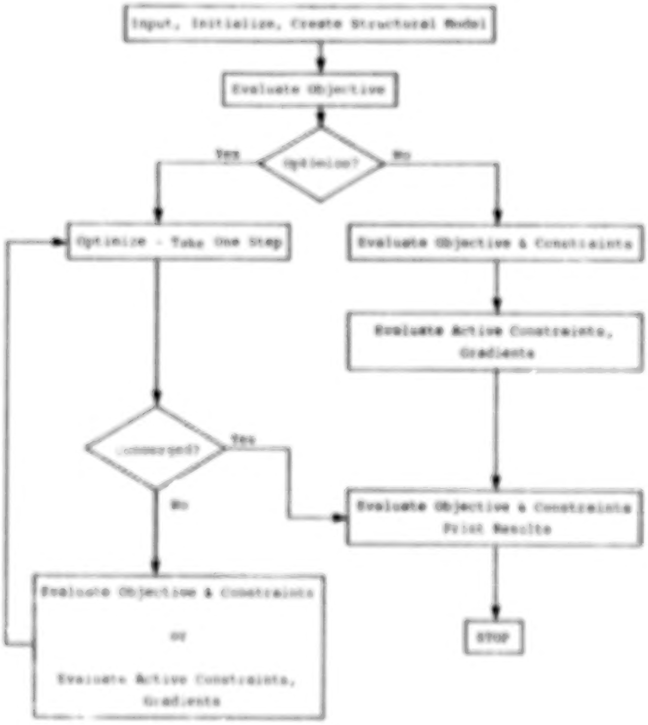
Input, Initialize, Create Structural Model
Evaluate Objective
Optimize?
Yes
No
Optimize - Take One Step
Evaluate Objective & Constraints
Evaluate Active Constraints, Gradients
Converged?
Yes
No
Evaluate Objective & Constraints Print Results
Evaluate Objective & Constraints
or
Evaluate Active Constraints, Gradients
STOP

- Objective: Dimensionless chordwise center of pressure offset from desired position, $|x_{cp}/\bar{x}_{cp} - 1.0|$, for a given flight condition.
- Design Variables: Material principal axis directions, θ_i, for a given stacking sequence.
- Constraints: Displacements, $z/\bar{z}_s - 1.0 \le 0$, for a given set of load conditions

  Frequencies, $1.0 - \omega_r/\bar{\omega}_r \le 0$

  Flutter Speeds, $g_r - \bar{g}_r \le 0$, at fixed speed and altitude.

Figure 1

STRUCTURAL MODEL

The example fin is illustrated in figure 2. It is made up of a graphite/epoxy composite with the stacking sequence as given in the figure. The fin is modeled with triangular bending elements. These are the elements described in reference 2, with modifications for anisotropic materials as given in reference 3. For each element, the orientation of the material principal axes with respect to the element local coordinate axes can be specified. For a given region of the fin, these angles can be specified so that a single angle variable governs the overall orientation. Two such regions, governed by design variables θ_1 and θ_2, are shown in the figure. The outer portion of the fin is inactive for tailoring purposes. The fin is anchored to a fixed node at the hinge line just inboard of the root by a beam-rod whose stiffness properties model the stiffness of the fin actuator and the body backup structure.

To update the design, the fin stiffness matrix for the active regions must be recreated. This is a relatively simple task, since the updating affects only the rotation matrices that transform the element constitutive matrices from principal axes to local coordinate axes. Gradients of the stiffness matrices are obtained analytically by differentiating the expressions for these matrices with respect to the orientation angles. Calculations for the constraints and their gradients follow well-known procedures and will not be discussed here. Reference 1 can be consulted for additional information.

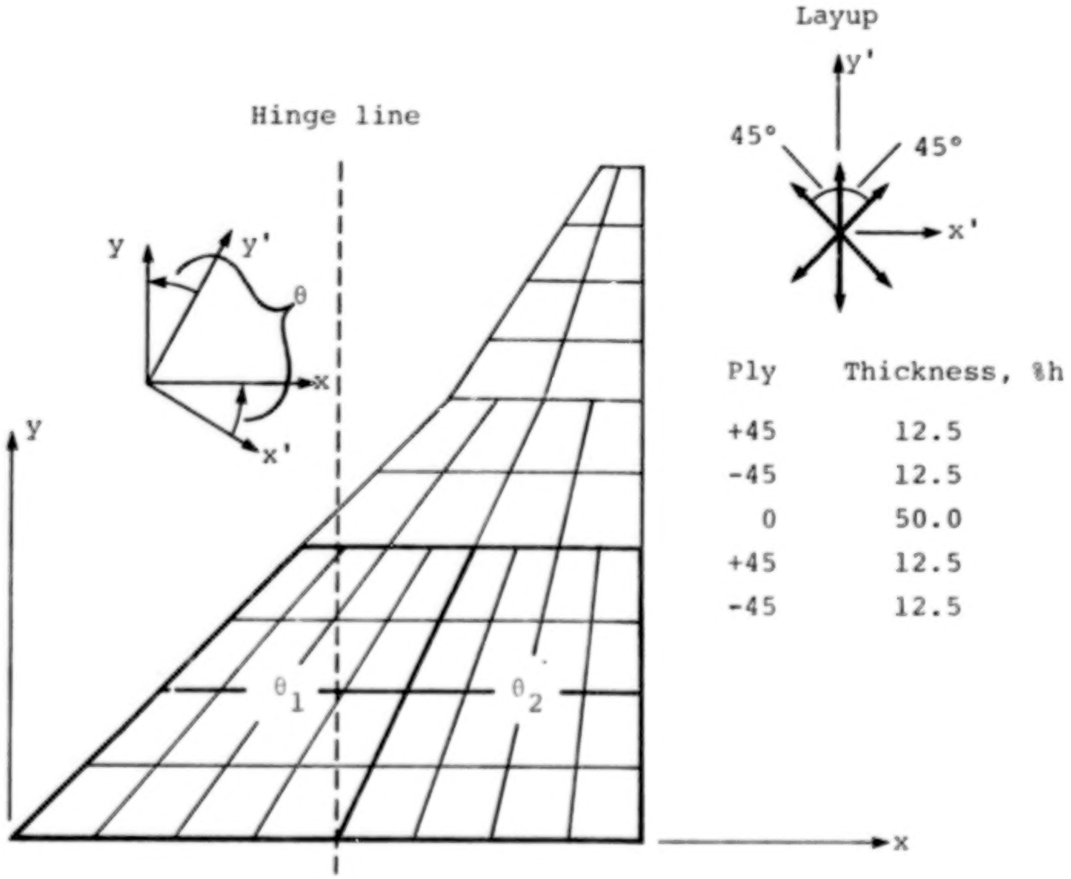

Ply	Thickness, %h
+45	12.5
-45	12.5
0	50.0
+45	12.5
-45	12.5

Figure 2

AERODYNAMIC LOAD CALCULATION

The aerodynamic load prediction method (ref. 4) applies to a fin attached to an axisymmetric body. The missile components are represented by distributions of singularities derived from supersonic linear theory. The missile body is modeled with linearly varying supersonic line sources and line doublets. In a finned section, the lifting surfaces and the body portion spanned by the lifting surfaces are modeled with planar supersonic lifting panels. Fin thickness effects can be represented, if desired, by planar source panels. The panel strengths are obtained by satisfying the flow tangency conditions at a set of control points, one for each panel. In addition, the fin loads include nonlinear augmentations due to fin leading and side edge flow separation at high angles of attack, and (for canard fins) nonlinear loads resulting from vortices formed on the forebody for the proper combination of forebody length and angle of attack. The tangency boundary condition satisfied on the fin includes the changes in streamwise slope caused by elastic fin deformation.

To compute the fin deformation, the aerodynamic loads at the control points are interpolated to loads at the structural node points in a scheme that preserves overall fin load and moments. Since the fin loads are in general nonlinear functions of fin deflection, an iterative process, described in detail in reference 1, is used to produce consistent fin deformations and loads. The resultant chordwise center of pressure location is then used to calculate the objective. Gradients of the objective are computed by finite differencing.

The static aerodynamic description of the example fin is given in figure 3. The following flight condition was assumed: An included angle of attack of 15.4 deg, a roll angle of 0.0 deg, a Mach number of 1.6, and an altitude of 30,000 ft. The fin is undeflected. A vertical plane of symmetry is assumed, and the body has an ogive nose up to the fin leading edge. No thickness or nonlinear effects are included in this model.

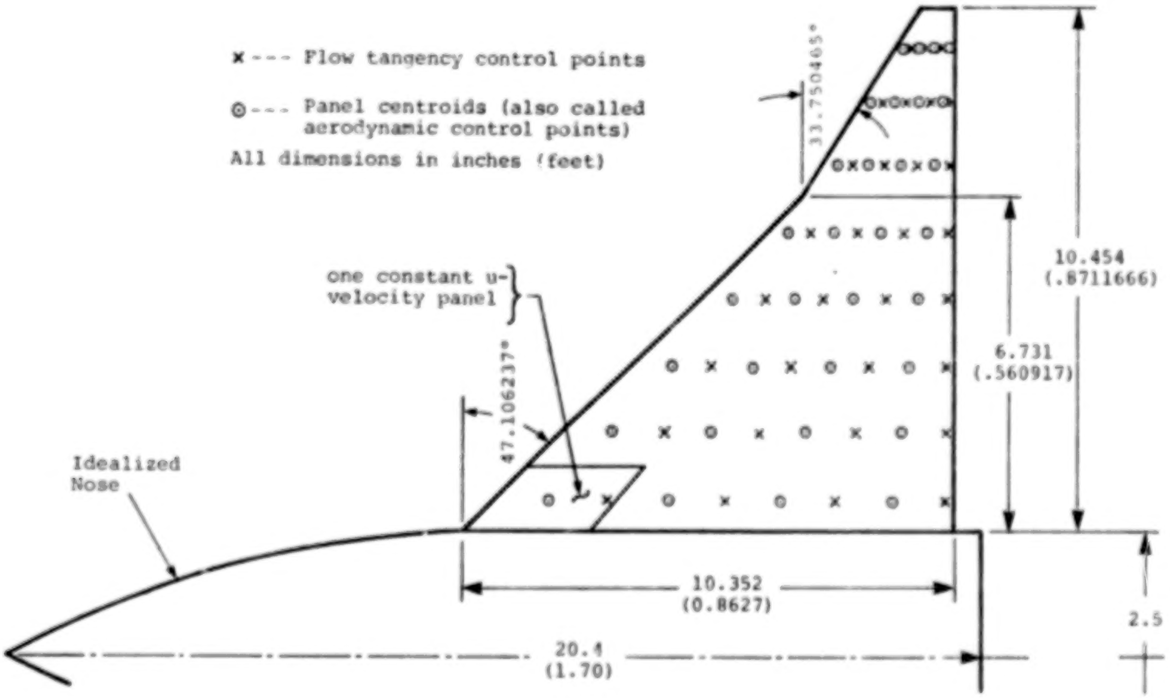
x --- Flow tangency control points
⊙ --- Panel centroids (also called aerodynamic control points)
All dimensions in inches (feet)
33.750465°
10.454
(.8711666)
one constant u-velocity panel
6.731
(.560917)
47.106237°
Idealized Nose
10.352
(0.8627)
2.5
20.4
(1.70)

Figure 3

FLUTTER CONSTRAINT

A flutter constraint was the only one considered in this example. The results of a flutter analysis at a Mach number of 1.4 are shown in figure 4, which presents a velocity-damping plot at a match-point altitude of 43,500 ft. Structural damping of 3% is assumed, so the match-point flutter speed is given by the g = 0.03 crossover of the first-mode branch. The flutter constraint requires that the damping parameter g for this branch be less than 0.03 at this speed and altitude.

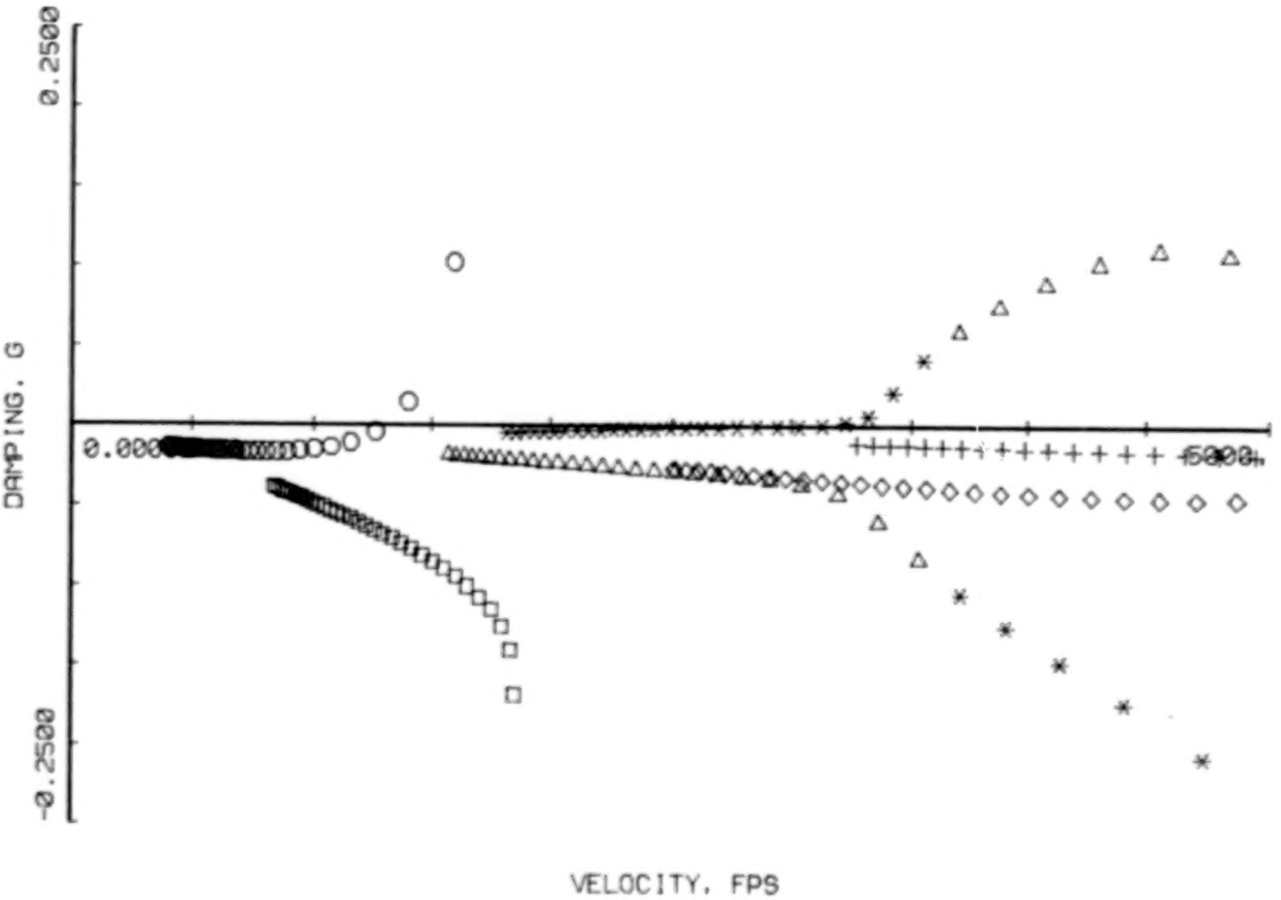

Figure 4

PARAMETRIC SURVEY

To provide some indication of the behavior of the fin as the principal-axis orientations are varied, the analysis-only option of the computer program was exercised. The angles θ_1 and θ_2 were linked to form a single design variable. Figure 5 displays the variation of x_{cp}. In view of the nature of the rotation matrix that transforms each element constitutive matrix from principal-axis to local coordinate directions (see Eq. (4) of ref. 1), the quasiharmonic nature of this variation is not surprising. The location of x_{cp} for the same fin made of aluminum is also shown.

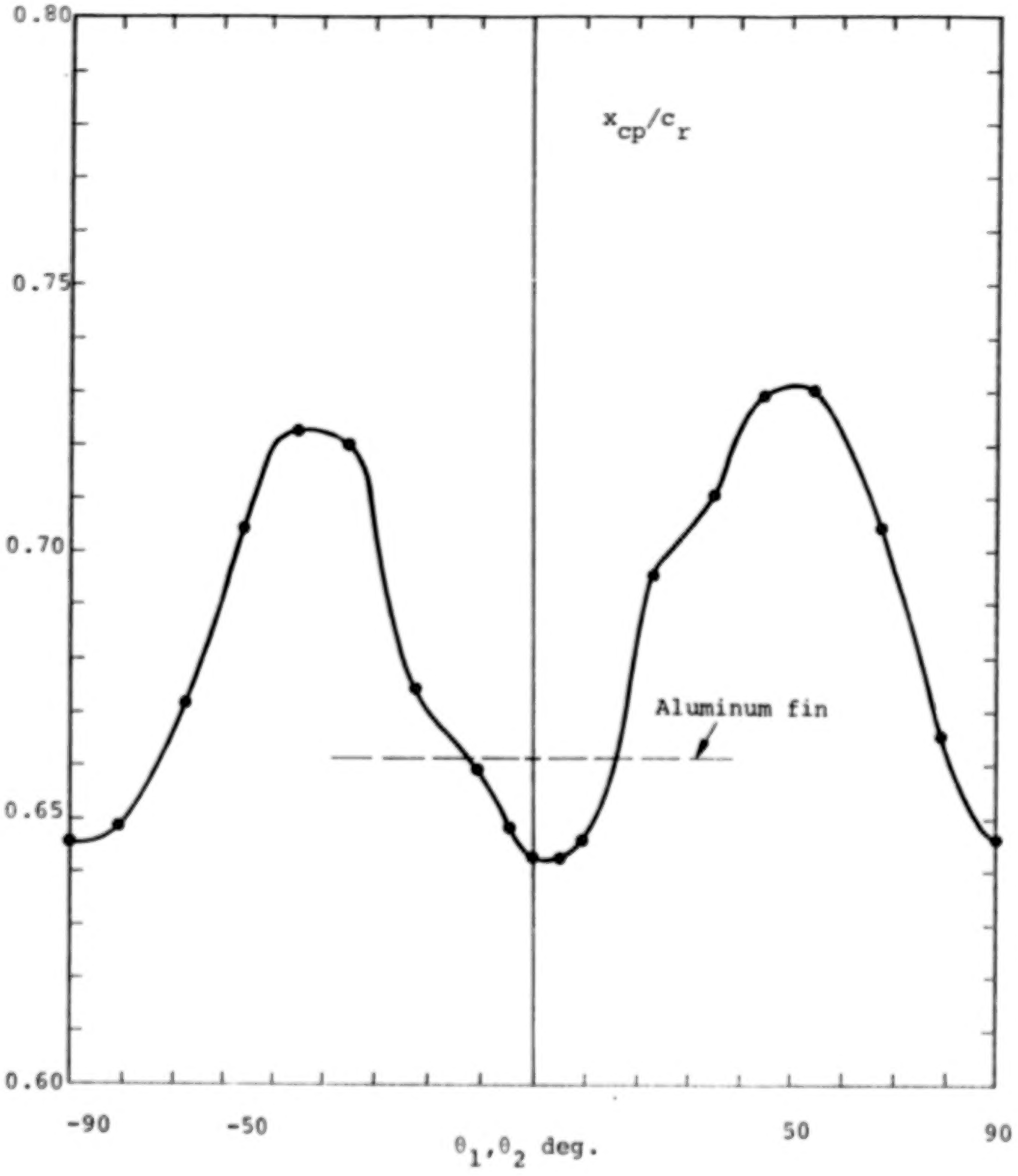

Figure 5 .

FIN DEFORMATIONS

Figure 6 presents perspective plots of the deformed fins for selected values of θ. The view in these figures is outboard in the x-y plane defined in figure 2, so the undeformed fin would be seen as a straight line. With θ near +45 deg or -45 deg, the chordwise flexibility is near maximum, which corresponds to the maximum shift in x_{cp}. Contrary to what might be expected, however, the fin chordwise bending is concave, rather than convex. This reduces the fin loading near the leading edge, so the center of pressure moves aft. Since the center of pressure is always aft of the hinge line, the fin also has a nose-down rigid-body rotation, which also appears in the plots.

When θ_1 and θ_2 are allowed to be independent, the curve in figure 5 becomes the intersection of the $\theta_1 = \theta_2$ plane with the x_{cp} surface. This surface was not mapped extensively, but enough analyses were performed to suggest that the surface resembles the shape of an egg carton, where the minima of figure 5 are the bottoms of valleys, and the maxima are the tops of peaks.

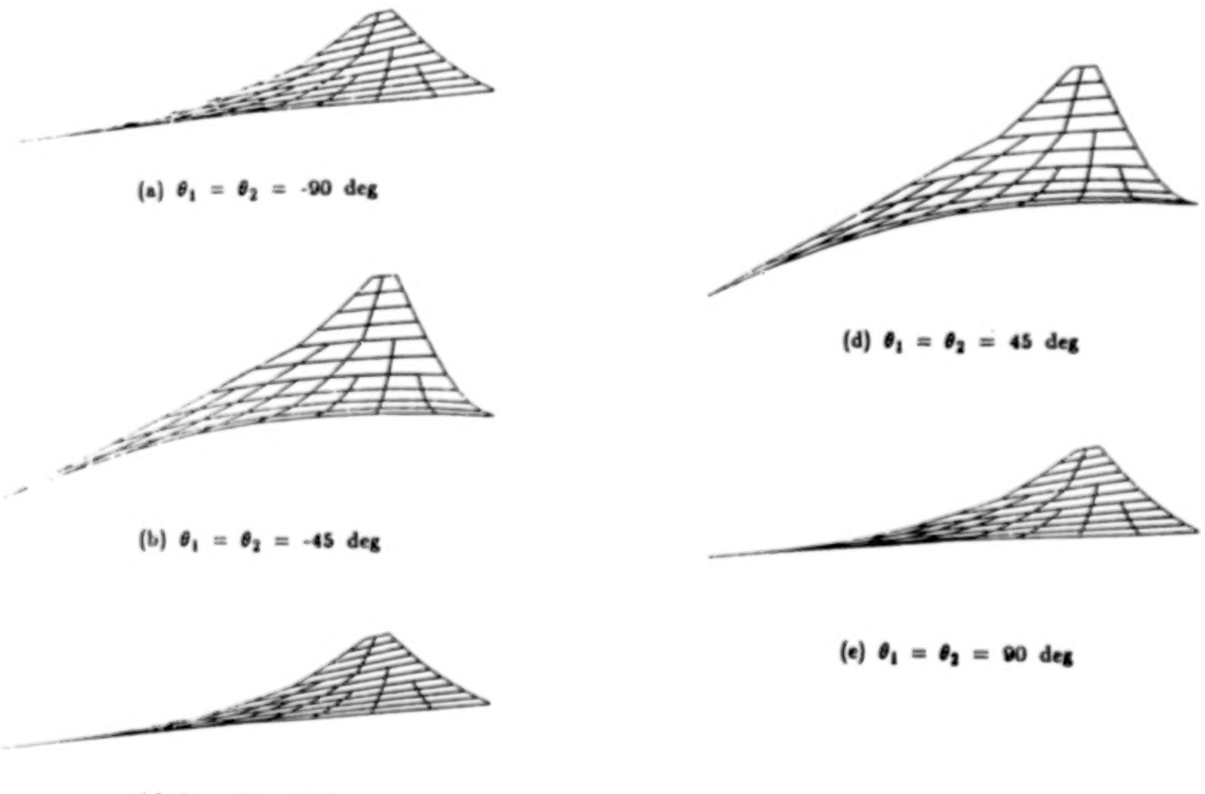

(a) $\theta_1 = \theta_2 = -90$ deg

(b) $\theta_1 = \theta_2 = -45$ deg

(c) $\theta_1 = \theta_2 = 0$ deg

(d) $\theta_1 = \theta_2 = 45$ deg

(e) $\theta_1 = \theta_2 = 90$ deg

Figure 6

OPTIMIZATION EXAMPLE 1

In the first optimization example, θ_1 and θ_2 were linked to form a single design variable. The desired value of x_{cp}, measured from the fin leading edge at the root, was set to 60% of the root chord c_r. The initial value of θ was 0.7 rad, or 40.1 deg. The flutter constraint, fixing the critical-mode crossover at a Mach number of 1.4 and an altitude of 43,500 ft, was also imposed. The iteration history for this example is shown in figure 7. In five iterations, the minimum at $\theta = 3.43$ deg was found. This corresponds very well with the curve of x_{cp} versus θ in figure 6. Attempts to reach the minimum near $\theta = 90$ deg were not successful because the flutter constraint was violated.

The optimization subroutine CONMIN (ref. 5) was used in all of the optimization examples.

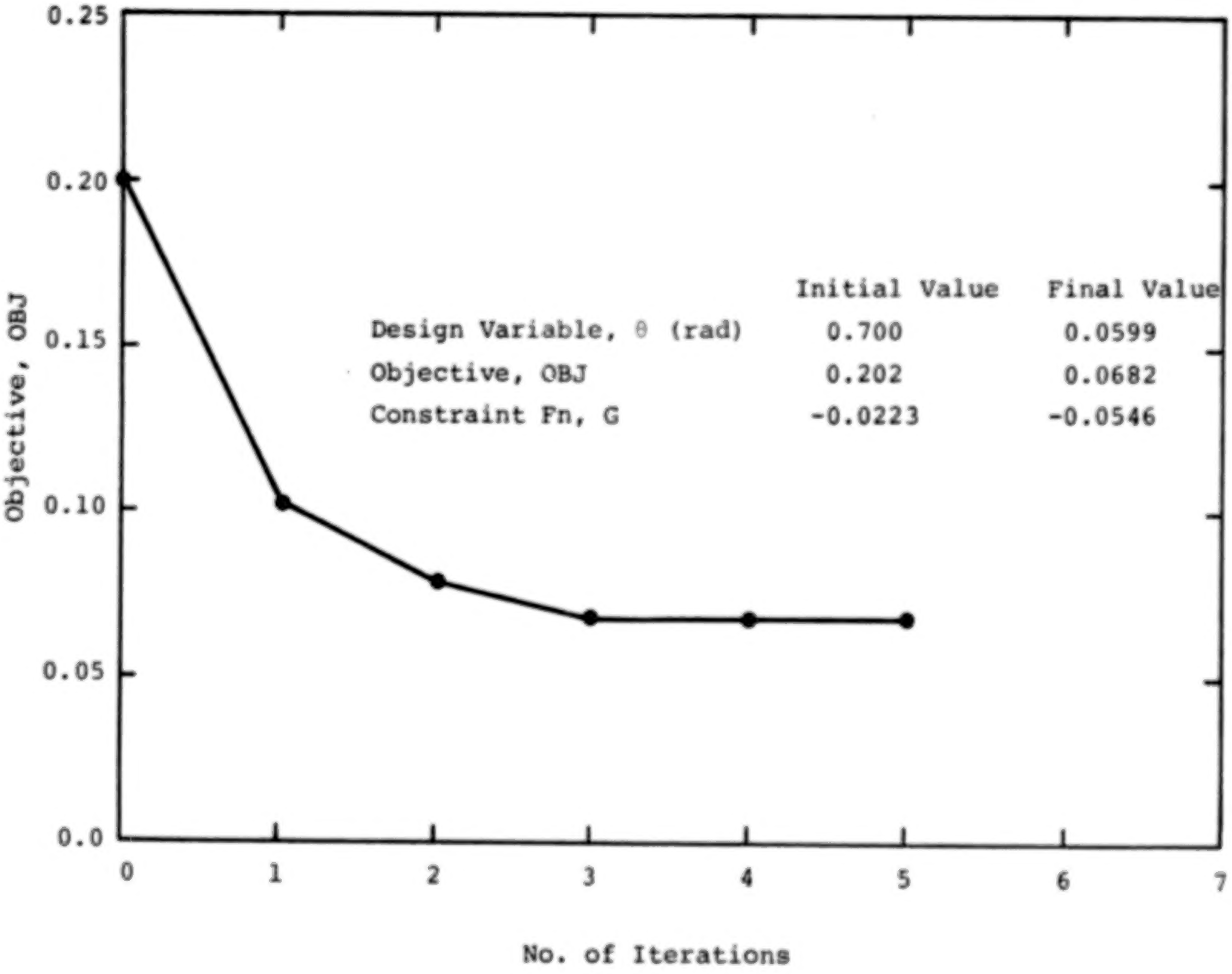

	Initial Value	Final Value
Design Variable, θ (rad)	0.700	0.0599
Objective, OBJ	0.202	0.0682
Constraint Fn, G	-0.0223	-0.0546

Figure 7

OPTIMIZATION EXAMPLE 2

An iteration history for the second optimization example is shown in figure 8. Here θ_1 and θ_2 were unlinked, and the flutter constraint was removed. The initial values of θ_1 and θ_2 were 0 deg and 45 deg, respectively. Convergence was achieved in five iterations with $\theta_1 = 0.334$ deg and $\theta_2 = 1.53$ deg. This is clearly the valley near the origin in design space suggested by figure 5.

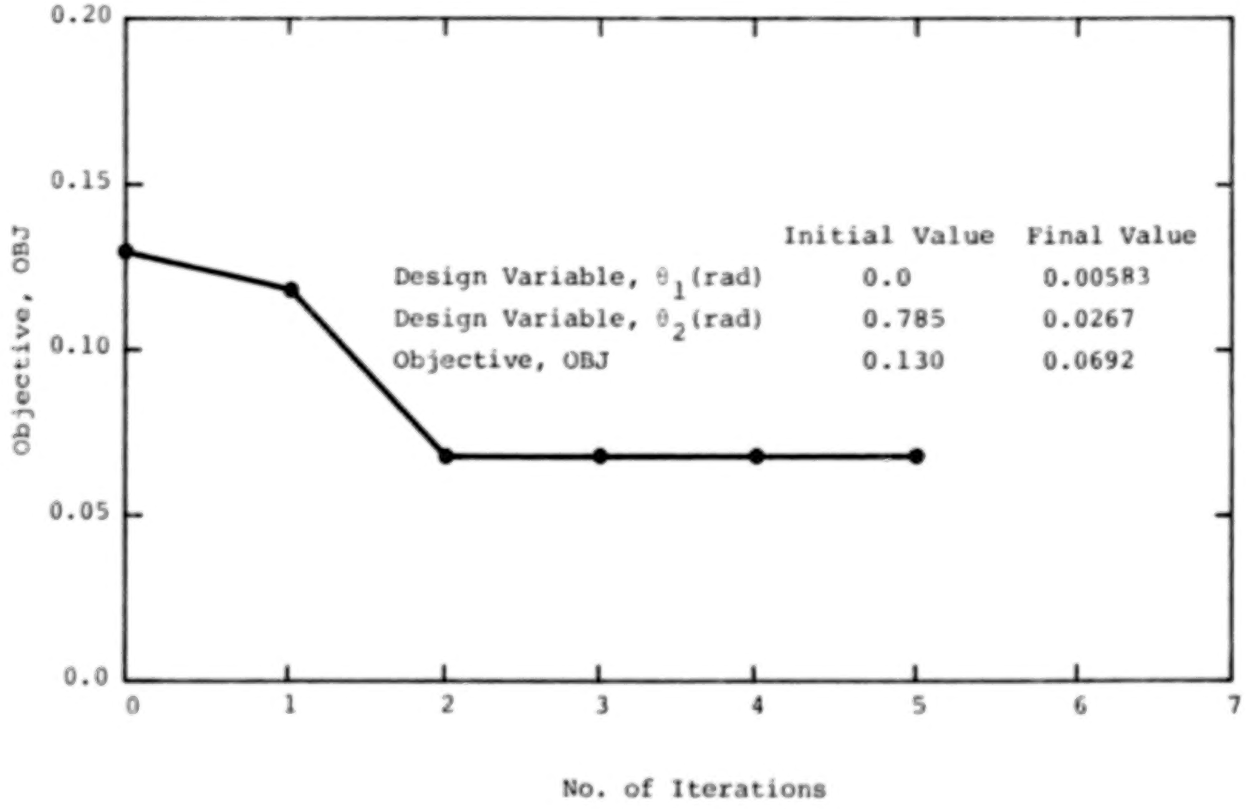

	Initial Value	Final Value
Design Variable, θ_1(rad)	0.0	0.00583
Design Variable, θ_2(rad)	0.785	0.0267
Objective, OBJ	0.130	0.0692

Figure 8

OPTIMIZATION EXAMPLE 3

The third optimization example is an attempt to find a neighboring valley in the design space. The starting point was at $\theta_1 = 10$ deg, $\theta_2 = 70$ deg, with no constraints other than side constraints on the design variables. The iteration history for this example is shown in figure 9. The minimum found here is at $\theta_1 = 2.20$ deg, $\theta_2 = 92.5$ deg, a neighboring valley with a minimum not quite as low as that near the origin.

Ironically, the best design -- the one with the most forward location of the center of pressure -- is the one initially chosen, with the "zero-deg" plies in the spanwise direction. From the standpoint of tailoring, this example is clearly not a very attractive one, since the movement of the center of pressure is not substantial. Different layups, and particularly those with more bending-twist coupling, would produce more appealing results.

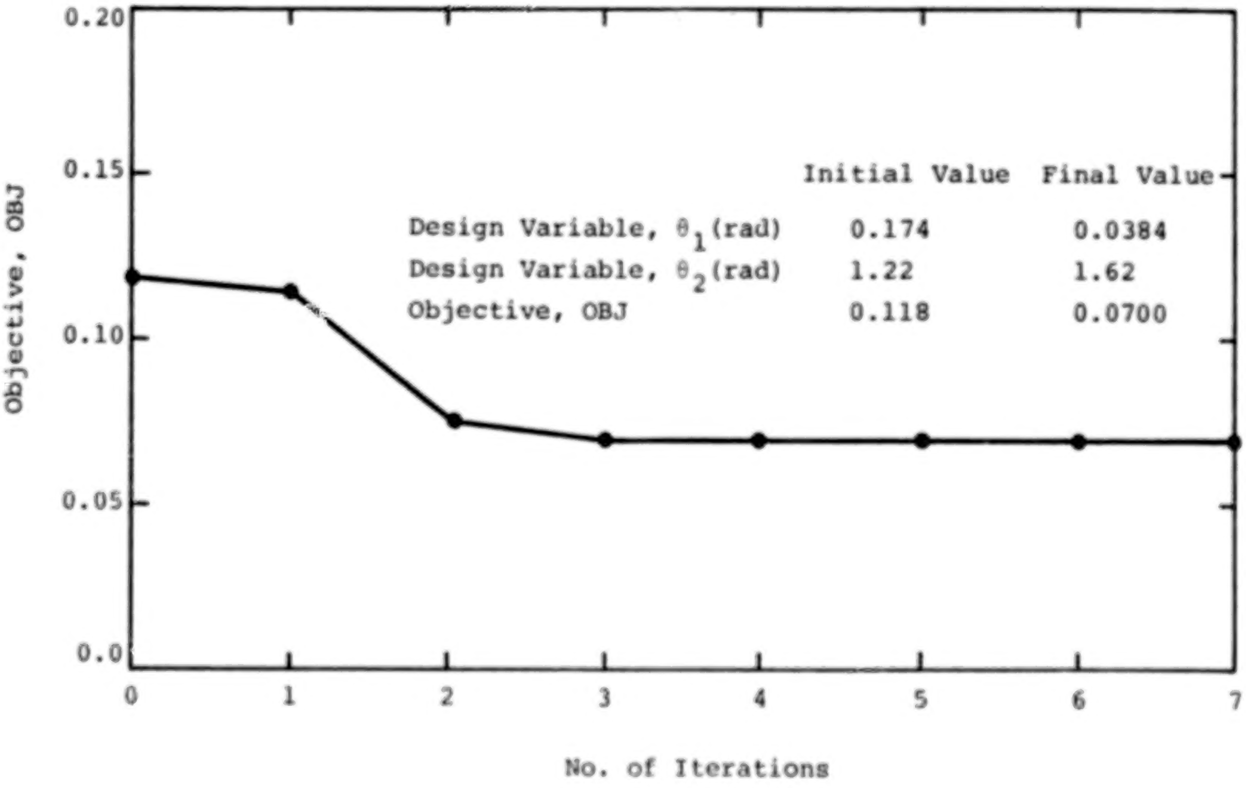

	Initial Value	Final Value
Design Variable, θ_1(rad)	0.174	0.0384
Design Variable, θ_2(rad)	1.22	1.62
Objective, OBJ	0.118	0.0700

Figure 9

REFERENCES

1. Dillenius, M. F. E. and McIntosh, S. C., Jr.: Aeroelastic Procedure for Controlling Hinge Moments. AIAA Paper 88-0528, presented at the AIAA 26th Aerospace Sciences Meeting (Reno, Nevada), January 1988.

2. Przemieniecki, J. S.: Theory of Matrix Structural Analysis. McGraw Hill, New York, 1968.

3. Zienkiewicz, O. C.: The Finite Element Method. McGraw-Hill (UK), London, 1977.

4. Dillenius, M. F. E.: Program LRCDM2, Improved Aerodynamics Prediction Program for Supersonic Canard-Tail Missiles with Axisymmetric Bodies. NASA CR-3883, April 1985.

5. Vanderplaats, G. N.: CONMIN - A Fortran Program for Constrained Function Minimization. User's Manual. NASA TM X-62,282, August 1973. Addendum, May 1978.

ACKNOWLEDGEMENTS

The work described in this paper was performed as a Phase I Small Business Innovation Research (SBIR) project sponsored under NAVAIR Contract N00019-86-C-0032 and is being continued as a Phase II SBIR project under NAVAIR Contract N00019-88-C-0071.

BLANK PAGE

EFFECTS OF NONLINEAR AERODYNAMICS AND STATIC AEROELASTICITY ON MISSION PERFORMANCE CALCULATIONS FOR A FIGHTER AIRCRAFT

Gary L. Giles
NASA Langley Research Center
Hampton, VA

Kenneth E. Tatum
Planning Research Corporation
Hampton, VA

Willard E. Foss, Jr.
NASA Langley Research Center
Hampton, VA

INTRODUCTION

During conceptual design studies of advanced aircraft, the usual practice is to use linear theory to calculate the aerodynamic characteristics of candidate rigid (nonflexible) geometric external shapes. Recent developments and improvements in computational methods, especially computational fluid dynamics (CFD), provide significantly improved capability to generate detailed analysis data for the use of all disciplines involved in the evaluation of a proposed aircraft design.

This paper describes a multidisciplinary application of such analysis methods to calculate the effects of nonlinear aerodynamics and static aeroelasticity on the mission performance of a fighter aircraft concept. The aircraft configuration selected for study was defined in a previous study using linear aerodynamics and rigid geometry. The results from the previous study are used as a basis of comparison for the data generated herein. Aerodynamic characteristics are calculated using two different nonlinear theories, potential flow and rotational (Euler) flow. The aerodynamic calculations are performed in an iterative procedure with an equivalent plate structural analysis method to obtain lift and drag data for a flexible (nonrigid) aircraft. **These static aeroelastic data are then used** in calculating the combat and mission performance characteristics of the aircraft. Comparisons are given between data obtained using conventional methods in the earlier study and the data obtained herein using more rigorous analytical methods.

- **Status**

  Aircraft conceptual design studies based on linear aerodynamic theory and rigid geometric shape

- **Objective**

  To calculate the effects of nonlinear aerodynamics and static aeroelasticity on the mission performance of a fighter aircraft concept

- **Outline**
  - **Configuration definition**
  - **Analytical tools and procedures**
  - **Static aeroelastic results**
  - **Mission performance results**

ARTIST'S CONCEPTION OF TVC AIRCRAFT

This study needed a configuration which would demonstrate the applicability of the methods to realistic geometries, e.g., a complete fighter aircraft. The aircraft chosen needed to provide some complexity without introducing difficulties which would detract from the research goals of the study.

A conceptual drawing of the aircraft selected is shown in the figure. The design incorporates many advanced technologies, including the concept of Thrust-Vector-Control (TVC). The TVC aircraft is a tailless, twin-engine vehicle utilizing multi-axis thrust vectoring for directional control and trim at supersonic speeds, both in cruise (Mach=2.0) and maneuver. The leading- and training-edge devices are intended for subsonic maneuver, take-off and landing.

The configuration is the result of conceptual design studies, and only limited experimental data for the aircraft exist, all for the rigid-body case. Experimental aerodynamic data for both the rigid and deformed shapes would be desirable for comparison with calculated data. The combination of a moderate-to-high wing loading for modern fighters and a relatively thin wing provided the potential for significant aeroelastic effects. Also, the use of thrust vectoring, instead of a horizontal tail, for trim and control eliminated the difficulties of analyzing multiple lifting surfaces, a problem inherent in many current production CFD codes. The simplicity of description coupled with potentially large physical effects made the TVC aircraft a desirable test-bed for the current study.

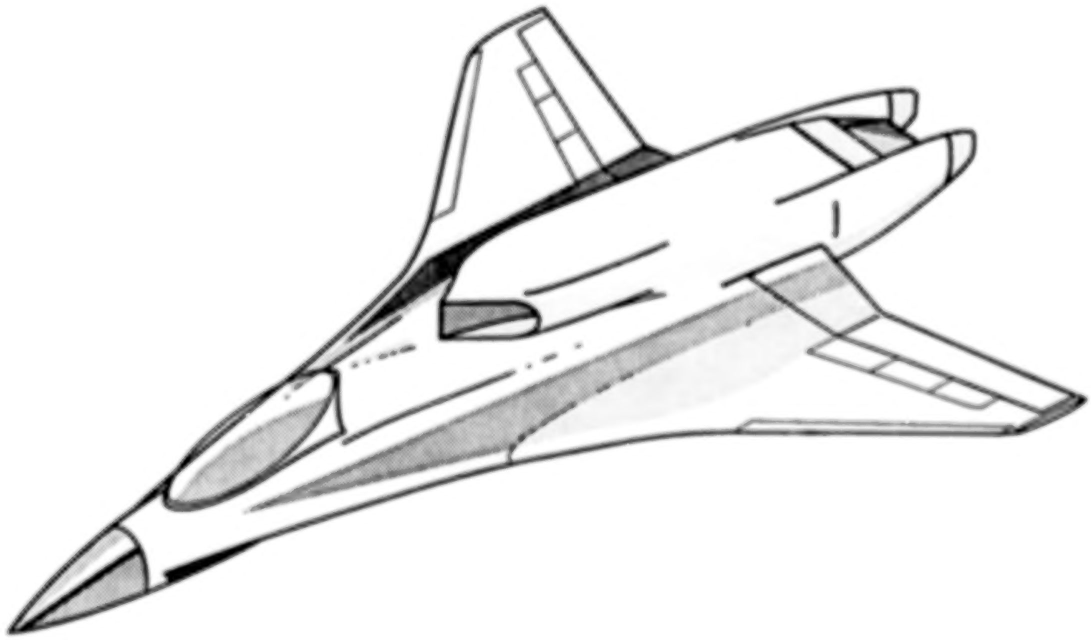

DISCRETIZED MODELS OF THE TVC AIRCRAFT

The TVC aircraft geometry is maintained at NASA Langley in a configuration geometry database which provides a standardized definition of the external geometry as shown at the top of the figure. The fuselage is defined by sets of points which describe the cross-section shapes at specified stations along the length of the fuselage. Lifting surfaces, such as wings, are defined by sets of points which describe airfoil cross sections at specified span locations. In the region of the wing-body intersection, the points on the fuselage are located to provide a smooth transition between the fuselage and wing.

The geometric input data required by the nonlinear aerodynamic analysis programs are illustrated at the bottom of the figure. Geometry data are interpolated from the database geometry at selected cross sections from the nose to the rear of the vehicle. A zero-thickness sheet is defined aft of the wing trailing edge and used for wake calculations. A geometry manipulation program, Ref.1, was used in conjunction with various splining techniques to generate the smooth planar cross-section cuts from the original wireframe definition. The same geometric definition is used for both nonlinear aerodynamic analysis programs used in this study. Note that the inlet geometry could not be represented exactly with the aerodynamic codes used in this study.

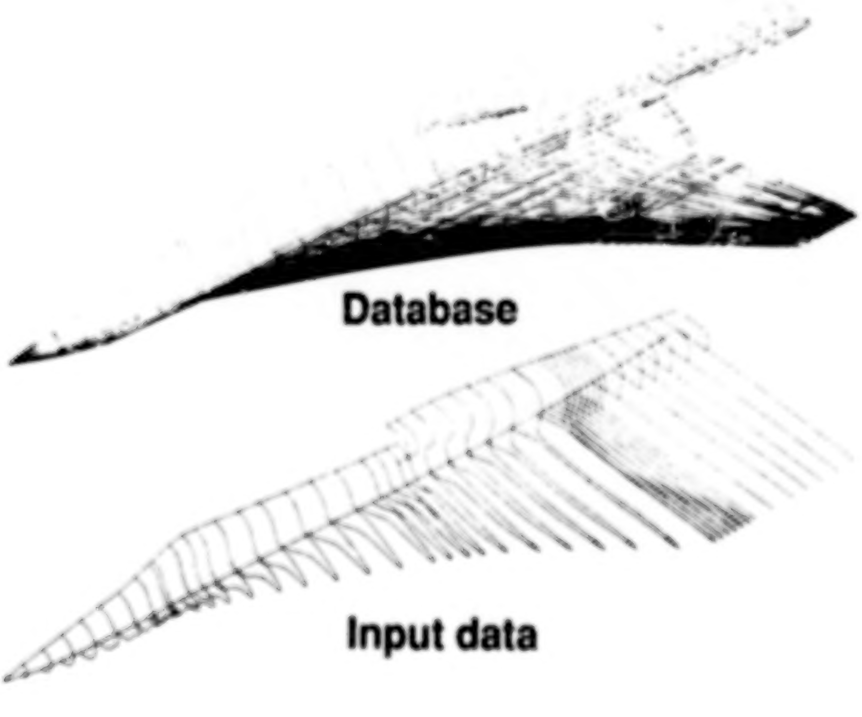

AERODYNAMIC ANALYSIS METHODS

The mission analyses in this study were based on force estimates from three different aerodynamic analysis tools. The baseline mission predictions utilized linear aerodynamic theories with the assumption that the drag is separable into components, e.g. skin friction, wave, etc. (Refs. 2 to 7). Using a "Mach-box" representation of the rigid wing, the induced drag was obtained from linear integral equations and an estimate of attainable leading-edge suction. Far-field wave drag was computed by the supersonic area rule.

In an effort to improve the force predictions, two nonlinear aerodynamic analysis methods were used. The first, SIMP (Ref. 8), solves the conservation-law form of the steady full potential equation by an implicit spatial marching technique. Finite differences are used to discretize the differential equation. The second code, EMTAC (Ref. 9), solves the unsteady Euler equations by a similar spatial marching technique. The discretization is by finite volume flux balancing. Both codes use the same geometry input and grid generation routines. The codes are capable of computing supersonic flow fields for complex geometries, including mass flow into inlets.

The Euler equations include fewer assumptions than the potential equations and, as such, are presumed to be more accurate. However, they also require more computer resources, as would be expected.

- **Linear theory**
  - **Wave drag: supersonic area rule**
  - **Drag-due-to-lift: integral equations**

- **Nonlinear full potential theory (SIMP)**
  - **Finite difference spatial marching**
  - **3D steady inviscid conservation law**

- **Euler theory (EMTAC)**
  - **Finite volume spatial marching**
  - **3D nonlinear inviscid equations**

STRUCTURAL ANALYSIS METHOD

The structural analysis method, Ref. 10, used for this study is implemented in a computer program referred to as ELAPS (Equivalent Laminated Plate Solution). This method requires only a small fraction of the volume of input data compared to a corresponding **finite-element** structural model. The resulting reduction in numerical model preparation is important during early stages of design where many candidate configurations are being assessed. The wing structure is represented as an equivalent plate in this formulation. The planform geometry of the structural box is defined by multiple trapezoidal segments as shown in the figure. A cross-sectional view of a typical segment is also shown. The wing depth, h, camber definition, zc, and cover skin thicknesses, t, are all defined in polynomial form over the planform of a segment.

The Ritz method is used to obtain an approximately stationary solution to the variational condition of the energy of the structure and applied loads. In this method, the wing deflection is assumed to be represented in polynomial form as given for the bending deflection by

$$W = C_{00}+C_{10}x^1+C_{20}x^2+C_{01}y^1+ \dots +C_{mn}x^m y^n \qquad (1)$$

The Ritz solution is used to determine the numerical values of the set of unknown coefficients, C_{mn}, which minimize the total energy. The solution, given in the form of Eq.(1), provides a continuous functional definition of the wing deflection over the planform. This continuous definition expedites the interface of the structural and aerodynamic calculations.

ELAPS - Equivalent Laminated Plate Solution

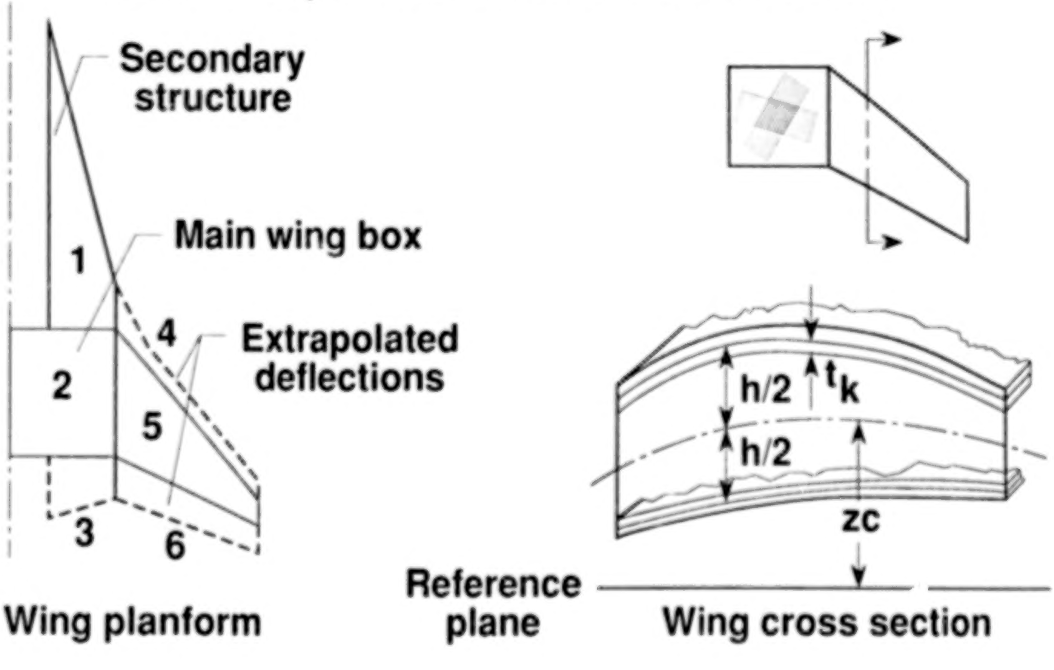

MISSION ANALYSIS METHOD

A computer program which calculates the mission radius and maneuverability characteristics of combat aircraft, Ref. 11, is used in this study. This program has been used at the Langley Research Center to assess mission performance of proposed configurations and to indicate associated research programs which would be expected to yield the most beneficial improvements, Ref. 12. The program can be used (1) in an analysis mode to determine the performance characteristics of a given configuration or (2) in a sizing mode to determine the configuration size in terms of takeoff gross weight, wing loading, and thrust-to-weight ratio that best meets all the mission performance constraints. Only the analysis mode is used in this study.

A variety of military missions can be specified by using a desired combination of modules to calculate performance data for take-off, climb, cruise, loiter, dash, combat, descent, reserves, and landing segments of a mission profile. The definition of the aircraft is given in terms of propulsion system characteristics, aerodynamic characteristics, along with size and weight of the vehicle. The propulsion characteristics are precomputed, usually from data supplied by an engine manufacturer. The aerodynamic characteristics are represented in terms of lift and drag coefficients as functions of aircraft angle of attack and flight Mach number. The size of the aircraft is defined in terms of the wing area, the size and number of engines, and the take-off gross weight.

- **Program used at Langley Research Center to calculate mission radius and maneuverability characteristics of military aircraft**
- **Flight segments used**

Takeoff	**Climb**	**Cruise**
Loiter	**Dash**	**Combat**
Descent	**Reserves**	**Landing**

- **Inputs to program**
  - **Propulsion**
    (engine decks)
  - **Aerodynamics**
    (C_L and C_D vs. α and M)
  - **Aircraft size**
    (wing area, takeoff gross weight)

COMPUTING ENVIRONMENT

This study is typical of multidisciplinary analysis/design efforts in that several existing computer programs are used with each program being operated by a disciplinary specialist. The computer programs used in this study resided on several different computers as indicated on the figure. No attempt was made to convert all programs to reside on a single machine. Instead, procedures were set up to accommodate communication of data between the various machines and programs. The required interfaces between the programs were written so as to minimize the volume of data that was transmitted between computers.

The size and location of the computers used included a MicroVAX II on an engineer's desktop, the CYBER 800 series computers at the NASA Langley central computer site, and the more powerful CYBER 205 and CRAY 2 required by the nonlinear aerodynamic programs. The CRAY 2 is part of the NAS computer complex located at NASA-Ames.

Computer program	Computer	Operating system
GEOM	CYBER 800 series	NOS
Middleton-Carlson	CYBER 800 series	NOS
Harris wave drag	CYBER 800 series	NOS
SIMP	CYBER 205	VSOS
EMTAC	CRAY 2	UNICOS
ELAPS	MicroVAX II	VMS
Mission analysis	CYBER 800 series	NOS

TVC MISSION DEFINITION

The primary mission for the TVC is one of **high-altitude** interdiction. The aircraft was designed to cruise at Mach 2 with a radius of 500 nautical miles. A payload of 2900 lbs. is expended at the radius station. Combat requirements are for one and a half sustained turns at Mach 2 at an altitude of 40,000 ft. with an ultimate maneuver criteria of **8.1 g load factor.** The mission performance calculations used the following fuel allowances. The takeoff fuel allowance is taken to be the fuel required to operate the engines for one-half minute at the maximum augmented thrust level and then for one minute at the maximum non-augmented thrust level. Fuel allowance for combat is the amount required to meet the combat requirements given above. The reserve fuel allowance is the fuel required to loiter for 20 minutes at sea level.

The majority of the mission is performed with the aircraft at Mach 2 cruising conditions (outbound and inbound). Combat conditions occur for a small percentage of time. The relative time spent in each of these conditions has a considerable impact on the performance results presented later.

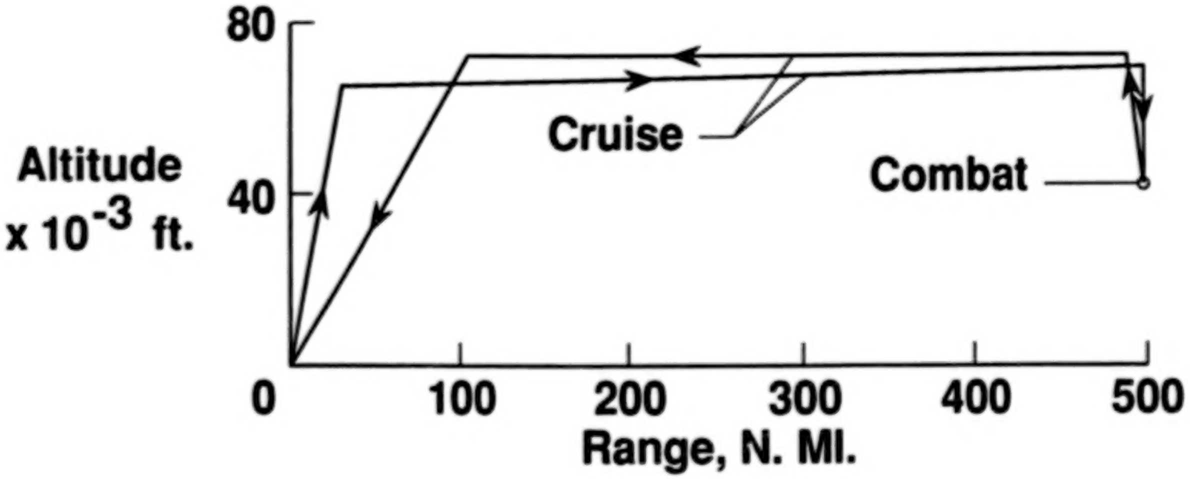

- **Cruise Mach number = 2.0**
- **Payload = 2900 lbs; expended at radius station**
- **Combat is for 1 1/2 turns at max. sustained turn rate at Mach number = 2.0 and altitude = 40 000 ft**

FLEXIBLE WING AERO/STRUCTURAL ANALYSIS PROCEDURE

A flow chart of the iterative procedure to arrive at the aeroelastically deformed shape of a wing at a specified flight condition is shown in the figure. A detailed discussion of the original development of this procedure is given in reference 13. The process is initiated with the geometric shape determined during the conceptual design studies taken to be the shape of the flexible aircraft at cruise. This baseline shape is analyzed at cruise to yield the jig (fabrication) shape, and at maneuver for an initial estimate of the elastic maneuver loads. Application of these maneuver loads to the jig shape produces an initial approximation to to the elastic maneuver shape. Iteration proceeds by computing loads on the current maneuver shape approximation and applying these loads to the jig shape. At each aerodynamic load analysis the maneuver lift is maintained by adjusting the aircraft angle of attack. Convergence is achieved when the calculated air loads are consistent with the structural deflection from the jig shape. The converged aerodynamic characteristics are then used in mission analysis calculations.

The continuous definition of the deformed wing shape used in ELAPS expedites the interface between the aerodynamics and structures programs. An equivalent load vector corresponding to the number of unknown displacement function coefficients, Eq. 1, is required for analysis of the equivalent plate structure. This load vector is formed by integrating the product of the aerodynamic pressure and displacement function terms over each portion of the aerodynamic grid on the wing surface. In the structures-to-aero interface, these continuous, analytic definitions of displacements are evaluated at each point of the aerodynamic input geometry and used directly to generate a deformed configuration.

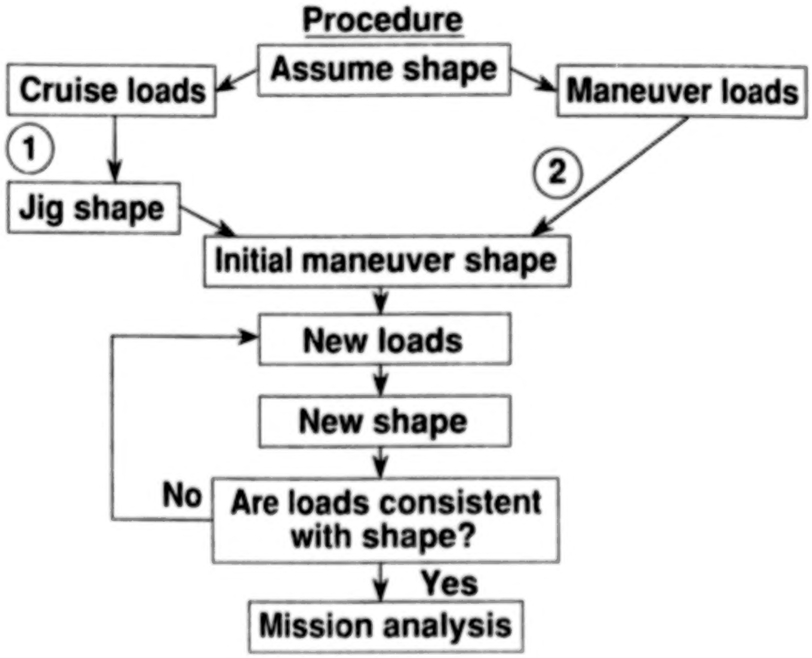

CONVERGED STRUCTURAL DISPLACEMENTS

During this design study, the thickness distribution of the wing cover skins was sized initially using loads on the rigid cruise shape at the 8.1g load factor. The deflection, calculated in the aeroelastic analysis, of this first structural model, herein referred to as wing 1, caused an inboard shift of the aerodynamic pressures and a corresponding reduction in stress levels in the cover skins. The thickness of the wing skins was then resized using the 8.1g aeroelastic loads. This wing with resized (reduced thickness) skins is referred to as wing 2.

A reduction in aircraft weight, as a result of going from wing 1 to wing 2, is not included in subsequent performance calculations. The aircraft weight was estimated using weight equations which inherently include the effect of reduced structural loads resulting from aeroelastic deformation.

The converged structural deformations at 8.1g load factor for wing 2 as computed by SIMP/ELAPS are shown in the figure. The maximum deflection (measured from the baseline cruise geometry) was 20.01 inches at the wing tip trailing edge. The loading caused the wing to twist 6.08 degrees, leading edge down. Similar results were obtained by EMTAC/ELAPS with the maximum deflection increasing to 21.37 inches.

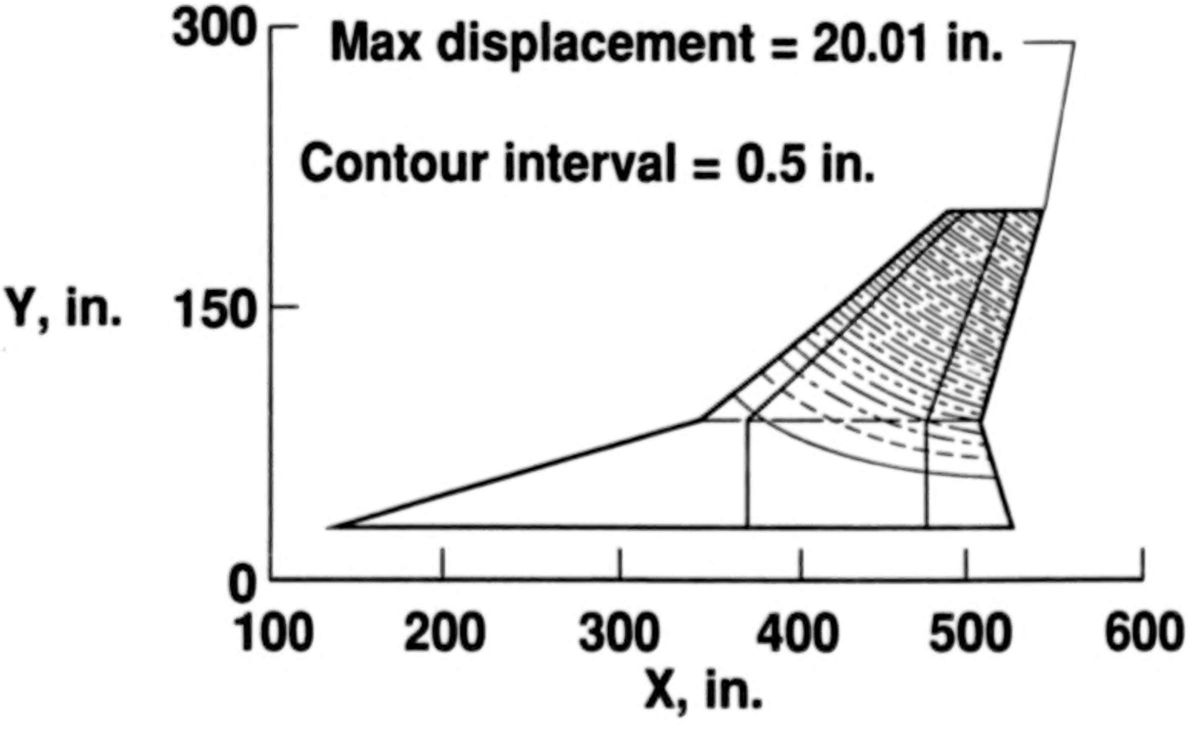

AERODYNAMIC CROSS-PLANE GRID

The level of detail of the analytical representation used in the solution of the aerodynamic flow equations is illustrated in this figure. A representative cross-plane grid at a specific body station is shown for one of the deformed wing geometries computed by SIMP. Both SIMP and EMTAC employ streamwise marching schemes to integrate the flow equations on successive planes, such as the one shown. A conical flow similarity solution is generated to start the calculation on a plane near the nose of the aircraft, which is assumed to be sharp, thereby allowing an attached bow shock wave. This starting solution defines the incoming flow for the next plane a small step downstream. By repetitively stepping (marching) from one plane to the next, the entire length of the body is traversed. On each plane a two-dimensional grid is constructed about the body cross-section, as shown, and a numerical difference approximation to the flow equations is solved for the dependent variables(s), which for EMTAC are the density, velocity components, and internal energy. Pressure can then be directly computed from these quantities using the ideal gas law. In SIMP the velocity components are computed by numerically differentiating the velocity potential. Pressure and density are then computed by the ideal gas law and the Bernoulli equation. Thus, at each longitudinal station down the body surface, the flow variables, such as pressure, are computed at discrete locations on the body surface and off the surface in the flow field.

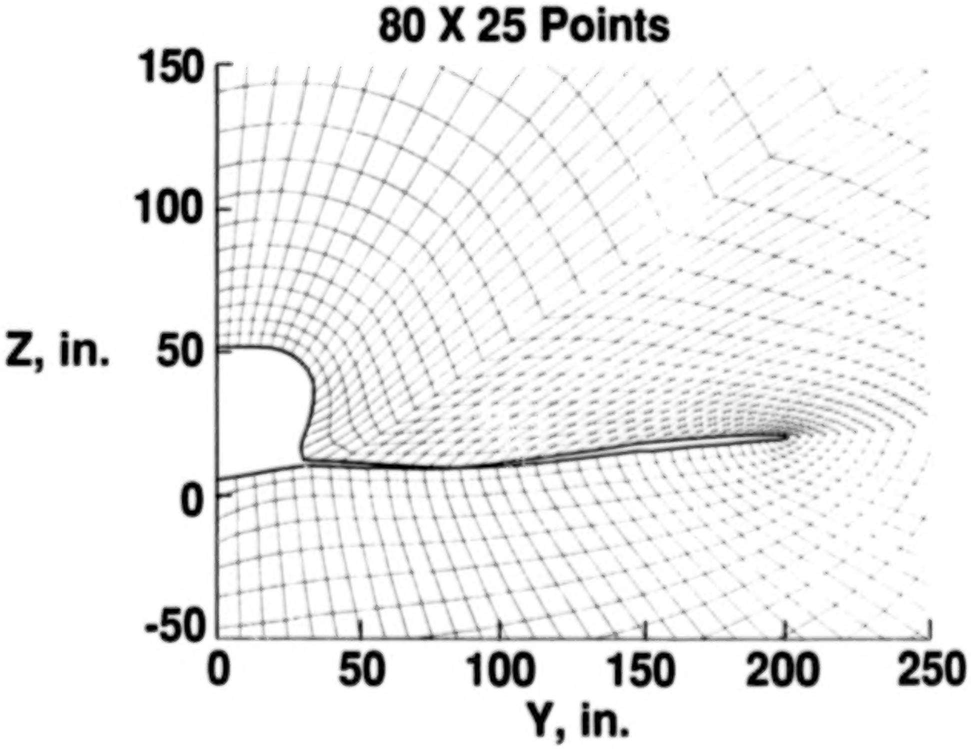

DETAILS OF THE AERODYNAMIC FLOW FIELDS

By using grids such as the one shown in the previous figure, the nonlinear aerodynamic codes provide a high degree of resolution of the flow fields about the aircraft. The contour plots of cross-plane pressure shown in this figure are representative of the detail attainable with SIMP and EMTAC. Such plots allow the calculated loads/pressures to be interpreted in light of the physics being modeled by the differential equations. For example, an upper-surface cross-flow shock wave is predicted by SIMP, evident in the concentration of isobars near Y=100. However, EMTAC does not indicate a shock impinging on the wing. Such localized differences in the flow field contribute to differences in the overall load distributions and resulting deflections in the aeroelastic calculations. While each aerodynamic code gave substantially different computed flow features (i.e. shocks, expansions, etc.), the overall character of each of these flow fields did not change significantly during the aeroelastic iterations with a given aerodynamics code. Even at the high maneuver conditions (8.1g's) where large structural deflections were computed, the overall character of the flow fields did not change, however the relative magnitudes or strengths of the aerodynamic pressures were affected by the deflections.

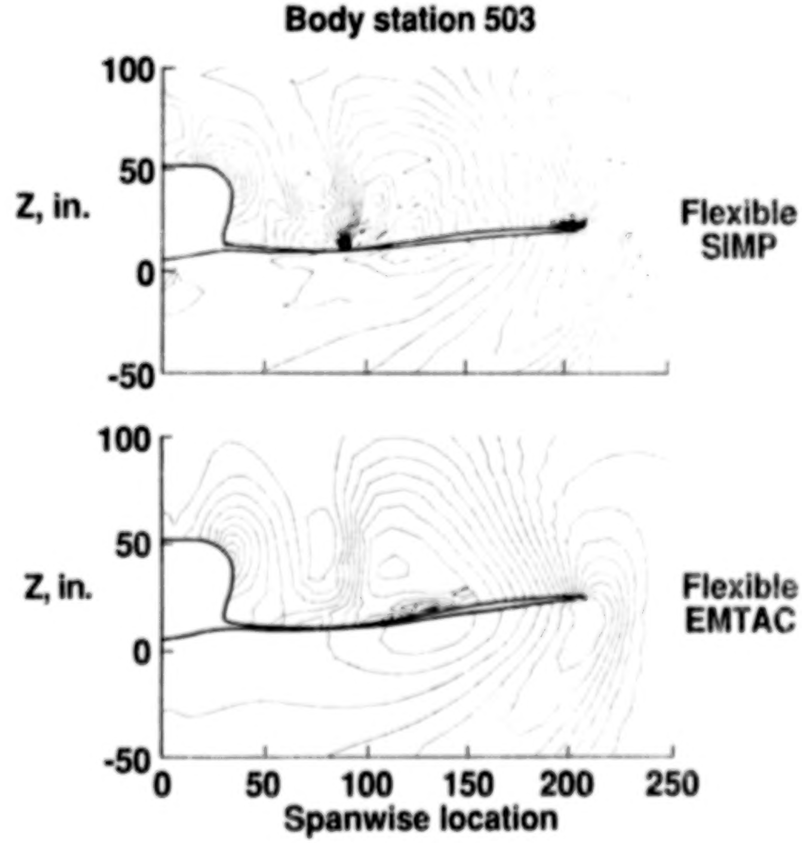

COMPARISON OF SPANWISE PRESSURE DISTRIBUTIONS

The aerodynamics and structural analysis codes were coupled through the aerodynamic loads as represented by pressure coefficient distributions over the wing surface. Representative spanwise pressure variations are shown in this figure as computed by SIMP and EMTAC at specific axial (body) stations. Two of these distributions are for the baseline rigid geometry while the third is for the aeroelastically deformed solution as computed by EMTAC/ELAPS. Each plot is part of the overall solution at a vehicle lift coefficient of approximately 0.361, however the section lift coefficient at each body station changes due to axial shifts of the load distribution produced by different aerodynamic theories and from the aeroelastic deformations.

A significant feature of these distributions is the unloading of the outboard wing region due to the static aeroelastic deformation. Also significant is the more physically realistic loading computed by EMTAC as opposed to SIMP in the region of the wing tip. At the high lift conditions required for **maneuver, the assumption of potential theory is questionable,** and, while this study has shown usable results from a potential flow code, indications are that the more complete theory, represented by the Euler equations, provides more reliable results.

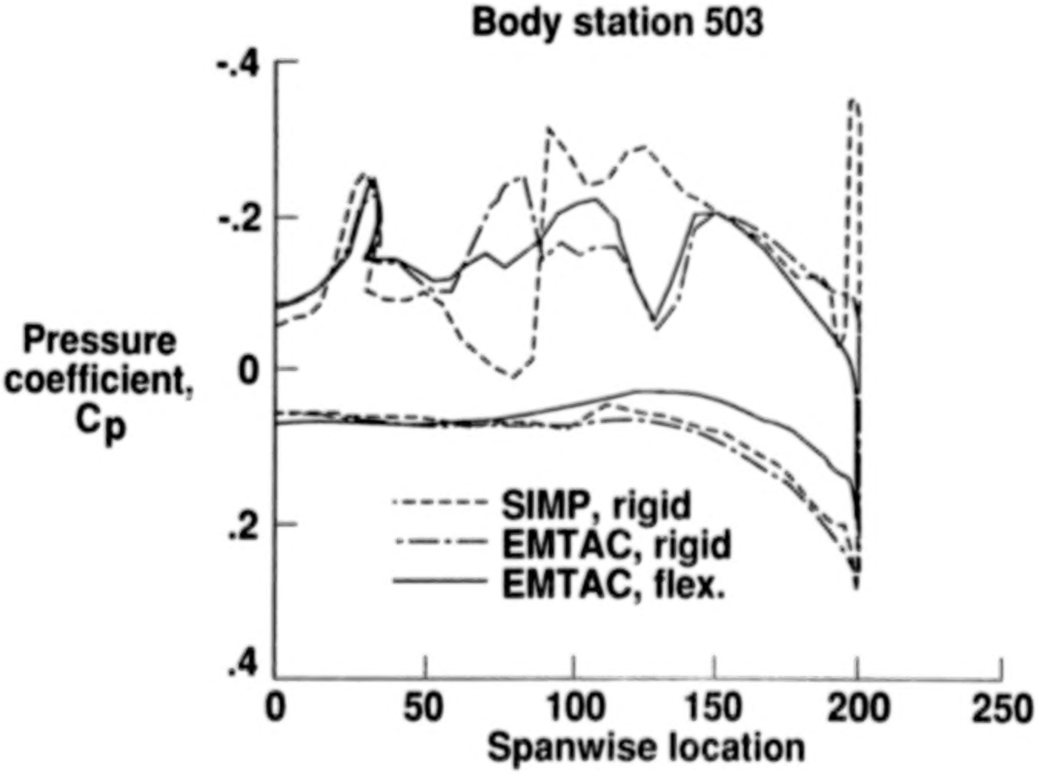

FORCE PREDICTIONS FOR THE TVC AIRCRAFT

As the pressure distributions are key quantities in the static aeroelastic computations, the integrated pressures in the forms of drag and lift are key quantities in performance calculations. The solid curve shown in the figure is the drag polar computed by the baseline linear aerodynamic theory, including the induced drag (often referred to as drag-due-to-lift) and the wave drag, assumed to be a constant at a given Mach number. Selected nonlinear aerodynamic calculations are shown by the symbols for both rigid and flexible geometries. At low lift coefficients, the difference in results between nonlinear aerodynamic theories, including the effects of static aeroelasticity, is negligible and single symbols are shown to indicate the drag increment predicted by nonlinear theory. At higher lifts, however, the differences are noticeable with progressively higher drag predicted by SIMP and EMTAC, with rigid and flexible geometries. In particular, for the case of a flexible wing, the drag coefficient from aeroelastic calculations using EMTAC (Euler theory) is about 0.0025 greater than that calculated using SIMP (Full potential theory).

Note that while the linear theory assumes separable wave and induced drag, the nonlinear theories include both of these components in the calculation of a single drag value.

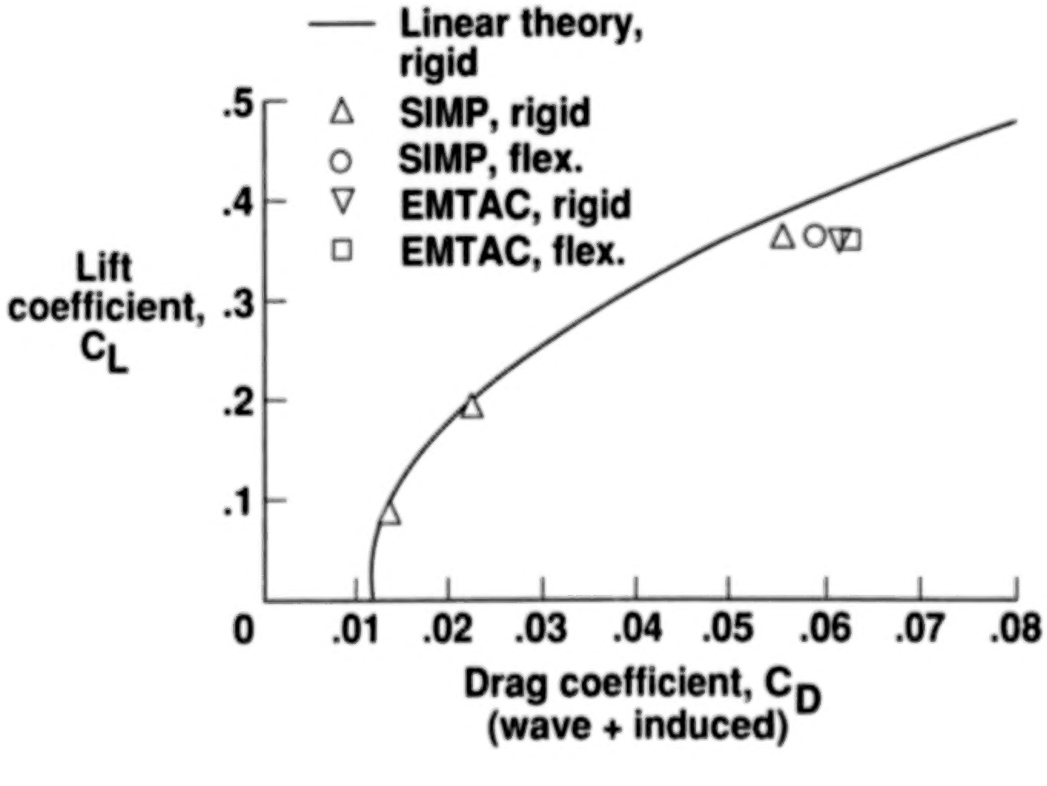

AERODYNAMIC DATA FOR PERFORMANCE ANALYSIS

The required aerodynamic input to the mission analysis program consists of the lift, drag, and angle of attack variations for the specified mission. These three variables are related as shown in the figure for the baseline linear theory prediction and the SIMP and EMTAC predictions for the rigid and flexible geometries. The angle of attack is an input to SIMP and EMTAC and the C_L is computed from the integrated pressures. The C_D shown includes the estimated skin friction and roughness drag. These latter two components were identical to those used in the original linear theory calculations. An analysis code solving the Navier-Stokes (viscous) equations would couple these effects with the wave and induced drag components and eliminate this approximation.

The curves shown for the nonlinear rigid/flexible cases were derived by curve fitting the values obtained from a limited set of computations since this was a research project, not an aircraft development project. Basic assumptions for the curve-fits were: 1.) the nonlinear predictions converged to the same values at low lift, and 2.) both the C_L/alpha and C_L/C_D curves were of second order. As might be expected, the linear predictions are the most optimistic and include nonlinear theory and/or static aeroelasticity results in degradation of the available lift and increase in predicted drag.

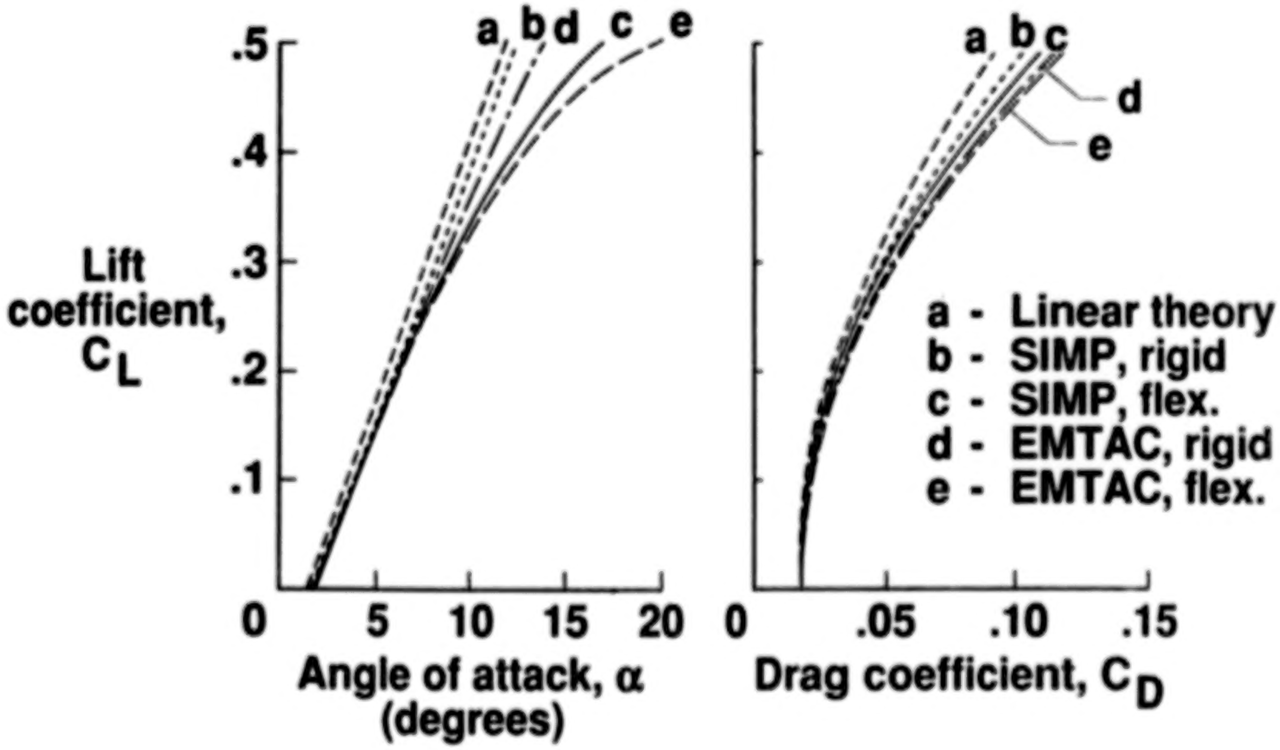

COMBAT PERFORMANCE OF THE TVC AIRCRAFT

The effect of nonlinear aerodynamics and static aeroelasticity on the combat performance of the TVC aircraft is indicated on the figure. The specific power, P_s, is a measure of the energy maneuverability of an aircraft for combat. This parameter is a direct function of the difference between the thrust and the drag. The load factor for maximum sustained turning occurs where the specific power is equal to zero. At a greater load factor, the specific power is negative and the aircraft is not able to sustain the flight condition. The increased drag levels of the nonlinear aerodynamic and the non-rigid structural considerations result in lower sustained load factors and associated turn rates. The decrease in load factor is from a value of 8.1g's to about 7.1g's. In addition to the loss in maneuvering capability, the amount of fuel used during combat is increased from 1000 lbs. to 1143 lbs. Consequently, the fuel available to cruise is reduced and as a result the mission radius capability is reduced.

As indicated, using the different nonlinear aerodynamic theories result in the largest reduction in calculated combat performance, with aeroelasticity contributing a somewhat smaller increment. Consideration of aeroelasticity often has a significant effect on maximum roll rate characteristics of a fighter aircraft, Refs. 14 and 15. However, the roll rate characteristics of the TVC aircraft were not calculated in this study.

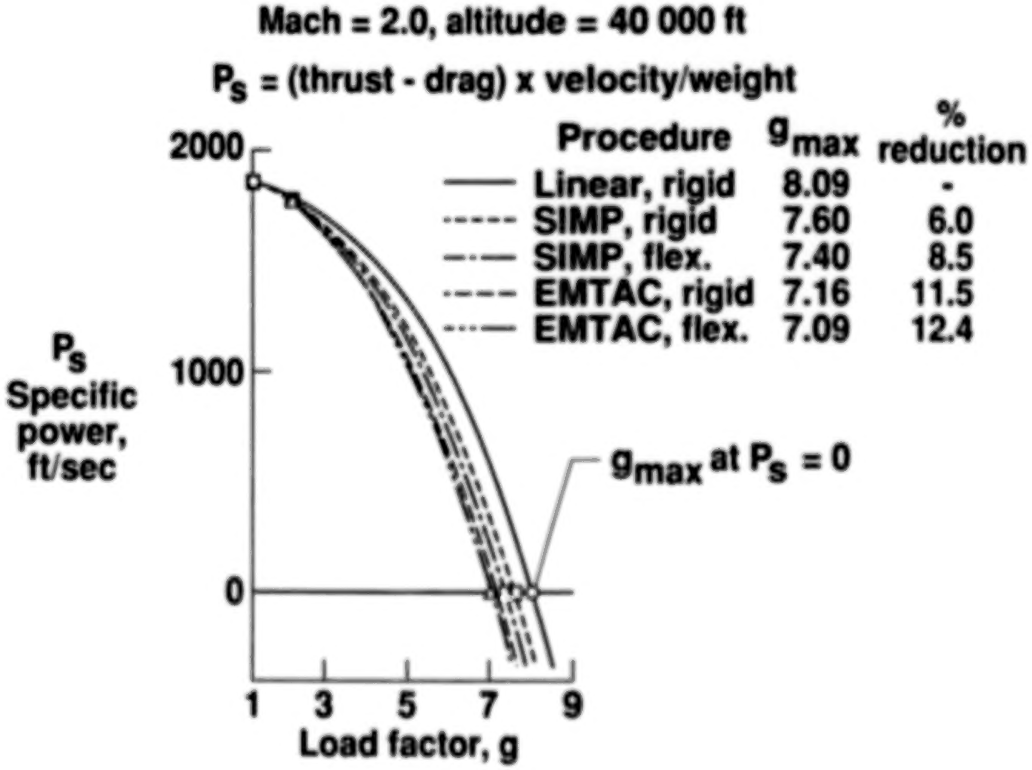

MISSION PERFORMANCE OF THE TVC AIRCRAFT

The increased drag levels estimated for the nonlinear aerodynamics and for the flexible structural considerations result in mission radius losses of up to 68 N.Mi. Approximately 75 percent of each of the losses is due to the reduced cruise efficiency as a direct result to the increased drag estimates given by the nonlinear codes. The remaining 25 percent of each of the losses is due to the reduction in available cruise fuel associated with the increased combat fuel allowance.

As would be expected for this particular mission, the effect of aeroelasticity on aircraft range is minimal. However, for a mission in which a large percentage of total time is spent in combat conditions, including the effects of aeroelasticity in design and analysis could become important.

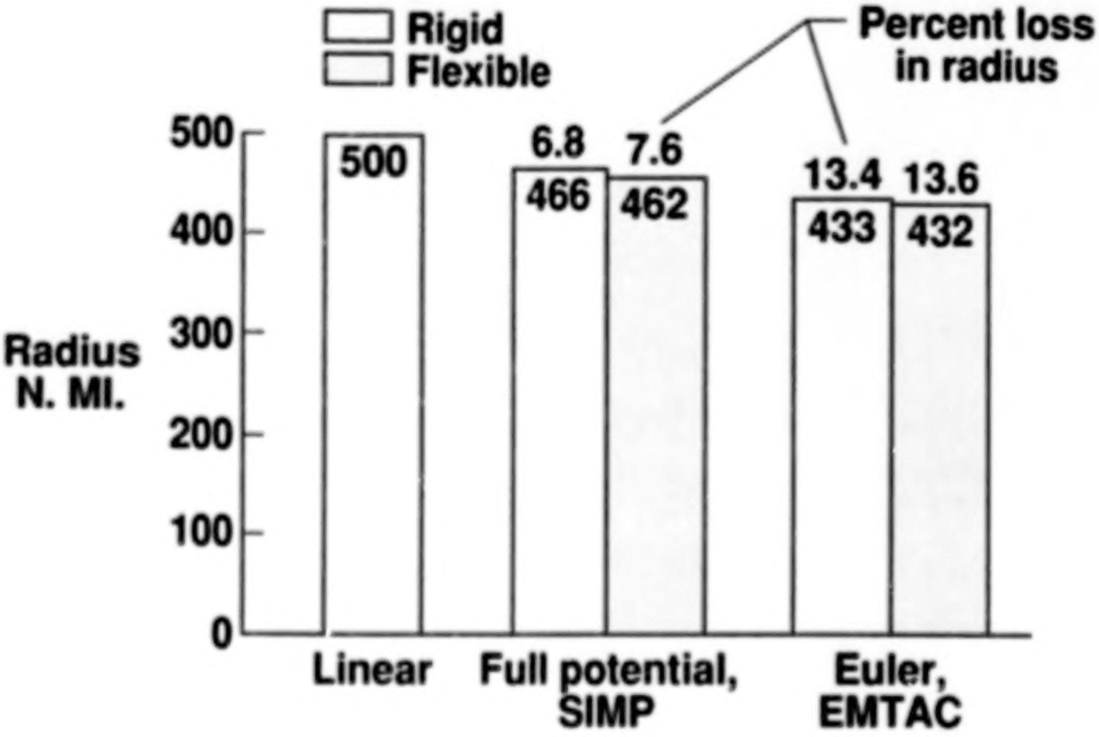

CONCLUDING REMARKS

A multidisciplinary analysis procedure has been developed that includes aerodynamic, structural and performance calculations. Use of this procedure is demonstrated by analyzing the effects of nonlinear aerodynamics and static aeroelasticity on the performance of a TVC fighter aircraft. Representation of the wing structure as an equivalent plate allows aeroelasticity considerations to be included early in the design process before a finite element model is available. In addition, the continuous definition of the wing deformation permits the interface to the aerodynamics programs to be written in a simple but general manner. Two programs, one based on full potential theory and the other based on Euler theory, were incorporated to provide a comparison of the effect on the calculated aerodynamic characteristics. There were significant differences in the pressure fields and the Euler theory predicted higher overall drag than full potential theory.

The aircraft performance was affected primarily by aerodynamic theory rather than aeroelastic effects. The combined effect gave a maximum loss in sustained load factor of 12% and a mission radius loss of 14% compared with linear aerodynamic calculations on a rigid aircraft. The cost-effectiveness of using these more rigorous analytical procedures for preliminary design must be determined by individual design organizations. As is demonstrated, this procedure provides the capability to provide refined design data. However, the potential for these data to provide improvements in the final aircraft design must be assessed in view of the practical limitations imposed by budget and calendar time for a particular project

- **Multidisciplinary analysis procedure developed that includes aerodynamic, structural, and performance calculations**
- **Equivalent plate structural representation expedites aeroelastic calculations**
- **Significant differences in pressure fields with improvements in aerodynamic modeling (linear, full potential, Euler)**
- **Performance affected primarily by aerodynamic theory; maximum sustained load factor loss = 12%
mission radius loss = 14%**
- **Cost-effectiveness of procedure decided by user**

REFERENCES

1. Hall, J. F.; Neuhart, D. H.; and Walkley, K. B.: An Interactive Graphics Program for Manipulation and Display of Panel Method Geometry. NASA CR 166098, March 1983.

2. Sommer, S. C.; and Short, B. J.: Free-Flight Measurements of Turbulent-Boundary-Layer Skin Friction in the Presence of Severe Aerodynamic Heating at Mach Numbers from 2.8 to 7.0. NACA TN 3391, 1955.

3. Harris, R. V., Jr.: An Analysis and Correlation of Aircraft Wave Drag. NASA TM X-947, 1964.

4. Carlson, H. W.; and Middleton, W. D.: A Numerical Method for the Design of Camber Surfaces of Supersonic Wings With Arbitrary Planforms. NASA TN D-2341, 1964.

5. Sorrells, R. B.; and Miller, D. S.: Numerical Method for Design of Minimum-Drag Supersonic Wing Camber With Constraints on Pitching Moment and Surface Deformation. NASA TN D-7097, 1972.

6. Carlson, H. W.; and Miller, D. S.: Numerical Methods for the Design and Analysis of Wings at Supersonic Speeds. NASA TN D-7713, 1974.

7. Middleton, W. D.; and Lundry, J. L.: A System for Aerodynamic Design and Analysis of Supersonic Aircraft. NASA CR 3351-3354, 1980.

8. Shankar, V.; Szema, K-Y; and Bonner, E.: Full Potential Methods for Analysis/Design of Complex Aerospace Configurations. NASA CR 3982, May 1986.

9. Szema, K-Y; Chakravarthy, S.; and Shankar, V.: Supersonic Flow Computations Over Aerospace Configurations Using an Euler Marching Solver. NASA CR 4085, July 1987.

10. Giles, G. L.: Further Generalization of an Equivalent Plate Representation for Aircraft Structural Analysis. NASA TM 89105, February 1987.

11. Foss, W. E., Jr.: A Computer Technique for Detailed Analysis of Mission Radius and Maneuverability Characteristics of Fighter Aircraft. NASA TP 1837, March 1981.

12. Coen, P. G.; and Foss, W. E., Jr.: Computer Sizing of Fighter Aircraft. NASA TM 86351, January 1985.

13. Tatum, K. E.; and Giles, G. L.: Integrating Nonlinear Aerodynamic and Structural Analysis for a Fighter Configuration. AIAA Paper No. 87-2863. Presented at the 1987 AIAA/AHS/ASEE Aircraft Design, Systems and Operations Meeting, St. Louis, Missouri, Sept. 14-16, 1987.

14. Static Aeroelasticity in Combat Aircraft. AGARD Report No. 725, January 1986.

15. Static Aeroelastic Effects on High Performance Aircraft. AGARD Conference Proceedings No. 403, July 1987.

OPTIMUM STRUCTURAL DESIGN WITH STATIC AEROELASTIC CONSTRAINTS

K. B. Bowman[1], **R. V. Grandhi**[2], **and F. E. Eastep**[3]

---

[1] Aerospace Engineer, Air Force Wright Aeronautical Lab.*, WPAFB, Ohio

[2] Assistant Professor, Mechanical Systems Engineering, Wright State University, Dayton, Ohio

[3] Professor, Aerospace Engineering, University of Dayton, Dayton, Ohio

* Now the Wright Research Development Center

INTRODUCTION

In this paper, the static aeroelastic performance characteristics, divergence velocity, control effectiveness and lift effectiveness are considered in obtaining an optimum weight structure. A typical swept wing structure is used with upper and lower skins, spar and rib thicknesses, and spar cap and vertical post cross-sectional areas as the design parameters. Incompressible aerodynamic strip theory is used to derive the constraint formulations, and aerodynamic load matrices. A Sequential Unconstrained Minimization Technique (SUMT) algorithm is used to optimize the wing structure to meet the desired performance constraints.

- MINIMUM WEIGHT DESIGN OF LIFTING SURFACES
- DIVERGENCE SPEED
- LIFT EFFECTIVENESS
- CONTROL EFFECTIVENESS
- FORWARD AND AFT SWEPT WINGS
- STRIP THEORY AERODYNAMICS

STATIC AEROELASTIC ANALYSIS

The equation of equilibrium is given in Equation 1. The divergence velocity is computed by setting the initial angle of attack and the flap setting to zero in Equation 1. The aerodynamic influence coefficient matrix [A] is computed using the strip aerodynamics. The lift effectiveness is the ratio of flexible to rigid lift and is computed by setting the flap angle in the equilibrium equation to zero, and is given in Equation 2. The rolling of an aircraft is affected by the raising and/or lowering of a flap located on the wing. Control effectiveness is the measure of the rolling moment produced by a flexible wing to that produced by a rigid wing at an angle of attack equal to zero, and is given in Equation 3.

$$[K]\{u\} = q[A]\{u\} + q[A^r]\{\alpha^r\} + q[A^f]\{\delta\} \qquad (1)$$

$$E^L = \frac{q\{h\}^T[A^r]\{\alpha^r\} + q\{h\}^T[A]\{u\}}{q\{h\}^T[A^r]\{\alpha^r\}} \qquad (2)$$

$$E^C = \frac{q\{p\}^T[A^f]\{\delta\} + q\{p\}^T[A]\{u\}}{q\{p\}^T[A^f]\{\delta\}} \qquad (3)$$

SENSITIVITY ANALYSIS

Mathematical optimization techniques involve computation of the search direction for finding the optimum. This involves gradients of the constraints and the objective function with respect to the design variables. In the following, gradients of the aeroelastic behavior constraints are given. Calculation of the objective function gradient with respect to the design variables is straight forward. The divergence gradients are computed using the left and right eigenvectors. The aerodynamic matrices do not vary with the design variables.

$$\frac{dq}{dx} = \frac{\{v\}^T \frac{d[K]}{dx} \{u\}}{\{v\}^T [A] \{u\}} \tag{4}$$

$$\frac{dE^L}{dx} = \frac{\{h\}^T [A] \frac{d\{u\}}{dx}}{\{h\}^T [A^r] \{\alpha^r\}} \tag{5}$$

$$\frac{dE^C}{dx} = \frac{\{p\}^T [A] \frac{d\{u\}}{dx}}{\{p\}^T [A^f] \{\beta\}} \tag{6}$$

OPTIMIZATION PROBLEM

The structural weight was minimized with limitations on divergence velocity, lift effectiveness and control effectiveness. The design variables were upper and lower skin thicknesses, cross-sectional areas of vertical posts and spar caps, and spar and rib thicknesses. Lower bounds were imposed on the design variables. The optimization problem was solved using quadratic extended interior penalty function method with Newton's method of unconstrained minimization. The computer program NEWSUMT-A was used.

Minimize the structural weight, f(x) subject to

$$g_j(\mathbf{x}) = G_j(\mathbf{x}) - \mathrm{G_j} \geq 0 \quad j = 1, 2, \ldots, m \tag{7}$$

and

$$x^l_i \leq x_i \quad i = 1, 2, \ldots, n \tag{8}$$

NUMERICAL RESULTS

The wing shown in Figure 1 is modelled with quadrilateral membrane elements for the upper and lower skins, shear panels for the ribs and webs, and rod elements for the spar caps and vertical posts. The structure consists of 66 elements, and it is made of aluminum with Young's modulus of 10.5×10^6 psi, $\nu = 0.3$, and a weight density of 0.1 lb/in^3. The wing is swept through 30 degrees representing typical forward-swept wing configurations. The wing shown has a 180 in. semispan, a constant chord of 50 in. (i.e. untapered), and a symmetric airfoil.

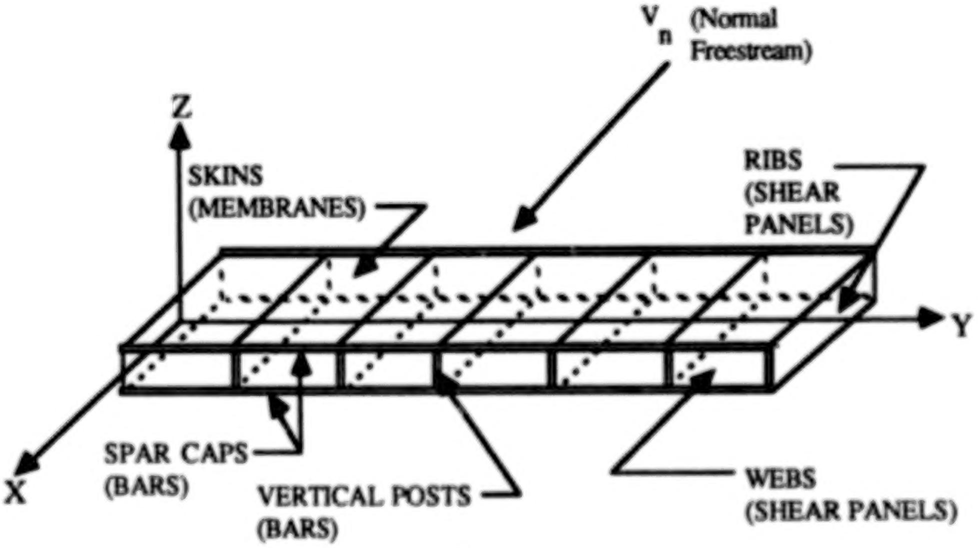

Figure 1. Built-Up Wing Configuration

Fig. 2 shows lift effectiveness and control effectiveness plotted against velocity. For this forward-swept configuration control reversal is higher than the divergence velocity. The divergence velocity is 515 ft/sec, and the control reversal (where the effectiveness goes to zero) is approximately at 1375 ft/sec. The typical nature of this plot is due to $\frac{q_R}{q_D} > 1$ as reported in Principles of Aeroelasticity by Bisplinghoff and Ashley.

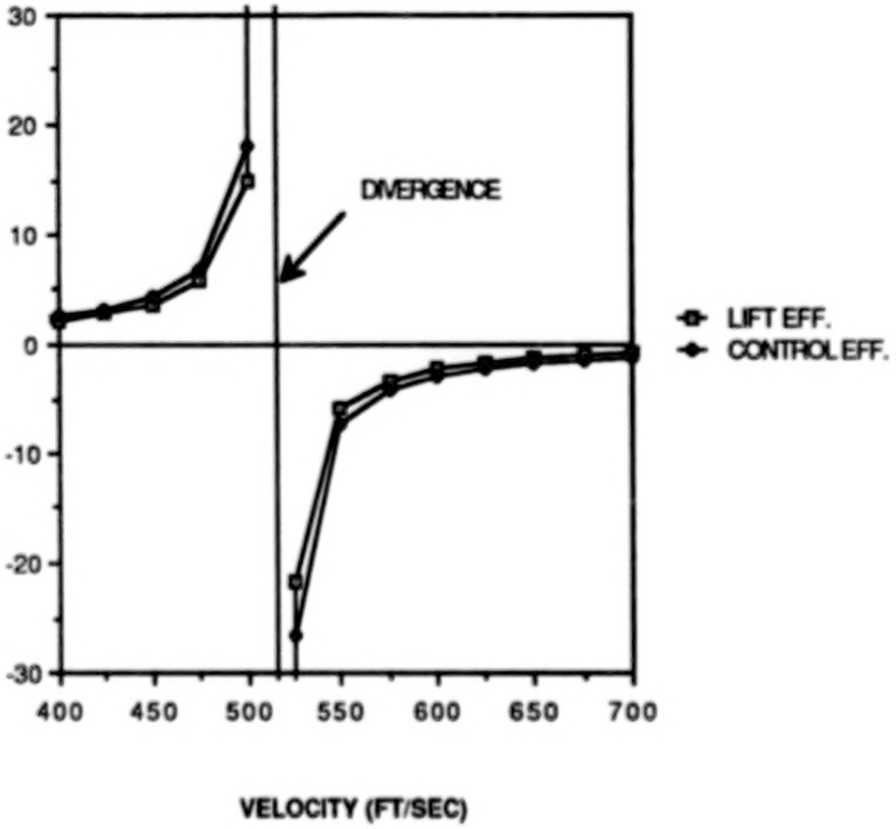

Figure 2. Control Effectiveness and Lift Effectiveness vs. Velocity

Initially the structural weight was minimized by imposing a lower limit on the divergence velocity. The divergence speed increased to 550.00 ft/sec from the reference design value of 515.06 ft/sec. A comparison of the optimum structure's divergence speed to NASTRAN analysis revealed less than a couple of percent difference at the initial and final designs. The convergence to the optimum is smooth as shown in Fig. 3.

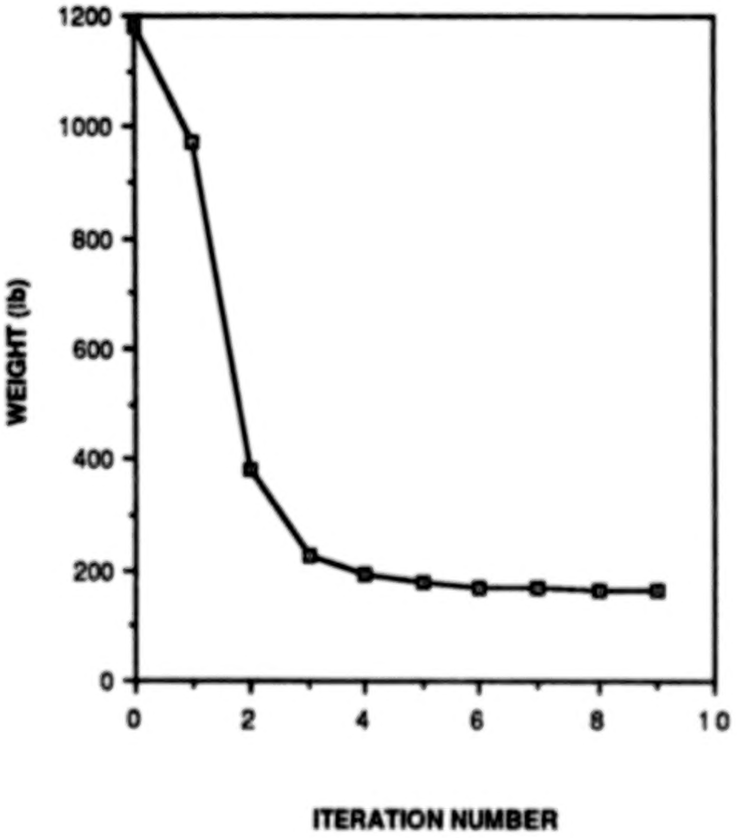

Figure 3. Design Iteration History for Divergence Constraint

The lift effectiveness and control effectiveness were calculated at the flight speed of 373.96 ft/sec, and were monitored as the divergence speed was increased. Several divergence velocities were considered for minimizing the structural weight. Fig. 4 shows the optimum weight vs. divergence velocity. The divergence speed lower limit was increased from 500 to 675 ft/sec. The optimum weight monotonically increased with the divergence velocity requirement. Lift effectiveness and control effectiveness both decreased with an increase in the divergence speed as shown in Fig. 4.

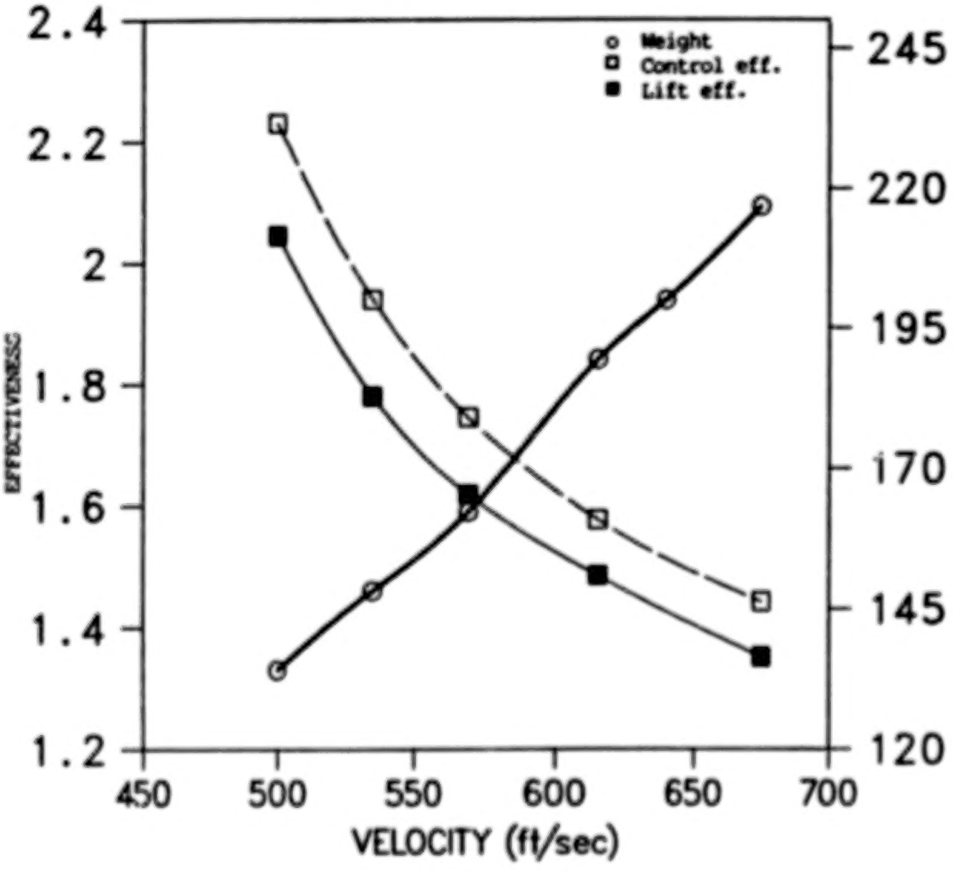

Fig. 4 Optimum Weight, Lift Effectiveness and Control Effectiveness vs. Divergence Velocity

The wing was optimized with two constraints imposed at a time to explore the opposite trend of the effectiveness values and divergence speeds with the increase of structural weight. The structure was optimized such that the divergence velocity be above 550 ft/sec and lift effectiveness above 2.0. The initial weight of the structure with all design variables set to 1.0 was 1180.80 lbs and the optimum structure had a divergence value of 560.57 ft/sec, a lift effectiveness of 2.71, and a weight of 225.46 lbs. Optimization with control effectiveness in place of lift effectiveness yielded a divergence of 550.03 ft/sec, a control effectiveness of 3.18, and a weight of 168.17 lbs.

Finally all three constraints were applied to this wing concurrently. Retaining the same constraint values as mentioned above, the structure was optimized and converged to an optimum design after six iterations. The final weight was 249.63 lbs with a divergence speed of 573.36 ft/sec, a lift effectiveness of 2.53, and a control effectiveness of 2.62. Table 1 presents the optimum performance values obtained for different combinations of constraints.

Table 1. Optimization Results

CONSTRAINTS	OPTIMUM			
	q_{DIV} (ft/sec)	E^L	E^C	Weight (lb)
$q_{DIV} \geq 550.0$ ft/sec	550.00			154.54
$q_{DIV} \geq 550.0$ ft/sec $E^L \geq 2.0$	560.60	2.71		225.46
$q_{DIV} \geq 550.0$ ft/sec $E^C \geq 2.0$	550.00		3.18	168.17
$q_{DIV} \geq 550.0$ ft/sec $E^L \geq 2.0$ $E^C \geq 2.0$	573.36	2.53	2.62	249.63

CONCLUSIONS

The divergence velocity of forward-swept wing configurations is the primary characteristic that must be improved. An increase in the structural stiffness of a wing will prevent a low divergence speed, but results in an increase of aircraft weight. Also an increase in divergence velocity affected the decrease of lift effectiveness and control effectiveness. Optimization of a wing for the three static aeroelastic constraints involves careful selection of the constraint limits. The studied wing had an initial weight of 1180.9 lbs, and lift and control effectiveness values of 1.11 and 1.12 respectively. Following the optimization process that set constraint limits on the effectiveness values of 2.0 and 550.0 ft/sec on divergence speed, the wing weighed 249.63 lbs, satisfying all constraints. The above results demonstrate the capability and feasibilty of optimizing for all three constraints concurrently, rather than one at a time.

- MINIMUM WEIGHT DESIGN IS PERFORMED FOR STATIC AEROELASTIC CONSTRAINTS
    - INCREASE IN DIVERGENCE SPEED RESULTS IN A DECREASE OF EFFECTIVENESS VALUES
    - CAREFUL SELECTION OF STATIC AEROELASTIC CONSTRAINT VALUES WILL RESULT IN SUCCESSFUL OPTIMIZATION
- PRESENT APPROACH USED NEWSUMT-A PROGRAM
- ULTIMATE GOAL IS TO DEVELOP OPTIMALITY TECHNIQUES

BIBLIOGRAPHY

1. Bisplinghoff, R.L, Ashley, H., Principles of Aeroelasticity, John Wiley and Sons, Inc., New York, 1962, pp. 196.

2. Bisplinghoff, R.L, Ashley, H., and R. L. Halfman, Aeroelasticity, Addison-Wesley Publishing Company, Massachusetts, 1957, pp. 11-13, 474 - 506.

3. Bohlmann, J.D., Eckstrom, C.V., and Weisshaar, T.A., "Aeroelastic Tailoring for Oblique Wing Lateral Trim," AIAA/ASME/ASCE/AHS 29th Structures, Structural Dynamics and Materials Conference, Williamsburg, Virginia, AIAA-88-2263, April 18-20, 1988.

4. Eastep, F.E., "Structural Optimization With Static Aeroelastic Constraints," Flight Dynamics Laboratory, Wright-Patterson Air Force Base, December 1987.

5. Eastep, F.E., Venkayya, V.B., and Tischler, V.A., "Divergence Speed Degradation of Forward Swept Wings with Damaged Composite Skin," *Journal of Aircraft*, Vol. 21, No. 11, November 1984, pp 921-923.

6. Grandhi, R.V., Thareja, R., and Haftka, R.T., "NEWSUMT - A: A General Purpose Program for Constrained Optimization Using Constraint Approximations," ASME Journal of Mechanisms, Transmissions, and Automation in Design, Vol. 107, March 1985, pp 94-99.

7. Lerner, E. and Markowitz, J., "An Efficient Structural Resizing Procedure for Meeting Static Aeroelastic Design Objectives," AIAA/ASME 19th Structures, Structural Dynamics and Materials Conference, Bethesda, Md., Paper 78-471, April 3-5, 1978, pp. 65-71.

8. Schmit, L.A., and Thornton, W.A., "Synthesis of an Airfoil at Supersonic Mach Number," NASA-CR-144, 1, 4, 1965

9. Shirk, M.H., Hertz, T.J., and Weisshaar, T.A., "A Survey of Aeroelastic Tailoring- Theory, Practice, and Promise," *Journal of Aircraft*, Vol. 23, No. 1, January 1986, pp 6-18.

10. Weisshaar, T.A, "Forward Swept Wing Static Aeroelasticity," AFFDL-TR-79-3087, Air Force Flight Dynamics Laboratory, June 1979.

OPTIMUM DESIGN OF SWEPT-FORWARD HIGH-ASPECT-RATIO GRAPHITE-EPOXY WINGS

M. J. Shuart
NASA Langley Research Center
Hampton, Virginia

R. T. Haftka
Virginia Polytechnic Institute and State University
Blacksburg, Virginia

R. L. Campbell
NASA Langley Research Center
Hampton, Virginia

INTRODUCTION

The efficiency of aerospace structures is evaluated by many criteria that may include performance, structural weight, and cost. Anisotropic composite materials have characteristics that are useful for the design of innovative aerospace structures. These materials are well-known for their high strength- and stiffness-to-weight ratios. Lightweight composite structures also can have unique response characteristics that enable the design of innovative structural concepts. An example of these characteristics is the beneficial bending/twisting coupling response of the graphite-epoxy wing skins for the swept-forward X-29 wing (see Figure 1). Moreover, recent advances in materials and processing technologies indicate that composite structures may be fabricated for a lower cost when compared to similar metallic structures. Additional research is needed to exploit the unique characteristics of composite structures to obtain structurally efficient, cost-effective designs.

This paper describes an analytical investigation of a swept-forward high-aspect-ratio graphite-epoxy transport wing. The objectives of this investigation were to illustrate an effective usage of the unique properties of composite materials by exploiting material tailoring and to demonstrate an integrated multidisciplinary approach for conducting this investigation.

X-29 ADVANCED TECHNOLOGY DEMONSTRATOR

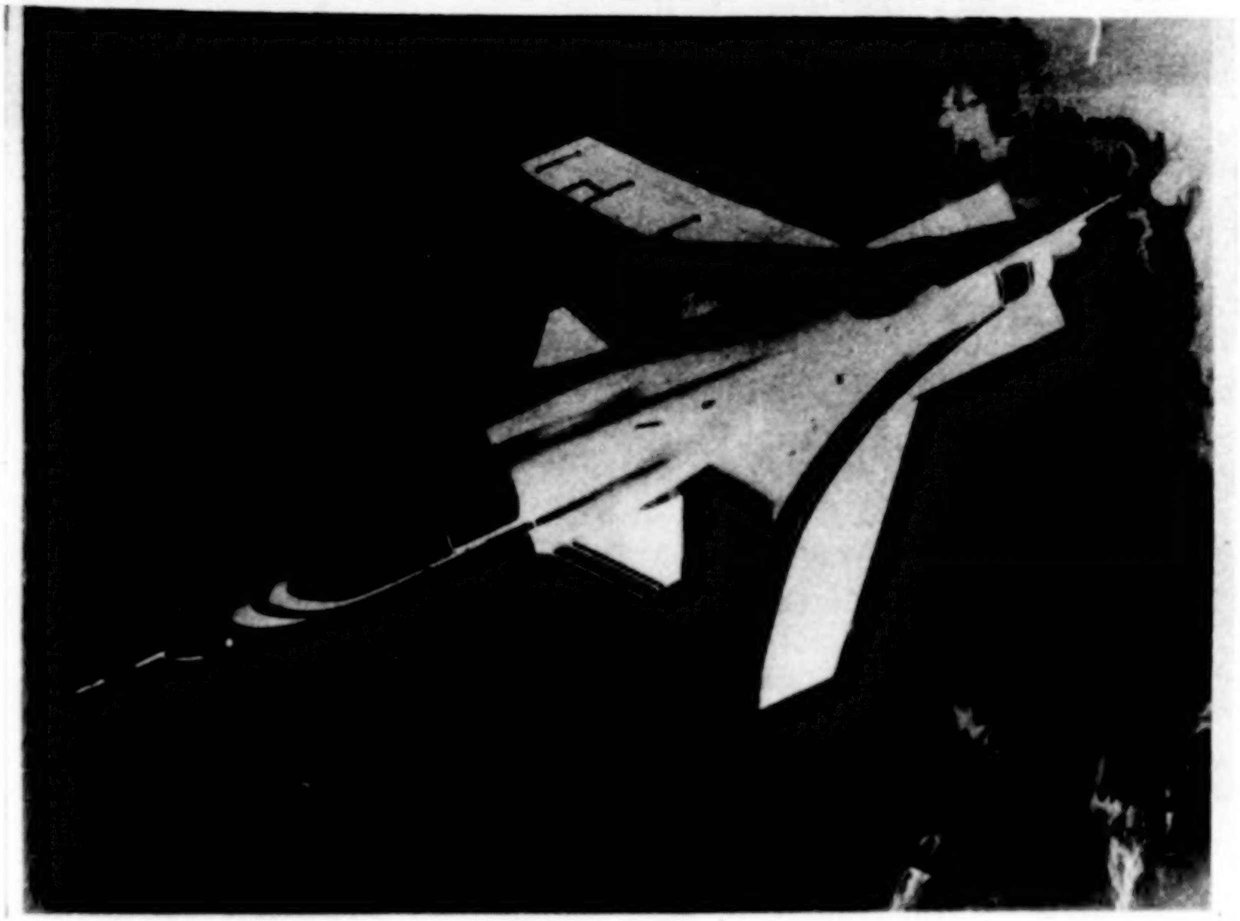

AN INTEGRATED APPROACH TO WING DESIGN

The integrated multidisciplinary procedure used in this investigation is illustrated in Figure 2. This procedure consists of an aerodynamic analysis, a structural analysis, and a structural optimization. The aerodynamic analysis of the wing configuration includes aeroelastic corrections to account for structural deformations and produces the wing loading. The structural analysis uses the wing loading to calculate stresses, strains, and deformations for the internal wing structure. The structural optimization compares these stresses, strains, and deformations against design constraints and perturbs the internal wing structure to obtain a minimum weight structural configuration that satisfies the design constraints. The optimized configuration is input to the aerodynamic analysis to update the wing loading, and the entire procedure is repeated to obtain a second optimized configuration. The second configuration is used as the final design.

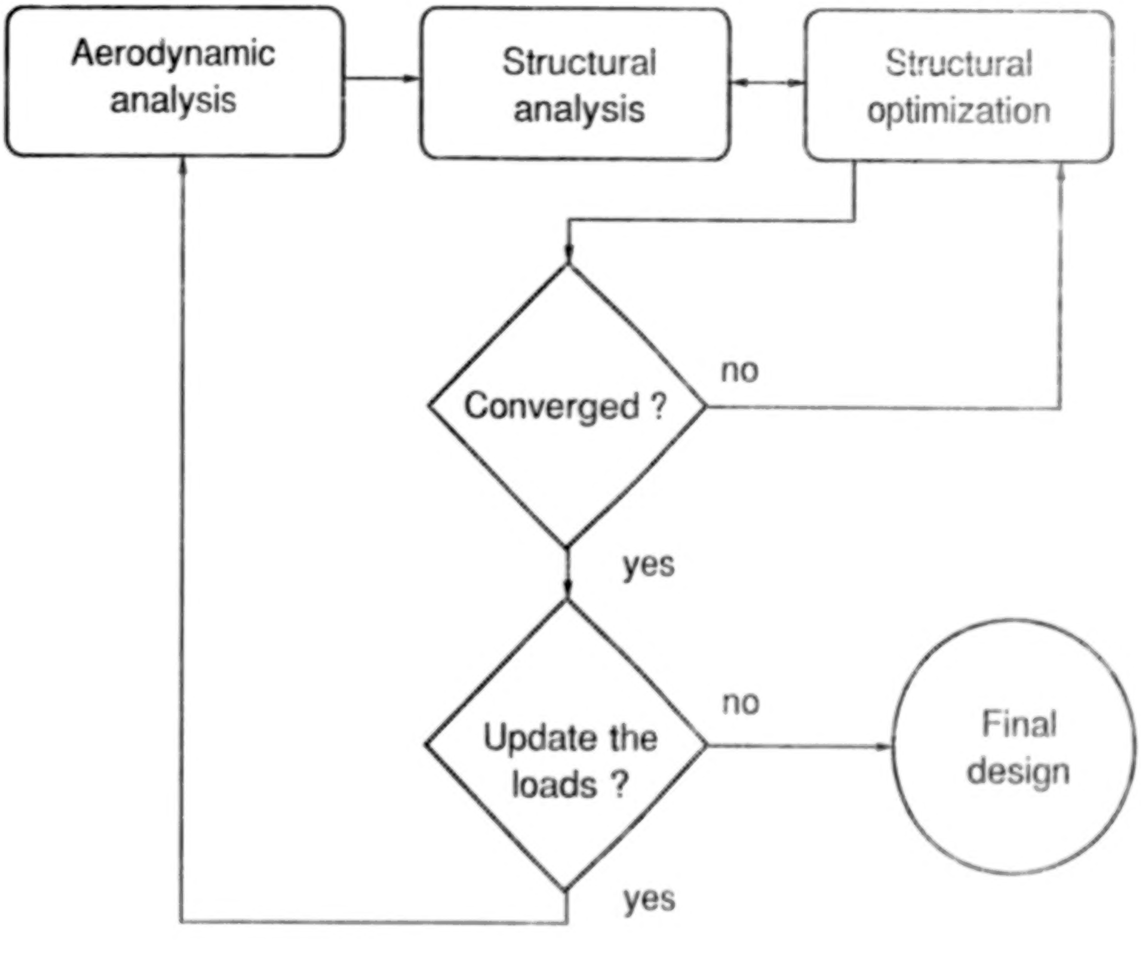

FORWARD SWEPT WING GEOMETRY

The wing geometry selected for this investigation is shown in Figure 3. The primary goal for the aerodynamic design of this wing was to reduce drag by natural laminar flow (NLF). Forward sweep appears to be advantageous for obtaining NLF since the flow along the leading edge of the wing would not be contaminated by the turbulent boundary layer from the fuselage. A moderate leading-edge sweep, -21°, was chosen in order to reduce the possibility of boundary layer transition due to cross-flow instabilities. The aspect ratio for this wing is 12. The flight conditions at the cruise design point were a Mach number of 0.78 and a lift coefficient of 0.55 at an altitude of 39,000 ft. The airflow is indicated by U on the figure. A parametric study of the effect of planform variations on wing shock strength and location was made at these flight conditions using the TAWFIVE full-potential wing-body computer code (ref. 1). The sweep of the leading and trailing edges of the wing from the root to about forty percent of the semispan was varied in an effort to reduce the shock strength over the inboard part of the wing. For the configurations examined, the best performance resulted from having a constant trailing-edge sweep for the entire wing and an unswept leading edge for the inboard portion of the wing. Airfoil geometry is determined using the pressure distributions at the three design stations indicated on the figure.

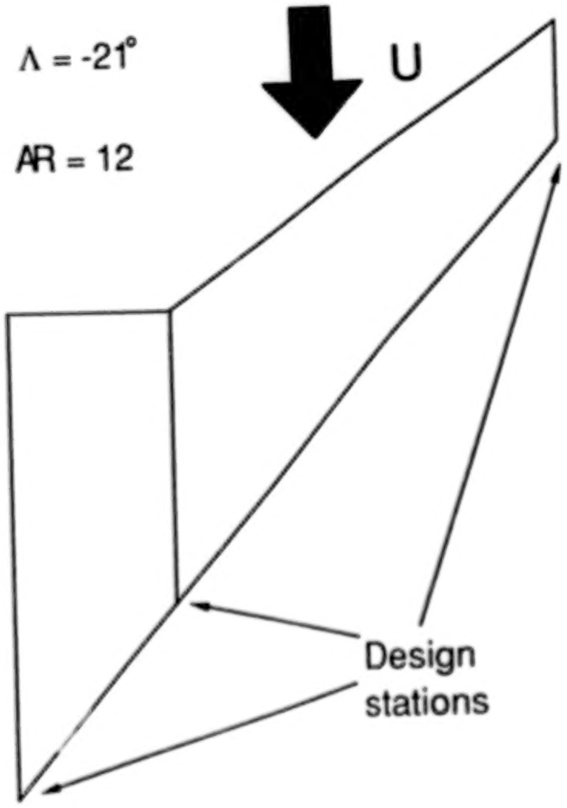

- Drag reduction through natural laminar flow
- Cruise design point:
  M=0.78, C_L=0.55, alt=39,000 ft
- TAWFIVE for planform design
  - full-potential wing-body code
  - reduce shock strength inboard

TRANSONIC AEROELASTIC PROGRAM SYSTEM (TAPS)

The aerodynamic loads were calculated using the Transonic Aeroelastic Program System (TAPS, ref. 2), and this system is illustrated schematically in Figure 4. The two main components of TAPS are an aerodynamic analysis code and an aeroelastic module. The TAWFIVE transonic wing-body code (ref. 1) was used for the aerodynamic calculations in this study. An initial aerodynamic analysis is made using specified flow conditions and the unloaded wing geometry. The resulting wing pressure coefficients are interpolated to the structural node locations, converted to lifting pressures using the free-stream dynamic pressure, and multiplied by input nodal areas to yield an array of nodal forces. This array is then multiplied by the structural flexibility matrix to obtain the vertical deflection at each node location. These static aeroelastic deflections are interpolated back to the wing planform locations needed for the aerodynamic analysis code. The deflected wing geometry is then analyzed in TAWFIVE to get a new estimate of the wing loading. The TAPS method updates the wing loading and deflections in this manner for a user-specified number of cycles. The calculations in this study were made using three aerodynamic-structural iterations.

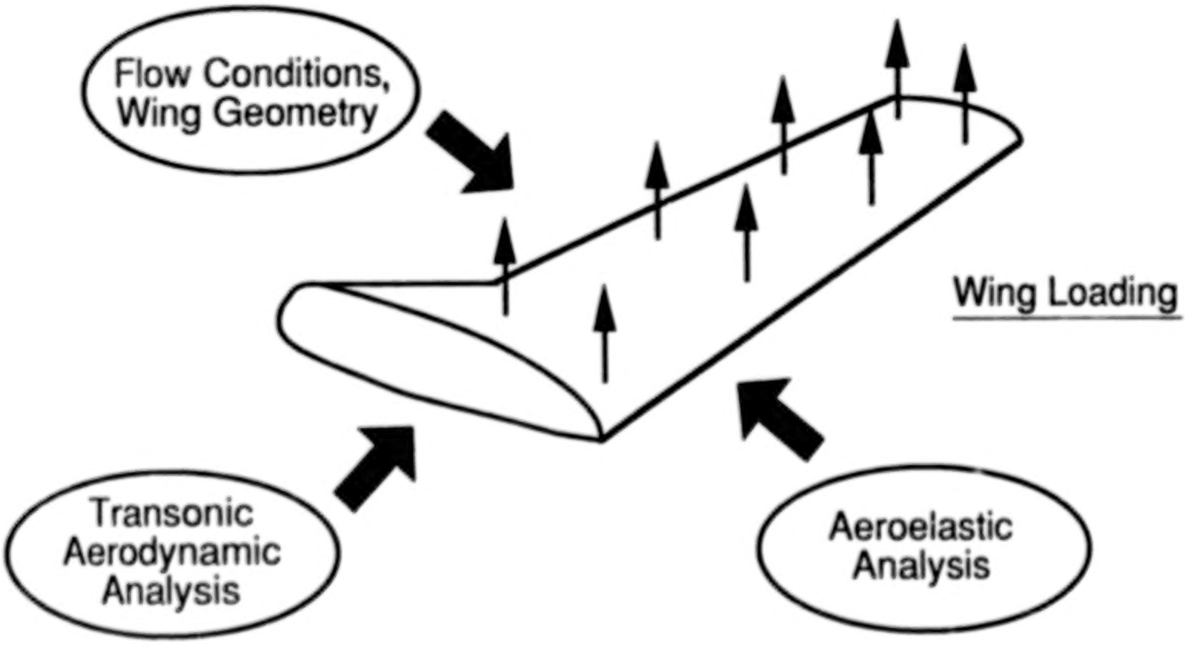

The loading conditions, design variables, and parameters for this high-aspect-ratio wing configuration are shown in Figure 5. Two loading conditions that significantly affect the response of a high-aspect-ratio wing were considered: a 2.5-g maneuver condition; and a gust-up condition. The 2.5-g maneuver condition was simulated by increasing the dynamic pressure at the cruise Mach number and angle of attack. The gust-up condition was simulated by modifying the angle of attack at the cruise Mach number. The loads obtained for these two conditions were multiplied by a 1.5 factor of safety. The graphite-epoxy wingbox consisted of orthotropic cover panel laminates, quasi-isotropic rib web laminates, and quasi-isotropic spar cap and spar web laminates. The design variables selected for optimization of the graphite-epoxy wingbox were material orientations for the cover panels (as determined by the laminate's 0° direction), ply thicknesses for the cover panel laminates, and cross-sectional areas for the spar caps. The parameters that were varied for this investigation were the number of spars, the number of ribs, the rib orientation with respect to the leading edge spar, and the graphite-epoxy material properties.

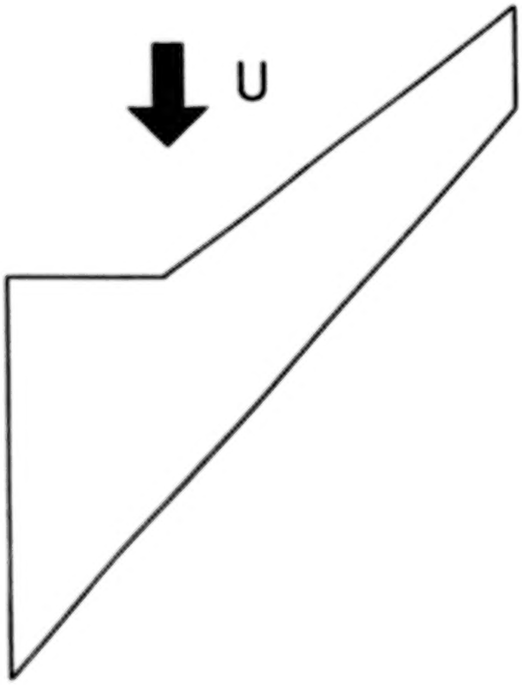

- Loading conditions
    - 2.5 G maneuver
    - gust up
- Design variables
    - material orientations
    - ply thicknesses
    - spar cap areas
- Parameters
    - number of spars
    - number of ribs
    - rib orientation
    - material properties

BENDING STIFFNESS VARIATIONS FOR AN ORTHOTROPIC LAMINATE

The tailorability of an orthotropic graphite-epoxy laminate is illustrated in Figure 6. The laminate described on the figure has 80 percent 0° plies, 10 percent ±45° plies, and 10 percent 90° plies when the 0° direction is parallel to the x-axis (θ=0°). The bending/torsional stiffnesses for this laminate change dramatically as the angle θ between the x-axis and the 0° direction varies from 0° to 180°. For example, the D_{11} bending stiffness value is more than an order of magnitude greater than all other values for θ=0° but is approximately the same as the D_{26} and D_{66} bending stiffness values for θ=70°. Also, the bending-torsion coupling term D_{16} critical for a forward-swept wing changes sign as θ is varied. In the present study, the wing tip was constrained to have zero twist deformation by the structural optimization module to guard against unfavorable bending-torsion coupling leading to aeroelastic instabilities. This constraint results in a selection of θ that uses anisotropy to cancel the unfavorable geometrical coupling inherent in a forward-swept wing.

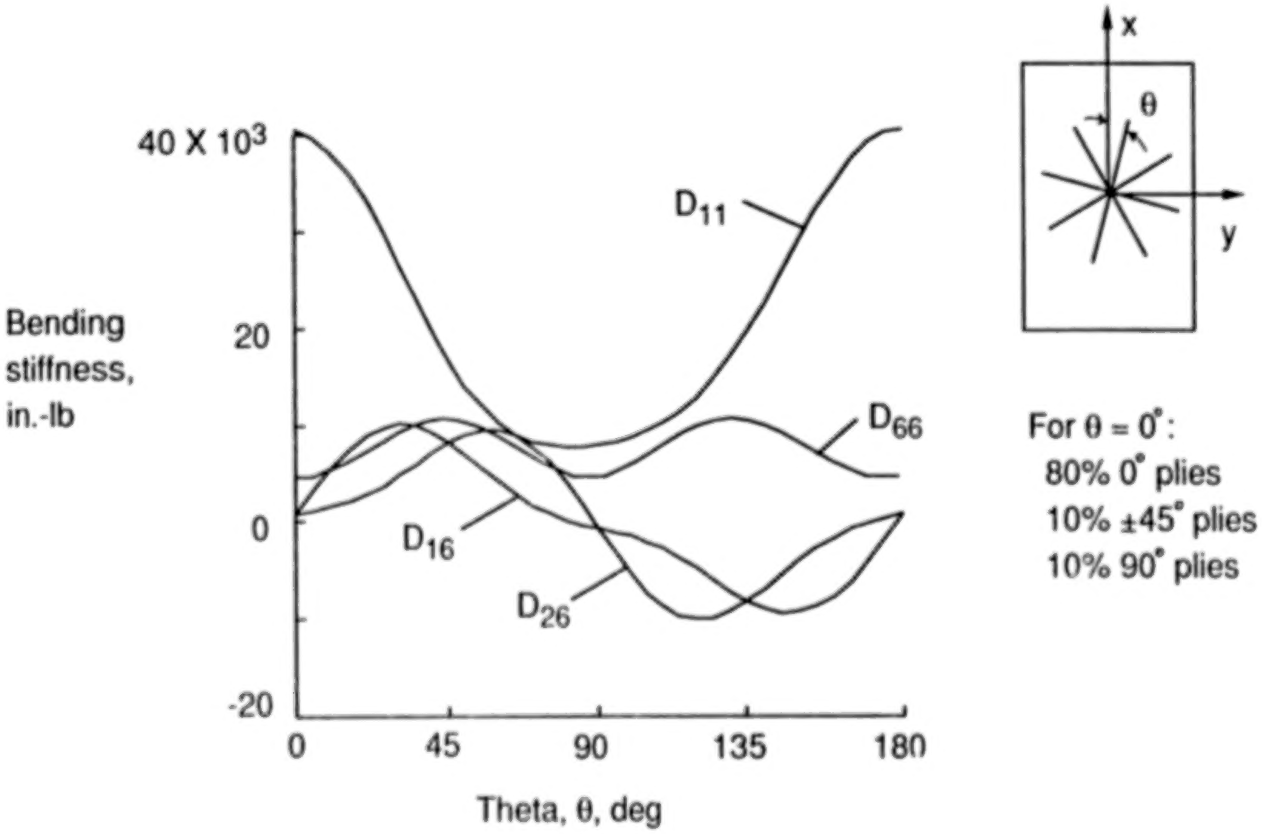

WING DESIGN OPTIMIZATION WITH AEROELASTIC CONSTRAINTS (WIDOWAC)

The structural optimization was carried out with a modified version of the WIDOWAC program (ref. 3), and this program is shown schematically in Figure 7. The program employs a built-up finite-element model of the wing consisting of membrane quadrilateral elements for cover panels and combinations of rod elements and shear elements for ribs and spars. A quadratic extended interior penalty function is used for the optimization. The structure was optimized subject to maximum strain constraints (e.g., $|\varepsilon| \leq 0.006$, $|\gamma| \leq 0.010$), minimum gage constraints (ply thickness ≥ 0.0074 in.), and side constraints that limited the percentage of ply thickness for any orientation to no less than 10 percent of the laminate thickness. To guard against aeroelastic instabilities two stiffness constraints were applied. The first stiffness constraint required a minimum torsional stiffness for the wing, and the second stiffness constraint mandated a zero or negative twist angle at the wing tip when the wing is subjected to each design load. The WIDOWAC program was used to obtain minimum weight designs for this wing configuration.

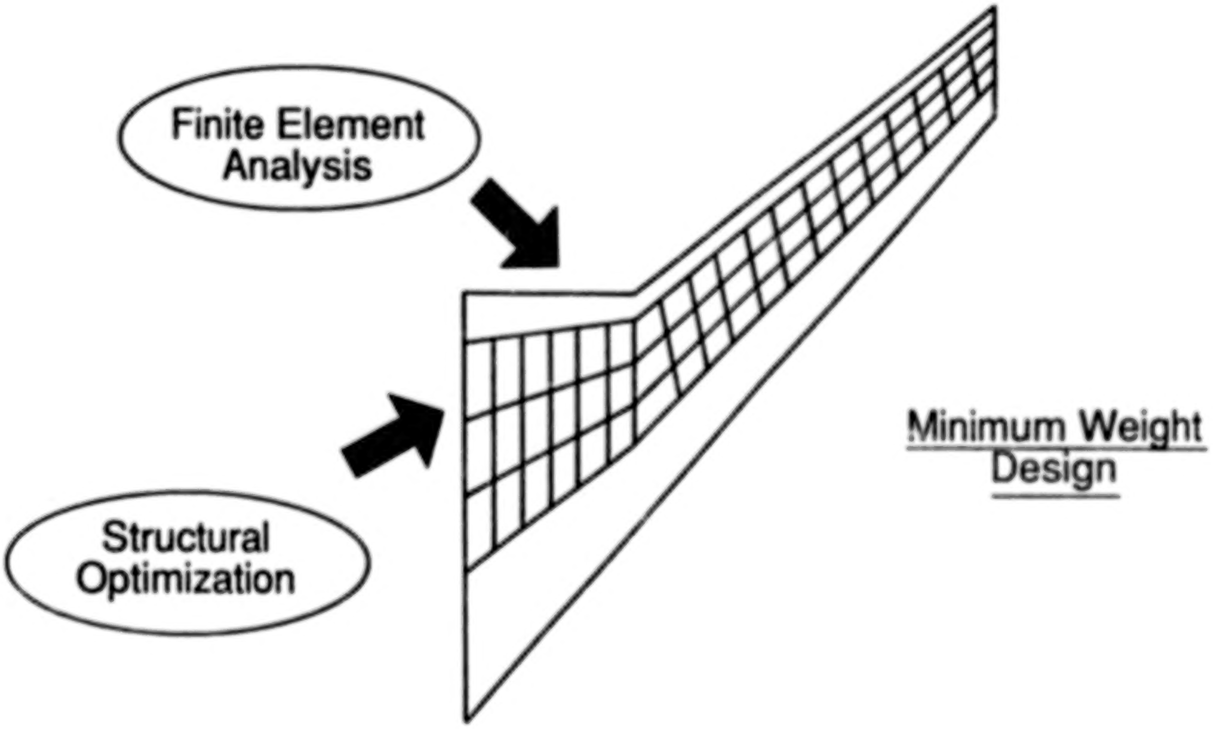

2-SPAR MODEL

Three wingbox models were used to investigate the effects of wingbox configuration on the configuration weight. These models are referred to as the 2-spar model, the 4-spar model, and the multi-spar/multi-rib model. These models were used to obtain results for configurations fabricated using either a state-of-the-art damage-tolerant graphite-epoxy material or an improved graphite-epoxy material. The state-of the-art graphite-epoxy material is referred to as the standard material. The improved material is not currently available but is assumed to have stiffness and strength properties that are 20% greater than the respective properties for the standard material. The 2-spar model is illustrated in Figure 8. This model is used to represent a wingbox configuration having leading and trailing edge spars and having ribs spaced 30 in. apart. The configuration has a total of twenty ribs. This configuration is typical of current wingbox configurations for transport aircraft.

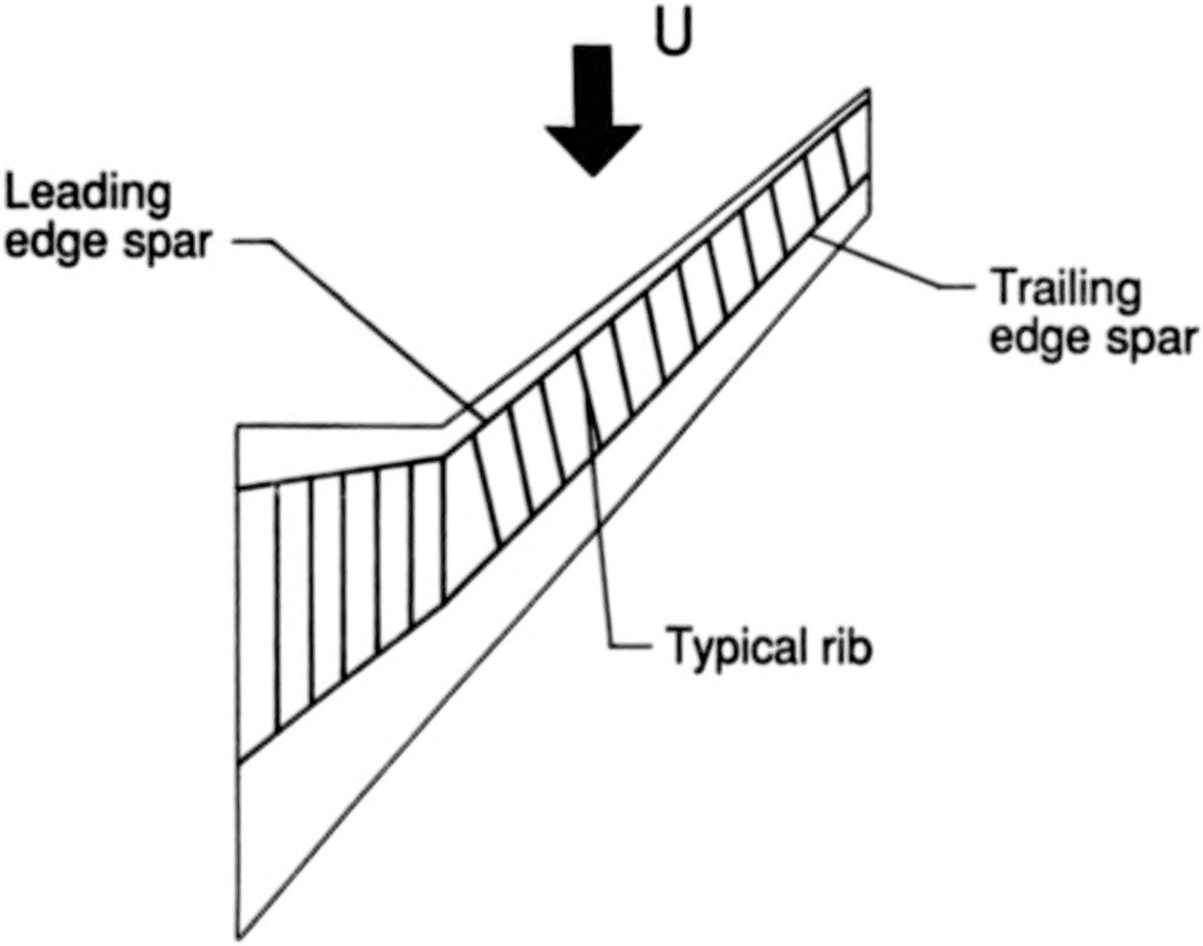

4-SPAR MODEL

The 4-spar wingbox model is shown in Figure 9. This model is used to represent a wingbox configuration having leading and trailing edge spars as well as two interior spars. The number of ribs for this model is minimized to seven.

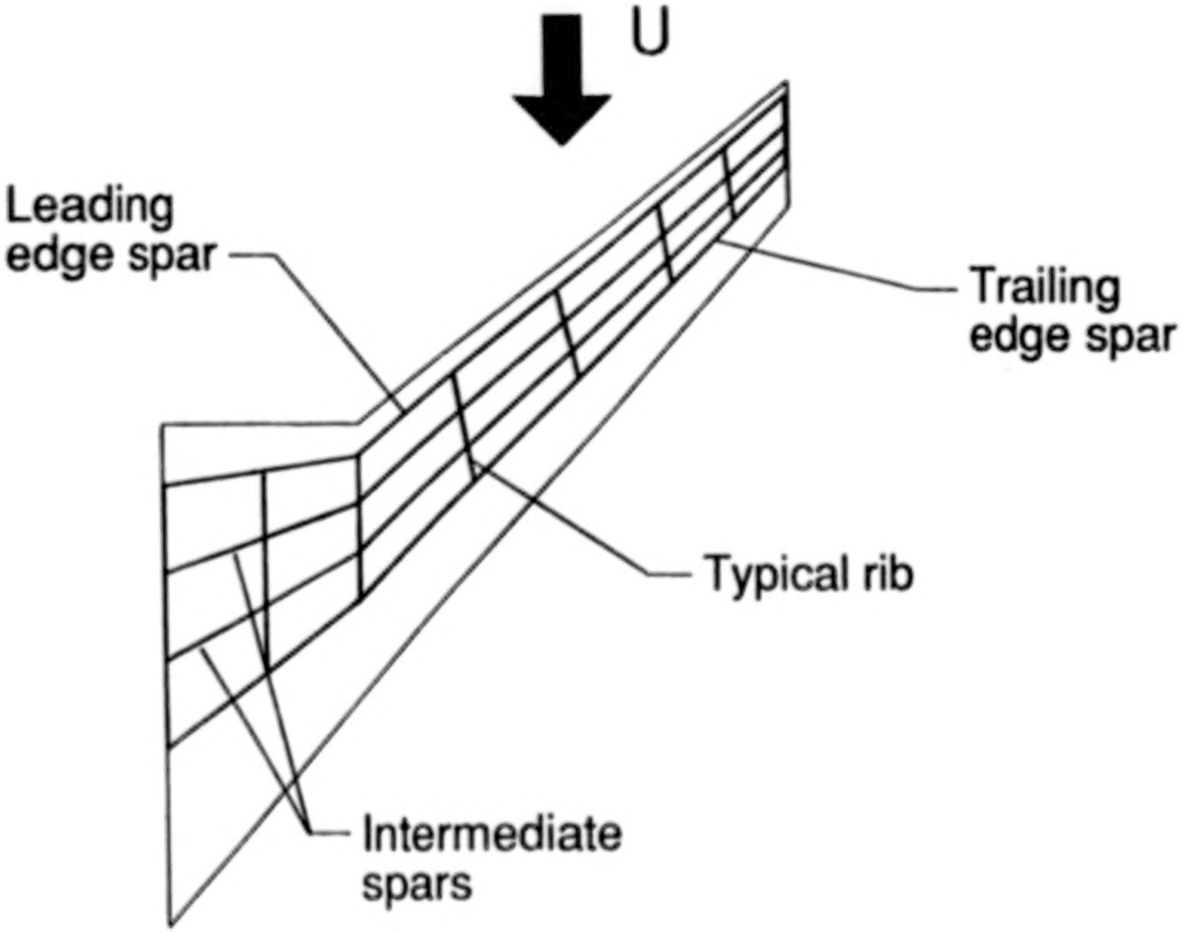

MULTI-SPAR/MULTI-RIB (MR/MS) MODEL

The multi-spar/multi-rib (MS/MR) model is shown in Figure 10. The MS/MR model is a combination of the 2-spar and the 4-spar models. The MS/MR model has a leading edge spar, a trailing edge spar, two interior spars, and ribs spaced 30 in. apart.

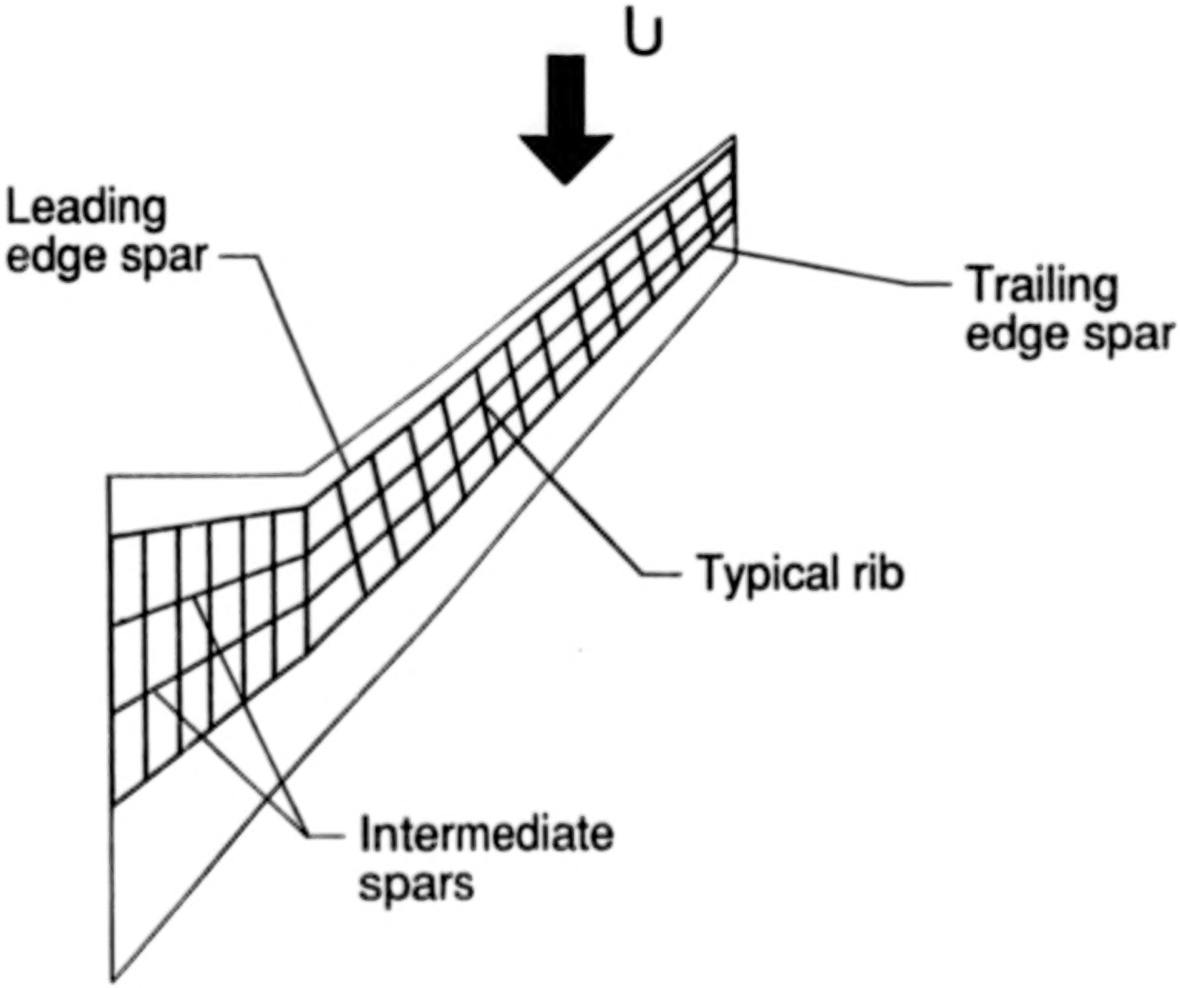

OPTIMIZED THICKNESS DISTRIBUTION FOR TOP COVER PANEL OF 2-SPAR WINGBOX

The wingbox models were used to determine cover panel thicknesses for the four regions of the wingbox, and results obtained using the 2-spar are shown in Figure 11. The wingbox regions are illustrated on the left side of the figure, and the top cover panel thicknesses for these regions are illustrated on the right side of the figure. The inboard orientation angle θ_i is the 0° material direction for regions 1 and 2; the outboard orientation angle θ_o is the 0° material direction for regions 3 and 4. Results for a configuration that uses the standard material are unshaded on the figure, and results for a configuration that uses the improved material are shaded on the figure. The values of θ_i and θ_o for both the standard and the improved materials indicate that significant bending-twisting coupling occurs for this configuration. The panel thickness results show regions 2 and 3 to be much thicker than regions 1 and 4, indicating that the region 2-3 interface is heavily loaded. Results for a configuration fabricated from an improved material show a 20 percent decrease in thickness that corresponds to the 20 percent increase in stiffness and strength properties.

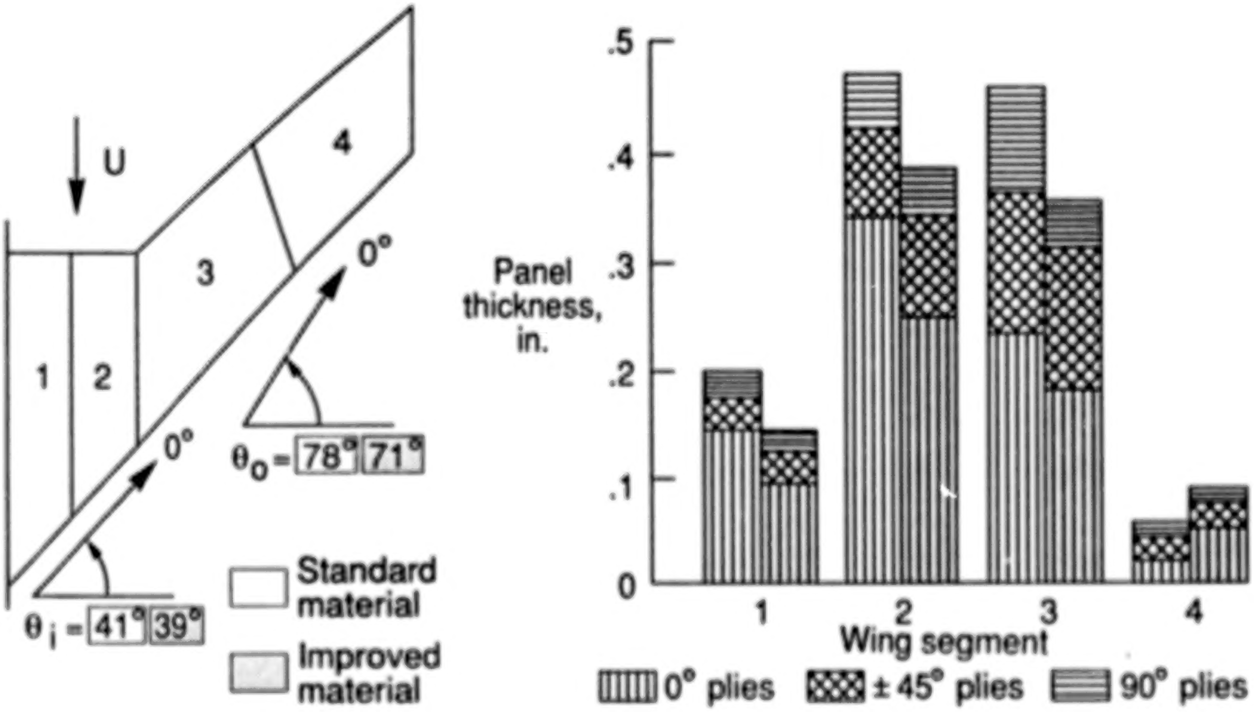

OPTIMIZED THICKNESS DISTRIBUTION FOR TOP COVER PANEL OF 4-SPAR WINGBOX

Results obtained using the 4-spar model are shown in Figure 12. The thicknesses for regions 1, 2, and 3 obtained using the 4-spar model are significantly less (e.g., 63 percent less, region 2) than the respective thicknesses obtained using the 2-spar model. Also, the percentages of ±45° and of 90° plies determined using the 4-spar model are approximately equal to the 10 percent minimum. These results for individual ply thicknesses suggest that the 4-spar configuration combines aeroelastic tailoring with an efficient internal structure to achieve a lightweight feasible design. Results for a configuration fabricated from an improved material show a 20 percent decrease in thickness that corresponds to the 20 percent increase in stiffness and strength properties.

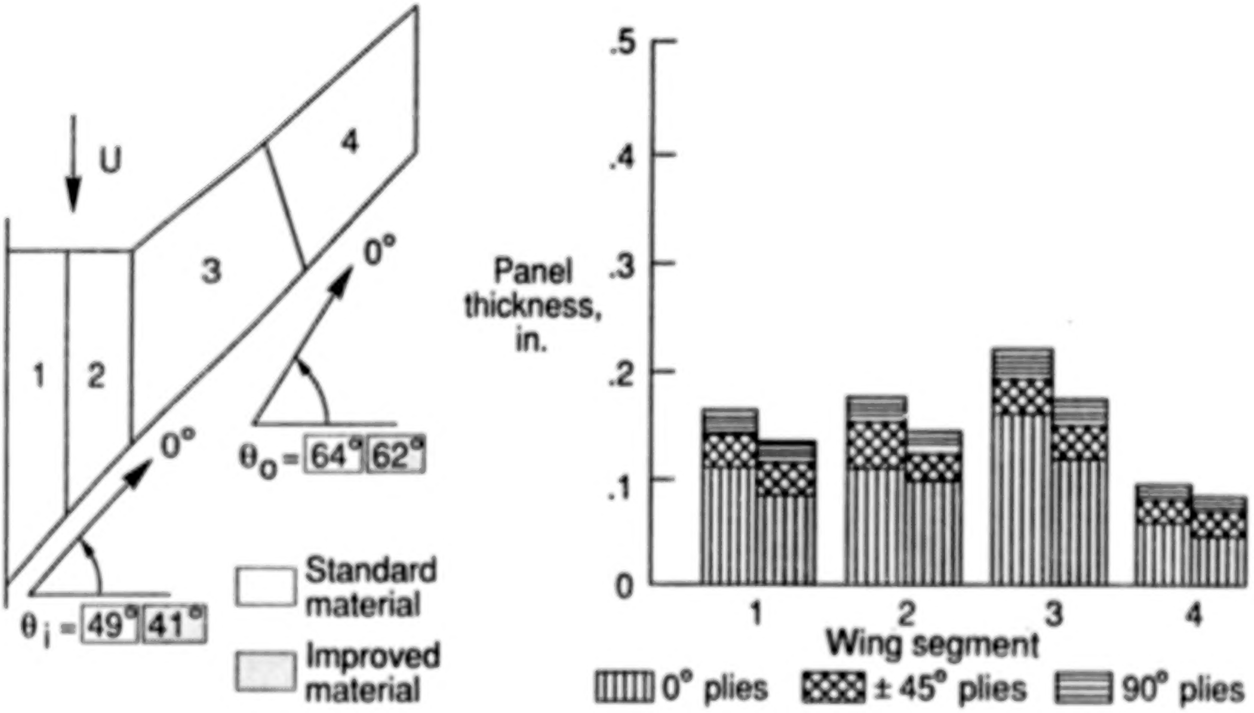

OPTIMIZED THICKNESS DISTRIBUTION FOR TOP COVER PANEL OF MULTI-SPAR/MULTI-RIB WINGBOX

Results obtained using the multi-spar/multi-rib (MS/MR) model are shown in Figure 13. The standard material or improved material thicknesses obtained using the MS/MR model are approximately the same as the respective thicknesses obtained using the 4-spar model. The MS/MR results suggest that the MS/MR configuration can be used to achieve lightweight feasible designs. However, the MS/MR configuration may be much more costly than the 4-spar configuration as determined by configuration part count. The MS/MR configuration has the same number of spars but has many more ribs than the 4-spar configuration. Typically, configuration cost increases with increasing part count.

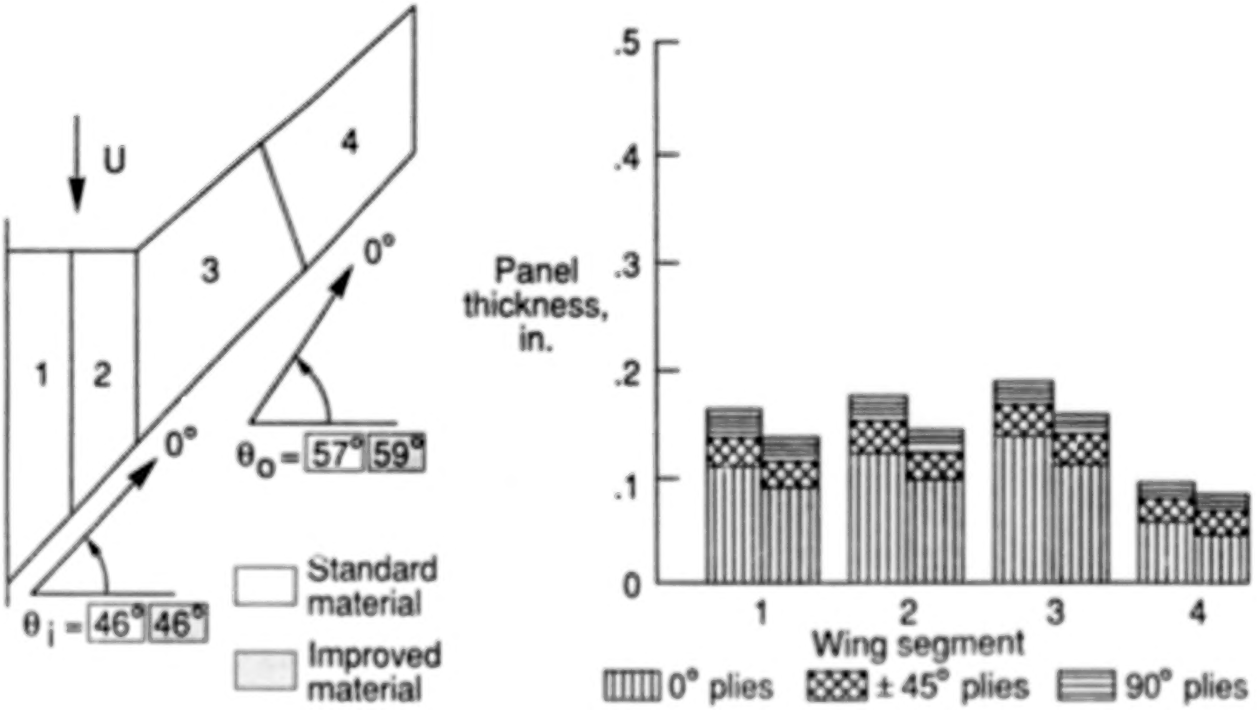

ORIENTED-RIB RESULTS: 2.5 G MANEUVER

The effect of rib angle on the wingbox configuration weight was investigated by changing the angle between ribs and the leading edge spar from 90° to 80° and then to 100°. Unfortunately, these changes apparently led to aeroelastic divergence instability which was evidenced by the high values for the tip twist angle after three aeroelastic iterations (Figure 14). A non-diverging design for the two rib-orientation configurations would have been possible if the aeroelastic analysis were a part of the optimization process. However, the extreme sensitivity to rib angles illustrates an inadequacy inherent in present deterministic design procedures. These procedures specify safety margins in terms of the applied loads. However, the present results indicate that a structure can have adequate load-based safety margins but lack a margin of safety with respect to small changes in the structure. These small changes may actually occur due to manufacturing tolerances and aging. A reliability-based design procedure with constraints on failure probabilities may avoid the inadequacy inherent in deterministic design procedures.

	Tip Twist, deg	
Orientation angle, deg	standard material	improved material
80	23.3	16.2
100	24.7	11.5

- Present model indicates divergence
- Model extremely sensitive
- Deterministic-based designs vs. reliability-based designs

OPTIMIZED WEIGHT FOR WINGBOX

The optimized weight for the three wingbox configurations is shown in Figure 15. Results are presented for configurations fabricated with the standard material and for configurations fabricated with the improved material. The results show that the 2-spar configuration is the heaviest of the configurations studied. This configuration satisfies the design constraints using thick tailored cover panels. The 4-spar and the MS/MR configurations are approximately 45 percent and 50 percent lighter, respectively, than the 2-spar configuration. The 4-spar and the MS/MR configurations combine an efficient internal structure with tailored cover panels to achieve feasible lightweight designs. The 4-spar configuration appears to be the best configuration of the configurations studied. The 4-spar configuration has approximately the same weight as the MS/MR configuration, but the 4-spar configuration is much simpler than the MS/MR configuration.

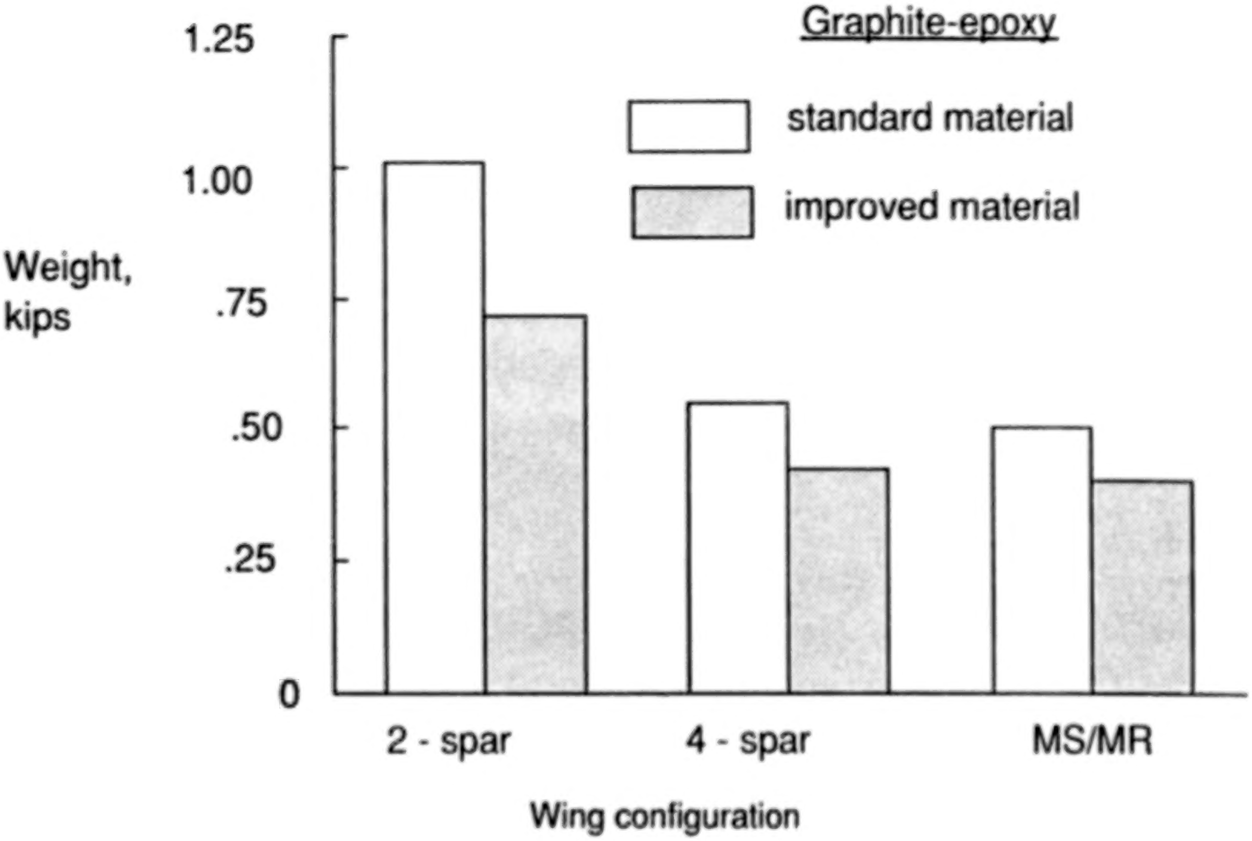

CONCLUDING REMARKS

An analytical investigation of a swept-forward high-aspect-ratio graphite-epoxy transport wing has been described. An integrated multidisciplinary procedure was discussed that included an aerodynamic analysis, a structural analysis, and a structural optimization. This procedure was used to study 2-spar, 4-spar, and multi-spar/multi-rib (MS/MR) wingbox configurations. Results were obtained for configuration fabricated from either a state-of-the-art damage-tolerant graphite-epoxy material or an improved graphite-epoxy material. The improved material had stiffnesses and strengths that were 20 percent greater than the corresponding properties for the state-of-the-art material.

The integrated procedure demonstrated the tailorability of composite structures for advanced concept wingbox configurations. Improved materials, tailorability, and efficient internal structure led to lightweight feasible designs. The designs appeared to be very sensitive to rib orientation. Ribs oriented at 80° or at 100° to the leading edge spar may lead to an aeroelastic divergence instability. The 4-spar and MS/MR configurations had approximately the same weight and were significantly lighter than the 2-spar configuration. The 4-spar configuration was the best of the configurations considered because the 4-spar configuration is both lightweight and simple.

REFERENCES

1. Melson, N. D.; and Streett, C. L.: TAWFIVE: A User's Guide. NASA TM-84619, September 1983.

2. Campbell, R. L.: Calculated Effects of Varying Reynolds Number and Dynamic Pressure on Flexible Wings at Transonic Speeds. Recent Experiences in Multidisciplinary Analysis and Optimization, NASA CP 2327, 1984, pp. 309-327.

3. Haftka, Rafael T; and Starnes, James H., Jr.: WIDOWAC(Wing Design Optimization with Aeroelastic Constraints): Program Manual. NASA TM X-3071, October 1974.

☆U.S. GOVERNMENT PRINTING OFFICE: 1989 -627-064/86027

NASA
National Aeronautics and Space Administration

Report Documentation Page

1. Report No. NASA CP-3031, Part 1	2. Government Accession No.	3. Recipient's Catalog No.

4. Title and Subtitle Recent Advances in Multidisciplinary Analysis and Optimization	5. Report Date April 1989
	6. Performing Organization Code
7. Author(s) Jean-François M. Barthelemy, Editor	8. Performing Organization Report No. L-16568
	10. Work Unit No. 506-43-41-01
9. Performing Organization Name and Address NASA Langley Research Center Hampton, Virginia 23665-5225	11. Contract or Grant No.
12. Sponsoring Agency Name and Address National Aeronautics and Space Administration Washington, DC 20546-0001 and Wright Research Development Center Wright Patterson AFB, OH 45433	13. Type of Report and Period Covered Conference Publication
	14. Sponsoring Agency Code

15. Supplementary Notes

Conference Co-Chairmen:
Jaroslaw Sobieski, NASA Langley Research Center
Laszlo Berke, NASA Lewis Research Center
Vipperla Venkayya, Air Force Wright Aeronautical Laboratory

16. Abstract

This three-part document contains a collection of technical papers presented at the Second NASA/Air Force Symposium on Recent Advances in Multidisciplinary Analysis and Optimization, held September 28-30, 1988 in Hampton, Virginia. The topics covered include: Helicopter Design, Aeroelastic Tailoring, Control of Aeroelastic Structures, Dynamics and Control of Flexible Structures, Structural Design, Design of Large Engineering Systems, Application of Artificial Intelligence, Shape Optimization, Software Development and Implementation, and Sensitivity Analysis.

17. Key Words (Suggested by Author(s)) Optimization Synthesis Systems Sensitivity Computers	18. Distribution Statement Unclassified - Unlimited Subject Category 05

19. Security Classif. (of this report) Unclassified	20. Security Classif. (of this page) Unclassified	21. No. of pages 542	22. Price A23

NASA FORM 1626 OCT 86

For sale by the National Technical Information Service, Springfield, Virginia 22161-2171

NASA-Langley, 1989

National Aeronautics and
Space Administration
Code NTT-4

Washington, D.C.
20546-0001

Official Business
Penalty for Private Use, $300

National Aeronautics and Space Administration
WASHINGTON, D.C. 20546

OFFICIAL BUSINESS
Penalty For Private Use, $300.00

POSTAGE AND FEES PAID
NATIONAL AERONAUTICS AND
SPACE ADMINISTRATION
PERMIT No. G27

U.S.MAIL

SPECIAL FOURTH CLASS MAIL
BOOK

11 001 CE-3C31-1 E9C417SCC237EL
GOVERNMENT PRINTING OFFICE
LIBRARY PROGRAMS SERVICE/SIIP
ACQUISITIONS SECTION
WASHINGTON DC 20401

NASA

POSTMASTER: **If Undeliverable (Section 158 Postal Manual) Do Not Return**

END

DATE FILMED

02-17-92